

SPINAL LIPOMA: DEVELOPING A BIOMARKER AND  
DEVELOPMENTAL  
MECHANISMS

Victoria Jane Jones

Thesis submitted for the degree of Doctor of Philosophy

Institute of Child Health,  
University College London

## **DECLARATION**

I, Victoria Jane Jones confirm that the work presented in this thesis is my own. Where information has been derived from other sources, I confirm that this has been indicated in the thesis.

## ABSTRACT

Lumbosacral lipomas (LSL) are a common form of closed spinal dysraphism occurring in 1 in 4000 live births. There is no established theory to explain origin, no animal models and no genetic or environmental association. In addition to the uncertainty that underlies the pathogenesis there are also unanswered clinical questions, with the timing of surgical intervention a difficult balance between prevention of neurological deterioration and avoidance of unnecessary surgery. Wykes et al. have demonstrated that not all children go onto develop symptoms in the first 10 years of life and therefore timing of surgery becomes an important issue. This thesis attempts to answer two questions – is there a biomarker that can be used to guide timing of surgery, and what is the underlying pathogenesis of LSL?

Samples of cerebrospinal fluid (CSF), blood and urine were collected from patients undergoing near total resection of LSL. High performance liquid chromatography/mass spectrometry (HPLC/MS) was used to determine the lipid profile of samples and a scoring system developed to correlate lipid results with severity of symptoms. In addition, Whole Genome Sequencing was performed on two families with familial cases of LSL and analysed in combination with Whole Exome Sequencing from two further individuals with LSL.

HPLC/MS confirmed a significant difference in phospholipids and targeted assay revealed lysophosphatidylcholine 18:2 and phosphatidylcholine 36:2 to be significantly different in CSF and blood samples respectively. These results not only have potential for development of a biomarker to guide clinical management but also hint at an underlying mechanism of neurological deterioration due to bioavailability of docosahexaenoic acid in CSF. Genetic analysis identified a number of different variants in LSL patients highlighting the complexity of pathogenesis. Identification of stop gain variants in *ADAMTS20* and *NDTS1* supports earlier work relating LSL pathogenesis to failure in neural crest differentiation and migration.

## IMPACT STATEMENT

This thesis represents the first steps in research that is hoped can lead to an improvement in the lives of children, and their families, born with lumbosacral lipoma (LSL). This can be achieved in several ways. Firstly, by validating the biomarker identified in this thesis and initiating its use in clinical practice. Children with LSL currently undergo prolonged clinical surveillance causing anxiety and uncertainty. Many end up undergoing complex spinal surgery that some children might not have ever needed. It is hoped this biomarker could reduce this uncertainty and even prevent children undergoing unnecessary surgery. Secondly, the identification of a possible mechanism by which some children progress more rapidly has led to the proposal of a medical treatment that might help to slow progression. Further research is required to confirm this potential, but, the simple medical treatment proposed could greatly impact on the lives of these children. Both biomarker and medical treatment require prospective trials to allow translation into clinical practice and this thesis clearly lays out the steps that would need to be done to achieve this.

In addition to the translational aspect of this thesis, insight is gained into the mechanisms underlying the pathogenesis and nature of LSL. Firstly, a clearer understanding of LSL as a pathology is demonstrated, separating it from the umbrella phrase 'closed spinal dysraphism' so commonly used in the literature. It is hoped that such insight may change the way genetic analysis is performed. Secondly, this thesis supports the hypothesis that LSL occurs from the maldifferentiation of caudal progenitor cells and highlights a number of different genes that may be involved in this process. The proposal is made that LSL occurs due to a disruption of at least two different pathways: one local to the development of the pathology and a second more global and fundamental to cellular function. Disruption to global cellular processes must be minor such that the individual does not suffer a significant metabolic dysfunction, yet in combination with disruption to caudal spinal cord development LSL will form. Experimental evidence is required to support a role of these genes highlighted in this thesis. However, there is potential that this work will lead to the development of an animal model of LSL which will accelerate our understanding of this pathology.

## CONTENT

|  |      |
|--|------|
| SECTION I  |      |
| 1. Abstract  | p3   |
| 2. Impact statement                                | p4   |
| 3. Content   | p5   |
| 4. List of Figures and Tables                      | p7   |
| 5. Acknowledgments                                 | p13  |
| 6. Abbreviations                                   | p14  |
| SECTION II: INTRODUCTION                           | p19  |
| SECTION III: METHODS                               |      |
| 1. Lipidomics                                      | p71  |
| 2. Targeted Assay                                  | p74  |
| 3. Genetics  | p84  |
| SECTION IV: DEVELOPING A BIOMARKER RESULTS         |      |
| 1. Lipidomics                                      | p86  |
| 2. Targeted Assay                                  | p123 |
| 3. Clinical Assessment and Correlation             | p140 |
| 4. Neurophysiology                                 | p160 |
| 5. Combined lipid analysis                         | p173 |
| 6. Discussion                                      | p177 |
| SECTION V: GENETICS RESULTS                        | p193 |
| 1. <i>RADIL/ARHGAP29</i>                           | p197 |
| 2. Familial LSL                                    | p207 |
| 3. Combined LSL cohort                             | p216 |
| 4. Comparison with the literature                  | p219 |
| 5. Discussion                                      | p221 |
| SECTION VI: DISCUSSION                             | p231 |
| 1. Strengths and Weaknesses: Biomarker Development | p234 |
| 2. Strengths and Weaknesses: Genetics              | p239 |
| 3. Further Work                                    | p244 |

## SECTION VII: SUPPLEMENTARY INFORMATION

|   |      |
|---|------|
| 1. Parent information sheet for biomarker development   | p269 |
| 2. Consent form for biomarker development   | p272 |
| 3. R scripts  | p273 |
| 4. Parent information sheet for genetics  | p275 |
| 5. Consent form for genetics  | p278 |
| 6. Patient clinical detail for biomarker development  | p279 |
| 7. 2x2 charts   | p281 |
| 8. Extended lipidomics database search  |      |
| a. Lipidomics 1: csf, plasma, urine   | p282 |
| b. Lipidomics 2: csf, plasma, urine   | p306 |
| 9. Extended plasma positive correlation results   | p326 |
| 10. Extended urine negative correlation results   | p329 |
| 11. Published paper: The pathology of lumbosacral lipomas:<br>macroscopic and microscopic disparity have implications for<br>embryogenesis and mode of clinical deterioration | p334 |
| 12. Published paper: Placode rotation in transitional lumbosacral<br>lipomas: are there implications for origin and mechanism of<br>deterioration?                            | p343 |

## LIST OF FIGURES AND TABLES

### FIGURES

|  |      |
|--|------|
| Figure II.1.i Primary and secondary neurulation  | p23  |
| Figure II.1.ii LSL MR images   | p39  |
| Figure II.1.iiia Histopathology of LSL (neuroectodermal cell types)  | p41  |
| Figure II.1.iiib Histopathology of LSL (mesodermal cell types)   | p42  |
| Figure II.1.iv Histopathology by LSL subtypes  | p43  |
| Figure II.1.v Phosphatidylcholine  | p58  |
| Figure II.1.vi Biosynthesis of PE and PC   | p59  |
| Figure II.1.vii Cleavage of phospholipids  | p61  |
| Figure II.1.viii Schematic representing clinical assessment of LSL patients  | p66  |
| Figure III.1.i Sample chromatogram   | p73  |
| Figure III.2.i Electrospray ionisation detection of phospholipid subclasses  | p74  |
| Figure III.2.ii Spectra of phosphatidylcholine   | p76  |
| Figure III.2.iii Spectra of phosphatidylethanolamine   | p76  |
| Figure III.2.iv Spectra of fragmentation of phosphatidylethanolamine   | p77  |
| Figure III.2.v Spectra of neutral loss scan for phosphatidylethanolamine   | p78  |
| Figure III.2.vi Chromatogram of phospholipid separation  | p79  |
| Figure III.2.vii Calibration curve for LPC standards   | p80  |
| Figure III.2.viii Position of scalp electrodes for TcMEPs and SSEPs  | p83  |
| Figure IV.1.i Volcano plot of CSF lipid: (Lipidomics 1: LSL versus control)  | p89  |
| Figure IV.1.ii Volcano plot of plasma lipid: (Lipidomics 1: LSL versus control)  | p92  |
| Figure IV.1.iii Volcano plot of urine lipid: (Lipidomics 1: LSL versus control)  | p94  |
| Figure IV.1.iva Volcano plot of CSF and plasma lipids: (Lipidomics 1: LSL versus control)  | p98  |
| Figure IV.1.ivb Comparison of mass charge ratio-retention time pairing between CSF and plasma samples (Lipidomics 1: LSL versus control) | p98  |
| Figure IV.1.v Volcano plot of CSF lipids: (Lipidomics 2: LSL versus control)   | p101 |
| Figure IV.1.vi Volcano plot of plasma lipids: (Lipidomics 2: LSL versus control)   | p103 |
| Figure IV.1.vii Volcano plot of urine lipids: (Lipidomics 2: LSL versus control)   | p106 |

|   |      |
|---|------|
| Figure IV.1.viii a Volcano plot of CSF and plasma lipids: (Lipidomics 2: LSL versus control)  | P108 |
| Figure IV.1.viii b Volcano plot of CSF and plasma lipids: (Lipidomics 2: LSL versus control) negative fold change only                                  | P108 |
| Figure IV.1.viii c Comparison of mass charge ratio-retention time pairing between CSF, plasma and urine samples (Lipidomics 2: LSL versus control)      | P110 |
| Figure IV.1.ix Volcano plot of CSF lipids: (Lipidomics 2: symptomatic versus asymptomatic)  | P113 |
| Figure IV.1.x Volcano plot of plasma lipids: (Lipidomics 2: symptomatic versus asymptomatic)  | P115 |
| Figure IV.1.xi Volcano plot of urine lipids: (Lipidomics 2: symptomatic versus asymptomatic)  | p118 |
| Figure IV.1.xii a Volcano plot of CSF and plasma lipids: (Lipidomics 2: symptomatic versus asymptomatic)  | p121 |
| Figure IV.1.xii b Comparison of mass charge ratio-retention time pairing between CSF and plasma samples (Lipidomics 2: symptomatic versus asymptomatic) | p122 |
| Figures IV.2.iva-e Chromatograms and spectra of PC 32:O-32:4  | p124 |
| Figure IV.2.va and b Targeted lipid results CSF: LSL versus control   | p127 |
| Figure IV.2.via and b Targeted lipid results plasma: LSL versus control   | p129 |
| Figure IV.2.vii Targeted lipid results urine: LSL versus control  | p130 |
| Figure IV.2.viii a and b Targeted lipid results CSF: symptomatic versus asymptomatic  | p132 |
| Figure IV.2.ix a and b Targeted lipid results plasma: symptomatic versus asymptomatic   | p134 |
| Figure IV.2.x a and b Targeted lipid results urine: symptomatic versus asymptomatic   | p136 |
| Figure IV.3.ia. Assessment of motor function in patients with LSL   | p144 |
| Figure IV.3.ib. Assessment of lower limb deformity in patients with LSL   | p145 |
| Figure IV.3.ic. Assessment of sensory loss in patients with LSL   | p146 |
| Figure IV.3.id. Assessment of lower limb pain in patients with LSL  | p147 |
| Figure IV.3.ie. Assessment of progression of symptoms in patients with LSL  | p148 |
| Figure IV.3.ii. Urological assessment in symptomatic LSL patients   | p149 |
| Figure IV.3.iii. Distribution of Total Clinical Score   | p150 |
| Figure IV.3.iv. Correlation of Total Clinical Score and LPC 22:3 in CSF   | p151 |
| Figure IV.3.v. Lipids in plasma with negative correlation with Total Clinical Score   | p152 |



|   |      |
|---|------|
| Figure IV.3.vi. Lipids in plasma with positive correlation with Total Clinical Score                            | p155 |
| Figure IV.3.vii. Lipids in urine with negative correlation with Total Clinical Score                            | p157 |
| Figure IV.3.viii.a Correlation of Total Clinical Score and PC/PE ratio in plasma samples                        | p158 |
| Figure IV.3.viii.b Correlation of Total Clinical Score and PC:PE ratio in CSF and urine samples.                | p159 |
| Figure IV.3.ix Correlation of Total Clinical Score and LPE/PE ratio in plasma samples                           | p165 |
| Figure IV.4.i ROC curve of BCR and CIC  | p166 |
| Figure IV.4.ii ROC curve of BCR and post-void residual percentage   | p167 |
| Figure IV.4.iii. Comparison between pre-operative and post-operative mean BCR and mean sphincter MEPs           | p168 |
| Figure IV.4.iv Lipids in CSF: abnormal versus normal BCR  | p170 |
| Figure IV.4.va and b Lipids in plasma: abnormal versus normal BCR   | p172 |
| Figure IV.4.vi Lipids in urine: abnormal versus normal BCR  | p183 |
| Figure IV.6.i. Summary of effects of altered intracellular PC/PE ratio  | p187 |
| Figure IV.6.ii Diagrammatic representation of PC and LPC  | p190 |
| Figure IV.6.iii.a. Comparison of targeted assay results from symptomatic LSL patients in CSF, plasma and urine  | p191 |
| Figure IV.6.iii.b. Comparison of targeted assay results from asymptomatic LSL patients in CSF, plasma and urine | p193 |
| Figure V.i Pedigree of two separate familial cases of LSL   | p194 |
| Figure V.ii. Pedigrees of Families 3 and 4  | p196 |
| Figure V.iii. String diagram of the neural crest differentiation pathway taken from Pathcards                   | p197 |
| Figure V.iv. String diagram of the adipogenesis superpathway taken from Pathcards                               | p203 |
| Figure V.1.i and ii. RNAscope of <i>RADIL</i> expression  | p206 |
| Figure V.1.iii. RNAscope of <i>ARHGAP29</i> expression  |      |

## **TABLES**

|   |     |
|---|-----|
| Table II.1.i Comparison of LSL subtypes   | p45 |
| Table III.2.i Total Clinical Score  | p81 |
| Table IV.1.ia Candidate lipids in CSF with highest p-values (Lipidomics 1: LSL versus control)                | p89 |
| Table IV.1.1b Candidate lipids in CSF with most negative log 2 fold change (Lipidomics 1: LSL versus control) | p89 |

|   |      |
|---|------|
| Table IV.1.ic Candidate lipids in CSF with most positive log 2 fold change (Lipidomics 1: LSL versus control)               | p90  |
| Table IV.1.iia Candidate lipids in plasma with highest p-values (Lipidomics 1: LSL versus control)                          | p92  |
| Table IV.1.iib Candidate lipids in plasma with most negative log 2 fold change (Lipidomics 1: LSL versus control)           | p92  |
| Table IV.1.iic Candidate lipids in plasma with most positive log 2 fold change (Lipidomics 1: LSL versus control)           | p93  |
| Table IV.1.iiia Candidate lipids in urine with highest p-values (Lipidomics 1: LSL versus control)                          | p95  |
| Table IV.1.iiib Candidate lipids in urine with most negative log 2 fold change (Lipidomics 1: LSL versus control)           | p95  |
| Table IV.1.iiic Candidate lipids in urine with most positive log 2 fold change (Lipidomics 1: LSL versus control)           | p96  |
| Table IV.1.iv Identification of lipids by Lipidmaps (Lipidomics 1: LSL versus control)                                      | p98  |
| Table IV.1.va Candidate lipids in CSF with highest p-values (Lipidomics 2: LSL versus control)                              | p100 |
| Table IV.1.vb Candidate lipids in CSF with most negative log 2 fold change (Lipidomics 2: LSL versus control)               | p101 |
| Table IV.1.vc Candidate lipids in CSF with most positive log 2 fold change (Lipidomics 2: LSL versus control)               | p101 |
| Table IV.1.via Candidate lipids in plasma with highest p-values (Lipidomics 2: LSL versus control)                          | p103 |
| Table IV.1.vib Candidate lipids in plasma with most negative log 2 fold change (Lipidomics 2: LSL versus control)           | p103 |
| Table IV.1.vic Candidate lipids in plasma with most positive log 2 fold change (Lipidomics 2: LSL versus control)           | p104 |
| Table IV.1.viia Candidate lipids in urine with highest p-values (Lipidomics 2: LSL versus control)                          | p106 |
| Table IV.1.viib Candidate lipids in urine with most negative log 2 fold change (Lipidomics 2: LSL versus control)           | p106 |
| Table IV.1.viic Candidate lipids in urine with most positive log 2 fold change (Lipidomics 2: LSL versus control)           | p107 |
| Table IV.1.viia and b Identification of lipids by Lipidmaps (Lipidomics 2: LSL versus control)                              | p109 |
| Table IV.1.ixa Candidate lipids in CSF with highest p-values (Lipidomics 2: symptomatic versus asymptomatic)                | p113 |
| Table IV.1.ixb Candidate lipids in CSF with most negative log 2 fold change (Lipidomics 2: symptomatic versus asymptomatic) | p114 |

|   |      |
|---|------|
| Table IV.1.ixc Candidate lipids in CSF with most positive log 2 fold change (Lipidomics 2: symptomatic versus asymptomatic)   | p114 |
| Table IV.1.xa Candidate lipids in plasma with highest p-values (Lipidomics 2: symptomatic versus asymptomatic)                | p116 |
| Table IV.1.xb Candidate lipids in plasma with most negative log 2 fold change (Lipidomics 2: symptomatic versus asymptomatic) | p116 |
| Table IV.1.xc Candidate lipids in plasma with most positive log 2 fold change (Lipidomics 2: symptomatic versus asymptomatic) | p117 |
| Table IV.1.xia Candidate lipids in urine with highest p-values (Lipidomics 2: symptomatic versus asymptomatic)                | p119 |
| Table IV.1.xib Candidate lipids in urine with most negative log 2 fold change (Lipidomics 2: symptomatic versus asymptomatic) | p119 |
| Table IV.1.xic Candidate lipids in urine with most positive log 2 fold change (Lipidomics 2: symptomatic versus asymptomatic) | p120 |
| Table IV.2.i Comparison of mean PC/PE ratios  | p138 |
| Table IV.2.ii.a Comparison of mean LPC/PC ratios  | p139 |
| Table IV.2.ii.b Comparison of mean LPE/PE ratios  | p139 |
| Table IV.3.i Total Clinical Score   | p143 |
| Table IV.4.i Summary of IONM results at initiation of surgery   | p162 |
| Table IV.5.i Summary of lipidomics results  | p173 |
| Table IV.5.ii Summary of targeted assay results   | p174 |
| Table IV.5.iii Summary of results from clinical correlation   | p174 |
| Table IV.5.iv Summary of comparison of results from different methods of analysis   | p175 |
| Table V.1.i Summary of all non-synonymous exonic variants in <i>RADIL</i>   | p198 |
| Table V.1.ii. Summary of variants likely to result in TFBS loss within the <i>RADIL</i> sequence in Family 1                  | p200 |
| Table V.1.iii. Summary of exonic non-synonymous variants in Family 2  | p201 |
| Table V.1.iv. Summary of variants likely to result in TFBS loss within the <i>RADIL</i> sequence in Family 2                  | p202 |
| Table V.1.v. Summary of variants likely to result in TFBS loss within the <i>ARHGAP29</i> sequence in Family 1                | p204 |
| Table V.1.vi. Summary of variants likely to result in TFBS loss within the <i>ARHGAP29</i> sequence in Family 2               | p205 |
| Table V.2.i. Summary of results from genetic analysis of whole genome sequencing from Family 1.                               | p208 |
| Table V.2.ii. Summary of candidate genes identified in Family 1 with stop gain variants                                       | p209 |
| Table V.2.iii. Summary of candidate genes identified in Family 1 with frameshift variants                                     | p210 |

|  |      |
|--|------|
| Table V.2.iv. Summary of candidate genes identified in Family 1 with single missense variants    | P211 |
| Table V.2.v. Summary of results from genetic analysis of whole genome sequencing from Family     | p213 |
| Table V.2.vi. Summary of candidate genes identified in Family 2 with single missense variants    | p215 |
| Table V.3.i. Summary of results from genetic analysis from all LSL individuals                   | p216 |
| Table V.3.ii. Summary of variants identified in <i>EIF4EBP1</i>                                  | p217 |
| Table V.3.iii. Summary of variants identified in <i>FRG2C</i>                                    | p218 |
| Table VI.1.i 'Problems and potential solutions at each stage of the biomarker research pipeline' | p238 |

## ACKNOWLEDGMENTS

This thesis would not have been possible without support from many people. Firstly, to my supervisors, Andrew Copp and Dominic Thompson for their ongoing support, understanding and inspiration. Secondly for technical support from a number of different people. Kevin Mills and Jenny Halqvist offered hours of support and advice in developing the targeted lipid assays. Jade Hawksworth and Sven Meckelmenn for sharing their knowledge and skills in lipidomics both in terms of lipid sample preparation and mass spectrometry as well as sharing their knowledge and algorithms for data analysis. Special thanks to Jade for such a warm welcome in Cardiff!

There are too many people to mention by name who helped with management of clinical patients. I am effusively grateful to all the doctors and nurses in the neurosurgery department at Great Ormond Street as well as physiotherapists, laboratory staff, anaesthetists and theatre staff. Special thanks must go to Lindy May whose vast knowledge of all the spina bifida patients in the department was invaluable. In addition, Ivan Jankovic for kindly sharing all her neurophysiology data collected over many years and Nikki Cohen and Tom Jacques for sharing their histopathology data and knowledge.

Genetic analysis would not have been possible without the support of Phil Stanier and once again Lindy May, who have been collecting DNA samples from spina bifida patients for many years prior to the start of my research. Phil kindly read through the genetics section of this thesis and offered much insight and advice in interpretation of the data. In addition, the GOSgene team and specifically Louise Ocaka for her help in preparing samples and teaching analysis techniques, as well as the HDBR for providing human fetal tissue and help with in situ analysis from Nadia Moreno.

Finally, all the work that underpins this thesis would have been possible without the support from my family and friends, specifically my husband for his patience and encouragement.

## ABBREVIATIONS

### A

ACMG = American College of Medical Genetics

#### Amino acid abbreviations

| Abbreviation | 1 letter abbreviation | Amino acid name             |
|--------------|-----------------------|-----------------------------|
| Ala          | A                     | Alanine                     |
| Arg          | R                     | Arginine                    |
| Asn          | N                     | Asparagine                  |
| Asp          | D                     | Aspartic acid               |
| Cys          | C                     | Cysteine                    |
| Gln          | Q                     | Glutamine                   |
| Glu          | E                     | Glutamic acid               |
| Gly          | G                     | Glycine                     |
| His          | H                     | Histidine                   |
| Ile          | I                     | Isoleucine                  |
| Leu          | L                     | Leucine                     |
| Lys          | K                     | Lysine                      |
| Met          | M                     | Methionine                  |
| Phe          | F                     | Phenylalanine               |
| Pro          | P                     | Proline                     |
| Pyl          | O                     | Pyrrolysine                 |
| Ser          | S                     | Serine                      |
| Sec          | U                     | Selenocysteine              |
| Thr          | T                     | Threonine                   |
| Trp          | W                     | Tryptophan                  |
| Tyr          | Y                     | Tyrosine                    |
| Val          | V                     | Valine                      |
| Asx          | B                     | Aspartic acid or Asparagine |
| Glx          | Z                     | Glutamic acid or Glutamine  |
| Xaa          | X                     | Any amino acid              |
| Xle          | J                     | Leucine or Isoleucine       |

AMT - aminomethyltransferase

ATP = adenosine triphosphate

### B

BAM = binary sequence alignment map

BCR = bulboavernosus reflex  
BGI = Beijing Genomics Institute  
BMP = bone morphogenetic proteins  
BTB = Broad-complex, Tramtrack and Bric a brac domain

## **C**

CADD = Combined Annotation Dependent Depletion  
CE = cholesterol ester  
CIC = clean intermittent catheterization  
CS = Carnegie Stage  
CSF = cerebrospinal fluid  
CT = CTP:phosphocholine cytidylyltransferase  
CTP = cytidine triphosphate  
Colleagues:  
    DT Dominic Thompson  
    NC Nikki Cohen  
    LM Lindy May  
    IJ Ivana Jankovic  
    NM Nadia Moreno  
    LR Liam Rasch  
CREBBP = CREB Binding Protein  
CREB = cAMP-response element-binding protein

## **D**

d8 = eight deuterium atoms  
dn = number of deuterium atoms in a molecule  
DAG = diacylglycerol  
DHA = docosahexaenoic acid  
DMPE = 1,2-Bis(dimethylphosphino)ethane  
DNA = deoxyribonucleic acid  
Dvl = disheveled  
Dd = double distilled water

## **E**

EMG = electromyography  
ERAD = endoplasmic reticulum associated degradation  
EDTA = ethylenediaminetetraacetic acid

## Elements

C = carbon

H = hydrogen

N = nitrogen

P = phosphate

O = oxygen

ES = electrospray ionization

eV = electron volts

## **F**

FGF = fibroblast growth factor

FOLR3 = folate receptor 3

Fs = frameshift

## **G**

GLDC = glycine decarboxylase

GOSH = Great Ormond Street Hospital

GlcNAc = *N*-acetyl-D-glucosamine

GlcAc = glucuronic acid

## **H**

H<sub>2</sub>O = water

H<sub>2</sub>O<sub>2</sub> = hydrogen peroxide

HDBR = Human Developmental Biology Resource

Het = heterozygous

Hom = homozygous

HPLC = high performance liquid chromatography

HSPG = heparan sulphate proteoglycan

## **I**

IGV = integrative genomics viewer

IPA = isopropyl alcohol (2-propanol)

IONM = intra-operative neurophysiology monitoring

## **K**

kb = kilobase



## L

Lipid Abbreviations:

| Abbreviation | Lipid                         |
|--------------|-------------------------------|
| MG           | Monoglycerol                  |
| DG           | Diglycerol                    |
| TG           | Triglycerol                   |
| MGDG         | Monogalactosyldiacylglycerol  |
| DGDG         | Digalactosyldiacylglycerol    |
| SQDG         | Sulfoquinovosyldiacylglycerol |
| PA           | Phosphatidic acid             |
| LPA          | Lysophosphatidic acid         |
| PC           | Phosphatidylcholine           |
| LPC          | Lysophosphatidylcholine       |
| PE           | Phosphatidylethanolamine      |
| LPE          | Lysophosphatidylethanolamine  |
| PG           | Phosphatidylglycerol          |
| LPG          | Lysophosphatidylglycerol      |
| PS           | Phosphatidylserine            |
| LPS          | Lysophosphatidylserine        |
| FA           | Fatty acid                    |
| NAE          | N-acyl ethanolmaine           |
| NAT          | N-acyl taurine                |
| CoA          | Acyl CoA                      |
| CAR          | Acyl carnitines               |
| CE           | Cholesterol esters            |
| Sph          | Sphingoid base                |

LMM = lipomyelomeningocele

LM = lipomeningocele

L:CAT = lecithin:cholesterol acyltransferase

LSL = lumbosacral lipoma

## M

MEP = motor evoked potential

MMC = myelomeningocele

MRC = medical research council

MRI = magnetic resonance imaging

MS = mass spectrometry

MTHFR = methylenetetrahydrofolate reductase

MTHFD = methylenetetrahydrofolate dehydrogenase

M/Z = mass charge ratio

mg = milligram

µg = microgram

ml = microlitre

µl = microlitre

## **N**

NBM = nil by mouth

NC = neural crest

ng = nanogram

NMP = neuromesodermal progenitor

NP = neurophysiology

NTD = neural tube defect

Nucleotides

A = adenine

C = cytosine

G = guanine

T = thymine

## **O**

OEIS = omphalocele, exstrophy, imperforate anus, spinal defects complex

## **P**

PAP = 3'-phosphoadenosine 5'-phosphate

PLA2 = phospholipase A2

PC = phosphatidylcholine

PE = phosphatidylethanolamine

PCP = planar cell polarity

PIP2 = phosphatidylinositol 4,5-bisphosphate

PPAR = peroxisome proliferator-activated receptors

PP-2 = Polymorphism Phenotyping version 2

## **R**

RNA = ribonucleic acid

ROC curve = receiver operator characteristic curve

ROCK = rho-associated protein kinase

RS id = reference SNPs cluster id

RT = retention time

Rpm = revolutions per minute

## **S**

SDR = selective dorsal rhizotomy

SIFT = Sorting Intolerance from Tolerance

SSEP = somatosensory evoked potential

SNV/SNP = single nucleotide variant/polymorphism

SCM = split cord malformation

Shh = sonic hedgehog

## **T**

TcMEP = transcranial motor evoked potential

TCS = Total Clinical Score

TFBS = transcription factor binding site

TNF = tumour necrosis factor

TGF = transforming growth factor

TRADD = TNF receptor type 1-associated death domain

TRAF2 = TNF receptor-associated factor 2

TSR = thrombospondin repeats

## **U**

UTI = urinary tract infection

## **V**

V = volts

VACTERL = vertebral anomaly, anal atresia, cardiac defect, trachea-oesophageal fistula, renal anomalies and limb abnormalities

Vertebra

C = cervical

T = thoracic

L = lumbar

S = sacral

VPS = ventriculoperitoneal shunt

## **W**

WGS = whole genome sequencing

WES = whole exome sequencing

## SECTION II

### 1. INTRODUCTION

#### **CONGENITAL BIRTH DEFECTS**

Congenital birth defects remain a major cause of morbidity and mortality around the world, with the World Health Organization estimating that 303,000 neonates die each year due to a congenital birth defect. Most of these deaths are due to severe birth defects such as heart defects, neural tube defects (NTDs) and Down's syndrome. Although there is established aetiology for many of these, for example trisomy 21 and Down's syndrome, approximately 50% of birth defects are of unknown causation, with many likely to be a combination of factors: genetic, environmental, nutritional and infectious [1].

An increase in antenatal screening, legalization of medical terminations and improvement/better understanding of nutrition over the 20<sup>th</sup> century has led to a significant decrease in the incidence of severe birth defects in the developed world. An example of this is the fall in overall prevalence of neural tube defects following the introduction and promotion of folic acid supplementation in the diet before and during early pregnancy [2]. However, the total incidence seems to be increasing with birth defects occurring in 1 in 49 births in the UK in 2009 [3]. A large number of milder defects with less obvious symptoms/presentation that may have gone undiagnosed prior to the development of CT and MR imaging and screening programs continue to persist within the population. Genetic causes of birth defects that do not alter an individual's fecundity are likely to remain prevalent in the population and as the incidence of more severe congenital defects is reduced, these milder defects and importantly their long-term management are likely to become an increasing topic of focus for the medical community.

#### **Congenital Birth Defects of the Central Nervous System**

As mentioned above, NTDs are one of the major causes of neonatal morbidity due to birth defect and account for 38% of all congenital birth defects involving the central nervous system [4]. Other developmental defects in the central nervous system can be divided based on failure of the developmental mechanisms resulting in the pathology: disorders of cell proliferation and differentiation within the cortex result in microcephaly; disorders of cell migration result in lissencephaly, heterotopia and microgyria. Due to the sensitive nature of development of the nervous system is it not uncommon for combined defects to be present, presenting as a spectrum of manifestations such as agenesis of the corpus callosum, porencephaly or schizencephaly [5].

## **DEVELOPMENTAL BIOLOGY OF THE LOWER SPINAL CORD AND VERTEBRAL COLUMN**

To consider neural tube defects in more detail, an understanding of the relevant developmental stages and processes is required. It should be noted that there is interspecies variation in development and that most mammalian experimental evidence comes from mouse embryos. Since mouse embryos are often used to model human neural tube defects, it is important to also consider where these developmental processes have been shown to, or even are assumed to, vary between these two species.

Initial conversion of the bilaminar embryo into a trilaminar structure is known as gastrulation. The result is three definitive germ layers and specification of two body axes: left-right and rostral-caudal. The dorsal layer of the bilaminar disc, known as the epiblast, migrates through the primitive streak and node generating the mesoderm and endoderm respectively. The epiblast cells remaining on the dorsal surface give rise to the ectoderm. In developmental pathologies where ectodermal, mesodermal and endodermal cell types exist in a disorganized fashion it is tempting to relate these pathologies to a disruption of gastrulation. However, it is now established that gastrulation only contributes to the three germ layers in the cranial and cervical region of the embryo above the level of the sixth somite [6]. The caudal spinal cord, the location of lumbosacral lipomas (LSL) and other forms of closed spinal dysraphism, arises from the 'tail-bud' region and a group of progenitor cells.

A distinct population of epiblast cells at the rostral end of the primitive streak (the primitive node) migrate caudally and ventrally to join the hypoblast layer, eventually replacing this primitive endoderm with the definitive gut endoderm [7]. The midline cells left in the wake of this migration are known as the head process, they are separated dorsally from the overlying epiblast to form a rod like structure located between the gut and neural tube, the notochord. In humans the notochord is commonly described as initially being hollow with openings at the dorsal epiblast/ectoderm layer and ventral endoderm layer. This is said to result in a communication between the amniotic cavity and the yolk sac known as the 'neurenteric canal' [8]. In mouse embryos the notochord forms via three distinct developmental origins but remains a solid structure and no such neurenteric canal has been recognized [9]. In both species the notochord has a dual function. It induces and patterns neighbouring neural and mesodermal tissue through the release of Shh thereby acting as a signalling centre. Following this role, it acts as a nucleation centre as sclerotomal cells condense around it to form the vertebral bodies, ultimately leaving the notochord remnant as the nucleus pulposus of intervertebral discs.

### **Primary and Secondary Neurulation**

The brain and spinal cord form from the ectoderm via two separate processes: primary and secondary neurulation. Primary neurulation is the principal process forming most of the embryonic neural tube. Initiation starts with an area of thickened pseudostratified epithelium in response to signals from the notochord and the formation of a medial hinge point at the hindbrain-spine junction. These morphological changes are tightly regulated by convergent extension (CE) displacement of cells. Both neurectoderm and adjacent mesodermal cells show a net lateral-to-medial displacement of cells, and as cells intercalate into the midline the embryo becomes both narrower and elongates along the cranio-caudal axis. CE cell movements are under the regulation of the Planar Cell Polarity pathway (PCP), a non-canonical Wnt/frizzled/dishevelled signalling pathway [10]. Mouse mutants in this pathway develop large open neural tube defects (craniorachischisis) due to a failure of initiation of neural tube closure associated with short but broad neural plates [11]. In addition, a number of variants in genes of the PCP pathway have been identified in large-scale genetic studies of neural tube defects in humans.

Through the process of CE the neuroepithelium generates bilateral neural folds that eventually fuse in the dorsal midline, completing closure of the neural tube. In mammals this fusion occurs at several locations along the cranio-caudal axis of the embryo with subsequent closure in adjacent areas resulting in “zippering” [12-16]. Failure of completion of this closure results in more localized open neural tube defects, myelomeningcele [13, 16].

During development, the mammalian embryo can be considered as two distinct parts, extending from the head to the cloaca is the trunk and from the cloaca to the most caudal aspect of the embryo is the tail. CE and axis elongation play important roles in the formation of both these regions, however different mechanisms and stem cell activity occur at the caudal end of the embryo. For example, gastrulation only contributes to the three germ layers up to somite 6 and CE contributes to elongation of the neural tube up to somite 20 [17]. In addition, it can be difficult to relate these developmental processes and divisions to final anatomy in adults.



Figure II.1.i. Schematic diagram representing the key steps present in both primary and secondary neurulation. A, secondary neurulation occurring in the tailbud. Mesenchymal cells aggregate, canalize and undergo transition to epithelial cells forming the secondary neural tube. B and C, stages of primary neurulation. B, neuroepithelium of the neural plate folds under the influence of CE cell movements before completely separating from the overlying epithelium forming the primary neural tube. Adjacent mesodermal cells congregate and segment to form somites. C, under the influence of Shh release from the notochord somites further divide into dermatomyotome and sclerotomes with the sclerotomes condensing around the spinal cord and notochord to form vertebrae. Taken from Jones et al 2019 [18].

Primary neurulation is believed to be responsible for formation of the spinal cord above the level of the conus medullaris. The conus medullaris, cauda equina and filum terminale are said to form via secondary neurulation. Secondary neurulation in humans occurs caudal to the posterior neuropore, from the level of somites 32 to 34 (corresponding to S3-5). The process initiates around 27 days post fertilization, approximately at the time of closure of the posterior neuropore. The secondary neural tube forms with medullary rosette formation and cavitation both occurring concomitantly. Unlike primary neurulation the caudal most neural tube does not form from neuroepithelial cells but rather multipotent mesenchymal tailbud cells. An important distinction being the overlying future epidermis remains intact throughout the process of secondary neurulation. The tailbud mesenchymal cells aggregate and condense with a radial arrangement

in the midline forming a medullary rosette. This structure fuses with the primary neural tube as the cells become apicobasally polarized, undergo mesenchymal to epithelial transition and ultimately undergo canalization to complete the spinal cord [12, 19-22] (Figure II.1.i). The lack of disturbance of the overlying epithelial layer during secondary neurulation results in disruption of this process causing pathologies covered in skin, as demonstrated by the closed spinal dysraphisms.

### **Junctional Neurulation Zone**

The junction between the primary and secondary neural tubes is not simply transverse in chick embryos. Instead, a transition zone has been identified with a clear demarcation between primary and secondary neural tubes as the caudal most primary neural tube extends dorsally and overlaps with the rostral most secondary tube extending ventrally [23]. It has been proposed that this region of the spinal cord forms via a different process to both primary and secondary neurulation dubbed 'junctional neurulation'. Within the same axial plane, dorsal Sox2 positive cells contribute to the very terminal part of the primary neural tube while ventral Sox2 negative cells undergo epithelial-mesenchymal transition and intercalate with the caudal mesenchymal cells forming the secondary neural tube. *Prickle 1* has been found to be expressed at this level and its inhibition results in NTDs in this region making this a candidate for a key role in junctional neurulation [24]. However, the same phenotype is not seen in mouse mutants. Instead partial loss of function of *Prickle 1* mimics the human condition Robinow syndrome which is characterized by growth restriction and vertebral segmentation abnormalities but not spinal dysraphism [25].

No transition zone is observed in mouse embryos, and therefore it is assumed to also not be present in humans [26]. Despite this, junctional neural tube defects have recently been described in a small number of case reports. Characteristically all these patients had a functioning spinal cord corresponding to regions of both primary and secondary neural tubes that appeared structurally intact but were separated by a band of non-neuronal tissue [27, 28].

### **Neuromesodermal Progenitor Cells**

Within the tailbud mesenchyme, a population of self-renewing progenitor cells have been identified that have the potential to differentiate into both neuroectodermal and mesodermal structures following in vitro formation of a "gastruloid" [29, 30]. These cells, known as neuro-mesodermal progenitors (NMPs), express both Sox2 and Brachyury, two transcription factors that can be considered master switches that regulate subsequent development of neuroectoderm and mesoderm respectively [31-33]. From as early as E8.5 in mouse embryos, cells co-expressing these two factors have been identified at the caudal lateral epiblast, the node streak border and the chordoneural hinge [21, 31, 34]. Although these initial experiments used in vitro mouse tissue, it is now possible to control differentiation of human embryonic stem cells, including through exposure to FGF and Wnt, to generate cells that also have the potential



of NMPs [32]. Regulation of differentiation by retinoic acid and Shh downregulate expression of *T/brachyury* and maintain expression of *Sox2* resulting in neural tissue. Alternatively, maintenance of Wnt signalling downregulates *Sox2* expression and NMPs differentiation towards a mesodermal fate [6, 32].

A simple division of an embryo into trunk and tail does not reflect the complexity of the developmental processes involved in axis elongation and, although NMPs have been localized to the tailbud, their contribution to neural and mesodermal development extends beyond the extent of secondary neurulation and associated tail structures. NMP derived cells have been identified within the trunk neural tube [35]. Given their location, their ability to differentiate into both mesodermal and neurectodermal structures, and their presumed role in secondary neurulation, maldifferentiation of NMPs is a prime candidate for the pathogenesis of LSLs and other closed spinal dysraphic conditions.

### **Axis Elongation**

Most of the experimental evidence to support the cellular and genetic mechanisms of axis elongation has come from chick, fish, amphibian and mouse models. As the only mammalian model, the mouse holds important parallels to human development,; however, it is worth noting the absence of a tail and the normal regression of caudal elements in humans makes caudal defects less obvious.

The NMP cell population is considered vital for axis elongation in the mouse. As mentioned above FGF and Wnt are required for the proliferation and multipotency of NMPs and specifically, null mutations in *Fgf8* or *Wnt3a* result in truncation of the body axis. This phenotype can be mimicked by disruption of retinoid levels. Excess retinoid exposure (a vitamin A derivative known to inhibit *Wnt3a* expression) results in early differentiation of cells within the tail-bud. Similarly mutations in *Cyp26a1*, an enzyme involved in retinoid metabolism cause a truncated axis [36]. It would seem a balance of both retinoic acid and Wnt signalling is required to promote NMP proliferation and maintain their multipotency. Loss of either signal will drive NMPs to differentiate either into neural or mesodermal tissue, the result being premature arrest of axis elongation. In addition, it seems as if the default state within the mouse tailbud is differentiation towards neural tissue, with axis truncation often associated with multiple abnormal neural tubes in the caudal region. During human development, children of a diabetic mother have an increased risk of caudal regression syndrome, this is mirrored in mouse models where retinoid exposure to embryos developing in a diabetic maternal environment show a predisposition for a truncated axis [37].

### **Neural Crest Cells**

Another population of cells that has been implicated in the formation of LSL, through a rare familial case, are the neural crest (NC) cells [38]. This population of cells is derived from the

neuroepithelium at the dorsal lip of the developing neural tube. At closure of the neural tube, these cells delaminate from the neuroepithelium, undergo epithelial to mesenchymal transition and migrate distal from the neural tube. They are pre-specified by the level of body axis from which they arise (e.g. cranial, vagal/cardiac and spinal crest), and become further specified by local cues to differentiate into a diverse range of cell types [39, 40]. In addition to BMPs, many factors involved in the induction of NC cells are also important in the generation of NMPs, namely FGFs and Wnt [41, 42]. Along the cranio-caudal axis of the embryo, NC cell populations are divided based on their fates. Some examples (but by no means an exhaustive list) include: cranial NC cells differentiating into bone and cartilage, trunk NC cells differentiating into sympathetic ganglia and neurons, cardiac NC cells differentiating into the spiral septum and semilunar valves of the heart, and vagal and sacral NC cells differentiating into enteric neurons [43]. Caudal NC cells arising from the secondary neural tube have not yet been identified in humans, and one of the most frequent NC derivatives, sensory ganglia, are not associated with the caudal most spinal cord. However, “secondary” NC cells are known to arise from the caudal most spinal cord in chick embryos, with differentiation restricted to melanocytes and glia [22, 44, 45].

In addition to the classical description of NC cell potential, there is also now increasing evidence that these cells are able to differentiate into a broader spectrum of cell types including, and relevant to the formation of LSLs, adipocytes [46-48]. In the absence of definitive proof that NC cells do not arise from the secondary neural tube in mammalian embryos, there remains the potential that maldifferentiation of this caudal population of NC cells is involved in the pathogenesis of closed spinal dysraphism.

### **Vertebral Development**

Spinal dysraphism is often referred to as spina bifida in reference to the failure of ossification of the posterior vertebral arch resulting in bifid spinous processes. Bony spina bifida can occur in the absence of any underlying spinal cord dysraphism; however, spinal dysraphic abnormalities more often than not do disrupt the process of vertebral formation, particularly that of the posterior elements.

Paraxial mesoderm, also known as the presomitic mesoderm, undergoes a process of segmentation under the control of both the segmentation clock and formation of a determination front: the clock and wave hypothesis. Unlike in the trunk, the paraxial mesoderm in the tailbud is derived from NMPs. A number of ‘clock’ genes are expressed in the paraxial mesoderm resulting in a molecular oscillator. After each cycle has finished and molecular expression has reached the anterior most extent of the presomitic mesoderm, a segment undergoes epithelization and buds off cranially and bilaterally to form a pair of symmetrical epithelial somites [49]. Antero-posterior gradients set up by FGF8 and retinoic acid create the determination front that helps to regulate the extent of each somite. Failure in this process will

result in segmentation defects that alter the number and size of vertebrae and are distinctly different from spinal dysraphism. With the exception of split cord malformations most dysraphic states are not associated with vertebral segmentation anomalies.

Sonic hedgehog released from the notochord functions as a morphogen to determine dorsoventral patterning of the paraxial mesoderm with *Pax1* and *Pax9* being expressed ventrally resulting in de-epithelisation of the somites and formation ventrally of the loose sclerotomal cells. The sclerotomes condense around the notochord and developing spinal cord to form the intervertebral discs and vertebral bodies respectively. More laterally the sclerotomes also undergo differentiation into cartilage and then bone, finally forming the vertebral arches and ribs [50]. Prior to final ossification, each sclerotome splits such that the rostral half of one sclerotome, and the caudal half of the one above, fuse together to form a single vertebral segment [51]. Failure of sclerotomal migration around the dorsal part of the neural tube often occurs due to mechanical obstruction by open spinal dysraphism. In the absence of an underlying spinal cord abnormality, faulty sclerotomal migration will result in isolated malformed or absent neural arches, as in isolated bony spina bifida occulta.

## OPEN SPINAL DYSRAPHISM

Spinal dysraphism is often also referred to as 'spina bifida' due to the associated bony defect. The term neural tube defect is also used interchangeably in the literature and encompasses cranial defects as well as spinal defects. Reflecting these multiple names, the term 'spinal dysraphism' is often taken to vaguely describe "congenital abnormalities of the vertebrae and spinal cord or nerve roots". However, the origin of the word dysraphism comes from 'raphe' meaning "a groove, ridge or seam in an organ or tissue, typically marking the line where two halves fused in the embryo". The term dysraphism therefore refers to a failure of this midline fusion and so strictly speaking is applicable to some, but not all congenital anomalies of the terminal spinal cord. Open defects remain distinct from closed defects in that the abnormality is not covered in skin, the neural tissue and meninges are exposed (*spina bifida aperta*) and these can reasonably be considered to be related to a defect in the process of primary neurulation, a failure of fusion of the dorsal neural tube.

The commonest pathologies that arise from this failure are myelomeningocele (MMC) and anencephaly in the spinal and cranial regions of the neural tube respectively. Craniorachischisis is the most extreme example, where failure of initiation of closure of the whole primary neural tube results in a defect that extends from just behind the forebrain to the end of the spinal cord. It is unclear if there are remnants of the secondary neural tube in these cases, however, the forebrain is often closed indicating a separate closure point at the most rostral part of the neural plate [52, 53].

Evidence for the mechanisms underlying these open neural tube defects (NTDs) come from two sources. Firstly a large number of genetic models of open NTDs have been established in mice with over 200 genes now associated with these pathologies. Secondly, this mouse data has been supported by large-scale genetic studies in human populations.

Mouse mutants for the PCP pathway disrupt CE resulting in a narrow, elongated neural plate and failure to initiation closure. The resulting severe craniorachischisis is also seen in humans and genomics studies have identified mutations in the human genes also involved in the PCP pathway: *CELSR1* and *SCRIB* [54]. In addition to this, milder NTDs have been found to be associated with possible disease causing variants in both core PCP genes and PCP-related genes, although a cause-and-effect relationship between the variants and the NTDs have rarely been demonstrated. These human variants in PCP genes of patients with myelomeningocele are always heterozygous whereas mouse models of craniorachischisis are homozygous, and heterozygous mouse mutants mostly demonstrate normal neural tube closure. This highlights the complexity of the molecular mechanisms involved in closure of the primary neural tube and disruption of the PCP pathway is unlikely to be the sole cause of pathology in most human cases [55].

The second pathway that has long had an association with NTDs is the folate one-carbon metabolism pathway. The UK MRC folic acid study in 1999 demonstrated a decrease in incidence of NTDs following 4 mg/day folic acid supplementation. Even before that study, folate deficiency had been associated with an increased incidence of NTDs. Folic acid is a substrate for the one-carbon metabolism pathway within mitochondria. Formate is then released from mitochondria into the cytoplasm and is involved in the synthesis of purine and pyrimidines as well as methylation of macromolecules such as lipids, proteins and DNA. The exact mechanism by which folate deficiency predisposes to NTDs on a population level is still debated, but with one likely mechanism being the limited availability to support sufficient cell proliferation [56]. Regardless, folic acid supplementation rescues multiple mouse models of NTDs [57].

In addition to the dietary intake of folic acid, genes coding for enzymes involved in folate metabolism have been implicated in NTDs following large-scale genetic analysis of NTD patients compared to control individuals. Polymorphisms in *MTHFR* and *MTFHD1* (cytosolic folate metabolism enzymes) give an increased risk of NTDs [58-60]. One further mitochondrial enzyme involved in one carbon metabolism (*MTHFD1L*) and two mitochondrial enzymes involved in the glycine cleavage system (*AMT* and *GLDC*) have also been associated with NTDs [61-63]. All these enzymes alter the amount of formate released from mitochondria and made available for further folate metabolism in the cytoplasm [64]. Interestingly, in knockout mouse models of the above human genes it is only loss of the mitochondrial enzymes that result in NTDs, suggesting that this part of one carbon metabolism must be the most sensitive [56, 61, 65-67].

Although folic acid supplementation early in pregnancy reduces the overall risk of open NTDs, some cases remain resistant, highlighting the multiple mechanisms likely to be involved in open NTDs [68]. It appears that the incidence of closed NTDs and specifically LSLs is unaffected by folic acid supplementation [69], although this is a tentative conclusion as there have been no prospective studies, and the available evidence is somewhat conflicting [70].

## **CLOSED CAUDAL SPINAL MALFORMATIONS**

As discussed above, 'spinal dysraphism' commonly refers to "congenital abnormalities of the vertebrae and spinal cord or nerve roots". Closed spinal dysraphism is usually considered to be any of those malformations covered with skin. Most of the pathologies commonly considered to fall under this category are related to disruption in secondary neurulation and not due to failure of midline fusion. In contrast to myelomeningocele and other open forms of spinal dysraphism, in which there are pan CNS changes e.g. Chiari II complex, closed dysraphic forms are generally locoregional malformations. LSL is a common form of pathology in the closed dysraphic category and will be discussed in detail below. There are a number of different pathologies that are also thought to arise from disruption of secondary neurulation, some of which are associated with LSL; that will be discussed here. In addition, although not a form of closed spinal dysraphism, closed bony spina bifida will also be discussed.

### **Spinal cord tethering**

By the time of completion of both primary and secondary neurulation, the neural tube terminates at the coccygeal region, however the embryo continues to grow rapidly with the mesodermal tissue growing at a faster rate than the developing spinal cord. This, combined with regression of some of the coccygeal elements of the spinal cord through apoptosis results in a relative ascent of the spinal cord during fetal growth such that, by the time of birth, the conus has attained its adult position at the first lumbar vertebra. When the spinal cord fails to 'ascend' in this fashion, the conus medullaris is described as low lying and the spinal cord as tethered [71]. A low-lying conus is diagnosed radiologically and is defined as being at or below the level of L2 [72]. The correlation between conus position and clinical symptoms is by no means clear. Although some patients with a low-lying spinal cord may manifest features of the Tethered Cord Syndrome due to stretching of the caudal spinal cord, cauda equina and nerve roots resulting in neurophysiological dysfunction, many can remain asymptomatic. Furthermore, the symptoms of Tethered Cord Syndrome can also occur without a low-lying conus, leading Yamada to define Tethered Cord Syndrome as "a stretch-induced functional disorder of the spinal cord with its caudal part anchored by inelastic structures." [73]

Tethered Cord Syndrome is a clinical, rather than radiological diagnosis and it can occur in association with almost all of the caudal spinal malformations, the most common being MMC where, even before the introduction of modern imaging techniques, it was noted that these patients often showed a neurological deterioration on forward flexion of the lumbar spine. The mechanism of tethering here simply results from the failure of the neuroepithelium of the neural tube to separate from the non-neural ectoderm, forming a placode and anchoring the spinal cord to the site of the defect. This is supported by observations of attenuation of the spinal cord diameter just above the placode in mouse models [74].

When a low lying conus occurs in the absence of MMC it is more likely to be the result of incomplete mesenchymal-to-epithelial transition of the caudal mesenchymal cells, with failure to separate the newly epithelialized cells of the secondary neural tube from the remaining mesenchyme [75]. When a low conus occurs in combination with closed caudal spinal defects such as LSL, this might be the result of direct tension from the fatty mass anchored to the subcutaneous fat as well as from disruption of secondary neurulation.

In summary, the term Tethered Cord Syndrome denotes a constellation of clinical symptoms and signs that may accompany any of the dysraphic states, and whilst the cause may be in part due to traction on the terminal spinal cord from the lesion, the likelihood that these symptoms may reflect a primary dysgenesis of the terminal spinal cord and nerve roots cannot be ignored.

### **Sacroccocygeal teratomas**

Sacroccocygeal teratomas are rare (1 in 40,000) and yet the commonest form of congenital solid tumour and the commonest congenital teratoma. They are more frequent in females (4:1) and can be divided into a number of different subtypes based on the histological appearance [76, 77].

The fact that sacroccocygeal teratomas are the most frequent congenital teratoma and are a caudal pathology has given rise to the idea that these teratomas may form from the tailbud/caudal cell mass due to altered local developmental signals. The caudal cell mass forms from undifferentiated mesenchymal tissue from the residual caudal primitive streak and primitive node and, even before the identification of NMPs, both in vivo and in vitro experiments demonstrated that the caudal cell mass is capable of differentiating into tissue form all three germ layers [75, 78]. This theory is supported by the absence of sacroccocygeal yolk sac tumours or choriocarcinomas which contradicts the previous assumptions of pathogenesis due to inappropriate primordial germ cell migration and survival [75, 79].

Sacroccocygeal teratomas have been referred to in the literature as being associated with LSL and thought to even arise from within the lipoma tissue [80, 81]. Indeed some have suggested that LSL are a form of benign sacroccocygeal teratoma [82]. While, like LSL, sacroccocygeal teratomas contain a diverse range of tissue, they are not described as consisting of mature adipocytes. LSLs represent a caudal pathology with maldifferentiation predominantly towards adipocytes whilst sacroccocygeal teratomas demonstrate multi-germ layer differentiation. The developmental signals that determine the pattern and degree of differentiation in both cases are unknown, but may yet be shown to be associated. It is worth noting that the published connection with NTDs seems to be spurious at best, with the frequency of association with sacroccocygeal teratomas no higher than other congenital defects [83].

### **Sacral agenesis and caudal regression**

As described above, the tailbud is important for axis elongation and specifically the NMP cells play a key role. Whilst many 'closed spinal dysraphisms' are said to be related to disruption of secondary neurulation, this process is closely related to axis elongation through the multipotency of NMPs and their differentiation towards either neural or mesodermal tissue, often with one occurring at the expense of the other. Gross abnormalities of axis elongation seem to extend beyond just the spectrum of NMPs with additional disruption of caudal endoderm development also resulting in a number of different syndromes (OEIS, Currarino and VACTERL association).

Variants of the proprotein convertase gene *PCSK5* have been identified in patients with VACTERL syndrome. The product protein cleaves and activates GDF11, and in mouse studies *Gdf11* regulates the downstream genes: *Mnx1* and members of the *Hox* gene family are involved in specification along the craniocaudal axis of the developing embryo [84]. Retinoid treatment in mouse embryos results in loss of expression of these two genes in the hindgut, leading to a caudal regression phenotype [85]. Similarly, mouse mutants resulting in loss of function of *Pcsk5* also give a phenotype with malformations comparable to Currarino or VACTERL association [86].

The extent of arrested axis elongation will also depend on the timing of disruption. In humans the mildest form of caudal regression syndrome is sacral dysgenesis; this pathology can occur in isolation and, if it just involves the most caudal sacrum, it may be asymptomatic. The more severe form comprises sacral agenesis with complete failure of development of the conus and cauda equina. In contrast to all other dysraphic states the spinal cord terminates at a higher level than usual in caudal regression (typically T12/L1) and has a characteristic blunted appearance. The commonest cause in humans is maternal diabetes with caudal regression syndrome being 24 times more common than in non-diabetic pregnancies [87]. Caudal regression syndrome is distinctly different from sirenomelia (mermaid syndrome), a condition characterized by failure of the lower limb bud field to separate early in development due to an abnormal umbilical artery, rather than disruption of axis elongation [88].

### **OEIS Syndrome**

OEIS syndrome is a rare group of defects associated with malformation of structures from the level of the diaphragm and below. It is also often referred to as cloacal exstrophy and typically consists of omphalocele, exstrophy, imperforate anus and spinal defects, with the commonest spinal deformity being terminal myelocystocele, and LSL being rarer [89]. In cases of terminal myelocystocele the end of the spinal cord is expanded, due to fluid filled distension of the neural tissue forming an ependyma lined 'trumpet'. OEIS has an incidence of 0.5-1 in 200,000 and no



hereditary pattern. It is considered to be part of a spectrum of congenital pathologies from epispadias and bladder exstrophy up to OEIS at the extreme [90, 91]. The presence of so many structural anomalies, including derivatives of both endoderm and mesoderm, along with the malformation of the caudal vertebrae and association with LSL, points towards early disruption of the tail bud and NMPs [92].

### **VACTERL Association**

VACTERL association, also known as VATER association is a combination of congenital defects: vertebral anomaly, anal atresia, cardiac defect, trachea-oesophageal fistula, renal anomalies and limb abnormalities. VACTERL association can be diagnosed if a patient has at least three of the mentioned congenital defects. Both the range and diversity of anomalies is wide leaving the potential for under diagnosis if clinical assessment is not completed in high-risk patients. The overall incidence is considered to be 1 in 10,000 to 40,000 [93]. Vertebral anomalies are thought to be the commonest association with frequency ranging from 60-95% between cases series. These vertebral defects can further be divided into a failure of formation defect (hemivertebrae, butterfly or wedge shaped vertebrae); failure of segmentation (fused or block vertebrae); or alternatively a combination of both [94, 95]. These vertebral defects occur throughout the spinal column. The incidence of myelomeningocele associated with VACTERL is low (5 cases detected on literature review) with the incidence of LSL even rarer (2 cases on literature review) [96, 97]. Unlike OEIS, the diversity of anomalies seen in this condition spread beyond disruption of the tailbud and secondary neurulation. Indeed, the lack of any established mechanism to account for the combination of anomalies, and the range of rare diseases associated with VACTERL, strongly indicates that there is no single unifying mechanism for the development of this group of associated pathologies. Any association of LSL with VACTERL may therefore be unlikely to yield useful information. More frequently than LSL is the presence of spinal cord tethering in VACTERL, with one series identifying up to 39% of cases requiring surgical intervention. This may reflect disruption of epithelial separation from caudal mesenchyme during secondary neurulation as discussed above. These cases all seem to be in the absence of any LSL [97].

### **Currarino Triad/Syndrome**

The Currarino Triad or Syndrome was first described by Currarino as a triad of an anorectal anomaly, presacral mass (either an anterior meningocele or teratoma) and a sickle shaped sacrum [98]. In actuality, a spectrum of severity is observed with only 1 in 5 cases exhibiting all three features and a range of other malformations being associated including gynaecological and renal anomalies as well as Hirschsprung's disease [99]. This is a rare syndrome with only 300 cases described in the literature although the variable penetrance of the disease suggests there may be many missed diagnoses. Female prevalence is 4 times that of males, although this may reflect the more frequent presentation of females with urinary/gynaecological

symptoms. The presence of familial cases has led to the identification of mutations in the *MNX1* (also known as *HLBX9*) gene accounting for autosomal dominance inheritance [100, 101]. The gene codes for a 403 amino acid protein made from 3 exons which is likely to be a homeo-domain containing transcription factor, however the exact function, binding and downstream effects of this protein are not yet established [99]. Despite the lack of detail about *MNX1*, a mouse model of Currarino Syndrome has been developed using etretinate (a teratogenic agent) that disrupts secondary neurulation resulting in abnormal differentiation of the tail bud mesenchyme leading to defects of the tailgut and neural tube [100]. However, direct knockout of *Mnx1* in mouse mutants results in foregut anomalies but no disruption of caudal development [102]. Thirty percent of cases of Currarino Syndrome are associated with LSL, suggesting that gross disruption of tailbud and NMP differentiation are likely to be the underlying cause for this Syndrome [103, 104].

### **Vertebral defects**

Isolated posterior vertebral arch defects covered in skin are often classed as spina bifida occulta but should not be considered as a closed NTD or closed spinal dysraphism. While posterior vertebral arch defects clearly occur with both closed and open NTDs, this is most likely due to a mechanical disruption of the cartilaginous differentiation and lack of ossification in the region immediately dorsal to the NTD. Similarly, where an intradural lipoma or fatty filum occurs in the absence of associated vertebral malformation, these are not considered to be NTDs, although the latter may still be due to maldifferentiation of the secondary neural tube precursors. In addition to these posterior vertebral arch defects, anterior arch and pedicle defects also exist in isolation, highlighting the different developmental and genetic mechanisms involved in vertebral development beyond neural tube formation.

Spina bifida occulta in the absence of underlying NTD most commonly occurs at the L5 and S1 vertebra with incomplete formation of their posterior arches. This abnormality is frequent in the general population (10-15%), it is mostly asymptomatic and should be regarded as a normal variant. These isolated vertebral defects are potentially due to genes related to somite and sclerotome development/differentiation rather than neurulation. For example, the *Patch* mouse, a null mutant of *Pdgfra* (coding for the protein platelet-derived growth factor receptor alpha) fails to undergo condensation of posterior vertebral arch elements resulting in a lack formation of further development of the posterior vertebral arches and a dorsal bony spina bifida defect across the entire spinal column, with a normal underlying spinal cord [105]. Another mouse model of isolated posterior vertebral arch defects is the double *Zic1/Gli3* mouse mutant, most likely due to downstream disruption of the *Shh* pathway [106].

Anterior vertebral defects often present with anomalous vertebral body morphology, such as a butterfly vertebra, and again there are specific mouse models that indicate the importance of individual genes in the development of the anterior vertebral components. In all cases the

neural tube and posterior vertebral arches remain unaffected whilst the anterior vertebrae show abnormality. The *Bapx* (*Nkx3.2*) mouse mutant lacks vertebral bodies and since *Bapx* is regulated by *Pax1* and *Shh* it is not surprising that the *Pax1* mouse mutant has a similar phenotype with additional loss of intervertebral discs [107, 108]. A third mouse model with mutant *Uncx4.1* indicates a separate genetic pathway involved in the development of the pedicles, transverse processes and proximal ribs. Although the adjacent neural tube seems to initially develop normally, the severe axial malformation is clearly not compatible with ventilation and life [109].

When present with NTDs, posterior vertebral defects are most likely due to mechanical disruption but concomitant pathology cannot be excluded. However, if more complex segmentation and anterior vertebral defects are present, this is often part of multi-system malformation syndromes such as the VACTERL association.

### **Other Closed Spinal Malformations**

A number of different rare, closed malformations are also associated with disruption of spinal cord development, but the exact developmental mechanisms are difficult to explain in the absence of animal models and results from genetic studies. Often these malformations are part of a clinical spectrum ranging from mild and asymptomatic to severe. Confounding matters are the multiple names and classifications that have arisen, as speculations have been made about their embryogenesis. Grouped together as neurenteric malformations are the related neurenteric cyst, fistula and sinus. Previously referred to as a subset of mediastinal cysts lined with gastrointestinal epithelium, published case reports have demonstrated a connection of these 'mediastinal cysts' to the spinal canal [110, 111]. Grouped under split cord malformations (SCM) are types I and II SCM. Other terms used in the literature include diastematomyelia/pseudodiplomyelia (for SCM type I), where two spinal cords are divided by a bony spur and reside within separate dural sacs, and diplomyelia/dimyelia (for SCM type II) where two apparently complete spinal cords are located within a single dura sac.

Bentley first proposed the theory of split notochord syndrome in 1960 to account for not only neurenteric malformations but also split cord malformations [112]. Others have extrapolated on this theory proposing potential mechanisms by which the notochord might be split. Beardmore hypothesized abnormal midline adhesions between the ectoderm and endoderm during gastrulation would prevent migration of a midline notochord and thus result in duplication [113]. Similarly, Feller (1929) and later Korff (1937) speculated that an abnormal cell rest associated with Henson's node would prevent midline migration of cells destined to form notochord and therefore splitting would occur resulting in two notochords. More recently, Row (2016) has demonstrated two separate progenitor populations present in the zebrafish tailbud and proposed that a similar arrangement in humans could account for two progenitor populations that fuse to form the definitive notochord [114]. Where this fusion fails split notochord syndrome

would result. However, no such populations are present in mice and so are unlikely to also be found in humans.

Bentley and Smith proposed that splitting of the notochord facilitates apposition of the midline ectoderm and endoderm with a spectrum of clinical presentations resulting, dependent on the degree of regression of this abnormal adhesion. As such, they argue that a split notochord syndrome could account for: prevertebral enteric cysts, postvertebral enteric cysts, posterior enteric sinus and posterior enteric remnants. The degree of the regression of this adhesion would also determine further development of surrounding tissue, with split spinal cord malformation at the most extreme, and anterior vertebral spina bifida at the mildest.

Split cord malformations have been seen in mouse mutants, although the underlying genetics remain unclear [115]. A split/bifid notochord is occasionally seen in PCP pathway mouse mutants at the far end of a spectrum that is normally associated with a flat, broad notochord [116] suggesting that disrupted CE might have a role to play in the pathogenesis. Beyond this, the proposals of how a split notochord could develop remain unsupported by experimental evidence and should be considered speculative.

#### **Persistent/accessory neurenteric canal**

Budde was the first to propose persistence of the neurenteric canal as a potential cause for neurenteric malformations. Although neurenteric malformations are well documented in humans, it remains debated as to whether a neurenteric canal ever forms, and since the proposed neurenteric canal communicates with the amniotic cavity via the primitive node and terminates near the coccyx, this theory could not account for more cranial lesions. Harriman subsequently proposed “sequestrational malformation of the neurenteric canal”, whilst Bremer coined the term “accessory neurenteric canal”. As mentioned, the existence of a neurenteric canal in humans is debated and there is no evidence that it forms in mouse embryos. Similarly there has been no experimental evidence of such an accessory structure [117]. Attempts have been made to surgically replicate such a developmental phenomenon in *Xenopus laevis*, *Gallus domesticus* and *Cynops pyrrhogaster* (Japanese fire belly newt) and these experiments have resulted in split cord syndrome; however, the significance of these experimental models remains unclear [118, 119].

Bremer speculated that an accessory neurenteric canal lying cranial to and persisting beyond the time frame of the definitive canal would result in ectopic endodermal tissue with potential connection to the dorsal skin. As with split notochord syndrome, the degree of regression and development of surrounding tissue would determine the end clinical presentation. Bremer went on to propose that this mechanism could account for diastematomyelia. By contrast Pang’s detailed histological assessment revealed mesenchymal remnants in diplomyelia and thus

speculated that an accessory neurenteric canal could account for all types of split spinal cord malformation, but again this is a hypothesis and is not supported by experimental data [120].

It is clear that there is a disparity between the clinical literature and experimental developmental biology that can only be solved by investigating the development of these structures (both normal and abnormal) in appropriately staged human embryos.

## **LUMBOSACRAL LIPOMAS**

LSL is a common form of closed spinal dysraphism but is classified as a rare disease, occurring in 1 in 4000 live births [121]. Diagnosis may be made on antenatal ultrasound but more usually at birth, or soon after, with a soft mass over the lumbosacral spine often associated with a number of different cutaneous manifestations: focal hirsutism, pigmentation, dermal sinus, capillary haemangioma. In addition, neonates may be noted to have signs of neuro-orthopaedic syndrome such as talipes equinovarus [80]. This pathology is slightly more common in male infants and seems to occur with the same frequency worldwide, although there might be some under-diagnosis and under reporting in developing countries [122, 123]. The term 'lipoma' is perhaps a misnomer, as it is used to describe a number of different pathologies, and yet LSL has its own highly specific features.

### **Anatomical features**

The aetiology and pathogenesis of LSL remains debated although clues can be derived from the anatomical appearance of the pathology. The lipoma tissue is closely adherent to the caudal spinal cord, at the level of the conus. The lower spinal cord is abnormal, splayed and forms a thickened placode at the junction with the lipoma tissue. LSLs are typically associated with a defect in the surrounding dura and a defect in the posterior vertebral arch (a spina bifida defect). These defects appear congenital in nature, as the lipoma tissue is not invasive or destructive. The lipoma tissue extends through these defects and is continuous with the overlying subcutaneous fat [124-126].

The exact anatomical location of the lipoma tissue in relationship to the conus, and more specifically the orientation of the placode, has led to the classification of LSLs into dorsal, caudal and transitional subtypes. A dorsal LSL is located dorsal to the spinal cord and above the level of the conus. A caudal LSL extends from the tip of the conus into the thecal sac. The terms filar lipoma or terminal lipoma are also often used in the literature to describe this configuration. A transitional LSL occupies an intermediate territory between dorsal and caudal types, the conus is always involved, the placode is commonly rotated and the lipomatous tissue may extend caudally to encompass elements of the cauda equina [124]. A more recently described subtype of the transitional LSL is a chaotic LSL where the lipoma tissue extends ventrally from the placode, extending beyond the dorsal root entry zone thus encompassing sensory nerve roots (Figure II.1.ii). Together the dorsal and caudal subtypes may be referred to as simple LSL, whilst the transitional/chaotic subtypes are referred to as complex [127, 128].

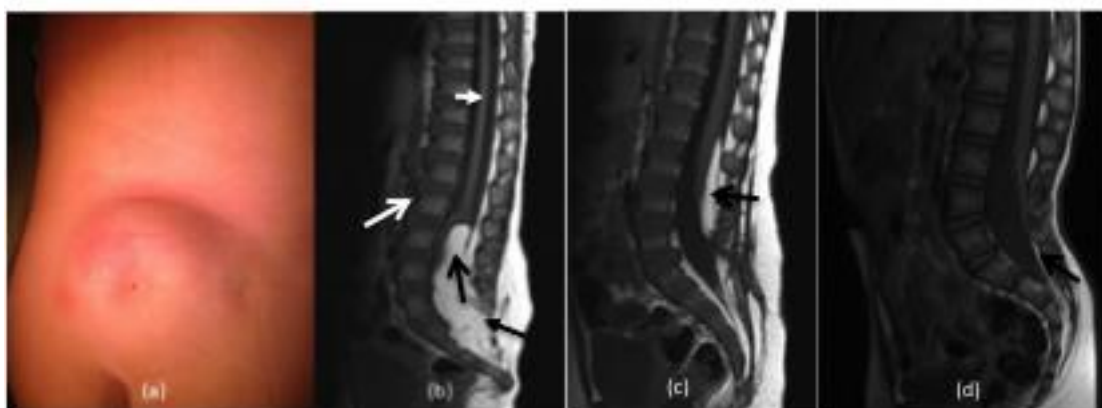


Figure II.1.ii. A, LSL with midline swelling and cutaneous dimple corresponding with a dermal sinus. B-D, Sagittal T1 MRI illustrating different anatomical subtypes of LSL based on their radiological appearance and relationship to the conus. B transitional, C dorsal, D caudal. Black arrow = LSL, closed head black arrow = defect/missing spinous processes (bony spina bifida), white arrow = vertebral bodies, closed head white arrow = spinal cord (Image taken from Jones et al 2019) [129].

In addition to their extension caudally, the transitional subtype often displays rotation of the neural placode in the left-right axis. Manifestation of the neuro-orthopaedic syndrome and cutaneous stigmata associated with underlying LSLs also often show a degree of laterality. This rotation results in some nerve roots being located more dorsally and having a longer course to their respective intervertebral foramina, often passing through the lipoma tissue. The contralateral nerve roots are located ventrally, often appear to be shorter and are rarely disrupted by the lipoma tissue. It is unclear whether this rotation is due to mechanical effects of the lipoma tissue during growth, although there is likely to be a significant congenital component with the nerve roots on either side being frequently irregular in size, number and point of attachment to the conus [80, 130, 131]. The full published paper from my own work on this topic can be found in Supplementary Information [129].

Alternatively, LSLs can be classified based on the relationship of the meninges to the defect in the posterior vertebral arch. Meninges that herniate outside the vertebral canal, with or without co-herniation of the lipoma placode and caudal spinal cord, can be referred to as lipomyelomeningoceles (LMM). Where no herniation occurs and the spinal cord, placode and meninges remain within the confines of the vertebral canal the LSL may be referred to as a lipomyelocele (LM).

### **Other lipoma masses**

The term lipoma or spinal lipoma is often used to describe LSLs but this does not allow for a distinction between different entities. LSL is not a malignant or invasive mass. Other lipoma masses can be found throughout the central nervous system and, in areas other than the caudal spinal cord, are rarely present at birth and are considered to be an acquired pathology.

These intradural lipomas are diagnosed in adulthood, most frequently occur in the thoracic spine and are characterized by mature adipocytes interspersed with thin fibrous septae [132]. Another condition that can be incorrectly classified as a spinal lipoma is the reactive expansion of epidural fat in response to corticosteroid: focal epidural lipomatosis.

The terms filar lipoma, terminal lipoma and caudal lipoma are often used interchangeably; in addition, the distinction between filar lipoma and fatty filum is often unclear. Filar lipomas that are not associated with vertebral or meningeal defects should be considered a separate pathology from caudal LSL. An abnormally thick filum terminale is found incidentally on MR imaging in up to 5% of the population [133]. In humans a filum less than 2 mm thick at the level of the L5/S1 intervertebral disc is rarely associated with caudal spinal cord dysfunction, and so should be considered normal variation. However, a fatty filum in combination with a low-lying conus may predispose to mechanical tethering and the appearance of clinical symptoms and signs of the Tethered Cord Syndrome.

### **Histopathology**

LSLs are also distinct from lipomas elsewhere in the body based on their histopathology [122]. The literature is unfortunately confused by the lack of clarity as to what constitutes a LSL, with publications instead using the overarching term 'lipoma' and often including intradural and fatty/thickened filum [80, 123, 134-136].

As with lipomas elsewhere, LSLs consist of mature adipocytes that are metabolically active but, in addition, the adipocytes of LSLs are surrounded by thickened bands of connective tissue interspersed with a diverse range of different cell types said to be derived from all three germ layers [137-139]. The largest review of histopathology was performed by Pierre-Kahn's group and published several times. The most recent publication includes 671 patients reviewed over a 22 year period. Importantly, this group included lipomas of the filum as well as LSLs and this might explain their finding of 77% of lesions containing more than just mature adipocytes and collagen bands [80, 123, 137]. Prior to this, Walsh published a much smaller series, of just 20 patients, although the inclusion criteria were even less strict and again a diverse group was considered, including intradural lipomas. Walsh noted "the presence of large, rather monotonous sheets of mature fat-cells and thick strands of connective tissue. Numerous thin-walled blood vessels were also seen", with 25% (five cases) demonstrating a more diverse range of cell types [135].

To address this inclusion of non-LSL lipomas in previous publications, histopathology reports from patients undergoing LSL resection surgery at GOSH were reviewed. Unlike previously published series, care was taken about the exact diagnosis of the pathology with exclusion of intradural lipoma, cases of fatty filum and teratomatous masses. Major differences compared to previous publications included the abundance of peripheral nerves, abnormal blood vessels and



striated muscle fibres within most of the GOSH patient samples (Figure II.1.iii). In addition, no evidence was found of cells of endodermal origin, most likely reflecting the stricter criteria used to define LSLs, rather than including the larger class of “lipomas”. The full published paper can be found in Supplementary Information [140].

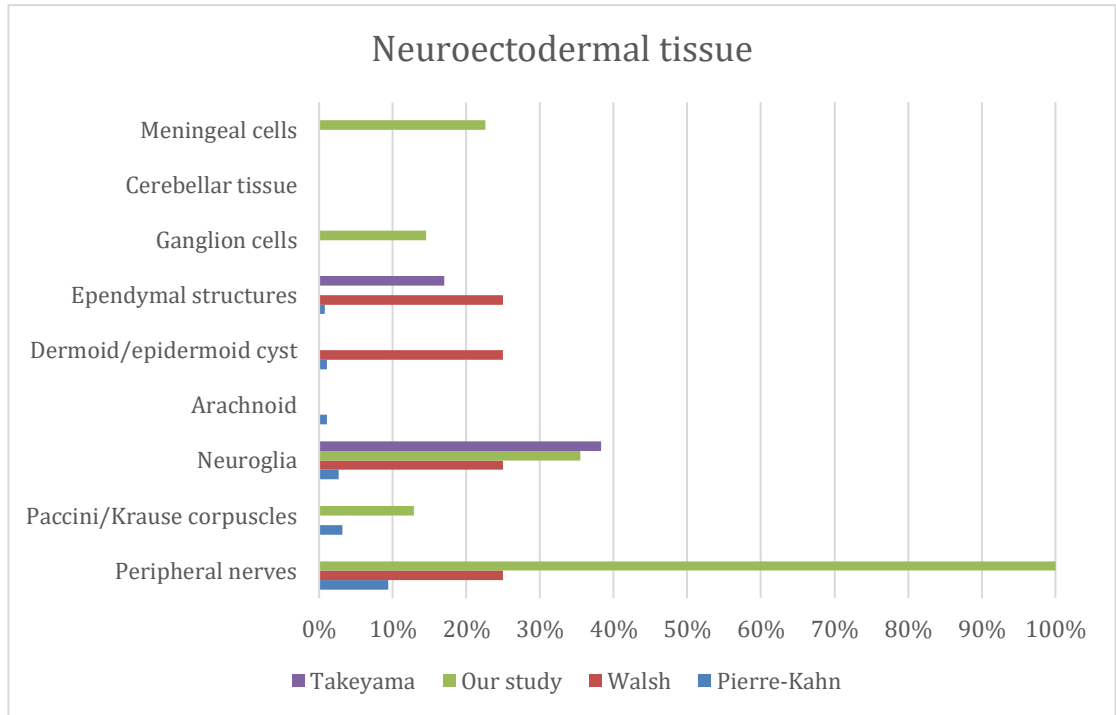


Figure II.1.iii.a Comparison with previously published data on frequency of cell types of neuroectodermal origin. Other publications: Takeyama et al 2006 [136], Walsh 1980 [135] and Pierre-Kahn et al 2008 [123].

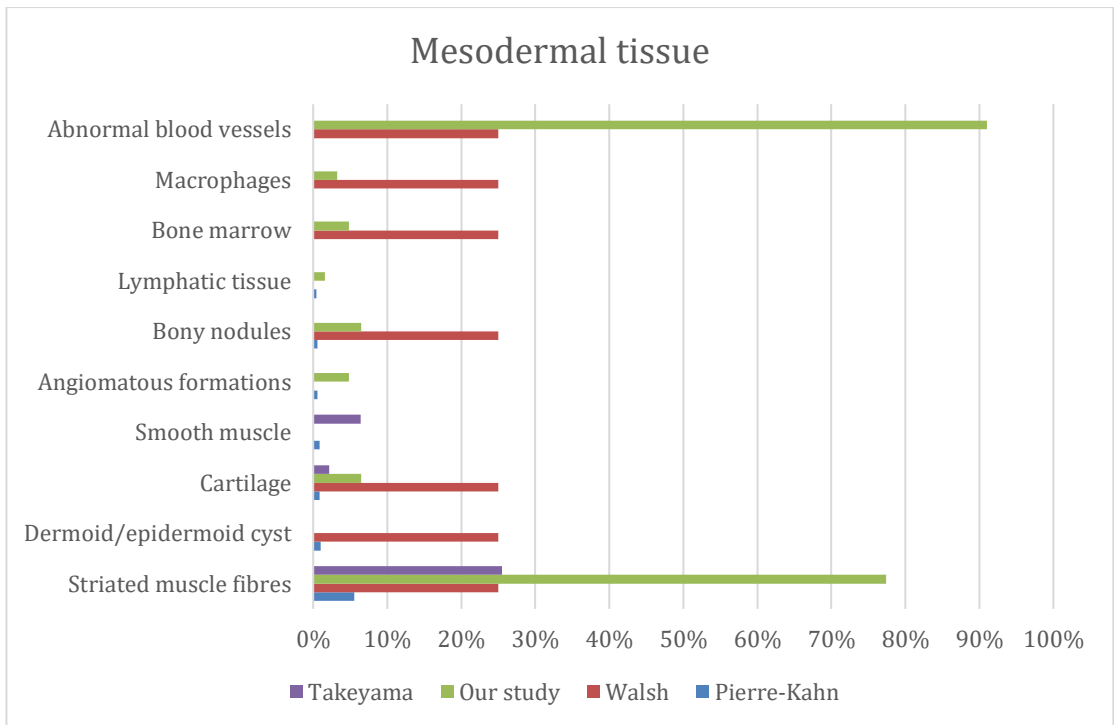


Figure II.1.iiib Comparison with previously published data on frequency of cell types of mesodermal origin. Figure published in Histopathology[140].

In addition to a comparison with the literature, LSL pathology samples from this GOSH cohort were also divided based on their anatomical features to determine if there was any association between the microscopic features observed and the macroscopic features used for subtype classification described above. Subtypes of LSL are often grouped together as those thought to be associated with primary neurulation (dorsal) and those associated with secondary neurulation (caudal, transitional and chaotic). Alternatively, the subtypes are described as simple (dorsal and caudal) or complex (transitional or chaotic). There was no significant difference (99% confidence interval) in the cellular diversity or degree of dysgenesis between the simple and complex subtypes, similarly there was no significant difference between the dorsal and other subtypes except for the presence of bone marrow being more frequent in the dorsal subtype (Figures II.1.iv). The significance of this finding is unclear. The anatomical and histological features are summarised in Table II.1.i.

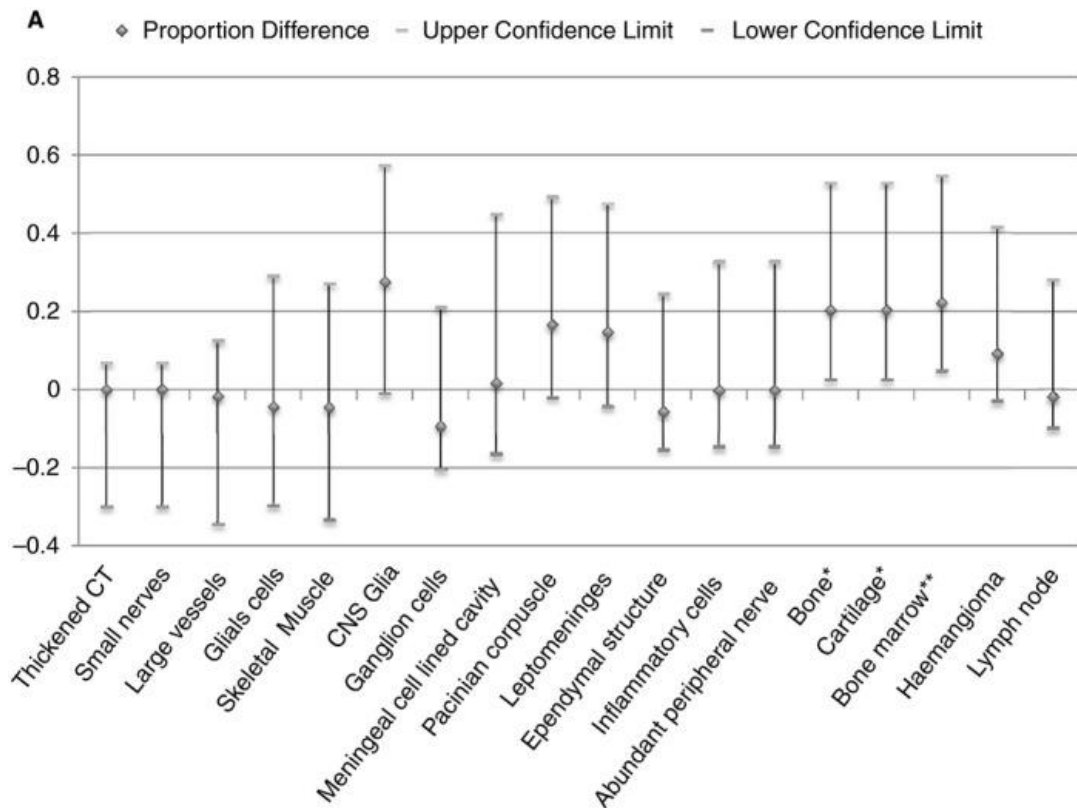


Figure II.1.iva, Subtypes of lipoma were grouped into those proposed to be due to a defect in primary neurulation (dorsal) and those proposed to be due to a defect in secondary neurulation (caudal, transitional and chaotic). Differences in proportion of different cell/tissue types detected were calculated along with 95% confidence intervals (CI) of the difference. \*Values which show significant difference at the 95% CI. This significance is lost at 99% CI for the presence of bone and cartilage but not bone marrow; \*\*difference = 0.222 (0.013, 0.635). Figure published in Histopathology[140].

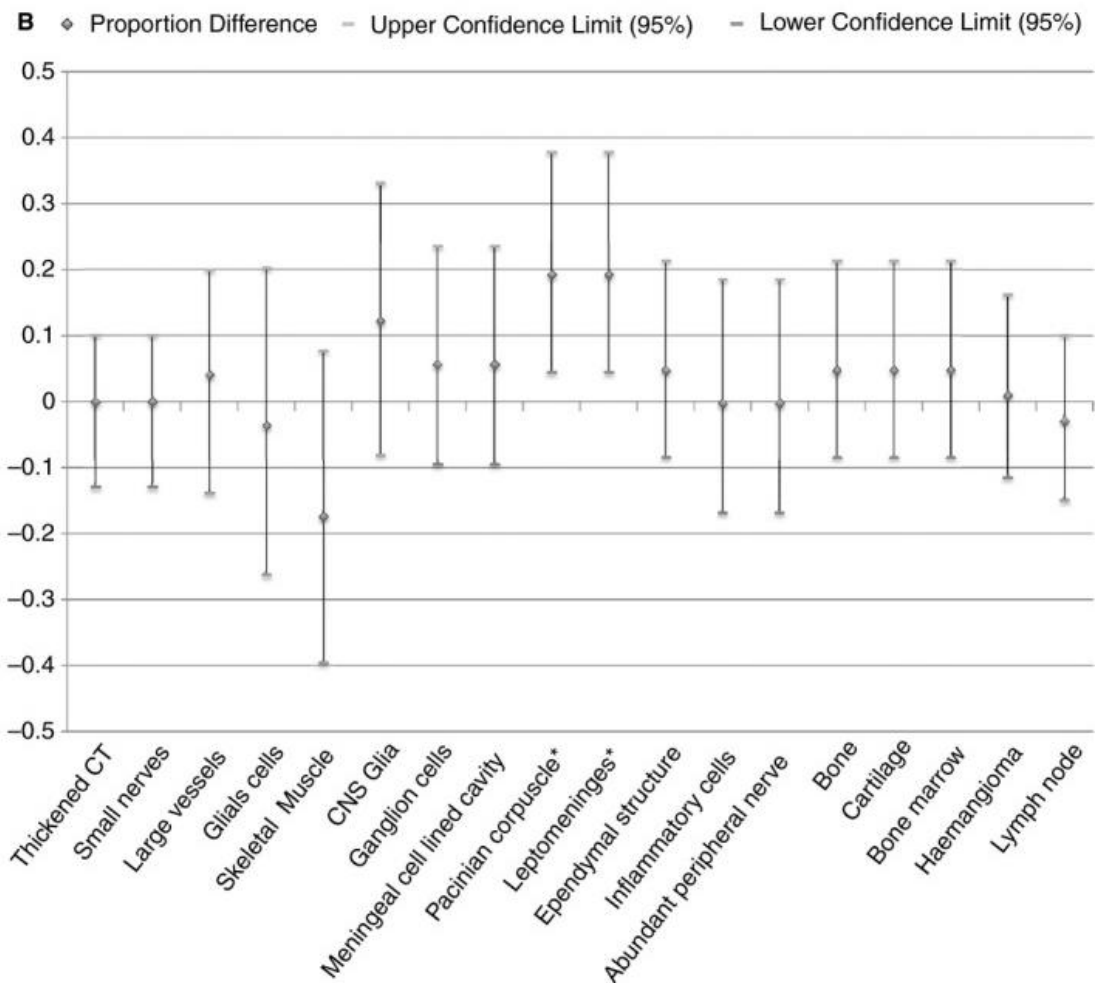


Figure II.1.ivb, Subtypes of the lipoma were grouped into 'simple' (dorsal and caudal) and 'complex' (transitional and chaotic). Difference in proportion of different cell/tissue types detected was calculated along with 95% CI of the difference. \*Values which show significant difference at the 95% CI. This significance is lost at 99% CI for the presence of Pacinian corpuscles and leptomeninges, difference = 0.192 (-0.014, 0.433). Figure published in Histopathology[140].

|                                   | <b>Simple</b>   | <b>Complex</b>   |
|-----------------------------------|---|--|
| <b>Previous classification</b>    | Dorsal, caudal*   | Transitional, chaotic  |
| <b>Characteristic location</b>    | Dorsal aspect of conus or caudal aspect of conus                                  | Extending from dorsal to caudal aspect of conus, extending ventrally                           |
| <b>Radiological features (MR)</b> | Associated with bony spina bifida<br>Preserved conus morphology                   | Associated with bony spina bifida<br>Conus poorly delineated<br>Rotation of the neural placode |
| <b>Histological features</b>      | Predominantly mature adipocytes<br>Cells of mesodermal and neuroectodermal origin | Predominantly mature adipocytes<br>Cells of mesodermal and neuroectodermal origin              |

Table II.1.i Comparison of location, radiological and histological features between simple and complex lumbosacral lipomas. MR, Magnetic resonance \*Lipomas of the filum terminale with intact conus. Table published in Histopathology[140].

### **Pathogenesis**

The above descriptions lead to two tentative conclusions. Firstly, since LSL is not an invasive or destructive pathology the malformation seen in the adjacent spinal cord/conus and the surrounding vertebrae and dura limit the timing of the initiation of LSL pathogenesis to prior to the completion of formation of these structures. Since LSLs are associated with the conus their formation is likely to be due to a disruption of the process of secondary neurulation. Nevertheless, a firm conclusion on this point is difficult at present, as there have only been case reports of prenatal diagnosis of LSL on ultrasonography and LSL is not routinely diagnosed at 20 week prenatal scans [141]. Secondly, the diversity of cell types within LSL tissue suggests inappropriate differentiation of either a stem cell or progenitor cell population. There are two such populations of cells that are present within the caudal embryo and are therefore likely candidates to contribute to the formation of LSLs: neuromesodermal progenitor cells (NMPs) and neural crest (NC) cells. As discussed above NMPs are thought to be vital in the formation of the secondary neural tube, whereas caudal NC cells have only been identified in chick embryos, where they only differentiate into melanocytes and glia [44, 45]. It is not yet known if NC cells arise from the secondary neural tube in mammalian embryos, although there is growing evidence to show that neural crest cells can differentiate into a larger number of cell types than originally thought, including adipocytes [46-48, 142].

To date only one animal model of LSL has been described. Ectopic expression of the gene *Gcm1* in the tailbud and caudal spinal cord of mouse embryos was achieved by linking the *Gcm1* coding sequence to a *Hoxa7* enhancer. All embryos developed an ectopic neural tube in the region of the tailbud/hind limb bud, resembling a split cord malformation. Strikingly, these

ectopic neural tubes were frequently associated with an adipocyte mass resembling a LSL at the caudal most tip. A quarter of fetuses were also found to have a caudal open NTD. *Gcm1* is the mammalian orthologue for the *Drosophila* gene *Glial cells missing*, which encodes a transcription factor. Gcm is involved in the control of the differentiation of progenitor cells into neuronal or glial cell lineages via regulation of *Hes5* and the Notch pathway [143]. *Gcm1* is expressed in the developing central nervous system in mouse embryos and in these transgenic mice overexpression in the tailbud down-regulates the expression of *Notch1* and *Tbx6*. It is proposed that this altered gene expression allows more cells to assume a neuroepithelial fate in the tailbud which ultimately results in the induction of additional secondary neural tubes [144].

It remains to be seen how representative of LSL this pathology is, both histologically and in terms of reflecting human pathogenesis. Unlike these transgenic mice, human LSLs are not typically associated with split cord malformation. However this formation of a lipoma mass associated with abnormal secondary neurulation indicates that cells within the tailbud have the potential to differentiate into adipocytes.

The ability of the self-renewing NMP cell population in the embryonic tail-bud to differentiate into a variety of neural and mesodermal derivatives, makes it a prime candidate for the origin of LSL. Moreover, the recent development of methods to study NMP differentiation in culture offers an opportunity to define the differentiation signals that might divert such cells towards adipocyte development. However, the observation of ectopic lipoma mass formation in the *Gcm1* model, in conjunction with structural defects of the low spinal neural tube (both primary and secondary), argues strongly for a more extensive maldifferentiation of NMPs, and is consistent with a fundamental defect of progenitor cell differentiation leading to spinal lipoma in humans.

A number of other less convincing models have been proposed over the decades to explain the pathogenesis of LSLs. These models are descriptive, taking into account changes in morphology, and lacking any form of genetic or biological basis. Accordingly, none of these hypotheses are supported by experimental evidence, and they are largely flawed in their assumption that LSL pathogenesis is related to disruption of primary rather than secondary neurulation. The fact that the dorsal subtype of LSL occurs above the level of the conus in a region that is said to correspond to the site of primary neurulation, has led to these suggestions that the pathogenesis of LSL is neither restricted nor exclusive to the disruption of secondary neurulation. It has therefore been assumed that dorsal LSLs must form from disruption of primary neurulation. However, this does not take into account the changes in anatomy that occur during development of the spinal cord, nor the overlap of NMPs extending into the trunk neural tube [35].

McLone *et al.* proposed the first model to explain the pathogenesis of LSL and described their theory of premature dysjunction. They proposed that prior to closure of the neural tube, the

ectoderm and neuroectoderm might separate resulting in the migration of paraxial mesoderm into the lumen of the open neural tube. Paraxial mesoderm cells would then differentiate into adipocytes forming the mass of the LSL [125]. A surgical model in the chick embryo designed to emulate this premature dysjunction with a unilateral incision to the neural fold resulted in a number of different developmental anomalies. Although, on the surface, these mimicked LSL formation, there was no histologically identifiable lipoma formation [145]. Moreover, this mechanism does not explain the presence of cells within the lipoma tissue of neuroectodermal origin.

Catala also proposed a model relating to disruption of primary neurulation by incomplete dysjunction, whereby failure of the ectoderm to separate completely from the neuroectoderm results in the formation of a dermal tract. The presence of this abnormal structure, they proposed, would disrupt normal development of the surrounding tissue including the spinal cord. To account for the diversity of cell types present in LSLs, Catala also proposed a double-hit model, suggesting that teratogenic cells might be present, including abnormal differentiation of the paraxial mesoderm into mature cell types derived from all three germ layers [146]. This hypothesis would suggest that a dermal sinus/pit should be associated only with dorsal LSLs; however, this has been found not to be the case [140].

To account for those LSLs associated with the conus, McLone and Naidich later proposed a role of the tailbud, and therefore disruption of secondary neurulation, in the formation of caudal LSLs [146]. Despite these different proposed models for the pathogenesis of dorsal versus caudal/transitional LSLs there is no significant difference in the diversity of cell types found in the two groups [140]. The above hypotheses lack detail or an experimental basis and, in the absence of an established and proven mechanism, there is scope to re-examine the theory of embryogenesis of LSL.

An alternative approach has been to review genetic variation either associated with a number of different syndromes with an incomplete penetrance of LSLs, or in large cohorts of patients with neural tube defects. As described above, when considering the histopathology of LSL, many of these genetic studies suffer from poor definition of LSL as a unique entity. Intradural lipomas, filar lipomas and teratomatous masses are often included in the analysis, thereby reducing the specificity of the findings. Morphological models have been discussed here. Genetic variants associated with LSL are discussed below, however, it is worth noting that in the absence of any identified genetic and/or molecular mechanism, the above descriptions of LSL pathogenesis remain speculative.

### **Genetics of LSL**

Unlike myelomeningocele (MMC), the underlying pathogenesis of LSL remains unestablished. Whilst there are hundreds of genes known to be associated with open spina bifida in mice and

accordingly a large number of animal models in mouse, sheep and rabbit, there is a conspicuous absence of any animal model for LSL. To date the literature hints at a range of different genes associated with LSL, but there is no consistency across publications.

There is also an inconsistency in the classification of spinal lipomas with fatty filum and intradural lipomas often being included in the same bracket. In addition, when considering large scale genetic studies, patients are often grouped together as cases of closed spinal dysraphism/closed neural tube defect or simply as lipoma. The terminology used in this section will follow the terms used in the publications reviewed. Unless a pathology is categorized as LSL or LMM/LM in a publication, there might be some ambiguity as to what kind of lipoma is being described.

### **Familial cases**

The absence of familial cases of LSL is notable with only a few examples appearing in the literature. Larrew et al published the first case of transgenerational inheritance of familial lumbosacral lipoma including whole exome sequencing and the identification of two variants (*RADIL* and *ARHGAP29* genes) in both the proband and affected father. They propose a digenic inheritance pattern[38]. The variants they identified were *RADIL* = c.2050G>T p.Ala684Ser and *ARHGAP29* = c.2590T>C p.Ser864Pro. They offered no detailed analysis of the likely protein product, and no SIFT and Polyphen-2 scores or CADD score for the identified variants.

*RADIL* codes for a Rap GTPase interactor, which is a 1075 amino acid protein containing Ras-associating and dilute domains, as well as a PDZ domain. *RADIL* is known to be vital in NC migration and cell adhesion in zebrafish. Knockout animals demonstrate multiple defects in NC cell lineages [147]. The variant identified by Larrew et al (Ala684Ser) in the family with LSL is located within the dilute domain [38].

*ARHGAP29* codes for Rho GTPase-activating protein 29, a 1261 amino acid protein containing zinc-finger and Rho-GAP domains. *Arhgap29* knockout mice do not survive beyond E9-10 demonstrating abnormally narrow blood vessel lumens [148]. *Arhgap29* binds Rasip1 which in turn inhibits the function of RhoA and subsequently inhibits the ROCK pathway. The ROCK/RhoA pathway has a role in tubulogenesis as well as a proposed larger role in regulation of cell shape, adhesion and migration [149-152]. It is worth noting that a detailed analysis of LSL histopathology highlighted abnormal blood vessels within the lipoma tissue [140]. The variant identified by Larrew et al (Ser864Pro) is located towards the end of the Rho-GAP domain [38]. In humans *ARHGAP29* has been implemented in non-syndromic cleft lip with/without cleft palate [153]. Consequently, a lot of experimental work has looked at the expression and function of *Arhgap29* in the developing head. Loss of function mouse mutants have increased adhesion within the palatal mesenchyme, with proposed reduced cell migration



due to disruption of a RhoA-dependent migration pathway including the protein IRF6 [154, 155].

Interestingly, there is a recognized functional interaction between RADIL and ARHGAP29. In human cell cultures, ARHGAP29 translocation to cell membranes was found to be dependent on interaction with RADIL. A truncated RADIL protein with a missing PDZ domain and C-terminus did not demonstrate the same interaction and translocation of ARHGAP29 was lost [149].

Seeds et al 1988 demonstrated a familial LMM at a 17 week prenatal ultrasound scan, in a fetus whose older sibling had been diagnosed with a LMM post-natally. However, the absence of further post-natal clinical detail and the description of the LMM as a teratomatous tumour highlights the inconsistency in classification of this pathology, and raises questions as to the actual diagnosis in this case[156]. Kannu et al identified two siblings with LMM. The parents were non-consanguineous. No genetic analysis was performed[157]. Finally, Hanaei et al described two identical twins with LSL but no previous family history. They did not offer any genetic analysis[158].

### **Syndromic cases**

In addition to the rare familial cases there have been a number of case reports of LSL associated with other rare genetic conditions. It remains to be determined if, as Occam's razor predicts, a unifying cause can be found or whether these cases are just coincidence.

Costain et al identified a case of LSL in Rubinstein-Taybi syndrome associated with mutation in *EP300*[159]. Hoshino et al describe a case of Schuurs-Hoeijmakers syndrome, a condition known to be associated with mutation in the *PACS1* gene, with delayed diagnosis of LMM. They highlight that constipation is a common symptom of Schuurs-Hoeijmakers syndrome, and speculate LMM may go undiagnosed in this rare condition[160]. Satyarthee et al described a case of LMM treated as a child but later found to have fusion of C2-3 spinous process, indicative of Klippel-Feil Syndrome. In addition the individual also had a split cord malformation[161]. Klippel-Feil is known to be associated with mutations in either *GDF6*, *GDF3* and *MEOX1*[162]. Girard et al have proposed the name PELVIS syndrome to describe a spectrum of large perineal haemangioma associated with congenital malformation (perineal haemangioma, external genitalia malformations, LMM, vesicorenal anomalies, imperforate anus, and skin tag) [163]. This has been supported by a number of case reports of large perineal haemangiomas and LMM, although genetic analysis has yet to be performed[163-165].

### **Associated congenital malformations**

There are a number of case reports of LMM associated with other congenital pathologies. For example, Franco et al describe a case of occipital encephalocele with LMM, Tetralogy of Fallot and Situs Inversus; no genetic analysis was offered in this case [166].

## **Syndromes and associations**

There are a number of associations and different syndromes said to be associated with LML.

OEIS syndrome is a rare group of defects typically consisting of omphalocele, exstrophy, imperforate anus and spinal defects, with the commonest spinal deformity being terminal myelocystocele and LSL being rarer [89, 91, 92].

VACTERL association is a combination of congenital defects: vertebral anomaly, anal atresia, cardiac defect, trachea-oesophageal fistula, renal anomalies and limb abnormalities [93-95]. Vertebral defects occur throughout the spinal canal with the incidence of LSL rare (2 cases on literature review) [96, 97].

The Currarino Syndrome/Triad consists of a sickle shaped sacrum, presacral mass (either a teratoma or anterior meningocele) and anorectal anomaly [98]. The presence of familial cases has led to the identification of mutations in the *MXN1* (also known as *HLXB9*) gene accounting for autosomal dominant inheritance [100, 101]. 30% of cases of Currarino are associated with LSL [103, 104]. Kwun et al described a case of siblings both fitting into the VACTERL association and Currarino syndrome spectrum; both siblings were found to have a LMM with terminal 7q deletion 7q36.1q36.3 and gain of 8q24.22q24.3. They propose candidate genes to account for the phenotype including *MXN1*, *SHH*, *HLXB9*, *PAXIP1*, *PEG1/MEST* and *KCNK9*[167].

Sacrococcygeal teratomas are the commonest form of congenital solid tumour [76, 77] and are often referred to in the literature as being associated with LSLs [80, 82, 168]. Despite this connection and the diverse range of tissue found within sacrococcygeal teratomas, they are not described as consisting of mature adipocytes and similarly the connection with dysraphism seems to be spurious at best, with the frequency of association with sacrococcygeal teratomas no higher than other congenital defects [83].

## **Non-syndromic neural tube defect genetic studies**

Large cohorts of patients with neural tube defects have been established with genetic samples stored allowing repeated sequencing of different suspect genes. These include an Italian group and a French-Canadian group. It is worth noting that the exact disease classification is often unclear in these cohorts, with intradural lipoma, lipoma of the filum or even spinal tethering being classified as neural tube defects. Since the pathogenesis of these subtypes may be distinct from LSL, the power of these studies remains to be questioned.

One of the main pathways known to be associated with NTDs as a whole is the planar cell polarity (or PCP) pathway, with several mouse models of NTDs caused by variants in genes coding for key PCP proteins [169]. The PCP pathway was first described in *Drosophila* with the

vertebrate equivalent consisting of a number of core proteins as part of the Frizzled/Flamingo system: the transmembrane Vangl1/2 and Frizzled proteins along with an atypical cadherin, Cesl1 [170]. In addition, there are three cytoplasmic proteins: Prickle, Disheveled (Dvl) and Ankrk6. There are also several downstream effectors of the PCP pathway: fuzzy, fritz and inturned [171]. The PCP pathway has a major role in convergent extension, as first demonstrated by disruption of Dvl function in *Xenopus* cells resulting in lamellopodia formation but no polarization, and so no organised orientation of epithelial cells [172]. Convergent extension is a vital developmental mechanism during neurulation [173].

De Marco et al reviewed 473 NTD cases, although it is unclear how many LSLs were included in this bracket. They resequenced disheveled 2 and disheveled 3 and identified one case of “lipoma” with a novel variant in DVL2 (p.Ala53Val) that was predicted to be damaging [174].

Merello et al reviewed 80 NTD cases and classified 39 as closed NTDs (including “meningocele, lipomyeloschisis, tethered cord and complex dysraphisms”). They resequenced VANGL1 and found one new variant in a case of “lipomyeloschisis”, that was absent in their controls. The variant p.Ala187Val was predicted to be possibly damaging by PolyPhen-2 but as tolerated by SIFT prediction [175].

Allache et al sequenced the coding region of the *CELSR1* gene (a gene coding for a cadherin associated with the planar cell polarity pathway) in 473 individuals with either neural tube defects or caudal agenesis. Six individuals with LMM/LM were identified with missense variants that were predicted to have a pathogenic role. The study also identified similar missense mutations in 3 patients with intradural lipomas, although this is likely to be a distinctly different pathology: there is no associated defect in the surrounding dura and bone and good evidence exists that intradural lipomas are an acquired condition [176].

Kibar et al sequenced the *VANGL2* gene in 673 individuals and identified missense variants in five closed neural tube defects. The lipomas associated with these defects were either lipoma or fibrolipoma of the filum [177].

De Marco et al sequenced *FZD3* and *FZD6* genes in 366 individuals. They identified one missense mutation in the *FZD6* gene, although this was in a complex phenotype with an intradural lipoma and an anterior thoracic meningocele amongst other defects. That does not fit with a classical description of a LSL [178].

Kousa et al reviewed the *TFAP2A-IRF6-GRHL3* genetic pathway that is known to be associated with orofacial clefting syndromes. They established a role for *IRF6* in neurulation in the mouse and reviewed human data from 3 cohorts, totaling 1209 individuals (50 with LMM), and identified the presence of a significant SNP in *IRF6* [179].

Wang et al reviewed 473 individuals with neural tube defects and identified a SNV in *PTK7* in one individual, although similar SNVs were also present in fatty filum and intradural lipoma[180].

It is clear from this review of publications that LSL does not have a simple monogenic autosomal dominant inheritance. The pathogenesis must therefore relate to a multiple hit model – potentially a combination of genetic and environmental factors. In addition, in the absence of functional studies relating a specific variant to disruption in relevant developmental pathways, such results need to be treated with a degree of scepticism.

### **Clinical presentation**

The diagnosis of LSL is most commonly made soon after birth due to the presence of a midline lumbosacral swelling, additional cutaneous manifestations such as haemangiomas, skin tags or atypical dimples and occasionally signs of neuro-orthopaedic syndrome. Up to 40% of patients may be ostensibly asymptomatic at birth [181]. Diagnosis is confirmed by MRI that is usually performed at 6-12 months. MR imaging allows classification of the subtype of the LSL and also presence of other associated features such as a low lying conus or syrinx [128]. All children diagnosed with LSL are at risk of developing significant neurological and urological disability with 70% showing deterioration over time [122, 130, 181]. Although an infant might appear to be ostensibly asymptomatic at the time of diagnosis, minor changes in neurological and urological function are difficult to assess in this group. As children age, it becomes easier to assess them for more subtle manifestations of LSL. Typical symptoms include mild weakness and/or altered sensation in one or both lower limbs, musculoskeletal deformity ranging from talipes equinovarus to mild internal rotation at the hip joint resulting in abnormal gait, and pain, either radicular in nature or lower back pain. Urological symptoms are particularly difficult to diagnose in the precontinent child and include urinary urgency, incontinence, poor stream, incomplete bladder emptying and recurrent UTIs. Therefore, careful paediatric urological assessment is essential in order to evaluate bladder function and identify subclinical abnormalities. When these symptoms are present, they can sometimes deteriorate rapidly, with implications for both renal function and long term continence. Although some radiological features have been found to correspond with symptoms, there are no long-term follow-up studies that identify consistent features that correlate with prognosis and risk of neurological or urological deterioration [129].

Rarely LSL is diagnosed as part of a syndrome or with a combination of other congenital malformations. There is never complete penetrance in these conditions, and it is the minority that present with associated LSL rather than the norm. It remains unclear whether these are incidental occurrences: perhaps the same teratogenic factor targeting multiple pathways/developmental processes, or whether there is a true association that might throw further light onto the pathogenesis of LSL.

## Treatment

Options for the treatment of LSL are either surgical or observational. Indeed, there remains controversy over the timing of surgery and this reflects the incomplete understanding, not only of the pathogenesis of LSL, but also the mechanisms underlying neurological and urological deterioration.

Subtotal resection of the lipoma tissue and untethering of the spinal cord has been the conventional treatment of choice, based on the assumption that mechanical tethering of the spinal cord to the lipoma tissue results in symptoms through traction on the terminal spinal cord due to growth, and therefore removing this factor will improve symptoms or at least halt progression [72, 182]. Parallels are drawn to patients with MMC who often develop Tethered Cord Syndrome as they grow. Their symptoms, similar to those of LSL patients, are worsened on forward flexion of the lumbar spine and are improved by simple untethering surgery. However, it is now known that children who undergo *subtotal* resection of LSL have a worse long term neurological/urological outcome than those children who are managed conservatively [181]. This suggests that either spinal cord tethering is not the main mechanism of disease progression or that surgical technique is ineffective. This remains a controversial observation with some experts pointing out that patient selection is key. Although there are no proven predictive factors through long-term follow up studies, certain features are considered to have a worse prognosis: including the transitional/chaotic subtype, the presence of syrinx in MR imaging and deformity present from birth [183].

Recent advances in intraoperative neurophysiological monitoring, and the lack of improvement in prognosis following subtotal resection (usually due to late re-tethering), have led to the proposal that, in order to achieve better and sustained long term outcomes a more radical excision of the lipoma is required combined with reconstruction of the neural placode and expansion of the terminal thecal sac [126-128, 184]. In this procedure lipoma tissue is meticulously dissected off the neural placode and nerve roots under neurophysiological monitoring to preserve function and reduce the risk of re-tethering. However these are lengthy procedures with increased operative risk to neurological and urological function as well as risk of wound related morbidity such as CSF leakage and wound infection. Proponents of this more radical technique argue that the increased operative risk is justified in order to reduce the risk of late deterioration due to re-tethering. Again, the assumption is that tethering is the primary mechanism for disease progression. Although near-total resection appears to be preferable to subtotal resection in the long term, there still remains a considerable controversy whether the surgical risk can be justified for ostensibly asymptomatic children, at least some of whom may not ultimately develop symptoms [127, 184]. In addition, it has been observed that, in the presence of abnormal appearing nerve roots, there is likely to be a degree of dysgenesis and therefore no amount of immaculate dissection will improve their function [129].

Current practice in the United Kingdom and Europe is more conservative than in the United States. Children are monitored regularly for any sign of neurological or urological deterioration, and if this occurs they are offered surgery to prevent further neurological/urological deterioration rather than improve symptoms that have already occurred [130].

### **Prognosis**

Potential mechanisms to explain might include, not necessarily in isolation: tethering, dysgenesis or ongoing disease processes due to factors released from the lipoma tissue itself. In addition, how an individual responds to these insults, and how this manifests itself in neurological deterioration, is likely to depend on a large number of variables including genetic variation, an individual's metabolome and even potentially nutritional status. Only one of these factors, tethering, is addressed by the current surgical management offered to patients and, as a result, surgery should not be considered a cure. Patients continue to require assessment following surgery and remain at risk of further deterioration.

### **Clinical Classification**

The terms symptomatic and asymptomatic are often used in the clinic and this practice is reflected in this thesis. Essentially all patients considered to be "symptomatic" are offered surgery. This includes all patients who appear to be developing a deterioration in urological function on bladder assessment. Some patients, however, may be considered to be "symptomatic" but not offered surgery. This includes, for example a child who is born with a musculoskeletal defect that is stable and is not developing any further clinical manifestation of LSL disease progression, or an older child who might have mild abnormalities on bladder function assessment but these seem to be stable on multiple assessments (surgery might have been declined at a younger age in this example and now considered not appropriate). As this group of stable "symptomatic" patients do not tend to undergo surgery they were not included in the dataset of this thesis. Therefore, all patients labelled as "symptomatic" in the Lipidomics and Targeted Lipid sections were children who underwent surgery with a detectable functional manifestation of LSL that was not considered to be stable. All these children are considered to be demonstrating a degree of disease progression, and thus surgery was offered.

A small subset of children underwent surgery while being classed as "asymptomatic". This was driven by either parent choice and socio-geographical concerns, or by radiological concerns such as the subtype of LSL or the presence of associated features such as a syrinx. This group did not include any stable patients with functional clinical manifestation of LSL.

In an attempt to clarify this classification a Total Clinical Score was developed. Again, children could be roughly divided into two categories – those with no functional manifestation of LSL and those with a functional manifestation that was considered to be progressing. It is of course difficult to identify progression in younger patients where less time has passed, and why a prognosis biomarker would be so useful for management of this disease. To account for this a score for progression was added to the TCS. All children undergoing surgery classed as

“symptomatic” were considered to show some degree of progression, the main trigger for offering surgery. However, some children demonstrated more rapid progression between clinical assessments (given 2 points), whilst some even developed notable progression detected by the child or parent between clinic visits which initiated expeditious clinical assessment (given 4 points). No children considered to be stable “symptomatic” were offered surgery during the timeframe of data collection and so none were included in the analysis.

## **LIPIDS**

### **Lipids in humans**

Lipids are a large and diverse group of biologically active molecules. They are characterized by long hydrocarbon chains and are largely soluble in organic solvents. Fahy has described 8 distinct classes of lipids based on chemical structure and hydrophilic/hydrophobic properties: fatty acids, phospholipids, glycerolipids, sterols, sphingolipids, phenols, saccharolipids and polyketides [185]. Each class of lipid is further divided into subclasses with thousands of different lipids existing based on different headgroups, hydrocarbon tail length, isomers, chimers and the presence of phosphorylated or oxidized molecules. Fatty acids, phospholipids, glycerolipids, sterols and sphingolipids are found in humans (the other lipid classes being predominantly present in bacteria, fungi and plants; although they can enter the human diet/are used as medication) with even length hydrocarbon chains [186]. The diverse number of lipids reflects their diverse roles within human biology. Phospholipids are particularly abundant, forming cell membranes, but in addition have a role in cell signalling, for example, the phosphorylation of phosphatidylinositol forms PIP<sub>2</sub>, a cellular second messenger. Sphingomyelin is located within the myelin sheath of the peripheral nervous system and sterol lipids include cholesterol and steroid hormones [187].

Lipids are abundant in the serum but also detectable in the cerebrospinal fluid (CSF) at approximately 1/500th of the serum total lipid content, normally in the range of 10-13 µl/mL [187]. The transport of lipids is well characterized in serum with lipoproteins binding hydrophobic lipids to aid transport. Lipoproteins have been identified in the CSF and it is proposed that lipids are present in the CSF either bound to such carrier molecules, within endosomes or alternatively, for the more amphipathic molecules, present free within CSF or as a micelle [188].

### **Likely role of lipids in LSL**

There has been no published data on the lipid profile of LSL tissue nor the profile of the surrounding cerebrospinal fluid. The adipocytes within LSLs have been described as mature and metabolically active [138]. As such, one would expect an abundance of triglycerides within the LSL tissue itself. In addition, the spinal cord and nerve roots contain myelin consisting of a phospholipid bilayer and sphingolipids. The presence of nerve dysfunction in LSL patients suggests some damage to the nerves located at or near the lipoma-placode interface. Although no lipid profile of nerve damage has been developed it seems appropriate to expect release of lipids both as free molecules and as micelles either from the adipose tissue or from damaged nervous tissue.

### **The role of lipids in LSL disease progression.**

Given the vast scope and diversity of lipids there are a number of possible roles they could play in LSL pathophysiology. Firstly, the presence of lipids detected in CSF (as well as plasma and to some extent urine) could reflect nerve damage either through tethering, inflammation or direct



injury to nerves caused by factors released from the lipoma tissue itself. There is, as of yet, no established description of the lipid changes that occur in CSF as the results of nerve damage, although, there are a large number of publications identifying altered lipids associated with nerve damage. It remains to be determined which of these lipids change as a direct result of nerve damage, perhaps being released by damaged cells, disruption of cell membrane and myelin sheaths, or through altered cellular processes.

Secondly, the lipid changes detected could reflect a disease process mediated by lipids causing disruption of nerve function and survival. As mentioned, lipids play an important role as second messengers and inflammatory mediators. An example of this is the association between hyperlipidaemia and nerve damage in [189]. Again, the exact mechanisms are not established, while this does appear to be a causative effect rather than reactive, the evidence is limited to a global rise in lipids rather than a mechanism associated with individual lipid subtypes.

Finally, there is a possibility that the changes in lipids observed in this study are not directly related to nerve function but rather are a by-product of the LSL tissue itself. Either through mechanical disruption of the blood spine barrier or through direct metabolic disruption of lipids synthesis.

### **Lipidomics**

Lipidomics and the study of lipids first arose in the 1960s, although advances in electrospray ionisation in the 1990s resulted in more reliable identification of lipids by mass spectrometry [190]. In 2003 Spener and Lagarde described lipidomics as “the full characterization of lipid molecular species and of their biological roles with respect to expression of proteins involved in lipid metabolism and function, including gene regulation” [191]. Lipids are a large and dynamic group of molecules. We are far from understanding all the intricacies of lipid interactions within the human body, including how lipids interact and are regulated by protein expression. It would not be possible to fully characterise the lipidome of a pathological disease state when the healthy human lipidome has not yet been completely described. Since a full understanding of human lipidomics as defined by Spener and Lagarde is likely to still take decades of active research it would not have been possible to complete a lipidomics report on LSL for a doctoral research project. The term ‘lipidomics’ is used in this thesis to describe the identification of mass charge ratio and retention time pairings that are likely to correspond to a specific lipid. The intention of lipidomics analysis was to confirm the viability of collection and extraction of lipids from human samples from patients with LSL. In addition, any identification of key lipids and differences between LSL and control patients, as well as between symptomatic and asymptomatic LSL patients would guide the development of a targeted lipid assay.

### **Phospholipids**

Phospholipids are ubiquitous in mammalian cells, contributing to cell and organelle membranes as well as having an important function in both cell signalling and metabolism. These amphipathic molecules have a non-polar hydrophobic glycerol backbone with a polar,

hydrophilic phosphate based head group (Figure II.1.v). Due to their amphipathic nature, extracellular transport of phospholipids is via three different methods. Firstly, via micelles, that may either be a single phospholipid layer with a non-polar fatty acid core and a polar head group outer surface, or an inverse micelle with a polar core and a fatty acid outer surface. Secondly, via soluble protein transporter molecules such as PC-TP (phosphatidylcholine specific transfer protein). Lastly phospholipids may be transported via artificially generated liposomes, a phospholipid bilayer surrounding an aqueous core, often also transporting polar molecules [192].

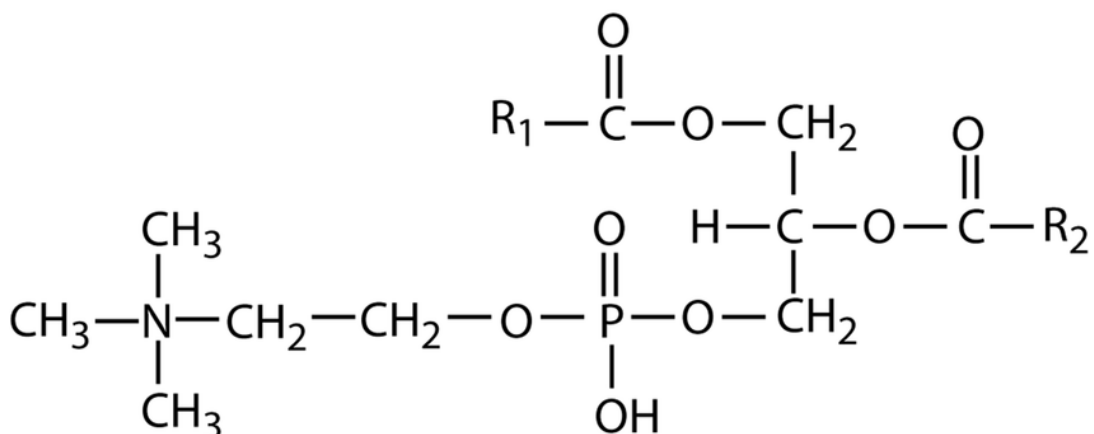


Figure II.1.v. Diagrammatic representation of a PC. R1 and R2 denote the aliphatic chains. These may be of variable length with or without double bonds. PE varies from PC only in the hydrogen residues on the terminal nitrogen rather than methyl groups.

### Synthesis

PC is the most abundant phospholipid in mammalian cell membranes, accounting for 40-50% of total phospholipids. PC is synthesised in all cells from choline, a vitamin B-like nutrient that is largely derived from diet. Adenosine and cytidine triphosphates (ATP, CTP) act as phosphate donors while diacylglycerol (DAG) acts as a glycerol donor. Synthesis is via the CDP-choline/Kennedy pathway and requires three enzymatic steps with the enzymes either cytosolic or associated with the nuclear and endoplasmic reticulum membranes. Two different isoforms exist of the enzyme CTP:phosphocholine cytidyltransferase (CT $\alpha$  and CT $\beta$ ), with predominant expression in the liver and central nervous system respectively (Figure II.1.vi).

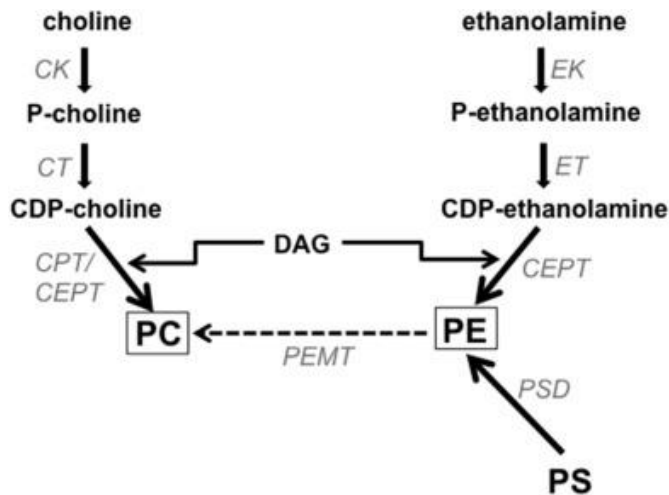


Figure II.1.vi. Biosynthesis of PE and PC are both via the Kennedy pathway with participation of choline/ethanolamine kinase and choline/ethanolamine transferase respectively. Both pathways rely on the final enzyme CEPT to convert CDP-substrate, through reaction with DAG, to the required phospholipid. PE is also synthesised from PS in mitochondria. PEMT converts PE to PC by methylation of the nitrogen residue. Figure taken from Van der Veen et al (2017)[193]. PC = Phosphatidylcholine, CK = choline kinase, CT = CTP:phosphocholine cytidylyltransferase, CPT = CDP-choline:1,2-diacylglycerol choline phosphotransferase, CEPT = CDP-choline:1,2-diacylglycerol choline/ethanolamine phosphotransferase, DAG = diacylglycerol, PE = Phosphatidylethanolamine, PS = phosphatidylserine, EK = ethanolamine kinase, ET = CTP:phosphoethanolaminecytidylyltransferase, PSD = phosphatidylserine decarboxylase, PEMT = phosphatidylethanolamine N-methyltransferase.

In addition to the Kennedy pathway, a small amount of PC can be synthesised directly from PE by the methylation of the terminal amine by the enzyme phosphatidylethanolamine N-methyltransferase, PEMT. AdoMet acts as a methyl group donor. This reaction occurs at mitochondria-associated membranes (MAM) of the endoplasmic reticulum. PEMT is predominantly present in hepatocytes but in addition is expressed in differentiating adipocytes [194]. The identification of PEMT and this alternative route for synthesis of PC from PE has highlighted the relationship between these two phospholipids and it is now known that the PC/PE ratio can affect a number of different cellular processes.

PE is the second most abundant phospholipid in mammalian cell membranes but is importantly the major contributor to the inner mitochondrial membrane, accounting for 40% of total phospholipid here. PE differs from PC only in the hydrogen atoms on the nitrogen part of the headgroup rather than the three methyl groups of PC. PE is synthesised via three different pathways, the two most significant pathways being, firstly, the CDP-ethanolamine/Kennedy pathway that closely mirrors the CDP-choline/Kennedy pathway with cytosolic ethanolamine kinase and transferase enzymes forming the CDP-ethanolamine substrate with both ATP and CTP acting as donors. The final step involves the ER associated CEPT enzyme that converts CDP-ethanolamine and DAG to PE. The second pathway occurs in the mitochondria with the

enzyme phosphatidylserine decarboxylase (PSD) solely associated with the outer aspect of the inner mitochondrial membrane. Phosphatidylserine is formed at MAM by two PS synthetase enzymes. Transport of PS to the inner mitochondrial membrane is then heavily dependent on ATP. After decarboxylation to PE, it is rapidly transported out of the mitochondria by an unknown mechanism. There is limited transportation of PE into mitochondria, and thus the PSD pathway is able to compensate for deficiency in the CDP-ethanolamine pathway, but not vice-versa.

As expected, mutations in a number of the different genes coding for the enzymes involved in synthesis of both PC and PE, frequently result in disruption of key metabolic processes and show embryonic lethality [193].

### **Function**

As mentioned above, PC and PE have a principal role in cell membrane formation with hydrophobic tails facing each other and hydrophilic headgroups forming the outer and inner surfaces of the phospholipid bilayer. However, the function of phospholipids extends beyond this structural role and many of the metabolic and signalling roles have now been identified. Due to the large variation in the length as well as number and location of double bonds in the fatty acid tails, there are also likely to remain a large number of roles of specific PC and PEs that are not yet established [195].

PC and PE are important in the synthesis and secretion of lipoproteins, including very low density lipoprotein, VLDL. VLDL is synthesised in the liver and is vital in the transport of triglycerides in plasma. Disruption of the PC/PE ratio not only alters VLDL secretion and causes accumulation of TAG in the liver, but also alters membrane stability in hepatocytes and reduced liver regeneration. It is important to note that patients with LSL do not suffer from any overt liver or metabolic disorder, and as such a global disruption in phospholipid/lipoprotein synthesis or lipid transport is unlikely to have a role in the formation or disease progression of LSL [193].

In addition to the role in the liver, PC and PE have been found to have a role in regulation of a number of different transcription factors: phospholipids are thought inhibit the function of SREBP 1a and 1c acting as a feedback loop to downregulate expression of lipogenic genes [196]. Another example is the specific function of PC 16:0/18:1 binding to PPAR $\alpha$  that results in upregulation of genes involved in lipid metabolism [197].

Phospholipids are also known to have a role in inflammation with one of the most established examples being a drop in PC associated with ulcerative colitis. Phosphatidylcholine is thought to regulate expression of NF- $\kappa$ B, and treatment with PC has been shown to reduce inflammation in this pathology [198]. More importantly, membrane phospholipids are broken down by the action of PLA2, hydrolyzing the sn-2 acyl bond and cleaving a fatty acid residue to generate arachidonic acid, an important pro-inflammatory mediator. In addition, the variable lysophospholipids generated by this reaction are likely to have diverse roles in cellular function based on their exact structure (Figure II.1.vii), [199].

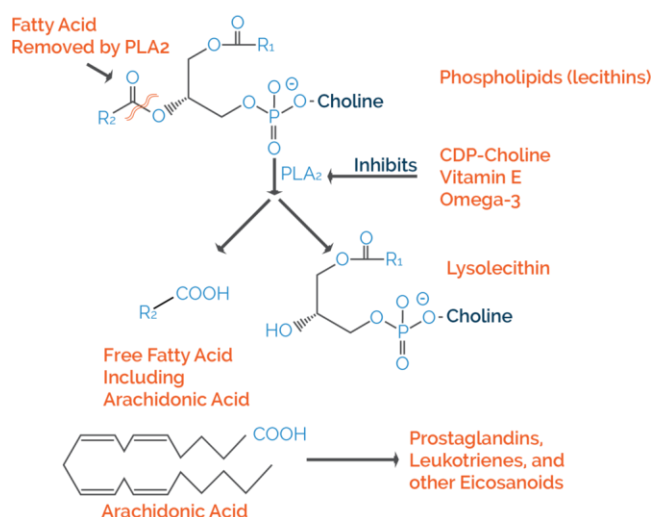


Figure II.1.vii. Enzymatic role of PLA<sub>2</sub> in the cleavage of phospholipids at the sn-2 acyl bond generating a free fatty acid and a lysophospholipid. The most biologically important free fatty acid is arachidonic acid, a precursor for a number of pro-inflammatory mediators.

The role of phospholipids in the central nervous system, beyond their contribution to plasma membrane and organelle stability, is still being established. However, a number of different phospholipids have been identified as being altered in disease states, including ALS, dementia and cerebral ischaemia. The exact mechanism underlying their role in these diseases is still the subject of active research [200, 201].

If altered levels of PC, PE or an imbalance in the PC/PE ratio are detected in LSL patients this could either reflect the role of phospholipids in the ongoing disease process, perhaps through local disruption of gene expression, or may be a side product such as from the destruction of cell membranes. In addition, an increased ratio of lysophospholipids to phospholipids would indicate increased activity of PLA<sub>2</sub> and therefore likely an increase in pro-inflammatory mediators.

## NEUROPHYSIOLOGY IN LSL

### **Anatomical basis of continence**

Control of bladder function is a complex process that continues to develop throughout early life. Three principal components of the nervous system need to co-ordinate and alternate between two states: storage and elimination.

Sensation of bladder stretch is via somatosensory afferent neurones of the pudendal nerve, but also visceral afferent neurones located in the pelvic plexus. Both pathways terminate in the sacral spinal cord. Sensation of stretch is predominantly carried by small myelinated A $\delta$  fibres that are thought to discharge during both stretch and bladder contraction contributing to the feedback control of micturition. In addition, larger unmyelinated C fibres solely respond to bladder filling/stretch. These fibres have high threshold levels which are thought not normally to be met in healthy physiological conditions, but this threshold is reduced by the introduction of toxins such as would be experienced in inflammation or infection. An important distinction between these two afferent pathways is that the A $\delta$  fibres synapse within the spinal cord so are likely to be disrupted if the spinal cord is injured, whilst the C fibres synapse directly with spinal efferent fibres, bypassing the spinal cord and thus rendering them relatively invulnerable [202]. In addition to the afferent component, the pudendal nerve also provides motor innervation to the external urethral sphincter with motor neurones originating from Onuf's nucleus in the ventral horn of the sacral spinal cord.

Parasympathetic pathways originate from the sacral intermediate grey matter at the sacral parasympathetic nucleus. Preganglionic fibres pass to the pelvic plexus and detrusor muscle, synapse and continue as short cholinergic post-ganglionic fibres that relax the internal urethral sphincter and contract the bladder wall respectively.

Sympathetic fibres originate from the intermediate horn of the lower thoracic spinal cord and descend as pre-ganglionic fibres to the inferior mesenteric plexus, synapse, and continue as post-ganglionic adrenergic fibres via the hypogastric and pelvic plexuses before terminating at the bladder wall, bladder base and internal urethral sphincter. These sympathetic fibres are both excitatory and inhibitory, resulting in contraction of the bladder base and internal urethral sphincter while at the same time causing relaxation of the bladder wall [203].

The exact mechanisms of faecal continence are less clear in comparison to urinary continence. The pudendal nerve plays a principal role in control of voluntary continence via the external anal sphincter, although this is supplemented by voluntary control of the puborectalis muscle directly from the nerve to levator ani originating from the S4 nerve root. Of note, pudendal nerve block does not stop the sensation of rectal distension. Instead, sensation is most likely mediated via visceral afferent fibres of the pelvic plexus. The sympathetic and parasympathetic systems work antagonistically to control the internal anal sphincter, with contraction and relaxation respectively. Anal sphincter control is supplemented by the recto-anal inhibitory reflex via the myenteric plexus: rectal distension causes relaxation of the internal anal sphincter and decreased anal resting pressure allowing defaecation. Defaecation is over-ruled by the recto-

anal contractile reflex that is mediated by voluntary somatic signals from the parasagittal motor cortex. Spinal cord injuries therefore disrupt both conscious awareness of faecal distension and control of the external anal sphincter, but do not disrupt the myenteric pathways involved in defaecation [204].

A good understanding of the underlying innervation and pathways involved in bladder and bowel continence is vital for the interpretation of intra-operative neurophysiological monitoring, although it is worth keeping in mind that considerable normal variation is demonstrated within the population [205].

### **Neurophysiological assessment of continence**

Sphincter motor evoked potentials (MEPs) follow transcranial stimulation and can be used to assess the efferent component of continence. Neurophysiological monitoring of the urethral sphincter is fraught with difficulty due to siting of the recording electrode and so the external anal sphincter (also innervated by the same sacral levels) is used as a surrogate for bladder sphincter function as well. Electrodes are placed on the anal sphincter and detect the function of both the descending motor spinal pathway and efferent motor neurones running in the pudendal nerve/inferior anal nerve to the external anal sphincter. Absent sphincter MEPs do not allow localisation of the injury beyond the descending motor pathway. Direct intra-operative stimulation of nerve roots can help to make this distinction although, if the sphincter MEPs remain absent with nerve root stimulation, this does not indicate whether or not there is concomitant spinal cord dysfunction.

In contrast, the bulbocavernosus reflex (BCR) is oligosynaptic and tests the somatic component of the sacral spinal cord, as well as the pudendal nerve. It is commonly used as part of the assessment in spinal cord injury where the glans penis or clitoris is squeezed and the anal sphincter is noted to contract (an “anal wink”), while bulbocavernosus contracts. An intact BCR indicates functioning lower motor neurone pathways (although there may be some damage to the spinal cord, the sacral reflexes are still functioning), whereas an absent BCR indicates damage to the nerve roots and therefore a lower motor neurone injury [206]. In the context of an unconscious child undergoing spinal surgery, electrodes are placed on the glans penis/clitoris and on the anal sphincter. The afferent pathway being tested is the dorsal nerve of the penis/clitoris and the efferent pathway the inferior anal nerve. Both afferent and efferent fibres are located in the pudendal nerve and the reflex arc is completed in the S2-4 segments of the sacral spinal cord [207]. Intra-operative neurophysiological monitoring of BCR therefore assesses the function of both nerve roots and sacral reflexes within the caudal spinal cord.

### **Neurophysiology in LSL surgery**

The current gold standard of surgical management for LSL children is near total resection of the LSL tissue with neurophysiological monitoring. Intraoperative monitoring includes transcranial motor evoked potentials (TcMEPs), somatosensory evoked potentials (SSEPs) and triggered electromyography (EMG). These are used to allow dissection of LSL tissue from nerve roots

with the aim of removing as much LSL tissue as possible without disrupting function of the conus and nerve roots. In addition, sphincter MEPs and the bulbocavernosus reflex (BCR) are monitored as a marker of the integrity of sphincter innervation [208]. Further detail of intra-operative neurophysiological monitoring can be found in the Methods Section. Although the benefits of such intraoperative monitoring are obvious it is unclear whether post-operative neurophysiological monitoring can be used as a guide to predict outcome following surgery. In addition, the assumption is often made that asymptomatic patients should have normal neurophysiology recordings, whilst symptomatic patients should have abnormal recordings, but this has not been formally tested in LSL patients.

Throughout this Chapter, all neurophysiology in LSL patients was performed under general anaesthesia at the time of LSL resection surgery and as such is considered as intra-operative neurophysiological monitoring. The terms pre-operative and post-operative are used to describe recordings taken prior to resection of the LSL tissue and at completion of resection respectively. All neurophysiology parameters were recorded as either normal, abnormal or absent on both the left and the right.

The terms symptomatic and asymptomatic are used to describe patients based on clinical assessment of both urological and neurological function. Due to the young age of the patients, both of these assessments are prone to inaccuracy (further description of these assessments can be found in the Methods Section) however, the decision to proceed with surgery remains largely based on these assessments. In an attempt to validate this approach, IONM data were reviewed to determine if the pre-operative neurophysiological measurements correlate with the clinical state of symptomatic/asymptomatic. It is proposed that while most asymptomatic patients have normal neurophysiological measurements, some clinically asymptomatic patients may have abnormal results. In addition, it is hypothesised that patients deemed clinically symptomatic should all have abnormal neurophysiological measurements and that these would be represented by a spectrum from moderately abnormal to severely abnormal/absent neurophysiological recordings in one or more parameters. Those patients with severely abnormal/absent NP recordings should correspond well with those patients who have grossly abnormal findings on clinical assessment; they would not benefit from a biomarker and are likely to have had confounding factors that would have skewed previous results. Ideally, development of a biomarker should focus on that group of patients who are asymptomatic but have abnormal NP results. Due to the small sample size this would generate, those patients deemed symptomatic but without grossly abnormal clinical findings or severely abnormal/absent NP results were also included in this cohort (Figure IV.4.i).

Sensory and motor nerve dysfunction assessed by MEPs and SSEPs usually correlate well with clinical findings [209]. In addition, no patients in the cohort had any sensory loss and only two patients had significant motor weakness. It is not yet established how sensitive BCR and sphincter MEPs are in assessing function, and more importantly in predicting longer-term outcomes in LSL patients. Ideally a neurophysiological measurement that is abnormal in asymptomatic patients and correlates with longer term outcomes would be useful in developing



a prognostically useful biomarker. The first aim was therefore to establish which of these tests was most reliable/sensitive in detecting disruption of nerve function before clinical symptoms became apparent. The next step was then to correlate these results with the targeted phospholipid assay.

It is currently not possible to accurately predict the clinical course of an individual with newly diagnosed LSL. As such, children with LSL are monitored closely with regular neurosurgical/physiotherapy assessment and bladder function assessment [181]. Many children go on to develop a neuropathic bladder with incomplete emptying, recurrent urinary tract infections and a risk of renal impairment. These children are managed with clean intermittent catheterisation [210]. As such, the need for clean intermittent catheterisation can be considered a robust clinical outcome measure. As previously discussed, less significant outcomes such as episodes of incontinence or mildly abnormal results on urodynamic assessment are less reliable measures. In terms of how a patient is affected by their disease, the likelihood of the need for future CIC should be considered as a major outcome that would alter the decision making process of whether to proceed with surgery or not. While the timing and decision to proceed with this surgery remains debated, once surgery has been performed further assessment and follow up is still required to know the long-term outcome from surgery. While it is possible to assess gross motor and sensory function post-operatively, subtle sphincter problems are not always apparent. Children undergo further bladder function assessment and still remain at risk of developing urological disability. This can lead to prolonged anxiety for both the child and parents.

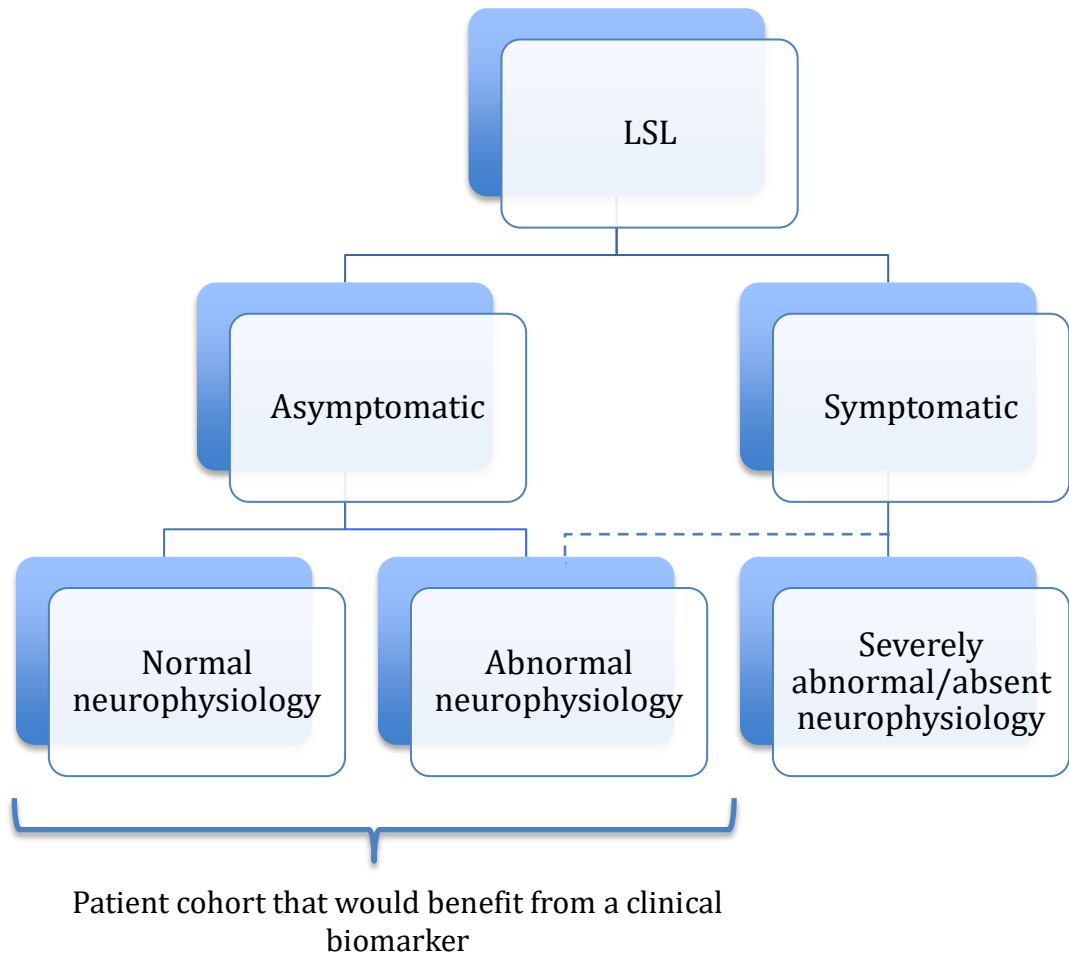


Figure II.1.viii. Schematic representing clinical assessment of LSL patients and how this potentially relates to intraoperative neurophysiology recordings. Patients who are deemed to be clinically asymptomatic could have normal or abnormal NP recordings; similarly patients who are clinically symptomatic may have different degrees of abnormal NP recordings. Those patients who are clinically asymptomatic are those that would benefit the most from a biomarker.

## **BIOMARKER DEVELOPMENT**

There are a number of different overlapping definitions of what constitutes a biomarker. For example, the World Health Organization uses the following definition: “almost any measurement reflecting an interaction between a biological system and a potential hazard, which may be chemical, physical, or biological. The measured response may be functional and physiological, biochemical at the cellular level, or a molecular interaction” (WHO 1993) [211].

Biochemical biomarkers are thought to have a particularly important role in neurological disorders where, once neurological deterioration is clinically detected, it is often too late to offer any reversible treatment. As such, the ultimate role of biomarkers in neurodegenerative disease is to identify a progressive disease process before clinical deterioration occurs, allowing early treatment and improving prognosis [212]. The same is true of LSLs where clinical assessment may ostensibly be normal but an underlying disease process may result in progressive neurological and urological symptoms in some patients but not in others.

It is important to note that while a biomarker needs to be measurable and reproducible it does not seek to explain the underlying disease process, nor does it need to be a single factor. Indeed, a combination of physical, biological and chemical factors may ultimately offer the most accurate reflection of any potential hazard.

In an attempt to establish a framework for biomarker development, Amur et al have described four different categories of biomarker: diagnostic, prognostic, predictive and response biomarkers. Each have their own specific contexts of use. The aims of this project have been to develop a prognostic biomarker to stratify patients in terms of risk of progression [213].

### **Features of a biomarker in LSL patients**

An ideal biomarker should be cheap, reliable and non-invasive with a low complication risk that is acceptable to patient/parents. Both sensitivity and specificity should be high [214]. Most importantly, a biomarker should be meaningful to clinical practice and make an improvement in patient care [215]. Ultimately a biomarker in LSL patients is likely to form only part of the clinical picture, allowing the clinician and parents to make an informed choice about treatment options.

Due to the young age at which most patients with LSL present, consideration needs to be given to the practicality of certain biomarkers. Although samples have been collected from CSF in this project, it is unlikely that a CSF-derived biomarker would be considered acceptable in this cohort, as young patients would require a general anaesthetic in order to collect this particular sample type. The benefit of collecting CSF samples in terms of biomarker development in LSL patients was based on the assumption that anything in great abundance or deficit in the CSF might also be detectable in plasma samples and therefore would give weight to a particular

candidate. In the absence of complete understanding of lipidome variation between different fluid compartments in the body, little further can be derived from CSF samples in terms of developing a biomarker, although CSF results can still be used to consider potential mechanisms of disease progression.

Plasma samples are easier to collect in young patients although this is still often a traumatic experience. There are limited complications and parents and patients are more likely to tolerate such an investigation. Urine samples are also readily available although there are also difficulties in collecting sterile samples, particularly from young patients. A urine biomarker would be clinically useful, however it has to be kept in mind that more symptomatic patients are likely to have urinary tract pathology such as infection or inflammation that would directly alter the urinary lipidome. Attempts have been made to mitigate this by excluding data from patients with grossly abnormal neurophysiology results. A blood test-based biomarker would generally be considered to be the most acceptable.

## RESEARCH QUESTIONS AND OVERVIEW OF THE THESIS

Two main controversies are associated with LSLs. Firstly, the timing of surgery. An absence of neurological and urological disability, without the need for surgery, is obviously the optimum outcome. Later surgery spares those children who did not ultimately require surgery and has lower surgical risks. However, there is little scope for recovering from any neurological/urological disability that has emerged and even near-total resection does not prevent further deterioration in all cases. Early surgery seems to offer the best chance to prevent clinical deterioration, but the complication rate is higher and, as not all children will ultimately require surgery, the ethical basis for offering this to all patients is questionable. Indeed, the promising outcome of early surgery may ultimately prove to be artefactual, due to the large number of asymptomatic patients included in the previous study on this topic [127, 128].

**The primary aim of this PhD project, therefore, was to develop a biomarker that could potentially optimize the need and timing of surgery.** This has been achieved through a number of different approaches. Firstly, lipidomics was used to determine whether differences in lipid composition of CSF, plasma or urine exist between control patients and LSL patients. Secondly, a targeted assay was developed based on the lipidomics results and comparison was made between symptomatic and asymptomatic LSL patients. Due to the difficulties in identifying symptoms in this age group, and the variation in severity of symptoms, a scoring system was developed and the targeted assay results were correlated with degree of severity of symptoms. Finally a surrogate for long-term outcome was identified (namely bulbocavernosus reflex) and targeted assay results were compared to this.

The second controversy surrounds the aetiology of LSL. A number of theories have been discussed above that are prevalent in the literature, although none offer a detailed cellular mechanism based explanation for the pathogenesis of LSL.

To initiate studies of a possible genetic basis of LSL, two familial cases of LSL were identified within our cohort of patients and genetic analysis was performed on these two families along with some additional sporadic LSL patients. These LSL patients were reviewed for evidence of genetic variants that have been previously discussed in the literature as being related to LSL. In addition, familial cases were reviewed for any inherited cause of LSL with particular focus on genes known to be associated with adipogenesis, neurulation and neural crest migration/differentiation.

The aims of this project laid out above have been met through testing the following null hypotheses:

There is no difference between the lipid profile of CSF/plasma/urine from children with LSL and control children

There is no difference between the lipid profile of CSF/plasma/urine from children with LSL demonstrating disease progression compared with children with LSL who appear clinically stable.

There is no difference in concentration of specific phospholipids in CSF/plasma/urine between children with LSL and control children

There is no difference in concentration of specific phospholipids in CSF/plasma/urine between children with LSL demonstrating disease progression compared with children with LSL who appear clinically stable.

There is no correlation between the degree of severity of disease progression and the concentration of specific phospholipids in CSF/plasma/urine from children with LSL.

There is no difference in concentration of specific phospholipids in CSF/plasma/urine between children with abnormal and children with normal intraoperative neurophysiological recordings.

There is no predicted functional genetic variation related to the formation of LSL within the genome of LSL individuals compared to the disease-free family member.

## SECTION III: METHODS

### 1. LIPIDOMICS

#### Sample Collection

Ethics approval was obtained from the Health Research Authority. REC reference: 15/WM/0249. IRAS project ID 171021. Consent was obtained from three groups of children. Group 1: children with LSL and confirmed neurological or urological deterioration on clinical and bladder function assessment/urodynamics; Group 2: children with LSL and no confirmed neurological or urological deterioration after thorough clinical and bladder function assessment/urodynamics; and Group 3: children with non-LSL related spinal pathology undergoing neurosurgery. All patients were recruited into the study with consent taken from parents prior to initial surgical intervention. Consent forms and information sheets provided to parents can be found in Supplementary Information.

Samples were collected at three specific time points. All patients were NBM for at least 8 hours prior sample collection. Firstly blood samples were collected at the initiation of anaesthesia, at the point of first cannulation of the patient. Samples were collected in a syringe, transferred to EDTA tubes and stored on ice in theatre. Secondly urine was collected following catheterization of the patient with a paediatric Foley catheter. The first urine within the catheter bag was collected under sterile conditions into a universal container and also stored on ice in theatre. Thirdly, CSF samples were collected at the point of opening of the dura. To minimize contamination with blood, care was made to keep the arachnoid intact. Hooks were used to elevate the arachnoid. A small incision was made in the arachnoid and a blunt 18G needle inserted into the subarachnoid space. Between 5-10 ml of CSF was collected into a sterile universal container and placed on ice. CSF sampling was performed by DT for LSL patients, and by a consultant paediatric neurosurgeon for control cases. Samples were all pseudonymised.

Samples were transferred to the laboratory. CSF and urine samples were aliquoted into Eppendorf tubes and stored at -80°C. Blood samples were decanted into Eppendorf tubes and spun in the centrifuge at 5°C for 20 minutes at 14000 rpm. The upper plasma phase was aliquoted into new Eppendorf tubes and, along with the lower cell phase, was stored at -80°C.

#### Lipid extraction

Lipid extraction was via a modified Bligh and Dyer method, optimised for plasma lipid extraction and modified for CSF and urine lipid extraction. The first phase was a propranolol/hexane extraction and preparation was done with glass tubes. 950 µl and 500 µl of HPLC grade H<sub>2</sub>O was added to 50 µl of plasma and 500 µl of CSF respectively. 1 ml of urine was used without any dilution. Glacial acetic acid was added to adjust the pH to between 3-4 (4 µl to plasma

samples and 3  $\mu$ l to CSF and urine). 2.5 ml of extraction mix was added (30:20:2 of propanol/hexane/acetic acid). Samples were vortexed, a further 2.5 ml of hexane were added then vortexed again. Samples were separated by centrifuge at 1500 rpm at 4°C for 5 minutes. The upper layer was collected, a further 2.5 ml of hexane added to the remaining bottom layer and vortexed then spun as previously. The second upper layer was collected and added to the first and together they were dried down using a vacuum drier at vacuum setting 200 (30°C, speed 30). The remaining bottom layer underwent Bligh and Dyer extraction with 3.75 ml of extraction solution (1:2 chloroform/methanol). Samples were vortexed and 1.25 ml chloroform added. Samples were vortexed again and 1.25 ml HPLC grade H<sub>2</sub>O added. Samples were vortexed once more then spun as above. The bottom layer was pipetted into a separate glass vial and dried down. Each dry sample was reconstituted in 200  $\mu$ l methanol, given a final vortex to ensure mixing and upper and lower phases were combined from each sample. The combined extraction mix was given a final spin through a column filter at 1300 rpm at 4°C for 15 minutes. Samples were stored at -80°C and prior to analysis internal standards were prepared using arachidonic acid d8 and DMPE (PE14:0) from Avanti and diluted to 10 ng in 10  $\mu$ l of methanol. 10  $\mu$ l of internal standard was added to each sample [216, 217].

#### **Liquid chromatography/Mass spectrometry**

Samples were run through an Accela Autosampler and 1250 pump using mobile phases A (80% water, 20% acetonitrile, 0.1% acetic acid and 4 mM ammonium acetate) and B (70% IPA, 30% acetonitrile, 0.1% acetic acid and 4 mM ammonium acetate). Lipids were separated in a C18 Accucore column (150 mm x 2.1 mm with 2.6  $\mu$ m silica particles), with a gradient such that lipids were separated with fatty acids eluting first followed by phospholipids and sphingomyelin then triglycerides and cholesterol esters (Figure III.1.i). Lipids were identified by ThermoFisher Orbitrap mass spectrometry in positive and negative electrospray mode with accuracy at 5 parts per million.



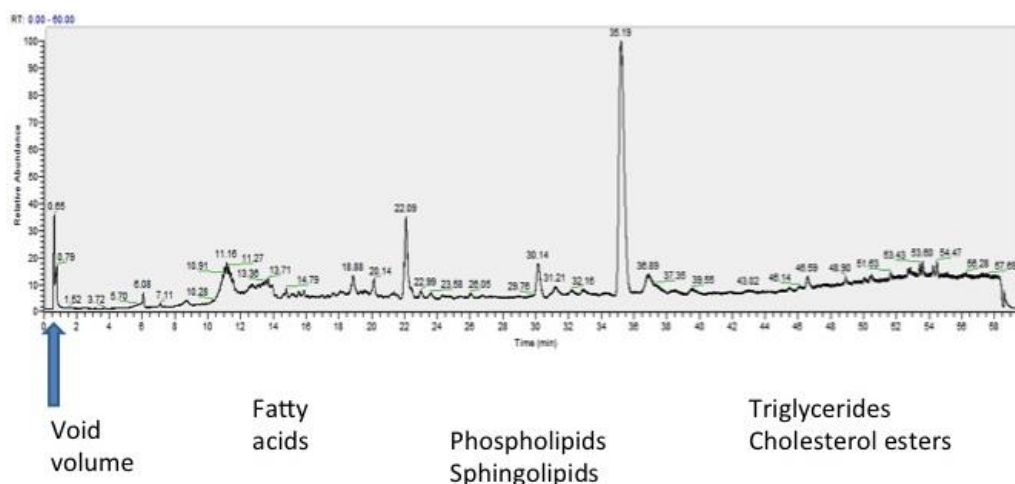


Figure III.1.i Sample chromatogram of a CSF sample taken from a control patient to demonstrate relative retention time of different lipid classes. Lipids with a retention time of less than 1 minute were within the void volume of the column.

Data are presented as spectra and chromatograms. Spectra plot  $m/z$  against intensity of ion signal on the y-axis, whilst chromatograms plot retention time against relative abundance on the y-axis. The intensity of ion signal loosely correlates with abundance of an ion. Depending on the type of mass spectrometer and the method of ion detection, different units can be used: counts per second (cps) or power of the signal sine wave (rms). However, there are many factors that can affect this value such as ease of ionization, size and velocity of the ion and signal decay. As a result, by convention, no unit is assigned to the signal intensity in publications [218, 219].

### Data processing

Total ion chromatograms were viewed in Xcalibur software to exclude any gross abnormalities. MS converter software generated mzXML files with centroid peak picking. XCMS package provided by Bioconductor was used with RStudio (RStudio, Inc) with the following setting: maximum tolerated  $m/z$  deviation in consecutive scans = 10 parts per million, chromatogram peak width 10 to 120 seconds, peak alignment with bandwidth set at 30 and width of overlapping  $m/z$  slices set at 0.005 and noise reduction with signal to noise ratio cutoff = 5 to produce .csv data file. The full R scripts can be found in supplementary information. Further data processing and analysis was completed in Excel (Microsoft). Mean values across extraction blanks were subtracted from test and control samples, log<sub>2</sub> fold change and p values were calculated using an unpaired t test. Volcano plots were generated using R studio. Lipids were identified through LipidMaps online database search with an accuracy set at 0.01M/Z [220].

## 2. TARGETED LIPID ASSAY

### Sample collection

Sample collection was as described above.

### Method development

Lipid standards were acquired from Matreya, Avantis and Sigma and prepared as 1 mg/50 ml chloroform:methanol (2:1). Initial mass spectrometry lipid identification was performed with sample injection and MS scan in both negative and positive electrospray modes, with the following settings: Cap 3,200 V, Cone 35 V, Desolv temperature 400°C, Desolv gas flow rate 800 L/Hr, source temp 120°C. Identified parent molecules were then interrogated with increasing collision energy with MSMS scan to detect daughter of fragments. To confirm phospholipid class, the head group needs to be detected. Head groups and expected daughter fragments in the appropriate ES mode were calculated using Brydwell.com. Where expected head groups were not detected, a neutral loss scan was performed using the calculated value of the head group (Figures III.2.i-v) [221].

| Phospholipid | ES-      | ES+      |
|--------------|----------|----------|
| PA           | Observed |          |
| PC           |          | Observed |
| PE           | Observed | Observed |
| LPC          |          | Observed |
| LPE          | Observed | Observed |

Figure III.2.i Phospholipid subclasses detected in different electrospray ionization modes. PA = phosphatidic acid, PC = phosphatidylcholine, PE = phosphatidylethanolamine, LPC = lysophosphatidylcholine, LPE = lysophosphatidylethanolamine. ES- = negative electrospray ionization, ES+ = positive electrospray ionization. All phospholipids tested observed in ES+ apart from PA.

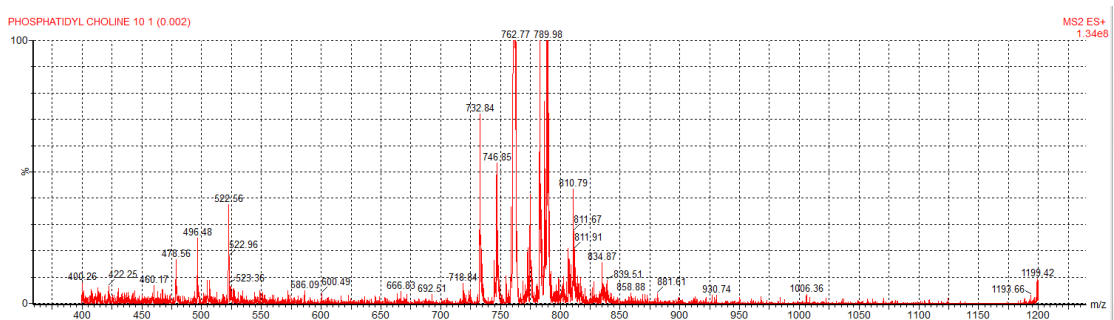
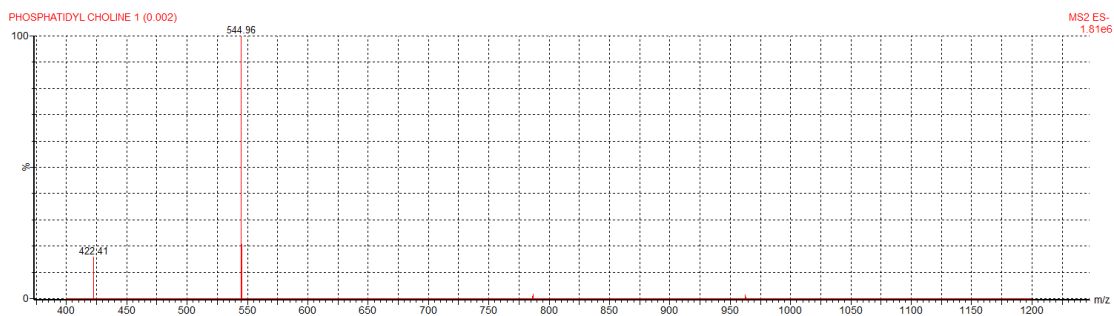


Figure III.2.ii Spectra comparing detection of PC in ES- mode (top spectrum) and ES+ mode (bottom spectrum). Note the intensity signal is 100-fold greater in ES+ mode and peaks show saturation.

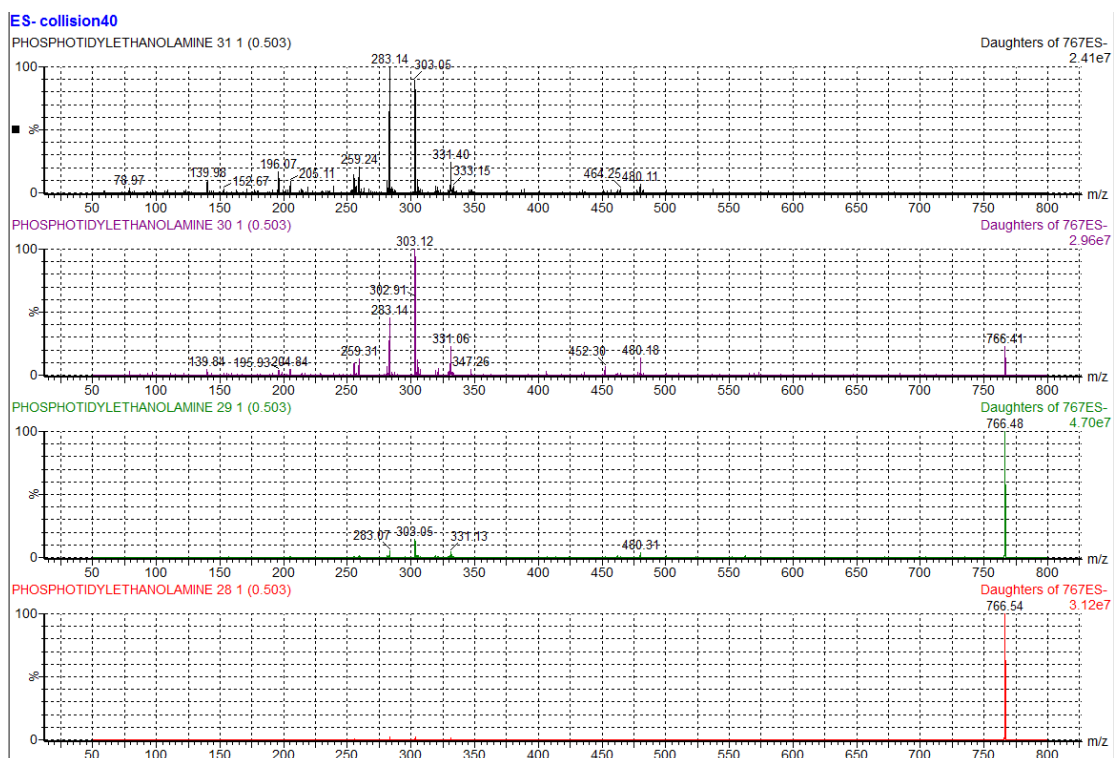


Figure III.2.iii Spectra of PE in ES- mode with increasing collision energy applied in 10 eV increases. Bottom spectrum shows detection of PE parent molecule at 10 eV collision energy. Top spectrum at 40 eV shows only daughter fragments.

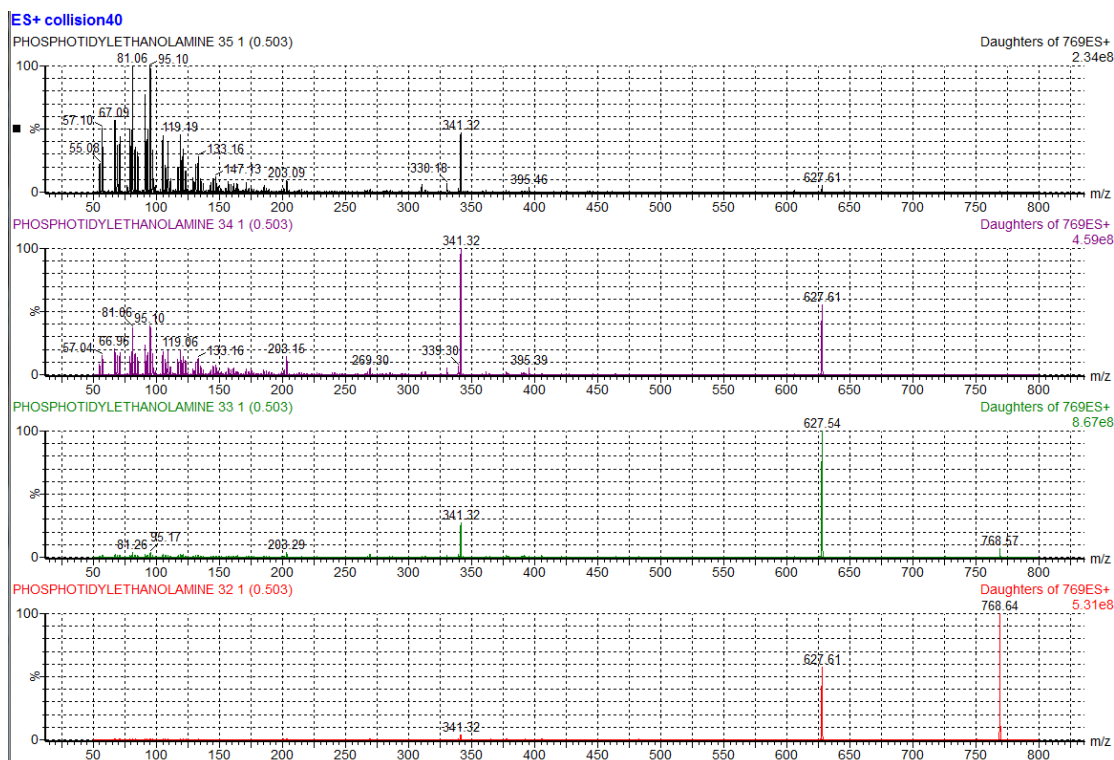


Figure III.2.iv. Spectra of PE in ES+ mode with increasing collision energy applied in 10 eV increases. Bottom spectrum shows detection of PC parent molecule at 10 eV collision energy. Top spectrum at 40 eV shows only daughter fragments. The positively charged PE head group (C<sub>2</sub>H<sub>9</sub>NO<sub>4</sub>P<sup>+</sup>) has an exact mass of 142.03. No head group is detected, however, a possible diacylglycerol like fragment is detected with mass 627.61. This fragment increases intensity signal at 20 eV collision energy and is almost undetectable by 40 eV collision energy. This corresponds with a daughter of 768.64 that is itself fragmented at higher collision energies. The head group is likely to be lost as a neutral molecule. Subtraction of this daughter m/z from the parent molecule m/z reveals mass of the neutral head group (768.64 - 627.61 = 141.03).

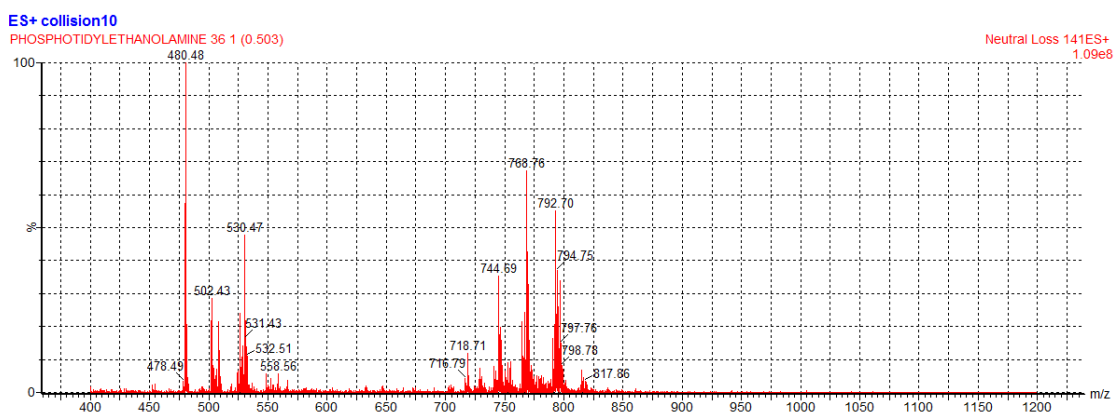


Figure III.2.v. Tandem MS demonstrating neutral loss scan of phosphatidylethanolamine in ES+ mode. Detection only of molecules that can be paired with a daughter fragment that is equal to the parent molecule minus head group fragment. Neutral loss scan set to 141.

### Lipid extraction

Three different methods of lipid extraction were compared to optimize the method. Firstly the modified Bligh-Dyer method described above, secondly the Fuchs method and thirdly a simplified Bligh-Dyer method as described below. Initial targeted assay method development steps were run with samples prepared from all three methods. There was no discernible difference in the detection or quality of signal so the simplified Bligh-Dyer method was used for final lipid extraction [222].

Higher concentrations of lipids in plasma samples led to saturation of the signal. Plasma volumes and extraction method was adjusted accordingly. Initially one tenth of the volumes in the simplified Bligh-Dyer method were used, however, the lower organic phase was small resulting in practical difficulties extracting this phase further. Instead the plasma samples were reconstituted in 240  $\mu$ l methanol then diluted 1 in 10 (24  $\mu$ l in 216  $\mu$ l methanol).

CSF and urine samples were prepared with the same method. 300  $\mu$ l of sample was added to 600  $\mu$ l of methanol with 0.0065 ng/ $\mu$ l of internal standard (LPE 15:0/18:1-d7). Samples were stored on dry ice for 10 minutes then placed in a sonication water bath for 5 minutes. 300  $\mu$ l of chloroform was added and samples were again placed on dry ice for 10 minutes. 300  $\mu$ l dd water was added, samples vortexed, a further 300  $\mu$ l of chloroform added and samples vortexed again. Samples were then centrifuged at 4°C for 10 minutes at 14000 rpm. The lower organic phase was transferred to a glass vial using a glass Pasteur pipette and either dried under high flow nitrogen or air dried in a fume cupboard overnight. Dried samples were reconstituted in 240  $\mu$ l of methanol. Plasma samples were prepared by the same method but with 30  $\mu$ l of plasma was added to 600  $\mu$ l of methanol with 0.65 ng/ $\mu$ l of internal standard. Every fifth sample was prepared as an extraction blank using 300  $\mu$ l or 30  $\mu$ l ddH<sub>2</sub>O for CSF/urine and plasma samples respectively.

### Lipid Separation and Detection

Samples were run through a Waters 717plus autosampler and 1525 Analytical Binary pump using mobile phases A (95% acetonitrile, 5% water, and 10 mM ammonium acetate) and B (50% acetonitrile, 50% water and 10 mM ammonium acetate). Lipids were separated in an Acquity UPLC BEH HILIC column (50 mm x 2.1 mm with 1.7  $\mu$ m Ethylene Bridged Hybrid particles), with a gradient such that lipids were separated with PE eluting first followed by PC then LPE and LPC (Figure III.2.vi). The method was optimized with a multiple reaction monitoring (MRM) mode to only detect lipid subclasses at known retention times. Lipids were identified by UPLC/Xevo TQ-S mass spectrometer (Waters Ltd., UK) in positive electrospray mode. Wash cycles and pre-samples were added to limit retention time drift seen.

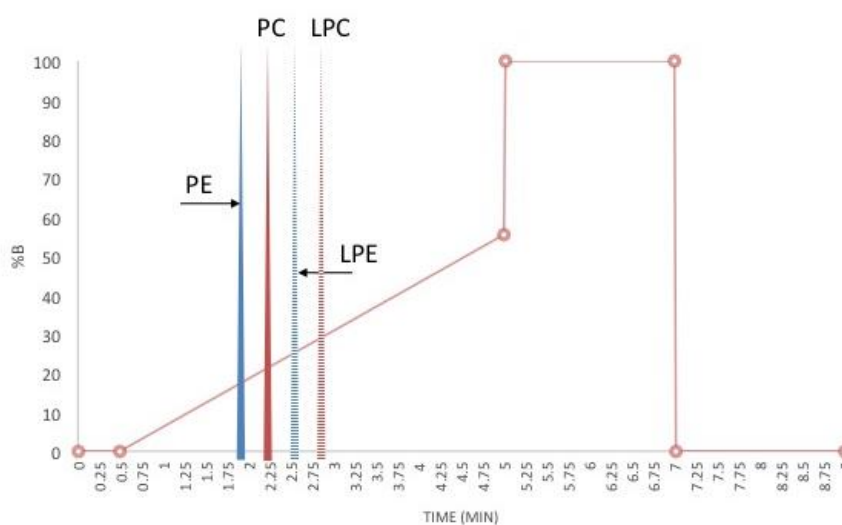


Figure III.2.vi. Change in mobile phase ratios and timing of elution of different phospholipid classes.

### Calibration curves

Values quoted throughout the Results section are in intensity of ion signal measured by mass spectrometry. This value has no units. To convert intensity into concentrations, calibration curves were calculated using an analyte standard mix of (LPC 18:0, 17:0, 16:0 and 14:0) such that each phospholipid subclass was present at the predetermined concentration. Initially concentrations ranging between 10 ng/ $\mu$ l and 0.1 ng/ $\mu$ l were used but most of these values showed saturation. The range was adjusted from 1 ng/ $\mu$ l to 0.01 ng/ $\mu$ l. Calibration curves were then plotted to determine the range and sensitivity of the mass spectrometer as well as to allow calculation of concentrations of different lipids. Concentrations above 0.8 ng/ $\mu$ l showed saturation, whilst concentrations below 0.2 ng/ $\mu$ l became less reliable (Figure III.2.vii). Since calculation of concentrations using this calibration curve adds error to values, intensity values were used for all analysis.

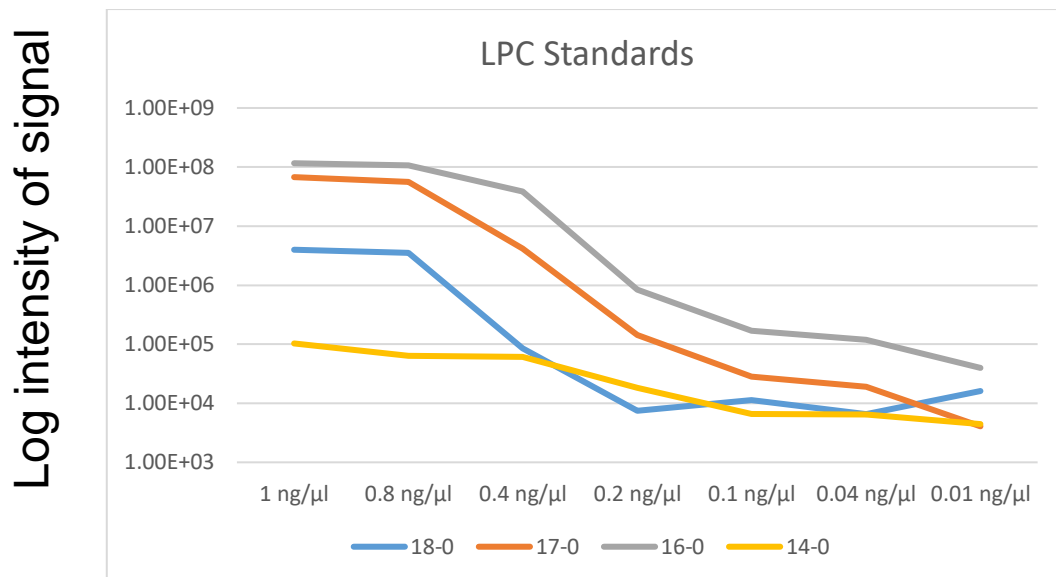


Figure III.2.vii. Calibration curve for LPC standards. Saturation of signal above 0.8 ng/μl. Signal becomes unreliable at low concentrations typically below log10e4 intensity.

### Data analysis

Chromatograms were analysed using TargetLynx 4.1 software (Waters). Peaks were selected for each phospholipid on a sample trace (standards were used where available but otherwise chromatograms were reviewed for optimum traces). TargetLynx was used to automatically select all subsequent peaks across samples then peak selection was reviewed, corrected and smoothed by hand as needed. The area under peaks was calculated to give a total intensity of signal and data was further analysed in SPSS (IBM).

The mean of extraction blanks was calculated and subtracted from other samples for each lipid. Lipids that subsequently had all sample values as negative or zero were excluded from further analysis. Samples were grouped according to clinical state: LSL or control and symptomatic or asymptomatic. Unpaired two tailed t-test was performed taking into account degree of variance within samples.

### Clinical Assessment

Patients were assessed in the clinic prior to surgery by a neurosurgeon (DT or myself).

Power was assessed as per MRC muscle grading score (5 = normal, 4 = mild weakness, 3 = loss of antigravity power, 2 = some movement noted, 1 = muscle contraction noted, 0 = no movement or muscle contraction noted). A score of 4 was considered to show mild weakness, a score of 3 or lower was considered as significant weakness. No patients had a score of 2 or less in any muscle groups. Sensation was assessed with light touch in relevant lower limb dermatomes. Sacral nerve roots 3-5 (around the anus were not routinely assessed in the out-

patient clinic). Gait was observed if the child was at walking age and any deformities noted. Patients were assessed post-operatively prior to discharge and in clinic at 2-3 months (by myself or part of the extended neurosurgical team).

### **Bladder Function Assessment**

Bladder assessment was performed by specialist urology nurses in the urology clinic according to a standardized proforma and reports were made available in the clinical notes. Assessment included a bladder diary documenting events of incontinence, urgency, bed-wetting, and confirmed events of urinary tract infection. Ultrasound of the bladder was performed to assess thickness of the bladder wall, and bladder volume pre and post micturition. In addition, a residual post-void percentage was calculated. Total bladder capacity was calculated as being equal to the sum of void volume and residual volume. The residual post-void percentage was then taken as residual volume over total bladder capacity. A percentage of twenty or below was considered to indicate a normal urological function [223].

In older children who were able to co-operate, full urodynamic assessment was performed including uroflowmetry (measure of the urine stream volume and flow) and cystometric testing (insertion of a manometer to measure pressure within the bladder as it fills and during micturition). Patients were assessed prior to surgery and again at 6 months post-operatively. Points were assigned to clinical and urological features to generate a Total Clinical Score (Table III.2.i). SPSS was used to calculate Spearman's rank correlation coefficient.



| <b>Motor</b>                        | <b>Deformity</b>                     | <b>Sensory</b>              | <b>Pain</b>         | <b>Progression</b>                | <b>Urinary</b><br>(1 point for each of the below)                |
|-------------------------------------|--------------------------------------|-----------------------------|---------------------|-----------------------------------|--|
| 0 = normal                          | 0 = no deformity                     | 0 = no sensory loss         | 0 = no pain         | 0 = suspected progression         |  |
| 1 = mild unilateral weakness        | 1 = mild unilateral deformity        |                             |                     |                                   | 1 = UTI,<br>CIC,<br>thick bladder wall,<br>large residual volume |
| 2 = significant unilateral weakness | 2 = significant unilateral deformity | 2 = unilateral sensory loss | 2 = unilateral pain | 2 = evidence of rapid progression |  |
| 3 = mild bilateral weakness         | 3 = mild bilateral deformity         |                             |                     |                                   |  |
| 4 = significant bilateral weakness  | 4 = significant bilateral deformity  | 4 = bilateral sensory loss  | 4 = bilateral pain  | 4 = very rapid progression        |  |

Table III.2.i. Total Clinical Score. Points were assigned to different clinical features. Motor weakness was considered mild if MRC motor grading of 4, and significant in MRC motor of grading 3 or less. Deformity was considered mild if no disruption to function or intervention was required (such as splinting for talipes). Progression of symptoms was a change in clinical assessment noted at 6 monthly intervals. Very rapid progression was considered to be a deterioration that was detected by the patient and/or parents such that out patient assessment was brought forward: for example multiple UTIs triggering repeat bladder function assessment. One point was assigned to each of the features on bladder function assessment. Urinary urgency and incontinence noted in bladder diaries were not assigned points since these symptoms are subjective and particularly difficult to assess in young children. Large residual volume was taken as a residual post-void percentage greater than 20%. Maximum total score 24.

## Neurophysiological Monitoring

Children with LSL undergoing near total resection under intraoperative neurophysiological monitoring (IONM) between 2015 and 2017 were included in this part of the study. As the aim was to see if IONM corresponds with longer-term outcome, a retrospective review was done. IONM was performed by IJ. Following induction of anaesthesia, subdermal needle electrodes were placed cranially for transcortical monitoring: at the CP3, CP4 and CPz positions for SSSEPs, and at C1/2 and C3/4 positions for TcMEPS (Figure III.2.viii).

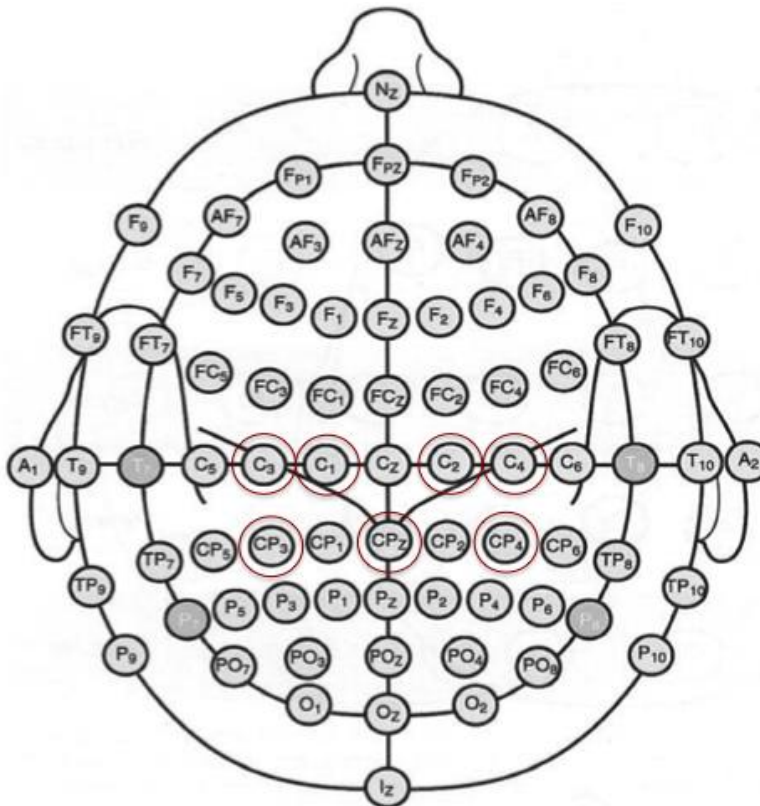


Figure III.2.viii. Position of scalp electrodes for TcMEPs and SSEPs. Diagram taken from Harner and Sannit 1974[224].

All peripheral needle electrodes were placed bilaterally. Peripheral sensory electrodes were placed at the posterior tibial nerve posterior to the medial malleolus and the common fibular nerve in the popliteal fossa. Motor electrodes were placed in tibialis anterior and abductor hallucis. Electrodes for sphincter MEPs were placed in the external anal sphincter, and for BCR were placed in the glans penis/clitoris as well as the external anal sphincter. Prior to the initiation of surgery, and after surgical opening of the dura, baseline IONM recordings were taken. In addition, BCR recordings were taken using post-tetanic potentiation to lower trigger threshold. Readings were taken from both left and right [224, 225].

BCR recording was initially classed as normal or absent pre-operatively as a baseline. These values were then compared with clinical assessment. Chi squared and Fisher's Exact Test were calculated using SPSS software package. Post-operative recordings were then taken as normal = same as pre-op (2), abnormal = noticeable difference from pre-op (1), or absent (0). Scores

from the left and right were summed to give a total out of 4. This allowed calculation of receiver operating characteristic (ROC) curves based on BCR score to identify the best score that correlates with outcome (need for CIC). ROC curves were also generated using SPSS. For the assessment of whether BCR corresponded with targeted assay, the pre-operative BCR was used. Patients with absent BCR results were excluded as this group represented an extreme. Since the data were taken from the beginning of the operation, there was no baseline for a comparison to be made. The baseline was taken as the side with the best recording. Therefore a BCR that was absent on one side but present on the contralateral side would get a score of 2. BCRs that were present bilaterally but with a noticeable reduction on one side would get a score of 3, and strong and equal BCR bilaterally would get a score of 4. For targeted assay t-tests scores of 2 and 3 were considered reduced, score of 4 was considered normal.

### 3. GENETICS

Ethics approval was obtained from the Health Research Authority (REC reference: 08/H0713/46 CRAC project ID 08ND09) as part of a pre-existing research project under PS. Consent was obtained from both parents for themselves and the child. Consent and parent information sheets from the original ethics approval are in Supplementary Information (author PS). Blood samples were collected by a neurosurgery nurse consultant (LM) in EDTA vacutainers and sent for DNA extraction in the GOSH laboratory. Once DNA extraction was complete samples were stored at -20°C. Sample concentration was measured by Qubit Fluorometer and integrity checked with agarose gel electrophoresis (1% agarose gel, 150 V, 40 minutes) before samples were sent to BGI (Beijing Genomics Institute) for completion of Whole Genome Sequencing.

#### Genetic Analysis

The Whole Genome Sequencing (WGS) data above was combined with Whole Exome Sequencing (WES) data previously generated under the project 08ND09 (“DNA sequence analysis to evaluate candidate genes for their aetiology in human birth defects”) by PS. Combined WGS/WES analysis was completed using the GOSgene pipeline. Data were provided by BGI as vcf files, that were uploaded into Ingenuity® Variant Analysis™ software version 3.1.20140902 from Ingenuity Systems. Ped files were generated with details of each family pedigree and also uploaded in Ingenuity. Autosomal dominant filters were set up for family 1 and 2. Confidence was set at allele fraction > 35, Call Quality >20, Read Depth >5. Common variant filter was set at 0.01% corresponding to a disease frequency of 1 in 10,000 based on the gnomAD database. Predicted deleterious filter was set to select only exonic variants and exclude synonymous variants.

BAM (binary sequence alignment map) files were uploaded into IGV and reviewed for artifact. There were insufficient samples to confirm candidate variants by Sanger Sequencing.

Following filtering of variants by Ingenuity, pathogenicity of variants was assessed by *in silico* programs Sorting Intolerance from Tolerance (SIFT), Polymorphism Phenotyping version 2 (Polyphen-2) and Combined Annotation Dependent Depletion score [226-228]. A review of these *in silico* algorithms can be found in Section VI.

Gene function, protein expression and known disease associations were then reviewed through published literature and online databases: the Human Proteome Map, Genecards, Ensembl, ClinVar and the Human Gene Mutation Database.

#### In situ hybridization

Initial *in situ* hybridization was performed by myself and LR. The majority of *in situ* hybridization thereafter was performed by NM. RNAscope probes for RADIL and ARHGAP29 as well as a control probe were designed by BioTechne. Human embryos were provided by the HDBR and were carefully viewed for correct staging and sliced into axial and sagittal sections, focusing on

the caudal spinal cord. Slides were heated to 60°C for 10 minutes then dewaxed in xylene and washed in ethanol. Slides were then covered in H<sub>2</sub>O<sub>2</sub> for 10 minutes then rinsed in ddH<sub>2</sub>O and washed in ethanol. Protease treatment was performed with Protease Plus at 40°C for 30 minutes followed by a ddH<sub>2</sub>O wash before the probe was added and the slides incubated for 2 hours at 40°C. Amplification washes were performed with amplification solutions provided by BioTechne, and staining with RED solution prior to drying and mounting. Routine haematoxylin and eosin counterstain was performed.

Microscopy was performed on a Leica DMI8 fluorescence microscope with photography using an IDS 3260 camera performed by NM.

## SECTION IV: DEVELOPING A BIOMARKER

### 1. LIPIDOMICS

Lipidomic results are represented in volcano plots of  $-\log(p\text{-value})$  against  $\log_2$  fold change. Each data point on the volcano plots corresponds to one mass charge ratio-retention time pair such that an identical mass charge ratio with a different retention time is represented by a separate data point. Due to the ionisation of lipids required for detection by mass spectrometry, each lipid may form a number of different adducts and so each lipid may be represented by a number of different data points. For this reason, the term lipid/lipid adduct is used to describe the volcano plot data points.

Throughout this section, volcano plots are presented with a y-axis division at 1.3 that corresponds to a p-value of 0.05. All marks above this line show a significant difference ( $p < 0.05$ ) in mean intensity of signal between control and test samples. The x-axis has two divisions at +2 and -2. These correspond to a difference in magnitude of 4 or more between control and test samples. A negative value on the x-axis corresponds to a lipid/lipid adduct that is more abundant in test samples, and a positive value corresponds to a lipid/lipid adduct that is more abundant in control samples.

All volcano plots are colour coded such that grey marks do not show any significance. Green marks show a large difference between control and test samples (greater than a magnitude of 4) but this does not reach significance ( $p > 0.05$ ). Blue marks represent lipid/lipid adducts that show a significant difference in mean intensity between control and test samples ( $p < 0.05$ ) but the magnitude of difference between the cohorts is small (less than a magnitude of 4). Red marks represent lipid/lipid adducts that show a significant difference in mean intensity between control and test samples ( $p < 0.05$ ) and a large magnitude of difference ( $> 4$  fold).

As mentioned, individual data points represent a mass charge ratio-retention time pair that corresponds to a lipid or lipid adduct. One lipid may be represented by several data points. Without injection of known standards and fragmentation of measured lipids it is impossible to confirm exactly which lipid is being measured. Identification of the 10 data points with the smallest p-value, with the largest negative  $\log_2$  fold change (most abundant in LSL patients) and with the largest positive  $\log_2$  fold change (most abundant in control patients) was attempted. Tabulated data that follows volcano plots gives one possible potential lipid that might account for each mass charge ratio-retention time pairing. This information has been taken from online database LipidMaps and should not be considered as definite confirmation of detection of an exact lipid.

Explanation of abbreviations used in lipid search results can be found in the Abbreviations section. Number annotation relates to the number of carbon atoms in each lipid type followed by the number of double bonds.

Where likely lipids are labelled as unknown this refers to either the database search not returning any potential matches within a M/Z of 0.01, or the only options that are presented are not found in humans (such as wax esters).

Two separate runs of lipidomics were completed. The first, Lipidomics 1, was a trial involving a small sample size of 3 LSL patients and 3 control patients. After confirmation that lipidomics was feasible on the collected samples, a further larger study was completed with 29 samples (11 control and 18 LSL patients, Lipidomics 2). Identification of lipids was attempted through on-line database search as described in the Methods section.

## LIPIDOMICS 1

For Lipidomics 1 the sample size was 3 control and 3 test patients. The test patients all had LSL, two classified as transitional and one as dorsal. All three patients had bladder symptoms in terms of urinary frequency, occasional incontinence and moderate post-micturition residual volumes. One LSL patient also had the bilateral musculoskeletal deformity, talipes equinovarus. Two control patients had cerebral palsy and were undergoing selective dorsal rhizotomy (SDR); both had spastic gaits but neither had any urinary symptoms. The final control patient had an untreated myelomeningocele and was undergoing delayed repair; she had lower limb weakness and had poor bladder control requiring catheterisation. Further clinical details of patients can be found in Supplementary Information.

## CSF

A total of 4761 lipids/lipid adducts were detected in CSF samples. Of those, 522 were significantly different between LSL and control patients ( $p < 0.05$ ) and 183 had a log<sub>2</sub> fold change of greater than 2 or less than -2 as well as being significantly different (Figure IV.1.i).

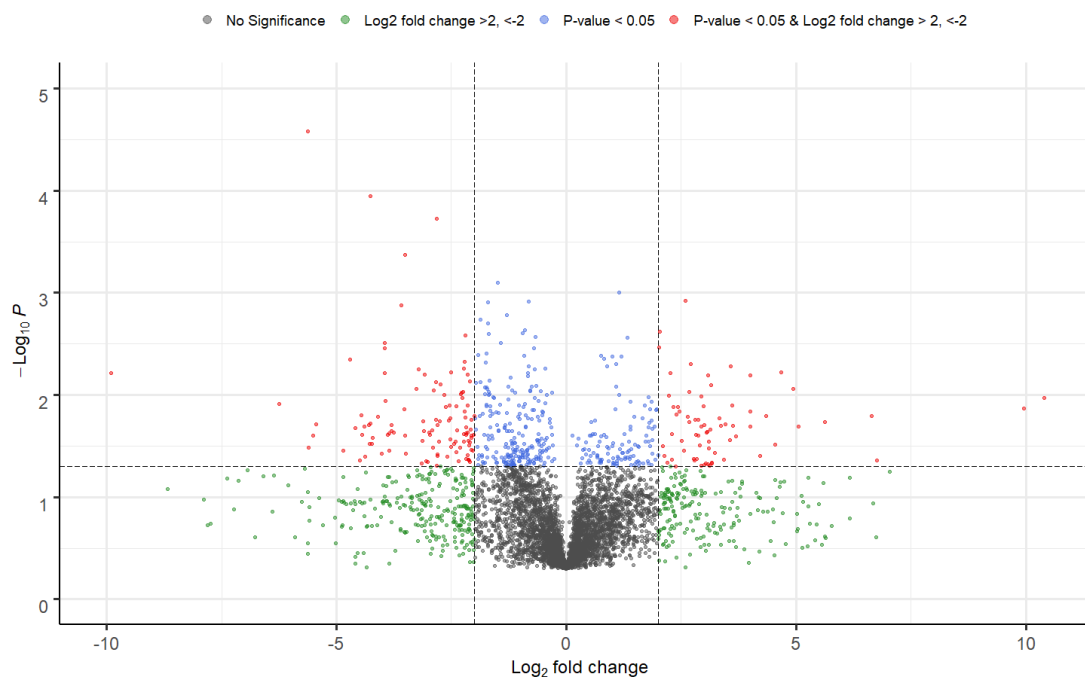


Figure IV.1.i. Volcano plot of potential lipid or lipid adducts detected in CSF samples from LSL and control patients. Attempted identification of lipids/lipid adducts marked in red with smallest p-value represented in Table IV.1.ia, with the most negative log<sub>2</sub> fold change (more abundant in LSL patients) represented in Table IV.1.ib and with the most positive log<sub>2</sub> fold change (more abundant in control patients) represented in Table IV.1.ic.



| <b>M/Z</b> | <b>RETENTION TIME</b> | <b>LIKELY LIPID</b> | <b>LOG2FOLD CHANGE</b> | <b>PVALUE</b> |
|------------|-----------------------|---------------------|------------------------|---------------|
| 351.14     | 3.82                  | LPIP(20:4)          | -5.62                  | 0.0000        |
| 470.21     | 3.98                  | unknown             | -4.27                  | 0.0001        |
| 501.38     | 14.62                 | TG(60:9)            | -2.83                  | 0.0002        |
| 568.44     | 19.50                 | LPA(26:0)           | 2.58                   | 0.0012        |
| 482.40     | 12.79                 | NAE(28:4)           | 2.03                   | 0.0024        |
| 407.26     | 17.24                 | PA(44:10(OH))       | -2.20                  | 0.0026        |
| 857.74     | 49.82                 | DG(50:1)            | 2.02                   | 0.0034        |
| 207.11     | 3.20                  | FA(12:3)            | -3.96                  | 0.0035        |
| 407.30     | 11.07                 | TG(46:5)            | -2.22                  | 0.0047        |
| 114.09     | 22.05                 | unknown             | 2.71                   | 0.0050        |

Table IV.1.ia Candidate lipids with highest p-values (rounded to 4 significant figures) and log 2 fold change of more than 2 or less than -2.

| <b>M/Z</b> | <b>RETENTION TIME</b> | <b>LIKELY LIPIDS</b> | <b>LOG2FOLD CHANGE</b> | <b>PVALUE</b> |
|------------|-----------------------|----------------------|------------------------|---------------|
| 326.38     | 25.62                 | unknown              | -9.90                  | 0.0061        |
| 729.47     | 16.51                 | unknown              | -6.24                  | 0.0123        |
| 351.14     | 3.82                  | LPIP(20:4)           | -5.62                  | 0.0000        |
| 228.20     | 3.68                  | unknown              | -5.61                  | 0.0328        |
| 717.56     | 14.37                 | CE(20:4)             | -5.51                  | 0.0249        |
| 686.46     | 16.50                 | LPE(30:1)            | -5.44                  | 0.0193        |
| 646.50     | 12.17                 | unknown              | -4.85                  | 0.0349        |
| 679.42     | 14.64                 | PG(28:2(OH))         | -4.59                  | 0.0209        |
| 693.48     | 12.05                 | PE(30:2(OH))         | -4.49                  | 0.0436        |
| 459.35     | 11.78                 | PA(48:0)             | -4.46                  | 0.0158        |

Table IV.1.ib Candidate lipids significantly different between LSL and control ( $p < 0.05$ ) with the most negative log 2 fold change (more abundant in LSL patients).

| <b>M/Z</b> | <b>RETENTION TIME</b> | <b>LIKELY LIPID</b> | <b>LOG2FOLD CHANGE</b> | <b>PVALUE</b> |
|------------|-----------------------|---------------------|------------------------|---------------|
| 454.33     | 18.30                 | SQDG(40:0)          | 10.40                  | 0.0107        |
| 425.30     | 15.27                 | MG(20:0)            | 9.96                   | 0.0135        |
| 627.58     | 47.85                 | unknown             | 6.76                   | 0.0441        |
| 649.57     | 50.54                 | TG(38:0)            | 6.64                   | 0.0161        |
| 517.36     | 20.12                 | PA(56:6(OH))        | 5.63                   | 0.0183        |
| 607.57     | 50.51                 | DG(36:0)            | 5.05                   | 0.0204        |
| 889.77     | 50.46                 | PE(O-46:1)          | 4.94                   | 0.0087        |
| 702.53     | 48.96                 | unknown             | 4.67                   | 0.0060        |
| 311.10     | 12.83                 | unknown             | 4.54                   | 0.0308        |
| 599.55     | 45.83                 | unknown             | 4.35                   | 0.0162        |

Table IV.1.ic Candidate lipids significantly different between LSL and control ( $p < 0.05$ ) with the most positive log<sub>2</sub> fold change (more abundant in control patients).

## PLASMA

A total of 4562 lipids/lipid adducts were detected in plasma samples. Of those, 348 were significantly different between LSL and control patients ( $p < 0.05$ ) and 60 had a log<sub>2</sub> fold change of greater than 2 or less than -2 as well as being significantly different (Figure IV.1.ii).

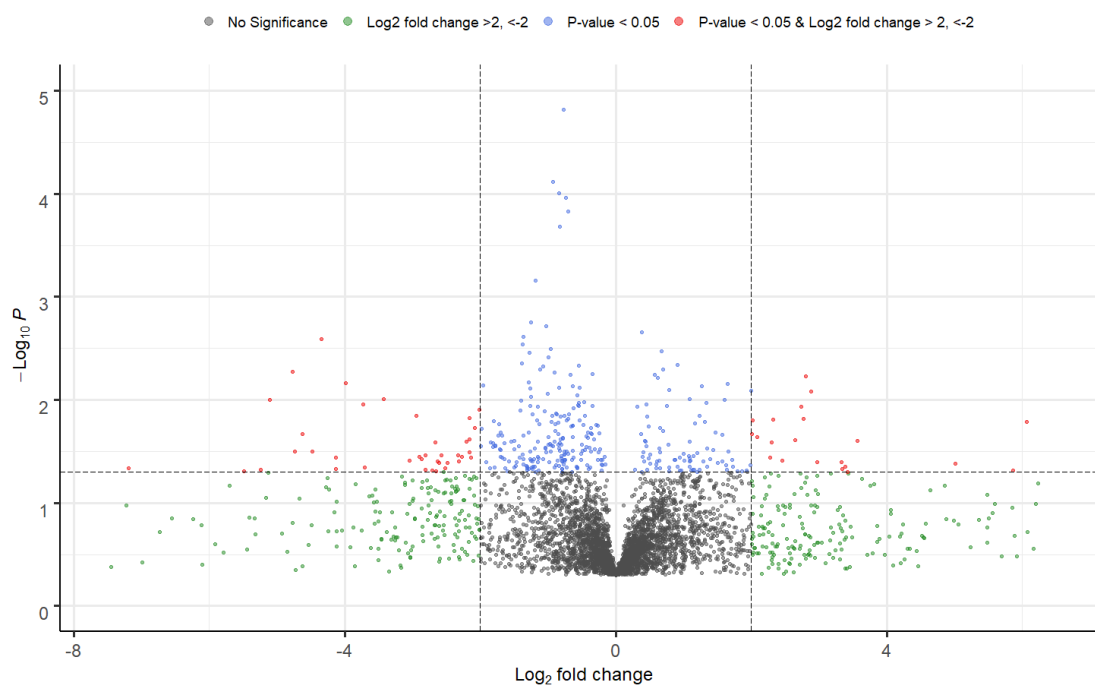


Figure IV.1.ii. Volcano plot of potential lipid or lipid adduct detected in plasma samples from LSL and control patients. Lipids/lipid adducts marked in red with smallest p-value represented in Table IV.1.ii.a, with the most negative log<sub>2</sub> fold change (more abundant in LSL patients) represented in Table IV.1.ii.b and with the most positive log<sub>2</sub> fold change (more abundant in control patients) represented in Table IV.1.ii.c.

| M/Z    | RETENTION TIME | LIKELY LIPID | LOG2FOLD CHANGE | PVALUE |
|--------|----------------|--------------|-----------------|--------|
| 482.36 | 14.47          | LPC(O-16:0)  | -4.34           | 0.0026 |
| 483.36 | 14.47          | PG(50:5)     | -4.77           | 0.0053 |
| 911.71 | 51.81          | PA(48:0(OH)) | 2.8             | 0.0059 |
| 634.45 | 18.5           | PE(28:1)     | -3.99           | 0.0069 |
| 864.71 | 40.53          | TG(52:8)     | 2.88            | 0.0082 |
| 764.9  | 16.81          | unknown      | -3.42           | 0.0099 |
| 678.48 | 26.18          | LPE(34:5)    | -5.11           | 0.01   |
| 651.37 | 15.26          | PA(34:0(OH)) | -3.73           | 0.0111 |
| 912.72 | 51.8           | PE(O-46:0)   | 2.73            | 0.0116 |
| 742.54 | 34.03          | PE(36:3)     | -2.01           | 0.0124 |

Table IV.1.ii.a Candidate lipids with highest p-values (rounded to 4 significant figures) and log 2 fold change of more or less than 2.

| M/Z    | RETENTION TIME | LIKELY LIPID | LOG2FOLD CHANGE | PVALUE |
|--------|----------------|--------------|-----------------|--------|
| 287.99 | 53.36          | unknown      | -7.19           | 0.0457 |
| 388.03 | 55.08          | TG(74:2)     | -5.49           | 0.049  |
| 725.54 | 35.55          | PE(32:0(OH)) | -5.24           | 0.0472 |
| 678.48 | 26.18          | LPE(34:5)    | -5.11           | 0.01   |
| 483.36 | 14.47          | PG(50:5)     | -4.77           | 0.0053 |
| 692.46 | 13.08          | LPE(32:4)    | -4.73           | 0.0318 |
| 384.19 | 13.2           | DGDG(20:1)   | -4.62           | 0.0216 |
| 406.33 | 12.76          | CAR(16:2)    | -4.48           | 0.0319 |
| 482.36 | 14.47          | SQDG(44:0)   | -4.34           | 0.0026 |
| 339.25 | 14.45          | unknown      | -4.13           | 0.0471 |

Table IV.1.ii.b Candidate lipids significantly different between LSL and control ( $p < 0.05$ ) with the most negative log2 fold change (more abundant in LSL patients).

| M/Z    | RETENTION TIME | LIKELY LIPID | LOG2FOLD CHANGE | PVALUE |
|--------|----------------|--------------|-----------------|--------|
| 634.04 | 56.71          | unknown      | 6.06            | 0.0163 |
| 702.5  | 37.92          | PC(O-28:0)   | 5.86            | 0.0485 |
| 873.65 | 45.48          | unknown      | 5.01            | 0.0419 |
| 634.04 | 53.15          | unknown      | 3.56            | 0.0252 |
| 552.04 | 53.86          | unknown      | 3.41            | 0.0497 |
| 676.47 | 15.6           | LPE(34:6)    | 3.39            | 0.0445 |
| 283.26 | 31.12          | FA(18:0)     | 3.34            | 0.047  |
| 513.42 | 50.34          | unknown      | 3.33            | 0.0404 |
| 805.61 | 13.55          | PE(38:2(OH)) | 2.97            | 0.0404 |
| 864.71 | 40.53          | TG(52:8)     | 2.88            | 0.0082 |

Table IV.1.iic Candidate lipids significantly different between LSL and control ( $p < 0.05$ ) with the most positive log<sub>2</sub> fold change (more abundant in control patients).

## URINE

A total of 5303 lipids/lipid adducts were detected in urine samples. Of those, 774 were significantly different between LSL and control patients ( $p < 0.05$ ) and 133 had a log<sub>2</sub> fold change of greater than 2 or less than -2 as well as being significantly different (marked red on volcano plot) (Figure IV.1.iii).

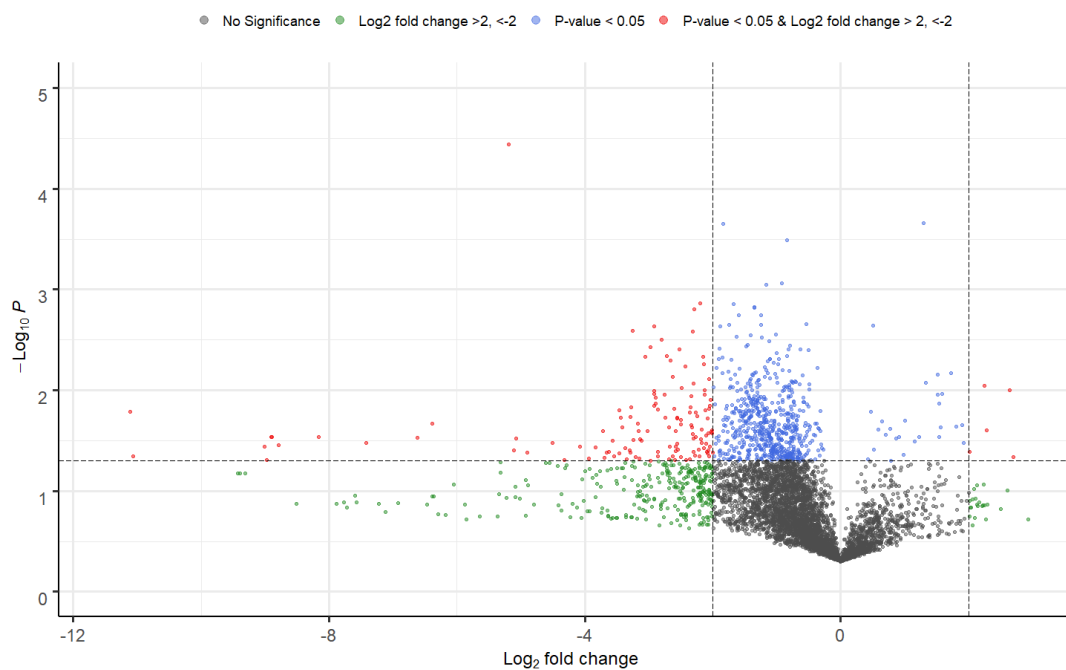


Figure IV.1.iii. Volcano plot of potential lipid or lipid adduct detected in urine samples from LSL and control patients. Lipids/lipid adducts marked in red with smallest p-value represented in Table IV.1.iiia, with the most negative log<sub>2</sub> fold change (more abundant in LSL patients) represented in Table IV.1.iiib and with the most positive log<sub>2</sub> fold change (more abundant in control patients) represented in Table IV.1.iiic.

| <b>M/Z</b> | <b>RETENTION TIME</b> | <b>LIKELY LIPID</b> | <b>LOG2FOLD CHANGE</b> | <b>PVALUE</b> |
|------------|-----------------------|---------------------|------------------------|---------------|
| 195.07     | 1.01                  | FA(10:1)            | -5.19                  | 0.0000        |
| 658.63     | 46.81                 | unknown             | -2.20                  | 0.0014        |
| 926.64     | 49.08                 | PE(P-48:6)          | -2.29                  | 0.0016        |
| 700.31     | 15.02                 | unknown             | -2.92                  | 0.0023        |
| 452.39     | 14.45                 | unknown             | -3.26                  | 0.0026        |
| 299.13     | 4.30                  | unknown             | -2.31                  | 0.0026        |
| 597.01     | 48.68                 | unknown             | -2.80                  | 0.0031        |
| 628.59     | 41.81                 | unknown             | -2.98                  | 0.0038        |
| 667.98     | 19.24                 | unknown             | -2.52                  | 0.0039        |
| 250.18     | 12.54                 | unknown             | -2.72                  | 0.0046        |

Table IV.1.iiia Candidate lipids with highest p-values (rounded to 4 significant figures) and log 2 fold change of greater than 2 or less than -2.

| <b>M/Z</b> | <b>RETENTION TIME</b> | <b>LIKELY LIPID</b> | <b>LOG2FOLD CHANGE</b> | <b>PVALUE</b> |
|------------|-----------------------|---------------------|------------------------|---------------|
| 570.31     | 5.20                  | unknown             | -11.11                 | 0.0164        |
| 695.39     | 3.67                  | LPA(34:6)           | -11.06                 | 0.0454        |
| 516.30     | 1.02                  | unknown             | -9.00                  | 0.0362        |
| 142.70     | 2.27                  | unknown             | -8.97                  | 0.0489        |
| 570.31     | 2.28                  | unknown             | -8.91                  | 0.0291        |
| 571.31     | 2.28                  | unknown             | -8.89                  | 0.0292        |
| 517.30     | 1.02                  | LPE(20:5)           | -8.78                  | 0.0349        |
| 572.31     | 2.28                  | LPE(22:2)           | -8.16                  | 0.0293        |
| 465.26     | 2.61                  | PI(38:5)            | -7.42                  | 0.0335        |
| 573.31     | 2.25                  | PA(24:1(OH))        | -6.62                  | 0.0296        |

Table IV.1.iiib Candidate lipids significantly different between LSL and control ( $p < 0.05$ ) with the most negative log2 fold change (more abundant in LSL patients).

| <b>M/Z</b> | <b>RETENTION TIME</b> | <b>LIKELY LIPID</b> | <b>LOG2FOLD CHANGE</b> | <b>PVALUE</b> |
|------------|-----------------------|---------------------|------------------------|---------------|
| 343.23     | 2.17                  | FA(22:5)            | 2.70                   | 0.0461        |
| 664.46     | 22.37                 | LPC(30:5)           | 2.64                   | 0.0100        |
| 357.11     | 1.27                  | unknown             | 2.28                   | 0.0251        |
| 201.12     | 1.48                  | FA(10:0)            | 2.25                   | 0.0090        |
| 151.04     | 7.88                  | unknown             | 2.01                   | 0.0411        |

Table IV.1.iic Candidate lipids significantly different between LSL and control ( $p < 0.05$ ) with the most positive log<sub>2</sub> fold change (more abundant in control patients)

Comparison was made between mass charge ratio-retention time pairs detected in CSF samples and plasma samples. There was a total of 6 data points that had a  $p < 0.05$  and a log<sub>2</sub> fold change of more than 2 or less than -2 in both CSF and plasma. None of these data points showed an exact match in properties between CSF and plasma samples. Variation was tolerated up to 0.04 for mass charge ratio and up to 3.5 minutes for retention time (Figure IV.1.iva). Candidates were further reduced to 4 once direction of log<sub>2</sub> fold change was taken into account (Figure IV.1.ivb).



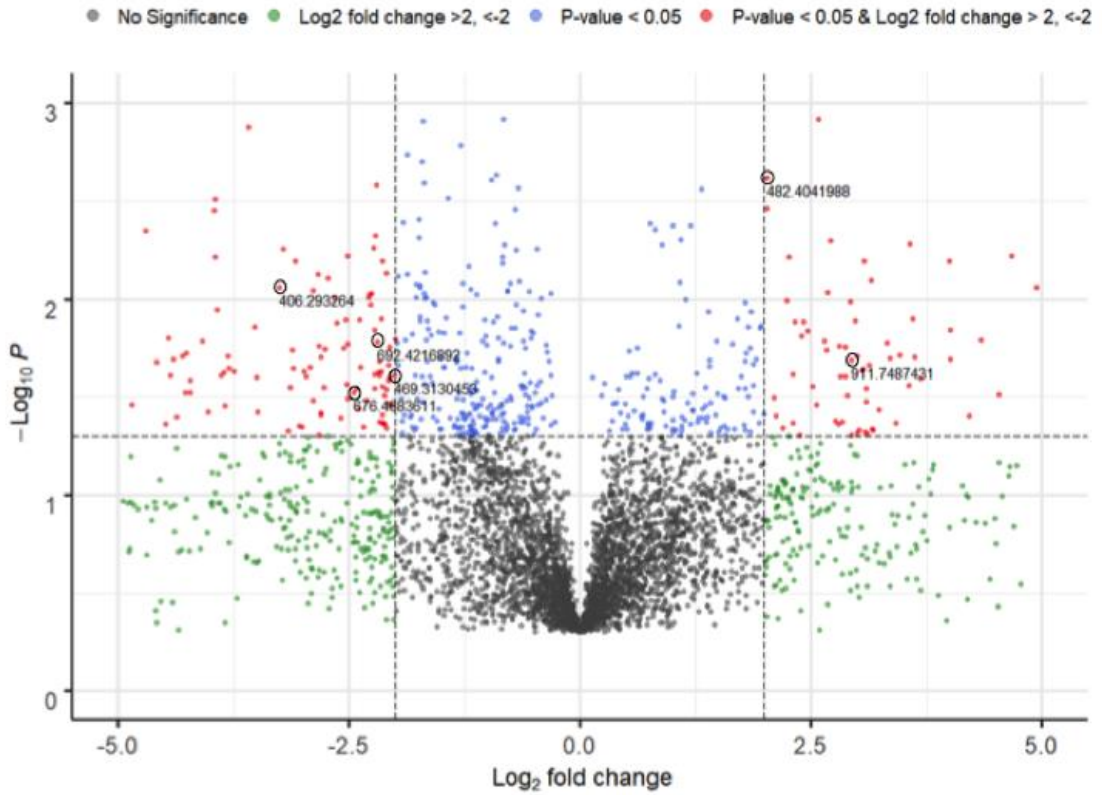


Figure IV.1.iva Volcano plot comparing mass charge ratio and retention time pairs identified in CSF and plasma samples. Mass charge ratio labelled on volcano plot for the best matches between CSF and plasma samples. Labels indicate the 6 lipids/lipid adducts that were detected in both CSF and plasma at significant levels. For identification see Table IV.1.iv.

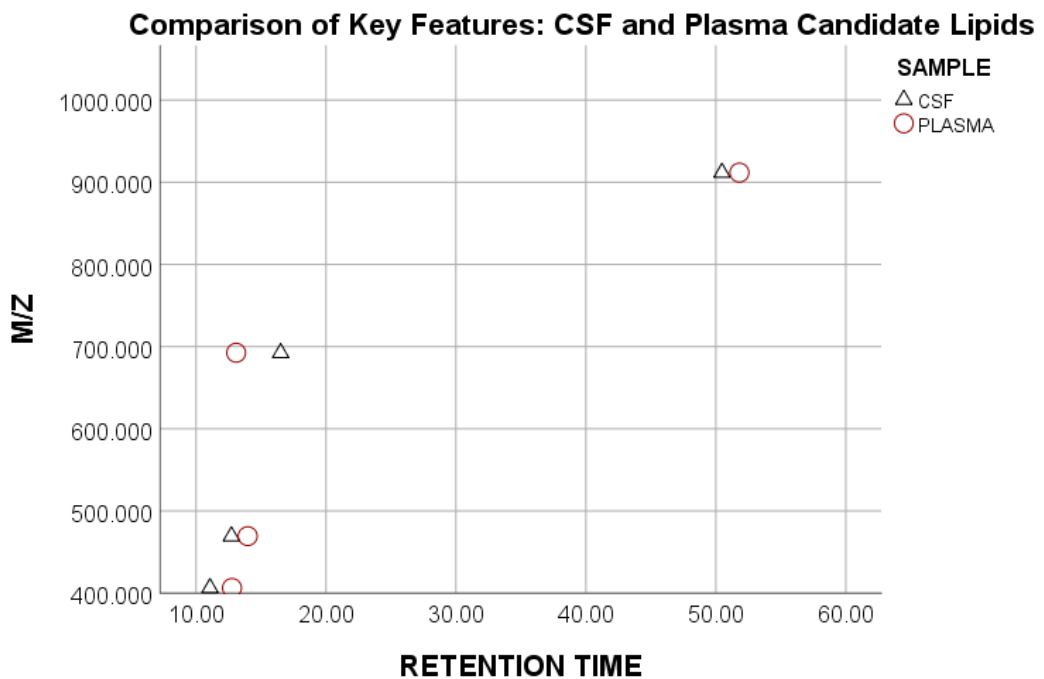


Figure IV.1.ivb Comparison of mass charge ratio-retention time pairing between CSF and plasma samples.

Three of the mass charge ratio-retention time pairs that were significantly different between control and LSL in both CSF and plasma were potentially identifiable via lipid database search (Table IV.1.iv). Only one mass charge ratio-retention time pair was also significantly different in urine samples, 469.313; this was identified as possibly being LPE 16:1.

| <b>M/Z</b> | <b>RETENTION TIME</b> | <b>LIKELY LIPID</b> | <b>LOG2FOLD CHANGE</b> | <b>PVALUE</b> |
|------------|-----------------------|---------------------|------------------------|---------------|
| 469.31     | 12.72                 | LPE(16:1)           | -2.01                  | 0.0245        |
| 692.42     | 16.51                 | PC(28:4)            | -2.19                  | 0.0166        |
| 911.75     | 48.96                 | TG(58:9)            | 2.93                   | 0.006         |

Table IV.1.iv Mass charge ratio-retention time pairs detected in both CSF and plasma that were significantly different between LSL and control samples with likely lipid as identified by LipidMaps.

## **LIPIDOMICS 2**

For Lipidomics 2 the sample size was 11 control and 18 test patients. Test patients all had LSLs, 2 classified as complex, 11 as transitional, 3 caudal and two as dorsal. One dorsal LSL was associated with a dermal sinus. Seven of the 18 LSL patients were classed as asymptomatic. Seven control patients had cerebral palsy and were undergoing selective dorsal rhizotomy (SDR), all 7 had spastic gaits but neither had any urinary symptoms. Four patients had myelomeningocele that was repaired at birth but were readmitted for revision of a blocked ventriculo-peritoneal shunt (VPS). One control patient had altered bladder function requiring catheterization. Further clinical details of patients can be found in Supplementary Information. The mean age of LSL patients was 17 months whereas for control patients it was 23 months. This reflects the fact that the blocked VPS patients and the SDR patients were slightly older at time of surgery than most LSL patients.

## **CSF**

A total of 4803 lipids/lipid adducts were detected in CSF samples. Of these, 1419 were significantly different between LSL and control patients ( $p < 0.05$ ) and 310 had a log<sub>2</sub> fold change of greater than 2 or less than -2 as well as being significantly different. Once mass charge ratio-retention time pairs that were only detected in one group were removed, this total was reduced further to 288 potential lipids (Figure IV.1.v).

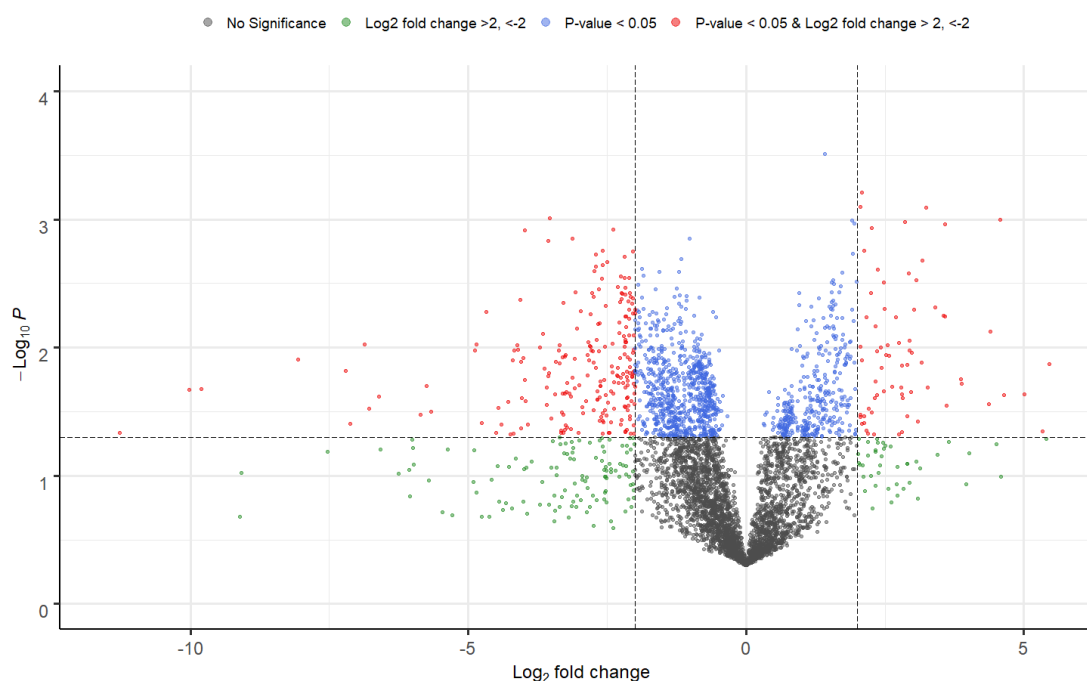


Figure IV.1.v. Volcano plot of potential lipids or lipid adducts detected in CSF samples from LSL and control patients. Attempted identification of lipids/lipid adducts marked in red with smallest p-value represented in Table IV.1.va, with the most negative log<sub>2</sub> fold change (more abundant in LSL patients) represented in Table IV.1.va and with the most positive log<sub>2</sub> fold change (more abundant in control patients) represented in Table IV.1.va. Sample size was 11 control and 15 test samples.

| M/Z    | RETENTION TIME | LIKELY LIPID | LOG2FOLD CHANGE | PVALUE |
|--------|----------------|--------------|-----------------|--------|
| 474.35 | 12.30          | CAR(20:2)    | 2.09            | 0.0006 |
| 663.47 | 12.47          | PA(32:1(OH)) | 2.06            | 0.0008 |
| 358.20 | 38.19          | NAT(14:0)    | 3.24            | 0.0008 |
| 805.62 | 18.68          | PA(42:0(OH)) | -3.53           | 0.0010 |
| 527.16 | 52.63          | LPI(10:0)    | 4.57            | 0.0010 |
| 716.38 | 9.84           | PE(30:4(OH)) | 2.86            | 0.0010 |
| 321.03 | 1.46           | unknown      | 3.58            | 0.0011 |
| 609.40 | 11.67          | unknown      | 2.26            | 0.0012 |
| 424.36 | 10.93          | unknown      | -2.39           | 0.0012 |
| 931.45 | 32.83          | PIP(36:8)    | -3.98           | 0.0012 |

Table IV.1.va Candidate lipids with highest p-values (rounded to 4 significant figures) and log<sub>2</sub> fold change of greater than 2 or less than -2.

| <b>M/Z</b> | <b>RETENTION TIME</b> | <b>LIKELY LIPID</b> | <b>LOG2FOLD CHANGE</b> | <b>PVALUE</b> |
|------------|-----------------------|---------------------|------------------------|---------------|
| 232.92     | 42.27                 | unknown             | -11.27                 | 0.0460        |
| 232.92     | 49.39                 | unknown             | -10.02                 | 0.0212        |
| 678.48     | 45.96                 | LPE(34:5)           | -9.80                  | 0.0210        |
| 540.45     | 50.13                 | NAT(30:1)           | -8.06                  | 0.0124        |
| 413.27     | 21.15                 | unknown             | -7.21                  | 0.0152        |
| 217.10     | 48.16                 | unknown             | -7.12                  | 0.0392        |
| 503.38     | 21.64                 | unknown             | -6.87                  | 0.0095        |
| 432.28     | 48.23                 | unknown             | -6.78                  | 0.0301        |
| 507.33     | 50.51                 | unknown             | -6.61                  | 0.0240        |
| 503.38     | 20.91                 | unknown             | -5.85                  | 0.0333        |

Table IV.1.vb Candidate lipids significantly different between LSL and control ( $p < 0.05$ ) with the most negative log2 fold change (more abundant in LSL patients).

| <b>M/Z</b> | <b>RETENTION TIME</b> | <b>LIKELY LIPID</b> | <b>LOG2FOLD CHANGE</b> | <b>PVALUE</b> |
|------------|-----------------------|---------------------|------------------------|---------------|
| 550.91     | 46.18                 | unknown             | 5.46                   | 0.0134        |
| 475.32     | 8.41                  | LPA(22:1)           | 5.33                   | 0.0452        |
| 507.33     | 47.27                 | unknown             | 5.01                   | 0.0231        |
| 372.28     | 11.35                 | NAE(18:0)           | 4.65                   | 0.0235        |
| 527.16     | 52.63                 | LPI(10:0)           | 4.57                   | 0.0010        |
| 649.45     | 11.28                 | PE(28:2)            | 4.37                   | 0.0276        |
| 443.33     | 33.94                 | unknown             | 3.89                   | 0.0190        |
| 232.92     | 49.07                 | unknown             | 3.61                   | 0.0286        |
| 358.20     | 33.62                 | NAT(14:0)           | 3.58                   | 0.0057        |
| 321.03     | 1.46                  | unknown             | 3.58                   | 0.0011        |

Table IV.1.vc Candidate lipids significantly different between LSL and control ( $p < 0.05$ ) with the most positive log2 fold change (more abundant in control patients)

## PLASMA

A total of 6873 lipids/lipid adducts were detected in plasma samples. Of those, 2891 were significantly different between LSL and control patients ( $p < 0.05$ ) and 609 had a log<sub>2</sub> fold change of greater than 2 or less than -2 as well as being significantly different. Once mass charge ratio-retention time pairs that were only detected in one group were removed, this total was reduced further to 591 potential lipids (Figure IV.1.vi). There were 11 control samples and 15 test samples.

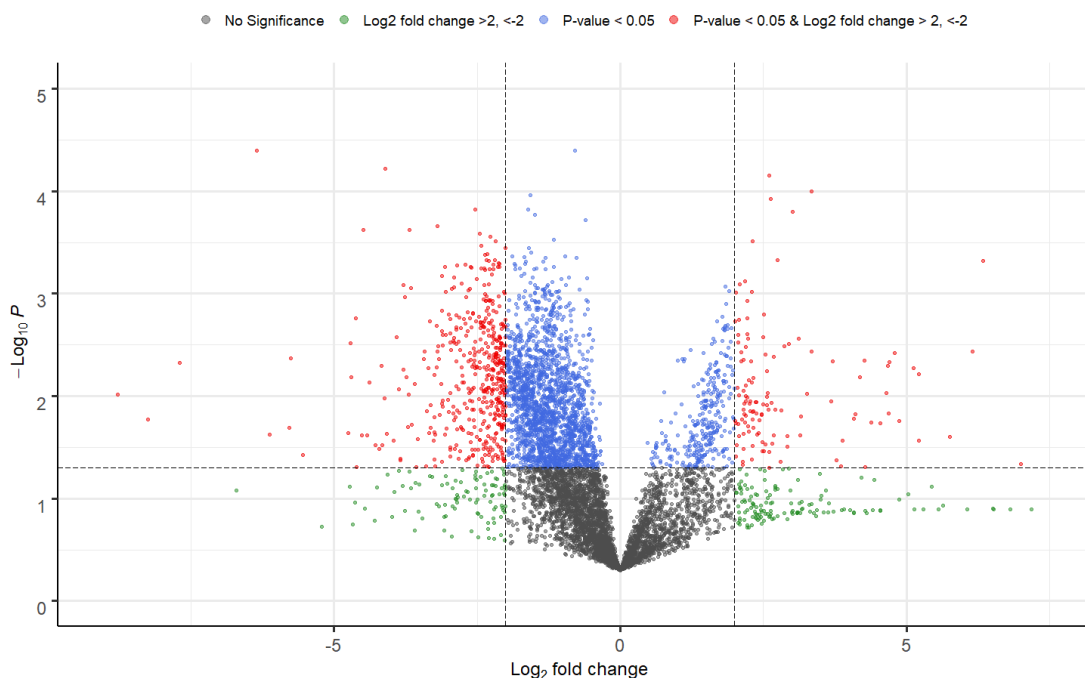


Figure IV.1.vi. Volcano plot of potential lipids or lipid adducts detected in plasma samples from LSL and control patients. Attempted identification of lipids/lipid adducts marked in red with smallest p-value represented in Table IV.1.via, with the most negative log<sub>2</sub> fold change (more abundant in LSL patients) represented in Table IV.1.vib and with the most positive log<sub>2</sub> fold change (more abundant in control patients) represented in Table IV.1.vic. Sample size was 11 control and 15 test samples.

| <b>M/Z</b> | <b>RETENTION TIME</b> | <b>LIKELY LIPID</b> | <b>LOG2FOLD CHANGE</b> | <b>PVALUE</b> |
|------------|-----------------------|---------------------|------------------------|---------------|
| 900.33     | 18.48                 | unknown             | -6.34                  | 0.0000        |
| 997.07     | 19.72                 | unknown             | -4.10                  | 0.0001        |
| 747.51     | 16.46                 | PG(34:2)            | 2.61                   | 0.0001        |
| 401.29     | 10.66                 | unknown             | 3.34                   | 0.0001        |
| 358.20     | 53.16                 | NAT(14:0)           | 2.63                   | 0.0001        |
| 591.35     | 10.56                 | MGDG(24:5)          | 3.02                   | 0.0002        |
| 925.65     | 8.83                  | PC(46:11)           | -3.19                  | 0.0002        |
| 753.56     | 44.04                 | LPC(34:6)           | -3.68                  | 0.0002        |
| 975.63     | 44.71                 | PI(O-44:6)          | -4.49                  | 0.0002        |
| 767.66     | 46.51                 | unknown             | -2.46                  | 0.0003        |

Table IV.1.via Candidate lipids with highest p-values (rounded to 4 significant figures) and log 2 fold change of greater than 2 or less than -2.

| <b>M/Z</b> | <b>RETENTION TIME</b> | <b>LIKELY LIPID</b> | <b>LOG2FOLD CHANGE</b> | <b>PVALUE</b> |
|------------|-----------------------|---------------------|------------------------|---------------|
| 722.50     | 34.71                 | PE(36:4)            | -8.78                  | 0.0097        |
| 454.34     | 7.48                  | NAT(24:2)           | -8.25                  | 0.0169        |
| 590.43     | 40.68                 | LPE(26:2)           | -7.69                  | 0.0048        |
| 900.33     | 18.48                 | unknown             | -6.34                  | 0.0000        |
| 634.45     | 34.05                 | PE(28:1)            | -6.13                  | 0.0236        |
| 699.53     | 21.31                 | DG(44:10)           | -5.75                  | 0.0043        |
| 395.36     | 12.28                 | MG(22:1)            | -5.54                  | 0.0375        |
| 715.04     | 52.29                 | unknown             | -4.75                  | 0.0229        |
| 513.35     | 17.06                 | unknown             | -4.71                  | 0.0030        |
| 602.57     | 44.41                 | unknown             | -4.70                  | 0.0066        |

Table IV.1.vib Candidate lipids significantly different between LSL and control ( $p < 0.05$ ) with the most negative log2 fold change (more abundant in LSL patients).

| M/Z    | RETENTION TIME | LIKELY LIPID | LOG2FOLD CHANGE | PVALUE |
|--------|----------------|--------------|-----------------|--------|
| 532.39 | 11.71          | NAT(30:5)    | 7.00            | 0.0463 |
| 358.20 | 18.69          | NAT(14:0)    | 6.34            | 0.0005 |
| 610.51 | 28.11          | unknown      | 6.16            | 0.0037 |
| 663.45 | 47.13          | PA(32:1(OH)) | 5.75            | 0.0252 |
| 665.44 | 10.35          | PG(28:1)     | 5.22            | 0.0274 |
| 773.49 | 10.45          | PA(O-40:6)   | 5.21            | 0.0061 |
| 328.22 | 8.50           | unknown      | 5.12            | 0.0053 |
| 436.31 | 21.14          | LPC(O-14:0)  | 4.79            | 0.0038 |
| 772.49 | 10.46          | PC(34:6)     | 4.71            | 0.0047 |
| 609.51 | 28.12          | TG(34:1)     | 4.69            | 0.0147 |

Table IV.1.vic Candidate lipids significantly different between LSL and control ( $p < 0.05$ ) with the most positive log<sub>2</sub> fold change (more abundant in control patients)



## URINE

A total of 5566 lipids/lipid adducts were detected in plasma samples. Of those, 1881 were significantly different between LSL and control patients ( $p < 0.05$ ) and 927 had a  $\log_2$  fold change of greater than 2 or less than -2 as well as being significantly different. Once mass charge ratio-retention time pairs that were only detected in one group were removed, this total was reduced further to 581 potential lipids (Figure IV.1.vii).

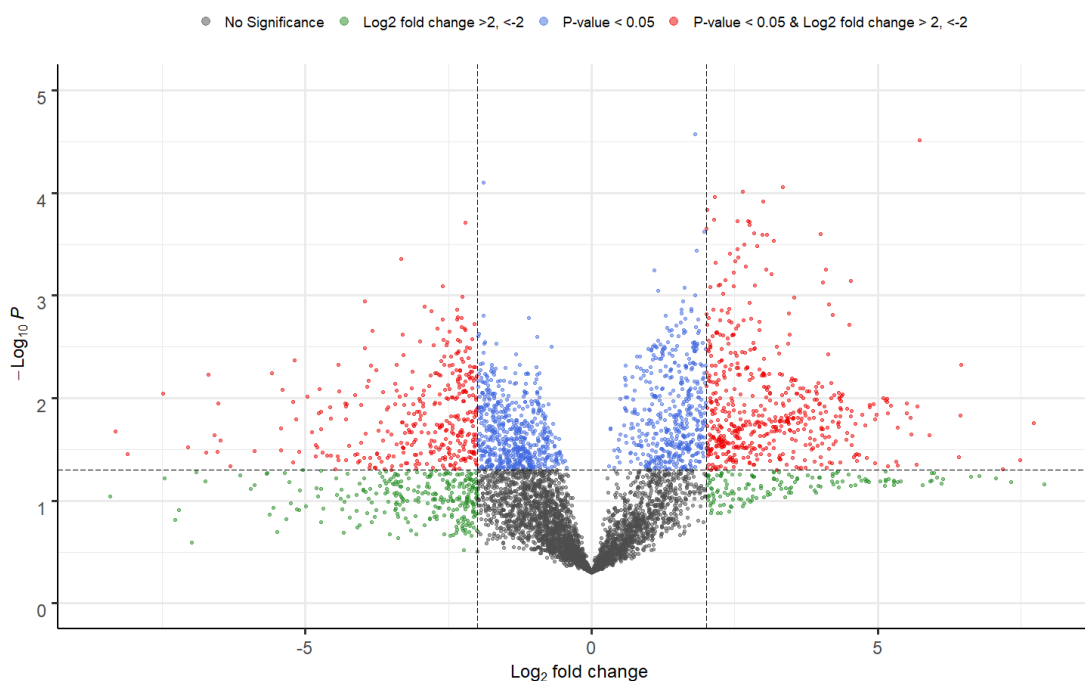


Figure IV.1.vii. Volcano plot of potential lipids or lipid adducts detected in urine samples from LSL and control patients. Attempted identification of lipids/lipid adducts marked in red with smallest p-value represented in Table IV.1.viia, with the most negative  $\log_2$  fold change (more abundant in LSL patients) represented in Table IV.1.viib and with the most positive  $\log_2$  fold change (more abundant in control patients) represented in Table IV.1.viic. Sample size was 8 control and 18 test samples.

| M/Z    | RETENTION TIME | LIKELY LIPID  | LOG2FOLD CHANGE | PVALUE |
|--------|----------------|---------------|-----------------|--------|
| 115.92 | 57.67          | unknown       | 5.72            | 0.0000 |
| 532.35 | 10.12          | unknown       | 2.15            | 0.0001 |
| 490.34 | 9.62           | unknown       | 2.02            | 0.0001 |
| 487.32 | 10.26          | unknown       | 2.14            | 0.0002 |
| 502.37 | 51.99          | unknown       | -2.21           | 0.0002 |
| 488.33 | 10.26          | CAR(18:0(OH)) | 2.01            | 0.0002 |
| 354.34 | 12.14          | NAE(20:1)     | 4.00            | 0.0003 |
| 606.43 | 10.37          | MGDG(22:1)    | 3.17            | 0.0003 |
| 619.44 | 11.92          | LPC(24:3)     | 2.54            | 0.0004 |
| 379.13 | 27.84          | unknown       | 2.56            | 0.0004 |

Table IV.1.viia Candidate lipids with highest p-values (rounded to 4 significant figures) and log 2 fold change of greater than 2 or less than -2.

| M/Z    | RETENTION TIME | LIKELY LIPID | LOG2FOLD CHANGE | PVALUE |
|--------|----------------|--------------|-----------------|--------|
| 299.01 | 43.08          | unknown      | -8.32           | 0.0212 |
| 722.50 | 44.51          | PE(36:4)     | -8.11           | 0.0350 |
| 703.00 | 45.47          | unknown      | -7.05           | 0.0299 |
| 349.18 | 49.29          | unknown      | -6.73           | 0.0340 |
| 500.36 | 9.87           | CAR(20:0)    | -6.69           | 0.0059 |
| 374.99 | 46.06          | unknown      | -6.59           | 0.0229 |
| 331.18 | 1.72           | FA(16:0)     | -6.54           | 0.0335 |
| 797.04 | 58.38          | unknown      | -6.53           | 0.0112 |
| 201.03 | 48.09          | unknown      | -6.49           | 0.0257 |
| 217.00 | 37.29          | unknown      | -6.32           | 0.0458 |

Table IV.1.viib Candidate lipids significantly different between LSL and control ( $p < 0.05$ ) with the most negative log2 fold change (more abundant in LSL patients).

| M/Z    | RETENTION TIME | LIKELY LIPID | LOG2FOLD CHANGE | PVALUE |
|--------|----------------|--------------|-----------------|--------|
| 244.95 | 50.56          | unknown      | 7.72            | 0.0175 |
| 330.34 | 12.90          | unknown      | 7.49            | 0.0399 |
| 791.55 | 17.27          | PG(36:2(OH)) | 7.18            | 0.0490 |
| 595.38 | 40.95          | MGDG(24:3)   | 6.45            | 0.0047 |
| 154.95 | 45.79          | unknown      | 6.45            | 0.0147 |
| 747.52 | 17.48          | PG(34:2)     | 6.41            | 0.0374 |
| 703.50 | 17.69          | PE(32:3)     | 5.90            | 0.0229 |
| 115.92 | 57.67          | unknown      | 5.72            | 0.0000 |
| 617.45 | 18.21          | MG(34:5)     | 5.69            | 0.0121 |
| 903.57 | 10.20          | SQDG(42:7)   | 5.68            | 0.0444 |

Table IV.1.viic Candidate lipids significantly different between LSL and control ( $p < 0.05$ ) with the most positive log<sub>2</sub> fold change (more abundant in control patients)

Comparison was made between mass charge ratio-retention time pairs detected in CSF samples and plasma samples. Of those mass charge ratio-retention time pairs that had a  $p < 0.05$  and a log<sub>2</sub> fold change of greater or less than 2, a total of 54 were detected in both CSF and plasma samples. This was further reduced to 37 once direction of log<sub>2</sub> fold change was taken into account. Nineteen candidate lipids/lipid adducts with the best match of features between CSF and plasma samples (a mass charge ratio of within 0.0005 and a retention time within 0.01 minutes) were then selected (Figures IV.1.viii.a and IV.1.viii.b).

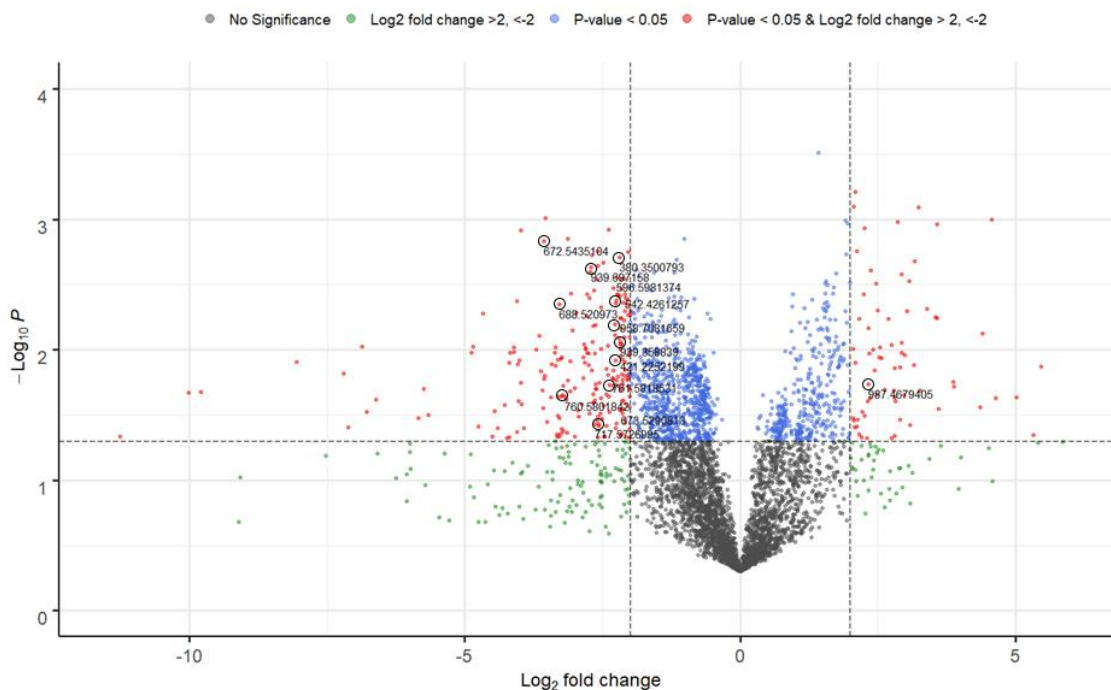


Figure IV.1.viii.a. Volcano plot comparing mass charge ratio-retention time pairs identified in CSF and plasma samples. Marks that represent mass charge ratio-retention time pairs that are closely matched between CSF and plasma samples, and show a significant difference between LSL and control patients, are labelled with the mass charge ratio as measured in CSF samples.

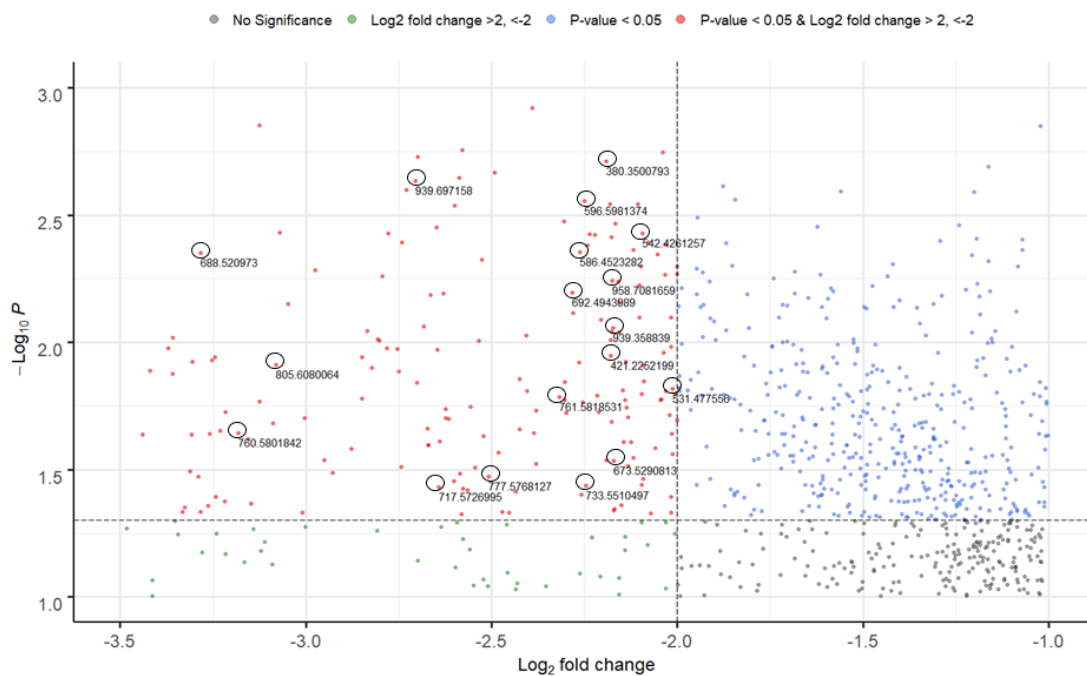


Figure IV.1.viii.b. Volcano plot highlighting mass charge ratio-retention time pairs with negative log 2 fold change. N.B. one mass charge-ratio retention time pair had a positive log 2 fold change and is not seen on Figure IV.1.viii.a.

Twelve of the mass charge ratio-retention time pairs that differed significantly between control and LSL in both CSF and plasma were potentially identifiable via lipid database search (Table IV.1.viii.a).

| M/Z    | RETENTION TIME | LIKELY LIPID | LOG2FOLDC HANGE | PVALUE |
|--------|----------------|--------------|-----------------|--------|
| 380.35 | 15.22          | NAE(22:2)    | -2.19           | 0.0020 |
| 688.52 | 10.19          | PC(30:0)     | -3.28           | 0.0045 |
| 692.49 | 11.44          | LPS(30:1)    | -2.28           | 0.0064 |
| 717.57 | 19.14          | PA(P-38:0)   | -2.64           | 0.0371 |
| 733.55 | 10.11          | PE(34:2)     | -2.25           | 0.0366 |
| 760.58 | 13.32          | PC(34:1)     | -3.18           | 0.0227 |
| 761.58 | 13.36          | PE(36:2)     | -2.32           | 0.0164 |
| 777.58 | 10.03          | PE(36:2(OH)) | -2.51           | 0.0337 |
| 805.61 | 13.22          | PE(38:2(OH)) | -3.08           | 0.0123 |
| 939.70 | 19.05          | MGDG(48:8)   | -2.17           | 0.0088 |

Table IV.1.viiiia Candidate lipids significantly different between LSL and control ( $p < 0.05$ ) with a log<sub>2</sub> fold change of less than -2 (more abundant in LSL) detected in both CSF and plasma samples. N.B. the one mass charge ratio-retention time pair with a positive log<sub>2</sub> fold change that was significantly different in both CSF and plasma samples was not identifiable via database search.

Seven candidate lipids were also detected in urine samples and were found to have a significant difference ( $p < 0.05$ ). Mass charge ratio was matched within 0.001 and retention time matched within 0.4 minutes (Figure III.1.viiiic). All candidate lipids were detected in positive electrospray mode and showed a negative log<sub>2</sub> fold change, more abundant in LSL samples. Four mass charge ratio-retention time pairings had potential matches on database search (Table IV.1.viiiib).

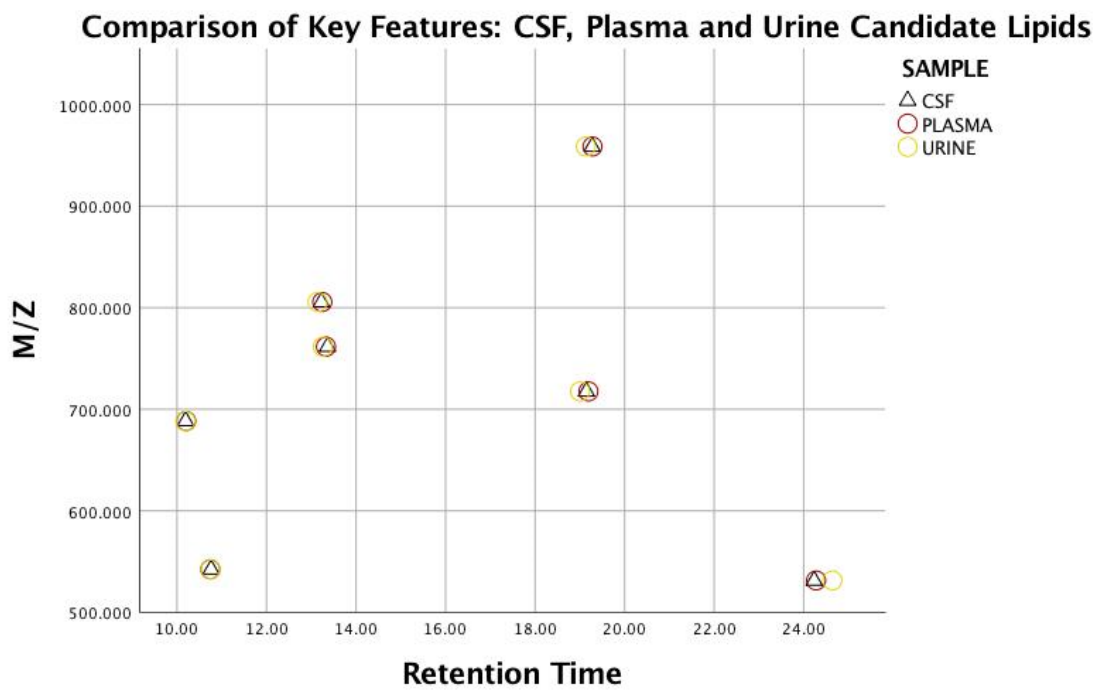


Figure IV.1.viiiic Comparison of mass charge ratio-retention time pairing between CSF, plasma and urine samples.

| LIKELY LIPID  | MZ      | RETENTION TIME | SAMPLE | LOG2FOLD CHANGE | PVALUE |
|---------------|---------|----------------|--------|-----------------|--------|
| PC (30:0)     | 688.521 | 10.19          | CSF    | -3.28           | 0.0045 |
|               | 688.521 | 10.20          | PLASMA | -2.34           | 0.0069 |
|               | 688.521 | 10.19          | URINE  | -1.92           | 0.0361 |
| PA (P-38:0)   | 717.573 | 19.14          | CSF    | -2.64           | 0.0371 |
|               | 717.573 | 19.19          | PLASMA | -3.19           | 0.0037 |
|               | 717.573 | 19.00          | URINE  | -4.03           | 0.0117 |
| PE (36:2)     | 761.582 | 13.36          | CSF    | -2.32           | 0.0164 |
|               | 761.582 | 13.33          | PLASMA | -2.22           | 0.0076 |
|               | 761.582 | 13.26          | URINE  | -2.92           | 0.0139 |
| PE (38:2(OH)) | 805.608 | 13.22          | CSF    | -3.08           | 0.0123 |
|               | 805.607 | 13.25          | PLASMA | -2.24           | 0.0069 |
|               | 805.607 | 13.14          | URINE  | -2.27           | 0.0204 |

Table IV.1.viii Log 2 fold change and p-values of mass charge ratio-retention time pairings in CSF, plasma and urine for potential lipids identified with LipidMaps database.

## **LIPIDOMICS 2 (SYMPTOMATIC V. ASYMPTOMATIC)**

From a total of 18 LSL patients, 11 were classified as symptomatic and 7 as asymptomatic. This was based on clinical assessment as discussed in the Methods section. Of the symptomatic patients, 3 had commenced clean intermittent catheterization (CIC) prior to surgery, 4 patients had recurrent UTIs and 5 had episodes of incontinence. Four patients had motor weakness, of which 2 had an associated lower limb deformity. Three patients reported limb pain prior to surgery but no patients had any lower limb loss of sensation. Further clinical details of patients can be found in Supplementary Information.

## **CSF**

A total of 4235 lipids/lipid adducts were detected in CSF samples. Of those, 528 were significantly different between samples taken from symptomatic and asymptomatic LSL patients ( $p < 0.05$ ) and 104 had a log<sub>2</sub> fold change of greater than 2 or less than - 2 as well as being significantly different. Once mass charge ratio-retention time pairs that were only detected in one group were removed, this total was reduced further to 87 potential lipids (Figure IV.1.ix).



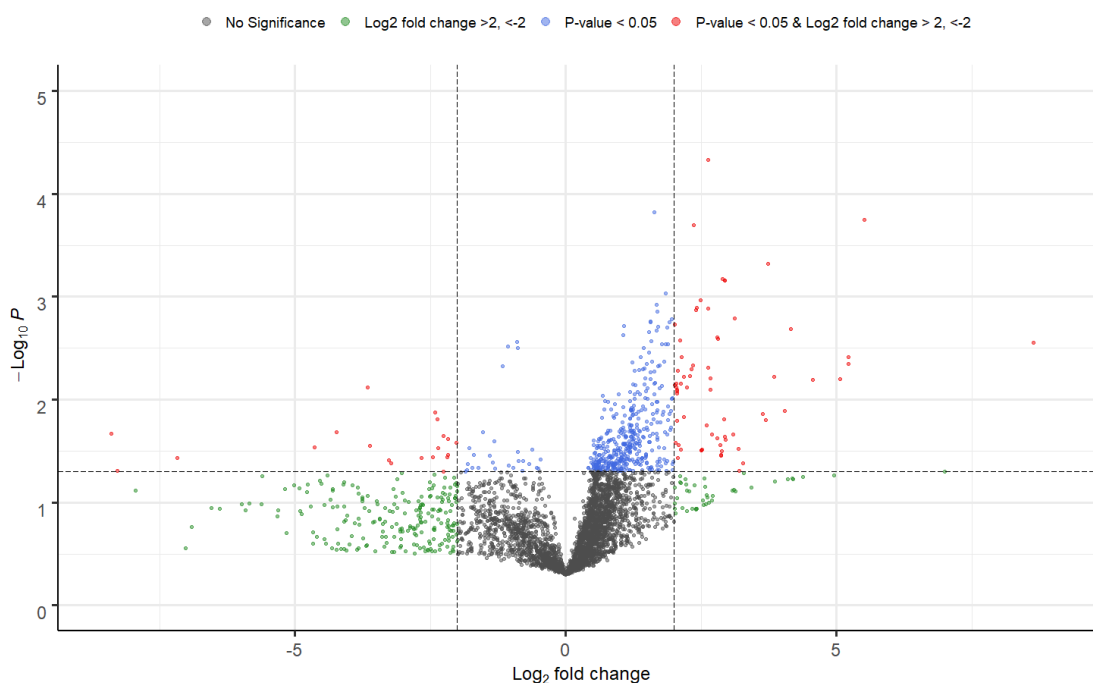


Figure IV.1.ix. Volcano plot of potential lipids or lipid adducts detected in CSF samples from symptomatic and asymptomatic LSL patients. Attempted identification of lipids/lipid adducts marked in red with smallest p-value represented in Table IV.1.ix.a, with the most negative log<sub>2</sub> fold change (more abundant in symptomatic LSL patients) represented in Table IV.1.ix.b and with the most positive log<sub>2</sub> fold change (more abundant in asymptomatic LSL patients) represented in Table III.1.ix.c. Sample size was 5 control and 10 test samples.

| M/Z    | RETENTION TIME | LIKELY LIPID | LOG2FOLD CHANGE | PVALUE |
|--------|----------------|--------------|-----------------|--------|
| 196.99 | 52.34          | unknown      | 3.51            | 0.0000 |
| 244.95 | 51.09          | unknown      | 2.63            | 0.0000 |
| 722.50 | 16.06          | PE(P-34:2)   | 5.52            | 0.0002 |
| 678.48 | 21.92          | LPE(34:5)    | 2.37            | 0.0002 |
| 507.33 | 13.43          | unknown      | 3.74            | 0.0005 |
| 617.47 | 21.44          | unknown      | 2.89            | 0.0007 |
| 634.45 | 29.85          | PE28:1       | 2.94            | 0.0007 |
| 349.18 | 48.23          | unknown      | 2.94            | 0.0007 |
| 763.56 | 48.94          | PC32:2(OH))  | 2.49            | 0.0011 |
| 670.61 | 47.77          | unknown      | 2.42            | 0.0013 |

Table IV.1.ix.a Candidate lipids with highest p-values (rounded to 4 significant figures) and log<sub>2</sub> fold change of greater than 2 or less than -2.

| M/Z    | RETENTION TIME | LIKELY LIPID | LOG2FOLD CHANGE | PVALUE |
|--------|----------------|--------------|-----------------|--------|
| 359.18 | 5.64           | unknown      | -8.40           | 0.0216 |
| 649.45 | 10.24          | PE(28:2)     | -8.28           | 0.0489 |
| 443.33 | 12.00          | unknown      | -7.17           | 0.0370 |
| 386.30 | 12.57          | unknown      | -4.64           | 0.0291 |
| 441.35 | 17.03          | unknown      | -4.23           | 0.0207 |
| 332.29 | 14.60          | NAE(20:3)    | -3.65           | 0.0076 |
| 630.43 | 14.66          | MGDG(24:3)   | -3.62           | 0.0282 |
| 703.00 | 43.52          | unknown      | -3.26           | 0.0386 |
| 595.38 | 41.84          | DG(32:6)     | -3.23           | 0.0414 |
| 739.48 | 7.94           | MGDG(30:1)   | -2.67           | 0.0370 |

Table IV.1.ixb Candidate lipids significantly different between symptomatic and asymptomatic LSL patients ( $p < 0.05$ ) with the most negative log<sub>2</sub> fold change (more abundant in symptomatic LSL patients).

| M/Z    | RETENTION TIME | LIKELY LIPID | LOG2FOLD CHANGE | PVALUE |
|--------|----------------|--------------|-----------------|--------|
| 590.43 | 49.61          | unknown      | 8.63            | 0.0028 |
| 722.50 | 16.06          | PE(O-34:3)   | 5.52            | 0.0002 |
| 283.26 | 57.68          | FA(18:0)     | 5.22            | 0.0039 |
| 715.04 | 54.82          | unknown      | 5.21            | 0.0045 |
| 431.30 | 8.48           | NAT(20:3)    | 5.07            | 0.0063 |
| 507.33 | 28.22          | unknown      | 4.56            | 0.0064 |
| 426.34 | 51.15          | NAE(24:4)    | 4.15            | 0.0021 |
| 634.45 | 36.90          | PE(28:1)     | 3.84            | 0.0060 |
| 388.25 | 51.26          | NAT(18:2)    | 3.69            | 0.0157 |
| 196.99 | 52.34          | unknown      | 3.51            | 0.0000 |

Table IV.1.ixc Candidate lipids significantly different between symptomatic and asymptomatic LSL patients ( $p < 0.05$ ) with the most positive log<sub>2</sub> fold change (more abundant in asymptomatic LSL patients).

## PLASMA

A total of 7298 lipids/lipid adducts were detected in CSF samples. Of those, 608 were significantly different between samples taken from symptomatic and asymptomatic LSL patients ( $p < 0.05$ ) and 157 had a  $\log_2$  fold change of greater than 2 or less than -2 as well as being significantly different. Once mass charge ratio-retention time pairs that were only detected in one group were removed, this total was reduced further to 137 potential lipids (Figure IV.1.x).

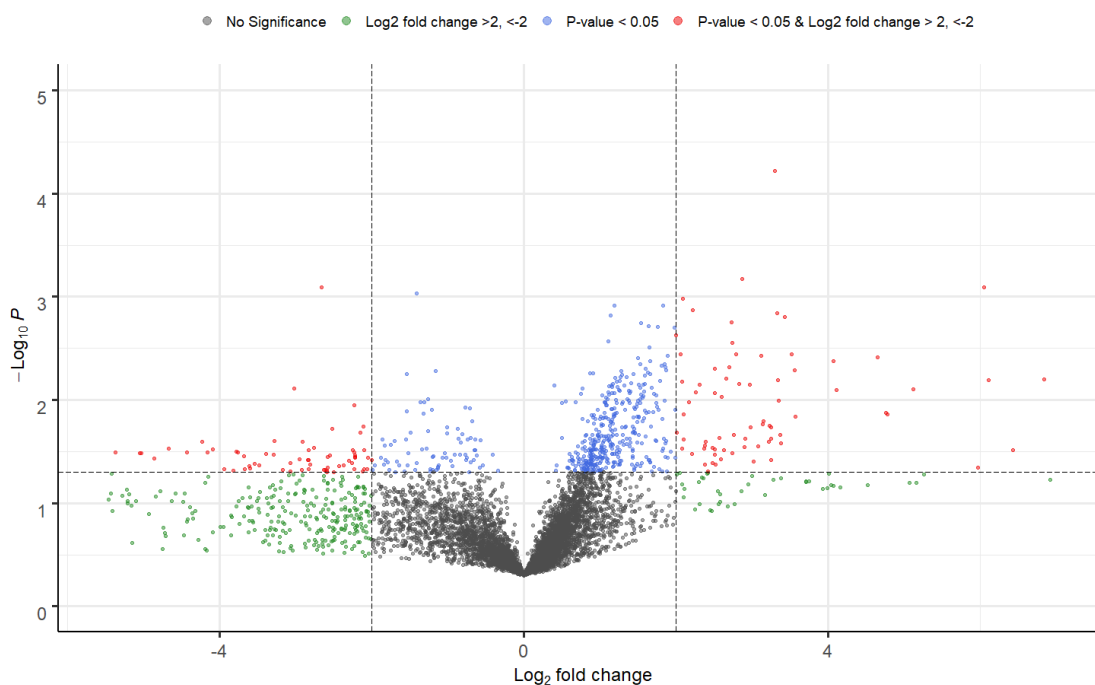


Figure IV.1.x. Volcano plot of potential lipids or lipid adducts detected in plasma samples from symptomatic and asymptomatic LSL patients. Attempted identification of lipids/lipid adducts marked in red with smallest  $p$ -value represented in Table IV.1.xa, with the most negative  $\log_2$  fold change (more abundant in symptomatic LSL patients) represented in Table IV.1.xb and with the most positive  $\log_2$  fold change (more abundant in asymptomatic LSL patients) represented in Table IV.1.xc. Sample size was 4 control and 9 test samples.

| M/Z    | RETENTION TIME | LIKELY LIPID   | LOG2FOLD CHANGE | PVALUE |
|--------|----------------|----------------|-----------------|--------|
| 758.53 | 25.25          | PE(34:0(OH))   | 3.30            | 0.0001 |
| 335.28 | 9.89           | unknown        | 2.87            | 0.0007 |
| 916.74 | 51.68          | TG(56:10)      | -2.66           | 0.0008 |
| 196.99 | 48.82          | unknown        | 6.05            | 0.0008 |
| 906.72 | 32.22          | PG(44:1)       | 2.09            | 0.0010 |
| 608.54 | 21.33          | unknown        | 2.21            | 0.0014 |
| 967.70 | 11.66          | PI(P-46:3)     | 3.33            | 0.0014 |
| 842.65 | 20.64          | PE(P-46:6)     | 3.43            | 0.0016 |
| 778.60 | 21.93          | PC(34:0(OH))   | 2.73            | 0.0018 |
| 739.60 | 25.24          | PE(O-34:0(OH)) | 2.00            | 0.0024 |

Table IV.1.xa Candidate lipids with highest p-values (rounded to 4 significant figures) and log 2 fold change of greater than 2 or less than -2.

| M/Z    | RETENTION TIME | LIKELY LIPID   | LOG2FOLD CHANGE | PVALUE |
|--------|----------------|----------------|-----------------|--------|
| 833.76 | 53.73          | TG(50:1)       | -5.37           | 0.0321 |
| 219.33 | 53.52          | unknown        | -5.05           | 0.0328 |
| 678.48 | 47.37          | LPE(34:5)      | -4.87           | 0.0371 |
| 748.57 | 32.33          | PC(O-36:5)     | -4.67           | 0.0294 |
| 869.75 | 53.09          | unknown        | -4.23           | 0.0253 |
| 913.70 | 53.74          | PE(46:4(OH))   | -3.94           | 0.0468 |
| 885.72 | 53.11          | unknown        | -3.82           | 0.0485 |
| 854.80 | 53.73          | unknown        | -3.78           | 0.0319 |
| 748.59 | 35.97          | PE(36:0)       | -3.76           | 0.0325 |
| 874.72 | 53.75          | PC(O-42:1(OH)) | -3.68           | 0.0352 |

Table IV.1.xb Candidate lipids significantly different between symptomatic and asymptomatic LSL patients ( $p < 0.05$ ) with the most negative log2 fold change (more abundant in symptomatic LSL patients).

| M/Z    | RETENTION TIME | LIKELY LIPID | LOG2FOLD CHANGE | PVALUE |
|--------|----------------|--------------|-----------------|--------|
| 757.52 | 25.25          | DG(44:9)     | 6.84            | 0.0063 |
| 299.18 | 5.58           | unknown      | 6.43            | 0.0307 |
| 734.53 | 7.98           | PE(34:1(OH)) | 6.11            | 0.0064 |
| 196.99 | 48.82          | unknown      | 6.05            | 0.0008 |
| 663.45 | 43.63          | PA(32:1(OH)) | 4.78            | 0.0137 |
| 375.25 | 11.99          | MG(18:3)     | 4.76            | 0.0134 |
| 576.36 | 13.08          | PE(24:1(OH)) | 4.65            | 0.0038 |
| 634.45 | 51.95          | PE(28:1)     | 4.07            | 0.0042 |
| 507.33 | 52.31          | unknown      | 3.57            | 0.0144 |
| 558.42 | 8.21           | unknown      | 3.56            | 0.0052 |

Table IV.1.xc Candidate lipids significantly different between symptomatic and asymptomatic LSL patients ( $p < 0.05$ ) with the most positive log2 fold change (more abundant in asymptomatic LSL patients).

## URINE

A total of 5156 lipids/lipid adducts were detected in urine samples. Of those, 753 were significantly different between samples taken from symptomatic and asymptomatic LSL patients ( $p < 0.05$ ) and 185 had a  $\log_2$  fold change of greater than 2 or less than -2 as well as being significantly different. Once mass charge ratio-retention time pairs that were only detected in one group were removed this total was reduced further to 172 potential lipids (Figure IV.1.xi).

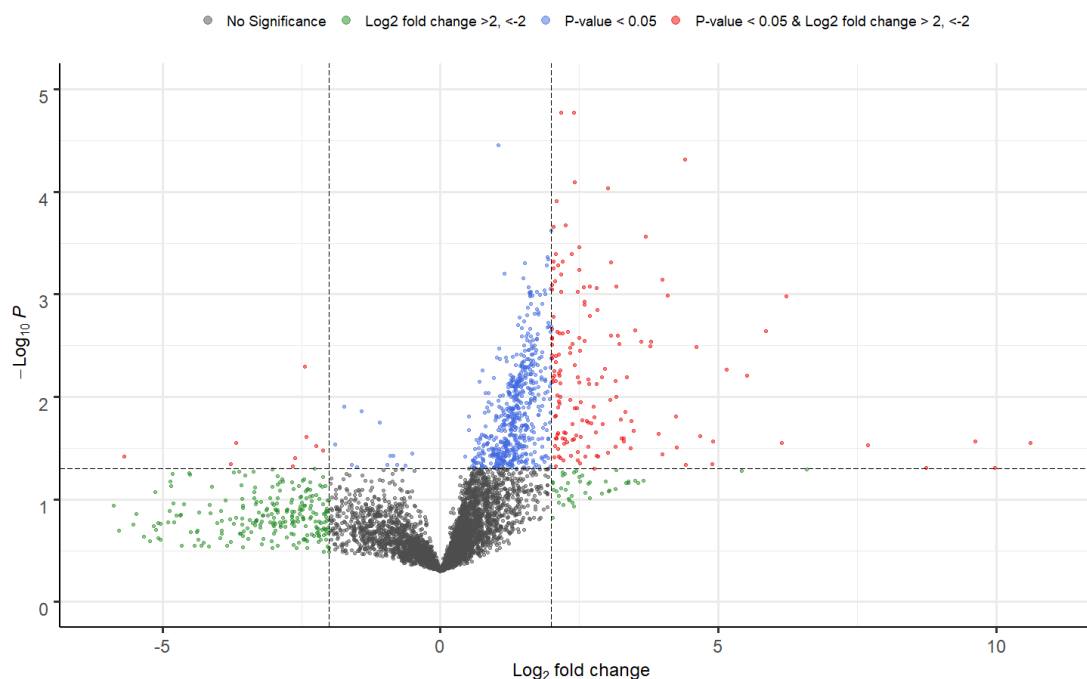


Figure IV.1.xi. Volcano plot of potential lipids or lipid adducts detected in urine samples from symptomatic and asymptomatic LSL patients. Attempted identification of lipids/lipid adducts marked in red with smallest  $p$ -value represented in Table IV.1.xia, with the most negative  $\log_2$  fold change (more abundant in symptomatic LSL patients) represented in Table IV.1.xib and with the most positive  $\log_2$  fold change (more abundant in asymptomatic LSL patients) represented in Table IV.1.xic. Sample size was 6 control and 10 test samples.

| M/Z    | RETENTION TIME | LIKELY LIPID | LOG2FOLD CHANGE | PVALUE |
|--------|----------------|--------------|-----------------|--------|
| 201.03 | 10.64          | unknown      | 3.70            | 0.0003 |
| 299.01 | 49.05          | FA(10:2)     | 4.00            | 0.0007 |
| 325.18 | 9.60           | unknown      | 4.40            | 0.0000 |
| 326.19 | 9.60           | unknown      | 3.01            | 0.0001 |
| 340.20 | 10.64          | unknown      | 3.07            | 0.0005 |
| 384.18 | 3.61           | unknown      | 2.81            | 0.0009 |
| 392.34 | 13.49          | unknown      | 2.41            | 0.0000 |
| 416.21 | 3.61           | unknown      | 2.58            | 0.0009 |
| 417.21 | 3.61           | unknown      | 2.68            | 0.0008 |
| 470.22 | 3.60           | unknown      | 2.03            | 0.0005 |

Table IV.1.xia Candidate lipids with highest p-values (rounded to 4 significant figures) and log 2 fold change of greater than 2 or less than -2.

| M/Z    | RETENTION TIME | LIKELY LIPID | LOG2FOLD CHANGE | PVALUE |
|--------|----------------|--------------|-----------------|--------|
| 341.27 | 12.27          | unknown      | -5.69           | 0.0380 |
| 249.15 | 8.78           | unknown      | -3.77           | 0.0449 |
| 531.39 | 11.70          | MG(28:3)     | -3.67           | 0.0281 |
| 552.53 | 34.14          | unknown      | -2.66           | 0.0473 |
| 651.41 | 10.49          | LPG(30:6)    | -2.61           | 0.0395 |
| 312.26 | 13.07          | unknown      | -2.44           | 0.0051 |
| 325.06 | 0.74           | unknown      | -2.41           | 0.0246 |
| 560.36 | 15.68          | LPE(22:0)    | -2.23           | 0.0299 |
| 323.19 | 6.61           | unknown      | -2.12           | 0.0336 |

Table IV.1.xib Candidate lipids significantly different between symptomatic and asymptomatic LSL patients ( $p < 0.05$ ) with the most negative log2 fold change (more abundant in symptomatic LSL patients).

| M/Z    | RETENTION TIME | LIKELY LIPID | LOG2FOLD CHANGE | PVALUE |
|--------|----------------|--------------|-----------------|--------|
| 816.64 | 18.95          | PC(38:1)     | 10.62           | 0.0282 |
| 835.62 | 49.70          | PA(46:5)     | 9.98            | 0.0492 |
| 860.67 | 18.73          | PC(40:1(OH)) | 9.63            | 0.0270 |
| 424.28 | 16.37          | unknown      | 8.74            | 0.0494 |
| 548.41 | 48.79          | LPE(24:0)    | 6.23            | 0.0010 |
| 728.59 | 19.42          | PC(O-34:1)   | 6.14            | 0.0280 |
| 590.43 | 38.35          | unknown      | 5.86            | 0.0023 |
| 806.58 | 47.37          | unknown      | 5.52            | 0.0062 |
| 816.52 | 10.33          | PS(40:7)     | 5.15            | 0.0054 |
| 684.56 | 19.67          | DG(40:7)     | 4.91            | 0.0272 |

Table IV.1.xic Candidate lipids significantly different between symptomatic and asymptomatic LSL patients ( $p < 0.05$ ) with the most positive log2 fold change (more abundant in asymptomatic LSL patients).

Comparison was made between mass charge ratio-retention time pairs detected in CSF samples and plasma samples. There were a total of 11 data points that had a  $p < 0.05$  and a log2 fold change of greater than 2 or less than -2 in both CSF and plasma samples. This was further reduced to 9 once direction of log2 fold change was taken into account. None of these data points showed an exact match in properties between CSF and plasma samples. Variation was tolerated up to 1.2 minutes for retention time, reducing the data points further to 3 (Figures IV.1.xiia and b). Only one potential match was made on database search, 590.426 (LPE 26:2). A similar mass charge ratio-retention time pair was detected in urine samples and was significantly different between symptomatic and asymptomatic patients.



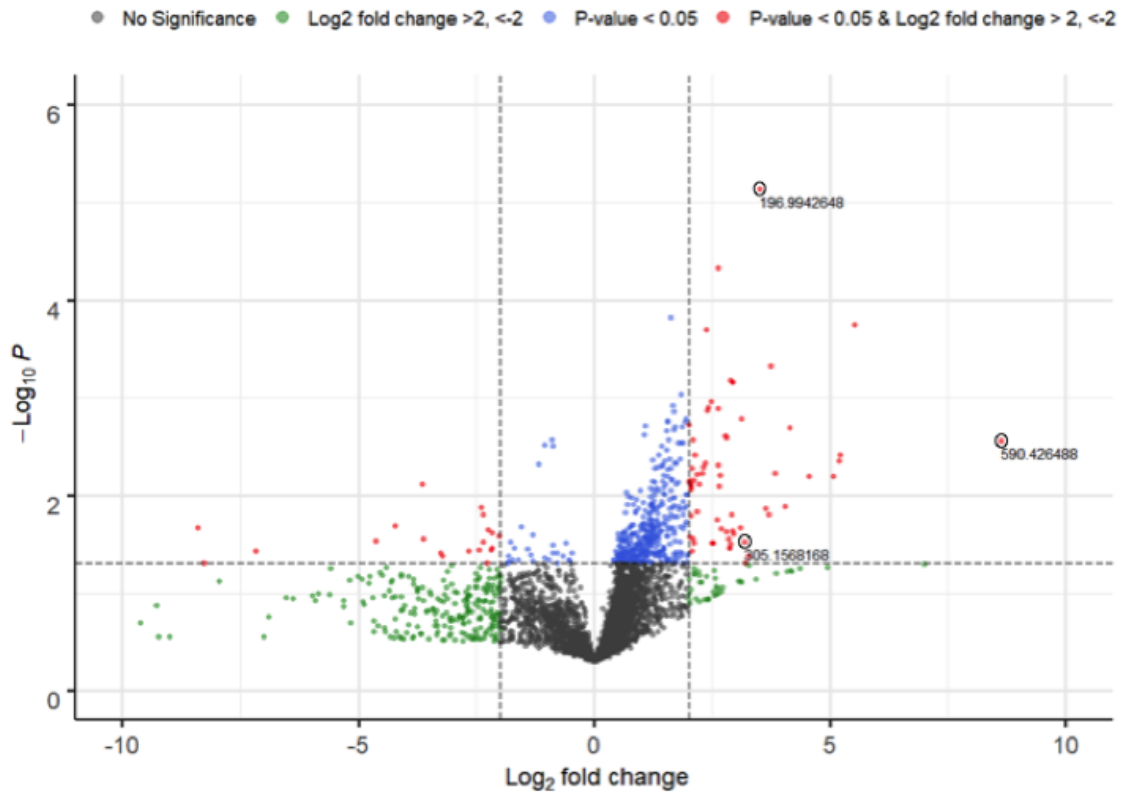


Figure IV.1.xiia Volcano plot comparing mass charge ratio-retention time pairs identified in CSF and plasma samples. Marks that represent mass charge ratio-retention time pairs that are closely matched between CSF and plasma samples, and show a significant difference between symptomatic and asymptomatic patients, are labelled with the mass charge ratio as measured in CSF samples.

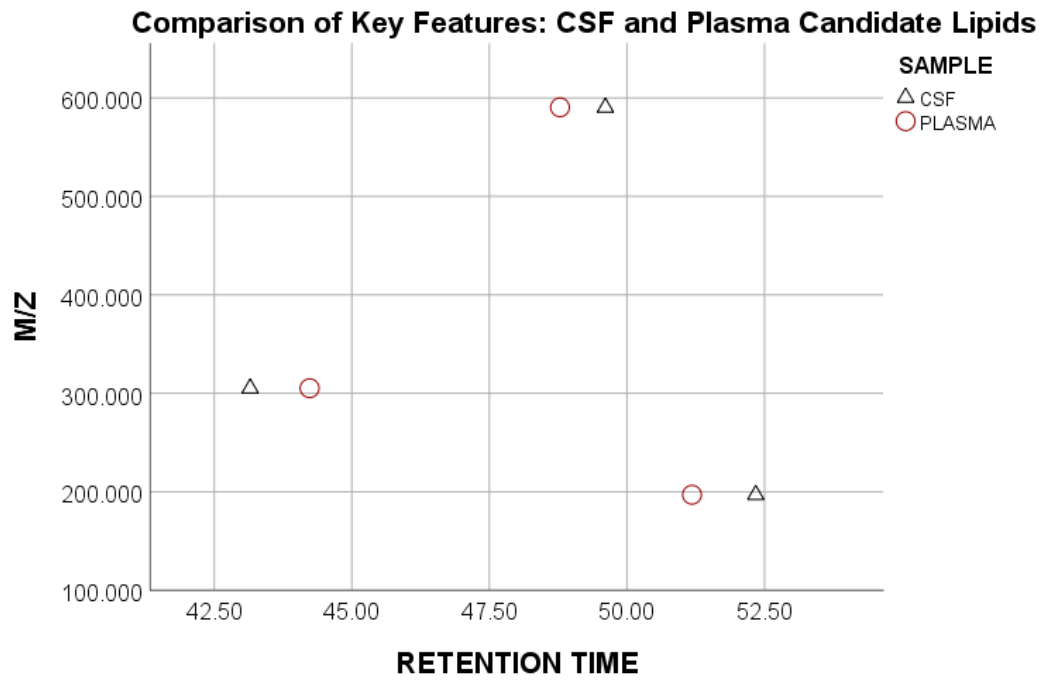


Figure IV.1.xiib Comparison of mass charge ratio-retention time pairings between CSF and plasma samples.

## TARGETED PHOSPHOLIPID ASSAY

A targeted assay was developed for PC/LPC and PE/LPE as described in the Methods section. A total of 175 phospholipids were separated and identified by high performance liquid chromatography and mass spectrometry (Figure IV.2.iv). Data from both control and test groups were normally distributed so t-test was used to generate p-values.

Samples were collected from a total of 41 patients undergoing neurosurgical procedures. CSF samples were omitted from 7 patients (due to contamination of CSF with blood at the time of collection); plasma samples were absent from 11 patients (due to difficulties in obtaining venous access at the time of intervention); and urine samples were absent from 15 patients (due to non-catheterisation of patients peri-operatively).

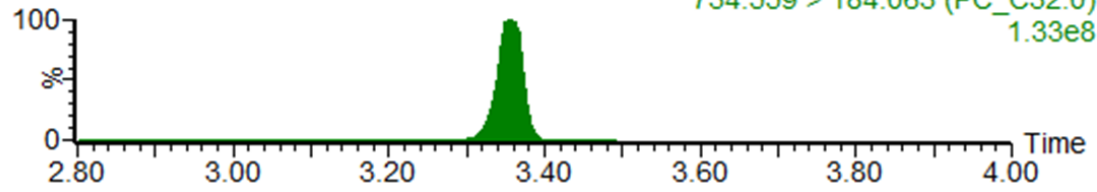
A total of 29 patients were diagnosed with a LSL on magnetic resonance imaging prior to surgery. Twelve cases were control patients taken largely from patients with myelomeningocele undergoing shunt insertion or with cerebral palsy undergoing selective dorsal rhizotomy.

Twenty-two patients were classed as being symptomatic based on neurological and urological assessment in the outpatient setting. Seven patients were considered to be asymptomatic. A breakdown of all patient features can be found in Supplementary Information.

Targeted assay results were compared against the complete database search results from Lipidomics 2. As mentioned previously, these database searches were limited to the 10 smallest p-values, the 10 most negative log<sub>2</sub> fold changes, and the ten most positive log<sub>2</sub> fold changes. The complete database search results can be found in Supplementary Information.

CSF\_181218\_194

2: MRM of 21 Channels ES+  
734.559 > 184.063 (PC\_C32:0)  
1.33e8



CSF\_181218\_194 449 (3.353)

2: MRM of 21 Channels ES+  
1.33e8

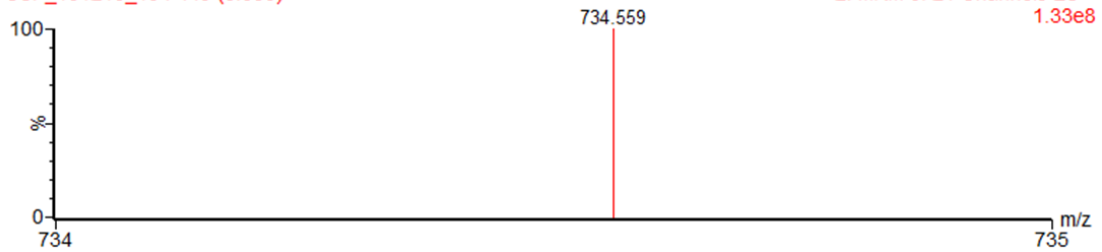
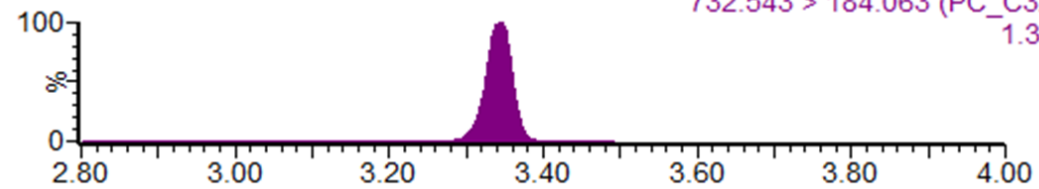


Figure IV.2.iva CSF PC32:0. Chromatogram (top) and spectrum (bottom) of PC 32:0

CSF\_181218\_194

2: MRM of 21 Channels ES+  
732.543 > 184.063 (PC\_C32:1)  
1.32e8



CSF\_181218\_194 447 (3.342)

2: MRM of 21 Channels ES+  
1.32e8

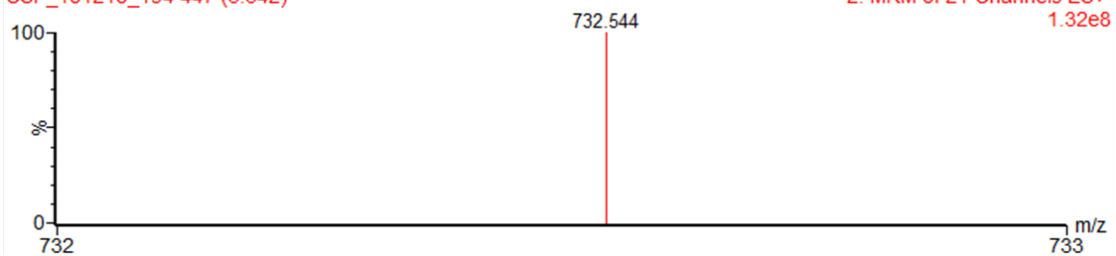


Figure IV.2.ivb CSF PC32:1 Chromatogram (top) and spectrum (bottom) of PC 32:1

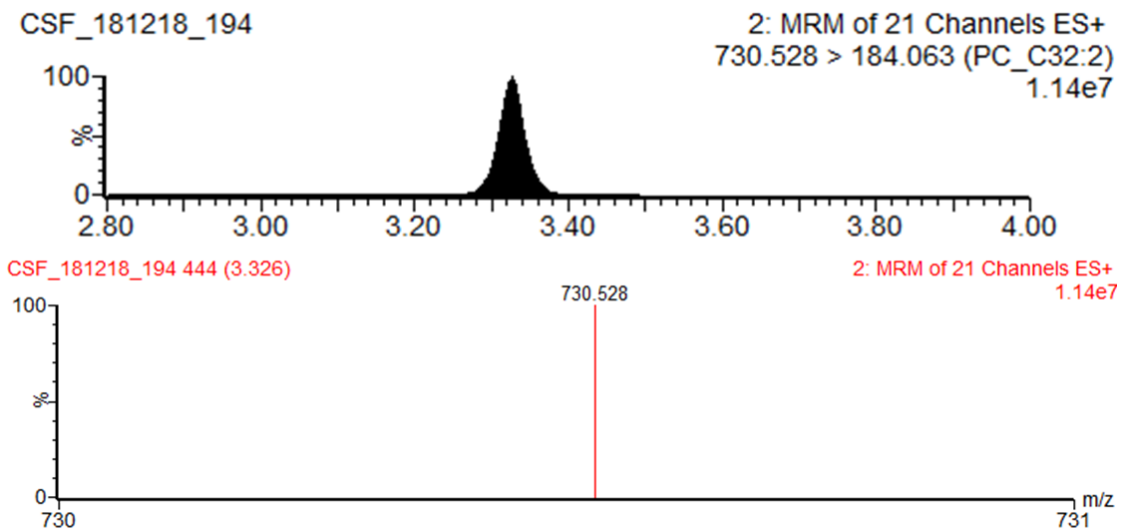


Figure IV.2.ivc CSF PC32:2 Chromatogram (top) and spectrum (bottom) of PC 32:2

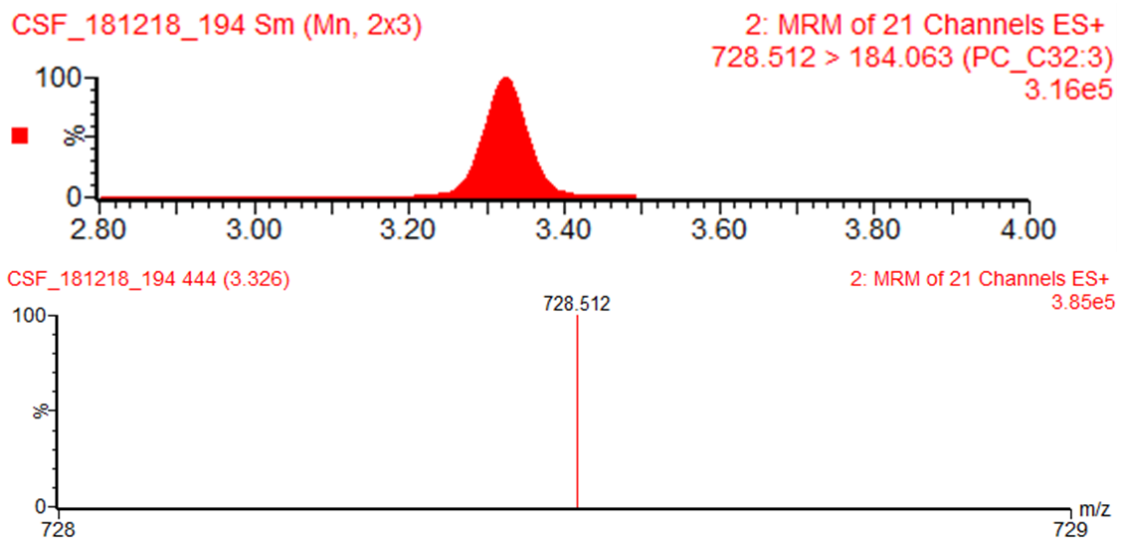


Figure IV.2.ivd CSF PC32:3 Chromatogram (top) and spectrum (bottom) of PC 32:3

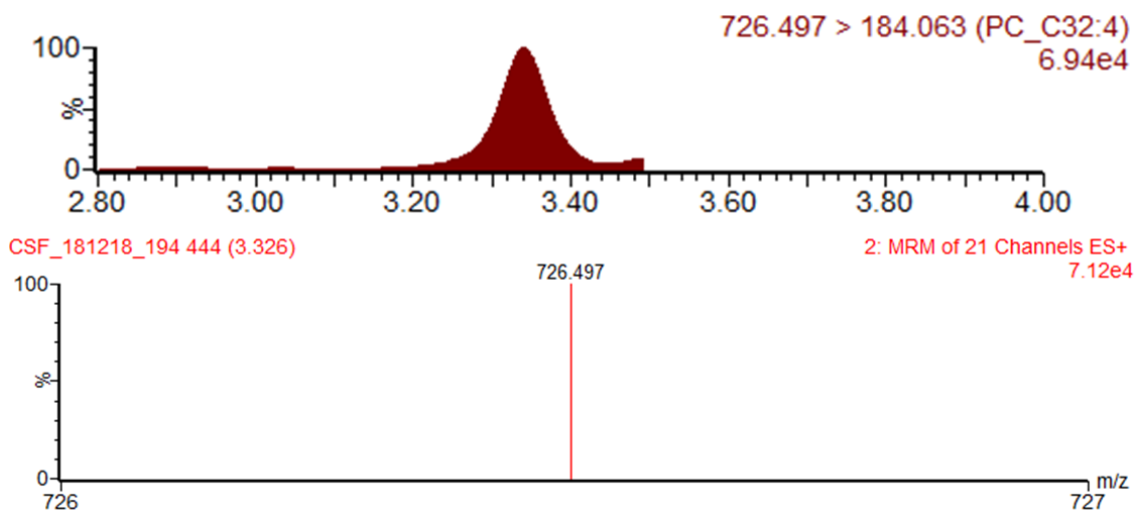


Figure IV.2.ive CSF PC32:4 Chromatogram (top) and spectrum (bottom) of PC 32:4

Sample chromatogram and spectrum traces, taken from CSF samples. In total, 175 different lipids were separated and identified by high performance liquid chromatography and mass spectrometry (LPE 12-26, PE 32-43, LPC 12-26, PC 24-44 were each detected with 0 to 4 double bonds in the fatty acid tail). Figure IV.2.iva shows the chromatogram generated for the targeted assay of the specific lipid PC 32:0 which is known to have the parent mass of 734.559 and a choline head group mass of 184.063, annotated as 734.559>184.063 (PC\_C32:0). The y-axis is a measure of percentage of the maximum intensity of the signal generated for this specific parent-daughter pairing; the maximum intensity detected is below mass annotation. The x-axis shows retention time in minutes. The underlying spectrum corresponds with the peak signal on the chromatogram and confirms detection of the mass of the PC32:0. Figures IV.2.ivb-e show the same data for: PC32:1, PC32:2, PC32:3 and PC32:4 respectively.

## CSF

Twenty-four of the lipids showed a significant difference between LSL and control patients in CSF samples. These differences were largely seen in the PCs (Figures IV.2.va and b). LPC 26:1 was the only one of the significantly different lipids detected by targeted assay that corresponded with the possible lipid matches based on database search of mass charge ratio-retention time pairs generated by Lipidomics 2, LSL versus control, in CSF samples.

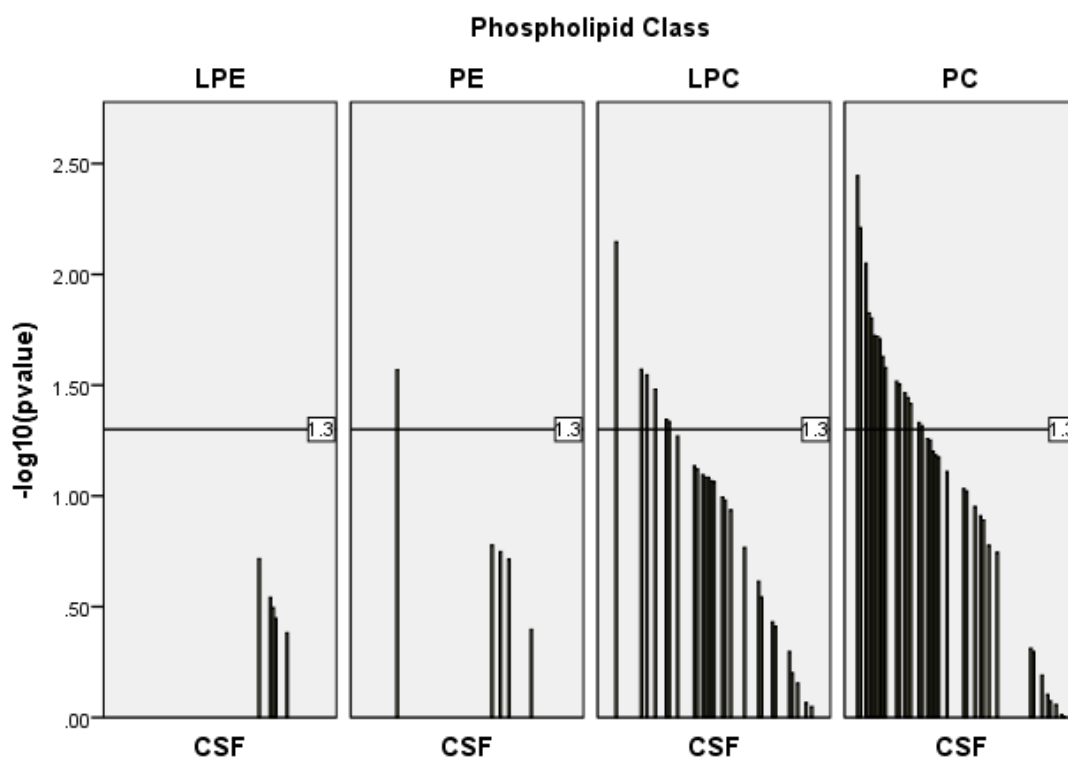


Figure IV.2.va Targeted phospholipid assay comparing means between control and LSL patients. Index line marks 1.3 ( $p=0.05$ ). Significantly different lipids between LSL and control: PCs 32:0 ( $p=0.0036$ ), 44:3 ( $p=0.0062$ ), 44:4 ( $p=0.0089$ ), 44:2 ( $p=0.0149$ ), 42:1 ( $p=0.0158$ ), 40:1 ( $p=0.0189$ ), 42:0 ( $p=0.0190$ ), 38:1 ( $p=0.0196$ ), 42:3 ( $p=0.0235$ ), 40:0 ( $p=0.0264$ ), 38:0 ( $p=0.0304$ ), 38:2 ( $p=0.0313$ ), 42:4 ( $p=0.0342$ ), 44:1 ( $p=0.036$ ), 40:2 ( $p=0.0383$ ), 36:0 ( $p=0.0467$ ), 40:3 ( $p=0.0483$ ); LPC 26:0 ( $p=0.0071$ ), 26:1 ( $p=0.0268$ ), 24:0 ( $p=0.0284$ ), 22:0 ( $p=0.0330$ ), 18:0 ( $p=0.0452$ ), 24:1 ( $p=0.0462$ ); and PE 36:2 ( $p=0.0270$ ).

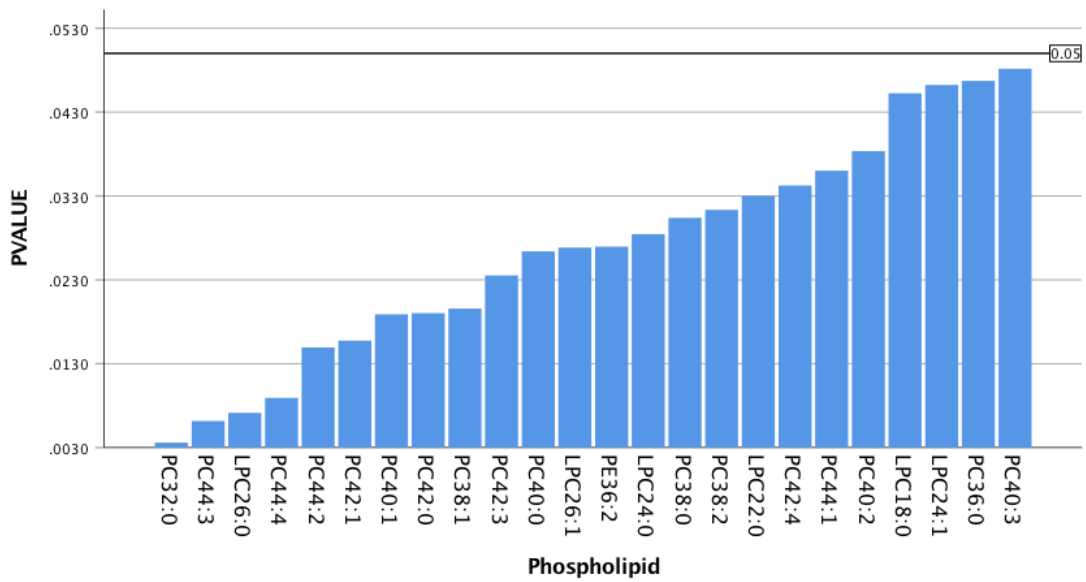


Figure IV.2.vb Summary of phospholipids identified by targeted assay with a significant difference ( $p < 0.05$ ) between LSL and control cases in CSF samples. Note: phospholipids are ranked from smallest p-value (most significant; on the left side) to largest p-value (least significant; on the right side).



## PLASMA

Five of the lipids showed a significant difference between LSL and control patients in plasma samples. These differences were largely seen in the LPCs (Figures IV.2.via and b). None of the significantly different lipids detected by targeted assay corresponded with the possible lipid matches based on database search of mass charge ratio-retention time pairs generated by Lipidomics 2, LSL versus control, in plasma samples.

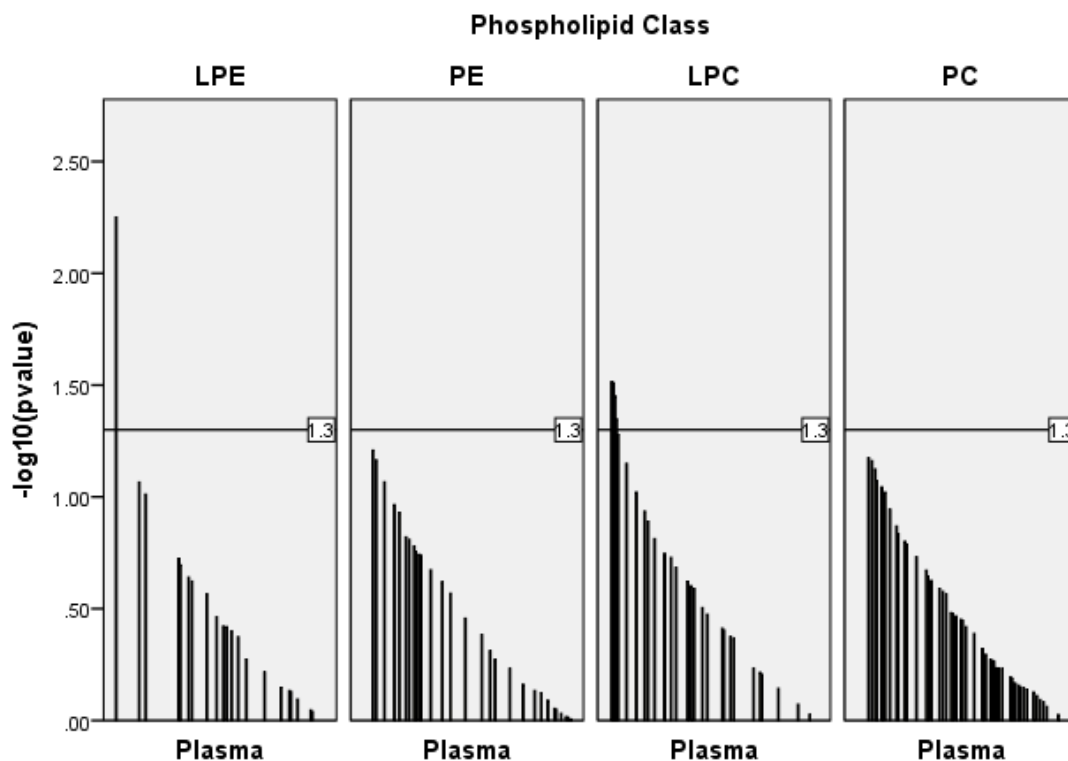


Figure IV.2.via Targeted phospholipid assay comparing means between control and LSL patients. Index line marks 1.3 ( $p=0.05$ ). Significantly different lipids between LSL and control: LPE 26:4 ( $p=0.0056$ ); and LPEs 16:2 ( $p=0.0306$ ), 22:3 ( $p=0.0309$ ), 14:1 ( $p=0.0354$ ), 16:4 ( $p=0.0449$ ).

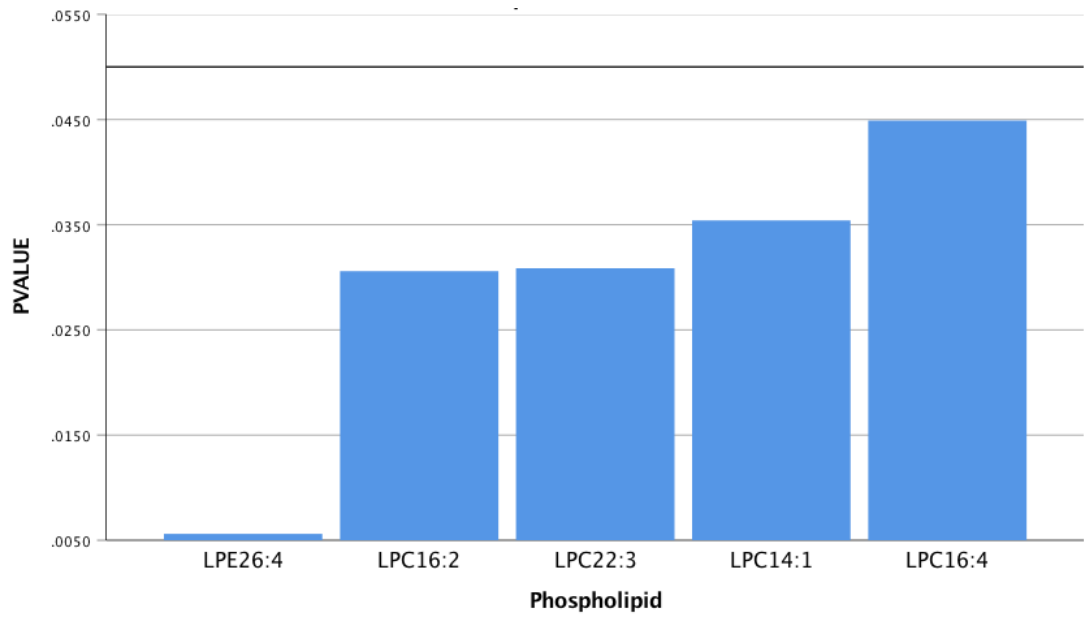


Figure IV.2.vib Summary of phospholipids identified by targeted assay with a significant difference ( $p < 0.05$ ) between LSL and control cases in plasma samples. Note: phospholipids are ranked from smallest p-value (most significant; on the left side) to largest p-value (least significant; on the right side).

## URINE

None of the lipids measured by targeted assay showed a significant difference between LSL and control patients in urine samples (Figure IV.2.vii).

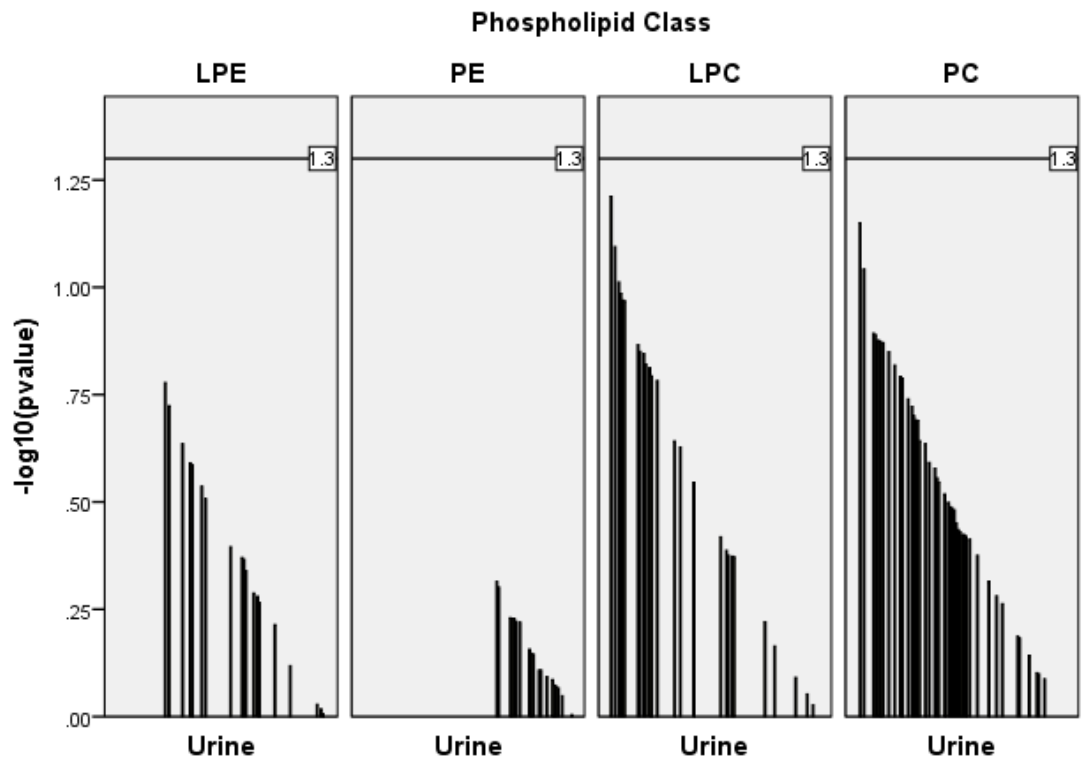


Figure IV.2.vii Targeted phospholipid assay comparing means between control and LSL patients. Index line marks 1.3 ( $p=0.05$ ). There were no significantly different lipids between LSL and control in urine samples.

## SYMPTOMATIC V. ASYMPTOMATIC

### CSF

Twelve of the lipids showed a significant difference between symptomatic and asymptomatic patients in CSF samples. These differences were largely seen in both the PCs and LPCs (Figures IV.2.viii a and b). None of the significantly different lipids detected by targeted assay corresponded with the possible lipid matches based on database search of mass charge ratio-retention time pairs generated by Lipidomics 2, symptomatic versus asymptomatic, in CSF samples.

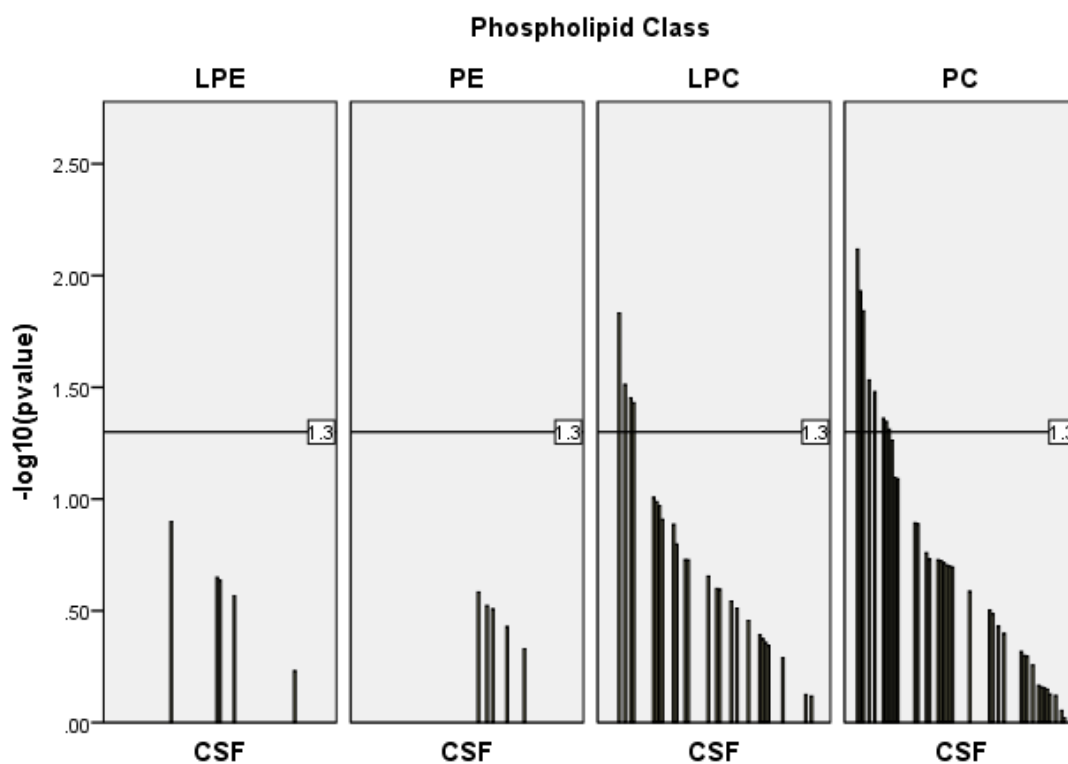


Figure IV.2.viii a Targeted phospholipid assay comparing means between control and LSL patients. Index line marks 1.3 ( $p=0.05$ ). Significantly different lipids between symptomatic and asymptomatic: PCs 44:4 ( $p=0.0076$ ), 42:1 ( $p=0.0117$ ), 38:0 ( $p=0.0144$ ), 44:1 ( $p=0.0293$ ), 44:0 ( $p=0.0331$ ), 42:0 ( $p=0.0435$ ), 44:2 ( $p=0.0450$ ), 36:0 ( $p=0.0488$ ); and LPCs 18:0 ( $p=0.0147$ ), 18:2 ( $p=0.0307$ ), 22:3 ( $p=0.0353$ ), 24:4 ( $p=0.0371$ ).

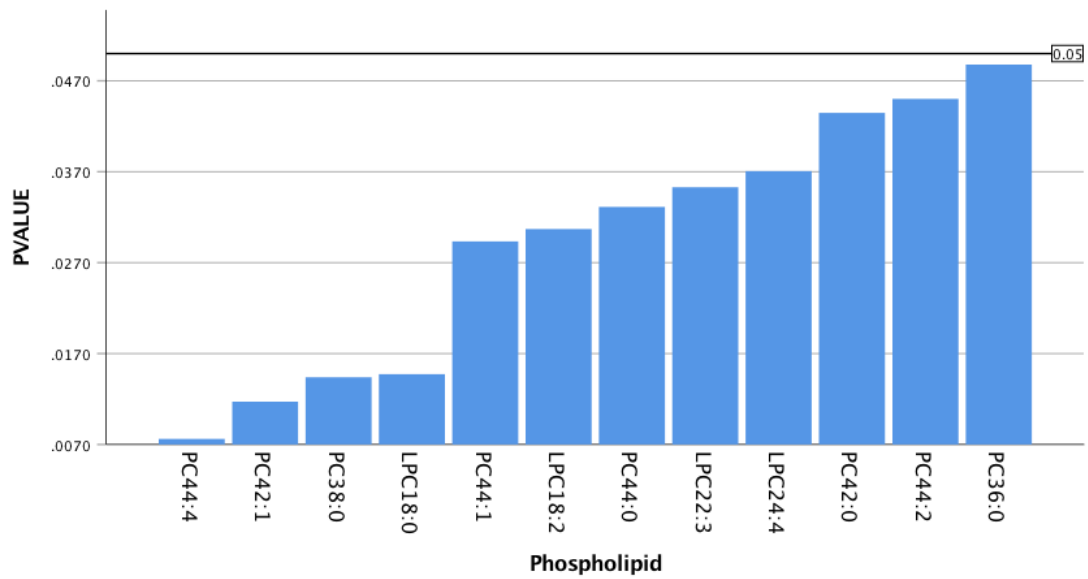


Figure IV.2.viiiB Summary of phospholipids identified by targeted assay with a significant difference ( $p < 0.05$ ) between symptomatic and asymptomatic cases in CSF samples. Note: phospholipids are ranked from smallest p-value (most significant; on the left side) to largest p-value (least significant; on the right side).

## PLASMA

Twenty of the lipids measured showed a significant difference between symptomatic and asymptomatic patients in plasma samples. These differences were largely seen in both the PCs and PEs (Figures IV.2.ix.a and b). None of the significantly different lipids detected by targeted assay corresponded with the possible lipid matches based on database search of mass charge ratio-retention time pairs generated by Lipidomics 2, symptomatic versus asymptomatic, in plasma samples.

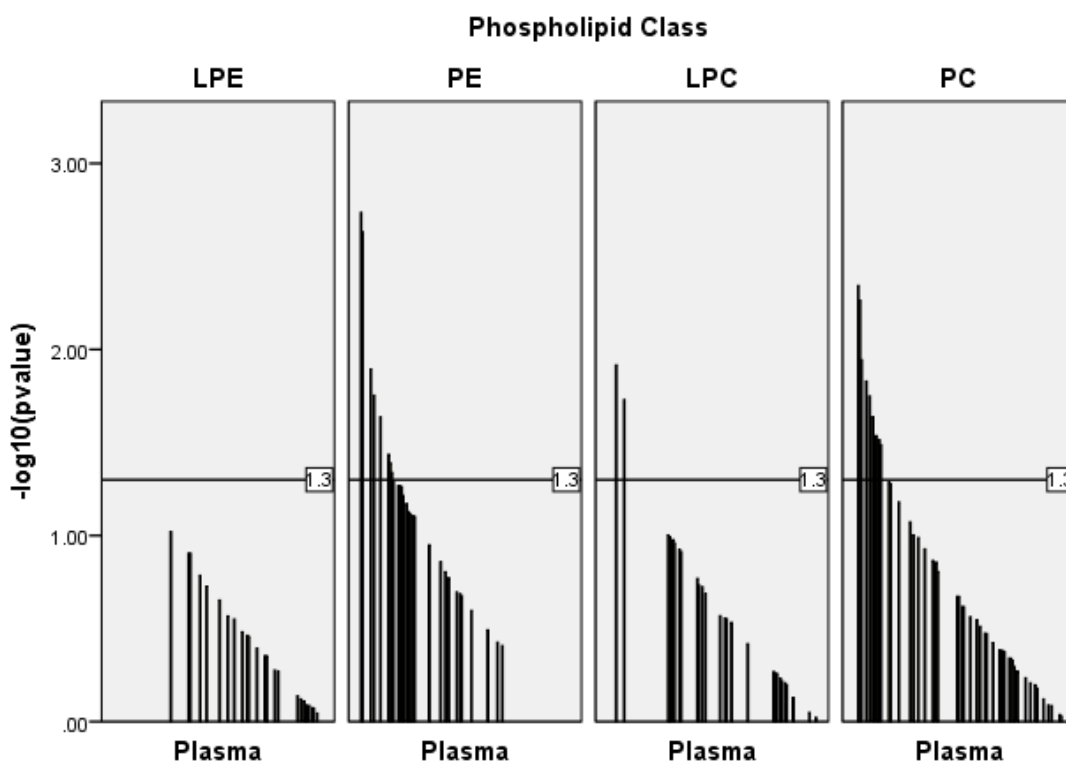


Figure IV.2.ix.a Targeted phospholipid assay comparing means between control and LSL patients. Index line marks 1.3 ( $p=0.05$ ). Significantly different lipids between symptomatic and asymptomatic: PCs 32:2 ( $p=0.0045$ ), 24:4 ( $p=0.0055$ ), 32:3 ( $p=0.0114$ ), 34:4 ( $p=0.0148$ ), 32:4 ( $p=0.0291$ ), 28:2 ( $p=0.0305$ ), 32:0 ( $p=0.0307$ ), 36:2 ( $p=0.0325$ ); LPCs 16:0 ( $p=0.0121$ ), 14:1 ( $p=0.0186$ ); and PE 42:1 ( $p=0.0018$ ), 32:3 ( $p=0.0023$ ), 36:4 ( $p=0.0127$ ), 38:4 ( $p=0.0231$ ), 40:4 ( $p=0.0366$ ), 38:2 ( $p=0.0409$ ), 40:0 ( $p=0.0459$ ).

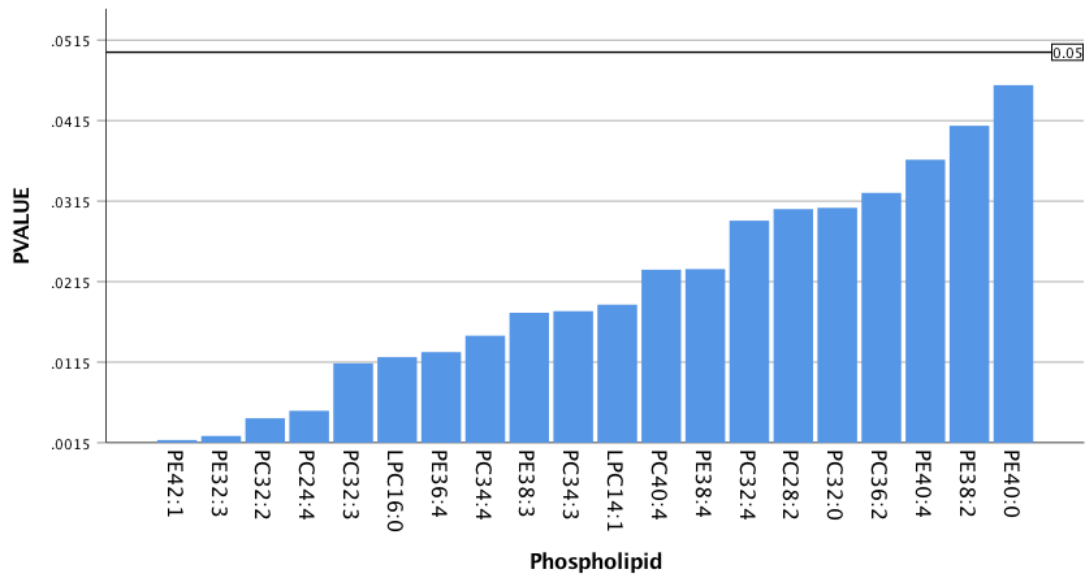


Figure IV.2.ixb Summary of phospholipids identified by targeted assay with a significant difference ( $p < 0.05$ ) between symptomatic and asymptomatic cases in plasma samples. Note: phospholipids are ranked from smallest p-value (most significant; on the left side) to largest p-value (least significant; on the right side).

## URINE

Thirteen of the lipids measured showed a significant difference between symptomatic and asymptomatic patients in urine samples. These differences were only seen in PCs (Figures IV.2.xa and b). PC 34:1 was the only significantly different lipid detected by targeted assay that corresponded with the possible lipid matches based on database search of mass charge ratio-retention time pairs generated by Lipidomics 2, symptomatic versus asymptomatic, in urine samples.

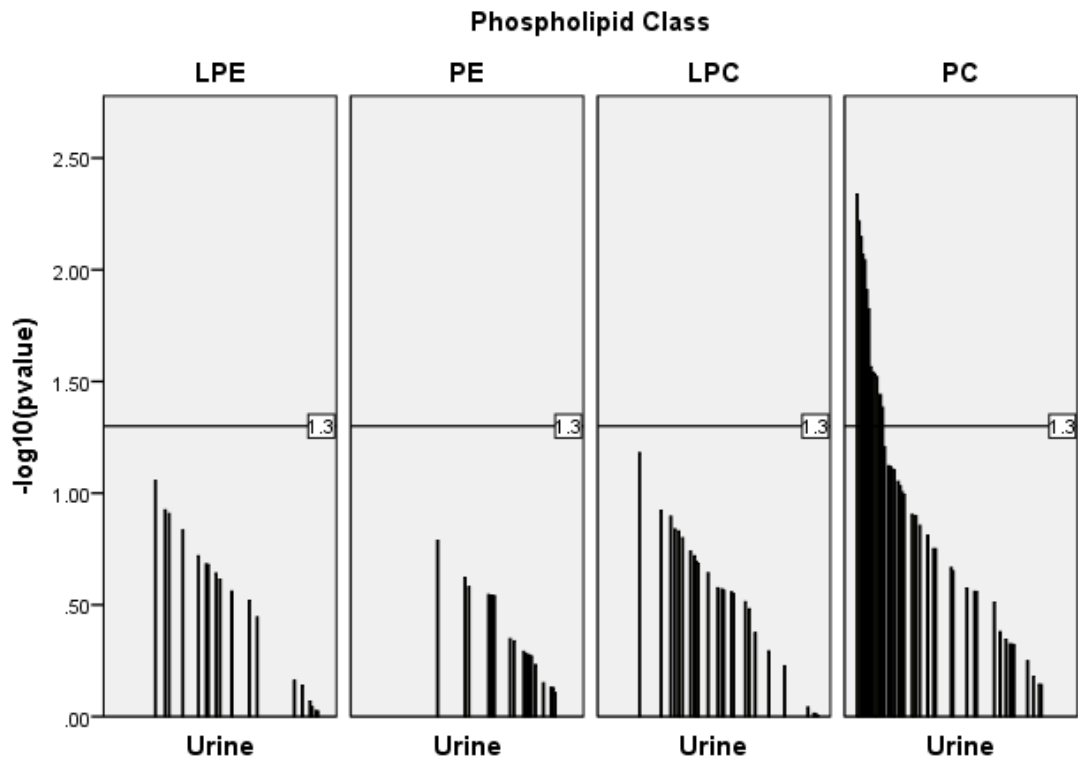


Figure IV.2.xa Targeted phospholipid assay comparing means between control and LSL patients. Index line marks 1.3 ( $p=0.05$ ). Significantly different lipids between symptomatic and asymptomatic: PCs 36:4 ( $p=0.0046$ ), 34:2 ( $p=0.0061$ ), 38:4 ( $p=0.071$ ), 36:3 ( $p=0.0086$ ), 34:1 ( $p=0.0091$ ), 36:2 ( $p=0.0123$ ), 34:4 ( $p=0.0150$ ), 28:1 ( $p=0.0272$ ), 32:2 ( $p=0.0288$ ), 30:2 ( $p=0.0293$ ), 28:0 ( $p=0.0302$ ), 40:4 ( $p=0.0363$ ), 32:4 ( $p=0.0413$ )



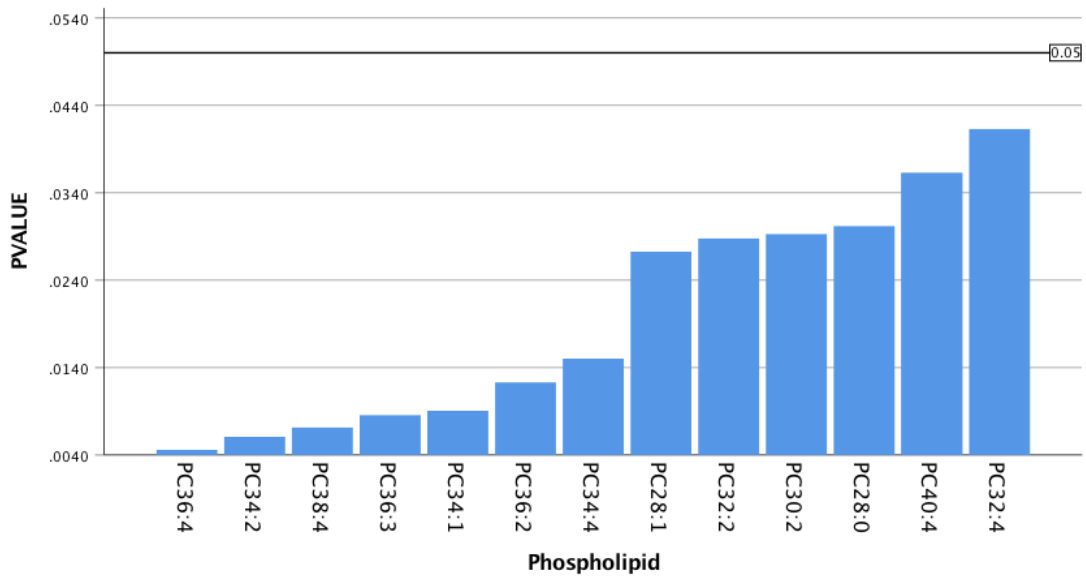


Figure IV.2.xb Summary of phospholipids identified by targeted assay with a significant difference ( $p < 0.05$ ) between symptomatic and asymptomatic cases in plasma samples. Note: phospholipids are ranked from smallest p-value (most significant; on the left side) to largest p-value (least significant; on the right side).

### PC/PE Ratio

Total PC and LPC values were calculated along with total PE and LPE to generate a total PC/PE ratio. Mean ratios were then compared between LSL and control and between symptomatic and asymptomatic patients.

All values were greater than one, representing an abundance of PC in comparison to PE in all sample types. There was a significant difference in the PC/PE ratio between LSL and control patients in CSF samples and between symptomatic and asymptomatic LSL patients in both CSF and plasma samples (Table IV.2.i).

| Sample | LSL        | Control   | pvalue |
|--------|------------|-----------|--------|
| CSF    | 11989.8085 | 5845.5322 | 0.013  |
| Plasma | 33.6843    | 278.6951  | 0.087  |
| Urine  | 61.8541    | 224.9202  | 0.086  |

| Sample | Symptomatic | Asymptomatic | pvalue |
|--------|-------------|--------------|--------|
| CSF    | 13443.1947  | 6176.2639    | 0.045  |
| Plasma | 25.2646     | 71.5731      | 0.001  |
| Urine  | 51.5368     | 87.6475      | 0.491  |

Table IV.2.i Comparison of mean PC/PE ratios between LSL and control patients and symptomatic and asymptomatic LSL patients.

Within CSF samples, PC is even more abundant compared to PE in the symptomatic LSL patients when compared to the asymptomatic patients. However, this relationship is reversed in plasma samples with PC being more abundant in asymptomatic patients. The same pattern is seen in LSL versus control samples, although this does not reach significance.

### LPC/PC AND LPE/PE RATIO

Total PC and LPC values were calculated along with total PE and LPE to generate a total LPC/PC ratio and LPE/PE ratio. Mean ratios were then compared between LSL and control and between symptomatic and asymptomatic patients (Tables IV.2.ii.a and b).

| Sample | LSL   | Control | pvalue |
|--------|-------|---------|--------|
| CSF    | 0.04  | 0.09    | 0.058  |
| Plasma | 0.76  | 0.68    | 0.152  |
| Urine  | 0.031 | 0.043   | 0.249  |

| Sample | Symptomatic | Asymptomatic | pvalue |
|--------|-------------|--------------|--------|
| CSF    | 0.04        | 0.06         | 0.124  |
| Plasma | 0.77        | 0.69         | 0.247  |
| Urine  | 0.03        | 0.032        | 0.886  |

Table IV.2.ii.a Comparison of mean LPC/PC ratios between LSL and control patients and symptomatic and asymptomatic LSL patients.

All values of LPC/PC ratio were less than 1, representing an abundance of PC in comparison to LPC in all sample types. There was no significant difference in the LPC/PC ratio between LSL and control patients or between symptomatic and asymptomatic LSL patients in any of the sample types.

| Sample | LSL  | Control | pvalue |
|--------|------|---------|--------|
| CSF    | 0.59 | 0.96    | 0.58   |
| Plasma | 0.06 | 0.15    | 0.29   |
| Urine  | 9.8  | 4.9     | 0.51   |

| Sample | Symptomatic | Asymptomatic | pvalue |
|--------|-------------|--------------|--------|
| CSF    | 0.55        | 0.73         | 0.59   |
| Plasma | 0.05        | 0.08         | 0.15   |
| Urine  | 13.04       | 1.69         | 0.22   |

Table IV.2.ii.b Comparison of mean LPE/PE ratios between LSL and control patients and symptomatic and asymptomatic LSL patients.

All values of LPE/PE ratio were also less than 1, representing an abundance of PE in comparison to LPE in all sample types. There was no significant difference in the LPE/PE ratio between LSL and control patients or between symptomatic and asymptomatic LSL patients in any of the sample types.

### 3. CLINICAL ASSESSMENT AND CORRELATION

LSLs are diagnosed at or near birth, usually with clinical assessment followed by confirmation of pathology on magnetic resonance imaging. LSLs are associated with a number of different cutaneous manifestations that are readily identifiable referred to as the stigmata of spinal dysraphism: e.g. focal hirsutism, dilated cutaneous blood vessels, cutaneous appendages, dermal pit and swelling over the sacral region. In addition to cutaneous manifestations at birth, children may be born with musculoskeletal deformity, talipes equinovarus or disparity in lower limb length/size. Such deformities are part of the spectrum of neuro-orthopaedic syndrome. The other features of this syndrome include motor weakness and altered sensation in the lower limbs. These features are often mild and problematic to diagnose at birth and may remain difficult to assess in infants and toddlers [124].

As well as controlling lower limb power and sensation, the sacral component of the spinal cord involved in LSL is important in the control of both micturition and defaecation. As a result, children may develop problems with incomplete bladder emptying, detrusor-sphincter dyssynergia and incontinence. Incomplete emptying can result in recurrent UTIs and discomfort but may ultimately lead to structural changes within the urinary system. Neuropathic bowel may present with constipation, overflow incontinence or recurrent soiling. As with motor and sensory function, mild bladder and bowel dysfunction is difficult to reliably assess in very young, precontinent patients. Despite this subtle presentation in young children, there is a potential to develop significant neurological and/or urological disability [210].

A hallmark of a symptomatic LSL that might benefit from surgery is a patient whose symptoms are progressively worsening. It is assumed that there is an on-going disease process that needs to be halted in these cases and, as such, these patients would derive the most benefit from surgery as in this scenario mechanical traction rather than primary dysplasia is the more likely mechanism for deterioration. In an attempt to identify new or evolving deficits children are assessed every 6 months by a neurosurgeon, neuro-physiotherapist and with formal urology assessment in the context of an MDT clinic.

To date the assessment of patients with LSL have principally taken into account two factors: firstly, is there evidence of any clinical manifestation of the LSL (excluding cutaneous manifestation at birth); and secondly, is there any evidence of progression or development of new clinical manifestations. A patient who is found not to have any clinical manifestations of their LSL is referred to as asymptomatic (this is even though some of the clinical manifestations may be picked up on bladder function tests and are therefore clinical signs not symptoms). A patient who has any abnormal results on clinical assessment or investigation is labelled as symptomatic [181].

Predominantly, in the United Kingdom, patients who are labelled as symptomatic are offered surgery whereas a watch-and-wait approach is adopted for asymptomatic patients. Alternatively a symptomatic patient, perhaps a child born with talipes equinovarus, but showing no suggestion of development of other clinical manifestations might be labelled as stable and continue to be monitored before the decision to proceed with surgery is made.

This binary division in clinical management does not reflect the degrees of severity of the neuro-orthopaedic syndrome or loss of bladder function. By reviewing the clinical features of individual patients in detail, and correlating this with lipid measurements by targeted assay, there is potential for identification of lipids that show strong correlation with symptoms and therefore may have a stronger sensitivity as a biomarker.

The above lipidomics and targeted phospholipid assay analysis was based on the division of patients into symptomatic and asymptomatic. Clinical assessment of LSL patients was conducted in the clinic setting and included neurological assessment by a neurosurgeon and neuro-physiotherapist, and urological assessment with a bladder diary, bladder ultrasound and urodynamics. Further detail can be found in the Section III.2.

Reviewing clinical features in detail will allow confirmation as to whether the label of symptomatic or asymptomatic is accurate. Clinical features were then combined to give a Total Clinical Score. The aim of this was to identify any correlation between lipids detected by targeted assay and severity of clinical features. A lipid that correlates well with the severity would be promising as a potential biomarker especially if changes in that lipid could be detected prior to the worsening of clinical features.

A total of 29 patients with LSL were assessed prior to surgery and, of these, 17 patients had complete pre-operative neurological and urological assessment sufficient to generate a Total Clinical Score. Reasons for incomplete pre-operative assessment included difficulties performing complete assessment on patients in the out-patient setting, parent wishes to proceed with surgery before complete investigations and unavailable patient information due to assessments completed in other institutions or abroad. Clinical categories measured were: power, sensation, pain, deformity, progression and urology. A maximum of four points was assigned to each clinical category to ensure equal weighting, giving a maximum possible score of 24. Urgency and incontinence were excluded from scoring in the urological assessment as these were deemed unreliable due to the young age of the patients at time of assessment. Individual Total Clinical Scores can be found in Table IV.3.i. Comparison was made between those patients designated as asymptomatic or symptomatic and the results of their clinical assessment.

| ID | Clinical Status | Residual volume | UTIs | Incont | Urgency | CIC | Thick Bladder Wall | Motor deficit | Sensory loss | Pain | Deformity | Rapid prog | Total Clinical Score | Age at surgery (mons) |
|----|-----------------|-----------------|------|--------|---------|-----|--------------------|---------------|--------------|------|-----------|------------|----------------------|-----------------------|
| 1  | Symptomatic     | 1               | 1    | 1      | 0       | 0   | 1                  | 1             | 0            | 0    | 0         | 0          | 4                    | 27                    |
| 2  | Symptomatic     | 0               | 0    | 1      | 1       | 0   | 0                  | 0             | 0            | 4    | 0         | 0          | 4                    | 42                    |
| 3  | Asymptomatic    | 0               | 0    | 0      | 0       | 0   | 0                  | 0             | 0            | 0    | 0         | 0          | 0                    | 31                    |
| 4  | Asymptomatic    | n/a             | 0    | 0      | 0       | 0   | n/a                | 0             | 0            | 0    | 0         | 0          | n/a                  | 53                    |
| 5  | Symptomatic     | n/a             | 1    | 0      | 0       | 0   | n/a                | 3             | 0            | 0    | 2         | 0          | n/a                  | 49                    |
| 6  | Asymptomatic    | n/a             | 0    | 0      | 0       | 0   | n/a                | 0             | 0            | 0    | 0         | 0          | n/a                  | 25                    |
| 7  | Symptomatic     | 1               | 1    | 0      | 0       | 1   | 0                  | 2             | 0            | 2    | 0         | 2          | 9                    | 36                    |
| 8  | Asymptomatic    | 0               | 0    | 0      | 0       | 0   | 0                  | 0             | 0            | 0    | 0         | 0          | 0                    | 18                    |
| 9  | Asymptomatic    | 0               | 0    | 0      | 0       | 0   | 0                  | 0             | 0            | 0    | 0         | 0          | 0                    | 30                    |
| 11 | Symptomatic     | 1               | 0    | 1      | 1       | 0   | 0                  | 1             | 0            | 0    | 1         | 2          | 5                    | 56                    |
| 12 | Asymptomatic    | 0               | 0    | 0      | 0       | 0   | 0                  | 0             | 0            | 0    | 0         | 0          | 0                    | 13                    |
| 14 | Symptomatic     | 0               | 1    | 0      | 0       | 0   | 0                  | 0             | 0            | 2    | 0         | 0          | 3                    | 13                    |
| 15 | Symptomatic     | 0               | 1    | 0      | 0       | 0   | 1                  | 3             | 0            | 0    | 3         | 0          | 8                    | 26                    |
| 17 | Symptomatic     | n/a             | 0    | 0      | 0       | 1   | n/a                | 0             | 0            | 0    | 0         | 2          | n/a                  | 32                    |
| 21 | Asymptomatic    | 0               | 0    | 0      | 0       | 0   | 0                  | 0             | 0            | 0    | 0         | 0          | 0                    | 11                    |
| 23 | Symptomatic     | 1               | 0    | 1      | 0       | 0   | 0                  | 0             | 0            | 0    | 0         | 0          | 1                    | 30                    |
| 26 | Symptomatic     | n/a             | 0    | 0      | 0       | 1   | n/a                | 0             | 0            | 0    | 0         | 0          | n/a                  | 28                    |
| 27 | Symptomatic     | n/a             | 1    | 1      | 0       | 0   | n/a                | 1             | 0            | 0    | 0         | 0          | n/a                  | 15                    |
| 30 | Symptomatic     | 1               | 1    | 0      | 0       | 1   | 0                  | 0             | 0            | 0    | 0         | 4          | 7                    | 32                    |
| 33 | Symptomatic     | 0               | 0    | 1      | 0       | 0   | 0                  | 0             | 0            | 0    | 0         | 0          | 0                    | 19                    |
| 35 | Symptomatic     | n/a             | 0    | 1      | 0       | 0   | n/a                | 1             | 0            | 0    | 0         | 0          | n/a                  | 25                    |
| 38 | Symptomatic     | n/a             | 0    | 1      | 0       | 0   | n/a                | 1             | 0            | 0    | 0         | 0          | n/a                  | 18                    |

|    |             |     |   |   |   |   |     |   |   |   |   |   |     |    |
|----|-------------|-----|---|---|---|---|-----|---|---|---|---|---|-----|----|
| 39 | Symptomatic | 0   | 0 | 0 | 0 | 0 | 0   | 1 | 0 | 0 | 0 | 0 | 1   | 28 |
| 40 | Symptomatic | 0   | 0 | 0 | 0 | 0 | 0   | 0 | 0 | 2 | 0 | 0 | 2   | 19 |
| 41 | Symptomatic | 1   | 0 | 0 | 0 | 0 | 0   | 0 | 0 | 0 | 0 | 0 | 1   | 25 |
| 42 | Symptomatic | n/a | 0 | 0 | 0 | 0 | n/a | 2 | 0 | 2 | 1 | 0 | n/a | 33 |
| 43 | Symptomatic | n/a | 0 | 0 | 0 | 0 | n/a | 1 | 0 | 0 | 1 | 0 | n/a | 27 |
| 44 | Symptomatic | n/a | 1 | 0 | 0 | 0 | n/a | 0 | 0 | 0 | 1 | 0 | n/a | 34 |

Table IV.3.i. Total clinical score based on sum of clinical findings. Points allocated as follows: residual volume 1 = > 20%; UTIs 1 = laboratory confirmed urinary tract infections; incont (incontinence) 1 = episodes of wetting; urgency 1 = patient reporting sensation of pending micturition; CIC 1 = clean intermittent catheterisation initiated; thick bladder wall 1 = abnormal bladder wall thickness noted on bladder ultrasonography; motor deficit 1 = mild unilateral weakness, 2 = significant unilateral weakness, 3 = mild bilateral weakness, 4 = significant bilateral weakness; sensory loss 0 = normal sensation on clinical assessment; pain 2 = unilateral radicular pain, 4 = bilateral radicular pain; deformity 1 = mild unilateral deformity, 2 = significant unilateral deformity, 3 = mild bilateral deformity, 4 = significant bilateral deformity; rapid prog (progression) 2 = noted at routine assessment, 4 = rapid progression requiring expeditious clinical assessment; n/a = results not available

### Neurological assessment

All asymptomatic patients had normal neurological assessment. A large number (38%) of patients who were classed as symptomatic also had no abnormal findings on neurological assessment (Figures IV.3.ia-e).

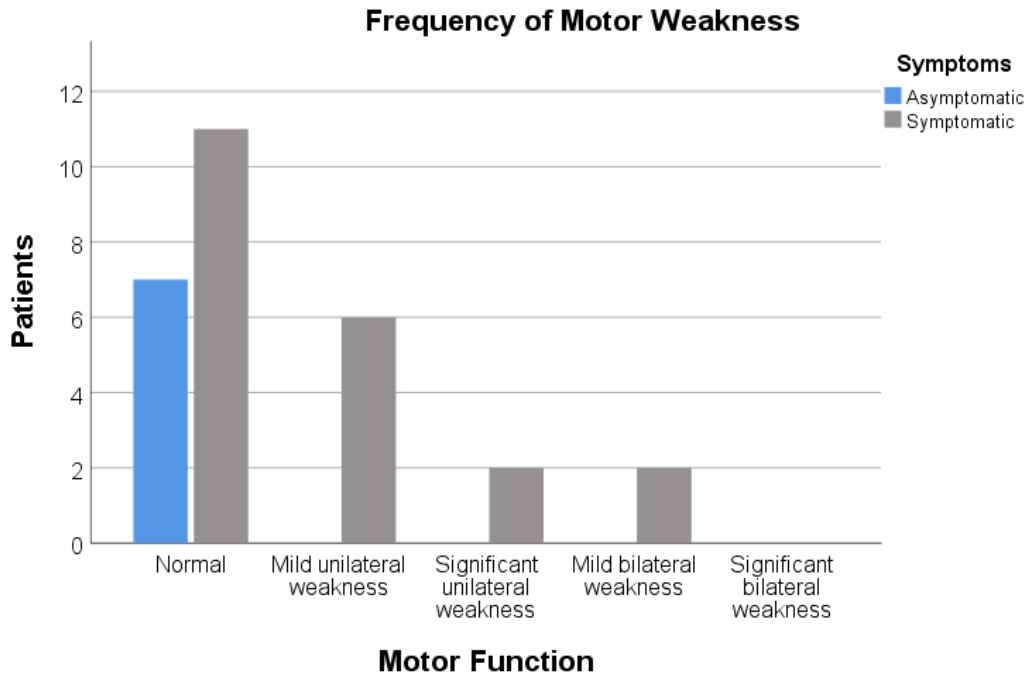


Figure IV.3.ia. Assessment of motor function in patients with LSL. Points were assigned to patients based on the severity of motor weakness: normal = 0, mild unilateral weakness = 1, significant unilateral weakness = 2, mild bilateral weakness = 3, significant bilateral weakness = 4. Comparison is made between symptomatic and asymptomatic patients.



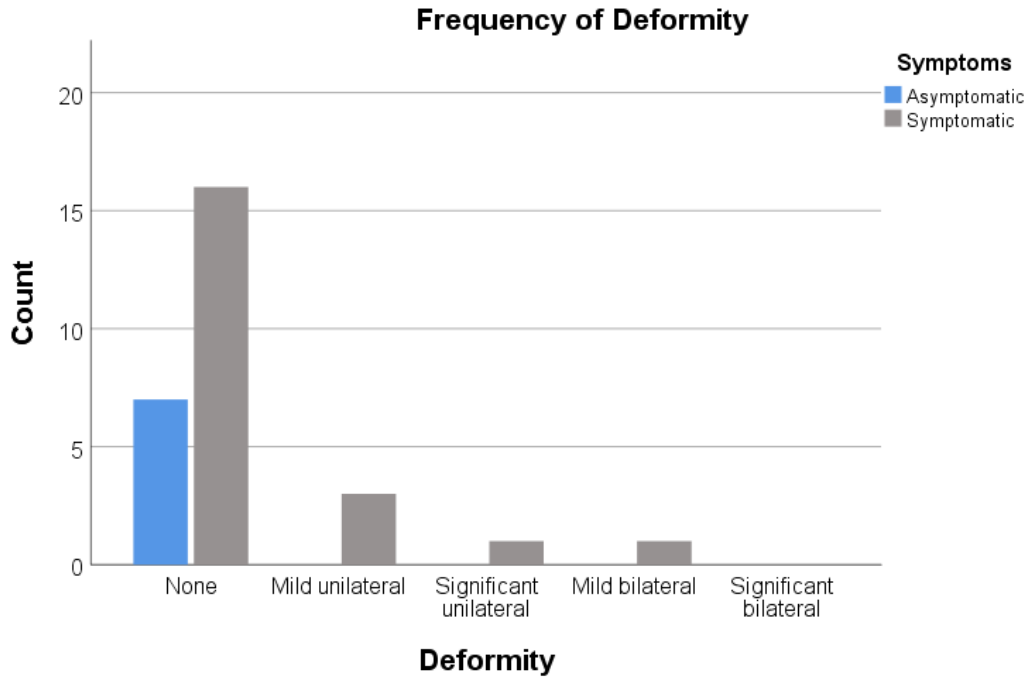


Figure IV.3.ib. Assessment of lower limb deformity in patients with LSL. Points were assigned to patients based on the severity of deformity: none = 0, mild unilateral = 1, significant unilateral = 2, mild bilateral = 3, significant bilateral = 4. Comparison is made between symptomatic and asymptomatic patients.

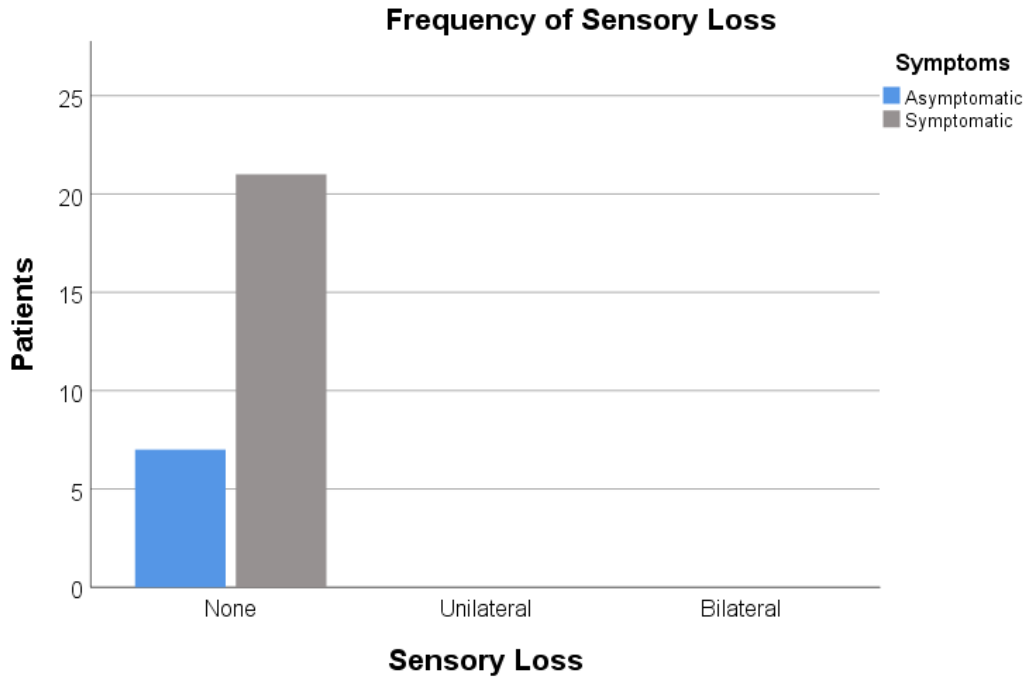


Figure IV.3.ic. Assessment of sensory loss in patients with LSL. Points were assigned to patients based on the extent of sensory loss: normal = 0, unilateral = 2, bilateral = 4. Comparison is made between symptomatic and asymptomatic patients.

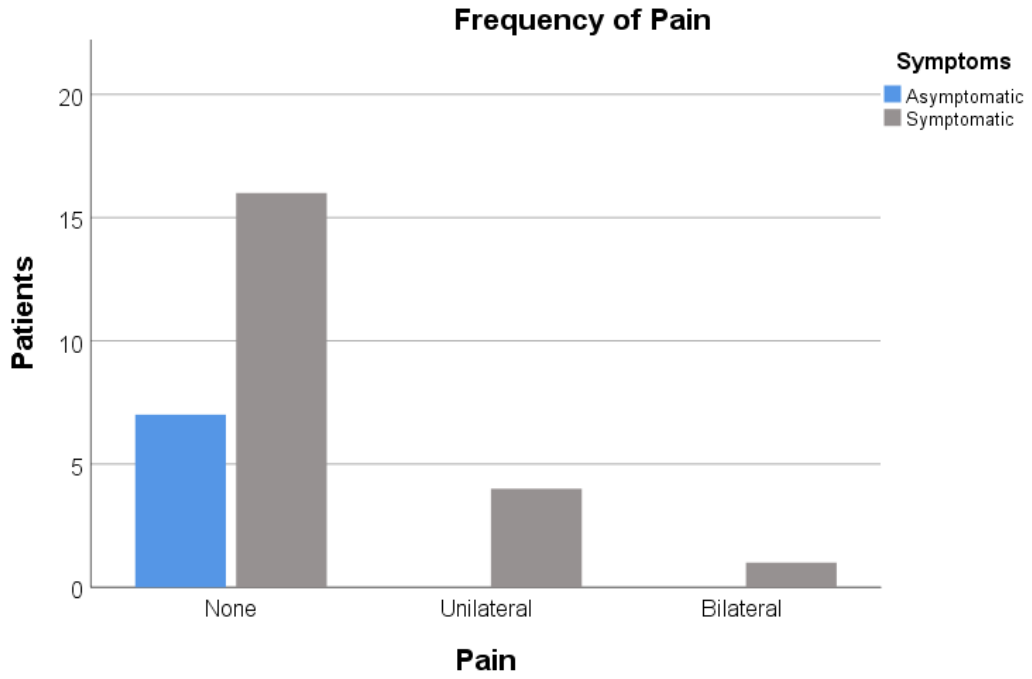


Figure IV.3.id. Assessment of lower limb pain in patients with LSL. Points were assigned to patients based on the extent of pain: none = 0, unilateral = 2, bilateral = 4. Comparison is made between symptomatic and asymptomatic patients

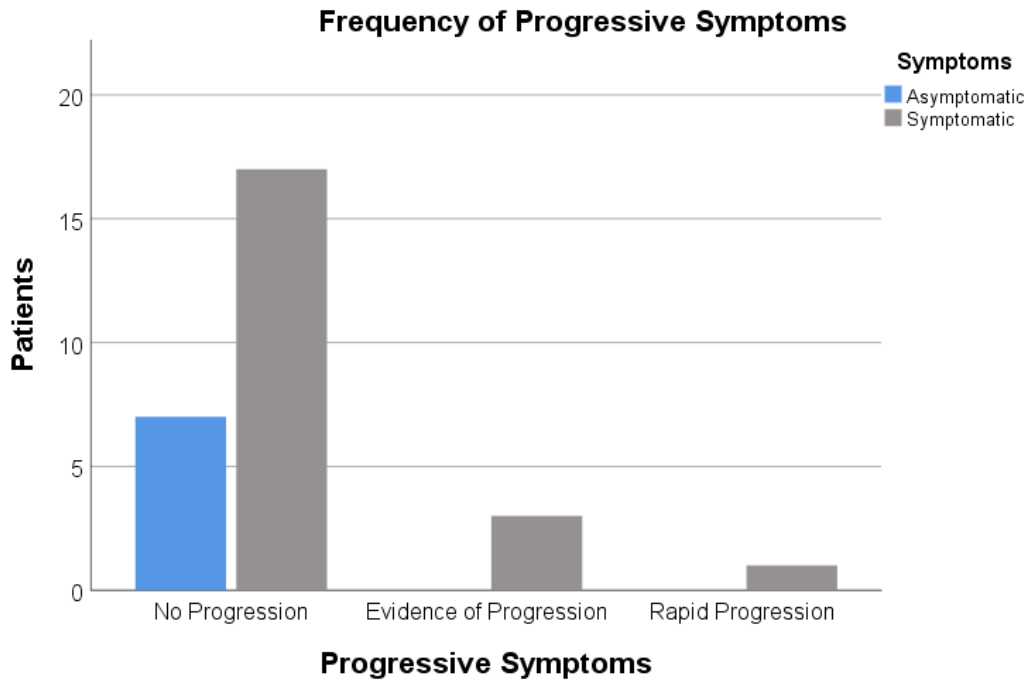


Figure IV.3.ii. Assessment of progression of symptoms in patients with LSL. Points were assigned to patients based on the extent of progression: none = 0, evidence of progression = 2, rapid progression = 4. Comparison is made between symptomatic and asymptomatic patients.

#### **Urological assessment**

All patients designated as asymptomatic had normal urological assessment although symptoms such as urgency and incontinence are difficult to assess in such a young cohort. Symptomatic patients had a range of different symptoms as well as signs identified following ultrasound investigation. Two symptomatic patients had no urological features on assessment (Figure IV.3.ii).

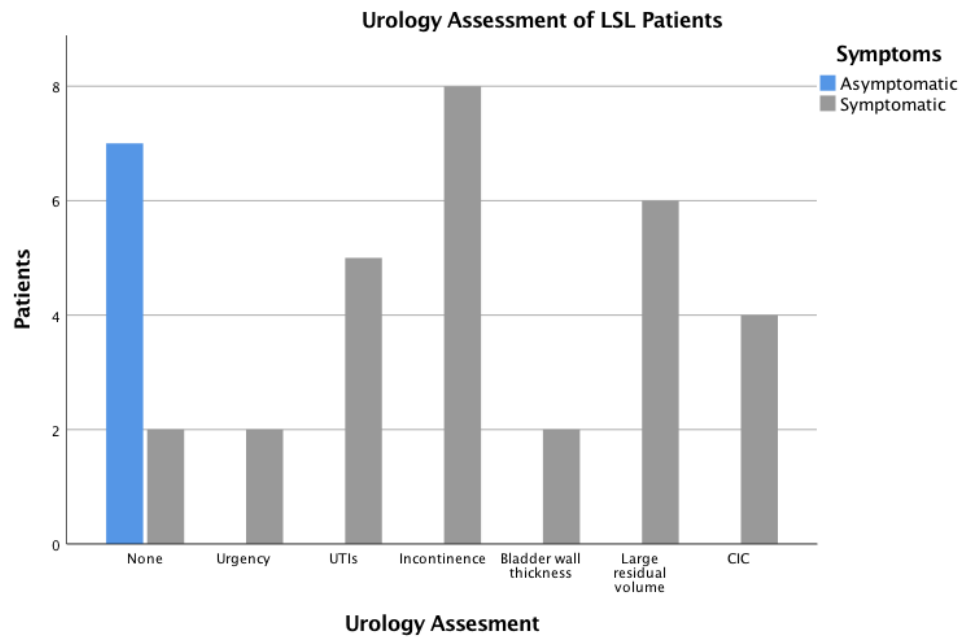


Figure IV.3.ii. Urological assessment in symptomatic LSL patients. UTI = urinary tract infection. CIC = clean intermittent catheterisation. One point was assigned to patients for each of the features identified on urological assessment with the exception of urgency and incontinence as these were deemed to be too subjective to be reliable.

The Total Clinical Score ranged from 0 to 9 with a mean of 2.76, a median of 0 and a positive skew distribution (Figure IV.3.iii). All asymptomatic patients scored 0, one symptomatic patient also scored 0. The Total Clinical Score (TCS) was correlated with targeted assay results in CSF, plasma and urine. The aim was to identify phospholipids that correlated well, either positively or negatively, with the TCS. Due to the skewed distribution, Spearman's rank correlation coefficient was used to determine significance.

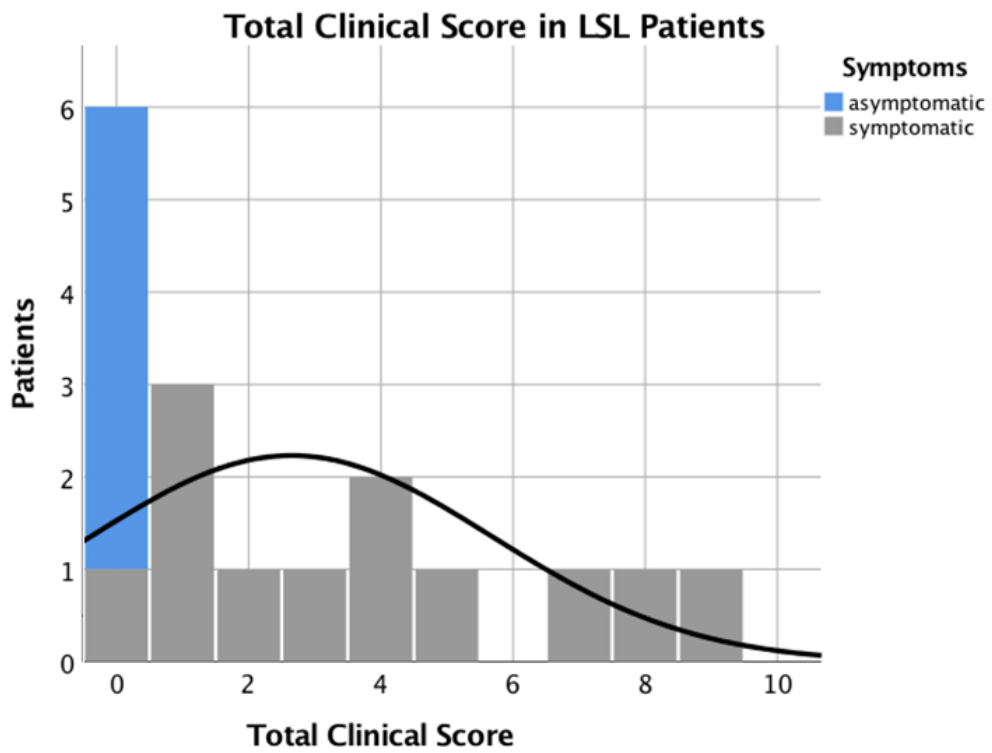


Figure IV.3.iii. Distribution of Total Clinical Score showing a positive skew. Black line indicates a normal distribution.

## CSF

Seventy-four phospholipids were detectable in CSF samples. One had a positive correlation with the Total Clinical Score (Figure IV.3.iv).

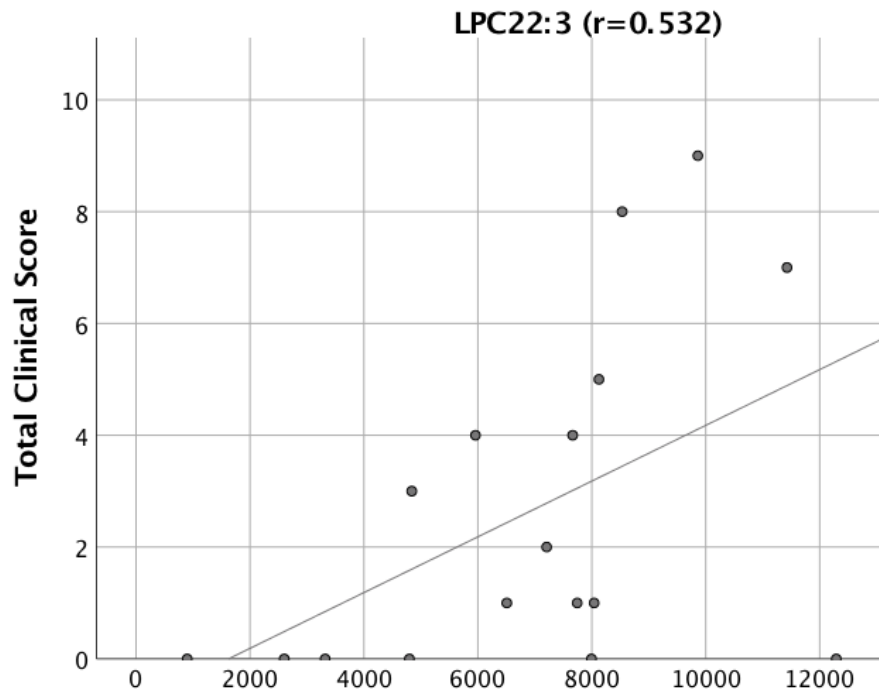


Figure IV.3.iv. Correlation of Total Clinical Score and intensity of signal of LPC 22:3 in CSF as per targeted assay ( $p=0.028$ ).

LPC 22:3 was also found to be significantly different on direct comparison between asymptomatic and symptomatic patients in CSF samples by targeted assay but was not identified in the top  $p$  values or  $\log_2$  fold changes for mass charge ratio-retention time pairings in Lipidomics 2.

## PLASMA

One hundred and thirty-four phospholipids were detected in plasma samples. When analysed against Total Clinical Score, five had a negative Spearman correlation coefficient less than -0.52, with 2 showing strong negative correlation ( $p < 0.01$ ) and 3 showing moderate negative correlation ( $p < 0.05$ , Figure IV.3.v).

### Plasma Phospholipids: Negative Correlation with Total Clinical Score

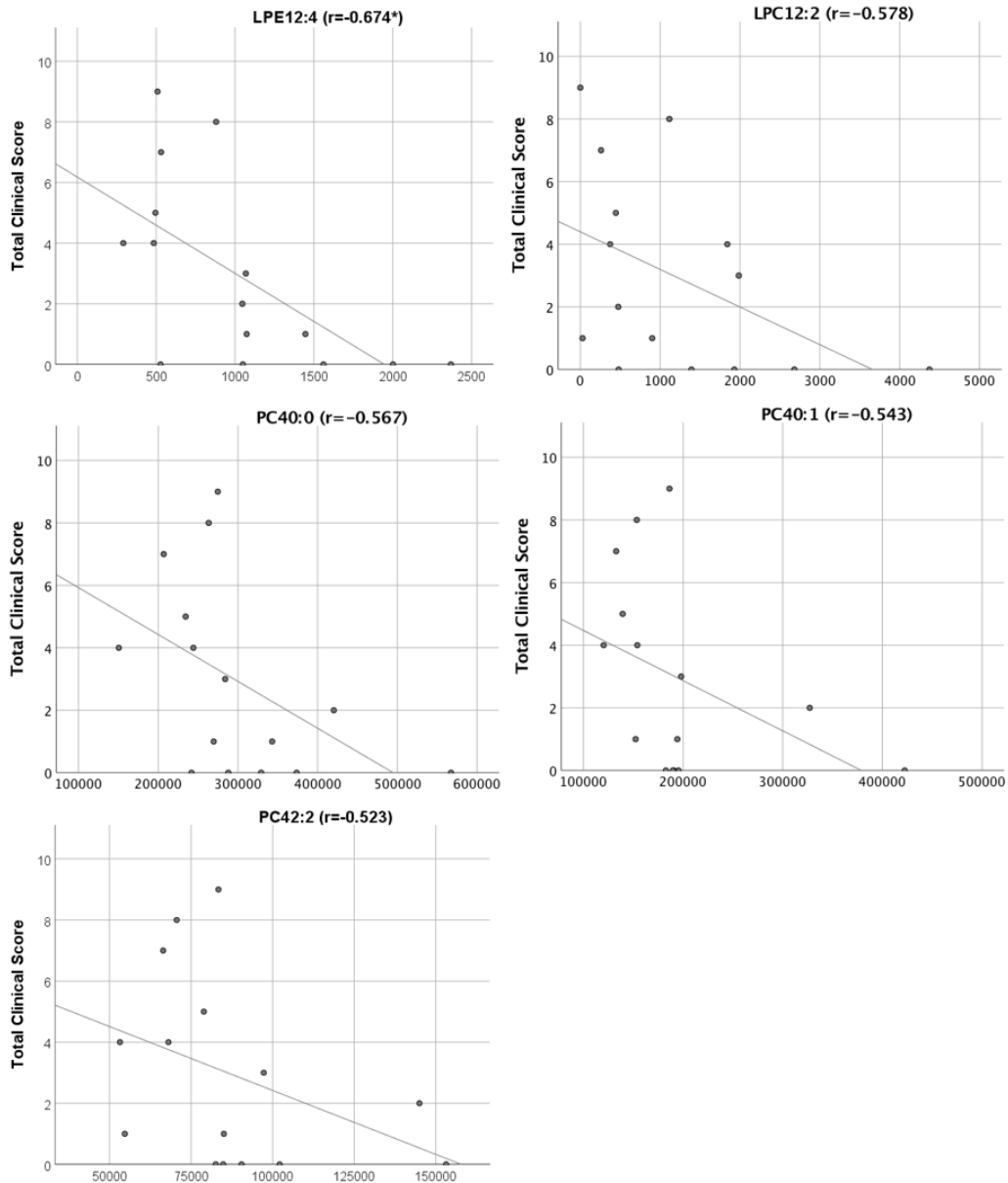


Figure IV.3.v. Five lipids showing negative correlation with Total Clinical Score (\* indicates  $p < 0.01$ ).

Of the 5 lipids that showed negative correlation with the Total Clinical Score, none showed a significant difference in plasma samples on targeted assay or lipidomics.



Nineteen phospholipids had a positive Spearman correlation coefficient greater than 0.52, with 4 showing strong positive correlation ( $p < 0.01$ ) and 15 showing moderate positive correlation ( $p < 0.05$ , Figure IV.3.vi).

### Plasma Phospholipids: Positive Correlation to Total Clinical Score

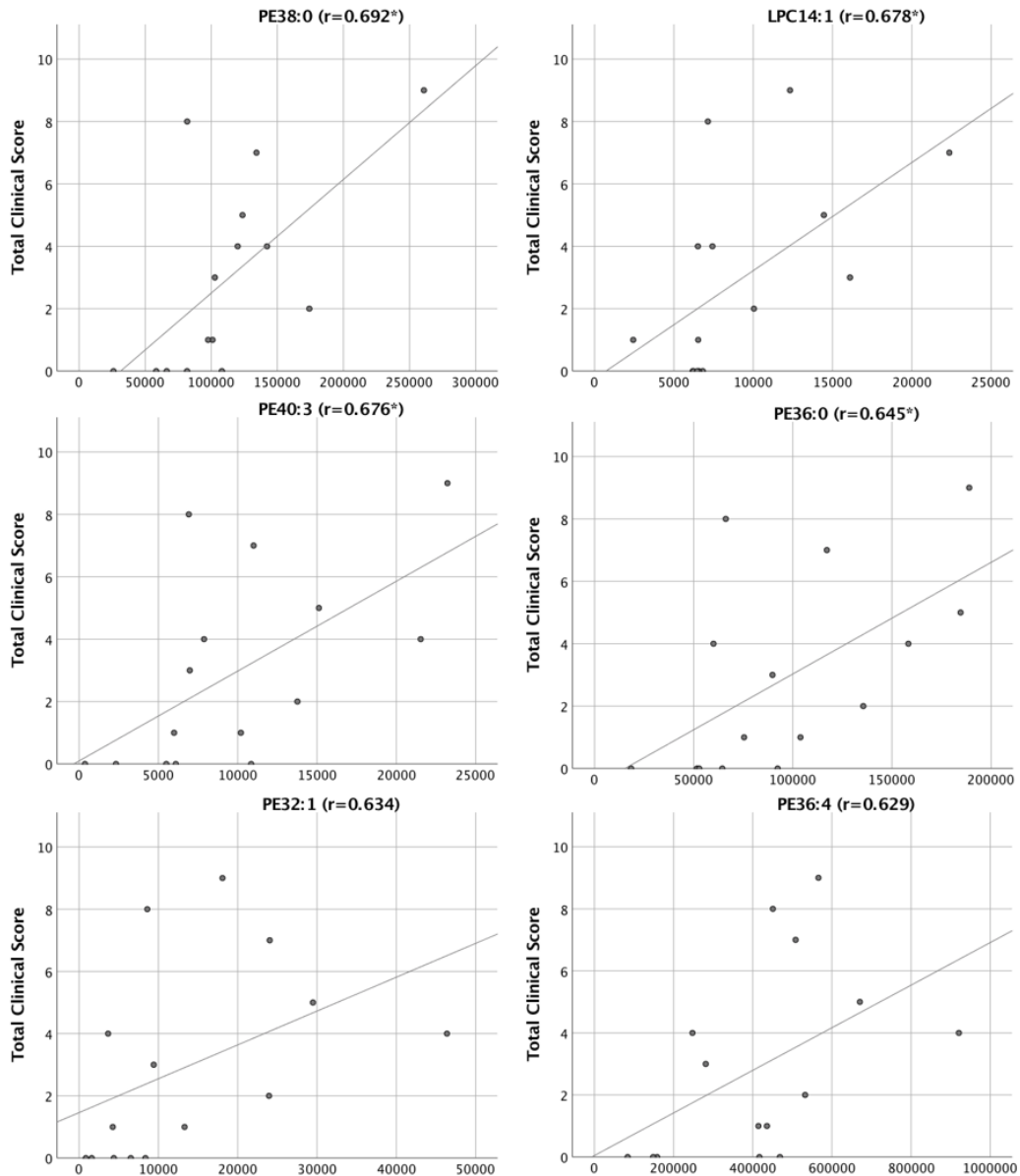


Figure IV.3.vi. Top 6 lipids in plasma samples showing positive correlation with Total Clinical Score. \* indicates  $p < 0.01$ . For other lipids see Supplementary Information.

Of the 19 lipids that showed positive correlation in plasma samples with the Total Clinical Score, one lipid was significantly different between LSL and control patients as well as between symptomatic and asymptomatic patient in plasma samples on targeted assay, LPC14:1. In addition, a further nine lipids showed a significant difference between symptomatic and

asymptomatic LSL patients in plasma samples on targeted assay (PE 32:3, 36:4, 38:2, 38:3, 38:4, 40:4 and PC 34:4, 36:2, 40:4). PE36:4 also came up as a possible match in Lipidomics 2 (LSL versus control).

## URINE

One hundred and fourteen phospholipids were detected in urine samples. Thirty had a negative Spearman correlation coefficient less than -0.57, with 1 showing strong negative correlation ( $p < 0.01$ ) and 29 showing moderate negative correlation ( $p < 0.05$ ). There was no significant positive correlation between phospholipids detected in urine samples and Total Clinical Score (Figure IV.3.vii).

### Urine Phospholipids: Negative Correlation to Total Clinical Score

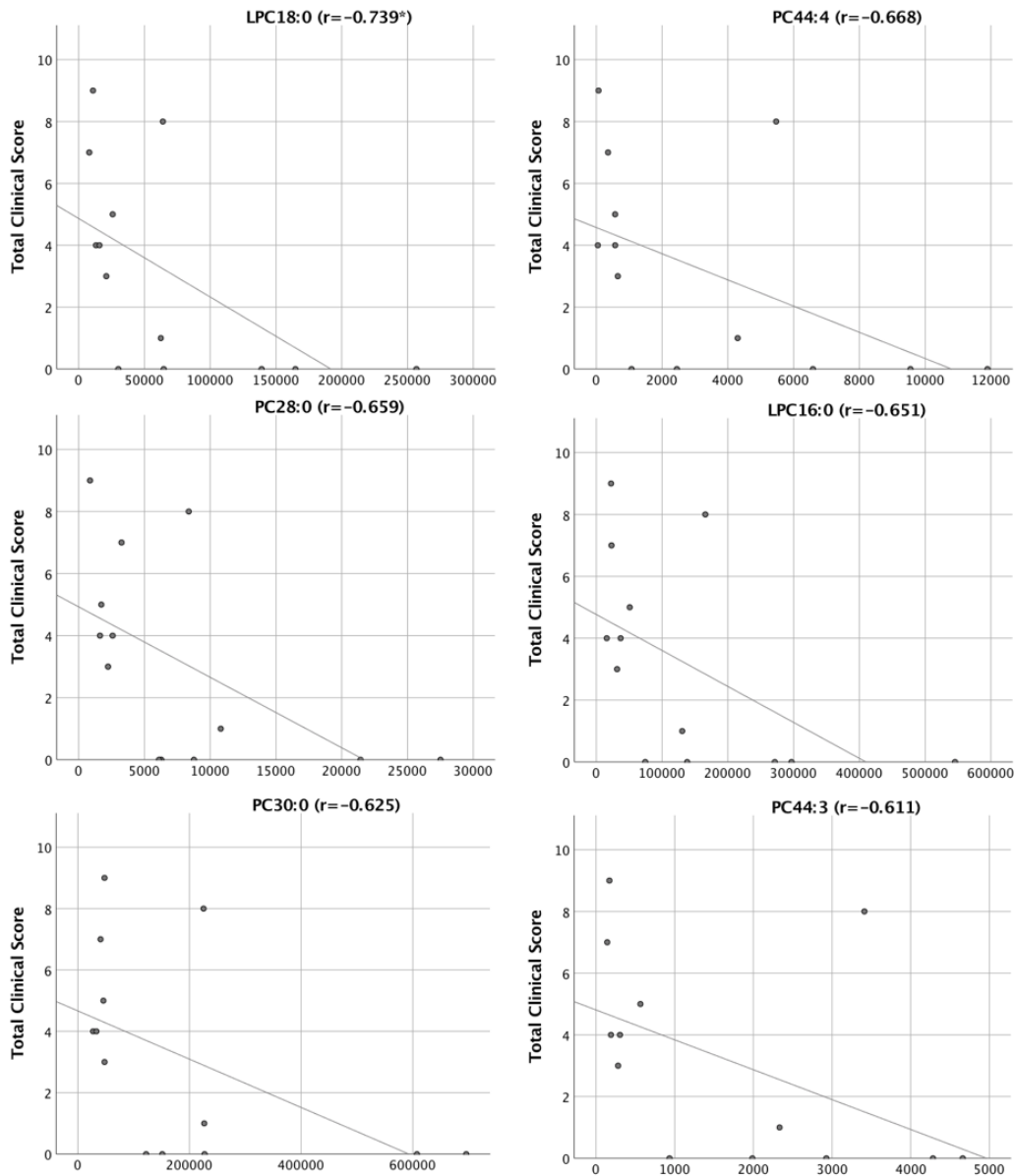


Figure IV.3.vii. Top 6 lipids in urine samples showing negative correlation with Total Clinical Score. \* indicates  $p < 0.01$ . For other lipids see Supplementary Information.

Of the 30 lipids that showed negative correlation in urine samples with the Total Clinical Score, nine also showed a significant difference between symptomatic and asymptomatic LSL patients

in urine samples on targeted assay (PC28:0, 28:1, 32:2, 32:4, 34:2, 34:4, 36:3, 36:4, and 38:4).  
In addition PC30:0 was also a potential match in Lipidomics 2 (LSL versus control).

### PC/PE RATIO

Total PC and PE values were calculated and a PC/PE ratio determined as discussed previously. There was a significant negative correlation with Total Clinical Score in plasma samples ( $p=0.031$ ). CSF and urine samples both showed a positive correlation with the PC:PE but this was not significant (Figures IV.3.viii a and b).

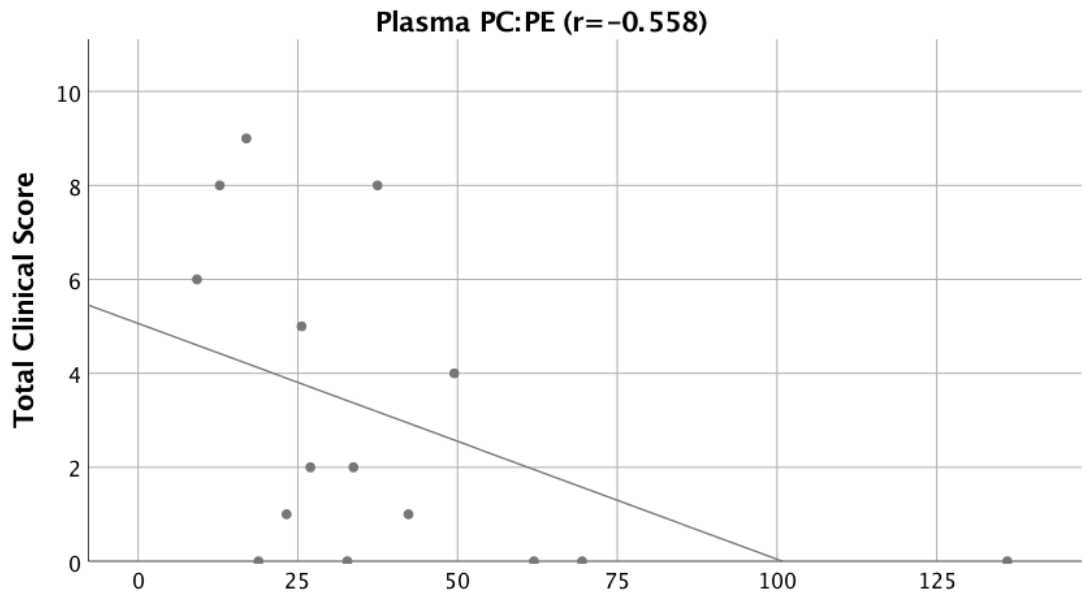


Figure IV.3.viii a Correlation of Total Clinical Score and PC/PE ratio in plasma samples.

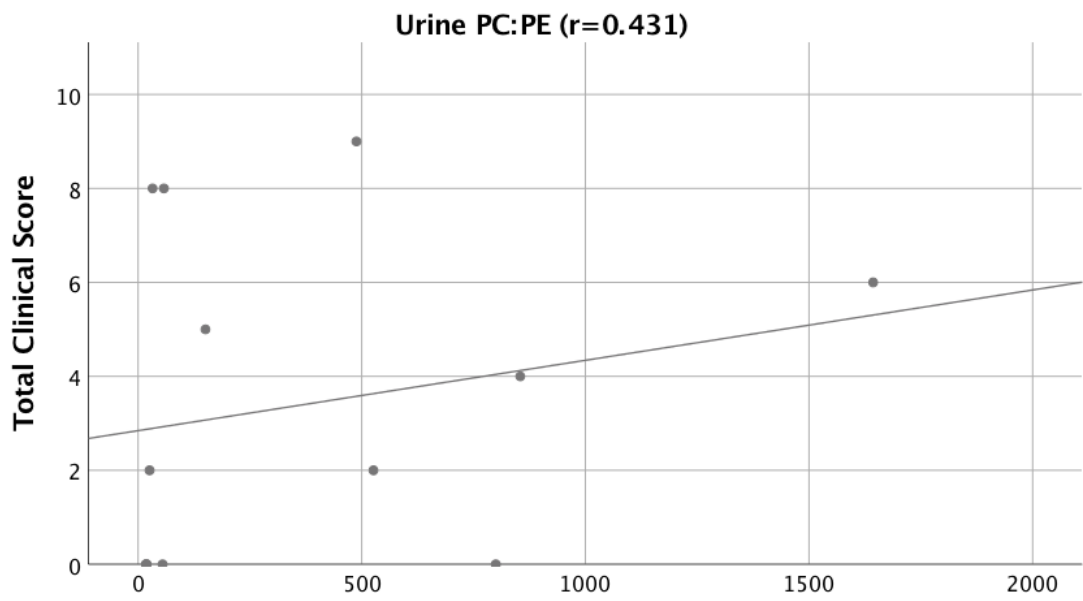
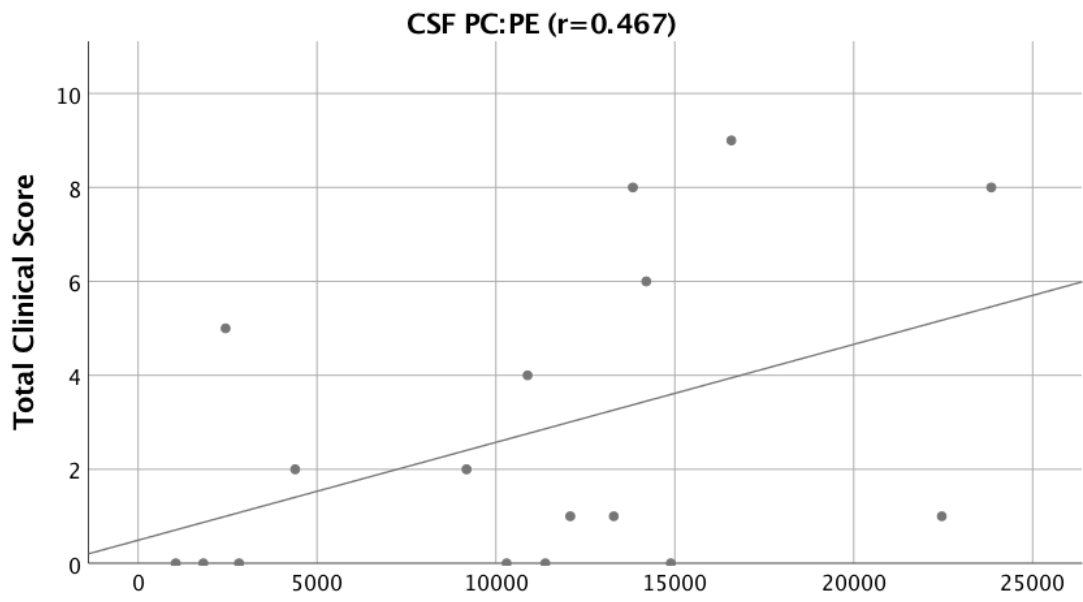


Figure IV.3.viii**b** Correlation of Total Clinical Score and PC:PE ratio in CSF and urine samples. Neither sample type shows significant correlation (CSF  $p=0.059$  and urine  $p=0.451$ ).

### LPC/PC and LPE/PE RATIOS

Total PC and LPC values were calculated along with total PE and LPE to generate a total LPC/PC ratio and LPE/PE ratio. Ratios were then correlated with the Total Clinical Score. There was no correlation with the TCS and LPC/PC ratio in any sample types ( $p>0.05$ ). In plasma samples there was a negative correlation between the TCS and LPE/PE ratio (Figure IV.3.ix).

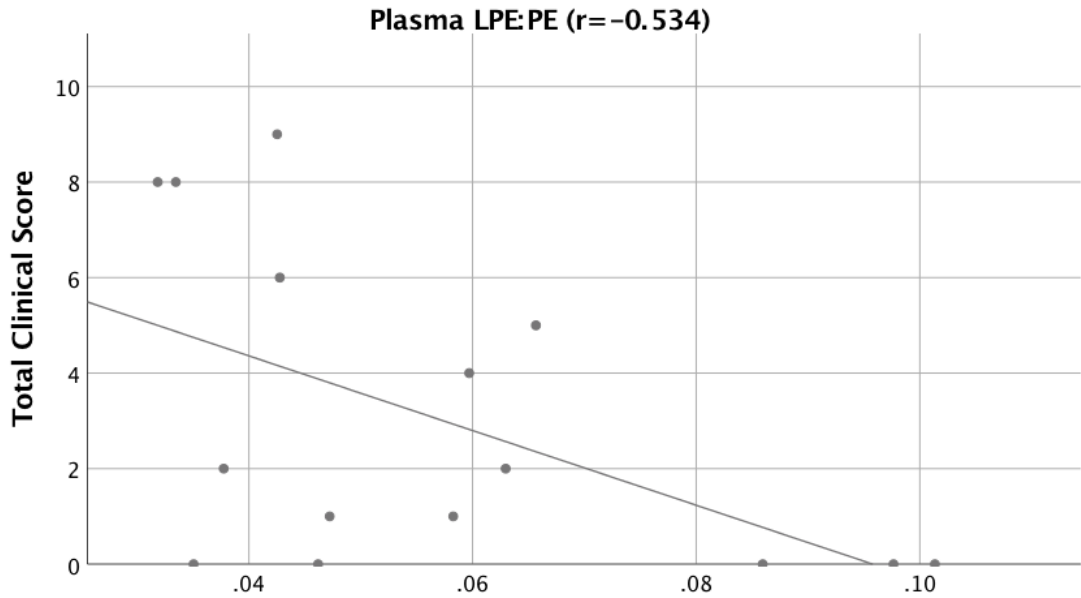


Figure IV.3.ix Correlation of Total Clinical Score and LPE/PE ratio in plasma samples ( $p=0.04$ ).

#### 4. NEUROPHYSIOLOGY

LSL is a dynamic pathology with the long term potential for children to develop urological and/or neurological disability. Regular assessment is required to ensure the safety of the upper renal tract as well as to optimise continence with many patients requiring clean intermittent catheterization in order to achieve these objectives. Assessment of young children is difficult and consists of a combination of clinical assessment, bladder and kidney imaging. There is no formal quantification or scoring of bladder function assessment that guides clinical management with expert interpretation required to make clinical decisions.

Neurophysiological monitoring is routinely used intra-operatively in an attempt to ensure maintenance of nerve function during surgery and prevent unintentional neurological injury [208]. Following near total resection of LSL, children still require prolonged follow-up to ensure that neurological and urological function are maintained. Although the role of intra-operative neurophysiology monitoring (IONM) in LSL surgery is now reasonably established, how this corresponds with pre-operative symptoms and longer-term outcome in LSL is unclear.

The pre-operative clinical state is particularly difficult to assess with the median age of children in this study being 26 months at the time of surgery. Of particular concern is the ability to detect evolving urological dysfunction in children who are still in nappies and children being able to cooperate sufficiently to allow accurate measurements of void and residual volumes. There is potential for IONM to add to the overall clinical picture, giving a more definitive assessment of caudal spinal cord and nerve root function. In addition, IONM might in itself be useful as an objective measure or biomarker to predict longer-term outcome, although as this is an intraoperative procedure this is only relevant to patients who have already undergone surgery.

To address the usefulness of invasive neurophysiology measurements as a biomarker of subsequent clinical progression, this study addressed several questions: Do pre-operative neurophysiology measurements correspond with the clinical classification of patients as asymptomatic or symptomatic? Do post-operative neurophysiological measurements correspond with long-term outcomes? Do any phospholipids measured by targeted assay correspond with any or all components of the neurophysiology assessment?

A total of 31 patients underwent LSL surgery with intraoperative neurophysiological monitoring, during the period 2015-2017. This timeframe was selected to allow subsequent follow-up to assess outcome. Patients who had missing results, most often due to technical reasons, were excluded. Patients who did not have local follow-up were also excluded. Recordings were taken once the patient was anaesthetised but prior to the commencement of surgery (pre-operative) and after completion of near total resection of the LSL tissue (post-operative). All IONM was performed by IJ. The mean age at time of surgery was 50 months with a median of 26 months. Eleven children were in nappies at the time of surgery and eleven children had already commenced CIC. Patients were classed as symptomatic based on a full clinical assessment,



including both neurological and urological assessment. A patient who was still in nappies could still be considered asymptomatic if there was good evidence of improving bladder control (long periods of a dry nappy), commencement of potty training with beginning to develop ability to empty bladder on command, and residual post void percentage < 20%. Of the 31 patients, 22 were classed as symptomatic and 9 as asymptomatic.

Twenty-four children had a 'normal' baseline BCR, of which five had already commenced CIC. Twenty-six children had a 'normal' baseline Sphincter MEP, of which eight had already commenced CIC. All patients assessed had normal sensory electrophysiology, whilst 26 out of 31 patients' motor recordings were normal. A summary of clinical features and IONM results can be found in Table IV.4.i.

### **Pre-operative IONM and clinical assessment**

The first aim was to address the question: do the clinical terms "symptomatic" and "asymptomatic" accurately reflect the pre-operative neurophysiological assessment of patients? As no baseline was available at the beginning of surgery, all components of IONM were classified as being either present or absent. If all components were present the IONM was considered to be 'normal', if one or more component was absent the IONM was considered to be 'abnormal'. In addition, individual components of pre-operative IONM were compared with clinical classification. BCR, sphincter MEPs, SSEPs and TcMEPs were also considered to be 'normal' or 'abnormal' depending on whether they were present or absent respectively.

2x2 tables were generated and can be found in Supplementary Information. As the sample size was small and some cells had a count of less than five, Fisher's Exact Test was performed rather than a Chi-squared test. These results can be seen at the bottom of Table IV.4.i.

| Patient No.    | Clinical | BCR   | Sphincter MEPs | TcMEPs | SSEPs | Total IONM |
|----------------|----------|-------|----------------|--------|-------|------------|
| 1              | Nappies  | +     | +              | +      | +     | +          |
| 2              | CIC      | +     | +              | +      | +     | +          |
| 3              | CIC      | -     | -              | +      | +     | -          |
| 4              | Nappies  | -     | +              | +      | +     | -          |
| 5              | Nappies  | +     | +              | +      | +     | +          |
| 6*             | Dry      | +     | +              | +      | +     | +          |
| 7              | CIC      | -     | +              | +      | +     | -          |
| 8              | CIC      | +     | +              | +      | +     | +          |
| 9              | Wetting  | +     | +              | +      | +     | +          |
| 10             | Nappies  | +     | -              | +      | +     | -          |
| 11*            | Dry      | +     | +              | +      | +     | +          |
| 12             | Dry      | +     | +              | +      | +     | +          |
| 13             | CIC      | +     | +              | +      | +     | +          |
| 14             | CIC      | -     | +              | +      | +     | -          |
| 15*            | Dry      | +     | +              | -      | +     | -          |
| 16             | Dry      | +     | +              | +      | +     | +          |
| 17*            | Nappies  | +     | +              | -      | +     | -          |
| 18*            | Dry      | +     | +              | +      | +     | +          |
| 19*            | Dry      | +     | +              | +      | +     | +          |
| 20*            | Nappies  | +     | +              | +      | +     | +          |
| 21*            | Nappies  | +     | +              | +      | +     | +          |
| 22             | Nappies  | +     | +              | +      | +     | +          |
| 23*            | Nappies  | +     | +              | +      | +     | +          |
| 24             | Nappies  | +     | +              | -      | +     | -          |
| 25             | CIC      | -     | +              | +      | +     | -          |
| 26             | CIC      | +     | +              | +      | +     | +          |
| 27             | CIC      | +     | +              | +      | +     | +          |
| 28             | Dry      | +     | -              | -      | +     | -          |
| 29             | CIC      | -     | -              | +      | +     | -          |
| 30             | CIC      | -     | -              | -      | +     | -          |
| 31             | Nappies  | +     | +              | +      | +     | +          |
| Fisher's Exact |          | 0.077 | 0.286          | 0.613  |       | 0.418      |

Table IV.4.i. Summary of IONM results at the initiation of surgery. CIC = Clean intermittent catheterisation. Patient No. marked with an \* indicate those patients who were considered to be asymptomatic. Fisher's Exact Test 2-sided p-values quoted at the bottom of each column.

No association was found between symptoms and total pre-operative IONM ( $p=0.418$ ). Similarly, no association was found between symptoms and BCR ( $p=0.077$ ), Sphincter MEP ( $p=0.286$ ), or TcMEPs ( $p=0.613$ ). As all patients had 'normal' SSEPs it was not possible to perform Fisher's Exact Test.

### **BCR/sphincter MEPs and long-term outcome**

To generate receiver operator characteristic (ROC) curves and determine the optimum predictive power of IONM, an IONM score needed to be generated, and an outcome determined. Post-operative IONM was compared to the baseline pre-operative IONM. This allowed further classification of each IONM category as either present, reduced or absent and scores 2,1 and 0 to be assigned respectively. Left and right-sided results were summed to give a total score of 4 for each of BCR and Sphincter MEPs. Due to the timeframe of the study two different outcomes were considered: the need for initiation of CIC and abnormal post residual void percentage at 3-month follow-up assessment. The need for initiation of CIC was considered to be the most significant in terms of patient experience and so this was selected as the outcome state first. ROC curves were plotted with BCR and Sphincter MEPs scores against the outcome to determine the optimum threshold of BCR and Sphincter MEP scores at predicting the outcome. Post-operative BCR measurements of 3 or more were the most predictive of not needing to initiate CIC with a maximum sensitivity of 80% (Figure IV.4.i). This score could only be achieved by normal intra-operative neurophysiological measurements on both sides, or a normal measurement on one side and a reduced (but not absent) measurement on the contralateral side.

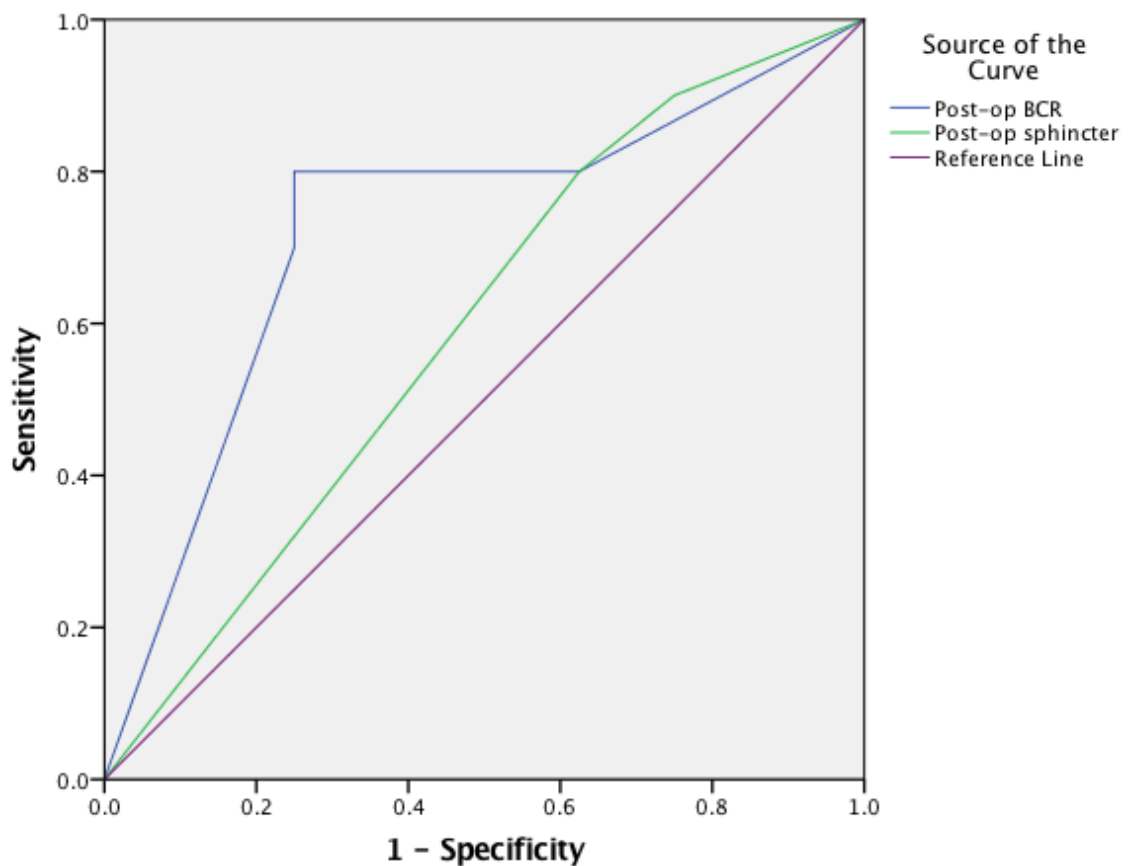


Figure IV.4.i ROC curve of the predictive value of post-operative BCR for not needing clean intermittent catheterisation at the time of urological follow up at 3 months. BCR has both a higher sensitivity and specificity when compared to sphincter MEPs. Reference line represents results produced by ties.

As described in Section III.2 the residual post-void percentage was calculated and a value of less than or equal to 20% was taken as an indication of normal bladder function. This does not take into account other parameters that are assessed during bladder function assessment. There was a low predictive value of both BCR and sphincter MEPs in predicting a normal post-void percentage post-operatively (Figure IV.4.ii).

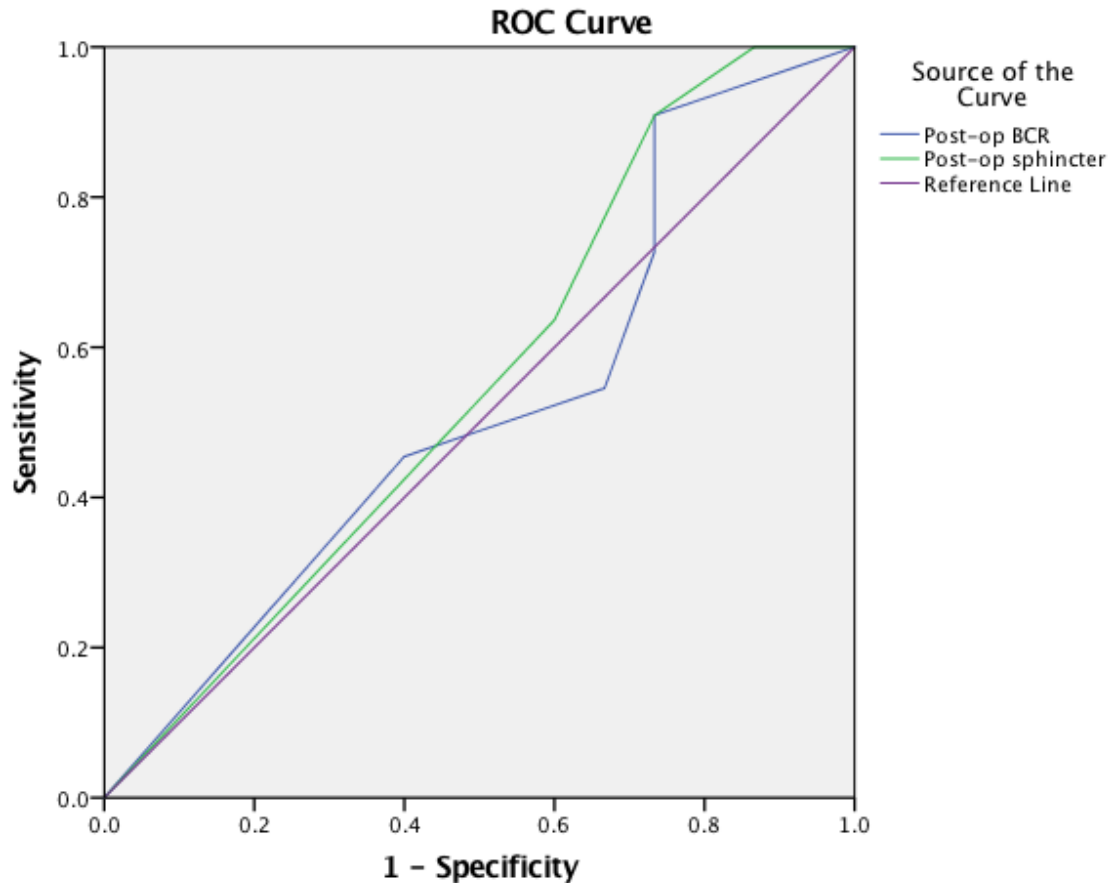


Figure IV.4.ii. ROC curve of the predictive value of post-operative BCR for normal post-void residual percentage at the time of urological follow up at 3 months. Both BCR and sphincter MEPs approximate to the reference line indicating a low predictive value and a sensitivity and specificity close to chance.

These data suggest that BCR is a more sensitive measure of neurological function than Sphincter MEPs and may indicate neurological damage before it becomes clinically apparent.

#### **Intra-operative assessment**

IONM is performed to minimise neurological injury during invasive spinal procedures such as LSL surgery. BCR and sphincter MEPs are considered to be a more sensitive measurement of neurological function as the pathways involved are the first to become disrupted in nerve and spinal cord damage. It is likely that a mild degree of nerve damage often happens during these operations. To support the above hypothesis that BCR is a more sensitive measure of neurological function than Sphincter MEPs pre-operative and post-operative IONM results were compared. As post-operative IONM was scored on a 4-point system, a new system was developed for scoring pre-operative IONM to match this. In lieu of an external baseline, the contralateral recordings were considered as a baseline such that if one side was notably less than the other it would score 1. Absent recordings scored 0 and 'normal' recordings scored 2. As before left and right sides were summed to give a total score of 4.

A paired two-tailed t-test was performed to compare mean pre-operative BCR with mean post-operative There was a mean drop from 3.19 to 2.32 in BCR recordings with a significant difference of  $p = 0.003$ . Comparison was also made between pre-operative Sphincter MEPs and post-operative measurements. There was a mean drop from 3.26 to 3.10 with no significant difference between these two values  $p = 0.283$  (Figure IV.4.iii).

A greater and significant difference between pre- and post-operative BCR recordings supports the hypothesis that BCR is a more sensitive measure of intraoperative neurophysiology than sphincter monitoring.

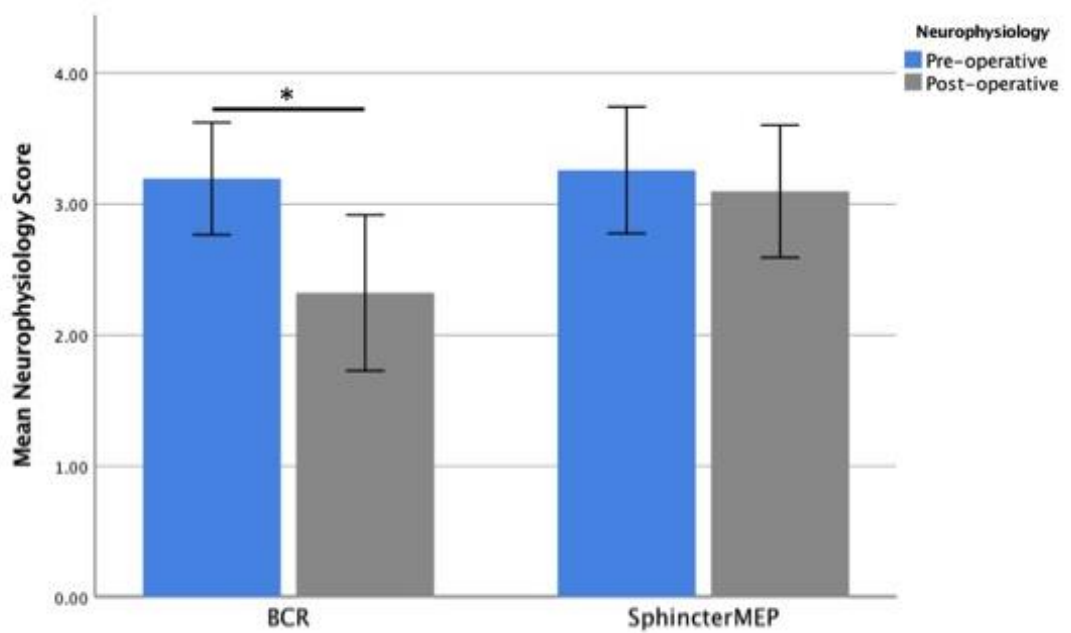


Figure IV.4.iii. Comparison between pre-operative and post-operative mean BCR and mean sphincter MEPs. BCR shows a significant difference between pre- and post-operative. Error bars at 95% confidence interval.

**Abnormal BCR v. normal BCR**

Of those patients with LSL that were recruited and had samples collected for targeted lipid assay, baseline BCR recordings (after general anaesthesia and prior to initiation of surgery) were considered to be normal in 11 patients and abnormal in 9 patients. The remaining 11 LSL patients did not have complete intra-operative neurophysiology data collected.

**CSF**

Targeted assay results were compared between those patients with normal and patients with abnormal BCR recordings at the beginning of surgery. There were no significantly different lipids in CSF samples between abnormal BCR and normal BCR recordings in patients (Figure IV.4.iv). Combined PC and PEs were calculated to generate a PC/PE ratio as previously. There was no significant difference in the ratio between the abnormal BCR group and the normal BCR. Similarly, LPC/PC and LPE/PE ratios were calculated and there was no significant difference in these ratios between the two groups in CSF samples.



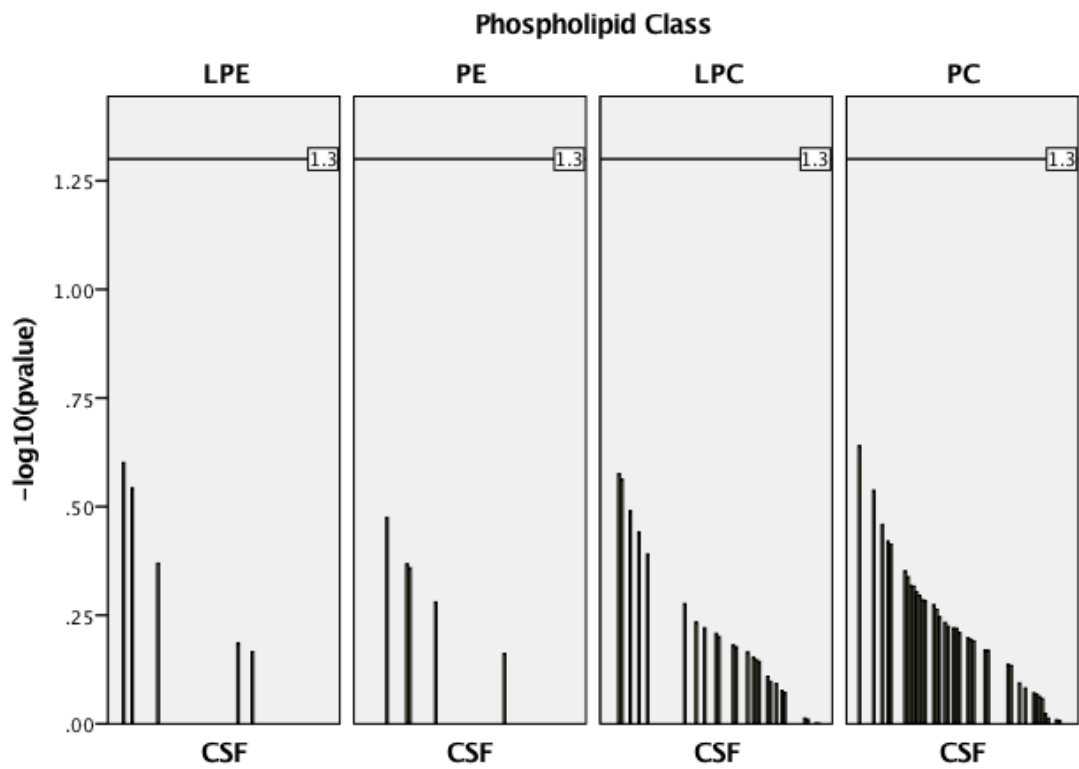


Figure IV.4.iv. Targeted phospholipid assay comparing means between patients with abnormal BCR recordings at the beginning of surgery and patients with normal BCR recordings at the beginning of surgery. Index line marks 1.3 ( $p < 0.05$ ).

## Plasma

Targeted assay results were compared between those patients with normal and patients with abnormal BCR recordings at the beginning of surgery. There were 13 significantly different lipids in plasma samples between abnormal BCR and normal BCR recordings in patients (Figures IV.4.va and b).

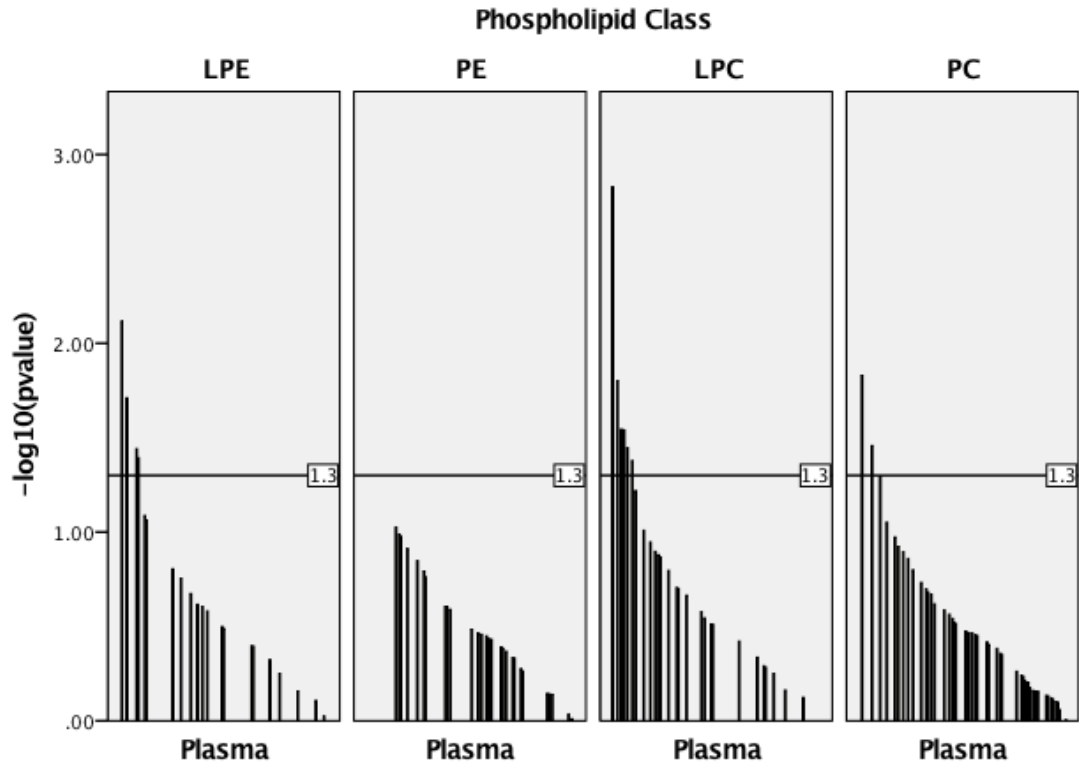


Figure IV.4.va. Targeted phospholipid assay comparing means between patients with abnormal BCR recordings at the beginning of surgery and patients with normal BCR recordings at the beginning of surgery. Index line marks 1.3 ( $p < 0.05$ ). Significantly different lipids found in plasma between abnormal and normal BCR recordings: LPE 18:4 ( $p=0.0076$ ), 18:3 ( $p=0.0195$ ), 16:4 ( $p=0.0363$ ), 20:0 ( $p=0.0405$ ); LPC 18:3 ( $p=0.0015$ ), 18:2 ( $p=0.0158$ ), 16:3 ( $p=0.0286$ ), 18:0 ( $p=0.0287$ ), 20:0 ( $p=0.0288$ ), 18:4 ( $p=0.0358$ ), 18:1 ( $p=0.0419$ ); and PC 28:1 ( $p=0.0148$ ), 32:1 ( $p=0.0350$ ).

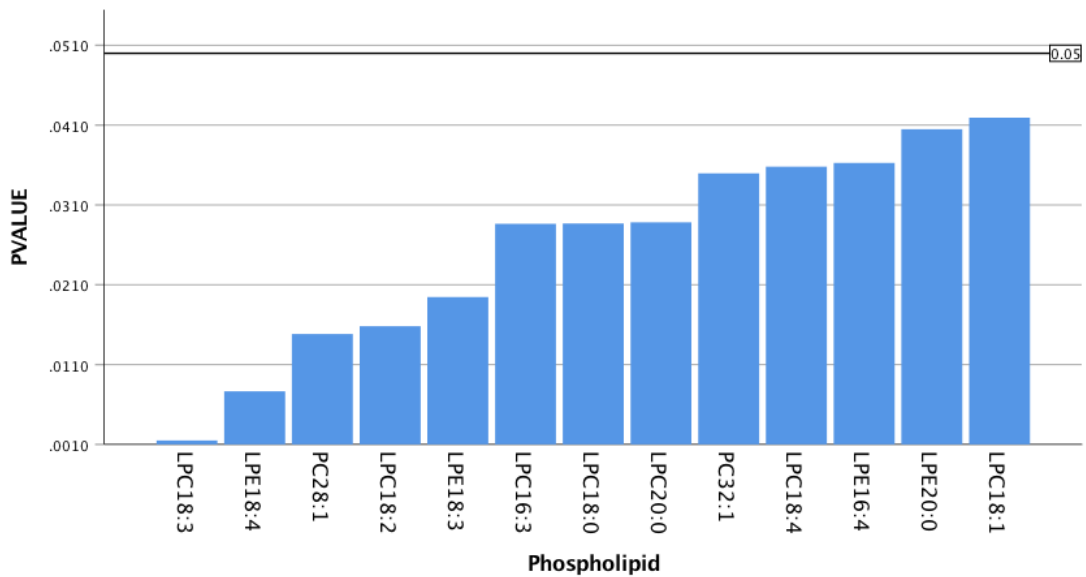


Figure IV.4.vb. Summary of phospholipids identified by targeted assay with a significant difference ( $p < 0.05$ ) in plasma samples between abnormal BCR and normal BCR recordings in patients. Note: phospholipids are ranked from smallest p-value (most significant; on the left side) to largest p-value (least significant; on the right side).

Three patients with grossly abnormal BCR recordings were removed from the data set and the analysis repeated. All of these 3 patients were considered to be clinically symptomatic, two required CIC prior to surgery and the third had multiple episodes of incontinence. Four phospholipids were significantly different in plasma samples between those patients that had normal BCR recordings and those patients that had moderately abnormal BCR recordings: LPE 18:3 ( $p=0.018$ ), LPC 18:3 ( $p=0.029$ ), LPE 18:4 (0.036) and PE 34:3 ( $p=0.046$ ).

Combined PC and PEs were calculated to generate a PC/PE ratio as previously. There was no significant difference in the ratio between the abnormal BCR group and the normal BCR. Similarly, LPC/PC and LPE/PE ratios were calculated and there was no significant difference in these ratios between the two groups in plasma samples.

## Urine

Targeted assay results were compared between those patients with normal and patients with abnormal BCR recordings at the beginning of surgery. There was 1 significantly different lipid in urine samples between abnormal BCR and normal BCR recordings in patients (Figure IV.4.vi).

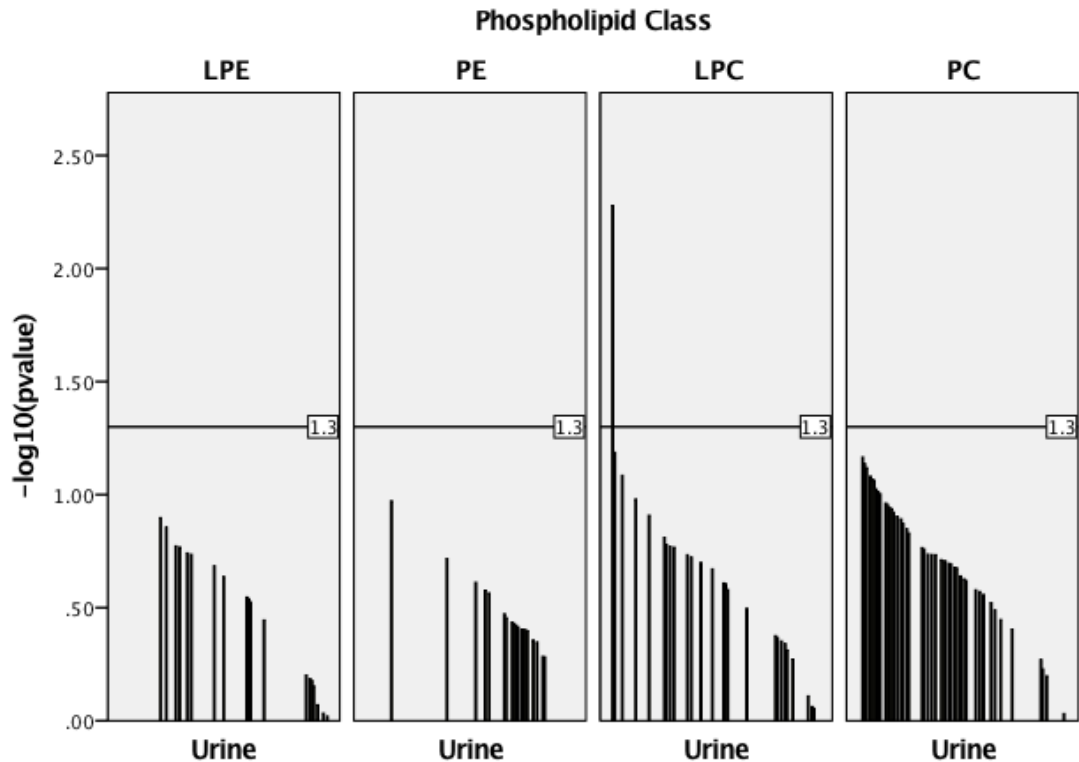


Figure IV.4.vi. Targeted phospholipid assay comparing means between patients with abnormal BCR recordings at the beginning of surgery and patients with normal BCR recordings at the beginning of surgery. Index line marks 1.3 ( $p < 0.05$ ). Significantly different lipid LPC 24:1 ( $p = 0.0053$ ) identified in urine samples.

As previously, the same 3 patients with grossly abnormal BCR recordings were removed from the data set and the analysis repeated. LPC 24:1 ( $p = 0.037$ ) remained significantly different in urine samples between those patients that had normal BCR recordings and those patients that had moderately abnormal BCR recordings.

Combined PC and PEs were calculated to generate a PC/PE ratio as previously. There was no significant difference in the ratio between the abnormal BCR group and the normal BCR. Similarly, LPC/PC and LPE/PE ratios were calculated and there was no significant difference in these ratios between the two groups in urine samples. There was however a significant difference in the LPE/LPC ratio between abnormal and normal BCR recordings pre-operatively ( $p = 0.04$ ). This same difference was not seen in plasma or CSF samples but it was also present once patients with grossly abnormal BCR recordings were removed from the cohort ( $p = 0.043$ ).

## 5. COMBINED ANALYSIS RESULTS

Results from Lipidomics and Targeted Assays were compared to establish key candidates for a LSL prognostic biomarker. Any lipids that were significantly different in CSF samples, and also found to be significantly different in plasma and urine in Lipidomics, are highlighted below. Similarly any lipids significantly different in CSF samples, and also found to be significantly different in plasma and urine in Targeted Assay, are also highlighted. Due to the criterion that would have to be met for the above to be a meaningful biomarker: no metabolism of key lipids between different fluid compartments, lipids will also be reviewed with focus on an individual fluid compartment. For example, CSF results are compared across Targeted Assay, Clinical Correlation and BCR results. Any lipids identified as candidate biomarkers are then compared with the extended Lipidomics database search results, and candidates are discussed in more detail in terms of the evidence supporting a role as a biomarker and evidence from the literature supporting a potential mechanisms in LSL disease progression.

### Lipidomics

Lipids potentially identified in Lipidomics 1 and Lipidomics 2 as being significantly different in all three sample types: CSF, plasma and urine are summarised below (Table IV.5.i).

| Lipid Class | Lipidomics 1 | Lipidomics 2: LSL versus control | Lipidomics 2: symptomatic versus asymptomatic |
|-------------|--------------|----------------------------------|---|
| PE          | LPE 16:1     | PE 36:2<br>PE 38:2 (OH)          | LPE 26:2                                      |
| PC          | PC 28:4      | PC 30:0                          |   |
| PA          |              | PA (P-38:0)                      |   |
| TG          | TG 58:9      |                                  |   |

Table IV.5.i. Summary of data from Lipidomics Results. Lipids were detected in all three sample types. As discussed in Section IV.1, lipids were identified by database search and should not be considered definitive confirmation of an exact lipid.

No single lipid was highlighted in both Lipidomics 1 and Lipidomics 2. Similarly, no single lipid was highlighted in both LSL versus control and symptomatic versus asymptomatic samples.

### Targeted Lipid Assay

No lipids were detected by targeted assay as being significantly different in all three sample types: CSF, plasma and urine. Results summarised below are those lipids that were significantly different in plasma and urine samples (Table IV.5.ii).

| Lipid Class | Targeted Assay:<br>LSL versus control | Targeted Assay:<br>symptomatic versus asymptomatic |
|-------------|---------------------------------------|--|
| LPE         | -                                     | -  |
| PE          | -                                     | -  |
| LPC         | -                                     | -  |
| PC          | -                                     | PC 32:2, 32:4<br>PC 34:4<br>PC 36:2<br>PC 40:4     |

Table IV.5.ii. Summary of data from Targeted Assay Results.

No lipids were detected as being significantly different in more than one sample type in LSL versus control samples. Candidate lipids do not correspond with potential results highlighted by Lipidomics in Table IV.5.i. The extended database of potential identity of lipids detected by Lipidomics was reviewed for any potential matches with the targeted assay results. The closest match to any of the lipids listed in Table IV.5.ii was PC (40:4(OH)). However, this potential match was in CSF not plasma or urine.

### Targeted Lipid Assay, Clinical Assessment and Neurophysiology

No lipids showed good correlation in all three sample types between clinical score and lipid signal intensity. Three lipids showed correlation in both plasma and urine samples (Table IV.5.iii). No lipids were significantly different in more than one sample type when compared to BCR results.

| Lipid Class | Positive Correlation Plasma<br>Negative Correlation Urine | Negative Correlation Plasma and<br>Urine |
|-------------|---|--|
| LPE         |   |  |
| PE          | PE 40:4   |  |
| LPC         |   |  |
| PC          | PC 36:2   | PC 42:2                                  |

Table IV.5.iii. Summary of results from clinical correlation. N.B. BCR results are not shown as no lipids were significantly different in more than one sample type.

Candidate lipids did not correspond with potential results highlighted by Lipidomics in Table IV.5.i. Comparison was made with the extended Lipidomics database. The closest match to any

of the lipids listed in Table IV.5.iii was PC (P-42:2). However, this potential match was in plasma samples only and not in urine.

Finally, comparison was made between LSL versus control, symptomatic versus control, clinical correlation and BCR results. The below results show those lipids that are highlighted in more than one analysis but within the same sample type (Table IV.5.iv).

| <b>Sample Type</b> | <b>Targeted assay:<br/>LSL versus control</b>               | <b>Targeted assay:<br/>symptomatic<br/>versus<br/>asymptomatic</b>                                  | <b>Clinical correlation</b>   | <b>BCR</b> |
|--------------------|---|---|---|------------|
| CSF                | LPC18:0*<br>PC 36:0<br>PC 42:0, 42:1<br>PC 44:1, 44:2, 44:4 | LPC 18:0*<br>LPC 22:3*<br>PC 36:0<br>PC 42:0, 42:1<br>PC 44:1, 44:2, 44:4                           | LPC 22:3*   |            |
| Plasma             | LPC 14:1*   | LPC 14:1*<br>PC 34:3<br>PC 36:2*<br>PC 40:4<br>PE 32:3<br>PE 36:4<br>PE 38:2, 38:3, 38:4<br>PE 40:4 | LPC 14:1*<br>PC 34:3<br>PC 36:2*<br>PC 40:4<br>PE 32:3<br>PE 36:4<br>PE 38:2, 38:3, 38:4<br>PE 40:4 |            |
| Urine              |   | PC 28:0, 28:1<br>PC 32:2, 32:4<br>PC 34:2, 34:4<br>PC 36:2*, 36:3, 36:4<br>PC 38:4                  | PC 28:0, 28:1<br>PC 32:2, 32:4<br>PC 34:2, 34:4<br>PC 36:2*, 36:3, 36:4<br>PC 38:4                  |            |

Table IV.5.iv. Summary of comparison of results from different methods of analysis. Lipids are only listed if they demonstrate significant difference by more than one method of analysis. No lipids identified by a significant difference between BCR results were also identified by another means of analysis. \* denotes those lipids identified as potential candidate lipids by more than one method of analysis and/or in more than one sample type and will be reviewed in more detail.

Candidate lipids do not correspond with potential results highlighted by Lipidomics in Table IV.5.i. Comparison with the extended Lipidomics database search did not reveal any matches of the above highlighted lipids.

Although the BCR results did not correspond with any of the other targeted assay results, the only lipid significantly different between abnormal and normal BCR results in urine samples was also detected as being significantly different in urine in Lipidomics 1. In addition, LPC18:0 was significantly different in plasma samples between abnormal and normal BCR and was significantly different between both LSL and control and between symptomatic and asymptomatic patient CSF samples on targeted assay.



## 6. DISCUSSION

### Lipidomics

Lipidomics is a feasible method for detection of lipids in samples obtained from LSL patients, although as stressed earlier this method does not fit the formal definition of lipidomics. Thousands of different mass charge ratio-retention time pairs were generated, however, due to the ionization of lipids required to allow mass spectrometry detection, each individual lipid is likely to account for more than one data point. With this method it is not possible to be certain which data points refer to the same lipid.

Knowledge of retention time patterns can guide identification; for example, fatty acids tend to have a low retention time. Similarly, use of database search allows accurate comparison of mass charge ratios with known (and extrapolated) masses of lipid adducts generated by electrospray ionization. When considering these database identification results, it is worth noting the significant number of unknowns – that is, mass charge ratios that are not matched within 0.01 or matches that are not biologically viable in humans. Explanation for these unknowns may include sensitivity and calibration of different mass spectrometers. In addition, lipid species that are not commonly identified and not usually present in human biology have been excluded. However, it is worth bearing in mind that the disease state may arise from abnormal lipid species that are not present in healthy humans. Ultimately, targeted assays are required for formal identification of any lipids detected through this method.

Database searches often generated a number of different potential matches for each data point. Tables in this Results section only highlight one potential match selected as the closest M/Z to that measured and the simplest adduct. A complete list of potential matches can be found under Supplementary Information.

Within Lipidomics 1, 55 lipids were potentially identified via database search and 34 of these were classed as phospholipids. Specifically, LPE16:1 was detectable in all sample types and showed a significant difference between LSL and control patients. LPE has previously been detected within CSF and is considered part of the normal CSF lipidome [229]. In addition, plasma LPE 16:1 has been found to be increased in obesity and is thought to have a possible role in mediating obesity-associated inflammation [230].

Within Lipidomics 2, phospholipids also represented the predominant lipid species matched on database search, with phospholipids accounting for 26 out of 47 identifiable lipids. In addition, all identifiable lipids found to be significantly different between LSL and control patients in CSF, plasma and urine were also identified as possible phospholipids, and were all more abundant in the LSL patients. The mass charge ratio of 469.313 (possible LPE16:1) detected in Lipidomics 1 was detected in Lipidomics 2 but did not show any significant difference between LSL and control samples.

Of note, when comparing LSL versus control patients there is an abundance of lipids/lipid adducts with increased intensity signal in LSL patients (demonstrated by volcano plots negatively skewed). In contrast, when comparing symptomatic versus asymptomatic patients there is an abundance of lipids/lipid adducts with increased intensity in asymptomatic patients

(demonstrated by volcano plots positively skewed). This difference raises the possibility that the asymptomatic patients may be producing some lipids that are protective, perhaps slowing disease progress in comparison to those symptomatic patients. Jende et al have identified that low levels of serum cholesterol (as is generated by medication with statins), increases the severity of nerve damage in patients with type 2 diabetes mellitus. They propose that the vital role of cholesterol in nerve function is disrupted by the low circulating levels, and thus the low availability, of this lipid [231]. Similarly an abundance of lipids vital for nerve structure and function could conceivably provide protection against disease states by optimising the availability of important lipids.

As already mentioned this method does not fulfil the strict definition of 'lipidomics', nor does it allow for the exact identification of lipid species. However, lipids are detectable in CSF samples taken from LSL patients, and there are significant difference between LSL patients and control cases. Lipids were also detected in plasma and urine samples.

Analysis to compare CSF, plasma and urine samples was completed. The importance underlying this analysis was that plasma and urine samples are more readily available in young children and their collection is much less invasive than collecting CSF. Ideally a biomarker would be detectable in samples that are relatively easy to collect and do not require significant intervention, with its own associated risks. The analysis that was done was simplistic and did not take into account the complexity of metabolism of lipids. It is conceivable that accumulation of a particular lipid in the CSF may contribute towards disease progression and that, with this accumulation, there might be a deficit in plasma. Similarly, a lipid present in the CSF might be further metabolised and present as a different lipid species within plasma and urine. Without a complete understanding of the LSL disease process, this degree of analysis is not possible. However, these results highlight that some lipids are significantly different in all three sample types between LSL and control patients, and the fact that phospholipids are the predominant lipid species on database search indicates that further research should focus on the exact identification of these phospholipids with a targeted assay.

### **Targeted Phospholipid**

A number of PC/LPCs and PE/LPEs are significantly different between LSL and control patients in CSF and plasma samples but not in urine samples. Only one of these lipids corresponds with the results from Lipidomics 2, LPC26:1. Within these different phospholipids, CSF samples demonstrated predominant differences in PC, with only 1 out of 24 significantly different phospholipids being PE 36:2. This is likely to reflect the more dominant role of PC in cell membrane structure whilst PE has a more dominant role in mitochondrial membrane structure. Within the plasma samples only LPC and LPE showed any significant difference. An increase in lysophospholipids may indicate increased activity in PLA2 which is considered to be a marker of inflammation in a number of different pathologies including some neurodegenerative such as Alzheimers [232]. However, reviewing the differences in LPC/PC or LPE/PE ratio gives a more

accurate assessment of PLA2 activity, and no significant difference was found in either of these ratios.

A number of different PC/LPCs and PEs are significantly different between symptomatic and asymptomatic LSL patients in CSF, plasma and urine samples. Only one of these lipids corresponds with the results from Lipidomics 2, PC34:1. Within the CSF samples the significant differences were only seen in PC and LPC, again likely to reflect to important role of PC as a structural component of cell membranes and possibly indicating damage to cell membranes, including neurons located at the LSL placode. Within plasma samples, significant differences were found in PC, LPC and PE. These plasma results were markedly different from the LPE and LPC found in the LSL versus control group. Within urine samples the significantly different phospholipids were all PC.

With a large number of different phospholipids being detected in different samples types, it is impossible to know if any/all of these are contributing to clinical deterioration in patients or if these phospholipids are a side product of ongoing nerve damage. Ultimately, further in vitro neurophysiological experiments, perhaps patch clamping neurons in cell culture to elicit any changes in electrophysiological properties that might develop when neurons are exposed to a different milieu of phospholipids, could indicate a causative rather than a responsive role to these differences in phospholipids.

The specific role of individual phospholipids in terms of nerve damage and cellular processes are still a topic of active research, and with the large degree of variation present in phospholipids, are likely to remain so for some considerable time. However, there are examples of particular roles of individual phospholipids that might be pertinent to the disease progression of LSL. For example, LPC 16:0 found to be significantly raised in symptomatic LSL patients ( $p=0.012$ ), is known to have a role in mediating glucose uptake in adipocytes [233]. Increased glucose uptake into the LSL tissue in the vicinity of the LSL placode could potentially result in less glucose locally available to neurons and therefore disrupt function. Decreased glucose uptake is known to contribute to Alzheimer's disease and nerve function has been shown to improve after correcting glucose uptake into neurons in the *Drosophila* model of Alzheimer's [234].

The differences between these targeted assay results and the lipidomics results (Section IV.1) highlight the inaccuracy of the 'shotgun' lipidomics and database search technique. The targeted assay offers a more precise measure of preselected lipids without the ambiguity over which exact lipid species are being detected.

A direct comparison between CSF in the LSL versus control group and symptomatic versus asymptomatic groups reveals a number of phospholipids that are significantly different in both: PC44:1, PC44:4, PC42:1, PC38:0, PC 36:0, LPC 18:0. Again, these were all PC perhaps indicating underlying nerve cell membrane damage.

None of the lipids significantly different in CSF samples from the LSL versus control group were also significantly different in plasma samples or urine samples. Similarly, none of the lipids significantly different in CSF samples from the symptomatic versus asymptomatic group were

also significantly different in plasma samples or urine samples. This limits the use of a phospholipid in plasma or urine as a biomarker to solely being a correlation with the disease state (which does not exclude the usefulness of a biomarker). The lack of the same phospholipids being detected in CSF, plasma and urine is likely to reflect the metabolism of lipids between the different fluid compartments within the body and, since the complete human lipidome is not yet established, this lack of similarity between fluid compartments should not yet be dismissed until we have a better understanding of lipid metabolism.

In terms of phospholipid ratios, much published research has considered intracellular levels of PC/PE. It is unclear how this may translate to measurements taken from CSF, plasma and urine. Indeed the normal range for hepatic cellular PC/PE is considered to be between 1.5 and 2.0 [193]. The PC/PE ratios measured in all sample types in the present study were substantially outside this range, raising the possibility that the method used for measurement of PE is not as sensitive as that for PC. These results may well be spurious. If they are genuine they may be a consequence of altered CSF phospholipid metabolism by the LSL tissue. Alternatively these results could represent a normal spectrum, especially in plasma, with no significant difference between LSL and control cases but substantially more PCs in asymptomatic LSL cases. Perhaps some PCs have a protective effect.

There was no significant difference when comparing the LPC/PC and LPE/PE ratios between LSL and control and between symptomatic and asymptomatic patients. This suggests that there is no significant increase in PLA2 activity that in turn indicates no increase in pro-inflammatory markers. However, a more accurate assessment could be done of PLA2 activity by directly measuring this enzyme [235]. In addition, the results may be confounded by two main factors. Firstly the control group also had pathology and some were undergoing prolonged surgery in which one would expect some inflammatory response (SDR cases). Although the CSF samples were taken near the beginning of surgery to mitigate intraoperative changes these cases cannot be considered equivalent to healthy controls. Unfortunately there is not much scope for obtaining CSF samples from healthy children. Secondly, the division of LSL patients into symptomatic and asymptomatic generates artificially polar opposites and does not take into account different degrees of severity or rate of progression of symptoms. More accurate clinical assessment of patients is required to see if there is any correlation between degree of severity of symptoms and differences in PC and PEs.

### **Clinical assessment and correlation**

Generating a Total Clinical Score potentially offers a more sensitive way of assessing patients and allows correlation between intensity of lipid signal identified by mass spectrometry and number/severity of findings on clinical assessment. Only one lipid in CSF correlates with the Total Clinical Score. In plasma samples, some lipids from each of the four lipid subclasses (LPC, PC, LPE and PE) show correlation with the Total Clinical Score. Of note, the PCs predominantly show a negative correlation whilst the PEs show a positive correlation. In urine samples, a larger number of lipids from all four subclasses, except LPE, also correlate with the

Total Clinical Score. Of note, only negative correlation is seen between urine samples and the Total Clinical Score. This corresponds with the positive skew seen on Lipidomics 2 (symptomatic versus asymptomatic) volcano plot results.

LPC22:3, the only lipid showing significant correlation with the Total Clinical Score in CSF, did not show any significant correlation in plasma or urine samples. Only one lipid had a significant negative correlation in both plasma and urine samples: PC42:2. In addition, PE40:4 and PC36:2 showed a significant positive correlation in plasma ( $r = 0.590$  and  $0.567$  respectively) but in urine the correlation was negative ( $r = -0.563$  and  $-0.589$  respectively).

The abundance of lipids showing correlation in urine with the Total Clinical Score may simply reflect common complications in the urinary system in those patients with higher scores. For example, inflammation from clean intermittent catheterisation and recurrent urinary tract infections are likely to alter the lipid profile of urine. However, although it might be reasonable to expect some changes within the plasma with particular severe cases of urinary tract infection/inflammation, it is difficult to explain a negative correlation in urine and a positive correlation in plasma of the same phospholipid entirely through mechanisms of urinary tract infection/inflammation.

As with both the Lipidomics and Targeted Assay Results, the statistical analysis is limited by the sample size. In addition, at low levels of intensity, the mass spectrometry measurements become less reliable. As such, levels less than  $10e^4$  should be considered with caution, particularly in cases where all measurements of a lipid are less than  $10e^4$ . However, where there is a large range of measured intensities with only a small number of low-level intensities measured, low-level intensities could be approximated to 0 and are likely to not significantly alter the calculated correlation coefficient.

With the above in mind a number of lipids have been selected that demonstrate both good correlation and reliable measurement by mass spectrometry and will be compared with the Lipidomics and Targeted Assay Results in more detail (see Combined Analysis section).

The negative correlation seen in plasma samples of the PC/PE ratio supports the observation that those lipids that show significant negative correlation are predominantly PCs whilst those lipids that show significant positive correlation are predominantly PEs. The negative correlation with the PC/PE ratio indicates relatively less of an abundance of PCs as symptoms worsen in relationship to a relative increase in PEs as symptoms worsen.

The absence of significant difference in the PC/PE ratio in CSF samples raises the question as to whether this altered phospholipid ratio could ultimately be related to the underlying mechanism of disease progression in LSL. Although the CSF correlation is not statistically significant, it is positive with relatively more abundant PCs than PEs in the CSF. It seems unlikely that the PC/PE ratio would have an effect on nerve function when significant differences are predominantly seen in the plasma. However, this does not exclude the usefulness of the PC/PE ratio as a potential biomarker.

As mentioned previously, most research into the PC/PE ratio has been on intracellular levels in hepatocytes (Figure IV.6.i). In the absence of gross metabolic disturbances in LSL patients it seems unlikely that the extracellular PC/PE ratios measured are having major impact on the pathways illustrated. It is unclear how changes in this ratio in CSF and plasma might correlate with intracellular levels in neurons and adipocytes. In addition, there is no evidence regarding the robustness of the blood-spinal cord barrier in LSL. The fact that different phospholipids show different directions of correlation, and that the PC/PE ratio shows a different direction of correlation between CSF and plasma samples suggests that the blood-spinal cord barrier is essentially intact.

The only significant difference seen in LPE/PE ratio was seen in plasma. The negative correlation here corresponds with relatively less LPE as symptoms increase. This fits a model of decreased PLA2 activity as symptoms worsen, although the lack of similar changes in the LPC/PC ratio questions whether this does reflect PLA2 activity or another mechanism.

LPEs are likely to have a range of different actions, some of which are as yet undetermined. Similarly, arachidonic acid (a product of PE hydrolysis by PLA2) has a role as an inflammatory mediator, a signalling molecule and vasodilator. With this diverse range of actions of these two related molecules, it is difficult to ascribe a direct mechanism to this observation, although this does not exclude the use of the LPE/PE ratio as a biomarker. A more detailed metabolomics analysis of samples from LSL patients would give more insight into the exact mechanisms that might be involved.

The use of the Total Clinical Score has highlighted further lipids that are worth exploring in more detail to determine if they might function as a useful biomarker. However, it is worth noting that as symptoms worsen and become more obvious in LSL patients it is only right to expect disruption of bladder function and consequent alterations in urine sample lipid levels and even plasma lipid levels as a result of inflammatory pathways [236]. A biomarker that is only predictive once a patient has developed such clinical signs is obviously of little use. Ideally an accurate test of nerve function needs to be done on those patients with a low TCS to determine if there is any degree of neurological disruption. Correlation with such neurophysiological measurements could potentially offer identification of a cohort of patients who have little or no symptoms (and therefore changes in plasma and urinary phospholipids are less likely to be attributed to urinary tract inflammation/infection) but are ultimately at risk of neurological deterioration. These are the patients who would most benefit from a biomarker. Neurophysiological testing in LSL patients will be discussed in the next results section: Neurophysiology.

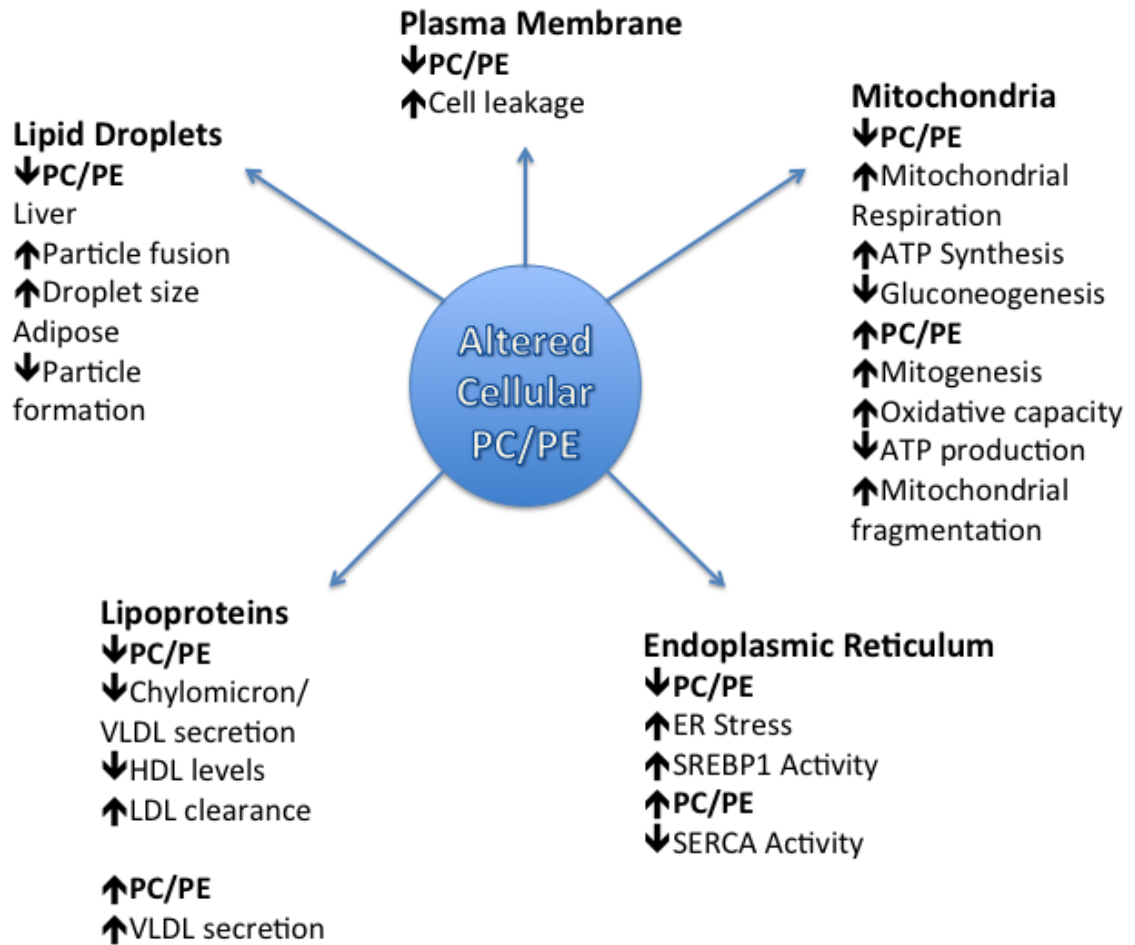


Figure IV.6.i. Summary of effects of altered intracellular PC/PE ratio adapted from Van der Veen et al 2017. PC = phosphatidylcholine, PE = phosphatidylethanolamine, ATP = adenosine triphosphate, VLDL = very low density lipoprotein, HDL = high density lipoprotein, LDL = low density lipoprotein, ER = endoplasmic reticulum, SREBP1 = sterol regulatory binding protein 1, SERCA = sarco/endoplasmic reticulum Ca<sup>2+</sup>ATPase

### Neurophysiology

Neurophysiological monitoring has been reviewed in LSL patients undergoing near-total resection of LSL tissue. Firstly, the different neurophysiological parameters were compared to clinical classification as symptomatic or asymptomatic. There was no significant association between symptoms and pre-operative neurophysiology results. This can either suggest that neurophysiology is unreliable or that pre-operative clinical assessment is unreliable. Due to the known difficulties assessing the age group that LSL patients fall into at diagnosis, the latter should certainly be considered to be true, although this does not show that neurophysiological monitoring is reliable.

MEPs and SSEPs are generally considered to be a reliable method for assessing motor and sensory function in patients and are known to correspond well with clinical assessment [209]. Within this LSL cohort, transcranial MEPs did not correspond with pre-operative clinical assessment, again perhaps highlighting the unreliability of clinical assessment. SSEPs were all recorded as normal, however, clinical assessment of sensory function in this age group is particularly difficult especially in non-verbal patients and is often not documented. As such, SSEPs were not compared directly with clinical assessment. Neither BCR nor sphincter MEPs demonstrated a significant association with clinical assessment, which may also highlight the difficulty in the relevant clinical assessment – here the difficulties in detecting subtle changes in bladder function before patients become obviously symptomatic. However, as mentioned previously, this does not confirm the accuracy of these two neurophysiological monitoring methods.

These data demonstrate that baseline intraoperative neurophysiology does not correspond with the clinical status of a child with LSL. However, there is a strong association with both BCR and sphincter MEPs and residual post-void percentage. This association is stronger with BCR when compared to sphincter MEPs. Current clinical practice does take into account the residual post-void percentage but due to the recognised inaccuracies with this assessment in a young cohort this parameter is rightly taken into consideration with the rest of the clinical assessment to allow a patient to be viewed as a whole. Even complete urodynamic assessment, which was unavailable in the majority of this cohort, has been shown not to correspond with continence or need for CIC [210]. These results suggest that perhaps more weight should be given to the residual post-void percentage when assessing LSL patients. In addition, the BCR appears to be more sensitive than sphincter MEPs.

The BCR neurophysiology shows more deterioration intra-operatively when compared to sphincter MEPs suggesting this is a more sensitive assessment of disruption of nerve function. It is, in particular, the sacral segment and inter-neurons of the sacral spinal cord that the BCR is able to assess beyond the sphincter MEPs [237]. Indeed the BCR is known to be better than clinical assessment at identifying dysfunction in the sacral spinal cord reflex arc and has been found to be abnormal even in asymptomatic adult patients with suspected neuropathic sacral lesions [238]. It is therefore not surprising that the BCR offers a more sensitive intra-operative assessment of nerve function in LSL patients undergoing near-total resection of LSL tissue.

This sensitivity of BCR monitoring is also reflected in the positive predictive value of this test. Patients who undergo near total resection of LSL with an abnormal BCR at the end of surgery are likely to require initiation of clean intermittent catheterisation post-operatively. This test has an optimum sensitivity of 80% and specificity of 75% and is more accurate than the use of sphincter MEPs in predicting urological outcome from surgery. This supports other recently published reports that show BCR is predictive of long-term urological outcome following untethering surgery in a range of different paediatric spinal pathologies [239]. These results suggest that BCR might provide an objective assessment of urological prognosis in initial evaluation of children with complex dysraphism.



Interestingly, neither BCR nor sphincter MEPs had a positive predictive value for residual post-void percentage at 3 months following near-total resection of LSL. Again, this is likely to highlight the inconsistencies in clinical assessment that persist post-operatively as the patients remain young. Although there is a range of different parameters that are considered during urodynamic assessment and bladder function assessment, there is no scoring method or way of quantifying the sum of all these results. A skilled urologist is required to interpret the results and suggest ongoing management. From a patient and parent perspective, an important outcome is not the individual results from such assessments but rather whether the child requires clean intermittent catheterisation. These results demonstrate the complexity of bladder assessment and although there is no direct association with individual components of the bladder assessment there is good association with the important outcome of the need for clean intermittent catheterisation, a significant outcome in terms of psychosocial as well as health care costs.

Taking the post-operative BCR as the most predictive marker of long-term outcome following LSL surgery raises the question as to whether the BCR can itself be used as a biomarker, or measure of early neurological dysfunction prior to development of symptoms. As discussed in the Methods Section, the young children who present with LSL, and require assessment, are particularly difficult subjects for BCR. The BCR is often diminished at this age and a process of temporal summation is required (repetitive stimulation to reach acceptable recordable levels). In addition, all research in this age group has been done under sedation and general anaesthesia with tightly controlled pharmacological parameters [240]. A biomarker that requires general anaesthesia and prolonged monitoring is not ideal.

The neurophysiological findings were reviewed to identify any association between BCR and targeted lipid profile. No significant difference was found in CSF samples and, as such, no assumptions can be made about any potential mechanisms that might associate lipid levels with early nerve dysfunction. However, a number of PCs, LPCs and LPEs were found to be significantly different in plasma samples between those patients with an abnormal BCR and those with a normal BCR on intra-operative monitoring prior to the initiation of surgery. These lipids will be reviewed in more detail in the Combined Analysis Section. Only one lipid was found to be significantly different in urine samples. This latter finding is reassuring as on correlation with the Total Clinical Score there was an abundance of lipids in urine samples that reached significance. Presumably a number of these urinary lipids were directly attributable to concomitant urinary tract pathology such as urinary tract infection. The removal of grossly abnormal patients from the cohort allows focus on the group of patients that would most benefit from the development of a biomarker (although it does reduce the sample size and so the statistical power). In addition, it removes these potentially confounding factors, such as urinary tract infections/inflammation, and this is reflected in the lack of a large number of significantly different phospholipids in urine samples.

Ideally, for optimum development of a biomarker, the cohort to be analysed would be only those patients with no or mild BCR changes, and who are either asymptomatic or mildly symptomatic.

This has been done and has highlighted a number of lipids that remain significantly different in both plasma and urine. These particular lipids, along with the results from Lipidomics 2, the Targeted Lipid Assays and Total Clinical Scoring will be reviewed in more detail to identify the most promising potential biomarker in the following section: Combined Analysis.

### **Combined**

No clear candidate biomarker stands out from the Lipidomics results although the frequency of phospholipids appearing to be significantly different between groups guided further targeted assay development. Of note there are different results between Lipidomics 1 and 2 highlighting difficulties with small sample sizes and reproducibility of results. Although lipidomics generates a large amount of data, transferring this to biomarker development is difficult and can only at best exist as a “molecular signature of structurally unidentified markers” [214]. There is no potential for developing insight into the disease process. The process of lipidomics is complex, time consuming and requires specific expertise not readily available in clinical laboratories. By comparison, targeted assays are more precise and reproducible. It is important to note that none of the candidates highlighted as most promising biomarkers from targeted assay analysis were also found to be significantly different on lipidomics database search.

### **Individual candidate lipids**

LPCs consist of a range of different fatty acids at the sn-1 position of the glycerol backbone of the phospholipid, with 16, 18 and 20 being the most abundant number of carbons in the fatty acid chains. Synthesis is directly via enzymatic action of PLA2 on membrane PCs, hydrolyzing the sn-2 position [199]. Alternatively, synthesis occurs via the lectithin:cholesterol acyltransferase pathway with esterification of free cholesterol to generate cholesterol esters. As with PLA2, PCs are used as an acyl donor with transesterification at the sn-2 position resulting in LPC as a byproduct (Figure IV.6.ii). Of note, PLA2 can be activated in vitro during the process of lipid extraction giving artificially high levels of LPC [241].

All LPCs are thought to act on the lysophospholipid receptors, in particular with high affinity for GPR4 and G2A. GPR4, a Gi/o protein coupled receptor is ubiquitous in humans with activation resulting in increased DNA synthesis, serum-responsive element, mitogen protein kinase and phospholipase C activity. Due to the diverse range of responses, the exact physiological role of GPR4 remains unknown. The G2A receptor is also a Gi/o protein coupled receptor but is principally expressed in the thymus, spleen and bone marrow [242].

In addition to a role in intracellular messaging, LPCs are also the preferred carrier of docosahexaenoic acid across the blood brain barrier. Docosahexaenoic acid (DHA) is a fundamental fatty acid required for central nervous system development and function, with deficiencies associated with Alzheimer's, Parkinson's and depression [243, 244].

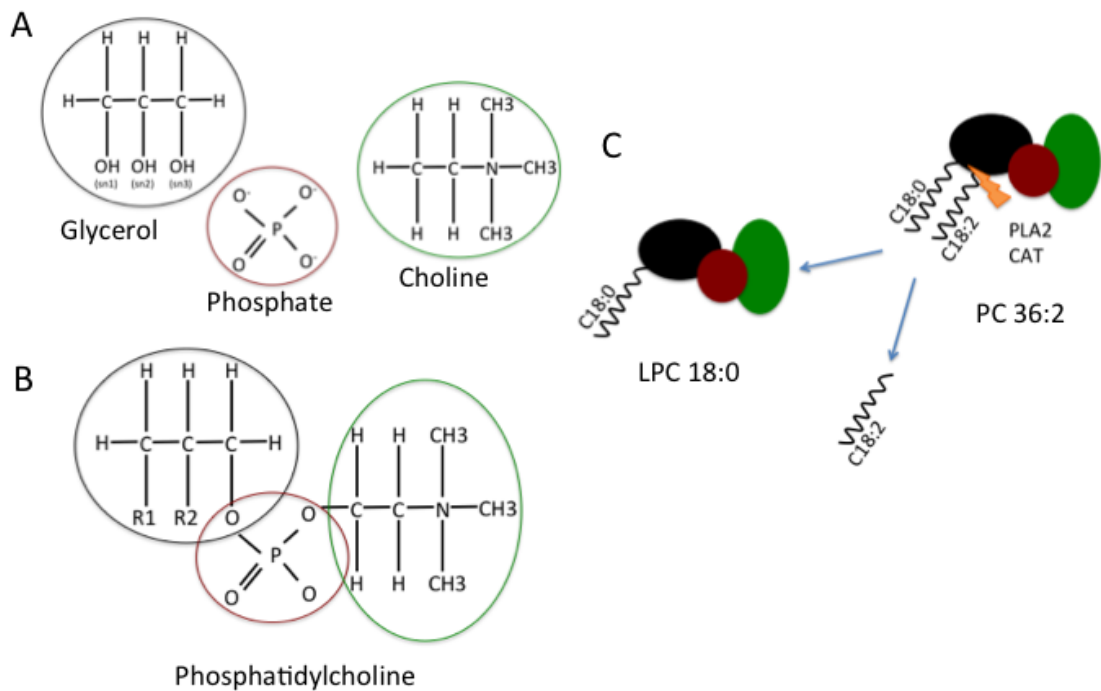


Figure IV.6.ii Diagrammatic representation of PC and LPC. Figure IV.6.iiA. Components of PC molecules. The glycerol molecule has 3 hydroxyl groups: numbers sn1, sn2 and sn3. Figure IV.6.iiB. PC. R1 and R2 are fatty acid tails at the sn1 and sn2 positions respectively. The sn1 position (R1) most commonly holds a saturated fatty acid chain, whilst the sn2 position (R2) most commonly holds an unsaturated fatty acid chain. In the case of LPC, only the sn1 position is occupied and sn2 remains a hydroxyl group. Figure IV.6.iiC. Enzymatic action of both PLA2 and CAT on PC results in cleavage and loss of the sn2 position fatty acid tail. The end products include a LPC and a free fatty acid that may be incorporated into other molecules such as a cholesterol ester in the case of CAT.

### LPC 14:1

LPC 14:1 consists of a 14 carbon fatty acid, with myristoleic acid (derived from milk fats) located at the sn-1 position. It has been detected and quantified in plasma [245]. LPC 14:1 is not known to be associated with any disease states and there is no published detection in CSF. This supports results where significant differences were only detected in plasma. The correlation with the Total Clinical Score was positive and strong ( $r=0.678$ ) and the p-values on targeted assay, LSL versus control and symptomatic versus asymptomatic, were 0.035 and 0.019 respectively. However, the intensity of signal was low with more than half of LPC 14:1 detection below  $10e4$ , making measurements less reliable.

The lack of established evidence as to the role of LPC 14:1 in normal physiological states and the low levels detected makes this a less good candidate for further testing as a potential biomarker.

### **LPC 18:0**

LPC 18:0 consists of an 18 carbon fatty acid, with stearic acid (derived from coco butter, sesame oil and animal fats) located at the sn-1 position. As stearic acid is one of the most abundant fatty acids in humans, it follows that LPC 18:0 is also abundant. LPC 18:0 is expressed in all tissues and has been quantified in blood and CSF of adults at concentrations of 47.54  $\mu\text{M}$  and 0.069  $\mu\text{M}$  respectively. In infants, plasma levels range between 12 and 31.9  $\mu\text{M}$  [245-247].

LPC 18:0 has been associated with a number of different pathologies as a potential biomarker, including lower levels detected in maternal serum in cases of fetal congenital heart disease [248], and high levels of LPC 18:0 in urine in adolescent obesity [249]. In all these cases LPC 18:0 forms part of a spectrum of metabolites and only brief attempts, if any, have been made to explain its presence. In terms of neurological disease, LPC 18:0 has been identified as being present at significantly lower levels in plasma of patients with schizophrenia when compared with healthy twins. In addition, there is a correlation with grey matter density in the lateral temporal surfaces, and medial occipital and parietal regions of the brain, as well as with cognitive function [250]. This supports evidence that LPCs are required for transport of DHA to support brain function. More importantly, Morita et al detected LPC 18:0 in CSF samples and noted increased in CSF levels in patients with invasive pathologies of the central nervous system, such as haematological malignancy or carcinoma. These higher levels may represent deregulation of LPC transport into the CSF, with associated disruption of the blood-brain barrier (or blood-spine barrier) [251].

In the present study, LPC 18:0 is more abundant in control samples and is detected at reliable levels in CSF with means between  $1.7 \times 10^6$  and  $5.9 \times 10^6$  in LSL and control samples respectively. LPC 18:0 is more abundant in asymptomatic patients, and was detected at reliable levels in CSF with means between  $1.2 \times 10^6$  and  $3.4 \times 10^6$  in symptomatic and asymptomatic patient samples respectively. Interestingly, this fits with a model of disruption of the blood-spine-barrier, as mentioned above, in asymptomatic patients. Alternatively, this also fits with a model of increased DHA transport into the central nervous system, perhaps having a protective role on neurological function in asymptomatic patients. LPC 18:0 is also detected as being significantly different between patients with normal and abnormal BCR recordings in plasma samples (but not in CSF samples). LPC 18:0 is more abundant in abnormal BCR patients (mean  $7.2 \times 10^7$ ) compared to normal BCR patients ( $5.6 \times 10^7$ ). This difference was lost when patients with grossly abnormal clinical assessment and absent BCR recordings were excluded from the data set.

### **LPC 22:3**

Little is known about this LPC, it has not been previously detected or quantified in plasma or CSF. A positive correlation was demonstrated against the Total Clinical Score, and on comparison between symptomatic and asymptomatic patients. However, most detection was below  $10^5$  therefore making measurement unreliable.

### **PC 36:2**

Most PCs have a saturated fatty acid chain at the sn-1 position and an unsaturated fatty acid chain on sn-2, although this is not invariable. A number of different combinations of fatty acids can therefore result in the same PC 36:2: for example, PC 18:0/18:2, PC 18:1/18:1, PC 20:0/16:2. In addition, the location of double bonds in the unsaturated fatty acyl chain can vary with the most frequent locations: 9Z and 11Z. The method used here does not allow distinction between these different subtypes of PC 36:2. One of the most abundant PC 36:2 lipids is likely to be PC 18:1(11Z)/18:1(9Z) based on the abundance of vaccenic acid and oleic acid in the human diet (from animal and butter fats as well as olive oil) [193, 245]. The synthesis and function of PCs is summarized in the Section IV.2. PC 36:2 has been detected and quantified in plasma and urine samples in a number of different studies in adults with a normal range 200-300  $\mu\text{M}$  and 0.0021-0.045  $\mu\text{mol}/\text{mmol}$  creatinine, respectively [252, 253]. Plasma levels have been quantified as slightly lower in infants 183-244  $\mu\text{M}$  [247]. As with LPC 18:0, PC 36:2 has been associated with obesity, specifically identified as being lower in blood in cases of weight loss in childhood obesity [254]. Badaho-Singh also detected low levels in maternal blood in cases of fetal congenital heart disease [248].

Targeted assay of asymptomatic versus symptomatic patient plasma samples shows PC36:2 to be more abundant in symptomatic patients (means  $9.2 \times 10^5$  versus  $1.5 \times 10^6$ ,  $p=0.03$ ). This is supported by a positive correlation in plasma with the Total Clinical Score Correlation,  $r=0.567$ . Detection of PC 36:2 in plasma was at reliable levels and mostly greater than  $10^6$ . PC 36:2 was also detected in urine samples at reliable levels, mostly greater than  $10^5$ . The correlation with the Total Clinical Score was negative,  $r=-0.589$ .

In view of a possible structure of PC 36:2 being PC 36:2 (18:0/18:2), LPC 18:0 and LPC 18:2 were reviewed in more detail since both are likely products of hydrolysis of PC 36:2 by PLA2 or transesterification of PC 36:2 by the L:CAT pathway. As mentioned above, LPC 18:0 was more abundant in CSF samples of asymptomatic patients compared to symptomatic patients. The same was true of LPC 18:2. Both LPC 18:0 and 18:2 were more abundant in plasma samples of patients with abnormal BCR results ( $p=0.029$  and  $0.0158$  respectively). As with PC 36:2, LPC 18:0 also shows strong negative correlation with the Total Clinical Score in urine samples  $r=-0.739$ , although most levels measured were below  $10^5$  making this a less reliable

measurement. It is conceivable that the same method that limits excretion of both PC 36:2 and LPC 18:0 in the urinary system may also limit the availability of LPC 18:0 for transport of DHA to the central nervous system, causing a relative increase of PC 36:2 in the plasma and lower levels of LPC 18:0 in the urine and CSF in symptomatic patient. Alternatively, asymptomatic patients have lower levels of PC 36:2 in the plasma but higher associated levels of LPC 18:0 in the CSF and urine (Figures IV.6.iiia and b).

#### Symptomatic LSL patient

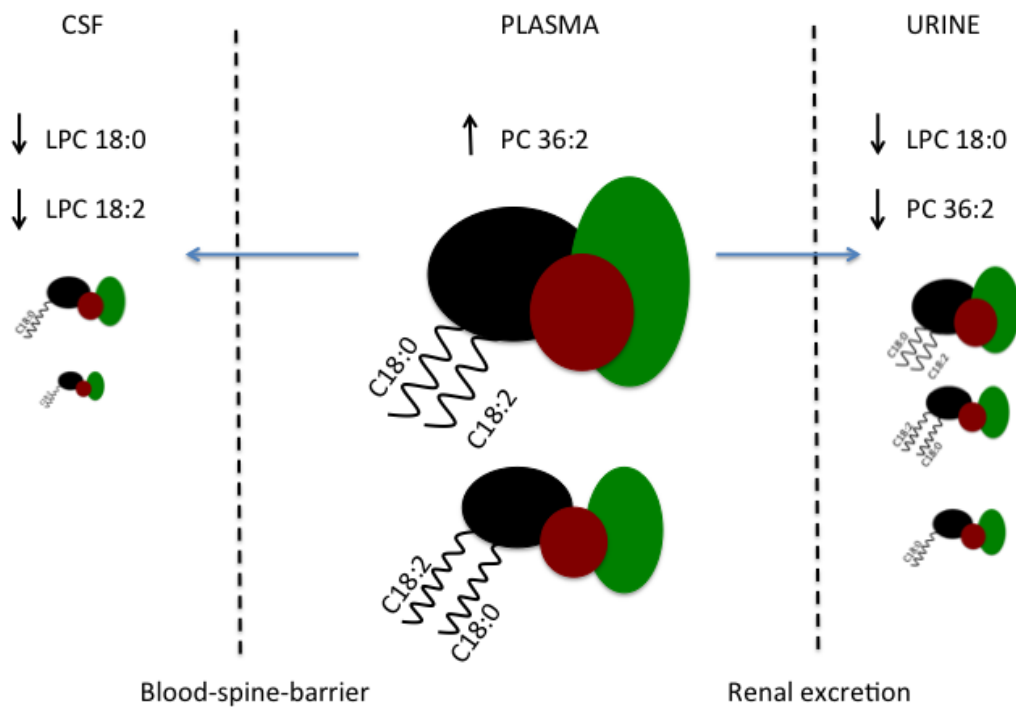


Figure IV.6.iiia. Comparison of targeted assay results from symptomatic LSL patients in CSF, plasma and urine. PC 36:2 may be present as both PC 36:2 (18:0/18:2) and PC 36:2 (18:2/18:0) with the former being more abundant due to the predominance of saturated fatty acid chains at the sn1 position. Both LPC 18:0 and LPC 18:2 are therefore potential breakdown products from the actions of either PLA2 or CAT at the sn2 position.

### Asymptomatic LSL patient

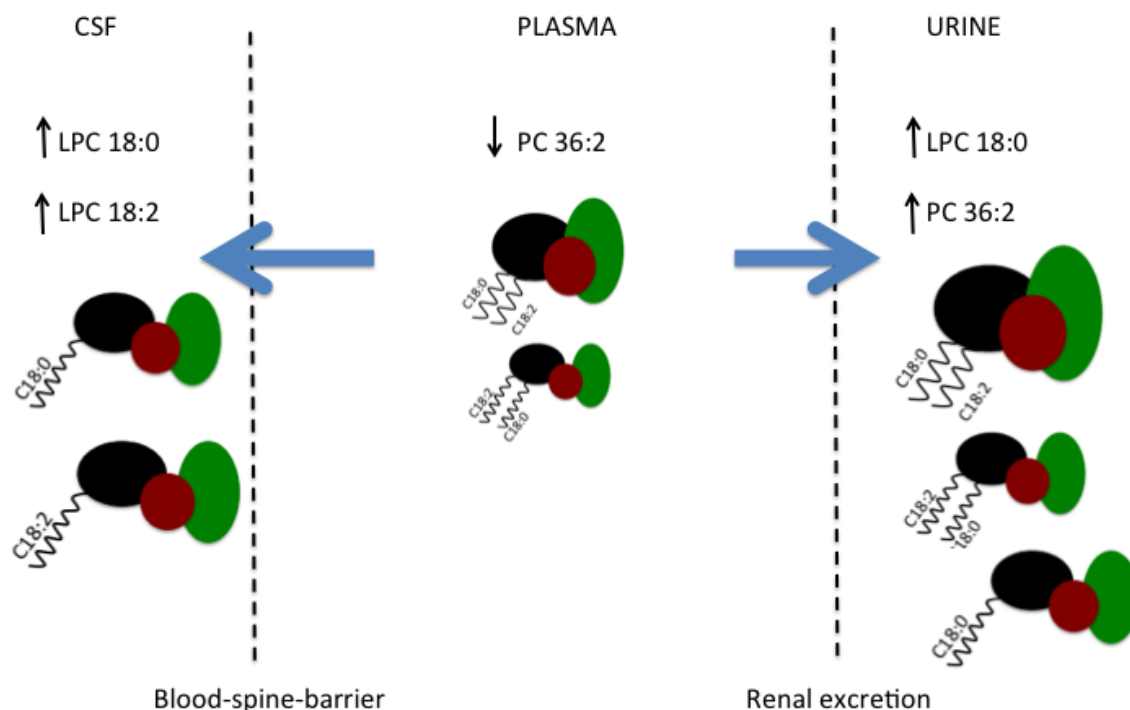


Figure IV.6.iii.b. Comparison of targeted assay results from asymptomatic LSL patients in CSF, plasma and urine. LPCs are known to be involved in the transport of DHA across the blood-brain-barrier/blood-spine-barrier. Renal excretion of phospholipids is poorly understood. Compared to symptomatic patients, it is proposed that increased conversion of PC 36:2 into LPC 18:0 and LPC 18:2 allows greater availability for both these LPCs to enter both the CSF and urine, accounting for lower levels of PC 36:2 in the plasma. LPCs' vital role in transport of DHA into the CSF suggests a mechanism whereby LPCs may maintain neurological function in a disease state.

The combination of PC 36:2 in plasma and LPC 18:0 in CSF samples holds the most promise for future development of a biomarker and further experiments to validate this will be discussed later. Neither PC 36:2 nor LPC 18:0 were detected as being significantly different in any of the samples types in either Lipidomics 1 or 2 or extended database search. Measurement of BCR and excluding grossly abnormal cases aims to eliminate confounding factors, however, the resulting small sample size and lack of abnormal results in CSF samples brings into question the validity of any results generated this way.

Initially the assumption was made that a promising biomarker would have to show significant difference in both CSF and plasma to have any possibility of relating a potential biomarker to underlying disease mechanisms. The fact that lipid metabolism is not completely understood, and the differences in the lipidome between fluid compartments not completely documented,

makes interpretation of lipid differences between fluid compartments complex. However, some of the lipids highlighted in all three fluid compartments can be easily linked by established mechanisms and future biomarker development should focus here. It is worth noting that the mechanism of disease progression in LSL is unlikely to be simple, with overall phospholipid profile, particularly in CSF, representing the balance of a number of different concomitant mechanisms.



## SECTION V: GENETICS

Two familial cases of LSL were identified amongst the GOSH lipoma cohort (Figure V.i). Blood samples were taken, and with consent, whole genome sequencing was performed. The analysis undertaken is detailed in Section III. In addition two further families with a LSL proband and an extended family history of spina bifida aperta or spinal deformity underwent whole exome sequencing and were included in the analysis (Figure V.ii). All cases of LSL (total of 6) were combined for a separate genetic analysis.

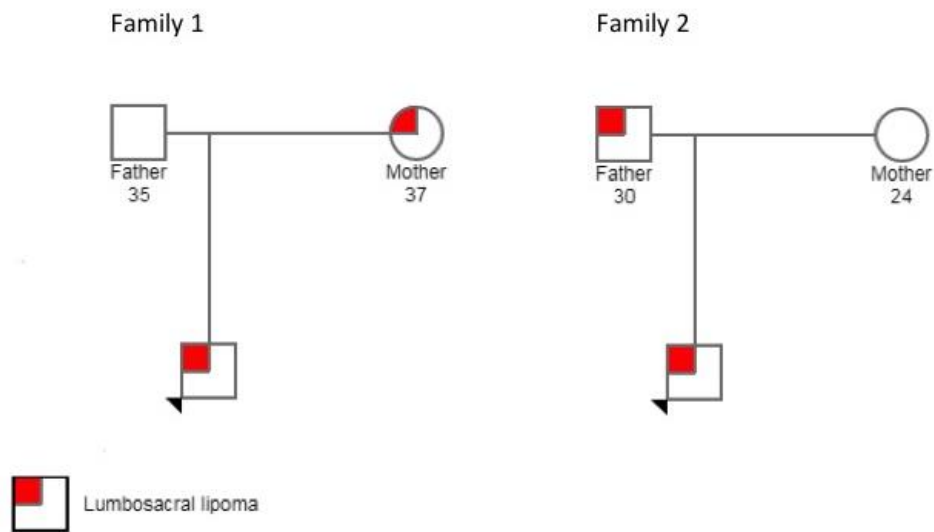
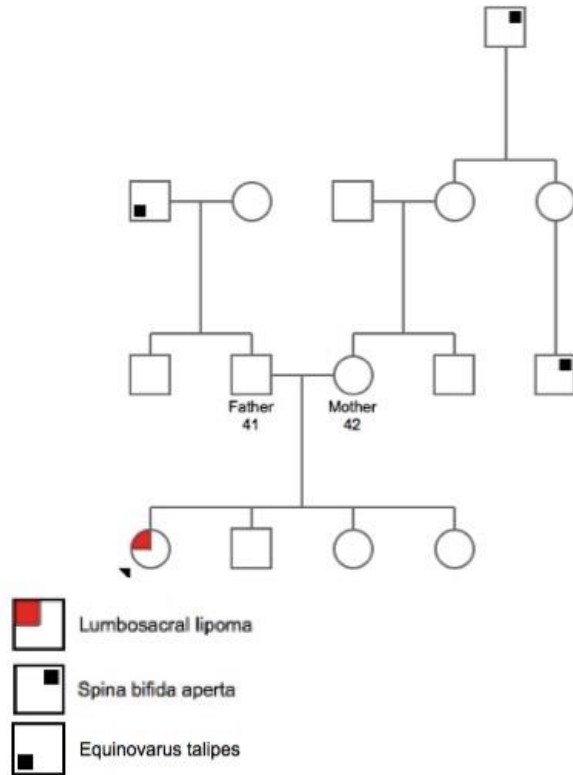


Figure V.i. Pedigree of two separate familial cases of LSL. Family 1: male proband with affected mother, all direct family members of European descent. Family 2: male proband with affected father, all direct family members of African descent. Arrowhead marks proband

Family 3



Family 4

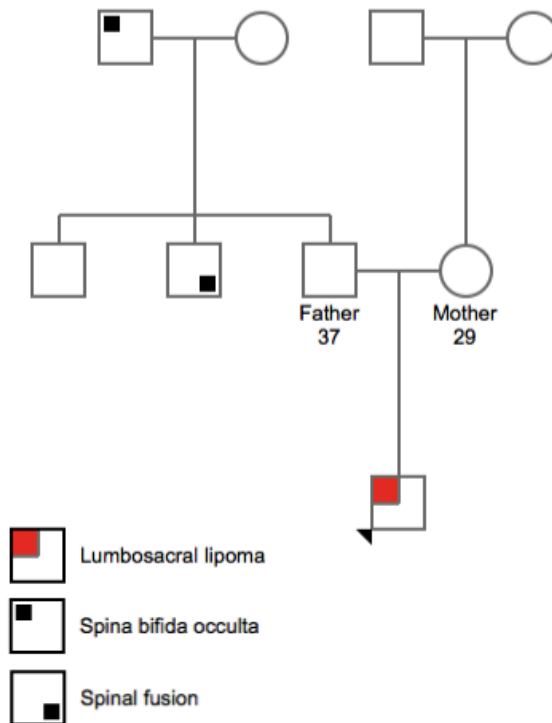


Figure V.ii. Pedigrees of Families 3 and 4. Family 3: female proband with unaffected parents. Both maternal great grandfather and maternal second cousin had spina bifida aperta. Paternal grandfather had equinovarus talipes Family 4: male proband with unaffected parents. Paternal grandfather had spina bifida occulta other than LSL. Arrowhead marks proband.

Results from whole genome/exome sequencing were analysed in three different ways. Firstly, in view of the previous finding by Larrew et al, all sequences of RADIL and ARHGAP29 were reviewed in detail, including intronic variants and variants in promoter regions.

Secondly, two family triplets with two cases of LSL were reviewed for any autosomal dominant variants present in both affected individuals but not in controls. Genes were filtered based on likelihood of being genetic cause of the pathology. This included comparing variants to known databases and *in silico* predictions systems (SIFT, PolyPhen-2, CADD and gnomAD). Any exonic variant with either a SIFT Function prediction of 'damaging', a PolyPhen-2 Function prediction of 'probably/possibly damaging', a CADD score of >20 and a gnomAD Frequency of <0.01% was considered in more detail. Candidates were then further reviewed based on location of variant, product protein and any likely disruption in function. Candidate genes were reviewed in the literature to identify any known association with neural tube defects or adipogenesis. Finally, any association of that gene with an alternative pathology was identified.

Thirdly, the extended cohort of patients including six affected individuals was reviewed for any variants present only in affected individuals with a low GnomAD frequency and filtered as described above.

By this method the combined analysis of six LSL individuals highlighted 829 variants in 703 genes. This included many variants that had unknown CADD scores, GnomAD frequency or *in silico* prediction. To further limit these variables, each gene was further reviewed for biological function and compared to the literature for evidence of involvement in either neural crest differentiation, adipogenesis or any previous documented association with neural tube defects (Figures V.iii and iv). Details of genes and products were taken from Ensemble and Genecards, and where relevant specific papers have been referenced.

Variants are annotated as per standard genetic annotation with p.Q312\* indicating the protein product with the amino acid at position 312 normally being Q (glutamine) but in this variant not being transcribed resulting in truncation of the protein at that location (indicated by \*). A full explanation of amino acid abbreviations can be found in the Abbreviations section.

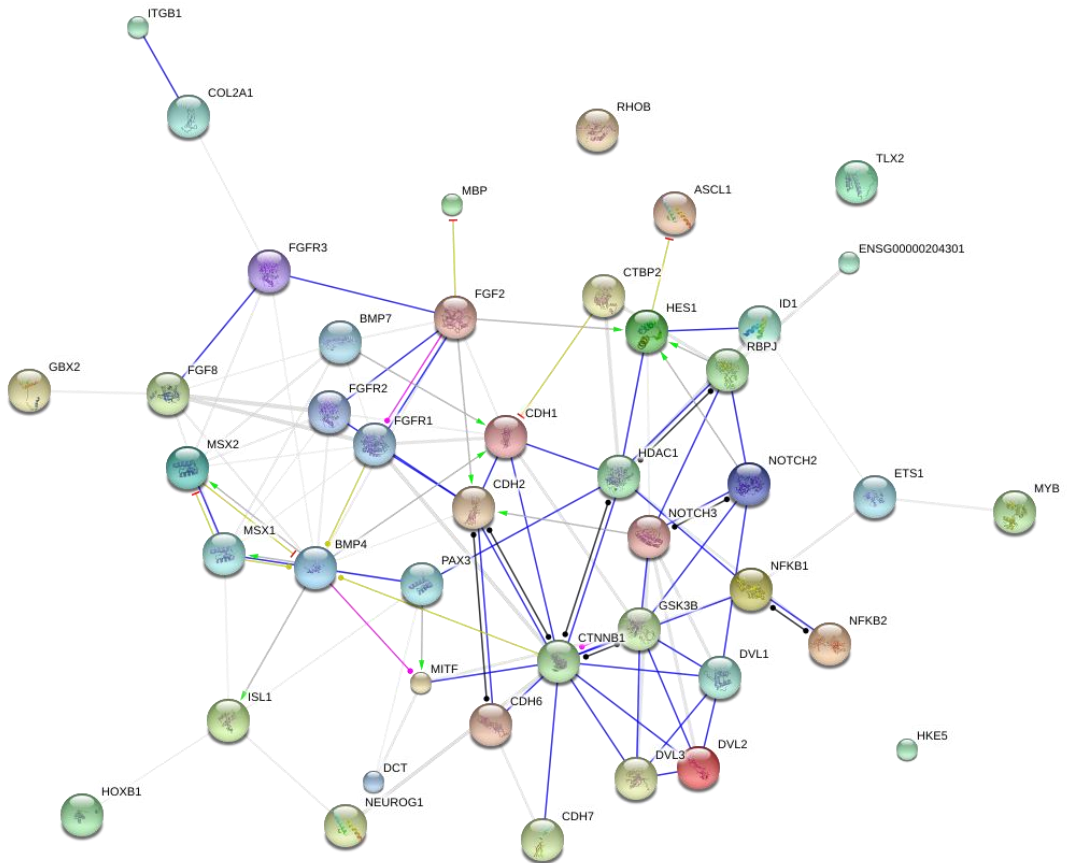


Figure V.iii. String diagram of the neural crest differentiation pathway taken from Pathcards. A total of 102 genes are known to have a role in neural crest differentiation.

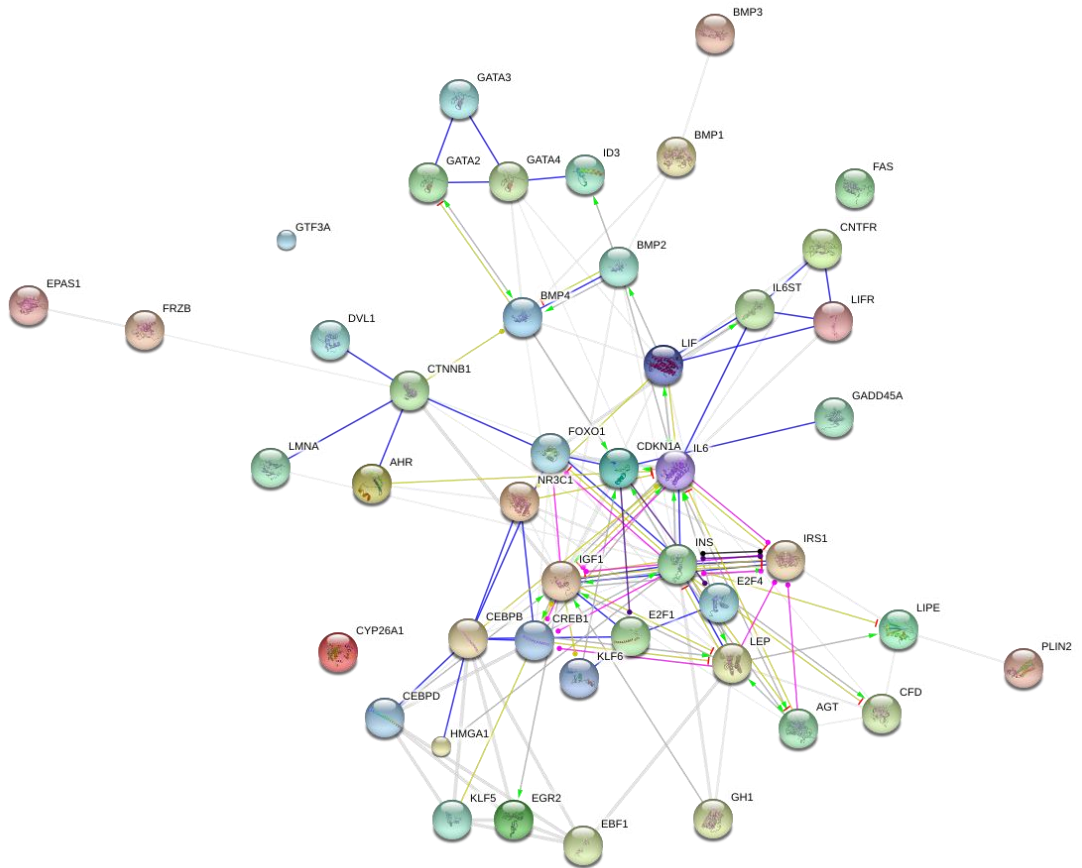


Figure V.iv. String diagram of the adipogenesis superpathway taken from Pathcards. A total of 123 genes are known to have a role in adipogenesis.

## 1. *RADIL* and *ARHGAP29*

All LSL patients were reviewed for the same variants as identified by Larrew et al, as well as any other exonic variants [38]. As whole genome sequence data (rather than whole exome sequence data) was only available for familial cases these were further reviewed for any non-exonic variants. Inheritance filters were not restricted to autosomal dominant inheritance since the digenic inheritance pattern would be lost by this filter. In situ hybridization was performed for both *RADIL* and *ARHGAP29* expression in human embryos in the developing caudal spinal cord as further supporting evidence for their possible role in LSL pathogenesis.

### *RADIL*

None of the families or LSL individuals had the same variant (Ala684Ser) as described in Larrew et al. A total of 325 variants were identified in the LSL cohort, of which twelve were exonic and seven were non-synonymous (Table V.1.i). The most abundant exonic variant after filtering was p.S886G which was homozygous in 5 cases and heterozygous in 1 case. This is a common variant (GnomAD > 99%) with *in silico* prediction models suggesting this it is unlikely to be disease causing. Further assessment of the *RADIL* sequence shows that this variant is located distant to any known functional binding domain of the protein. This variant is unlikely to be responsible for formation of LSL.

The exonic variant with the highest CADD score (of 18.7) was p.S490L. This variant, along with all the other exonic variants detected, was located outside the protein domains of *RADIL*. As previously, all *in silico* function prediction models predicted this variant to be not disease causing.

| Amino acid variant | Homozygotes | Heterozygotes | SIFT      | PP-2   | CADD | GnomAD frequency |
|--------------------|-------------|---------------|-----------|--------|------|------------------|
| S490L              |             | 1             | Tolerated | Benign | 18.7 | 3.30             |
| T968A              |             | 1             | Tolerated | Benign | <10  | 11.19            |
| H412D              | 1           | 3             | Tolerated | Benign | <10  | 25.14            |
| D239N              | 1           | 4             | Tolerated | Benign | <10  | 25.10            |
| S886G              | 5           | 1             | Tolerated | Benign | <10  | 99.64            |
| P946L              |             | 1             | Tolerated | Benign | <10  | 2.16             |
| L938P              |             | 2             | Tolerated | Benign | <10  | 32.17            |

Table V.1.i. Summary of all non-synonymous exonic variants in *RADIL* in LSL cohort (n=6). Explanation of amino acid annotation can be found in the Abbreviations section.

Reviewing the combination of SIFT function, Polyphen-2 Function, CADD score and GnomAD Frequency, it seems unlikely that any of these *RADIL* variants are candidates for further review regarding the pathogenesis of LSL.

The majority of other variants in the *RADIL* gene were intronic and none had a CADD score >20. Nineteen variants were in the promoter region of *RADIL*; these will be discussed separately in the individual families, as none of these variants were identified in all of the cohort.

## Family 1

Three exonic variants were detected on whole genome sequencing: p.S886G, p.D239N and p.H412D. Features of these variants are the same as in Table V.2.i. The control individual was homozygous for p.S886G but had neither of the other variants. None of these variants localized to a functional domain within the RADIL protein.

Eight variants were detected in the *RADIL* promoter region and are predicted to result in loss of transcription factor binding sites (TFBS). As demonstrated below, all but one of these variants was present in LSL cases and absent in the control case, despite being relatively prevalent in the general population based on the GnomAD frequency (Table V.1.ii).

| LSL cases | Control case | Potential TFBS loss   | GnomAD frequency |
|-----------|--------------|---|------------------|
| Het; Het  | -            | ARID3A, <b>FOXI1</b> , <b>FOXL1</b> , <i>Nkx2-5</i>               | 47.05            |
| Het; Het  | -            | ETS1, <b>GATA2</b> , Hlhf   | 28.26            |
| Het; Het  | -            | <i>Nkx2-5</i> , <i>Nkx3-2</i>                                     | 28.61            |
| Het; Het  | -            | ARID3A, <b>FOXL1</b> , <i>Nkx2-5</i> , <i>Pdx1</i> , <i>Prrx2</i> | 28.91            |
| Het; Het  | -            |   |                  |
| Het; -    | Het          | NFIC  |                  |
| Het; Het  | -            |   | 50.70            |
| Het; Het  | -            | <i>Esrrb</i> , <i>Myf</i> , <i>NR4A2</i> , <i>Pax2</i>            |                  |

Table V.1.ii. Summary of variants likely to result in TFBS loss within the *RADIL* sequence. Listed potential TFBSs are based on sequence analysis and predicted binding by Ingenuity and does not take into account known or experimental evidence to support interaction. Transcription factors highlighted in bold are known to have a role in adipogenesis. Transcription factors italicized are known to have general roles in development not associated with adipogenesis. None of the transcription factors are known to have a role in neurulation or NC cell migration or differentiation.



## Family 2

Eight exonic variants were detected, of which one was synonymous. As previously mentioned the p.S886G variant was present as in all LSL cases, and in keeping with its high GnomAD frequency was also homozygous in the control. A number of the variants were heterozygous in the control case and only heterozygous in one lipoma case making these unlikely to be pathological variants (Table V.1.iii). All variants are located outside the known functional domains.

| Amino acid variant | LSL cases | Control case | SIFT      | PP-2   | CADD | GnomAD frequency |
|--------------------|-----------|--------------|-----------|--------|------|------------------|
| S490L              | Het; -    | Het          | Tolerated | Benign | 18.7 | 3.30             |
| T968A              | Het; -    | Hom          | Tolerated | Benign | <10  | 11.19            |
| H412D              | Hom; Het  | -            | Tolerated | Benign | <10  | 25.14            |
| D239N              | Hom; Het  | Het          | Tolerated | Benign | <10  | 25.10            |
| S886G              | Hom; Hom  | Hom          | Tolerated | Benign | <10  | 99.64            |
| P946L              | Het; -    | Het          | Tolerated | Benign | <10  | 2.16             |
| L938P              | Het; -    | Hom          | Tolerated | Benign | <10  | 32.17            |

Table V.1.iii. Summary of exonic non-synonymous variants in Family 2. All variants were also identified in the LSL cohort analysis. Of note here is the frequency of variants within the control individual making many of these variants unlikely to be disease causing (although with digenic inheritance pattern they cannot be excluded).

Eighteen variants were detected in the promoter region of *RADIL*. Unlike Family 1 all promoter variants were also present in the control case (Table V.1.iv).

| LSL cases | Control case | Potential TFBS loss  | GnomAD frequency |
|-----------|--------------|--|------------------|
| Het; -    | Het          | ETS1, <b>GATA2</b> , Hltf  | 28.26            |
| Hom; Het  | Het          | <i>Nkx2-5</i> , <i>Nkx3-2</i>  | 28.61            |
| Hom; Het  | Het          | ARID3A, <b>FOXI1</b> , <b>FOXL1</b> , <i>Nkx2-5</i>                        | 47.05            |
| Het; -    | Het          | <i>YY1</i>   |                  |
| Hom; Het  | Het          | ARID3A, <b>FOXL1</b> , <i>Nkx2-5</i> , <i>Pdx1</i> ,<br><i>Prrx2</i>       | 28.91            |
| Hom; Het  | Het          |  | 29.25            |
| Hom; Hom  | Hom          | <i>MZF1</i>  | 50.80            |
| - ; -     | Het          | <b>FOXC1</b>   | 20.01            |
| Hom; Hom  | Hom          | <b>FOXC1</b> , <i>FOXO3</i> , HNF1B  | 48.26            |
| Het; -    | Het          |  | 33.57            |
| Het; Hom  | Het          | ETS1, Pax2, <b>HIF1A</b>   | 14.66            |
| Hom; Hom  | Hom          |  | 48.60            |
| Het; -    | Het          | NFIC   | 77.18            |
| Hom; Hom  | Hom          | <i>ZEB1</i>  | 48.14            |
| Het; Het  | Hom          |  | 50.70            |
| Hom; Hom  | Hom          | Esrrb, Myf, NR4A2, <i>Pax2</i>   | 66.35            |
| Het; Hom  | Het          | NFIC   |                  |
| Het; -    | Hom          | CEBPA, <b>FOXL1</b> , <i>Nkx2-5</i> , Nobox,<br><i>Pdx1</i> , <i>Prrx2</i> | 35.82            |

Table V.1.iv. Summary of variants likely to result in TFBS loss within the *RADIL* sequence in Family 2. Listed potential transcription factors are based on sequence analysis and predicted binding by Ingenuity and does not take into account known or experimental evidence to support interaction. Transcription factors in bold are known to have a role in adipogenesis. Transcription factors italicized are known to have general roles in development not associated with adipogenesis. None of the transcription factors are known to have a role in neurulation or neural crest cell migration or differentiation.

Potential TFBS loss for variants that were detected in both LSL cases were reviewed in more detail to determine the likelihood of involvement in the pathogenesis of LSL. The variant with the lowest GnomAD frequency across both families is predicted to result in TFBS loss of HIF1A. HIF1A is activated by the CREBBP/EP300 complex and has a role in adipogenesis, although there is no known association between any of these three proteins and RADIL in adipogenesis [255].

## Gene Expression

RNASCOPE expression of *RADIL* in human embryos, focusing on the caudal-most body region, was performed between CS13 and CS16 with samples provided by HDBR (Figure V.1.i and ii). There is faint detection of *RADIL* throughout the neural tube with some expression in the paraxial mesoderm at CS16.

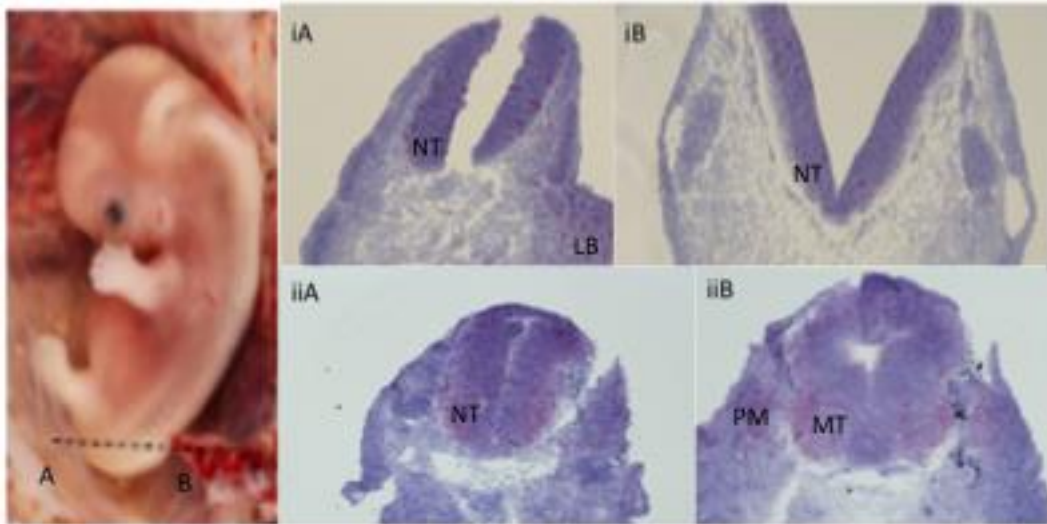


Figure V.1.i and ii. RNAScope of *RADIL* expression in human embryos with haematoxylin and eosin (H&E) counter stain. Magnification x10. Positive expression indicated by dark pink staining. Axial sections were taken through the caudal region such that two sections of neural tube were visible (A and B). iA, most caudal section of neural tube at CS13. iB, more cranial section through caudal neural tube at CS13. iiA, most caudal section of neural tube at CS16. iiB, more cranial section through caudal neural tube at CS16. NT = neural tube, LB = limb bud, MT = motor tract (within neural tube), PM = paraxial mesoderm.

## **ARHGAP29**

Analysis of *ARHGAP29* variants in all LSL cases revealed 173 variants. None of these corresponded with the variant (Ser864Pro) detected by Larrew et al. Two variants were exonic of which one was synonymous. The variant p.G1191D was homozygous in all LSL individuals which reflects the GnomAD frequency of 94.4%. The variant is located distant from the known *ARHGAP29* protein domains and, as such, the *in silico* prediction models suggest this to be benign. Four variants were in the promoter region of *ARHGAP29* and predicted to cause TFBS loss. These will be discussed separately in the individual families as none of these variants were identified in all of the cohort.

### **Family 1**

Exonic variants were as discussed for the group analysis. Of note, the one non-synonymous exonic variant was also homozygous in the control case.

There were four variants detected within the promoter region of *ARHGAP29* with predicted promoter loss. All were present in the control case and most had a relatively high GnomAD frequency (Table V.1.v).

| LSL cases | Control case | Potential TFBS loss     | GnomAD frequency |
|-----------|--------------|-------------------------|------------------|
| Het; -    | Het          | NFIC                    | 30.15            |
| Het, Het  | Het          |                         | 26.62            |
| Hom; Hom  | Hom          | <i>Nobox, Pdx1, YY1</i> | 97.17            |
| Hom; Hom  | Hom          | <b>FOXC1</b>            | 83.51            |

Table V.1.v. Summary of variants likely to result in TFBS loss within the *ARHGAP29* sequence in Family 1. Listed potential transcription factors are based on sequence analysis and predicted binding by Ingenuity and does not take into account known or experimental evidence to support interaction. Transcription factors highlighted in bold are known to have a role in adipogenesis. Transcription factors italicized are known to have general roles in development not associated with adipogenesis. None of the transcription factors are known to have a role in neurulation or neural crest cell migration or differentiation.

## Family 2

Exonic variants were as in combined analysis and Family 1. The variant p.G1191D was also homozygous in the control case. There were four variants with possible TFBS loss (Table V.1.vi). The potential TFBS loss of most interest is *Foxd3*. In the mouse, *Foxd3* is expressed in the dorsal neural tube and is an accepted marker of pre-migratory neural crest. Inhibition of *Foxd3* expression results in reduced expression of *Sox10*, a transcription factor vital for neural crest stem cell formation [256].

| LSL cases | Control case | Potential TFBS loss   | GnomAD frequency |
|-----------|--------------|---|------------------|
| Het; Hom  | Het          | NFIC  | 30.92            |
| Het, Het  | Het          | CTCF, <b>FOXC1</b> , <b>Foxd3</b> , <b>FOXI1</b> , <b>FOXL1</b> , RAD21 | 17.26            |
| Hom; Hom  | Hom          | <b>FOXC1</b>  | 87.34            |
| Hom; Hom  | Hom          | <i>Nobox</i> , <i>Pdx1</i> , <i>YY1</i>                                 | 97.56            |

Table V.1.vi. Summary of variants likely to result in TFBS loss within the *ARHGAP29* sequence in Family 2. Listed potential transcription factors are based on sequence analysis and predicted binding by Ingenuity and does not take into account known or experimental evidence to support interaction. Transcription factors highlighted in bold are known to have a role in adipogenesis.

## Gene Expression

RNASCOPE expression of *ARHGAP29* in human embryos, focusing on the caudal-most body region, was performed between CS13 and CS16 (Figure V.1.iii). Strong staining was noted around the lateral margins of the neural tube, as well as in the surface ectoderm (future epidermis).

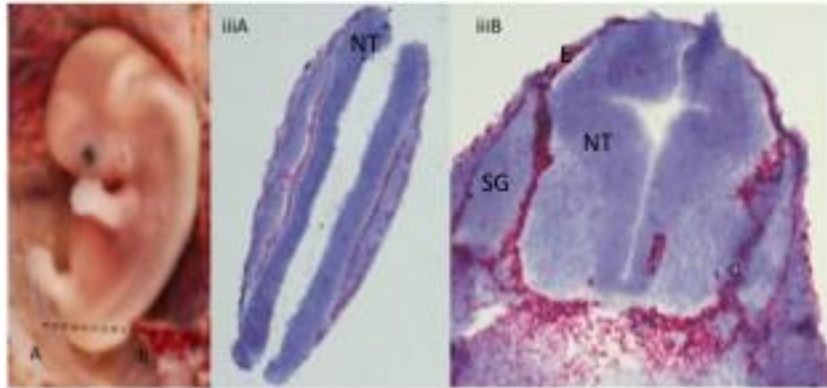


Figure V.1.iii. RNAScope of *ARHGAP29* expression in human embryos with haematoxylin and eosin (H&E) counter stain. Magnification x10. Positive expression indicated by dark pink staining. Axial sections taken through the caudal body region such that two sections of neural tube were visible (A and B). iiiA, most caudal section of neural tube at CS13. iiiB, more cranial section through caudal neural tube at CS16. NT = neural tube, SG = spinal ganglion, E = ectoderm.

## **2. FAMILIAL LSL**

### **Family 1**

The WGSs of Family 1 were reviewed applying an autosomal dominant inheritance filter limiting variants to those that are present in both LSL individuals and absent in the control family member. Two hundred and seventy variants were identified and were ranked from highest to lowest probability of being deleterious. A total of 15 variants were reviewed in more detail and are summarized below (Table V.2.i). Five variants were stop gain mutations resulting in a truncated product protein. Three variants were frameshift variants possibly resulting in no or limited function of the product protein beyond the point of the variant. The remaining seven variants were single nucleotide variants resulting in a single amino acid change. These 15 genes were all reviewed in terms of the location of the variant and how this relates to known functional domains in the product protein, detail of the function of the protein and any pathology previously attributed to variations in the gene. Finally any mention in the literature of the particular gene being associated with adipogenesis or neural tube defects was reviewed (Tables V.2.ii, iii and iv).

The 270 variants were further reviewed for any candidate genes that are known to have a role in adipogenesis, neural crest differentiation or neural tube formation. However, no further variants were flagged by this method.

| <b>GENE</b>                       | <b>Nucleotide Variant</b>          | <b>CADD Score</b> | <b>PP2</b> | <b>SIFT</b> | <b>GnomAD Frequency</b> |
|-----------------------------------|------------------------------------|-------------------|------------|-------------|-------------------------|
| <i>LRIG2</i>                      | SNV T→G                            | 38                |            |             |                         |
| <i>NDST1</i>                      | SNV C→T                            | 40                |            |             |                         |
| <i>SLC36A2</i>                    | Insertion CA                       |                   |            |             |                         |
| <i>FAM8A1</i>                     | SNV T→C                            | 24.6              | ++         | Damaging    | 0.003%                  |
| <i>TNFAIP3</i>                    | SNV C→T                            | 35                | ++         | Damaging    | 0.003%                  |
| <i>KIAA1324L</i>                  | Deletion CTC                       |                   |            |             |                         |
| <i>CLN8</i>                       | SNV C→T                            | 32                | ++         | Damaging    | 0.002%                  |
| <i>SYT15</i>                      | Deletion<br>GCCCTGGC               |                   |            |             |                         |
| <i>ADAMTS20</i>                   | SNV C→T                            | 39                |            |             |                         |
| <i>VRTN</i>                       | SNV G→A                            | 31                | +          | Damaging    | <0.0005%                |
| <i>C17orf107;</i><br><i>CHRNE</i> | Deletion<br>GGCGGCCCG<br>GGGGCCTCG |                   |            |             |                         |
| <i>ADGRL1</i>                     | SNV G→A                            | 24.7              | ++         | Damaging    |                         |
| <i>DEFB125</i>                    | SNV C→T                            | 34                |            |             | 0.002%                  |
| <i>SGSM1</i>                      | SNV C→T                            | 33                | +          | Damaging    | 0.002%                  |
| <i>ACOT9</i>                      | SNV G→A                            | 34                |            |             | 0.001%                  |

Table V.2.i. Summary of results from genetic analysis of whole genome sequencing from Family 1. Fifteen genes were highlighted as being most likely to be pathogenic based on the type of variant and comparison against genomics databases. PP2 = polyphen-2 Function prediction as either possibly damaging (+) or probably damaging (++), SIFT prediction as either damaging or tolerated. Empty squares indicate no prediction available by that particular prediction system.



### STOP GAIN VARIANTS

| Gene            | Protein Variant | Functional Domain Loss         | Evidence of role in adipogenesis | Association with neural tube defect | Associated pathology  | Protein Name, Function and Expression   |
|-----------------|-----------------|--------------------------------|----------------------------------|-------------------------------------|---|---|
| <i>LRIG2</i>    | L518*           | Immunoglobulin domains         | -                                | -                                   | Urofacial syndrome – neurogenic bladder but normal spinal MR [257, 258]   | Leucine-rich-repeats and immunoglobulin-like-domains 2<br>Role in neural cell signalling and cell cycle regulation [259]<br>Expressed in fetal bladder nerves [258]           |
| <i>NDST1</i>    | R211*           | Sulfotransfer                  | Forsberg et al [260]             | Pallerla et al [261]                | Holoprosencephaly [262]<br>Intellectual disability and epilepsy [263]<br><i>Congenital heart disease [264]</i><br><i>Cleft lip/palate [265]</i> | Bifunctional heparan sulfate N-deactylase/N-sulfotransferase 1<br>Heparan sulfate biosynthesis<br>Expressed throughout embryo and adult tissue [260]                          |
| <i>ACOT9</i>    | Q312*           | Hot dog (thioester hydrolysis) | -                                | -                                   | -   | Acyl-CoA thioesterase – likely fatty and amino acid metabolism in mitochondria [266]  |
| <i>ADAMTS20</i> | W1047*          | Thrombospondin type 1          | -                                | Nandadasa et al [267]               | -   | ADAM Metallopeptidase with thrombospondin type 1 motif 20 Secreted protein with role in cell migration [268](Somerville 2003)<br>Fetal expression in dorsal neural tube [269] |
| <i>DEFB125</i>  | R38*            | Defensin $\beta$ 2             | -                                | -                                   | -   | Defensin $\beta$<br>Immune response against invading organisms [270]  |

Table V.2.ii. Summary of candidate genes identified in Family 1 with stop gain variants. Both affected individuals were heterozygous for the variant but the variant was absent in the control parent. Protein variants annotated as amino acid abbreviation as in control parent/amino acid position/\* indicating truncation of protein at that position. Functional domain loss refers to known domains only. Associated pathology in italics indicates non-human experimental evidence.

### FRAMESHIFT VARIANTS

| Gene                                       | Protein Variant | Functional Domain Loss   | Evidence of role in adipogenesis        | Association with neural tube defect | Associated pathology                      | Protein Name, Function and Expression   |
|--|-----------------|--|---|-------------------------------------|---|---|
| <i>SLC36A2</i>                             | E395fs          | -  | Cell surface marker of adipocytes [271] | -                                   | -   | PAT2<br>pH-dependent proton-coupled amino acid transport (glycine, alanine and proline)<br>Expressed in kidney and adipocytes [271-273]               |
| <i>C17orf107</i>                           | E361fs          | -  | -                                       | -                                   | -   | -   |
| <i>CHRNE</i><br>( <i>promoter region</i> ) |                 | LIC (Ligand-gated Ion Channel)<br>Neurotransmitter-gated ion-channel transmembrane | -                                       | -                                   | Congenital myasthenic syndrome [274, 275] | Cholinergic receptor nicotinic epsilon subunit<br>Part of acetylcholine receptor in neonates<br>Expressed at neuromuscular junction in neonates [276] |
| <i>KIAA1324L</i>                           | G914fs          | Terminal glycine residues  | -                                       | -                                   | -   | -   |

Table V.2.iii. Summary of candidate genes identified in Family 1 with frameshift variants. Both affected individuals were heterozygous for the variant but the variant was absent in the control parent. Protein variants annotated as amino acid abbreviation as in control parent/amino acid position/fs indicating shift of coding sequence for rest of protein. Functional domain loss refers to known domains only located after the position of the variant and therefore disruption of the coding sequence of that domain.

### MISSENSE VARIANTS

| Gene           | Protein Variant | Located within Domain  | Evidence of role in adipogenesis | Association with neural tube defect | Associated pathology   | Protein Name, Function and Expression  |
|----------------|-----------------|--|----------------------------------|-------------------------------------|--|--|
| <i>FAM8A1</i>  | I288T           | RDD domain   | -                                | -                                   | -  | Family with sequence similarity 8 member A1, Role in ERAD<br>Expression throughout adult [277]   |
| <i>TNFAIP3</i> | R141C           | OUT domain (possible protease)   | Dorransoro et al 2013 [278]      | -                                   | -  | TNF Alpha Induced Protein 3 Zinc-finger protein and ubiquitin-editing enzyme, involved in NF-κB pathway [278]                          |
| <i>CLN8</i>    | R70C            | TRAM LAG1 CLN8 domain  | -                                | Oren et al 2019 [279]               | Elevated sphingolipids and phospholipids in brain CLN8 disease (neuronal ceroid lipofuscinoses) [280]. | CLN8<br>Transmembrane protein with role in lipid synthesis and lysosome biogenesis [280].<br>Expressed in central nervous system [281] |
| <i>VRTN</i>    | R440Q           | -  | -                                | -                                   | <i>Vrtn-null mice display abnormal somitogenesis and fewer thoracic vertebrae [282].</i>               | Vertebrae development associated<br>Expressed in developing somites<br>Development of thoracic vertebrae [282]                         |
| <i>ADGRL1</i>  | S1253F          | Latrophilin domain (G-protein coupled receptor associated with secretion). | -                                | -                                   | -  | Latrophilin 1<br>Adhesion G protein coupled receptor expressed in the brain<br>Synapse formation and brain development [283]           |
| <i>SGSM1</i>   | R59W            | RUN domain   | -                                | -                                   | -  | Small G protein signalling modulator 1<br>Expressed in central nervous system [284].   |

Table V.2.iv. Summary of candidate genes identified in Family 1 with single missense variants. Both affected individuals were heterozygous for the variant but the variant was absent in the control parent. Protein variants annotated as amino acid abbreviation as in control parent/amino acid position/new amino acid variant. Domains listed if variant located within a specific known domain. Associated pathology in italics indicates non-human experimental evidence. ERAD = endoplasmic reticulum associated degradation.

## **Family 2**

Family 2 was reviewed as described above for Family 1. Two hundred and eighty four variants were identified and were analysed separately, firstly as those with the highest probability of being deleterious; and secondly as those with the highest probability of being involved in the formation of LSL through analysis of their known function and interactions.

A total of 16, all single nucleotide, variants were considered most likely to be disease causing and are summarized below (Table V.2.v). These 16 genes were all reviewed in terms of the location of the variant and how this relates to known functional domains in the product protein, detail of the function of the protein and any pathology previously attributed to variations in the gene. Finally any mention in the literature of the particular gene being associated with adipogenesis or neural tube defects was reviewed (Table V.2.vi).

The 284 variants were further reviewed for any candidate genes that are known to have a role in adipogenesis, neural crest differentiation or neural tube formation. Two further variants were flagged by this method.

| <b>GENE</b>    | <b>Variant</b> | <b>CADD Score</b> | <b>PP2</b> | <b>SIFT</b> | <b>GnomAD Frequency</b> |
|----------------|----------------|-------------------|------------|-------------|-------------------------|
| <i>HEATR5B</i> | SNV A → T      | 29.7              | ++         | Damaging    |                         |
| <i>AADA2L2</i> | SNV G → A      | 24.8              | ++         | Damaging    |                         |
| <i>MYLK4</i>   | SNV C → A      | 29.8              | +          | Damaging    |                         |
| <i>TRAF2</i>   | SNV C → T      | 31                | +          | Damaging    |                         |
| <i>FXD4</i>    | SNV T → A      | 24                |            |             |                         |
| <i>TGFB2</i>   | SNV T → C      | 28.6              | ++         | Damaging    |                         |
| <i>PAN2</i>    | SNV C → A      | 34                | +          |             | 0.001%                  |
| <i>ZNF747</i>  | SNV G → A      | 23.5              | +          | Damaging    |                         |
| <i>KCNG4</i>   | SNV C → G      | 27.4              | +          | Damaging    | 0.002%                  |
| <i>HYDIN</i>   | SNV T → C      | 28.9              |            |             |                         |
| <i>NOD2</i>    | SNV G → T      | 29.1              | ++         | Damaging    |                         |
| <i>KRT28</i>   | SNV G → T      | 28.1              | ++         | Damaging    |                         |
| <i>EMILIN3</i> | SNV T → C      | 24.5              | +          | Damaging    |                         |
| <i>COL6A1</i>  | SNV G → A      | 23.1              | ++         | Damaging    |                         |
| <i>CCT8</i>    | SNV G → A      | 28.4              | +          | Damaging    |                         |
| <i>CBR3</i>    | SNV G → T      | 32                | ++         | Damaging    |                         |

Table V.2.v. Summary of results from genetic analysis of whole genome sequencing from Family 2. Sixteen genes were highlighted as being most likely to be pathogenic based on the type of variant and comparison against genomics databases. PP2 = polyphen-2 Function prediction as either possibly damaging (+) or probably damaging (++), SIFT prediction as either damaging or tolerated. Empty squares indicate no prediction available by that particular prediction system, or that the gnomAD frequency is unknown.

## MISSENSE VARIANTS

| Gene           | Protein Variant | Located within Domain                                 | Evidence of role in adipogenesis | Association with neural tube defect | Associated pathology | Protein Name, Function and Expression   |
|----------------|-----------------|---|----------------------------------|-------------------------------------|----------------------|---|
| <i>HEATR5B</i> | V501D           |   | -                                | -                                   |                      | HEAT Repeat Containing 5B protein<br>Expressed throughout body  |
| <i>AADA2L2</i> | G187R           | Abhydrolase<br>Abhydrolase 3                          | -                                | -                                   |                      | Arylacetamide deacetylase Like 2 protein<br>Expressed in skin [285]   |
| <i>MYLK4</i>   | D323Y           |   | -                                | -                                   |                      | Myosin light chain kinase family member 4<br>Role in muscle development<br>Expressed in muscle  |
| <i>TRAF2</i>   | P186L           | zf-TRAF domain  |                                  | Wang et al 2015 [286]               |                      | TNF receptor-associated factor 2<br>Role in numerous pathways: cell death, cell proliferation, inflammation, NF- $\kappa$ B, JNK, p38 pathways [287]. |
| <i>FXD4</i>    |                 | ATP1G1/PLM/MAT 8 domain                               | -                                | -                                   |                      | FXD domain containing ion transport regulator 4<br>Modulation of Na/K-ATPase<br>Expressed in kidney [288]   |
| <i>TGFB2</i>   | L78P            | TGFB propeptide domain                                | Wang et al 2012 [289]            | Mayanil et al 2006 [290]            |                      | Transforming growth factor beta role in a number of different pathways  |
| <i>PAN2</i>    | R571L           | Peptidase C19 Ubiquitin carboxyl-terminal transferase | -                                | -                                   |                      | PAN2 is an adenylase involved in degradation of mRNA  |
| <i>ZNF747</i>  | P15S            | -   | -                                | -                                   |                      | Voltage-gated potassium channel largely expressed in adrenal glands   |
| <i>KCNG4</i>   | V308L           | Ion transport domain                                  |                                  |                                     |                      |   |
| <i>HYDIN</i>   | E1488G          | -   | -                                | -                                   |                      | HYDIN Axonemal Central Pair Apparatus Protein involved in cilia motility and expressed in the testes  |

**MISSENSE VARIANTS continued**

| <b>Gene</b>    | <b>Protein Variant</b> | <b>Located within Domain</b>             | <b>Evidence of role in adipogenesis</b> | <b>Association with neural tube defect</b> | <b>Associated pathology</b> | <b>Protein Name, Function and Expression</b>  |
|----------------|------------------------|--|---|--|-----------------------------|---|
| <i>NOD2</i>    | A891S                  | -  | -                                       | -  | Inflammatory bowel disease  | Nucleotide binding oligomerization domain containing 2 protein plays a role in immune response  |
| <i>KRT28</i>   | L255I                  | Filament domain                          | -                                       | -  | -                           | Keratin family protein expressed in the testes contributing to the cytoskeleton of epithelial cells   |
| <i>EMILIN3</i> | Y42C                   | -  | -                                       | -  | -                           | Elastin microfibril enhancer 3<br>Expressed in tailbud of mice at E8.5-9.5, later expressed in developing gonads and osteogenic mesenchyme [291]  |
| <i>COL6A1</i>  | R68H                   | Von Willebrand factor type A domain      | -                                       | -  | -                           | Collagen type VI alpha 1 subunit<br>Contributes to the heterotrimeric collagen VI, a major component along neural crest migratory pathways<br>Role in neural crest cell differentiation [292] |
| <i>CCT8</i>    | S131F                  | All major domains of the product protein | -                                       | -  | -                           | Chaperonin-containing T-complex protein subunit 8<br>Expressed throughout the body<br>Role in protein synthesis   |
| <i>CBR3</i>    | G83W                   | All major domains of the product protein | Chang 2012 [293]                        | -  | -                           | Carbonyl reductase 3  |

Table V.2.vi. Summary of candidate genes identified in Family 2 with single missense variants. Both affected individuals were heterozygous for the variant but the variant was absent in the control parent. Protein variants annotated as amino acid abbreviation as in control parent/amino acid position/new amino acid variant. Domains listed if the variant located within a specific known domain. Associated pathology in italics indicates non-human experimental evidence.

### 3. COMBINED LSL COHORT

The combined cohort of LSL patients (familial and sporadic cases) was reviewed for variants that were prevalent in the cohort but had a low GnomAD frequency and for variants that were selected by genetic filtering to be likely disease causing. Nine genes were selected in total that showed significant variants (Table V.3.i). A number of genes had multiple variants (Tables V.3.ii and iii).

| Gene            | Variant | Cases        | CADD | PP2 | SIFT      | GnomAD |
|-----------------|---------|--------------|------|-----|-----------|--------|
| <i>PNPLA7</i>   | D589N   | 1 het        | 34   | +   | Damaging  | 0.001% |
| <i>PTPRG</i>    | A286V   | 4 hom        | <10  |     |           |        |
| <i>SMAD6</i>    | R57H    | 2 het        | 24.6 | +   | Tolerated |        |
| <i>KCTD15</i>   | E280*   | 1 het        | 48   |     |           |        |
| <i>FOLR3</i>    | Y107*,  | 5 het; 1 hom |      |     |           |        |
| <i>EIF4EBP1</i> | R63W    | 5 het        | 35   | ++  | Damaging  | 0.001% |
| <i>DVL2</i>     | R590Q   | 1 het        | 21.1 | +   | Tolerated | 0.001% |
| <i>ANKRD26</i>  | A186S   | 1 het        | 23   | ++  | Damaging  | 0.001% |
| <i>FRG2C</i>    | R160fs* | 6 het        | 19.8 |     |           |        |

Table V.3.i. Summary of results from genetic analysis of whole genome sequencing and whole exome sequencing from all LSL individuals. Nine genes were highlighted as being most likely to be pathogenic based on the type of variant and comparison against genomics databases. PP2 = polyphen-2 Function prediction as either possibly damaging (+) or probably damaging (++), SIFT prediction as either damaging or tolerated. Empty squares indicate no prediction available by that particular prediction system. Hom = homozygous, Het = heterozygous. Total cases 6.

*PNPLA7* codes for the patatin like phospholipase domain containing 7 protein. The variant is located within the CAP ED domain which is an effector domain for a group of transcription factors. *PNPLA7* is expressed in adipocytes and hydrolyses lysophosphatidylcholines [294, 295].

*PTPRQ* codes for the protein tyrosine phosphatase receptor type Q, a member of type III receptor-like protein-tyrosine phosphatase family, and is largely expressed in adipocytes. Overexpression of *PTPRQ* causes reduced differentiation of mesenchymal stem cells into adipocytes [296]. This variant is located outside of the known domains.

*SMAD6* is expressed in the dorsal spinal cord of the chick embryo and plays a role in neuronal differentiation via the Wnt/ $\beta$ -catenin pathway [297]. Zhang et al demonstrated methylation of *SMAD6* (and other genes associated with the epithelial-to-mesenchymal transition) in a pedigree of multiple neural tube defect individuals [298]. The Smad6 protein is known as an inhibitory



smad (I-smad) due to its role in inhibiting TGF-  $\beta$  signalling, a protein involved in regulation of adipogenesis [299]. This variant is located outside of the known domains.

*KCTD15* codes for the potassium channel tetramerization domain containing 15 protein. Different roles of *KCTD15* include inhibition for NC formation through interaction with TFAP2A [300], and adipogenesis [301]. Smaldone et al also demonstrated that the C-terminus of the *KCTD15* was particularly important in the stabilization of the functional domain containing N-terminus [301]. This stop gain variant is located within 3 amino acids of the C-terminus of the product protein.

*FOLR3* codes for the Folate 3 receptor. Whilst folate is known to have an important role in the prevention of neural tube defects, little is known about *FOLR3*. Unlike the other two folate receptors, *FOLR3* is predicted to be a secreted protein expressed mainly in the bone marrow and spleen [302]. Findley et al reviewed the role of mutations in the folate receptors in cases of myelomeningocele and identified 5 new variants in *FOLR3* (four insertion/deletions and one stop gain variant) [303]. This frameshift variant was the result of a TA insertion.

*EIF4EBP1* gene encodes eukaryotic translation initiation factor 4E-binding protein that represses translation through interaction with eIF4E. eIF4EBP1/2 double knockout mice demonstrated accelerated adipogenesis [304]. Multiple variants across LSL individuals were identified in *EIF4EBP1* all within the functional domain of the protein (Table V.3.ii).

| Variant | Cases | CADD  | PP2 | SIFT       | GnomAD |
|---------|-------|-------|-----|------------|--------|
| D55H    | 2 het | 32    | ++  | Damaging   |        |
| R56W    | 2 het | 35    | ++  | Damaging   |        |
| R63W    | 5 het | 35    | ++  | Damaging   | 0.001  |
| S65L    | 5 het | 34    | ++  | Damaging   | 0.001  |
| P71L    | 4 het | 32    | ++  | Damaging   |        |
| S85A    | 5 het | <10   | -   | Tolerated  |        |
| M91fs*  | 5 het |       |     |            |        |
| M91T    | 5 het | <10   | -   | Activating |        |
| R99S    | 4 het | 11.43 | -   | Tolerated  |        |

Table V.3.ii. Summary of variants identified in *EIF4EBP1*. PP2 = polyphen-2 Function prediction as either benign (-) possibly damaging (+) or probably damaging (++), SIFT prediction as either damaging, tolerated or activating. Empty squares indicate no prediction available by that particular prediction system. Hom = homozygous, Het = heterozygous. Total cases 6.

*DVL2* encodes the protein disheveled segment polarity protein 2 which is part of the PCP pathway. De Marco et al demonstrated the presence of *DVL2* variants in a human population of

neural tube defects (they do not make distinctions within the diagnosis), and supported this with murine evidence that *dv12* *-/-* mice have thoracic spina bifida [174]. This variant is located within the Dsh C domain of the protein product.

*ANKRD26* is expressed throughout the body and the product protein ANKRD26 (Ankyrin repeat domain 26) is likely to function in cell signalling. Fei et al demonstrated that *Ankrd26**-/-* mouse embryo fibroblasts have a higher rate of spontaneous adipogenesis [305]. There is no association between *ANKRD26* and neural tube defects. This variant is located within multiple domains near the N-terminus of the protein product.

Multiple variants were identified in *FRG2C* (Table V.3.iii). All but D9N were located within or caused frame shift across the *FRG2C* functional domain. The likelihood of these variants causing altered protein function is difficult to assess due to a disparity between different prediction algorithms. Little is known about the exact function of the *FRG2C*, FSHD region gene 2 family C member, however, it has been found to be expressed at increased levels in mesenchymal stem cells in ankylosing spondylitis stem cells, a group of cells known to have a greater tendency towards osteogenesis [306].

| Variant | Cases | CADD  | PP2 | SIFT      | GnomAD |
|---------|-------|-------|-----|-----------|--------|
| R160fs* | 6 het | 19.8  |     |           |        |
| D9N     | 5 het | <10   | ++  | Tolerated |        |
| D143G   | 5 het | <10   | ++  | Tolerated |        |
| R156C   | 6 het | 15.4  | -   | Damaging  |        |
| L210M   | 4 het | 12.95 | +   | Tolerated |        |

Table V.3.iii. Summary of variants identified in *FRG2C*. PP2 = polyphen-2 Function prediction as either benign (-) possibly damaging (+) or probably damaging (++), SIFT prediction as either damaging or tolerated. Empty squares indicate no prediction available by that particular prediction system. Hom = homozygous, Het = heterozygous. Total cases 6.

#### **4. COMPARISON WITH THE LITERATURE**

All genes previously described as being associated with LSL were reviewed in the combined cohort of LSL patients. Any exonic variants were further reviewed.

##### ***TFAP2A-IRF6-GRHL3***

Fifty-two variants were identified in *TFAP2A* with one being exonic, although this variant was synonymous. Seventy-nine variants were identified in *IRF6* with one being exonic, and this variant was also synonymous. One hundred and thirteen variants were identified in *GRHL3* with 6 being exonic: 3 synonymous and 3 non-synonymous. The variant p.T408M was present in one affected individual. The SIFT Function prediction was that this protein would be damaging and this is supported by both the PolyPhen-2 Function prediction (possibly damaging) and CADD score (29.6) and gnomAD Frequency of 2.3%. Further analysis of the *GRHL3* gene locates this variant to outside the CP2 domain

##### ***PTK7***

Five hundred and four variants were identified in *PTK7* with two being exonic, although both these variants were synonymous.

##### ***CELSR1/VANGL1/VANGL2***

Six hundred and eighty three variants were identified in *CELSR1* with 20 being exonic, although nine of these variants were synonymous. Two variants were highlighted as being potentially damaging. Variant p.S664W is a common variant (gnomAD Frequency 92.3%) and accordingly is homozygous in four of six affected individuals. The PolyPhen-2 Function Prediction is 'Probably Damaging' and this is supported by the location of the variant to the cadherin repeat-like domain of the protein. Variant p.E2903Q is also a common variant (gnomAD Frequency 22.5%). The SIFT Function Prediction is damaging, however the PolyPhen Function Prediction is Benign and the location of the variant is distant to any of the known domains.

One hundred and eighty five variants were identified in *VANGL1* with 2 being exonic. Of note the variant p.S336\* was present in two individuals and is a stop gain variant resulting in a truncated protein. The CADD score is notably high at 36.

Forty-seven variants were identified in the *VANGL2* gene of which 3 were exonic, although, all 3 were synonymous.

### ***EP300***

Two hundred and fifteen variants were identified in the EP300 gene of which 4 were exonic. One was synonymous, two are predicted to be tolerated/benign, and the last variant was only present in one individual but results in loss of function of one allele.

### ***FZD6***

One hundred and twenty four variants were identified in the FZD6 gene of which 3 were exonic and all were synonymous.

### **SUMMARY**

Variants in GRHL3, VANGL1 were deemed to be particularly likely to be disease causing. Both these genes and their related pathways have been associated with LSL in large-scale genetic studies, although the incidence of identified variants is always low in these studies. Although the LSL cohort here is small, the results reflect these larger studies. Multiple different heterozygous variants across a number of different genes show an association with the disease.

## 5. DISCUSSION

The Larrew paper does not offer any *in silico* analysis of the variants detected, nor do they discuss the location or likely biological impact that the variants they identified might have on protein function. In the absence of functional *in vitro* models demonstrating altered protein function as a result of the variant(s), or an animal model with these variants inserted causing the disease phenotype, it is difficult to extrapolate their data further. With a proposed digenic inheritance pattern, the GnomAD frequency becomes less relevant, although a variant in one gene that was very abundant in the population would result in variants of the second gene mimicking an autosomal dominant inheritance pattern.

Neither of the variants published by Larrew were identified in either the familial LSL cases or in the LSL cohort. The most likely disease causing variant was in *RADIL*, S490L, and was located outside of the known functional protein domains. This variant was only heterozygous in one LSL individual yet also heterozygous in a control individual. *In silico* prediction did not support any of the variants in *RADIL* or *ARHGAP29* as being disease causing. These negative results do not contradict the findings by Larrew et al but rather support the model of LSL being a multigene disease, possibly with different pathogenic variants present in different affected individuals, as is thought to be the case in open NTDs.

The fact that *RADIL* has been shown to be required for normal neural crest cell migration in zebrafish, and that *ARHGAP29* and *RADIL* interact, is in keeping with a possible neural crest cell origin of LSL. RNAscope demonstrates that both genes are expressed in and around the caudal neural tube, consistent with expression in neural crest. As discussed in Section II, caudal neural crest cells associated with secondary neurulation have only been identified in chick embryos and their fate is restricted to glia and melanocytes. If there is a human population of caudal neural crest cells it seems feasible that failure of their migration and maldifferentiation could be one of the factors involved in LSL pathogenesis.

### Family 1

There are two strong candidates for the pathogenesis of LSL identified in this family: *NDST1* and *ADAMST20*.

#### ***NDST1***

The *NDST1* protein is important in the sulfation of *N*-acetyl-D-glucosamine during the synthesis of heparan sulfate proteoglycans (HSPGs). HSPGs are a group of 17 different molecules all with a core protein and two or more heparan sulfate sugar chains covalently attached. They are present either as membrane bound, secreted into the extracellular matrix or within secretory vesicles. Synthesis is within the Golgi apparatus of most cells and is dependent on a number of different enzymes resulting in sulfation and epimerization at different positions along the polysaccharide

chains. The regulation of the exact pattern of sulfation and epimerization seems to depend on the cell type [307]. In addition, it is this pattern of residues, especially the negatively charged sulfate residues, which alters the specificity of interactions of the product HSPG. Variations in the protein core, number and length of polysaccharide chains and associated residues result in the large number of different functions associated with HSPG: cell migration, signalling and motility, protease regulation, development of morphogen gradients and inflammatory and coagulation pathways [308].

The first steps of HSPG synthesis involve the addition of xylose to serine residues on core proteins. The xylose is then extended into a tetrasaccharide with the addition two galactoses and glucuronic acid. The sugar chains are further extended by alternate additions of *N*-acetyl-D-glucosamine (GlcNAc) and glucuronic acid (GlcAc) by the ExtI3, Ext1 and Ext2 enzymes. Ndst1 has a bifunctional role to remove the acetyl group from the GlcNAc sugars and replace with sulfate (N-deacetylase/N-sulfotransferase). The GlcAc sugars are firstly epimerized (conversion of glucuronic acid to iduronic acid) and then sulfate is added by *O*-sulfotransferase enzymes. Not all sugars undergo sulfation, but when sulfation does occur it tends to be in clusters generating NS domains where protein ligands bind [309].

*NDST1* is a 70 kb gene located on chromosome 5. The product protein bifunctional heparan sulfate N-deactylase/N-sulfotransferase 1 consists of 882 amino acids and folds to form a spherical protein consisting of 5 parallel  $\beta$  sheets, 8 anti-parallel  $\beta$  sheets and a random coil resulting in a cleft that holds PAP (3'-phosphoadenosine 5'-phosphate). PAP acts as the sulfate donor with the cleft being large enough to receive the polysaccharide chain to be sulfated as well. This sulfotransferase site is formed from amino acids 580-880 [310]. The deacetylase site has not yet been established, although variants in cysteine 486 abolishes or increases deacetylase activity [311].

There are four *NDST* genes in humans: *NDST1* and 2 are expressed throughout adult and embryo tissues, whereas *NDST3* and 4 seem to have a more restricted expression [312]. *NDST1* has a specific role in development, as indicated by animal knockouts. Ringval et al were the first group to demonstrate a mammalian knockout with *Ndst1*<sup>-/-</sup> mice. They demonstrated neonatal death due to a respiratory distress syndrome and incomplete penetrance of cranial and eye defects [313]. Pan et al further expanded the phenotype in mice describing a range of optic abnormalities from coloboma to anophthalmia, dependent on FGF signalling [314]. Later, the same group added to the phenotype describing cleft lip, face and palate and split sternum as well as a low penetrance of neural tube defects (5%) and delayed ossification. They also identified a role for *Ndst1* in NC cell survival [261, 264].

Lanner et al demonstrated the vital role of HSPG in regulating FGF receptor signalling and subsequently embryonic stem cell differentiation [315]. Similarly, Forsberg et al demonstrated

*Ndst1*<sup>-/-</sup> *Ndst2*<sup>-/-</sup> embryonic stem cells failed to differentiate into adipocytes and neural cells [260].

Despite the evidence for essential function of *Ndst1* in mouse mutants, no human homozygous null mutations have been identified, possibly indicating lethality of this genotype. Homozygous missense mutations localized to the sulfotransferase domain have been demonstrated in eight individuals with intellectual disability and variable ataxia, seizures and short stature, whilst one individual has been identified with compound heterozygous mutations in *NDST1*, who had additional cranial nerve dysfunction and a bifid uvula [316].

The heterozygous stop gain variant detected in this family should result in a truncated protein with absent active domains. The subsequent reduced sulfation of GlcNAc sugars on HSPG is likely to disrupt function including FGF signalling. Clearly, from the animal studies above, a homozygous stop gain variant as this is unlikely to be compatible with life. Although there is no evidence of *NDST1* being associated with LSL in the literature, the fact that it is expressed in embryonic tissue, is important in stem cell differentiation and NC survival, and that there is a low penetrance of NTDs with homozygous null mutants makes it a promising candidate for further investigation. In addition, since LSL is unlikely to be a simple autosomal dominant genetic condition, two possibilities need to be considered. Firstly a second acquired mutation in the unaffected allele may result in a homozygous cells localized in the region of LSL formation. Secondly, this variant may predispose individuals to the formation of LSL either through an additional environmental factor or other, different genetic variants affecting the same pathways.

### ***ADAMTS20***

*ADAMTS20* codes for a secreted zinc metalloprotease containing 15 thrombospondin type I repeats (TSR). There are 26 members of the ADAMTS family of secreted proteases with all having a metalloproteinase domain, disintegrin domain, a cysteine rich region, and multiple TSRs. Despite the similarities, these proteins are associated with a range of different pathologies ranging from Ehlers Danlos syndrome (*ADAMTS2*) to thrombotic thrombocytopenic purpura (*ADAMTS13*) [317].

The *ADAMTS20* gene is located on chromosome 12 and is 199 kilobases long. *ADAMTS9* is an important homolog with the same exonic sequence [268]. The product protein is large, with an 1910 amino acid sequence and a more complex C-terminal GON domain compared to the other ADAMTSs. Llamazares expressed a truncated protein with a functional metalloprotease domain; there was loss of hydrolysis function suggesting the C-terminus is vital for this role [318].

In the mouse, *Adamts20* is 69% identical to human *ADAMTS20* with a shorter reading frame and fewer TSRs. Both mouse and human genes include the terminal GON domain [268]. Expression

is in the neural tube at E9.5-11.5, then lateral to the neural tube particularly in the region of the developing hind limbs at E11.5. Expression precedes markers for neural crest cells suggesting *Adamts20* is expressed in mesenchymal cells that regulate neural crest cell migration. Rao et al identified stop gain variants, with loss of the functional c-terminus, in the belted (bt) mouse which has localized loss of pigmentation more dorsally than ventrally around the trunk in the region of the hind limbs. They proposed this was most likely due to reduced NC cell migration and differentiation into melanocytes in this region [269]. Silver et al reviewed the role of *adamts20* in NC migration and differentiation and found that neither specification nor migration of NC cells was disrupted but rather there was reduced survival of neural crest derived melanoblasts in *Adamts20*<sup>-/-</sup> mice. The localized phenotype is thought to be due to a smaller number of melanoblasts arising from more distal neural crest cells making this particular group more sensitive to cell death [319].

Nandadasa proposed a role of *adamts20* in ciliogenesis and identified one case of NTD. They specifically identified binding of *adamts9* to heparan sulfate. They did not review the relationship between *Adamts20* and heparan sulfate but propose that both *adamts20* and *adamts9* are likely to bind directly to HSPG in vivo [267].

*Adamts20* function has also recently been found to be disrupted by loss of post-translational modification of the TSR domains by mutations in  $\beta$ 3-glucosyltransferase gene. The resultant phenotype of Peters Plus Syndrome has remarkable similarities to the mouse *ndst1*<sup>-/-</sup> described above [320]. In addition, three cases of PPS have been described with associated spina bifida defects [321].

The heterozygous stop gain variant identified in this family is located just over half way through the amino acid sequence and so results in significant loss at the c-terminal end of the protein including the TSRs and the unique functioning GON domain only present in *ADAMTS20* and *ADAMTS9*. There is no established link between *ADAMTS20* and *NDST1*, although the proposed regulation of *ADAMTS20* by HSPG in the embryo, and the fact that both are expressed and have an important role during NC development, suggests that both genes may be involved in the same pathway, which may regulate NC cell migration, differentiation and survival. In addition variants have been identified in humans and mice respectively that are associated with neural tube defects.

## **Family 2**

There are four strong candidates for the pathogenesis of lumbosacral lipomas identified in this family: *TRAF2* and *TGFB2* were identified through genetic filtering and *CREBBP* and *MTHFD1* were considered likely to be related to possible disease mechanisms.



## **TRAF2**

*TRAF2* codes for the protein TNF receptor-associated factor 2, a 501 amino acid protein that has a role in TNF signalling and subsequently cell survival and death. The protein has several well documented domains including a ring finger domain that binds NF- $\kappa$ B, a c-terminal TNFR2 binding region and five zinc-finger domains [322]. The variant identified in Family 2, p.P186L, can be localized to one of the zinc finger domains and is predicted to be disease causing by *In silico* prediction.

TRAF2 forms a complex with TRADD (TNF receptor type 1-associated death domain) and TNF $\alpha$  and RIP proteins. This complex is usually involved in the formation of necrosomes and cell necrosis. Binding of TRAF2 has an inhibitory affect on this pathway [323]. The same pathway can also activate JUN kinase and I $\kappa$ B kinase signalling cascades, leading to the upregulation of Wnt10b, a member of the Wnt family known to block adipogenesis [287].

In keeping with a role in moderating cell death, knockout in mouse models is lethal and not compatible with survival. Cell culture experiments demonstrate increased cell death [323].

TRAF2 is expressed throughout the human body, but interestingly, there is increased expression in adult rat spinal cord following induced spinal cord injury [324].

Despite the previously described role in moderating cell death, it has been proposed that TRAF2 plays a direct role in stimulating apoptosis following interaction with phosphorylated IRE1a in maternal diabetes. In this way, it may contribute to the mechanism underlying an increased incidence of NTDs in this population [286].

With so many diverse interactions it seems unlikely that a TRAF2 variant will be the sole cause of LSL pathogenesis, although multiple variants in associated pathways could lead to the final pathology.

## **TGFB2**

The product protein, transforming growth factor beta2 (TGF $\beta$ 2), is part of a large superfamily of growth factors. It has been specifically implicated in the inhibition of adipocyte formation from stem cells[289]. Although TGF $\beta$ 2 does not have an established role in neural tube defect formation, Mayanil et al have proposed regulation of TGF $\beta$ 2 by Pax3 in murine development such that *Pax3*(-/-) mice have significantly lower levels of TGF $\beta$ 2 transcripts[290]. The T $\rightarrow$ C single nucleotide variant is a missense mutation resulting in protein variant p.L78P that is located within in the TGFB propeptide region of the gene. The CADD score is 28.6 and the gnomAD frequency unknown.

## **CREBBP**

*CREBBP* codes for CREB Binding Protein, a 2442 amino acid protein that acts as a transcriptional co-activator with p300 and histone acetyltransferase. CREB is also known as cAMP-response element-binding protein. CREBBP has multiple zinc finger domains as well as a bromodomain, histone acetyltransferase domain and CREB and DNA binding domains [325]. Single nucleotide nonsense variants throughout the protein, including between domains, have been associated with Rubinstein-Taybi Syndrome. The variant found in this family, P911L, is located between the CREB binding domain and Bromodomain. Despite this location, it is still predicted to be disease causing as are SNVs found in this region in Rubinstein-Taybi Syndrome [326]. As mentioned earlier, one case of LSL has been identified in Rubinstein-Taybi Syndrome [159], although this was associated with a mutation in *EP300*.

Together with p300 (the protein product of *EP300*) and histone acetyltransferase, CREBBP modifies chromatin structure and acetylates proteins. It has an important role in cell proliferation and differentiation during development but also functions as a tumour suppressor gene [325]. Reflecting this role in development, *Crebbp* is expressed throughout the neural tube in the mouse embryo at E8.5, although predominantly in the dorsal neural tube. By E9.5 it has localized to the neural tube in the tail region. Later it is expressed more globally in the heart, liver, lungs, vasculature and skin [325].

Heterozygous mutant mice demonstrate skeletal anomalies whilst homozygous deletions are associated with NTDs [327]. *p300*<sup>+/-</sup> mice die in utero with anencephaly and a modest association between these two genes and spina bifida in human populations has been documented. However, the researchers did not clearly specify the phenotype within the diagnosis of spina bifida [328].

Both CREBBP and p300 are likely to play a vital role in adipocyte differentiation through their activation of PPAR $\gamma$  in adipocytes [329]. Any involvement in LSL formation is therefore likely to be a gain of function mutation.

## **MTHFD1**

*MTHFD1* codes for methylenetetrahydrofolate dehydrogenase, a cytosolic enzyme involved in one carbon metabolism (discussed in the Section II.1). MTHFD1 consists of a 935 amino acid sequence with multiple domains reflecting its trifunctionality. The variant seen within Family 2 lies in three domains including the formate tetrahydrofolate ligase domain. This is a rare variant that is predicted to be damaging.

Reflecting its role in folate metabolism, purine/pyrimidine synthesis and macromolecule methylation, MTHFD1 is expressed throughout the body. Homozygous mouse mutants are embryonically lethal, whilst heterozygous mutants have widespread metabolic disorders [330].

Multiple SNVs have been associated with conotruncal heart defects (a group of congenital heart defects associated with failure of cardiac neural crest migration and differentiation) [331]. There is also an increased risk of NTDs [58, 60, 332].

As discussed in Section II.1, the mechanism by which folate metabolism contributes to NTDs is unclear, although a likely mechanism is less availability of purines/pyrimidines for cellular proliferation. This mechanism might also account for insufficient NC differentiation in conotruncal heart defects. It seems mutations in this pathway increases the risk of multiple pathologies depending on cofounding variants in the individual [331, 333].

### **Conclusion**

Familial cases of LSL are rare with genetic analysis of trios (proband and both affected and unaffected parents) even rarer. The analysis of these two families has not revealed any single candidate that appears relevant to both families. However, a number of the variants are located in areas of the product protein that are predicted to alter function. The candidates can be broadly divided into two categories: those that are expressed in the dorsal neural tube during development (*CREBBP*, *ADAMTS20*) and those that are expressed more globally but are vital to basic cell processes like cell survival, folate metabolism or HSPG synthesis (*TRAF2*, *TGFB2*, *NDST1* and *MTHFD1*). It is also striking to note that, like *ARHGAP29*, a number of these genes are also associated with cleft lip/palate defects (*MTHFD1*, *NDST1*). Ultimately the next steps to validate any involvement in the LSL disease process is functional experiments of the variants identified. This will be discussed in more detail in the Section VI.

### **Combined LSL Cohort**

The three most striking variants are the multiple variants found within the *EIF4EBP1* gene, the presence of the same TA deletion in *FOLR3* in all LSL patients and the highly predicted deleterious stop gain variant in *KCTD15*. Little more is known about *FOLR3* than what is discussed above.

#### ***EIF4EBP1***

*EIF4EBP1* is the eukaryotic translation initiation factor 4E binding protein gene, a 2,986 kb gene consisting of 3 exons. The product protein 4EBP1, or 4E binding protein 1, is important in regulation of translation of mRNA for the eIF4E protein which in turn is involved in regulation of translation at a cellular level. The 4EBP1 protein binds to the protein cap of EIF4E mRNA competitively with eIF4G. When eIF4G is bound to eIF4E mRNA translation and polypeptide chain initiation is triggered. When 4EBP1 is bound this process is blocked.

4EBP1 is further regulated through phosphorylation with key serine and threonine residues undergoing phosphorylation (Thr37, Thr46, Ser65, Thr70, Ser 83, Ser101 and Ser112) which reduces binding of the mRNA. One of the variants present in five of the LSL individuals was the

serine to leucine variant at residue 65. Physiological stress, TNF $\alpha$  and activation of p53 all reduce phosphorylation, increase binding to eIF4E, sequester eIF4E in the nucleus and ultimately decrease translation of eIF4E [334].

*EIF4EBP1* is ubiquitously expressed throughout the body and the protein is located within both the nucleus and cytoplasm. Despite this 4EBP1 does not seem to be essential for cell survival. A 4EBP1/2 double KO mouse displays increased adiposity in response to diet as well as increased adipogenesis in mouse embryonic fibroblasts stimulation in cell culture [304].

Although there is a clear association between *EIF4EBP1* and adipogenesis the lack of localized expression fails to explain the embryogenesis of lumbosacral lipoma. Although the abundance of rare variants within our cohort is surprising it does seem unlikely that this particular gene in isolation has an important role to play.

### ***KCTD15***

The KCTD15 protein has 283 amino acids, a BTB domain and a conserved C-terminus across species (RIKQEPLD) that undergoes sumoylation [335]. Uniquely, KCTD15 is thought to be involved in both the regulation of adipogenesis and differentiation of NC cells. KCTD15 binds directly to AP2 $\alpha$  limiting its transcriptional activity that subsequently inhibits the activity of C/EBP $\alpha$  and adipogenesis. Decreased AP2 $\alpha$  activity also inhibits c-kit expression and wnt/ $\beta$ -catenin signalling resulting in inhibition of NC cells [300, 336]. It is expressed in the neural plate of zebrafish, and at the edges of the neural plate and presumptive NC cells in *Xenopus*. Knockout or inhibition in both these species result in expansion of early NC domains and abnormal NC related structures [336-338].

SUMOylated KCTD15 and wildtype KCTD15 have no functional difference. However, the protein is deSUMOylated by acetylation of the P (proline) residue, and deSUMOylated KCTD15 shows less inhibition of neural crest cells [339]. In addition to this role in SUMOylation, the C-terminus has been found to be important in stabilizing the rest of the KCTD15 protein and particularly the BTB domain in cell culture experiments [301]. The variant present in one LSL individual in this cohort is a stop gain variant just before this proline residue. Loss of this residue is likely to affect the SAS (SUMOylation-acetylation switch) with loss of deSUMOylation positively regulating protein activity.

One control individual was homozygous for this variant. This is in keeping with more than one gene contributing to the pathogenesis of LSL. Alternatively this also highlights the problems with *in silico* predictions. Despite a CADD score of 48 this variant does not relate to any disease state in the homozygous individual.

## CONCLUSION

As with the familial LSL cases, there was no one outstanding gene that could be considered to be the most likely to be disease causing. Again, this fits with the model of LSL occurring as a result of multiple variants along several different developmental pathways. Genes were specifically filtered based on published evidence to support a role in three distinct pathways/processes: adipogenesis, neural crest cell regulation and neurulation. With the large number of variants detected, and hundreds of genes related to these three processes, it is not surprising that some positive results were generated. However, on top of these established processes there were also a number of genes that have general roles in cellular function i.e. *EIF4EBP1*, and just like the association with carbon one metabolism in open NTDs, perhaps subtle affects on multiple essential cell processes leave particular developmental processes vulnerable.

### **The Role of the Extracellular Matrix in LSL Pathogenesis**

The extracellular matrix, ECM, is a component of the body tissue that exists outside cells and is densely packed with a large and diverse number of structural proteins. A fibrous collagen dense band, the basement membrane, lines the neuroepithelium. The most abundant of these ECM proteins are the laminins and (their receptors, integrins), cadherins, collagen and proteoglycans. Each of these are large families of proteins made up of different arrangement of subunits, different ligands and in different states of post-translational modification (such as sulfonation of the proteoglycans). With this large potential for variation within the composition of the ECM our understanding remains incomplete but it is clear that the ECM offers much more than just structural support during development. There is good experimental evidence to support the role of the ECM in not only migration but also in the regulation of the fundamental developmental processes of proliferation and differentiation of progenitor cells, highlighting the ECMs vital role in morphogenesis during development. Importantly, the ECM is likely to play a key role in coordinating all these processes during development to ensure complete organogenesis and final tissue shape [340].

Examples of the role of proteoglycans in neural development includes blocking prelecan (a proteoglycan usually associated with providing structural support to the basement membrane) in mouse embryos resulting in exencephaly and reduced progenitor proliferation [341]. These morphological changes are likely to be mediated through a reduction in FGF and Hh signalling [342]. Similarly, the glypican null mouse has inhibited FGF signalling, and syndecan (a proteoglycan known to interact with integrin) demonstrates increased neural progenitor proliferation in knockout zebrafish [343].

Laminins and their receptors, the integrins, have also been found to regulate FGF signalling. An increase in laminin expressions has been shown to stimulate differentiation into neural stem cells and promote their proliferation and survival [344-346]. Importantly, a difference has been identified in laminins within the basement membrane identified along the cranio-caudal axis of mouse embryos with a significantly different composition around the future lumbar and sacral

spinal cord [347]. This highlights the potential for different regulation of proliferation and differentiation of progenitor cells along the length of the developing spinal cord. The laminins also seem to play a role in cell movement and shape through the disruption of interkinetic nuclear migration, as well as the co-ordination of movement of sheets of cells [348, 349].

As with the proteoglycans and laminins, integrins have also been found have a role in controlling proliferation of progenitor cells, through their regulation of the MAPK signalling pathway, as well as EGF and FGF signalling [350, 351].

Furthermore, current research topics are highlighting our incomplete understanding of how the ECM manipulates developing cells. The ECM is a dynamic structure changing not only protein composition but also nanotopographical structural arrangement and stiffness [352, 353]. Both of these elements are able to regulate progenitor cells, indicating how incomplete our understanding of this system is.

Considering this vital yet subtle role the ECM appears to play in neurodevelopment it seems unsurprising that the WGS of familial LSL patients has highlighted a number of different genes involved in the formation and regulation of ECM composition. In the absence of a strong hereditary pattern, it seems likely that subtle disruption in the ECM may perpetuate other disruptions during secondary neurulation resulting in LSL. The existence of an animal model of LSL would allow in depth analysis of the differences that are likely to be present in the caudal most embryo during secondary neurulation, and will undoubtedly throw new light of the mechanisms of the pathogenesis of LSLs. However, in the absence of such a model, it is hoped that as we learn more about the ECM during development more clues may be elicited as to the origins of this pathology.

## SECTION VI: GENERAL DISCUSSION

These hypotheses laid out in the introduction have been addressed in the thesis in a number of ways:

**There is no difference between the lipid profile of CSF/plasma/urine from children with LSL and control children**

Lipidomics was used to compare samples from control and LSL children; a large number of potential lipids were found to be significantly different between these two small groups. Database searches were used to attempt to identify these potential lipids.

**There is no difference between the lipid profile of CSF/plasma/urine from children with LSL demonstrating disease progression compared with children with LSL who appear clinically stable.**

Lipidomics was used to compare samples from children with LSL demonstrating disease progression compared with children with LSL who appear clinically stable; a large number of potential lipids were found to be significantly different between these two small groups. Database searches were used to attempt to identify these potential lipids.

**There is no difference in concentration of specific phospholipids in CSF/plasma/urine between children with LSL and control children**

A targeted phospholipid assay was developed and used to compare samples from control and LSL children; a number of phospholipids (predominantly phosphatidylcholines) were found to be significantly different between these two groups in CSF and plasma.

**There is no difference in concentration of specific phospholipids in CSF/plasma/urine between children with LSL demonstrating disease progression compared with children with LSL who appear clinically stable.**

A targeted phospholipid assay was developed and used to compare samples from children with LSL demonstrating disease progression compared with children with LSL who appear clinically stable; a number of phospholipids (predominantly PCs) were found to be significantly different between these two groups in CSF, plasma and urine.

**There is no correlation between the degree of severity of disease progression and the concentration of specific phospholipids in CSF/plasma/urine from children with LSL.**

A Total Clinical Score was developed to describe the severity of disease progression and correlation was drawn between this score and phospholipid concentrations. CSF samples showed positive correlation to a single LPC, plasma showed both positive and negative correlation to both PCs and Pes, and urine showed only negative correlation with a number of PCs.

**There is no difference in concentration of specific phospholipids in CSF/plasma/urine between children with abnormal and children with normal intraoperative neurophysiological recordings.**

BCR was determined to be the most predictive of long-term follow-up outcome in LSL patients undergoing surgical resection of LSL tissue. There was no difference in specific phospholipids in

CSF samples between children with abnormal and normal BCR recordings. Only a small number of PCs were found to be different in plasma and urine sample.

**There is no predicted functional genetic variation related to the formation of LSL within the genome of LSL individuals compared to the disease-free family member.**

Whole genome sequencing was performed on probands and parents in two families with apparent familial LSL. A number of different genes were identified that are predicted to have a functional mutation that might contribute to the pathogenesis of LSL.

The aims of this project were also met. Lipidomics was performed on samples of CSF, plasma and urine from LSL patients undergoing spinal surgery. A number of differences were identified between samples from LSL and control patients. Classification of the most significant groups into lipids classes by database search found phospholipids to be particularly different between the two cohorts.

A targeted assay was developed for PC/LPC and PE/LPE. Differences were found once again between LSL and control patients but also between symptomatic and asymptomatic LSL patients. A large number of PCs were significantly different in urine samples, which may have reflected many of the symptomatic patients having urinary pathology. To address this a Total Clinical Score was designed to score patients based on the number and severity of symptoms. Targeted assay results were correlated with the TCS and again a number of phospholipids showed significant correlation.

As this correlation was based on identified clinical symptoms, it does not add any prognostic value but is rather descriptive of a known state. Ultimately to validate any of these lipids as a biomarker, a longer-term follow-up study is required with sample collection near diagnosis (rather than at the time of surgery), and regular assessment thereafter. In the absence of the time available for this kind of study a surrogate for long-term outcome was considered by reviewing IONM. This added two aspects to the project. Firstly, identification of a group of patients that had grossly abnormal IONM, all of which corresponded with particularly high TCS, were identified and excluded from the data. Secondly, the BCR was found to predict urological outcome suggesting that this might be a particularly sensitive measure of neurological function before symptoms develop. A number of LPCs and LPEs were identified as being significantly different and importantly, the number of significantly different lipids in urine samples was greatly reduced reflecting the deselection of patients at the extreme end.

Many of the PLs identified by the above methods were different between methods, although a few lipids remained significantly different across analytical methods. Focus on these lipids was used to create a model explaining the difference seen between symptomatic and asymptomatic patients: higher levels of LPC18:0 in CSF, as found here in asymptomatic patients, reflects increased availability of DHA in the CNS which supports nerve function. This is likely to just be



one of many aspects that determines whether a patient develops symptoms. Further validation of the identified PLs should include the other lipids identified in plasma samples as this is the simplest and most reliable method of obtaining samples from patients. In addition, a valid biomarker does not necessarily have to be related to a disease mechanism.

The results obtained by these methods should be considered just the first step in the development of a biomarker. Similarly, the above DHA availability mechanism described remains speculation and requires rigorous investigation before this can be incorporated into clinical practice.

Genetic samples were reviewed from six LSL patients to identify any supporting evidence for genes identified in the literature. In keeping with LSL being related to multiple different genes, a number of significant variants were noted in this cohort but not in all the genes published.

Familial cases were reviewed for any autosomal dominant inherited variants. Results were different between the two families. Variants were divided broadly into the categories of disruption of neural crest cell migration/differentiation and disruption of fundamental cellular processes that occur throughout the body.

All six cases of LSL were also reviewed for any variants common to the group, since multiple genes causing a disease could be missed on autosomal dominant filters applied to familial cases. Again a number of genes were identified that broadly fit into the above two categories.

Throughout this project, one assumption needed to be made that could have considerable effects on the results: what exactly is a LSL. The definition used throughout this thesis is a fatty mass, containing cells of both mesodermal and neuroectodermal origin, attached to the caudal spinal cord, extending through a defect in the posterior vertebral arch (spina bifida) and continuous with the subcutaneous fat. The assumption was that fatty filum/filar lipoma in the absence of any bony spina bifida was not LSL. Similarly, in the critique of published genetics pertaining to LSL, the terms closed spinal dysraphism, spina bifida occulta or spinal lipoma are frequently used without qualifying exactly which pathologies are included in this bracket. The assumption that isolated bony spina bifida, intradural lipoma as well as filar lipomas are incorrectly included in these analyses, and are fundamentally different pathologies, may not hold to be true. Perhaps a bony spina bifida occurs through the same process yet maldifferentiating progenitor cells subsequently regress just leaving the bony defect. Moreover, an intradural lipoma could occur due to the same process, just triggered at a different time point. And thus a paradox: without a fundamental understanding of the pathogenesis of LSL we are not able to define the exact spectrum of this pathology and, in the absence of including all relevant cases in analysis, we are not able to identify the underlying mechanisms. Thus, we are hampered in developing a model to explain the pathogenesis.

## 1. STRENGTHS AND WEAKNESSES: BIOMARKER DEVELOPMENT

### Lipidomics

Two main techniques were used to identify candidate biomarkers: lipidomics and targeted phospholipid assay, both using HPLC/MS. Lipidomics as a research technique is still in early stages of development. The main weakness of this approach is the large amount of data that is generated that is difficult to meaningfully interpret. For example, each M/Z that is measured by MS reflects a lipid that has been ionized by electrospray ionization (it is this process that allows amphipathic lipids to be detected by MS). Adducts are added to the lipids based on the availability within the mobile phase during HPLC. As a result, a number of different adducts can potentially form for the same lipid. In addition, as the mobile phase changes during separation, these adducts may potentially also change. Lipidomics does not offer identification of these adducts and lipids but rather detects a M/Z that corresponds with multiple adducts forming from each lipid[354]. Database search, that takes into account the types of adducts that are likely to form, is required to identify possible lipids that correspond with the M/Z. These database results are based on expected adducts rather than observed adducts [220, 355, 356]. The only way to identify a lipid is through a targeted lipid assay with fragmentation patterns predetermined by analysis of standards.

A method such as this requires a large sample size to limit type II errors with regression models. The number of subjects per variable should be two per independent variable [357]. Since it is not clear from lipidomic data how many adducts are present for an individual lipid (dependent variables) and in the absence of a complete understanding of the human lipidome for each fluid compartment measured (again many lipids measured may be dependent on each other), this calculation is difficult. Lipidomics data identified thousands of different M/Z RT pairs. The prevalence of LSL is 1 in 4000, which corresponds to 180 cases in the UK each year [124]. With just over half having surgery, and therefore amenable to CSF collection, it would take 10 years to collect 1000 samples in the UK alone. This size of study would have to be done as an international collaboration which is difficult and expensive to set up, requires multiple different ethics approvals and becomes much harder to regulate collection and sample preparation/storage/transport

The statistical tests as performed in the study were not ideal for this sample size. Multiple t-tests were run which will result in false positives, particularly with a p cut off set at 0.05. Without correction of the alpha-level, 1 in 20 variables will, by chance, show significant difference at this level. However, this should be considered as a guide towards the first steps of developing a biomarker rather than a definitive result. The databases that are used to identify potential lipids can be filtered based on the ES mode and suspected adducts based on the mobile phase. After filtering, a high number of unknowns are still generated and this can vary based on whether

comparison is made with standard based data or predictive databases [220, 355, 356]. Lack of full understanding of the human lipidome and how this varies makes analyzing data near impossible. Examples that might affect the lipidome include when and what the patient last ate, particularly with babies, if they are breastfed or not, the time of day and the level of stress [358]. Attempts were made to control for some of these factors in sample collection.

With so many variables present and small sample sizes, the interpretation and statistical analysis of lipidomics was limited to identify the lipid class most of interest to develop a targeted assay.

### **Sample collection**

Every effort was made to be consistent with sample collection and storage, although some variation inevitably occurred. For example, samples collected near the beginning of the project were stored for longer than others at -80°C prior to analysis. This could have resulted in degradation/oxidation of older samples [359].

All patients were nil-by-mouth (NBM) prior to surgery. For most cases this was at least 8 hours. LSL surgery was always commenced with the patient arriving in the anaesthetic room at 8.30 am. The actual time point of sample collection beyond this varied based on a number of practicalities within theatre. This was not true for control cases although they were all also NBM prior to surgery.

Blood samples were collected prior to initiation of intravenous anaesthesia (this was not always possible if the patient was particularly difficult to cannulate). CSF samples were collected at the same point during the operation, although this was variable based on a number of practicalities within theatre/timing of anaesthetic/preparation of IONM, complexity of the case/age of patient. The arachnoid was left intact and a needle inserted under direct observation to collect an uncontaminated sample, this was not the same for all control procedures performed by other neurosurgeons. For example, a MMC patient with a blocked VPS had CSF aspirated at the point of insertion of a new VPS. Visible contaminant was present within some CSF samples from control patients. These samples could have been centrifuged to separate out the cells. This was not done but, in any event, would not have removed any extracellular lipids that were present in plasma that might have contaminated CSF.

Urine was collected mostly at the point of catheterization, although, when this was not possible (if the child had an empty bladder on catheterization), samples were collected later during the procedure. Although the concentration of urine is tightly regulated, this is with the aim of maintaining blood concentrations: urine can be very dilute or concentrated depending on the patient's fluid state. When samples were collected at the same time, after the same period of being NBM, this attempted to control the variable. Samples collected later in surgery were often more dilute, due to intravenous fluid given during surgery. Measuring the specific gravity of urine

samples would have helped identify dilute urine, although this was normally obvious by looking at the colour of urine. For the most accurate measurement of urine lipids, a total 24 hour urine collection could have been performed (ideally before surgery). This was not practical, especially in young children still using nappies. To account for this variation in sample collection, blood samples from LSL patients should be considered to have the least variation and therefore be of the most value.

### **Targeted assay**

During the lipid extraction process for targeted assay, ideally only glass tubes should have been used [360]. Unfortunately a suitable centrifuge that was able to spin glass tubes was not available and Eppendorfs were used for a brief period during the lipid extraction process. Extracted lipids were then stored in methanol in glass vials.

A particular step during the lipid extraction process was the removal of the lower lipid phase, which took a degree of dexterity, blowing bubbles through the upper phase to ensure none is accidentally aspirated. There was therefore a risk of contamination with proteins in the end sample. It is theoretically possible that a protein could potentially fragment to give the same parent/daughter M/Z seen in the targeted assays of phospholipids, therefore giving a false positive result.

Once lipids were extracted from samples, they were stored at  $-20^{\circ}\text{C}$ . For samples to be analysed they were loaded into an auto-injector tray which was chilled to  $5^{\circ}\text{C}$ . Samples were then injected one at a time and analysed. The total protocol took near to 24 hours, meaning that samples were left at a higher temperature for a significant amount of time. As mentioned before, this may have led to oxidation and degradation of lipids, particularly in samples analysed towards the end of the cycle [359].

A MS algorithm was written to fragment phospholipids and detect daughter/parent molecules with predetermined M/Zs. These values were initially based on direct injection of known phospholipid standards. Standards were not available for all targeted phospholipids, so many of the results had to be extrapolated. For example the same PC with one more double bond in the fatty acid chain would have a M/Z of 2.02 less (the mass of the two hydrogen ions lost by forming an extra double bond).

MS measures the intensity of a signal for a particular M/Z at a particular time point. To calculate the total intensity of signal, measurements over a number of adjacent time points need to be aligned and the area under the curve calculated. This value has no units: it is a measure of intensity of signal. To convert these values into a recognizable unit, calibration curves were created from standards with increasing dilution. For the purposes of statistical analysis, the intensity of signal was used as this limited error that would have occurred when converting values

to a unit; especially where the standard used was not the same as the lipid being analysed. Where combination of intensities gave a bifid peak, these were smoothed with a Targetlynx algorithm. A smoothed bifid peak would not have been as accurate as a single peak. The quality of the traces for LPE/PE were marginally worse than for LPC/PC.

Although the variables being considered by targeted assay were smaller than in lipidomics, the critique of statistical analysis used remains the same: the sample size was smaller than the number of variables and it is difficult to classify variables as dependent or independent, since the human lipidome is not fully understood. Using a p-value of less than 0.05 would still have generated 5% of lipids appearing significantly different, by chance.

### **Clinical assessment**

Clinical assessment when symptoms are subtle is always subjective and particularly difficult when the patient is in the non-verbal age group. This is also true when relying on carers to report symptoms such as urgency and incontinence. For this reason, these components of bladder function assessment were omitted from the TCS. Assessment of bladder emptying and post-micturition residual volumes was dependent on the full cooperation of the patient. At times, however, this can be difficult to assess, even if a very young child is fully compliant. To account for these variations in clinical assessment, IONM was reviewed.

### **IONM**

Subdermal electrode placement and monitoring were performed by the same experienced individual (IJ). Sphincter MEPs and BCR are usually only described as present or absent. There is no established baseline for what is a normal recording, especially in very young children. A sequence of multiple stimulations were used to optimize recordings prior to the initiation of formal monitoring. An untested scoring system was used to compare bilateral impulses, and between pre- and post-operative recordings, to give three different states: normal, abnormal or absent. This method has not been validated. The categorization of abnormal was used when there was a notable deterioration in recording between pre and post-operative IONM or if there was a notable difference between left and right. It was possible that an 'abnormal' recording was perfectly normal for that individual.

Neurophysiology data was recorded intra-operatively prior to resection and post-resection. Ideally further data points would have been collected. Intra-operative recordings prior to opening the dura could have been used as a baseline to allow comparison for further recordings. Additionally, neurophysiological assessment at follow-up would have allowed a more robust assessment of the validity and prognostic value of neurophysiological monitoring. In the absence of such comprehensive data the intra-operative recording prior to resection had to be considered as a baseline to allow assessment of changes in neurophysiology immediately following resection. In addition, changes in this baseline on contralateral sides was used to score the available data as

robustly as possible. It is acknowledged that that additional data points would have greatly improved the quality of this data.

### **Biomarker development**

Development of a biomarker can be divided into five distinct stages: discovery, validation, clinical translation, evaluation and implementation. This section focuses on the discovery stage while the latter stages will be discussed in more detail under the section Future Work. Ioannidis and Bossuyt have produced a thorough critique of all stages of the biomarker research pipeline, as summarized below (Table VI.1.i).

| Current problems                         | Potential solutions                     |
|--|---|
| Poor design, conduct, and analysis       | Methodological rigor                    |
| Unaccounted multiplicity                 | Appropriate use of statistics           |
| Small studies                            | Larger, collaborative studies           |
| Extreme case selection                   | Proper case-control or cohort selection |
| Non-rigorous exploratory nature of study | More rigorous training of scientists    |
| Poor reporting                           | Use of reporting standards              |
| Selective reporting                      | Preregistration                         |
| Spin in interpretation                   | Careful editorial and peer-review       |

Table VI.1.i. Adaptation of figure: 'Problems and potential solutions at each stage of the biomarker research pipeline' from Ioannidis and Bossuyt 2017[361]. Problems and solutions encountered during the biomarker discovery phase.

Attempts have been made to address each of these points where possible, in particular through thorough study design, and excluding extreme cases such as in BCR analysis. Exclusion of outliers was done based in clinical presentation/findings but was not done by reviewing overall lipid profile. One patient had significantly higher levels of lipids in all three sample types. This patient could have been excluded but, in view of the small sample size, the decision was made to keep the data in the analysis.

Acknowledgement needs to be made of the many negative results that were generated and that, out of necessity, only positive results have been mainly discussed. Little can be done about the sample size and there was no scope for collaboration to increase sample size, during the time-scale of this doctorate. In view of the small sample size, multivariate regression models are less reliable and, as multiple comparisons of means was performed, there is an increased risk of type 2 error. Ultimately the next stages of biomarker development need to be completed before a biomarker for LSL can be translated into clinical practice.

## 2. STRENGTHS AND WEAKNESSES: GENETICS

Genomics, much like lipidomics, suffers from the generation of a large amount of data that is difficult to interpret. This is worsened by the large number of publications claiming associations with pathology but not supported by functional studies. For example, reference SNV cluster identities (RS IDs) are assigned to any new variant detected in the genome. These are often listed as demonstrating an association with a disease in particular genes but, with so many genes being reviewed by WGS/WES, it is not surprising that some variants might be more common in diseased individuals. These RS ids do not take in to account the variant, where in the gene it is located (exonic, intronic, promoter region), whether it is exonic, nor how it might affect protein function. To assess effect on protein function, a number of different *in silico* prediction algorithms have been developed [226, 227, 362]. Unfortunately different algorithms of the same SNV may generate contradictory results or are not supported by further functional studies. Being selective about methods would allow many of the variants identified in this study to be published individually, as potentially pathogenic, but this is disingenuous and distracts from the prime aim of understanding the underlying developmental biology.

### Sample Collection

Samples were collected over a number of years. Some degradation was noted in the samples and one sample had to be recollected. Some of the samples were small (particularly from young children) and it was not possible to aliquot them. Ideally, aliquots of extracted DNA would have been stored to complete Sanger sequencing and confirm any variants identified. In addition, familial LSL cases only had samples collected from the proband, the affected parent and the unaffected parent. Ideally a large number of controls would have been collected from siblings and grandparents. Even more ideal would have been the identification of an extended family tree with more than two cases of LSL. This has never been described in the literature. Histopathology was not available to confirm the diagnosis in non-proband family members.

### Sequencing

Throughout the sequencing process there are several technical reasons why there might be mistakes in identifying bases: read errors. These can be due to the read depth, and can occur as a result of crosstalk, phasing errors, T fluorophore accumulation, decay, mixed clusters and boundary effects [363]. The Illumina process of next generation sequencing relies on random fragmentation of DNA to create a single stranded DNA library of templates. Adapters are then added to the DNA templates and amplification results in multiple sequences of the same fragments. If these DNA templates co-locate, they are amplified together resulting in a mixed cluster of sequences and subsequent inconsistencies in the read [364]. The amplified single stranded sequences are paired with fluorescently labelled 3'-blocked nucleotides and the emission frequencies detected to identify the base [363]. Crosstalk occurs when the emission frequencies from the dye used to identify the nucleotides overlap: thus G can be mistaken for T

and C for A [365]. In addition, the intensity of these signals is harder to read towards the end of a fragment resulting in read errors more frequently at the edges (boundary effect) [366]. If a base is missed, the result is a lag in the read, or a phase error. Alternatively, if an additional base is added, then the sequencing shows a pre-phase error [365]. The latter may occur due to incomplete cleavage of the generated fluorescently labelled nucleotides, which can particularly occur towards the end of a read resulting in T fluorophore accumulation [364].

It is estimated that as many as 1 in 12 single nucleotide variants are a result of read errors [367]. This is compared with Sanger sequencing where the error rate is as low as  $10^{-5}$  per base [368]. Accuracy was improved by read depth: resequencing several times to increase the coverage. Attempts are made to identify and reduce these read errors by sequence quality control performed by BGI as part of their WGS service. Some errors are easier to detect than others, such as T fluorophore accumulation [364].

To check for such artifacts, BAM files were loaded into IGV and the sequence of candidate genes reviewed in detail. The familial cases and the sporadic cases were sequenced separately at different facilities, making batch contamination impossible. Similarly, by applying the autosomal dominant filter in Ingenuity, only variants present in the two affected individuals and absent from the healthy parent were flagged. The same read error occurring in just the two affected individuals but not the control is less likely (although not impossible).

### **Analysis**

Analysis was performed on Ingenuity using an autosomal dominant filter for familial cases. The proposed digenic inheritance pattern suggested by Larrew et al for *RADIL* and *ARHGAP29* would not be detected by this method, as the unaffected parent could be a carrier for one gene [38]. Similarly, control samples were limited to healthy parents although, in a model of digenic/multigenic inheritance, these controls may well have carried many but not all of the required variants, thus blinding the study to many potential variants.

The main problem when identifying possible disease causing variants in a genetic sequence is the sheer amount of genetic information within the human genome. It is thought that a single person's genome includes millions of variants, and as many as 1 in 8 base pairs may be considered a variant, even though exomes account for only 2% of the genome [369]. A distinction needs to be made between normal variants and variants that are abnormal/result in loss of function. A further distinction then needs to be made between those loss of function variants that cause disease and those that do not. What is damaging to a gene is not necessarily pathogenic. To answer these questions a number of algorithms, pipelines and *in silico* prediction systems have been designed.



Every effort has been made to follow all the stages of variant prioritization: conservation, constraint, mode of inheritance, allele frequency and penetrance. Conservation refers to the presence of identified variants in other species: a variant in a highly conserved gene is thought to be more disruptive to gene function rather than a variant in a gene that shows a lot of variability across populations and between species. This is the principle of the SIFT function [226]. Unfortunately, it is known that many genes have both highly conserved and non-conserved regions and pathogenic variants have been found in both. To address the lack of functional biological information, protein structure is taken into consideration in the PolyPhen-2 model [227]. Both of these models assume stop gain variants resulting in a truncated protein and frameshift variants to be maximally damaging. Stop gain variants do not necessarily alter protein function especially when located near the c-terminus. Where this was encountered in the genetics results for *KCTD15*, the literature was reviewed in detail to determine if such a stop gain variant could relate to loss of function. An example of where a frame shift variant does not cause disease is a common frameshift variant found in ABO blood grouping proteins [370]. Overall the false positive rates are high for both these models: with 219 and 154 variants falsely classified as disease causing in PolyPhen-2 and SIFT respectively in an individual human genome [370].

'Gene constraint' is an approach that takes a more detailed look at gene function and takes into consideration the number of variants within a gene that do not result in loss-of-function and their frequency within the population. A gene with many variants that do not alter function, and that are common in the population, is said to have low constraint and new variants are considered less likely to be disease causing. A gene is said to be constrained if it has fewer common functional variants. The CADD (Combined Annotation Dependent Depletion) score was used to assess gene constraint. CADD is only designed to assess SNVs and deletions/insertions, and since it is based on level of variation the results may be skewed by local mutation rates. In addition, it only takes into consideration function of the gene, and so should not be considered a measure of whether a variant is pathogenic [228, 362].

For mode of inheritance, the assumption was made that for familial cases the putative causal gene variants were autosomal dominant. For the extended cohort this was unlikely to be true and so no assumptions were made. Similarly, for penetrance the assumption was made that for familial cases this was complete, whilst for the extended cohort no such assumptions were made.

Allele frequency was compared to the largest available dataset of human genetic information: gnomAD. This database was generated from 125,748 exomic sequences and 15,708 genomic sequences. Although this dataset spans the global population there are deficiencies: specifically the Native American population is underrepresented. The larger majority of this genetic data came from adults with chronic disease such as dementia, type 2 diabetes or cardiovascular disease. The population is far from healthy, although individuals with severe childhood disease were excluded, along with second degree relatives or closer. The assumption when using such

databases is that loss of function variants should be naturally filtered out of the population and therefore have a lower allele frequency, especially in comparison to synonymous variants. Within the gnomAD database, almost 450,000 variants predicted with a high-confidence to be loss of function variants were identified. That is more than three per individual [371].

It is difficult to assess the accuracy of these tools since many of them are based or 'trained' on existing databases of known disease causing variants. Therefore, to use known variants to test these *in silico* predictions is circular and not a true measure of performance. An attempt has been made to assess their accuracy of identifying a benign variant by selecting variants in the ExAC database of frequency above 1% and less than 25%. The assumption is made that these common variants are most likely to be benign (although an example where this is not true is the *CFRT* gene, where variants in the European population, as common as 5%, protect against cholera when heterozygous and yet when homozygous cause cystic fibrosis). Regardless, this study found the specificity of SIFT to be 63%, CADD 64% and Poly-Phen-2 75% reflecting a high false positive rate [372]. A 1% difference in specificity corresponds with 100 false classifications of variants.

Other steps that can improve variant prioritization include phenotype matching to known clinical genetic databases such as ClinVar and the Human Gene Mutation Database. These databases suffer from inaccurate classification of LSL as a unique pathology with neither lipomyelomeningocele nor lumbosacral lipoma recognized in either database. For large datasets with many controls, burden testing can be performed. Here individual genes of question are reviewed for the number of variants throughout the whole gene and compared to their frequency in the control population. Many rare variants suggest that the suspected variant is less likely to result in loss of function [370].

The final step is variant interpretation which involves reviewing the variant in detail in relationship to the gene and potential mechanisms that may link variant (damaging) gene function to disease causation. This has been done in the final stages of analysis, in the Genetics Discussion. However, it is worth noting two points. This final step is dependent on expert opinion and literature review and is vulnerable to investigator bias. Secondly, the 2012 CLARITY Challenge highlighted how different investigators performing this final stage can yield different results [373]. ACMG consensus guidelines have been generated that should be followed in the application of variant prioritization and interpretation in the clinical setting [374]. However, this is not designed for multigenic complex disorders nor for the identification of new disease causing genes in research.

A large number of variants were noted in both familial cases and in the LSL cohort. Clearly not all of these can be disease causing, as suggested by the *in silico* predictions. By necessity, variants were filtered based on known mechanisms assumed to be associated with LSL. The assumption

that there must be a variant in genes for adipogenesis doesn't necessary follow since adipocytes are mature and normal. The identification of *RADIL* and *ARHGAP29* as causative variants for LSL by Larrew et al led to genes being filtered based on their function in NC migration/differentiation/specification which generated a number of positive results [38]. As mentioned in the critique of the Larrew paper, only functional studies of the variants identified can confirm a relationship with LSL. Unfortunately a multigenic inheritance, rather than a digenic inheritance pattern might require multiple other variants/polymorphisms to give a phenotype and as yet these are not established

By their nature such large data sets are subject to investigator bias. Current data-mining methods need to be directed by prior knowledge and often ultimately result in the researcher looking for what they 'want to see'. Both the genomics and lipidomics data presented in this thesis should be considered just a step in understanding the pathogenesis and disease progression processes of LSL. To validate this work further, functional experimentation is required.

### 3. FUTURE WORK

#### **Biomarker Development**

This doctoral project has covered the discovery phase of biomarker development for LSL. The next stage is validation and needs to be carried out prospectively. Approximately 180 children are diagnosed in the UK with LSL each year [124]. Ideally a large scale national research project should be set up to recruit all these cases, for blood samples to be taken at diagnosis, and all clinical features documented. To control for variation within the blood lipidome, all patients should be NBM for at least 6 hours prior to sample collection. This would be a multicenter research project that would require co-ordination of neurosurgery departments to standard clinical assessment and documentation of features. Patients should initially be followed up for five years with an end point being either the decision to proceed with surgery or the time limit of the study.

Lipids would be extracted from samples and analysed by targeted lipid assay as described in the Methods section, but with optimisation for the PCs of interest: LPC 14:1, LPC18:0-18:4, PC 32:1 and 36:0-36:2. This optimization would include purchasing and injecting standards of all these lipids to confirm detection methods and develop calibration curves with the standards in increasing concentrations from between 0.1ng/μl and 0.8ng/μl in 0.05ng/μl intervals. This would allow accurate measurement of lipid concentrations. After five years, ROC curves would be plotted to calculate the level of each of the lipid's sensitivity and specificity in predicting the outcome: decision to proceed with surgical intervention. Moreover, the clinicians making the management decisions would need to be 'blinded' to all information relating to the lipidomics findings for their patients. Such a large-scale study is key to minimizing bias [361].

If this validation was successful, and confirmed the sensitivity and positive predictive value of one or all of the chosen lipids, the next step would be a further prospective clinical trial. Again all LSLs diagnosed in the UK would need to be recruited and patients randomized to two groups: biomarker group and control group. Ideally recruitment should last at least 2 years to give a sample size of over 300. The control group would follow current best practice, whereas the biomarker group would have blood sampling for biomarker analysis at the time of diagnosis. Biomarker lipids would then be measured and a report generated for the responsible neurosurgeon with the advice to proceed with surgery or continue to monitor. Due to the lack of evidence to support clinical management of LSLs, some parents might decide to continue to 'watch and wait', while some parents might push for surgery despite biomarker results suggesting their child was low risk. It would not be ethical to deny these options based on the current evidence, and so such children would need to be excluded from the trial. All surgery offered to patients should be near-total resection with IONM. Three groups (control, biomarker with surgery, biomarker without surgery) would continue to be monitored, again initially for the first 5 years, with regular clinical assessment and bladder function assessment. At the 5 year end point of the trial, all three cohorts would be assessed in terms of neurological and urological outcome. Importantly,

for this biomarker to be adopted into clinical practice there would need to be better outcomes in the biomarker group than in the control group. This would happen if the biomarker indicated surgery prior to any other clinical assessment, and if the number of children having surgery was less than in the control group. Although patients might deteriorate beyond 5 years of age, a blood test at diagnosis that predicts that a child will remain stable for the first 5 years of life would be a meaningful addition to a patient's assessment. Ideally both trials would continue to follow patients until they reach adulthood.

### **Mechanisms of disease progression**

Separate from the translational application of a biomarker is the understanding of the underlying mechanisms of disease progression. The model proposed in Section III.5 highlights the differences in PC36:2 and LPC 18:0/18:2 between symptomatic and asymptomatic patients. Further confirmation of these differences could come from the biomarker validation study described above. In addition, the proposed mechanism of less DHA available in symptomatic patients could be tested by a direct assay for DHA in remaining CSF samples. This would be covered by current ethics approval and patient consent. Support for the proposed model with lower levels of DHA in CSF in symptomatic patients would lend itself to a simple clinical trial to improve outcomes. Low CSF DHA has been found to be associated with progression in Alzheimer's disease whilst dietary supplementation of DHA corresponds with an increase in CSF DHA and a decrease in Alzheimer progression biomarkers [375]. Several trials have looked at DHA supplementation in the under-5 population and neurocognitive function [376]. This is a safe, over the counter supplementation often given to children in fish oil tablets. A simple double-blind randomized control trial could be performed with two cohorts taking 200mg DHA per day or placebo. Ideally recruitment should be 50 patients per group and from the time of diagnosis, although care would need to be taken such that this trial did not overlap with any biomarker study. Patients would be assessed at 6 monthly intervals as is normal practice with LSL patients. Patients where the decision was made that they should have surgery should continue medication until the end of a five-year period. The two cohorts would be compared for the outcome: change in clinical state and decision to proceed with surgery.

If low levels of LPC18:0 in CSF do correspond with low DHA levels, it is unlikely that this is the sole cause of deterioration in LSL patients. Availability of DHA is likely to be just one factor that influences outcome. Also, if low levels are due to problems transporting DHA rather than the absolute amount of DHA, the above study would not necessarily yield a positive result. More can be learnt about the disease process through proteomics, firstly, of CSF and secondly of the lipoma tissue itself. Ethics approval for proteomics of CSF samples from LSL patients is already in place and CSF samples from LSL patients have been prepared from remaining aliquots from the biomarker work. However, due to mass spectrometry equipment failure it was not possible to complete CSF proteomics before writing. In addition, proteomics of lipoma tissue could be performed. Particular proteins of interest include PNPLA7 that is expressed in mature adipocytes

and hydrolyses LPC. A variant coding for p.D589N was detected in one LSL patient who underwent genetic analysis. Such a variant might hydrolyse LPC less than 'normal' PNPLA7, in and around the lipoma tissue, making more LPC available for DHA and so rendering this patient less likely to be symptomatic.

### **Genetics**

As mentioned above it was not possible to do Sanger sequencing to confirm the sequence of likely disease causing variants. Ideally this should be done following additional sample collection from the involved individuals. In the absence of obtaining additional familial cases, the data generated here could be added to databases such as Genematcher and Matchmaker Exchange to pool data from other LSL research projects. Although, as also described above, the problems with classifying LSL may convolute the results.

Blood samples have been collected from GOSH patients under the ongoing project 08ND09 (led by PS), and about 30 of these patients have LSL. Depending on available funding WGS could be completed on this cohort, or alternatively Sanger sequencing could be performed on the ten genes listed below along with *RADIL* and *ARHGAP29*. It is unlikely that such results would yield a definitive answer as to the genetic causes of LSL but instead add to the overall picture.

To fully understand the impact of genetic variants in LSL patients, some functional work needs to be carried out. All the evidence suggests that multiple genes are associated with LSL as is the case with open NTDs. These genes can broadly be divided into two categories: firstly genes involved in basic cellular function and secondly genes with expression localized to the site of LSL development. Just as disruption or deficiency in folate metabolism is known to increase the risk of NTDs, despite folate metabolism being a global process throughout the body, the same is likely to apply in LSL. Little can be gained from assessing the expression during development of genes involved in basic cellular function, apart from confirming global expression as expected. Instead, it would be interesting to see how progenitor cells with these variants might alter their behaviour in cell culture experiments. Gene editing by CRISPR/Cas9 could be used to introduce the new variants identified in *EIF4EBP1*, *MTHFD1*, *TGFB2* and *TRAF2* into three different cell types: NMPs, NC progenitor and pre-adipocytes. Cells would then be induced to differentiate as per standard cell culture protocols and any disruption of this usual differentiation noted.

With the second group, genes expressed local to the site of formation of LSL, many of these already have gene expression studies in other species showing expression in the dorsal/ caudal neural tube and surrounding mesoderm. Where this animal work is incomplete, such as for *Kctd15* expression in the mouse embryo, in situ hybridisation could be done to confirm expression. Similarly, expression of the genes *KCTD15*, *ADAMST20*, *CREBBP* in human embryos during and soon after secondary neurulation would argue a stronger case for their involvement in LSL pathogenesis.

It is apparent from reviewing the genes, where loss of function knockout models already exist, that none of these genes in isolation cause LSL in animal models. Therefore it would be interesting to generate heterozygous double knockouts for the two pairs of genes identified in familial cases: from Family 1 *NDST1* and *ADAMTS20* and from Larrew et al *RADIL* and *ARHGAP29* and assess the embryos for any evidence of NTDs [38].

The function of *FOLR3* is harder to assess since it is known not to exist in mice. Human data shows that it is an excreted protein mainly expressed in the spleen and bone marrow so in situ hybridization of the neural tube in human embryos is unlikely to yield any expression (although not impossible) [302]. More meaningful studies of *FOLR3* are also complicated by its unknown function in humans. The assumption could be made that *FOLR3* has a role in transport of folate in the blood. To do any functional human experiments a number of volunteers would have to have their *FOLR3* gene sequenced and confirmed as 'normal'. These individuals could then be compared with the LSL individuals carrying the *FOLR3* variant. Once *FOLR3* status was known, the volunteers/patients could be divided into two cohorts: one with normal *FOLR3* and one with the LSL variants. Both groups could be given folic acid and their folate levels compared before and after supplementation.

### **Final thoughts**

This project has taken the initial steps towards developing a biomarker to aid clinical management of children with LSL. Further validation and translation are required to bring this biomarker into clinical practice. Although a biomarker does not need to explain disease mechanism, the lipids highlighted in this study have led to a model suggesting that DHA might have a role in limiting symptoms. This is not likely to be the main cause of disease progression but rather one of many factors. A simple trial of DHA supplementation to children with LSL may improve their outcomes. It is important to keep in mind that the main mechanism of disease progression in LSL remains undetermined. If clinical manifestation of LSL is due to dysgenesis of the conus and nerves roots, near-total resection of the lipoma tissue, regardless of how immaculate, will not improve function. However, if nerve function is altered by factors released by the lipoma tissue, such as PLPLA7 hydrolysing LPCs, then lipoma debulking will be of benefit. LSL is a complex pathology and the most likely scenario is that many factors contribute to the observed variation between individuals in deterioration after diagnosis. We are still far from fully understanding this pathology. The genetics study of LSL patients has also taken steps towards a better understanding the pathogenesis of LSL. A number of potential candidate genes have been identified that would be interesting to study in more detail. The pattern that seems to be emerging is of a number of genes contributing to the formation of LSL: firstly those genes that are locally expressed, and might disrupt NC cells or NMPs, and secondly a number of genes that disrupt important cellular processes, but not enough to be incompatible with life.

1. Secretariat, W.H.O., *Birth Defects*. 2010.
2. Eichholzer, M., O. Tönz, and R. Zimmermann, *Folic acid: a public-health challenge*. The Lancet, 2006. **367**(9519): p. 1352-1361.
3. Boyd, P.A., et al., *Monitoring the prenatal detection of structural fetal congenital anomalies in England and Wales: register-based study*. J Med Screen, 2011. **18**(1): p. 2-7.
4. Hadzagic-Catibusic F., M.H., Uzicanin S., Heljic S., Zubcevic S., Merhemic Z., Cengic A., Kulenovic E., *Congenital malformations of the central nervous system: clinical approach*. Journal of Basic Medical Sciences, 2008. **8**: p. 356-360.
5. Verity C., F.H., ffrench-Constant C., *Congenital Abnormalities of the central nervous system*. J Neurol Neurosurg Psychiat, 2003. **74**: p. 13-18.
6. Gouti, M., V. Metzis, and J. Briscoe, *The route to spinal cord cell types: a tale of signals and switches*. Trends in Genetics, 2015. **31**(6): p. 282-289.
7. Kwon, G.S., M. Viotti, and A.K. Hadjantonakis, *The endoderm of the mouse embryo arises by dynamic widespread intercalation of embryonic and extraembryonic lineages*. Dev Cell, 2008. **15**(4): p. 509-20.
8. Muller, F. and R. O'Rahilly, *The primitive streak, the caudal eminence and related structures in staged human embryos*. Cells Tissues Organs, 2004. **177**(1): p. 2-20.
9. Yamanaka, Y., et al., *Live imaging and genetic analysis of mouse notochord formation reveals regional morphogenetic mechanisms*. Dev Cell, 2007. **13**(6): p. 884-96.
10. Tissir, F. and A.M. Goffinet, *Planar cell polarity signaling in neural development*. Curr Opin Neurobiol, 2010. **20**(5): p. 572-7.
11. Ybot-Gonzalez, P., et al., *Convergent extension, planar-cell-polarity signalling and initiation of mouse neural tube closure*. Development, 2007. **134**(4): p. 789-99.
12. Copp, A.J. and N.D. Greene, *Neural tube defects--disorders of neurulation and related embryonic processes*. Wiley Interdiscip Rev Dev Biol, 2013. **2**(2): p. 213-27.
13. Greene, N.D. and A.J. Copp, *Neural tube defects*. Annu Rev Neurosci, 2014. **37**: p. 221-42.
14. Ybot-Gonzalez, P., Cogram, P., Gerrelli, D., Copp, A.J., *Sonic hedgehog and the molecular regulation of mouse neural tube closure*. Development, 2002. **129**: p. 2507-2517.
15. Cearns, M.D., et al., *Microtubules, polarity and vertebrate neural tube morphogenesis*. Journal of Anatomy, 2016. **229**(1): p. 63-74.
16. Schoenwolf, G.C., Smith, J.L., *Mechanisms of neurulation: traditional viewpoint and recent advances*. Development, 1990. **109**: p. 243-270.
17. Roszko, I., P. Faure, and L. Mathis, *Stem cell growth becomes predominant while neural plate progenitor pool decreases during spinal cord elongation*. Developmental Biology, 2007. **304**(1): p. 232-245.
18. Jones V.J., G.N.D.E., Copp, A.J., *Genetics and developmental biology of closed dysraphic conditions*. In *Occult Spinal Dysraphism*, eds. RS Tubbs, RJ Oskouian, JP Blount, WJ Oakes, 2019: p. 325-344.
19. Durdag, E., et al., *Pathological evaluation of the filum terminale tissue after surgical excision*. Childs Nerv Syst, 2015. **31**(5): p. 759-63.



20. Kural, C., et al., *Histological structure of filum terminale in human fetuses*. J Neurosurg Pediatr, 2014. **13**(4): p. 362-7.
21. Cambray, N., Wilson, V., *Axial progenitors with extensive potency are localised to the mouse chordoneural hinge*. Development, 2002. **129**: p. 4855-4866.
22. Schoenwolf, G.C., Chandler, N.B., Smith, J.L., *Analysis of the Origins and Early Fates of Neural Crest Cells in Caudal Regions of Avian Embryos*. Developmental Biology, 1985. **110**: p. 467-479.
23. Schoenwolf, G.C., Delongo J., *Ultrastructure of secondary neurulation in the chick embryo*. Am J Anat, 1980. **158**(1): p. 43-63.
24. Dady, A., et al., *Junctional neurulation: a unique developmental program shaping a discrete region of the spinal cord highly susceptible to neural tube defects*. J Neurosci, 2014. **34**(39): p. 13208-21.
25. Liu, C., et al., *Null and hypomorph Prickle1 alleles in mice phenocopy human Robinow syndrome and disrupt signaling downstream of Wnt5a*. Biol Open, 2014. **3**(9): p. 861-70.
26. Schoenwolf, G.C., *Histological and ultrastructural studies of secondary neurulation in mouse embryos*. Am J Anat, 1984. **169**(4): p. 361-76.
27. Eibach, S., et al., *Unjoined primary and secondary neural tubes: junctional neural tube defect, a new form of spinal dysraphism caused by disturbance of junctional neurulation*. Childs Nerv Syst, 2017. **33**(10): p. 1633-1647.
28. Schmidt, C., et al., *Junctional neural tube defect in a newborn: report of a fourth case*. Childs Nerv Syst, 2017. **33**(5): p. 873-875.
29. Tzouanacou, E., et al., *Redefining the Progression of Lineage Segregations during Mammalian Embryogenesis by Clonal Analysis*. Developmental Cell, 2009. **17**(3): p. 365-376.
30. Turner, D.A., et al., *Wnt/-catenin and FGF signalling direct the specification and maintenance of a neuromesodermal axial progenitor in ensembles of mouse embryonic stem cells*. Development, 2014. **141**(22): p. 4243-4253.
31. Stemple, D.L., et al., *Loss of FGF-Dependent Mesoderm Identity and Rise of Endogenous Retinoid Signalling Determine Cessation of Body Axis Elongation*. PLoS Biology, 2012. **10**(10): p. e1001415.
32. Nusse, R., et al., *In Vitro Generation of Neuromesodermal Progenitors Reveals Distinct Roles for Wnt Signalling in the Specification of Spinal Cord and Paraxial Mesoderm Identity*. PLoS Biology, 2014. **12**(8): p. e1001937.
33. Henrique, D., et al., *Neuromesodermal progenitors and the making of the spinal cord*. Development, 2015. **142**(17): p. 2864-2875.
34. Cambray, N. and V. Wilson, *Two distinct sources for a population of maturing axial progenitors*. Development, 2007. **134**(15): p. 2829-2840.
35. Garriock, R.J., et al., *Lineage tracing of neuromesodermal progenitors reveals novel Wnt-dependent roles in trunk progenitor cell maintenance and differentiation*. Development, 2015. **142**(9): p. 1628-38.
36. Abu-Abed S., D.P., Metzger D., Beckett B., Chambon P., Petkovich M., *The retinoic acid-metabolizing enzyme, CYP26A1, is essential for normal hindbrain patterning, vertebral identity, and development and posterior structures*. Genes & Development, 2001. **15**: p. 226-240.
37. Lee, L.M., et al., *Perturbation of Retinoid Homeostasis Increases Malformation Risk in Embryos Exposed to Pregestational Diabetes*. Diabetes, 2017. **66**(4): p. 1041-1051.

38. Larrew, T., et al., *Transgenerational Inheritance of Familial Lipomyelomeningocele*. Journal of Child Neurology, 2017. **32**(14): p. 1118-1122.
39. Ahlstrom, J.D. and C.A. Erickson, *The neural crest epithelial-mesenchymal transition in 4D: a 'tail' of multiple non-obligatory cellular mechanisms*. Development, 2009. **136**(11): p. 1801-1812.
40. Newbern, J.M., *Molecular Control of the Neural Crest and Peripheral Nervous System Development*. 2015. **111**: p. 201-231.
41. Mayor R., G.N., Martinez C., *Role of FGF and Noggin in Neural Crest Induction*. Dev Biol, 1997. **189**: p. 1-12.
42. Vallin, J., et al., *Cloning and characterization of three Xenopus slug promoters reveal direct regulation by Lef/beta-catenin signaling*. J Biol Chem, 2001. **276**(32): p. 30350-8.
43. Graham, A., *The Neural Crest*. Current Biology. **13**.
44. Osorio, L., et al., *Neural crest ontogeny during secondary neurulation: a gene expression pattern study in the chick embryo*. Int J Dev Biol, 2009. **53**(4): p. 641-8.
45. Catala, M., Ziller C., Lapointe F., Le Douarin N.M., *The developmental potentials of the caudal most part of the neural crest are restricted to melanocytes and glia*. Mechanisms of Development, 2000. **95**: p. 77-87.
46. Billon, N., et al., *The generation of adipocytes by the neural crest*. Development, 2007. **134**(12): p. 2283-92.
47. Paylor, B., A.W. Joe, F.M.V. Rossi, D.R. Lemos, *In vivo characterization of neural crest-derived fibro/adipogenic progenitor cells as a likely substrate for craniofacial fibrofatty infiltrating disorders*. Biochemical and Biophysical Research Communications, 2014. **451**: p. 148-151.
48. Sowa, Y., et al., *Adipose stromal cells contain phenotypically distinct adipogenic progenitors derived from neural crest*. PLoS One, 2013. **8**(12): p. e84206.
49. Pourquie, O., *Vertebrate somitogenesis: a novel paradigm for animal segmentation?* Int J Dev Biol, 2003. **47**: p. 597-603.
50. Christ, B., Wilting, J., *From somites to vertebral column*. Am J Anat, 1992. **174**: p. 23-32.
51. Maroto, M., R.A. Bone, and J.K. Dale, *Somitogenesis*. Development, 2012. **139**(14): p. 2453-2456.
52. Sakai, Y., *Neurulation in the mouse: manner and timing of neural tube closure*. Anat Rec, 1989. **223**: p. 194-203.
53. O'Rahilly, R.M., F., *The two sites of fusion of the neural folds and the two neuropores in the human embryo*. Teratology, 2002. **65**: p. 162-170.
54. Robinson, A., et al., *Mutations in the planar cell polarity genes CELSR1 and SCRIB are associated with the severe neural tube defect craniorachischisis*. Hum Mutat, 2012. **33**(2): p. 440-7.
55. Juriloff, D.M. and M.J. Harris, *A consideration of the evidence that genetic defects in planar cell polarity contribute to the etiology of human neural tube defects*. Birth Defects Res A Clin Mol Teratol, 2012. **94**(10): p. 824-40.
56. Copp, A.J., P. Stanier, and N.D.E. Greene, *Neural tube defects: recent advances, unsolved questions, and controversies*. The Lancet Neurology, 2013. **12**(8): p. 799-810.
57. Fleming A., C.A.J., *Embryonic Folate Metabolism and Mouse Neural Tube Defects*. Science, 1998. **280**.

58. Etheredge, A.J., et al., *Maternal and infant gene-folate interactions and the risk of neural tube defects*. Am J Med Genet A, 2012. **158A**(10): p. 2439-46.
59. Amorim, M.R., et al., *Non-Latin European descent could be a requirement for association of NTDs and MTHFR variant 677C > T: a meta-analysis*. Am J Med Genet A, 2007. **143A**(15): p. 1726-32.
60. Brody, L.C., Conley M., Cox, C., Kirke P.N., McKeever P., Mills J.L., Molloy A.M., O'Leary V.B., Parle-McDermott A., Scott J.M., Swanson D., *A Polymorphism, R653Q, in the Trifunctional Enzyme Methylenetetrahydrofolate Dehydrogenase/Methenyltetrahydrofolate Cyclohydrolase/Formyltetrahydrofolate Synthetase Is a Maternal Genetic Risk Factor for Neural Tube Defects: Report of the Birth Defects Research Group*. Am J Hum Genet, 2002. **71**: p. 1207-1215.
61. Narisawa, A., et al., *Mutations in genes encoding the glycine cleavage system predispose to neural tube defects in mice and humans*. Hum Mol Genet, 2012. **21**(7): p. 1496-503.
62. Parle-McDermott, A., et al., *A common variant in MTHFD1L is associated with neural tube defects and mRNA splicing efficiency*. Hum Mutat, 2009. **30**(12): p. 1650-6.
63. Shah, R.H., et al., *Genetic association of the glycine cleavage system genes and myelomeningocele*. Birth Defects Res A Clin Mol Teratol, 2016. **106**(10): p. 847-853.
64. Pike, S.T., et al., *Mitochondrial C1-tetrahydrofolate synthase (MTHFD1L) supports the flow of mitochondrial one-carbon units into the methyl cycle in embryos*. J Biol Chem, 2010. **285**(7): p. 4612-20.
65. Beaudin, A.E., et al., *Maternal Mthfd1 disruption impairs fetal growth but does not cause neural tube defects in mice*. Am J Clin Nutr, 2012. **95**(4): p. 882-91.
66. Momb, J., et al., *Deletion of Mthfd1l causes embryonic lethality and neural tube and craniofacial defects in mice*. Proc Natl Acad Sci U S A, 2013. **110**(2): p. 549-54.
67. Pai, Y.J., et al., *Glycine decarboxylase deficiency causes neural tube defects and features of non-ketotic hyperglycinemia in mice*. Nat Commun, 2015. **6**: p. 6388.
68. Blencowe, H., et al., *Folic acid to reduce neonatal mortality from neural tube disorders*. Int J Epidemiol, 2010. **39 Suppl 1**: p. i110-21.
69. McNeely, P.D., Howes, W.J., *Ineffectiveness of dietary folic acid supplementation on the incidence of lipomyelomeningocele: pathogenetic implications*. J Neurosurg (Paediatrics 2), 2004. **100**: p. 98-100.
70. Esmaeili, A., et al., *Risk factors associated with lipomyelomeningocele: a case-control study*. Pediatr Neurosurg, 2013. **49**(4): p. 202-7.
71. Arthurs, O.J., et al., *Normal ascent of the conus medullaris: a post-mortem foetal MRI study*. J Matern Fetal Neonatal Med, 2013. **26**(7): p. 697-702.
72. Barson, *The vertebral level of termination of the spinal cord during normal and abnormal development*. J Anat, 1970. **106**: p. 489-497.
73. Yamada, S., et al., *Tethered cord syndrome: overview of diagnosis and treatment*. Neurol Res, 2004. **26**(7): p. 719-21.
74. Stiefel, D., Shibata, T., Meuli, M., Duffy, P.G., Copp, A.J., *Tethering of the spinal cord in mouse fetuses and neonates with spina bifida*. J Neurosurg, 2003. **99**(20): p. 206-213.

75. Griffith, C.M., Wiley, M.J., Sanders, E.J., *The vertebrate tail bud: Three germ layers from one tissue*. *Anat Embryol*, 1992. **185**: p. 101-113.
76. Swamy, R., N. Embleton, and J. Hale, *Sacrococcygeal teratoma over two decades: Birth prevalence, prenatal diagnosis and clinical outcomes*. *Prenatal Diagnosis*, 2008. **28**(11): p. 1048-1051.
77. Barksdale, E.M. and I. Obokhare, *Teratomas in infants and children*. *Current Opinion in Pediatrics*, 2009. **21**(3): p. 344-349.
78. Tam, P.P.L., *The histogenetic capacity of tissues in the caudal end of the embryonic axis of the mouse*. *J Embryol exp Morph*, 1984. **82**: p. 253-266.
79. Gatcombe, H.G., et al., *Primary retroperitoneal teratomas: a review of the literature*. *J Surg Oncol*, 2004. **86**(2): p. 107-13.
80. Pierre-Kahn, A., M. Zerah, D. Renier, G. Cinalli, C. Sainte-Rose, A. Lellouch-Tubiana, F. Brunelle, M. Le Merrer, Y. Giudicelli, J. Pichon, B. Kleinknecht, F. Nataf, *Congenital lumbosacral lipomas*. *Childs Nerv Syst*, 1997. **13**(6): p. 298-334.
81. Beuriat, P.A., et al., *Complete Reversibility of the Chiari Type II Malformation After Postnatal Repair of Myelomeningocele*. *World Neurosurg*, 2017. **108**: p. 62-68.
82. Koen, J.L., McLendon, R.E., George, T.M., *Intradural spinal teratoma: evidence for a dysembryonic origin*. *J Neurosurg*, 1998. **89**: p. 844-851.
83. Ein, S.H., Adeyemi, M.B., Mancner, K., *Benign sacrococcygeal teratomas in infants and children: a 25 year review*. *Ann Surg*, 1980. **191**(3): p. 382-4.
84. Young, T. and J. Deschamps, *Chapter 8 Hox, Cdx, and Anteroposterior Patterning in the Mouse Embryo*. 2009. **88**: p. 235-255.
85. Tsuda, T., et al., *PCSK5 and GDF11 expression in the hindgut region of mouse embryos with anorectal malformations*. *Eur J Pediatr Surg*, 2011. **21**(4): p. 238-41.
86. Szumska, D., et al., *VACTERL/caudal regression/Currarino syndrome-like malformations in mice with mutation in the proprotein convertase Pcsk5*. *Genes Dev*, 2008. **22**(11): p. 1465-77.
87. Garne, E., et al., *Spectrum of congenital anomalies in pregnancies with pregestational diabetes*. *Birth Defects Res A Clin Mol Teratol*, 2012. **94**(3): p. 134-40.
88. Stevenson, R.E., Jones, K.L., Phelan, M.C., Jones, M.C., Barr, M., Clericuzio, C., Harley, R.A., Benirschke, K., *Vascular steal: the pathogenetic mechanism producing sirenomelia and associated defects of the visera and soft tissues*. *Pediatrics*, 1986. **78**: p. 451-457.
89. Tokunaga, S., Morioka, T., Hashiguchi, K., Samura, K., Yoshida, F., Miyagi, Y., Yoshiura, T., Yamanouchi, T., Sasaki, T., *Double Lumbosacral Lipomas of the Dorsal and Filar Types Associated With OEIS Complex*. *Neurol Med Chir (Tokyo)*, 2009. **49**: p. 487-490.
90. Carey JC, G.B., Hall BD, *The OEIS complex (omphalocele, exstrophy, imperforate anus, spinal defects)*. *Birth Defects Orig Artic Sec*, 1978. **14**(6B): p. 253-63.
91. Kutzner, D.K., Wilson, W.G., Hogge, W.A., *OEIS complex (cloacal exstrophy): prenatal diagnosis in the second trimester*. *Prenat Diagn*, 1988. **8**(4): p. 247-53.
92. Smith, N.M., Chambers, H.M., Furness, M.E., Haan, E.A., *The OEIS complex (omphalocele-exstrophy-imperforate anus-spinal defects): recurrence in sibs*. *J Med Genet*, 1992. **29**: p. 730-732.

93. England, R.J., et al., *Improving the rigour of VACTERL screening for neonates with anorectal malformations*. Pediatric Surgery International, 2017.
94. Offiah, A., et al., *Pilot assessment of a radiologic classification system for segmentation defects of the vertebrae*. American Journal of Medical Genetics Part A, 2010. **152A**(6): p. 1357-71.
95. Giampietro, P.F., et al., *Clinical, Genetic and Environmental Factors Associated with Congenital Vertebral Malformations*. Molecular Syndromology, 2012.
96. Lubinsky, M., *The VACTERL Association as a disturbance of cell fate determination*. American Journal of Medical Genetics Part A, 2015. **167**(11): p. 2582-2588.
97. O'Neill, B.R., A.K. Yu, and E.C. Tyler-Kabara, *Prevalence of tethered spinal cord in infants with VACTERL*. Journal of Neurosurgery: Pediatrics, 2010. **6**(2): p. 177-182.
98. Currarino, G., Coln, D., Votteler, T., *Triad of Anorectal, Sacral, and Presacral Anomalies*. American Journal of Roentgenology, 1981. **137**(2): p. 395-398.
99. Lynch S.A., W.Y., Strachan T., Burn J., Lindsay S, *Autosomal dominant sacral agenesis: Currarino syndrome*. J Med Genet, 2000. **37**: p. 561-566.
100. Kubota, Y., Shimotake, T., Iwai, N., *Congenital Anomalies in Mice Induced by Etretinate*. Eur J Pediatr Surg, 2000. **10**(4): p. 248-51.
101. Andersson, E.R., R. Sandberg, and U. Lendahl, *Notch signaling: simplicity in design, versatility in function*. Development, 2011. **138**(17): p. 3593-612.
102. Li H., A.S., Jessell T.M., Edlund H., *Selective agenesis of the dorsal pancreas in mice lacking homeobox gene Hlxb9*. Nature Genetics, 1999. **23**: p. 67-70.
103. Kole, M.J., et al., *Currarino syndrome and spinal dysraphism*. Journal of Neurosurgery: Pediatrics, 2014. **13**(6): p. 685-689.
104. Martucciello, G., et al., *Currarino syndrome: Proposal of a diagnostic and therapeutic protocol*. Journal of Pediatric Surgery, 2004. **39**(9): p. 1305-1311.
105. Payne, J., Shibasaki, F., Mercola, M., *Spina Bifida Occulta in Homozygous Patch Mouse Embryos*. Developmental Dynamics, 1997. **209**: p. 105-116.
106. Aruga, J., Mizugishi, K., Koseki, H., Imai, K., Balling, R., Noda, T., Mikoshiba, K., *Zic1 regulates the patterning of vertebral arches in cooperation with Gli3*. Mechanisms of Development, 1999. **89**: p. 141-150.
107. Lettice, L.A., Purdie, L.A., Carlson, G.J., Kilanowski, F., Dorin, J., Hill, R.E., *The mouse bagpipe gene controls development of axial skeleton, skull, and spleen*. Developmental Biology, 1999. **96**: p. 9695-9700.
108. Rodrigo, I., et al., *Pax1 and Pax9 activate Bapx1 to induce chondrogenic differentiation in the sclerotome*. Development, 2003. **130**(3): p. 473-82.
109. Letiges M., N.L., Haenig B., Herrmann B.G., Kispert A., *The paired homeobox gene Uncx4.1 specifies pedicles, transverse processes and proximal ribs of the vertebral column*. Development, 2000. **127**: p. 2259-2267.
110. Neuhauser, E.B., Harris, G.B., Berrett, A., *Roentgenographic features of neurenteric cysts*. Am J Roentgenol, 1958. **79**(2): p. 235-40.
111. Jackson, F.E., *Report of a case of neurenteric cyst with associated chronic meningitis and hydrocephalus*. Journal of Neurosurgery, 1961. **18**(5): p. 678-682.
112. Bentley, J.F.R., Smith, J.R., *Developmental Posterior Enteric Remnants and Spinal Malformations: The Split Notochord Syndrome*. Arch Dis Childh, 1960. **35**(76-86).

113. Beardmore, H.E., Wiglesworth, F.W., *Vertebral anomalies and alimentary duplications. Clinical and embryological aspects.* Paediatric Clinics of North America, 1958: p. 457-474.
114. Row, R.H., et al., *The zebrafish tailbud contains two independent populations of midline progenitor cells that maintain long-term germ layer plasticity and differentiate in response to local signaling cues.* Development, 2015. **143**(2): p. 244-254.
115. Cogliatti, S.B., *Diplomyelia: caudal duplication of the neural tube in mice.* Teratology, 1986. **34**: p. 343-352.
116. Greene, N.D., Gerrelli D., Van Straaten H.W.M., Copp A.J., *Abnormalities of floorplate, notochord and somite differentiation in the loop-tail (Lp) mouse: a model of severe neural tube defects.* Mechanisms of Development, 1998. **73**: p. 59-72.
117. Rulle, A., et al., *On the Enigma of the Human Neurenteric Canal.* Cells Tissues Organs, 2018. **205**(5-6): p. 256-278.
118. Emura, T., Asashima, M., Hashizume, K., *An Experimental Animal Model of Split Cord Malformation.* Pediatric Neurosurgery, 2000. **33**: p. 283-292.
119. Rilliet, B., Schowing, J., Berney, J., *Pathogenesis of diastematomyelia: can a surgical model in the chick embryo give some clues about the human malformation?* Child's Nerv Syst, 1992. **8**: p. 310-316.
120. Pang, D., Dias, M.S., Mamdouha, A-B., *Split Cord Malformation: Part I: A Unified Theory of Embryogenesis for Double Spinal Cord Malformations.* Neurosurgery, 1992. **31**(3): p. 451-480.
121. Finn, M.A. and M.L. Walker, *Spinal lipomas: clinical spectrum, embryology, and treatment.* Neurosurg Focus, 2007. **23**(2): p. E10.
122. Lassman, L.P., C.C Michael James, *Lumbosacral lipomas: critical survey of 26 cases submitted to laminectomy.* J Neurol Neurosurg Psychiat, 1967. **30**: p. 174-181.
123. Zerah, M., . T. Roujeau, M. Catala., A. Pierre-Kahn, *Spinal Lipomas.* Spinal Bifida: Management and Outcome, 2008: p. 445-474.
124. Chapman, *Congenital intraspinal lipomas: anatomic considerations and surgical treatment.* Childs Brain, 1982. **9**(1): p. 37.
125. Naidich, T., D.G. McLone, S. Mutluer, *A new understanding of dorsal dysraphism with lipoma (lipomyeloschisis): radiologic evaluation and surgical correction.* Am J Roentgenol, 1983. **140**(6): p. 1065-78.
126. Pang, D., et al., *Surgical treatment of complex spinal cord lipomas.* Childs Nerv Syst, 2013. **29**(9): p. 1485-513.
127. Pang, D., Zovickian, J., Oviedo, A, *Long-Term Outcome of Total and Near-Total Resection of Spinal Cord Lipomas and Radical Reconstruction of the Neural Placode, Part II: Outcome Analysis and Preoperative Profiling.* Neurosurgery, 2010. **66**(2): p. 253-273.
128. Pang, D., J. Zovickian, and A. Oviedo, *Long-term outcome of total and near-total resection of spinal cord lipomas and radical reconstruction of the neural placode: part I-surgical technique.* Neurosurgery, 2009. **65**(3): p. 511-28; discussion 528-9.
129. Jones, V., Thompson, D., *Placode rotation in transitional lumbosacral lipomas - are there implications for origin and mechanism of deterioration.* Childs Nervous System, 2018.

130. Kulkarni, A.V., A. Pierre-Kahn, and M. Zerah, *Conservative Management of Asymptomatic Spinal Lipomas of the Conus*. Neurosurgery, 2004. **54**(4): p. 868-875.
131. Tortori-Donati, P., R. Andrea, R. Biancheri, Armando Cama, *Magnetic Resonance Imaging of Spinal Dysraphism*. Topics in Magnetic Resonance Imaging, 2001. **12**(6): p. 375-409.
132. Chaturvedi, S. and I. Pant, *Spectrum of histopathology in spinal lesions*. Astrocyte, 2016. **2**(4): p. 187.
133. Yundt, K.D., Park, T.S., Kaufman, B.A., *Normal diameter of filum terminale in children: in vivo measurement*. Pediatr Neurosurg, 1997. **27**(5): p. 257-9.
134. Lellouch-Tubiana, A., M Zerah, M Catala, N Brousse, A Pierre-Kahn, *Congenital Intraspinial Lipomas: Histological Analysis of 234 Cases and Review of the Literature*. Pediatr Dev Pathol, 1999. **2**(4): p. 346-352.
135. John W. Walsh, W.R.M., *Histological features of congenital lipomas of the lower spinal canal*. Journal of Neurosurgery, 1980. **52**: p. 564-569.
136. Takeyama, J., *Spinal hamartoma associated with spinal dysraphism*. Childs Nerv Syst, 2006. **22**: p. 1098-1102.
137. Dubowitz, V., L.J., R.B. Zachary, *Lipoma of the Cauda Equina*. Arch Dis Childh, 1965. **40**: p. 207-213.
138. Giudicelli Y., A.P.-K., AM Bourdeaux, P de Mazancourt, D Lacasa, JF Hirsch, *Are the metabolic characteristics of congenital intraspinal lipoma cells identical to, or different from normal adipocytes?* Childs Nerv Syst, 1986. **2**(6): p. 290-296.
139. Anderson, *Occult Spinal Dysraphism: A Series of 73 Cases*. Pediatrics. **55**(6): p. 826-835.
140. Jones V., W.V., Cohen N., Thompson D., Jacques T.S., *The pathology of lumbosacral lipomas: macroscopic and microscopic disparity have implications for embryogenesis and mode of clinical deterioration*. Histopathology, 2018.
141. Morel, B., et al., *Prenatal Sacral Anomalies Leading to the Detection of Associated Spinal Cord Malformations*. Fetal Diagnosis and Therapy, 2017.
142. Isern, J., et al., *The neural crest is a source of mesenchymal stem cells with specialized hematopoietic stem cell niche function*. Elife, 2014. **3**: p. e03696.
143. Hitoshi, S., et al., *Mammalian Gcm genes induce Hes5 expression by active DNA demethylation and induce neural stem cells*. Nat Neurosci, 2011. **14**(8): p. 957-64.
144. Nait-Oumesmar, B., Stecca, B., Fatterpekar, G., Naidich, T., Corbin, J., Lazzarini, R.A., *Ectopic expression of Gcm1 induces congenital spinal cord abnormalities*. Development, 2002. **129**: p. 3957-3964.
145. Li, Y.C., Shin, S.-H., Cho, B.-K., Lee, M.-S., Lee, Y.-J., Hong, S.-K., Wang, K.-C., *Pathogenesis of lumbosacral lipoma A test of the 'premature dysfunction' theory*. Pediatric Neurosurgery, 2001. **34**: p. 124-130.
146. Catala, M., *Why do we need a new explanation for the emergence of spina bifida with lipoma*. Childs's Nerv Syst, 1997. **13**: p. 336-340.
147. Smolen, G.A., et al., *A Rap GTPase interactor, RADIL, mediates migration of neural crest precursors*. Genes & Development, 2007. **21**(17): p. 2131-2136.
148. Barry, D.M., et al., *Rasip1-Mediated Rho GTPase Signaling Regulates Blood Vessel Tubulogenesis via Nonmuscle Myosin II* Novelty and Significance. Circulation Research, 2016. **119**(7): p. 810-826.

149. Post, A., et al., *Rap1 Spatially Controls ArhGAP29 To Inhibit Rho Signaling during Endothelial Barrier Regulation*. *Molecular and Cellular Biology*, 2015. **35**(14): p. 2495-2502.
150. Xu, K., et al., *Blood vessel tubulogenesis requires Rasip1 regulation of GTPase signaling*. *Dev Cell*, 2011. **20**(4): p. 526-39.
151. Xu, Q., et al., *MicroRNA-1291 promotes endometrial fibrosis by regulating the ArhGAP29-RhoA/ROCK1 signaling pathway in a murine model*. *Mol Med Rep*, 2017. **16**(4): p. 4501-4510.
152. Vicente-Manzanares, M., et al., *Non-muscle myosin II takes centre stage in cell adhesion and migration*. *Nat Rev Mol Cell Biol*, 2009. **10**(11): p. 778-90.
153. Savastano, C.P., et al., *Impact of rare variants in ARHGAP29 to the etiology of oral clefts: role of loss-of-function vs missense variants*. *Clinical Genetics*, 2017. **91**(5): p. 683-689.
154. Paul, B.J., et al., *ARHGAP29 Mutation Is Associated with Abnormal Oral Epithelial Adhesions*. *J Dent Res*, 2017. **96**(11): p. 1298-1305.
155. Biggs, L.C., et al., *Interferon regulatory factor 6 regulates keratinocyte migration*. *J Cell Sci*, 2014. **127**(Pt 13): p. 2840-8.
156. Seeds, J.W., Powers, S.K., *Early prenatal diagnosis of familial lipomyelomeningocele*. *Obstet Gynecol*, 1988. **72**(3): p. 469-71.
157. Kannu, P., C. Furneaux, and S. Aftimos, *Familial lipomyelomeningocele: a further report*. *Am J Med Genet A*, 2005. **132A**(1): p. 90-2.
158. Hanaei, S., et al., *Identical twins with lumbosacral lipomyelomeningocele*. *J Neurosurg Pediatr*, 2015. **15**(1): p. 92-5.
159. Costain, G., P. Kannu, and S. Bowdin, *Genome-wide sequencing expands the phenotypic spectrum of EP300 variants*. *Eur J Med Genet*, 2018. **61**(3): p. 125-129.
160. Hoshino, Y., et al., *Schuurs-Hoeijmakers syndrome in two patients from Japan*. *Am J Med Genet A*, 2019. **179**(3): p. 341-343.
161. Satyarthee, G.D., Kumar, A., *Klippel-Feil Syndrome Associated with Sacral Agenesis, Low Lying Cord, Lipomyelomeningocele and Split Cord Malformation Presenting with Tethered Cord Syndrome: Pentads Neural Tube Defects Spread along Whole Spinal Axis*. *J Pediatr Neurosci*, 2017. **12**(1): p. 51-54.
162. Bayrakli F., G.B., Yakicier C., Balaban H., Kartal U., Erguner B., Sagiroglu M.S., Yuksel S., Ozturk A.R., Kazanci B., Ozum U., Kars H.Z, *Mutation in MEOX1 gene causes a recessive Klippel-Feil syndrome subtype*. *BMC Genetics*, 2013. **14**(95).
163. Girard, C., Bigorre, M., Guillot, B., *PELVIS Syndrome*. *Arch Dermatol*, 2006. **142**(7): p. 884-888.
164. Shimizu, M., et al., *An infant with PELVIS (perineal hemangioma, external genital malformations, lipomyelomeningocele, vesicorenal abnormalities, imperforate anus, and skin tag) syndrome misdiagnosed as diaper rash*. *J Pediatr*, 2014. **165**(3): p. 634.
165. Goldberg N.S., H.A.A., Esterly N.B., *Sacral haemangiomas and multiple congenital abnormalities*. *Arch Dermatol*, 1986. **122**(6): p. 684-687.
166. Franco, A., et al., *A Rare Triad of Giant Occipital Encephalocele with Lipomyelomeningocele, Tetralogy of Fallot, and Situs Inversus*. *J Radiol Case Rep*, 2016. **10**(3): p. 36-46.
167. Kwun, Y., et al., *Phenotypic variability of a terminal 7q deletion/8q duplication in Korean siblings*. *Ann Lab Med*, 2015. **35**(5): p. 557-60.



168. Oliveria, S.F., E.M. Thompson, and N.R. Selden, *Lumbar lipomyelomeningocele and sacrococcygeal teratoma in siblings: support for an alternative theory of spinal teratoma formation*. Journal of Neurosurgery: Pediatrics, 2010. **5**(6): p. 626-629.
169. Lopez-Escobar, B., et al., *The non-canonical Wnt-PCP pathway shapes the mouse caudal neural plate*. Development, 2018. **145**(9).
170. Wong, L.L., Adler, P.N., *Tissue Polarity Genes of Drosophila Regulate the Subcellular Location for Prehair Initiation in Pupal Wing Cells*. Journal of Cell Biology, 1993. **123**(1): p. 209-221.
171. Simons, M. and M. Mlodzik, *Planar cell polarity signaling: from fly development to human disease*. Annu Rev Genet, 2008. **42**: p. 517-40.
172. Keller, R., et al., *Mechanisms of convergence and extension by cell intercalation*. Philos Trans R Soc Lond B Biol Sci, 2000. **355**(1399): p. 897-922.
173. Copp, A.J., N.D.E. Greene, and J.N. Murdoch, *Dishevelled: linking convergent extension with neural tube closure*. Trends in Neurosciences, 2003. **26**(9): p. 453-455.
174. De Marco, P., et al., *Genetic analysis of disheveled 2 and disheveled 3 in human neural tube defects*. J Mol Neurosci, 2013. **49**(3): p. 582-8.
175. Merello, E., Mascelli, S., Raso, A., Piatelli, G., Consales A., Cama, A., Kibar, Z., Capra, De Marco, P., *Expanding the mutational spectrum associated to neural tube defects: Literature revision and description of novel VANGL1 mutations*. Clinical and Molecular Teratology, 2014. **103**(1): p. 51-61.
176. Allache, R., et al., *Role of the planar cell polarity gene CELSR1 in neural tube defects and caudal agenesis*. Birth Defects Res A Clin Mol Teratol, 2012. **94**(3): p. 176-81.
177. Kibar, Z., et al., *Contribution of VANGL2 mutations to isolated neural tube defects*. Clin Genet, 2011. **80**(1): p. 76-82.
178. De Marco, P., et al., *FZD6 is a novel gene for human neural tube defects*. Hum Mutat, 2012. **33**(2): p. 384-90.
179. Kousa, Y.A., et al., *The TFAP2A-IRF6-GRHL3 genetic pathway is conserved in neurulation*. Hum Mol Genet, 2019.
180. Wang M., D.M.P., Merello E., Drapeau P., Capra V., Kibar Z., *Role of the Planar Cell Polarity Gene Protein Tyrosine Kinase 7 in Neural Tube Defects in Humans*. Birth Defects Res A Clin Mol Teratol, 2015. **103**: p. 1021-1027.
181. Wykes, V., D. Desai, and D.N. Thompson, *Asymptomatic lumbosacral lipomas-- a natural history study*. Childs Nerv Syst, 2012. **28**(10): p. 1731-9.
182. Reimann, A.F., B.J. Anson, *Vertebral level of termination of the spinal cord with a report of a case of sacral cord*. Anat Rec, 1944. **88**: p. 127-138.
183. Tu, A., A.R. Hengel, and D.D. Cochrane, *Radiographic predictors of deterioration in patients with lumbosacral lipomas*. J Neurosurg Pediatr, 2016. **18**(2): p. 171-6.
184. Pang, D., *Total Resection of Complex Spinal Cord Lipomas: How, Why, and When to Operate?* Neurol Med Chir (Tokyo), 2015. **55**(9): p. 695-721.
185. Fahy, E., *A comprehensive classification system for lipids*. The Journal of Lipid Research, 2005. **46**(5): p. 839-862.
186. Zhang, H., et al., *RNAi-based biosynthetic pathway screens to identify in vivo functions of non-nucleic acid-based metabolites such as lipids*. Nature Protocols, 2015. **10**(5): p. 681-700.

187. Fonteh, A.N., Harrington, R.J., Huhmer, A.F., Biringer, R.G., Riggins, J.N., Harrington, M.G., *Identification of disease markers in human cerebrospinal fluid using lipidomic and proteomic methods*. Disease Markers, 2006. **22**: p. 39-64.
188. Danik, M., Champagne, D., Petit-Turcotte, C., Beffert, U., Poirier, J., *Brain lipoprotein metabolism and its relation to neurodegenerative disease*. Crit Rev Neurobiol, 1999. **13**(4): p. 357-407.
189. David, W.S., Mahdavi, Z., Nance, M., Khan, M., *Hyperlipidemia and neuropathy*. Electromyography and Clinical Neurophysiology, 1999. **39**(4): p. 227-230.
190. Gross, R.W., *The evolution of lipidomics through space and time*. Biochim Biophys Acta Mol Cell Biol Lipids, 2017. **1862**(8): p. 731-739.
191. Spener F., L.M., *What is Lipidomics?* European Journal of Lipid Science and Technology, 2003. **105**: p. 481-482.
192. Vance, J.E., *Phospholipid synthesis and transport in mammalian cells*. Traffic, 2015. **16**: p. 1-18.
193. van der Veen, J.N., et al., *The critical role of phosphatidylcholine and phosphatidylethanolamine metabolism in health and disease*. Biochim Biophys Acta Biomembr, 2017. **1859**(9 Pt B): p. 1558-1572.
194. Cole, L.K. and D.E. Vance, *A role for Sp1 in transcriptional regulation of phosphatidylethanolamine N-methyltransferase in liver and 3T3-L1 adipocytes*. J Biol Chem, 2010. **285**(16): p. 11880-91.
195. Furse, S. and A.I. de Kroon, *Phosphatidylcholine's functions beyond that of a membrane brick*. Mol Membr Biol, 2015. **32**(4): p. 117-9.
196. Shimano, H. and R. Sato, *SREBP-regulated lipid metabolism: convergent physiology - divergent pathophysiology*. Nat Rev Endocrinol, 2017. **13**(12): p. 710-730.
197. Chakravarthy, M.V., et al., *Identification of a physiologically relevant endogenous ligand for PPARalpha in liver*. Cell, 2009. **138**(3): p. 476-88.
198. Treede, I., et al., *Anti-inflammatory effects of phosphatidylcholine*. J Biol Chem, 2007. **282**(37): p. 27155-64.
199. Burke, J.E. and E.A. Dennis, *Phospholipase A2 structure/function, mechanism, and signaling*. J Lipid Res, 2009. **50 Suppl**: p. S237-42.
200. Tracey, T.J., et al., *Neuronal Lipid Metabolism: Multiple Pathways Driving Functional Outcomes in Health and Disease*. Front Mol Neurosci, 2018. **11**: p. 10.
201. Xu, D., et al., *Increased arachidonic acid-containing phosphatidylcholine is associated with reactive microglia and astrocytes in the spinal cord after peripheral nerve injury*. Sci Rep, 2016. **6**: p. 26427.
202. Yoshiyama, M., Nezu, F.M., Yokoyama, O., De Groat, W.C., Chancellor, M., *Changes in micturition after spinal cord injury in conscious rats*. Urology, 1999. **54**(5): p. 929-933.
203. Yoshimura, N., Chancellor, M.B., *Neurophysiology of Lower Urinary Tract Function and Dysfunction*. Reviews in Urology, 2003. **5**(8).
204. Rao, S.S.C., *Pathophysiology of Adult Fecal Incontinence*. Gastroenterology, 2004. **126**: p. 14-22.
205. Carlucci, L., et al., *Functional variability of sacral roots in bladder control*. J Neurosurg Spine, 2014. **21**(6): p. 961-5.
206. Previnaire, J.G., *The importance of the bulbocavernosus reflex*. Spinal Cord Ser Cases, 2018. **4**: p. 2.

207. Wester, C., et al., *Validation of the clinical bulbocavernosus reflex*. *NeuroUrol Urodyn*, 2003. **22**(6): p. 589-91; discussion 591-2.
208. Pang, D., *Surgical management of complex spinal cord lipomas: how, why, and when to operate. A review*. *J Neurosurg Pediatr*, 2019. **23**(5): p. 537-556.
209. Walsh, P., N. Kane, and S. Butler, *The clinical role of evoked potentials*. *J Neurol Neurosurg Psychiatry*, 2005. **76 Suppl 2**: p. ii16-22.
210. Yerkes, E.B., et al., *Lipomyelomeningocele for the urologist: Should we view it the same as myelomeningocele?* *J Pediatr Urol*, 2017. **13**(4): p. 371 e1-371 e8.
211. Strimbu, K. and J.A. Tavel, *What are biomarkers?* *Current Opinion in HIV and AIDS*, 2010. **5**(6): p. 463-466.
212. Walker, A.L., S.Z. Imam, and R.A. Roberts, *Drug discovery and development: Biomarkers of neurotoxicity and neurodegeneration*. *Exp Biol Med* (Maywood), 2018. **243**(13): p. 1037-1045.
213. Amur, S., LaVange, L., Zinch, I., Buckman-Garner, S., Woodcock, J., *Biomarker Qualification: Toward a Multiple Stakeholder Framework for Biomarker Development, Regulatory Acceptance and Utilization*. *Clinical Pharmacology and Therapeutics*, 2015. **98**: p. 34-47.
214. Naylor, S., *Biomarkers current perspectives and future prospects*. *Expert Rev Mol Diagn*, 2003. **3**(5): p. 525-529.
215. Selleck, M.J., M. Senthil, and N.R. Wall, *Making Meaningful Clinical Use of Biomarkers*. *Biomark Insights*, 2017. **12**: p. 1177271917715236.
216. Bligh, E.G., Dyer, W.J., *A rapid method of total lipid extraction and purification*. *Can J Biochem Physiol*, 1959. **37**(8): p. 911-7.
217. O'Connor, A., et al., *LipidFinder: A computational workflow for discovery of lipids identifies eicosanoid-phosphoinositides in platelets*. *JCI Insight*, 2017. **2**(7): p. e91634.
218. Murray, K.K., et al., *Definitions of terms relating to mass spectrometry (IUPAC Recommendations 2013)*. *Pure and Applied Chemistry*, 2013. **85**(7): p. 1515-1609.
219. Todd, J.F.J., *Recommendations for nomenclature and symbolism for mass spectrometry*. *International Journal of Mass Spectrometry and Ion Processes*, 1995. **142**: p. 209-240.
220. Fahy, E., et al., *LipidFinder on LIPID MAPS: peak filtering, MS searching and statistical analysis for lipidomics*. *Bioinformatics*, 2019. **35**(4): p. 685-687.
221. Lydic, T.A., et al., *Complementary precursor ion and neutral loss scan mode tandem mass spectrometry for the analysis of glycerophosphatidylethanolamine lipids from whole rat retina*. *Anal Bioanal Chem*, 2009. **394**(1): p. 267-75.
222. Zhao, Z. and Y. Xu, *An extremely simple method for extraction of lysophospholipids and phospholipids from blood samples*. *J Lipid Res*, 2010. **51**(3): p. 652-9.
223. Chang, S.-J., et al., *Age- and gender-specific nomograms for single and dual post-void residual urine in healthy children*. *Neurourology and Urodynamics*, 2013. **32**(7): p. 1014-1018.
224. Park, J.H. and S.J. Hyun, *Intraoperative neurophysiological monitoring in spinal surgery*. *World J Clin Cases*, 2015. **3**(9): p. 765-73.
225. Legatt, A.D., Emerson, R.G., Epstein, C.M., MacDonald, D.B., Deletis, V., Bravo, R.J., Lopez, J.R., *ACNS Guideline: Transcranial Electrical Stimulation Motor Evoked Potential Monitoring*. *J Clin Neurophysiol*, 2016. **33**: p. 42-50.

226. Ng, P.C., *SIFT: predicting amino acid changes that affect protein function*. Nucleic Acids Research, 2003. **31**(13): p. 3812-3814.
227. Adzhubei, I., D.M. Jordan, and S.R. Sunyaev, *Predicting functional effect of human missense mutations using PolyPhen-2*. Curr Protoc Hum Genet, 2013. **Chapter 7**: p. Unit7 20.
228. Kircher, M., et al., *A general framework for estimating the relative pathogenicity of human genetic variants*. Nat Genet, 2014. **46**(3): p. 310-5.
229. Seyer, A., et al., *Annotation of the human cerebrospinal fluid lipidome using high resolution mass spectrometry and a dedicated data processing workflow*. Metabolomics, 2016. **12**: p. 91.
230. Del Bas, J.M., et al., *Impairment of lysophospholipid metabolism in obesity: altered plasma profile and desensitization to the modulatory properties of n-3 polyunsaturated fatty acids in a randomized controlled trial*. Am J Clin Nutr, 2016. **104**(2): p. 266-79.
231. Jende, J.M.E., et al., *Association of Serum Cholesterol Levels With Peripheral Nerve Damage in Patients With Type 2 Diabetes*. JAMA Netw Open, 2019. **2**(5): p. e194798.
232. Fonteh, A.N., et al., *Alterations in cerebrospinal fluid glycerophospholipids and phospholipase A2 activity in Alzheimer's disease*. J Lipid Res, 2013. **54**(10): p. 2884-97.
233. Yea, K., et al., *Lysophosphatidylcholine activates adipocyte glucose uptake and lowers blood glucose levels in murine models of diabetes*. J Biol Chem, 2009. **284**(49): p. 33833-40.
234. Niccoli, T., et al., *Increased Glucose Transport into Neurons Rescues Abeta Toxicity in Drosophila*. Curr Biol, 2016. **26**(17): p. 2291-300.
235. Leslie, C.C., Gelb, M.H., *Assaying Phospholipase A2 Activity*. Signal Transduction Protocols, 2004: p. 229-242.
236. Freigang, S., *The regulation of inflammation by oxidized phospholipids*. Eur J Immunol, 2016. **46**(8): p. 1818-25.
237. Granata, G., Padua, L., De Franco, P., Coraci, D., Rossi, V., *Electrophysiological study of the bulbocavernosus reflex: normative data*. Functional Neurology, 2013. **28**(4): p. 293-295.
238. Podnar, S., *Sphincter electromyography and the penilo-cavernosus reflex: are both necessary?* Neurourol Urodyn, 2008. **27**(8): p. 813-8.
239. Cha, S., et al., *Predictive value of intraoperative bulbocavernosus reflex during untethering surgery for post-operative voiding function*. Clin Neurophysiol, 2018. **129**(12): p. 2594-2601.
240. Kothbauer, K.F., Novak, K., *Intraoperative monitoring for tethered cord surgery: an update*. Neurosurg Focus, 2004. **16**(2).
241. Kunnen, S. and M. Van Eck, *Lecithin:cholesterol acyltransferase: old friend or foe in atherosclerosis?* J Lipid Res, 2012. **53**(9): p. 1783-99.
242. Ishii, I., et al., *Lysophospholipid receptors: signaling and biology*. Annu Rev Biochem, 2004. **73**: p. 321-54.
243. Sugasini, D., Yalagala, P.C.R., Goggin, A., Tai, L.M., Subbaiah, P.V., *Enrichment of brain docosahexaenoic acid (DHA) is highly dependent upon the molecular carrier of dietary DHA: lysophosphatidylcholine is more efficient than either phosphatidylcholine or triacylglycerol*. Journal of Nutritional Biochemistry, 2019. **74**.

244. Lagarde, M., Bernoud, N., Brossard, N., Lemaitre-Delauney, D., Thies, F., Croset, M., Lecerf, J., *Lysophosphatidylcholine as a Preferred Carrier Form of Docosahexaenoic Acid of the Brain*. Journal of Molecular Neuroscience, 2001. **16**.
245. Wishart, D.S., et al., *HMDB: a knowledgebase for the human metabolome*. Nucleic Acids Res, 2009. **37**(Database issue): p. D603-10.
246. Mandal, R., Guo, A.C., Chaudhary, K.K., Liu, P., Yallou, F.S., Dong, E., Aziat, F., Wishart, D.S., *Multi-platform characterization of the human cerebrospinal fluid metabolome: a comprehensive and quantitative update*. Genome Medicine, 2012. **4**.
247. Herberth, G., et al., *Endogenous metabolites and inflammasome activity in early childhood and links to respiratory diseases*. J Allergy Clin Immunol, 2015. **136**(2): p. 495-7.
248. Bahado-Singh, R.O., et al., *Metabolomic prediction of fetal congenital heart defect in the first trimester*. Am J Obstet Gynecol, 2014. **211**(3): p. 240 e1-240 e14.
249. Cho, K., et al., *Combined untargeted and targeted metabolomic profiling reveals urinary biomarkers for discriminating obese from normal-weight adolescents*. Pediatr Obes, 2017. **12**(2): p. 93-101.
250. Oresic, M., et al., *Phospholipids and insulin resistance in psychosis: a lipidomics study of twin pairs discordant for schizophrenia*. Genome Med, 2012. **4**(1): p. 1.
251. Morita, Y., Kurano, M., Sakai, E., Nishikawa, M., Sawabe, M., Aoki, J., Yatomi, Y., *Evaluation of Lysophospholipid Measurement in Cerebrospinal Fluid Samples using Liquid Chromatography-Tandem Mass Spectrometry*. Lipids, 2019. **54**(8): p. 487-500.
252. Trabado, S., et al., *The human plasma-metabolome: Reference values in 800 French healthy volunteers; impact of cholesterol, gender and age*. PLoS One, 2017. **12**(3): p. e0173615.
253. Bouatra, S., et al., *The human urine metabolome*. PLoS One, 2013. **8**(9): p. e73076.
254. Wahl, S., et al., *Childhood obesity is associated with changes in the serum metabolite profile*. Obes Facts, 2012. **5**(5): p. 660-70.
255. Jiang, C., et al., *HIF-1A and C/EBPs transcriptionally regulate adipogenic differentiation of bone marrow-derived MSCs in hypoxia*. Stem Cell Res Ther, 2015. **6**: p. 21.
256. Fujita, K., Ogawa, R., Ito, K., *CHD7, Oct3/4, Sox2, and Nanog control FoxD3 expression during mouse neural crest - derived stem cell formation*. The FEBS Journal, 2016. **283**(20): p. 3791-3806.
257. Roberts, N.A., et al., *Lrig2 and Hpse2, mutated in urofacial syndrome, pattern nerves in the urinary bladder*. Kidney Int, 2019. **95**(5): p. 1138-1152.
258. Stuart, H.M., et al., *LRIG2 mutations cause urofacial syndrome*. Am J Hum Genet, 2013. **92**(2): p. 259-64.
259. Wang, B., et al., *Downregulation of LRIG2 expression by RNA interference inhibits glioblastoma cell (GL15) growth, causes cell cycle redistribution, increases cell apoptosis and enhances cell adhesion and invasion in vitro*. Cancer Biol Ther, 2009. **8**(11): p. 1018-23.

260. Forsberg, M., et al., *Undersulfation of heparan sulfate restricts differentiation potential of mouse embryonic stem cells*. J Biol Chem, 2012. **287**(14): p. 10853-62.
261. Pallerla, S.R., et al., *Heparan sulfate Ndst1 gene function variably regulates multiple signaling pathways during mouse development*. Dev Dyn, 2007. **236**(2): p. 556-63.
262. Kim, A., et al., *Integrated clinical and omics approach to rare diseases: novel genes and oligogenic inheritance in holoprosencephaly*. Brain, 2019. **142**(1): p. 35-49.
263. Reuter, M.S., et al., *NDST1 missense mutations in autosomal recessive intellectual disability*. Am J Med Genet A, 2014. **164A**(11): p. 2753-63.
264. Pan, Y., et al., *Heparan sulfate expression in the neural crest is essential for mouse cardiogenesis*. Matrix Biol, 2014. **35**: p. 253-65.
265. Filipek-Gorniok, B., et al., *The NDST gene family in zebrafish: role of NDST1B in pharyngeal arch formation*. PLoS One, 2015. **10**(3): p. e0119040.
266. Tillander, V., et al., *Acyl-CoA thioesterase 9 (ACOT9) in mouse may provide a novel link between fatty acid and amino acid metabolism in mitochondria*. Cell Mol Life Sci, 2014. **71**(5): p. 933-48.
267. Nandadasa, S., et al., *Secreted metalloproteases ADAMTS9 and ADAMTS20 have a non-canonical role in ciliary vesicle growth during ciliogenesis*. Nat Commun, 2019. **10**(1): p. 953.
268. Somerville, R.P., et al., *Characterization of ADAMTS-9 and ADAMTS-20 as a distinct ADAMTS subfamily related to Caenorhabditis elegans GON-1*. J Biol Chem, 2003. **278**(11): p. 9503-13.
269. Rao, C., et al., *A defect in a novel ADAMTS family member is the cause of the belted white-spotting mutation*. Development, 2003. **130**(19): p. 4665-72.
270. Guo, M., et al., *Characterization of Rabbit Nucleotide-Binding Oligomerization Domain 1 (NOD1) and the Role of NOD1 Signaling Pathway during Bacterial Infection*. Front Immunol, 2017. **8**: p. 1278.
271. Ussar S., L.K.Y., Dankel S.M., Boucher J., Haering M-F., Kleinridders A., Thomou T., Xue R., Macotela Y., Cypess A.M., Tseng Y-H., Mellgren G., Kahn C.R., *ASC-1, PAT2, and P2RX5 are cell surface markers for white, beige, and brown adipocytes*. Science Translational Medicine, 2014. **6**(247).
272. Chen, Z., et al., *Structure, tissue expression pattern, and function of the amino acid transporter rat PAT2*. Biochemical and Biophysical Research Communications, 2003. **304**(4): p. 747-754.
273. Bermingham, J.R., Jr. and J. Pennington, *Organization and expression of the SLC36 cluster of amino acid transporter genes*. Mamm Genome, 2004. **15**(2): p. 114-25.
274. Finsterer, J., *Congenital myasthenic syndromes*. Orphanet J Rare Dis, 2019. **14**(1): p. 57.
275. Engel, A.G., *Genetic basis and phenotypic features of congenital myasthenic syndromes*. Handb Clin Neurol, 2018. **148**: p. 565-589.
276. Yampolsky, P., et al., *AChR channel conversion and AChR-adjusted neuronal survival during embryonic development*. Mol Cell Neurosci, 2008. **37**(3): p. 634-45.
277. Christianson, J.C., et al., *Defining human ERAD networks through an integrative mapping strategy*. Nat Cell Biol, 2011. **14**(1): p. 93-105.

278. Dorrnsoro, A., et al., *Identification of the NF-kappaB inhibitor A20 as a key regulator for human adipogenesis*. Cell Death Dis, 2013. **4**: p. e972.
279. Oren, M.S., et al., *Postnatal diagnosis of de novo complex der(8) in a boy with prenatal diagnosis of recombinant chromosome 8 syndrome*. Clin Case Rep, 2019. **7**(5): p. 898-902.
280. di Ronza, A., et al., *CLN8 is an endoplasmic reticulum cargo receptor that regulates lysosome biogenesis*. Nat Cell Biol, 2018. **20**(12): p. 1370-1377.
281. Lonka, L., Kyttala, A., Ranta, S., Jalanko, A., Lehesjok, A-E., *The neuronal ceroid lipofuscinosis CLN8 membrane protein is a resident of the endoplasmic reticulum*. Human Molecular Genetics, 2000. **9**(11): p. 1691-1697.
282. Duan, Y., et al., *VRTN is Required for the Development of Thoracic Vertebrae in Mammals*. Int J Biol Sci, 2018. **14**(6): p. 667-681.
283. Nazarko, O., et al., *A Comprehensive Mutagenesis Screen of the Adhesion GPCR Latrophilin-1/ADGRL1*. iScience, 2018. **3**: p. 264-278.
284. Yang, H.-J., et al., *Secondary neurulation of human embryos: morphological changes and the expression of neuronal antigens*. Child's Nervous System, 2013. **30**(1): p. 73-82.
285. Toulza, E., et al., *Large-scale identification of human genes implicated in epidermal barrier function*. Genome Biol, 2007. **8**(6): p. R107.
286. Wang, F., et al., *Dominant negative FADD dissipates the proapoptotic signalosome of the unfolded protein response in diabetic embryopathy*. Am J Physiol Endocrinol Metab, 2015. **309**(10): p. E861-73.
287. Kato M., K.M., *AP1- and NF-KB-binding sites conserved among mammalian WNT10B orthologs elucidate the TNFa-WNT10B signaling loop implicated in carcinogenesis and adipogenesis*. International Journal of Molecular Medicine, 2007. **19**: p. 699-703.
288. Geering, K., *Function of FXYP proteins, regulators of Na, K-ATPase*. J Bioenerg Biomembr, 2005. **37**(6): p. 387-92.
289. Wang, M.K., et al., *Different roles of TGF-beta in the multi-lineage differentiation of stem cells*. World J Stem Cells, 2012. **4**(5): p. 28-34.
290. Mayanil, C.S., et al., *Regulation of murine TGFbeta2 by Pax3 during early embryonic development*. J Biol Chem, 2006. **281**(34): p. 24544-52.
291. Schiavinato, A., et al., *EMILIN-3, peculiar member of elastin microfibril interface-located protein (EMILIN) family, has distinct expression pattern, forms oligomeric assemblies, and serves as transforming growth factor beta (TGF-beta) antagonist*. J Biol Chem, 2012. **287**(14): p. 11498-515.
292. Vitale P., B.P., Volpin D., Bonaldo P., Bressan G.M., *Mechanisms of transcriptional activation of the col6a1 gene during Schwann cell differentiation*. Mechanisms of Development, 2001. **102**: p. 145-156.
293. Chang, Y.C., et al., *Genetic variation in the carbonyl reductase 3 gene confers risk of type 2 diabetes and insulin resistance: a potential regulator of adipogenesis*. J Mol Med (Berl), 2012. **90**(7): p. 847-58.
294. Heier, C., et al., *The phospholipase PNPLA7 functions as a lysophosphatidylcholine hydrolase and interacts with lipid droplets through its catalytic domain*. J Biol Chem, 2017. **292**(46): p. 19087-19098.
295. Kienesberger, P.C., et al., *Identification of an insulin-regulated lysophospholipase with homology to neuropathy target esterase*. J Biol Chem, 2008. **283**(9): p. 5908-17.

296. Jung, H., Kim, W.K., Kim, D.H., Cho, Y.S., Park, S.G., Park, B.C., Lim, H.M., Bae, K-H., Lee, S.C., *Involvement of PTP-RQ in differentiation during adipogenesis of human mesenchymal stem cells*. Biochemical and Biophysical Research Communications, 2009. **383**(2): p. 252-257.
297. Xie, Z., et al., *Smad6 promotes neuronal differentiation in the intermediate zone of the dorsal neural tube by inhibition of the Wnt/beta-catenin pathway*. Proc Natl Acad Sci U S A, 2011. **108**(29): p. 12119-24.
298. Zhang, R., et al., *A unique methylation pattern co-segregates with neural tube defect statuses in Han Chinese pedigrees*. Neurol Sci, 2017. **38**(12): p. 2153-2164.
299. Miyazawa, K. and K. Miyazono, *Regulation of TGF-beta Family Signaling by Inhibitory Smads*. Cold Spring Harb Perspect Biol, 2017. **9**(3).
300. Zarelli, V.E. and I.B. Dawid, *Inhibition of neural crest formation by Kctd15 involves regulation of transcription factor AP-2*. Proc Natl Acad Sci U S A, 2013. **110**(8): p. 2870-5.
301. Smaldone, G., et al., *The essential player in adipogenesis GRP78 is a novel KCTD15 interactor*. Int J Biol Macromol, 2018. **115**: p. 469-475.
302. Shen, F., Wu, M., Ross, J.F., Miller D., Ratnam, M., *Folate receptor type gamma is primarily a secretory protein due to lack of an efficient signal for glycosylphosphatidylinositol modification: protein characterization and cell type specificity*. Biochemistry, 1995. **34**(16): p. 5660-5.
303. Findley, T.O., et al., *Mutations in folate transporter genes and risk for human myelomeningocele*. Am J Med Genet A, 2017. **173**(11): p. 2973-2984.
304. Le Bacquer, O., et al., *Elevated sensitivity to diet-induced obesity and insulin resistance in mice lacking 4E-BP1 and 4E-BP2*. J Clin Invest, 2007. **117**(2): p. 387-96.
305. Fei, Z., et al., *Ankrd26 gene disruption enhances adipogenesis of mouse embryonic fibroblasts*. J Biol Chem, 2011. **286**(31): p. 27761-8.
306. Xie, Z., et al., *Differential Expression Profiles of Long Noncoding RNA and mRNA of Osteogenically Differentiated Mesenchymal Stem Cells in Ankylosing Spondylitis*. J Rheumatol, 2016. **43**(8): p. 1523-31.
307. Kato, M., Wang, H., Bernfield, M., Gallagher, J.T., Turnbull, J.E. , *Cell surface syndecan-1 on distinct cell types differs in fine structure and ligand binding of its heparan sulfate chains*. J Biol Chem, 1994. **269**(29): p. 18881-90.
308. Sarrazin, S., W.C. Lamanna, and J.D. Esko, *Heparan sulfate proteoglycans*. Cold Spring Harb Perspect Biol, 2011. **3**(7).
309. Bishop, J.R., M. Schuksz, and J.D. Esko, *Heparan sulphate proteoglycans fine-tune mammalian physiology*. Nature, 2007. **446**(7139): p. 1030-7.
310. Kakuta, Y., Sueyoshi T., Negishi, M., Pedersen, L.C., *Crystal Structure of the Sulfotransferase Domain of Human Heparan Sulfate N-Deacetylase/N-Sulfotransferase*. Journal of Biological Chemistry, 1998. **274**(16): p. 10673-10676.
311. Bengtsson, J., Eriksson, I., Kjellen, L., *Distant Effects on Heparan Sulfate Structure by Different Active Site Mutations in NDST-1*. Biochemistry, 2003. **42**: p. 2110-2115.
312. Kusche-Gullberg, M., Eriksson, I., Pikas, D.M., Kjellen, L., *Identification and Expression in Mouse of Two Heparan Sulfate Glucosaminyl N-Deacetylase/N-Sulfotransferase Genes*. Journal of Biological Chemistry, 1998. **273**(19): p. 11902-11907.



313. Ringvall, M., et al., *Defective heparan sulfate biosynthesis and neonatal lethality in mice lacking N-deacetylase/N-sulfotransferase-1*. J Biol Chem, 2000. **275**(34): p. 25926-30.
314. Pan, Y., et al., *Heparan sulfate biosynthetic gene Ndst1 is required for FGF signaling in early lens development*. Development, 2006. **133**(24): p. 4933-44.
315. Lanner, F., et al., *Heparan sulfation-dependent fibroblast growth factor signaling maintains embryonic stem cells primed for differentiation in a heterogeneous state*. Stem Cells, 2010. **28**(2): p. 191-200.
316. Armstrong, L., Tarailo-Graovac, M., Sinclair, G., Seath, K.J., Wasserman, W.W., Ross, C.J., van Karnebeek, C.D.M., *A girl with developmental delay, ataxia, cranial nerve palsies, severe respiratory problems in infancy - Expanding NDST1 syndrome*. American Journal of Medical Genetics Part A, 2017. **173**(3): p. 712-715.
317. Mead, T.J. and S.S. Apte, *ADAMTS proteins in human disorders*. Matrix Biol, 2018. **71-72**: p. 225-239.
318. Llamazares, M., et al., *Identification and characterization of ADAMTS-20 defines a novel subfamily of metalloproteinases-disintegrins with multiple thrombospondin-1 repeats and a unique GON domain*. J Biol Chem, 2003. **278**(15): p. 13382-9.
319. Silver, D.L., et al., *The secreted metalloprotease ADAMTS20 is required for melanoblast survival*. PLoS Genet, 2008. **4**(2): p. e1000003.
320. Holdener, B.C., et al., *ADAMTS9 and ADAMTS20 are differentially affected by loss of B3GLCT in a mouse model of Peters Plus Syndrome*. Hum Mol Genet, 2019.
321. Faletra, F., et al., *Vertebral defects in patients with Peters plus syndrome and mutations in B3GALTL*. Ophthalmic Genet, 2011. **32**(4): p. 256-8.
322. Song, H.Y., Rothe, M., Goeddel, D.V., *The tumour necrosis factor-inducible zinc finger protein A20 interacts with TRAF1/TRAF2 and inhibits NF-kappaB activation*. Proc Natl Acad Sci U S A, 1996. **93**(13): p. 6721-5.
323. Petersen, S.L., et al., *TRAF2 is a biologically important necroptosis suppressor*. Cell Death Differ, 2015. **22**(11): p. 1846-57.
324. Xu, G., et al., *Up-regulation of TRAF2 Suppresses Neuronal Apoptosis after Rat Spinal Cord Injury*. Tissue Cell, 2017. **49**(5): p. 589-596.
325. Partanen, M., Motoyama, J., Chi-Chung, H., *Developmentally regulated expression of the transcriptional cofactors/histone acetyltransferases CBP and p300 during mouse embryogenesis*. Int J Dev Biol, 1999. **43**: p. 487-494.
326. Boot, M.V., et al., *Benign and malignant tumors in Rubinstein-Taybi syndrome*. Am J Med Genet A, 2018. **176**(3): p. 597-608.
327. Tanaka, Y., Naruse, I., Hongo T., Xu, M-J., Nakahata, T., Maekawa, T., Ishii, S. , *Extensive brain haemorrhage and embryonic lethality in a mouse null mutant of CREB-binding protein*. Mechanisms of Development, 95. **95**: p. 133-145.
328. Lu, W., et al., *Genes encoding critical transcriptional activators for murine neural tube development and human spina bifida: a case-control study*. BMC Med Genet, 2010. **11**: p. 141.
329. Takahashi, N., et al., *Overexpression and ribozyme-mediated targeting of transcriptional coactivators CREB-binding protein and p300 revealed their indispensable roles in adipocyte differentiation through the regulation of peroxisome proliferator-activated receptor gamma*. J Biol Chem, 2002. **277**(19): p. 16906-12.

330. MacFarlane, A.J., et al., *Mthfd1 is an essential gene in mice and alters biomarkers of impaired one-carbon metabolism*. J Biol Chem, 2009. **284**(3): p. 1533-9.
331. Zhu, H., et al., *Gene variants in the folate-mediated one-carbon metabolism (FOCM) pathway as risk factors for conotruncal heart defects*. Am J Med Genet A, 2012. **158A**(5): p. 1124-34.
332. Cai, C.Q., et al., *Association of neural tube defects with maternal alterations and genetic polymorphisms in one-carbon metabolic pathway*. Ital J Pediatr, 2019. **45**(1): p. 37.
333. Mills, J.L., et al., *Folate-related gene polymorphisms as risk factors for cleft lip and cleft palate*. Birth Defects Res A Clin Mol Teratol, 2008. **82**(9): p. 636-43.
334. Gingras, A.C., et al., *Hierarchical phosphorylation of the translation inhibitor 4E-BP1*. Genes Dev, 2001. **15**(21): p. 2852-64.
335. Stogios, P.J., et al., *Sequence and structural analysis of BTB domain proteins*. Genome Biol, 2005. **6**(10): p. R82.
336. Dutta, S. and I.B. Dawid, *Kctd15 inhibits neural crest formation by attenuating Wnt/beta-catenin signaling output*. Development, 2010. **137**(18): p. 3013-8.
337. Heffer, A., et al., *Generation and characterization of Kctd15 mutations in zebrafish*. PLoS One, 2017. **12**(12): p. e0189162.
338. Takahashi, C., et al., *Identification and characterization of Xenopus kctd15, an ectodermal gene repressed by the FGF pathway*. Int J Dev Biol, 2012. **56**(5): p. 393-402.
339. Zarelli, V.E. and I.B. Dawid, *The BTB-containing protein Kctd15 is SUMOylated in vivo*. PLoS One, 2013. **8**(9): p. e75016.
340. Long, K.R. and W.B. Huttner, *How the extracellular matrix shapes neural development*. Open Biol, 2019. **9**(1): p. 180216.
341. Giros, A., et al., *Perlecan controls neurogenesis in the developing telencephalon*. BMC Dev Biol, 2007. **7**: p. 29.
342. Park, Y., Rangel, C., Reynolds, M. M., Caldwell, M. C., Johns, M., Nayak, M., Welsh, J.R., McDermott, S., Datta, S., *Drosophila Perlecan modulates FGF Hedgehog signals to activate neural stem cell division*. Developmental Biology, 2003. **253**: p. 247-257.
343. Jen, Y.H., M. Musacchio, and A.D. Lander, *Glypican-1 controls brain size through regulation of fibroblast growth factor signaling in early neurogenesis*. Neural Dev, 2009. **4**: p. 33.
344. Flanagan, L.A., et al., *Regulation of human neural precursor cells by laminin and integrins*. J Neurosci Res, 2006. **83**(5): p. 845-56.
345. Hall, P.E., et al., *Laminin enhances the growth of human neural stem cells in defined culture media*. BMC Neurosci, 2008. **9**: p. 71.
346. Ma, W., et al., *Cell-extracellular matrix interactions regulate neural differentiation of human embryonic stem cells*. BMC Dev Biol, 2008. **8**: p. 90.
347. Copp, A.J., et al., *Regional differences in the expression of laminin isoforms during mouse neural tube development*. Matrix Biol, 2011. **30**(4): p. 301-9.
348. Araya, C., C. Carmona-Fontaine, and J.D. Clarke, *Extracellular matrix couples the convergence movements of mesoderm and neural plate during the early stages of neurulation*. Dev Dyn, 2016. **245**(5): p. 580-9.
349. Tsuda, S., et al., *FAK-mediated extracellular signals are essential for interkinetic nuclear migration and planar divisions in the neuroepithelium*. Journal of Cell Science, 2010. **123**(3): p. 484-496.

350. Campos, L.S., et al., *Beta1 integrins activate a MAPK signalling pathway in neural stem cells that contributes to their maintenance*. *Development*, 2004. **131**(14): p. 3433-44.
351. Leone, D.P., et al., *Regulation of neural progenitor proliferation and survival by beta1 integrins*. *J Cell Sci*, 2005. **118**(Pt 12): p. 2589-99.
352. Iwashita, M., et al., *Systematic profiling of spatiotemporal tissue and cellular stiffness in the developing brain*. *Development*, 2014. **141**(19): p. 3793-8.
353. Solanki, A., et al., *Controlling differentiation of neural stem cells using extracellular matrix protein patterns*. *Small*, 2010. **6**(22): p. 2509-13.
354. Fenn, J.B., Mann, M., Meng, C.K., Wong, S.F., Whitehouse, C.M., *Electrospray Ionization for Mass Spectrometry of Large Biomolecules*. *Science*, 1989. **246**: p. 64-73.
355. Cajka, T., Fiehn, O., *LC-MS-Based Lipidomics and Automated Identification of Lipids Using the LipidBlast In-Silico MS/MS Library*. In: Bhattacharya S. (eds) *Lipidomics*. *Methods Mol Biol*, 2017. **1609**: p. 149-170.
356. Kind, T., et al., *LipidBlast in silico tandem mass spectrometry database for lipid identification*. *Nat Methods*, 2013. **10**(8): p. 755-8.
357. Austin, P.C., Steyerberg, E.W., *The number of subjects per variable required in linear regression analyses*. *J Clin Epidemiol*, 2015. **68**(6).
358. Begum, H., et al., *Discovering and validating between-subject variations in plasma lipids in healthy subjects*. *Sci Rep*, 2016. **6**: p. 19139.
359. Zivkovic, A.M., et al., *Effects of sample handling and storage on quantitative lipid analysis in human serum*. *Metabolomics*, 2009. **5**(4): p. 507-516.
360. Ulmer, C.Z., et al., *Optimization of Folch, Bligh-Dyer, and Matyash sample-to-extraction solvent ratios for human plasma-based lipidomics studies*. *Anal Chim Acta*, 2018. **1037**: p. 351-357.
361. Ioannidis, J.P.A. and P.M.M. Bossuyt, *Waste, Leaks, and Failures in the Biomarker Pipeline*. *Clin Chem*, 2017. **63**(5): p. 963-972.
362. Rentzsch, P., et al., *CADD: predicting the deleteriousness of variants throughout the human genome*. *Nucleic Acids Res*, 2019. **47**(D1): p. D886-D894.
363. Ledergerber, C. and C. Dessimoz, *Base-calling for next-generation sequencing platforms*. *Brief Bioinform*, 2011. **12**(5): p. 489-97.
364. Whiteford, N., et al., *Swift: primary data analysis for the Illumina Solexa sequencing platform*. *Bioinformatics*, 2009. **25**(17): p. 2194-9.
365. Erlich, Y., et al., *Alta-Cyclic: a self-optimizing base caller for next-generation sequencing*. *Nat Methods*, 2008. **5**(8): p. 679-82.
366. Rougemont, J., et al., *Probabilistic base calling of Solexa sequencing data*. *BMC Bioinformatics*, 2008. **9**: p. 431.
367. Dohm, J.C., et al., *Substantial biases in ultra-short read data sets from high-throughput DNA sequencing*. *Nucleic Acids Res*, 2008. **36**(16): p. e105.
368. Shendure, J. and H. Ji, *Next-generation DNA sequencing*. *Nat Biotechnol*, 2008. **26**(10): p. 1135-45.
369. Lek, M., et al., *Analysis of protein-coding genetic variation in 60,706 humans*. *Nature*, 2016. **536**(7616): p. 285-91.
370. Eilbeck, K., A. Quinlan, and M. Yandell, *Settling the score: variant prioritization and Mendelian disease*. *Nat Rev Genet*, 2017. **18**(10): p. 599-612.
371. Karczewski, K.J., et al., *Variation across 141,456 human exomes and genomes reveals the spectrum of loss-of-function intolerance across human protein-coding genes*. *Broad Institute*, 2019.

372. Niroula, A. and M. Vihinen, *How good are pathogenicity predictors in detecting benign variants?* PLoS Comput Biol, 2019. **15**(2): p. e1006481.
373. Brownstein, C.A., Beggs, A.H., Homer, N., Merriman, B., Yu, T.W., Flannery, K.C., DeChene, E.T., Towne, M.C., *An international effort towards developing standards for best practices in analysis, interpretation and reporting of clinical genome sequencing results in the CLARITY Challenge.* Genome Biol, 2014. **15**(R53).
374. Richards, S., et al., *Standards and guidelines for the interpretation of sequence variants: a joint consensus recommendation of the American College of Medical Genetics and Genomics and the Association for Molecular Pathology.* Genet Med, 2015. **17**(5): p. 405-24.
375. Freund Levi, F., Vedin, I., Cederholm, T., Basun, H., Faxen Irving, G., Eriksson, M., Hjorth, E., Schultzberg, M., Vessby, B., Wahlund, L.O., Salem, N., Palmblad, J. , *Transfer of omega -3 fatty acids across the blood-brain barrier after dietary supplementation with a docosahexaenoic acid-rich omega-3 fatty acid preparation in patients with Alzheimer's disease: the OmegAD study.* J Intern Med, 2014. **275**(4): p. 428-36.
376. Meldrum, S. and K. Simmer, *Docosahexaenoic Acid and Neurodevelopmental Outcomes of Term Infants.* Ann Nutr Metab, 2016. **69 Suppl 1**: p. 22-28.

# Great Ormond Street

## Hospital for Children

NHS Foundation Trust

### Parent information sheet

**Project Title: Developing a biomarker for children with spinal lipoma**

#### **Invitation to take part in a research study**

Dear .....

#### **We are asking the parents of children with spinal lipoma whether they are happy for their child to take part in a research study.**

We are undertaking a research study to find out if there is a laboratory test that can be done to work out which children with spinal lipoma require early surgery. We are asking children who were born with this condition to take part in the study. This information sheet tells you what will happen if you and your child agree to take part. It is entirely up to you to decide if you want to take part and your child's care at the hospital will not be affected if you decide not to be involved.

#### **Why have I been approached?**

Children with spinal lipoma under the care of the hospital will be asked to take part in the study. We are asking your permission for your child to be involved in this study, so please read on to see what is involved.

#### **Who is doing the study?**

I am doing this study as part of a Doctor of Philosophy degree (PhD) at University College, London (UCL). Mr Thompson (your neurosurgeon) and Professor Copp (Professor of Developmental Neurobiology at the Institute of Child Health) will supervise the study.

#### **What's the purpose of the study?**

Spinal lipoma is a rare condition with each paediatric neurosurgical centre treating relatively small numbers of children. We know that urine and bowel function can be affected in some children, and as they grow up some children find it more difficult to join in sports at school or be as active as their friends due to difficulty with mobility or pain. This happens to some but not all children with spinal lipoma.

Current practice is to monitor children with this condition, over months and years, to see if they develop any of the symptoms. If symptoms do arise, surgery is then offered to stop things getting worse. The surgery cannot completely reverse the problem of spinal lipoma.

We could offer to operate on all children with spinal lipoma, even before they develop any symptoms. However, a certain number of children will never develop symptoms and therefore would have undergone unnecessary surgery.

We would like to develop a simple test – either a blood, urine or spinal fluid test – that will help us work out which children are most at risk of deterioration and would therefore benefit from early surgery. If children are negative for this test, we can be confident that delaying or never undertaking surgery will be the right course of action.

#### **What will happen during the study?**

Your child will attend his / her normal outpatient appointments with Mr Thompson and his team. Your child will be examined by Mr Thompson or another doctor as usual.

- At an outpatient appointment, or during pre-assessment for surgery, routine blood and urine tests are taken. We would like to use part of each sample, which is surplus to medical requirements, to analyse in the laboratory. Usually this will not involve any extra needles for your child! In the unlikely situation that we need to collect a further sample we will ask you and your child again if you are happy for this to be done.
- If your child has surgery, then routine spinal fluid samples are taken. We would like to use part of the sample, which is surplus to medical requirements, to analyse in the laboratory.

All samples will be stored and analysed for research at the Institute of Child Health.

### **What will happen to the samples after the study?**

Anonymous samples will be stored at the Institute of Child Health for 5 years. We would like to be able to use these samples in future ethically approved studies. Your child will not be able to be identified for any future studies the samples might be used in.

### **Do you have to take part?**

Neither you nor your child has to take part and if you do participate, you can withdraw from the study at any time should you so choose. A decision not to take part, or to withdraw, will not affect your child's care or the standard of care he / she receives.

### **How will the information be kept?**

- In accordance with the UK's Data Protections Act 1998, data collected regarding you and your child will be kept confidential and secure and used only for the purpose for which it is collected.
- Data will be stored on a computer in the Hospital and also on a computer in the Institute of Child Health. Each computer will be password protected.
- Information obtained will be kept by the Principal Investigator for 6 months after completion of the study after which time it will be deleted / shredded.
- All data are anonymous – each child will be given a study number by the clinical team who collect the samples. The research team will only know these numbers, not your child's name or any other means of personal identification.
- No-one apart from the clinical team and the research team will have access to information about your child.

### **Are there any risks to me or my child and what do I do if I am worried about the study?**

We do not anticipate there will be any risks in taking part in the study. The samples we need will be taken as part of routine collection in the clinic and theatre and so there will be no additional risk associated with this study. In the unlikely situation that we ask to take an extra blood sample, the risks of this are pain and bruising at the site.

### **What are the possible benefits for me and / or my child taking part?**

Taking part will not have any direct benefit to you or your child. However, in the future we hope to be able to help similar families with the data we collect.

### **What happens if I am worried about the study?**

If you have any questions about the study you can contact me as follows, and I will do my best to answer your concerns.

**Contact details:** Victoria Jones; Tel: XXXXXXXXXX

If you remain unhappy with my answer or want to complain formally you can contact the PALS office at Great Ormond Street Hospital.

**Who is supporting the study?**

The study is supported by GOSH Children's Charity, the neurosurgical team at the hospital and my PhD supervisor. All research in the NHS is assessed by an independent group called the Research Ethics Committee. This study has been assessed by NRES Committee West Midlands - Edgbaston who have given it a favourable opinion. Research Ethics Committees are involved to ensure the dignity, wellbeing, safety and rights of both you and your child are maintained throughout the study.

**Payment.**

Neither you nor your child will be paid for taking part in the study.

**What happens now?**

A number of families whose children are under the care of Mr Thompson at the hospital are being sent this information leaflet. If you and your child agree to take part, I will meet you when you come to clinic, to discuss the study further, answer any questions you may have and take consent from you

**Thank you for taking time to read this information sheet.**

Yours sincerely

Victoria Jones (Specialty Registrar, Neurosurgery)

**Centre Number:**

**Study Number:**

**Patient Identification Number for this trial:**

**PARENT CONSENT FORM FOR CHILD**

**Title of Project: Developing a Biomarker for Children with Spinal Lipoma**

**Name of Researcher:**

|   |   |  |
|---|---|--|
| 1 | I confirm that I have read and understand the information sheet provided dated July 2015 (version 2) for the above study. I have had the opportunity to ask questions and have had these answered satisfactorily.           |  |
| 2 | I understand my child's participation is voluntary and he/she is free to withdraw at any time and without providing a reason. I understand my child's medical care will not be affected by this decision.                   |  |
| 3 | <u>I understand</u> the purpose of the study and how much time is required of my child.   |  |
| 4 | <u>I understand</u> that relevant sections of the medical notes and samples or data collected during the study may be looked at by individuals from the Hospital team, and by researchers at the Institute of Child Health. |  |
| 5 | <u>I understand</u> that samples taken as part this study may be kept for future research on spinal lipoma.   |  |
| 6 | I agree to my child taking part in the above study.   |  |

**Please initial each box to indicate agreement**

\_\_\_\_\_  
Full name of Parent

\_\_\_\_\_  
Date

\_\_\_\_\_  
Signature

\_\_\_\_\_  
Full name of Researcher or  
person taking consent

\_\_\_\_\_  
Date

\_\_\_\_\_  
Signature

When completed: 1 for participant; 1 for researcher site file; 1 (original) to be kept in the medical notes



```

library(xcms)
# all samples
setwd("E:/.....")
myClass1 <- "c"
myClass2 <- "sol"
# peak picking using wavelet algorithm for peak detection (centWave)
xset <- xcmsSet (method="centWave",ppm=10, peakwidth=c(10,120), snthresh=5,
prefilter=c(10,20000), integrate=1, mzdif=0.001, fitgauss=FALSE, noise=20000,
scanrange=c(1,11485))
# peak alignment
xset <- group(xset, bw=30, mzwid=0.005, minfrac=0.5, minsamp=1)
# retention time correction
xset <- retcor(xset, method="obiwarp", profStep=0.05, response=20, center=1
,plottype="deviation")
#re-align
xset <- group(xset, bw=3, mzwid=0.005, minfrac=0.5, minsamp=1)
# fill in missing peak data
xset <- fillPeaks(xset)
# output results
reporttab <- diffreport(xset, filebase="Plasma_Vicky_neg")
#####
#repair files before use
require(xcms)
library(xcms)
library(caTools)
AllCDFs<-list.files(recursive=TRUE, pattern="mzxml", ignore.case=TRUE, full.names=TRUE)
checkAllcdfs<-function(Ftype="mzXML", nSlaves=1){
AllCDFs<-list.files(recursive=TRUE, pattern=Ftype, ignore.case=TRUE, full.names=TRUE)
if(nSlaves >1){
if(require(snow)){
cl <- makeCluster(nSlaves, type = "SOCK")
}
clusterEvalQ(cl, library(xcms))
unlist(clusterApply(cl, AllCDFs, checkCDFfile))
stopCluster(cl)
} else{
sapply(AllCDFs, checkCDFfile)
cat("\n")
}
}
checkCDFfile<-function(file, type=".mzXML"){
cat("\n")
cat(paste("Loading File:", file, sep=""))
xr<-xcmsRaw(file, profstep=0)
for(i in 1:length(xr@scanindex)){
scan<-getScan(xr, scan=i)
if(is.unsorted(scan[,"mz"]) == TRUE){
cat(" x ")
newfile<-sub(type, "-Fixed.mzdata", file, ignore.case=TRUE)
write.mzdata(xr, newfile)
file.copy(file, sub(type, ".OLD", file, ignore.case=TRUE))
unlink(file)
rm(list=ls())
gc()
return(1)
}
if(i == length(xr@scanindex)){
cat(" O ")
rm(list=ls())
gc()
}
}

```

```
return(0)
}
}
}
sapply(AIICDFs, checkCDFfile)
```

**Title of project:** Investigation of neural tube defects

### **Explanation**

We would like to invite you to participate in a research project. Before you decide, it is important that you understand why the research is being done and what it will involve. Ask us if there is anything that is not clear or if you would like more information. Take time to decide whether or not you wish to take part. Thank you for reading this.

### **What is the purpose of the study?**

It is not known why some babies are born with birth defects affecting the neural tube (future spine) such as spina bifida. We are researching this problem to help us find out about the cause. This involves the study of both normal and affected individuals. We want to understand why these defects occur so that we can help prevent them from happening in the future.

### **Why have I been chosen?**

Your baby has a birth defect. A small sample of blood (or saliva) for making DNA will be obtained from your child to help us study the genetic basis and inheritance of this defect. We also request a blood or saliva sample from the parent(s).

### **What will happen to the sample?**

The blood or saliva sample will be used to make DNA. The DNA will then be analysed in genetic studies for this project. At the end of this project, the DNA sample will be stored for later use in similar research, which will be dependant on future funding.

### **Do I have to take part?**

It is up to you to decide whether or not to take part. If you do wish to take part you will be given this information sheet to keep. You are still free to withdraw at any time and without giving a reason. This will not in any way affect the standard of care the Patient receives.

### **What will happen to me if I take part?**

If you do agree to take part in this study, treatment will remain exactly the same. Your donated blood sample will be used in a research project. The sample will be anonymous and used in a genetic study designed to determine the underlying cause of birth defects.

### **What are the possible benefits of taking part?**

There is no clinical benefit to the patient from taking part. The information we will obtain from this study may help us to prevent birth defects or improve treatments in the future.

### **What are the possible disadvantages and risks of taking part?**

Apart from the small discomfort associated with taking a blood sample, there are no additional disadvantages or risks attached to this study. Our study is a research project and may not identify the cause of the condition.

### **What if new information becomes available?**

It is possible that information relevant to you or your family could be discovered by this study. You will therefore be given the option on the consent form to say if you would like to be re-contacted via your hospital specialist. This would involve discussion with your hospital specialist and further tests including a new sample for DNA analysis.

### **Will my taking part in this study be kept confidential?**

All information that is collected about you during the course of the research will be kept strictly confidential and anonymous.

### **What will happen to the results of the research study?**

This study will take several years to complete. We anticipate that the results will increase our understanding of birth defects and allow the development of better screening and preventative treatments in the future. The results of this study may be published in the medical and scientific

literature. If the samples remain useful for a similar research project we will retain them in a fully anonymised form but with a link to the type of defect.

**Who is organizing and funding the research?**

This work is funded by a variety of medical charities including the Birth Defects Foundation and SPARKS. No member of staff is being paid to include you in this study.

**Who has reviewed the study?**

This research has been approved by the Great Ormond Street and Institute of Child Health Research Ethics Committee.

**Contact for Further Information**

Further information can be obtained from [REDACTED].

Thank you for taking part in this study. You will be given a copy of the information sheet and a signed consent form to keep.

---

## **Appendix 1A**

### **Neural Tube Defect Research Information Sheet**

Many babies are born with an anomaly, often called a birth defect, and in many cases we have no clear indication what has caused the problem. To be able to provide the most rational care and offer the possibility of prevention in the future, it will be necessary to perform detailed research. We are therefore asking for volunteers to help in this research. We would like to collect a small sample of blood or if possible saliva from the affected child. It would also be of great help if we could also take a similar sample from other relatives such as the mother, father and an unaffected brother or sister too. We will use the sample to make DNA so that we can then investigate genetic factors that we believe will be important. Our research will tell us if there is a link between these factors and the baby's anomaly.

Our research team is currently investigating some of the genetic factors that may cause or predispose to neural tube defects such as spina bifida. The neural tube is the term we use for the future spinal cord and is effectively a duct that relays nerves between different parts of the body to the brain. The neural tube forms very early in the baby's development, between 3 and 4 weeks after conception. The tube forms from a flat plate of cells that roll up like a scroll, joining first in the middle then zippering closed both towards the head and the lower back. Defects occur when the tube is unable to close properly, which in the UK happens in about 1 in every 1000 babies. The severity of the defect is governed by the position e.g. at the top or the bottom, and the degree of closure.

Previous research has shown that in about half of all cases, folic acid added to the diet can be of great benefit to preventing neural tube defects. It is not yet clear how this works or why it is not effective for all babies. Our research is to try to understand what causes these defects and why different babies have different types of neural tube defect. This will allow us to develop genetic tests and to direct efforts at prevention and cure much more effectively. Our research group has already identified several genes that we believe are likely to be the cause of the defect in some patients and they will be studied further. Our ongoing research will also generate new candidate genes to investigate as the work progresses.

Project Title: Investigation of neural tube defects

Researcher: [Redacted]

Please Fax completed form to: [Redacted]

Patient identification No.....

- 1. I have read and understand the attached Information Sheet.
- 2. I have been given the opportunity to ask questions and discuss this study.
- 3. I have received satisfactory answers to all my questions.
- 4. I agree to have a blood/saliva sample taken for DNA extraction.
- 5. I agree to my DNA sample being stored for future analysis.
- 6. I give permission for someone from the research team to look at my medical records to obtain information about this pregnancy and related medical information.
- 7. I would/would not\* like to be contacted if a diagnostic test that may have implications for my family becomes available. I understand that a diagnostic test will require discussion with my doctor and a fresh blood sample. (\*please delete as appropriate).

The study has been explained to me by (Consentor): \_\_\_\_\_

I understand that I am free to withdraw from the study at any time, without having to give a reason for with drawing and without affecting my future medical care.

I agree to take part in this study.

(Print NAME).....

Signed.....Date.....

Relationship e.g. patient/mother/father/brother/sister.....

(Print NAME of CONSENTOR).....

Signed.....Date.....

(PRINT INVESTIGATOR'S NAME).....

Investigator's signature.....Date: .....

Thank you for agreeing to participate in this research

| Patient ID | Diagnosis        | Clinical Status | Motor weakness         | Sensory deficit           | Deformity              | Progression | Urological assessment |
|------------|------------------|-----------------|------------------------|---------------------------|------------------------|-------------|-----------------------|
| 1*         | Dorsal LSL       | Symptomatic     | Mild unilateral        |                           |                        |             | Wetting               |
| 2*         | Transitional LSL | Symptomatic     |                        | Bilateral radicular pain  |                        |             | Wetting               |
| 3**        | Caudal LSL       | Asymptomatic    |                        |                           |                        |             | NAD                   |
| 4**        | Transitional LSL | Asymptomatic    |                        |                           |                        |             | NAD                   |
| 5*         | Transitional LSL | Symptomatic     | Mild bilateral         |                           | Mild bilateral         |             | UTIs                  |
| 6**        | Transitional LSL | Asymptomatic    |                        |                           |                        |             | NAD                   |
| 7          | Transitional LSL | Symptomatic     | Significant unilateral | Unilateral radicular pain |                        | Present     | CIC                   |
| 8**        | Transitional LSL | Asymptomatic    |                        |                           |                        |             | NAD                   |
| 9**        | Transitional LSL | Asymptomatic    |                        |                           |                        |             | NAD                   |
| 11**       | Transitional LSL | Symptomatic     | Mild unilateral        |                           | Significant unilateral | Present     | Wetting               |
| 12**       | Caudal LSL       | Asymptomatic    |                        |                           |                        |             | NAD                   |
| 14**       | Dorsal LSL       | Symptomatic     |                        | Unilateral radicular pain |                        |             | UTIs                  |
| 15**       | Transitional LSL | Symptomatic     | Mild bilateral         |                           | Mild bilateral         |             | UTIs                  |
| 17**       | Transitional LSL | Symptomatic     |                        |                           |                        | Present     | CIC                   |
| 21**       | Transitional LSL | Asymptomatic    |                        |                           |                        |             | NAD                   |
| 23**       | Caudal LSL       | Symptomatic     |                        |                           |                        |             | Wetting               |
| 26**       | Complex LSL      | Symptomatic     |                        |                           |                        |             | CIC                   |
| 27**       | Transitional LSL | Symptomatic     | Mild unilateral        |                           |                        |             | Wetting               |
| 30**       | Complex LSL      | Symptomatic     |                        |                           |                        | Rapid       | CIC                   |
| 33         | Transitional LSL | Symptomatic     |                        |                           |                        |             | Wetting               |
| 35         | Caudal LSL       | Symptomatic     | Mild unilateral        |                           |                        |             | Wetting               |
| 38         | Transitional LSL | Symptomatic     | Mild unilateral        |                           |                        |             | Wetting               |
| 39         | Transitional LSL | Symptomatic     |                        |                           | Mild unilateral        |             | NAD                   |

|    |                  |             |                        |                           |                 |      |
|----|------------------|-------------|------------------------|---------------------------|-----------------|------|
| 40 | Dorsal LSL       | Symptomatic |                        | Unilateral radicular pain |                 | NAD  |
| 41 | Complex LSL      | Symptomatic |                        |                           |                 | NAD  |
| 42 | Transitional LSL | Symptomatic | Significant unilateral | Unilateral radicular pain |                 | NAD  |
| 43 | Transitional LSL | Symptomatic | Mild unilateral        |                           | Mild unilateral | NAD  |
| 44 | Transitional LSL | Symptomatic |                        |                           | Mild unilateral | UTIs |

Clinical assessment of patients. \* denotes those samples used for Lipidomics 1 and 2, \*\* denotes those samples used for Lipidomics 2. All samples used for targeted assay analysis. LSL = lumbosacral lipoma, CP = cerebral palsy, CIC = clean intermittent catheterisation, UTI = urinary tract infection, NAD = no abnormality detected.



|          |              | BCR    |          | Total |
|----------|--------------|--------|----------|-------|
|          |              | Normal | Abnormal |       |
| Symptoms | Asymptomatic | 9      | 0        | 9     |
|          | Symptomatic  | 15     | 7        | 22    |
| Total    |              | 24     | 7        | 31    |

|          |              | Sphincter MEPs |          | Total |
|----------|--------------|----------------|----------|-------|
|          |              | Normal         | Abnormal |       |
| Symptoms | Asymptomatic | 9              | 0        | 9     |
|          | Symptomatic  | 17             | 5        | 22    |
| Total    |              | 26             | 5        | 31    |

|          |              | TcMEPS |          | Total |
|----------|--------------|--------|----------|-------|
|          |              | Normal | Abnormal |       |
| Symptoms | Asymptomatic | 7      | 2        | 9     |
|          | Symptomatic  | 19     | 3        | 22    |
| Total    |              | 26     | 5        | 31    |

|          |              | Total IONM |          | Total |
|----------|--------------|------------|----------|-------|
|          |              | Normal     | Abnormal |       |
| Symptoms | Asymptomatic | 7          | 2        | 9     |
|          | Symptomatic  | 12         | 10       | 22    |
| Total    |              | 19         | 12       | 31    |

Lipidomics 1: CSF top pvalue candidate lipids

| Input Mass | Matched Mass | Delta  | Name                       | Formula       | Ion        |
|------------|--------------|--------|----------------------------|---------------|------------|
| 351.14     | 351.1385     | 0.0015 | LPIP(20:4)                 | C29H52O15P2   | [M+2H]2+   |
| 351.14     | 351.1449     | 0.0049 | FA(18:1(OH,Ke2,Ep2,cyclo)) | C18H23O7      | [M-H]-     |
| 351.14     | 351.1449     | 0.0049 | FA(18:2(OH2,Ke2,Ep,cyclo)) | C18H23O7      | [M-H]-     |
| 351.14     | 351.1449     | 0.0049 | FA(18:2(OH2,Ke,Ep2,cyclo)) | C18H23O7      | [M-H]-     |
| 351.14     | 351.1449     | 0.0049 | FA(18:2(OH,Ke2,Ep2))       | C18H23O7      | [M-H]-     |
| 351.14     | 351.1449     | 0.0049 | FA(18:3(OH2,Ke2,Ep))       | C18H23O7      | [M-H]-     |
| 351.14     | 351.1449     | 0.0049 | FA(18:3(OH2,Ke,Ep2))       | C18H23O7      | [M-H]-     |
| 351.14     | 351.1449     | 0.0049 | FA(18:3(OH3,Ep2,cyclo))    | C18H23O7      | [M-H]-     |
| 351.14     | 351.1449     | 0.0049 | FA(18:3(OH3,Ke2,cyclo))    | C18H23O7      | [M-H]-     |
| 351.14     | 351.1449     | 0.0049 | FA(18:3(OH3,Ke,Ep,cyclo))  | C18H23O7      | [M-H]-     |
| 351.14     | 351.1449     | 0.0049 | FA(18:4(OH3,Ep2))          | C18H23O7      | [M-H]-     |
| 351.14     | 351.1449     | 0.0049 | FA(18:4(OH3,Ke2))          | C18H23O7      | [M-H]-     |
| 351.14     | 351.1449     | 0.0049 | FA(18:4(OH3,Ke,Ep))        | C18H23O7      | [M-H]-     |
| 351.14     | 351.1449     | 0.0049 | FA(18:4(OH4,Ep,cyclo))     | C18H23O7      | [M-H]-     |
| 351.14     | 351.1449     | 0.0049 | FA(18:4(OH4,Ke,cyclo))     | C18H23O7      | [M-H]-     |
| 351.14     | 351.1449     | 0.0049 | FA(18:5(OH4,Ep))           | C18H23O7      | [M-H]-     |
| 351.14     | 351.1449     | 0.0049 | FA(18:5(OH4,Ke))           | C18H23O7      | [M-H]-     |
| 351.14     | 351.1396     | 0.0004 | LPIP(20:2)                 | C29H52O15P2   | [M-2H]2-   |
| 470.21     | 470.2137     | 0.0037 | NAT(22:6)                  | C24H37NO4SCl  | [M+Cl]-    |
| 501.38     | 501.3833     | 0.0033 | TG(64:15)                  | C67H102O6     | [M+2H]2+   |
| 501.38     | 501.3797     | 0.0003 | PG(O-50:2)                 | C56H109O9PNa2 | [M+2Na]2+  |
| 501.38     | 501.3797     | 0.0003 | PG(P-50:1)                 | C56H109O9PNa2 | [M+2Na]2+  |
| 501.38     | 501.3809     | 0.0009 | TG(60:9)                   | C63H104O6Na2  | [M+2Na]2+  |
| 501.38     | 501.3797     | 0.0003 | FA(28:0(OH4,Ep))           | C28H53O7      | [M-H]-     |
| 501.38     | 501.3797     | 0.0003 | FA(28:0(OH4,Ke))           | C28H53O7      | [M-H]-     |
| 501.38     | 501.3716     | 0.0084 | MG(26:2)                   | C29H54O4Cl    | [M+Cl]-    |
| 501.38     | 501.3797     | 0.0003 | DG(24:0)                   | C28H53O7      | [M+For]-   |
| 501.38     | 501.3832     | 0.0032 | PG(O-54:6)                 | C60H107O9P    | [M-2H]2-   |
| 501.38     | 501.3832     | 0.0032 | PG(P-54:5)                 | C60H107O9P    | [M-2H]2-   |
| 501.38     | 501.3844     | 0.0044 | TG(64:13)                  | C67H102O6     | [M-2H]2-   |
| 568.44     | 568.4449     | 0.0049 | PE-Cer(d26:0)              | C28H63N3O6P   | [M+NH4]+   |
| 568.44     | 568.4337     | 0.0063 | LPA(26:0)                  | C29H63NO7P    | [M+NH4]+   |
| 568.44     | 568.4337     | 0.0063 | PA(O-26:0)                 | C29H63NO7P    | [M+NH4]+   |
| 568.44     | 568.4398     | 0.0002 | PI(54:0(OH))               | C63H125O14P   | [M+2H]2+   |
| 568.44     | 568.438      | 0.002  | TG(74:18)                  | C77H116O6     | [M+2H]2+   |
| 568.44     | 568.4356     | 0.0044 | TG(70:12)                  | C73H118O6Na2  | [M+2Na]2+  |
| 568.44     | 568.4312     | 0.0088 | Cer(t32:2)                 | C32H61NO4     | [M+2Na-H]+ |
| 568.44     | 568.4392     | 0.0009 | TG(74:16)                  | C77H116O6     | [M-2H]2-   |
| 482.4      | 482.3968     | 0.0032 | NAE(28:4)                  | C30H53NO2Na   | [M+Na]+    |
| 482.4      | 482.3944     | 0.0056 | NAE(26:1)                  | C28H55NO2     | [M+2Na-H]+ |
| 482.4      | 482.4004     | 0.0004 | NAE(30:6)                  | C32H52NO2     | [M-H]-     |
| 407.26     | 407.2669     | 0.0069 | LysoSM(d14:2)              | C19H40N2O5P   | [M+H]+     |
| 407.26     | 407.2669     | 0.0069 | LysoSM(t14:1)              | C19H40N2O5P   | [M+H-H2O]+ |
| 407.26     | 407.2569     | 0.0031 | PA(44:10(OH))              | C47H75O9P     | [M+2H]2+   |
| 407.26     | 407.268      | 0.008  | LysoSM(d14:1)              | C19H40N2O5P   | [M-H]-     |
| 407.26     | 407.258      | 0.002  | PA(44:8(OH))               | C47H75O9P     | [M-2H]2-   |
| 857.74     | 857.7358     | 0.0042 | PA(O-48:1)                 | C51H102O7P    | [M+H]+     |
| 857.74     | 857.7358     | 0.0042 | PA(P-48:2)                 | C51H102O7P    | [M+H]+     |

|        |          |        |                            |                |                        |
|--------|----------|--------|----------------------------|----------------|------------------------|
| 857.74 | 857.747  | 0.007  | PE-Cer(d48:1)              | C50H102N2O6P   | [M+H] <sup>+</sup>     |
| 857.74 | 857.7358 | 0.0042 | PA(O-48:0(OH))             | C51H102O7P     | [M+H-H2O] <sup>+</sup> |
| 857.74 | 857.747  | 0.007  | PE-Cer(t48:0)              | C50H102N2O6P   | [M+H-H2O] <sup>+</sup> |
| 857.74 | 857.747  | 0.007  | CerP(d50:2)                | C50H102N2O6P   | [M+NH4] <sup>+</sup>   |
| 857.74 | 857.7359 | 0.0041 | DG(50:1)                   | C53H102O5K     | [M+K] <sup>+</sup>     |
| 857.74 | 857.7359 | 0.0041 | TG(O-50:1)                 | C53H102O5K     | [M+K] <sup>+</sup>     |
| 857.74 | 857.7359 | 0.0041 | TG(P-50:0)                 | C53H102O5K     | [M+K] <sup>+</sup>     |
| 857.74 | 857.7369 | 0.0031 | PA(O-48:0)                 | C51H102O7P     | [M-H] <sup>-</sup>     |
| 857.74 | 857.7481 | 0.0081 | PE-Cer(d48:0)              | C50H102N2O6P   | [M-H] <sup>-</sup>     |
| 857.74 | 857.7392 | 0.0008 | CE(30:4)                   | C58H97O4       | [M+For] <sup>-</sup>   |
| 857.74 | 857.7392 | 0.0008 | WE(56:9)                   | C58H97O4       | [M+OAc] <sup>-</sup>   |
| 857.74 | 857.7481 | 0.0081 | SM(d46:0)                  | C50H102N2O6P   | [M-CH3] <sup>-</sup>   |
| 207.11 | 207.1027 | 0.0073 | FA(12:2(Ep,cyclo))         | C12H15O3       | [M-H] <sup>-</sup>     |
| 207.11 | 207.1027 | 0.0073 | FA(12:2(Ke,cyclo))         | C12H15O3       | [M-H] <sup>-</sup>     |
| 207.11 | 207.1027 | 0.0073 | FA(12:3(Ep))               | C12H15O3       | [M-H] <sup>-</sup>     |
| 207.11 | 207.1027 | 0.0073 | FA(12:3(Ke))               | C12H15O3       | [M-H] <sup>-</sup>     |
| 207.11 | 207.1027 | 0.0073 | FA(12:3(OH,cyclo))         | C12H15O3       | [M-H] <sup>-</sup>     |
| 207.11 | 207.1157 | 0.0057 | WE(10:0)                   | C10H20O2Cl     | [M+Cl] <sup>-</sup>    |
| 407.3  | 407.2921 | 0.0079 | LPA(O-18:0)                | C21H44O5P      | [M+H-H2O] <sup>+</sup> |
| 407.3  | 407.2938 | 0.0062 | NAT(18:1)                  | C20H43N2O4S    | [M+NH4] <sup>+</sup>   |
| 407.3  | 407.3038 | 0.0038 | PG(O-40:4)                 | C46H87O9P      | [M+2H] <sup>2+</sup>   |
| 407.3  | 407.3038 | 0.0038 | PG(P-40:3)                 | C46H87O9P      | [M+2H] <sup>2+</sup>   |
| 407.3  | 407.3026 | 0.0026 | TG(46:5)                   | C49H84O6Na2    | [M+2Na] <sup>2+</sup>  |
| 407.3  | 407.2965 | 0.0035 | PE-Cer(d42:3)              | C44H85N2O6PNa2 | [M+2Na] <sup>2+</sup>  |
| 407.3  | 407.2956 | 0.0044 | FA(28:8)                   | C28H39O2       | [M-H] <sup>-</sup>     |
| 407.3  | 407.3049 | 0.0049 | PG(O-40:2)                 | C46H87O9P      | [M-2H] <sup>2-</sup>   |
| 407.3  | 407.3049 | 0.0049 | PG(P-40:1)                 | C46H87O9P      | [M-2H] <sup>2-</sup>   |
| 407.3  | 407.3018 | 0.0018 | PG(68:9(OH))               | C74H126O11P    | [M-3H] <sup>3-</sup>   |
| 399.15 | 399.1519 | 0.0019 | LPA(12:0)                  | C15H31O7P      | [M+2Na-H] <sup>+</sup> |
| 399.15 | 399.1449 | 0.0051 | FA(22:5(OH,Ke2,Ep2,cyclo)) | C22H23O7       | [M-H] <sup>-</sup>     |
| 399.15 | 399.1449 | 0.0051 | FA(22:6(OH2,Ke2,Ep,cyclo)) | C22H23O7       | [M-H] <sup>-</sup>     |
| 399.15 | 399.1449 | 0.0051 | FA(22:6(OH2,Ke,Ep2,cyclo)) | C22H23O7       | [M-H] <sup>-</sup>     |
| 399.15 | 399.1449 | 0.0051 | FA(22:6(OH,Ke2,Ep2))       | C22H23O7       | [M-H] <sup>-</sup>     |
| 518.37 | 518.3605 | 0.0095 | LPE(22:1)                  | C27H53NO6P     | [M+H-H2O] <sup>+</sup> |
| 518.37 | 518.3606 | 0.0094 | CAR(22:2)                  | C29H53NO4K     | [M+K] <sup>+</sup>     |
| 518.37 | 518.3666 | 0.0034 | PI(P-50:6)                 | C59H105O12P    | [M+2H] <sup>2+</sup>   |
| 518.37 | 518.3743 | 0.0043 | PA(60:11(OH))              | C63H105O9P     | [M+2H] <sup>2+</sup>   |
| 518.37 | 518.3719 | 0.0019 | PA(56:5(OH))               | C59H107O9PNa2  | [M+2Na] <sup>2+</sup>  |
| 518.37 | 518.377  | 0.007  | NAE(30:6)                  | C32H53NO2Cl    | [M+Cl] <sup>-</sup>    |
| 518.37 | 518.3677 | 0.0023 | PI(O-50:5)                 | C59H105O12P    | [M-2H] <sup>2-</sup>   |
| 518.37 | 518.3677 | 0.0023 | PI(P-50:4)                 | C59H105O12P    | [M-2H] <sup>2-</sup>   |
| 284.29 | 284.2948 | 0.0048 | Sph(m18:1)                 | C18H38NO       | [M+H] <sup>+</sup>     |
| 284.29 | 284.2948 | 0.0048 | Sph(d18:0)                 | C18H38NO       | [M+H-H2O] <sup>+</sup> |
| 284.29 | 284.2959 | 0.0059 | Sph(m18:0)                 | C18H38NO       | [M-H] <sup>-</sup>     |
| 323.16 | 323.1554 | 0.0046 | LPI(22:6)                  | C31H51O12P     | [M+2H] <sup>2+</sup>   |
| 323.16 | 323.1606 | 0.0006 | PA(28:4(OH))               | C31H53O9PNa2   | [M+2Na] <sup>2+</sup>  |
| 323.16 | 323.1565 | 0.0035 | LPI(22:4)                  | C31H51O12P     | [M-2H] <sup>2-</sup>   |
| 353.16 | 353.1606 | 0.0006 | FA(18:0(OH,Ke2,Ep2,cyclo)) | C18H25O7       | [M-H] <sup>-</sup>     |
| 353.16 | 353.1606 | 0.0006 | FA(18:1(OH2,Ke2,Ep,cyclo)) | C18H25O7       | [M-H] <sup>-</sup>     |
| 353.16 | 353.1606 | 0.0006 | FA(18:1(OH2,Ke,Ep2,cyclo)) | C18H25O7       | [M-H] <sup>-</sup>     |

|        |          |        |                           |              |              |
|--------|----------|--------|---------------------------|--------------|--------------|
| 353.16 | 353.1606 | 0.0006 | FA(18:1(OH,Ke2,Ep2))      | C18H25O7     | [M-H]-       |
| 353.16 | 353.1606 | 0.0006 | FA(18:2(OH2,Ke2,Ep))      | C18H25O7     | [M-H]-       |
| 353.16 | 353.1606 | 0.0006 | FA(18:2(OH2,Ke,Ep2))      | C18H25O7     | [M-H]-       |
| 353.16 | 353.1606 | 0.0006 | FA(18:2(OH3,Ep2,cyclo))   | C18H25O7     | [M-H]-       |
| 353.16 | 353.1606 | 0.0006 | FA(18:2(OH3,Ke2,cyclo))   | C18H25O7     | [M-H]-       |
| 353.16 | 353.1606 | 0.0006 | FA(18:2(OH3,Ke,Ep,cyclo)) | C18H25O7     | [M-H]-       |
| 353.16 | 353.1606 | 0.0006 | FA(18:3(OH3,Ep2))         | C18H25O7     | [M-H]-       |
| 353.16 | 353.1606 | 0.0006 | FA(18:3(OH3,Ke2))         | C18H25O7     | [M-H]-       |
| 353.16 | 353.1606 | 0.0006 | FA(18:3(OH3,Ke,Ep))       | C18H25O7     | [M-H]-       |
| 353.16 | 353.1606 | 0.0006 | FA(18:3(OH4,Ep,cyclo))    | C18H25O7     | [M-H]-       |
| 353.16 | 353.1606 | 0.0006 | FA(18:3(OH4,Ke,cyclo))    | C18H25O7     | [M-H]-       |
| 353.16 | 353.1606 | 0.0006 | FA(18:4(OH4,Ep))          | C18H25O7     | [M-H]-       |
| 353.16 | 353.1606 | 0.0006 | FA(18:4(OH4,Ke))          | C18H25O7     | [M-H]-       |
| 353.16 | 353.1553 | 0.0047 | LPIP(20:0)                | C29H56O15P2  | [M-2H]2-     |
| 703.54 | 703.5385 | 0.0015 | PE-Cer(t36:2)             | C38H76N2O7P  | [M+H]+       |
| 703.54 | 703.5355 | 0.0045 | MGDG(30:0)                | C39H75O10    | [M+H]+       |
| 703.54 | 703.5424 | 0.0024 | WE(48:12)                 | C48H72O2Na   | [M+Na]+      |
| 703.54 | 703.5385 | 0.0015 | LPC(30:3)                 | C38H76N2O7P  | [M+NH4]+     |
| 703.54 | 703.5467 | 0.0067 | HexCer(t32:2)             | C38H75N2O9   | [M+NH4]+     |
| 703.54 | 703.54   | 0      | WE(46:9)                  | C46H74O2     | [M+2Na-H]+   |
| 703.54 | 703.5396 | 0.0004 | PE-Cer(t36:1)             | C38H76N2O7P  | [M-H]-       |
| 703.54 | 703.5396 | 0.0004 | SM(t34:1)                 | C38H76N2O7P  | [M-CH3]-     |
| 855.73 | 855.7313 | 0.0013 | PE-Cer(d48:2)             | C50H100N2O6P | [M+H]+       |
| 855.73 | 855.7201 | 0.0099 | PA(O-48:2)                | C51H100O7P   | [M+H]+       |
| 855.73 | 855.7201 | 0.0099 | PA(P-48:1)                | C51H100O7P   | [M+H]+       |
| 855.73 | 855.7313 | 0.0013 | PE-Cer(t48:1)             | C50H100N2O6P | [M+H-H2O]+   |
| 855.73 | 855.7201 | 0.0099 | PA(48:0)                  | C51H100O7P   | [M+H-H2O]+   |
| 855.73 | 855.7201 | 0.0099 | PA(O-48:1(OH))            | C51H100O7P   | [M+H-H2O]+   |
| 855.73 | 855.7201 | 0.0099 | PA(P-48:0(OH))            | C51H100O7P   | [M+H-H2O]+   |
| 855.73 | 855.7396 | 0.0096 | HexCer(d44:2)             | C50H99N2O8   | [M+NH4]+     |
| 855.73 | 855.7355 | 0.0055 | CE(30:2)                  | C57H100O2K   | [M+K]+       |
| 855.73 | 855.7202 | 0.0098 | DG(50:2)                  | C53H100O5K   | [M+K]+       |
| 855.73 | 855.7202 | 0.0098 | TG(O-50:2)                | C53H100O5K   | [M+K]+       |
| 855.73 | 855.7202 | 0.0098 | TG(P-50:1)                | C53H100O5K   | [M+K]+       |
| 855.73 | 855.7325 | 0.0025 | PE-Cer(d48:1)             | C50H100N2O6P | [M-H]-       |
| 855.73 | 855.7212 | 0.0088 | PA(O-48:1)                | C51H100O7P   | [M-H]-       |
| 855.73 | 855.7212 | 0.0088 | PA(P-48:0)                | C51H100O7P   | [M-H]-       |
| 855.73 | 855.7236 | 0.0064 | CE(30:5)                  | C58H95O4     | [M+Formate]- |
| 855.73 | 855.7236 | 0.0064 | WE(56:10)                 | C58H95O4     | [M+OAc]-     |
| 855.73 | 855.7325 | 0.0025 | SM(d46:1)                 | C50H100N2O6P | [M-CH3]-     |

#### Lipidomics 1: CSF top neglog2fc candidate lipids

| Input Mass | Matched Mass | Delta  | Name           | Formula      | Ion      |
|------------|--------------|--------|----------------|--------------|----------|
| 729.47     | 729.4661     | 0.0039 | PI-Cer(t28:1)  | C34H70N2O12P | [M+NH4]+ |
| 729.47     | 729.4712     | 0.0012 | PA(34:3)       | C39H70O10P   | [M+OAc]- |
| 729.47     | 729.4712     | 0.0012 | PA(O-34:4(OH)) | C39H70O10P   | [M+OAc]- |
| 729.47     | 729.4712     | 0.0012 | PA(P-34:3(OH)) | C39H70O10P   | [M+OAc]- |
| 729.47     | 729.4795     | 0.0095 | MGDG(28:2)     | C39H69O12    | [M+OAc]- |

|        |          |        |                            |               |              |
|--------|----------|--------|----------------------------|---------------|--------------|
| 351.14 | 351.1385 | 0.0015 | LPIP(20:4)                 | C29H52O15P2   | [M+2H]2+     |
| 351.14 | 351.1449 | 0.0049 | FA(18:1(OH,Ke2,Ep2,cyclo)) | C18H23O7      | [M-H]-       |
| 351.14 | 351.1449 | 0.0049 | FA(18:2(OH2,Ke2,Ep,cyclo)) | C18H23O7      | [M-H]-       |
| 351.14 | 351.1449 | 0.0049 | FA(18:2(OH2,Ke,Ep2,cyclo)) | C18H23O7      | [M-H]-       |
| 351.14 | 351.1449 | 0.0049 | FA(18:2(OH,Ke2,Ep2))       | C18H23O7      | [M-H]-       |
| 351.14 | 351.1449 | 0.0049 | FA(18:3(OH2,Ke2,Ep))       | C18H23O7      | [M-H]-       |
| 351.14 | 351.1449 | 0.0049 | FA(18:3(OH2,Ke,Ep2))       | C18H23O7      | [M-H]-       |
| 351.14 | 351.1449 | 0.0049 | FA(18:3(OH3,Ep2,cyclo))    | C18H23O7      | [M-H]-       |
| 351.14 | 351.1449 | 0.0049 | FA(18:3(OH3,Ke2,cyclo))    | C18H23O7      | [M-H]-       |
| 351.14 | 351.1449 | 0.0049 | FA(18:3(OH3,Ke,Ep,cyclo))  | C18H23O7      | [M-H]-       |
| 351.14 | 351.1449 | 0.0049 | FA(18:4(OH3,Ep2))          | C18H23O7      | [M-H]-       |
| 351.14 | 351.1449 | 0.0049 | FA(18:4(OH3,Ke2))          | C18H23O7      | [M-H]-       |
| 351.14 | 351.1449 | 0.0049 | FA(18:4(OH3,Ke,Ep))        | C18H23O7      | [M-H]-       |
| 351.14 | 351.1449 | 0.0049 | FA(18:4(OH4,Ep,cyclo))     | C18H23O7      | [M-H]-       |
| 351.14 | 351.1449 | 0.0049 | FA(18:4(OH4,Ke,cyclo))     | C18H23O7      | [M-H]-       |
| 351.14 | 351.1449 | 0.0049 | FA(18:5(OH4,Ep))           | C18H23O7      | [M-H]-       |
| 351.14 | 351.1449 | 0.0049 | FA(18:5(OH4,Ke))           | C18H23O7      | [M-H]-       |
| 351.14 | 351.1396 | 0.0004 | LPIP(20:2)                 | C29H52O15P2   | [M-2H]2-     |
| 717.56 | 717.5541 | 0.0059 | SM(t34:2)                  | C39H78N2O7P   | [M+H]+       |
| 717.56 | 717.5541 | 0.0059 | PE(O-34:3)                 | C39H78N2O7P   | [M+NH4]+     |
| 717.56 | 717.5541 | 0.0059 | PE(P-34:2)                 | C39H78N2O7P   | [M+NH4]+     |
| 717.56 | 717.5557 | 0.0043 | CE(20:4)                   | C47H76O2      | [M+2Na-H]+   |
| 717.56 | 717.5594 | 0.0006 | DG(O-42:6)                 | C45H78O4Cl    | [M+Cl]-      |
| 717.56 | 717.5594 | 0.0006 | DG(P-42:5)                 | C45H78O4Cl    | [M+Cl]-      |
| 717.56 | 717.5675 | 0.0075 | DG(40:4)                   | C44H77O7      | [M+Formate]- |
| 686.46 | 686.4521 | 0.0079 | LPE(30:1)                  | C35H70NO7PK   | [M+K]+       |
| 686.46 | 686.4521 | 0.0079 | PE(O-30:1)                 | C35H70NO7PK   | [M+K]+       |
| 686.46 | 686.4521 | 0.0079 | PE(P-30:0)                 | C35H70NO7PK   | [M+K]+       |
| 686.46 | 686.4578 | 0.0022 | HexCer(d30:2)              | C36H67NO8     | [M+2Na-H]+   |
| 686.46 | 686.4533 | 0.0067 | PC(O-26:0(OH))             | C34H70NO8PCl  | [M+Cl]-      |
| 646.5  | 646.4918 | 0.0082 | PE-Cer(d32:3)              | C34H69N3O6P   | [M+NH4]+     |
| 646.5  | 646.5052 | 0.0052 | CAR(30:4)                  | C39H68NO6     | [M+OAc]-     |
| 646.5  | 646.5086 | 0.0086 | NAT(32:0)                  | C36H72NO6S    | [M+OAc]-     |
| 679.42 | 679.4181 | 0.0019 | PG(28:2(OH))               | C34H64O11P    | [M+H]+       |
| 679.42 | 679.4192 | 0.0008 | PG(28:1(OH))               | C34H64O11P    | [M-H]-       |
| 679.42 | 679.4194 | 0.0006 | MGDG(26:1)                 | C35H64O10Cl   | [M+Cl]-      |
| 679.42 | 679.4111 | 0.0089 | PA(32:2)                   | C35H65O8PCl   | [M+Cl]-      |
| 679.42 | 679.4192 | 0.0008 | PA(30:1(OH))               | C34H64O11P    | [M+Formate]- |
| 679.42 | 679.4192 | 0.0008 | LPG(26:2)                  | C34H64O11P    | [M+OAc]-     |
| 679.42 | 679.4162 | 0.0038 | CL(66:10)                  | C75H124O17P2  | [M-2H]2-     |
| 679.42 | 679.4162 | 0.0038 | PIP(66:11(OH))             | C75H124O17P2  | [M-2H]2-     |
| 693.48 | 693.4701 | 0.0099 | PG(30:1)                   | C36H70O10P    | [M+H]+       |
| 693.48 | 693.4701 | 0.0099 | PG(P-30:1(OH))             | C36H70O10P    | [M+H]+       |
| 693.48 | 693.4701 | 0.0099 | PG(30:0(OH))               | C36H70O10P    | [M+H-H2O]+   |
| 693.48 | 693.4813 | 0.0013 | PE(30:2(OH))               | C35H70N2O9P   | [M+NH4]+     |
| 693.48 | 693.4712 | 0.0088 | PG(30:0)                   | C36H70O10P    | [M-H]-       |
| 693.48 | 693.4712 | 0.0088 | PG(O-30:1(OH))             | C36H70O10P    | [M-H]-       |
| 693.48 | 693.4712 | 0.0088 | PG(P-30:0(OH))             | C36H70O10P    | [M-H]-       |
| 693.48 | 693.4744 | 0.0056 | PE-Cer(d34:2)              | C36H71N2O6PCl | [M+Cl]-      |
| 693.48 | 693.4866 | 0.0066 | TG(38:4)                   | C41H70O6Cl    | [M+Cl]-      |

|        |          |        |                   |               |              |
|--------|----------|--------|-------------------|---------------|--------------|
| 693.48 | 693.4825 | 0.0025 | PE-Cer(t32:1)     | C35H70N2O9P   | [M+Formate]- |
| 693.48 | 693.4712 | 0.0088 | PA(32:0)          | C36H70O10P    | [M+Formate]- |
| 693.48 | 693.4712 | 0.0088 | PA(O-32:1(OH))    | C36H70O10P    | [M+Formate]- |
| 693.48 | 693.4712 | 0.0088 | PA(P-32:0(OH))    | C36H70O10P    | [M+Formate]- |
| 693.48 | 693.4825 | 0.0025 | SM(t28:1)         | C35H70N2O9P   | [M+OAc]-     |
| 693.48 | 693.4736 | 0.0064 | DG(38:9)          | C43H65O7      | [M+OAc]-     |
| 459.35 | 459.3469 | 0.0031 | MG(26:6)          | C29H47O4      | [M+H]+       |
| 459.35 | 459.3445 | 0.0055 | MG(24:3)          | C27H48O4Na    | [M+Na]+      |
| 459.35 | 459.3599 | 0.0099 | WE(28:2)          | C28H52O2K     | [M+K]+       |
| 459.35 | 459.3533 | 0.0033 | PA(52:6)          | C55H99O8P     | [M+2H]2+     |
| 459.35 | 459.3533 | 0.0033 | PA(P-52:6(OH))    | C55H99O8P     | [M+2H]2+     |
| 459.35 | 459.3509 | 0.0009 | PA(48:0)          | C51H101O8PNa2 | [M+2Na]2+    |
| 459.35 | 459.3509 | 0.0009 | PA(O-48:1(OH))    | C51H101O8PNa2 | [M+2Na]2+    |
| 459.35 | 459.3509 | 0.0009 | PA(P-48:0(OH))    | C51H101O8PNa2 | [M+2Na]2+    |
| 459.35 | 459.3421 | 0.0079 | MG(22:0)          | C25H50O4      | [M+2Na-H]+   |
| 459.35 | 459.348  | 0.002  | MG(26:5)          | C29H47O4      | [M-H]-       |
| 459.35 | 459.3544 | 0.0044 | PA(52:4)          | C55H99O8P     | [M-2H]2-     |
| 459.35 | 459.3544 | 0.0044 | PA(O-52:5(OH))    | C55H99O8P     | [M-2H]2-     |
| 459.35 | 459.3544 | 0.0044 | PA(P-52:4(OH))    | C55H99O8P     | [M-2H]2-     |
| 898.61 | 898.6015 | 0.0085 | PI(36:1(OH))      | C45H89NO14P   | [M+NH4]+     |
| 898.61 | 898.6086 | 0.0014 | PE(P-46:6)        | C51H90NO7PK   | [M+K]+       |
| 898.61 | 898.6098 | 0.0002 | PC(42:5)          | C50H90NO8PCl  | [M+Cl]-      |
| 898.61 | 898.6098 | 0.0002 | PC(O-42:6(OH))    | C50H90NO8PCl  | [M+Cl]-      |
| 898.61 | 898.6098 | 0.0002 | PC(P-42:5(OH))    | C50H90NO8PCl  | [M+Cl]-      |
| 898.61 | 898.6028 | 0.0072 | LacCer(d34:0)     | C46H89NO13Cl  | [M+Cl]-      |
| 898.61 | 898.6026 | 0.0074 | PI-Cer(t38:0)     | C45H89NO14P   | [M+Formate]- |
| 898.61 | 898.6179 | 0.0079 | PC(40:4(OH))      | C49H89NO11P   | [M+Formate]- |
| 898.61 | 898.6179 | 0.0079 | PS(O-42:4)        | C49H89NO11P   | [M+Formate]- |
| 898.61 | 898.6179 | 0.0079 | PS(P-42:3)        | C49H89NO11P   | [M+Formate]- |
| 898.61 | 898.6179 | 0.0079 | PE(42:4(OH))      | C49H89NO11P   | [M+OAc]-     |
| 736.45 | 736.4548 | 0.0048 | PS(34:5)          | C40H67NO9P    | [M+H-H2O]+   |
| 736.45 | 736.4524 | 0.0024 | LPS(32:4)         | C38H68NO9PNa  | [M+Na]+      |
| 736.45 | 736.4524 | 0.0024 | PC(30:4(OH))      | C38H68NO9PNa  | [M+Na]+      |
| 736.45 | 736.45   | 0      | LPS(30:1)         | C36H70NO9P    | [M+2Na-H]+   |
| 736.45 | 736.45   | 0      | PC(28:1(OH))      | C36H70NO9P    | [M+2Na-H]+   |
| 736.45 | 736.45   | 0      | PS(O-30:1)        | C36H70NO9P    | [M+2Na-H]+   |
| 736.45 | 736.45   | 0      | PS(P-30:0)        | C36H70NO9P    | [M+2Na-H]+   |
| 736.45 | 736.4559 | 0.0059 | LPS(34:6)         | C40H67NO9P    | [M-H]-       |
| 736.45 | 736.4406 | 0.0094 | PI-Cer(t30:2)     | C36H67NO12P   | [M-H]-       |
| 736.45 | 736.4406 | 0.0094 | PS(28:1)          | C36H67NO12P   | [M+OAc]-     |
| 942.6  | 942.5913 | 0.0087 | MIPC(d34:1)       | C46H89NO16P   | [M+H]+       |
| 942.6  | 942.5913 | 0.0087 | MIPC(t34:0)       | C46H89NO16P   | [M+H-H2O]+   |
| 942.6  | 942.5983 | 0.0017 | PE(50:12)         | C55H86NO8PNa  | [M+Na]+      |
| 942.6  | 942.5985 | 0.0015 | PC(44:7(OH))      | C52H90NO9PK   | [M+K]+       |
| 942.6  | 942.5985 | 0.0015 | PS(P-46:6)        | C52H90NO9PK   | [M+K]+       |
| 942.6  | 942.5915 | 0.0085 | LacCer(t36:2)     | C48H89NO14K   | [M+K]+       |
| 942.6  | 942.6018 | 0.0018 | PI-Cer(t40:0(OH)) | C46H92NO13P   | [M+2Na-H]+   |
| 942.6  | 942.5959 | 0.0041 | PE(48:9)          | C53H88NO8P    | [M+2Na-H]+   |
| 942.6  | 942.5925 | 0.0075 | MIPC(d34:0)       | C46H89NO16P   | [M-H]-       |
| 942.6  | 942.6077 | 0.0077 | PS(42:4(OH))      | C50H89NO13P   | [M+OAc]-     |

|        |          |        |                        |                |              |
|--------|----------|--------|------------------------|----------------|--------------|
| 343.22 | 343.218  | 0.002  | LPI(24:0)              | C33H67O12P     | [M+2H]2+     |
| 343.22 | 343.2126 | 0.0074 | FA(18:0(OH2,Ep2))      | C18H31O6       | [M-H]-       |
| 343.22 | 343.2126 | 0.0074 | FA(18:0(OH2,Ke2))      | C18H31O6       | [M-H]-       |
| 343.22 | 343.2126 | 0.0074 | FA(18:0(OH2,Ke,Ep))    | C18H31O6       | [M-H]-       |
| 343.22 | 343.2126 | 0.0074 | FA(18:0(OH3,Ep,cyclo)) | C18H31O6       | [M-H]-       |
| 343.22 | 343.2126 | 0.0074 | FA(18:0(OH3,Ke,cyclo)) | C18H31O6       | [M-H]-       |
| 343.22 | 343.2126 | 0.0074 | FA(18:1(OH3,Ep))       | C18H31O6       | [M-H]-       |
| 343.22 | 343.2126 | 0.0074 | FA(18:1(OH3,Ke))       | C18H31O6       | [M-H]-       |
| 343.22 | 343.2126 | 0.0074 | FA(18:1(OH4,cyclo))    | C18H31O6       | [M-H]-       |
| 343.22 | 343.2126 | 0.0074 | FA(18:2(OH4))          | C18H31O6       | [M-H]-       |
| 343.22 | 343.2279 | 0.0079 | FA(22:4(Ep,cyclo))     | C22H31O3       | [M-H]-       |
| 343.22 | 343.2279 | 0.0079 | FA(22:4(Ke,cyclo))     | C22H31O3       | [M-H]-       |
| 343.22 | 343.2279 | 0.0079 | FA(22:5(Ep))           | C22H31O3       | [M-H]-       |
| 343.22 | 343.2279 | 0.0079 | FA(22:5(Ke))           | C22H31O3       | [M-H]-       |
| 343.22 | 343.2279 | 0.0079 | FA(22:5(OH,cyclo))     | C22H31O3       | [M-H]-       |
| 343.22 | 343.2279 | 0.0079 | FA(22:6(OH))           | C22H31O3       | [M-H]-       |
| 691.42 | 691.4181 | 0.0019 | LPI(26:2)              | C35H64O11P     | [M+H-H2O]+   |
| 691.42 | 691.4293 | 0.0093 | PS(28:3)               | C34H64N2O10P   | [M+NH4]+     |
| 691.42 | 691.4285 | 0.0085 | PA(32:1)               | C35H67O8P      | [M+2Na-H]+   |
| 691.42 | 691.4285 | 0.0085 | PA(P-32:1(OH))         | C35H67O8P      | [M+2Na-H]+   |
| 691.42 | 691.4192 | 0.0008 | LPG(28:3)              | C35H64O11P     | [M+Formate]- |
| 691.42 | 691.4192 | 0.0008 | PA(30:2(OH))           | C35H64O11P     | [M+OAc]-     |
| 691.42 | 691.4162 | 0.0038 | CL(68:12)              | C77H124O17P2   | [M-2H]2-     |
| 470.21 | 470.2137 | 0.0037 | NAT(22:6)              | C24H37NO4SCL   | [M+Cl]-      |
| 649.45 | 649.4439 | 0.0061 | LPG(28:2)              | C34H66O9P      | [M+H]+       |
| 649.45 | 649.4439 | 0.0061 | PG(28:0)               | C34H66O9P      | [M+H-H2O]+   |
| 649.45 | 649.4439 | 0.0061 | PG(P-28:0(OH))         | C34H66O9P      | [M+H-H2O]+   |
| 649.45 | 649.4551 | 0.0051 | PE(28:2)               | C33H66N2O8P    | [M+NH4]+     |
| 649.45 | 649.4455 | 0.0045 | SQDG(66:9)             | C75H128O12SNa2 | [M+2Na]2+    |
| 649.45 | 649.445  | 0.005  | LPG(28:1)              | C34H66O9P      | [M-H]-       |
| 649.45 | 649.445  | 0.005  | PG(P-28:0)             | C34H66O9P      | [M-H]-       |
| 649.45 | 649.445  | 0.005  | LPA(30:1)              | C34H66O9P      | [M+Formate]- |
| 649.45 | 649.445  | 0.005  | PA(O-30:1)             | C34H66O9P      | [M+Formate]- |
| 649.45 | 649.445  | 0.005  | PA(P-30:0)             | C34H66O9P      | [M+Formate]- |
| 649.45 | 649.4562 | 0.0062 | PE-Cer(d30:1)          | C33H66N2O8P    | [M+Formate]- |
| 649.45 | 649.4562 | 0.0062 | SM(d26:1)              | C33H66N2O8P    | [M+OAc]-     |
| 678.48 | 678.4704 | 0.0096 | PE(30:1(OH))           | C35H69NO9P     | [M+H]+       |
| 678.48 | 678.4857 | 0.0057 | LPE(34:5)              | C39H69NO6P     | [M+H-H2O]+   |
| 678.48 | 678.4857 | 0.0057 | PE(P-34:4)             | C39H69NO6P     | [M+H-H2O]+   |
| 678.48 | 678.4704 | 0.0096 | PA(32:2(OH))           | C35H69NO9P     | [M+NH4]+     |
| 678.48 | 678.4858 | 0.0058 | CAR(34:6)              | C41H69NO4K     | [M+K]+       |
| 678.48 | 678.4716 | 0.0084 | PE(30:0(OH))           | C35H69NO9P     | [M-H]-       |
| 678.48 | 678.4717 | 0.0083 | HexCer(d30:1)          | C36H69NO8Cl    | [M+Cl]-      |
| 678.48 | 678.4798 | 0.0002 | HexCer(t28:0)          | C35H68NO11     | [M+Formate]- |
| 678.48 | 678.4716 | 0.0084 | CerP(t34:1)            | C35H69NO9P     | [M+Formate]- |
| 678.48 | 678.4716 | 0.0084 | LPC(26:1)              | C35H69NO9P     | [M+Formate]- |
| 678.48 | 678.4716 | 0.0084 | PC(P-26:0)             | C35H69NO9P     | [M+Formate]- |
| 678.48 | 678.4716 | 0.0084 | LPE(28:1)              | C35H69NO9P     | [M+OAc]-     |
| 678.48 | 678.4716 | 0.0084 | PE(P-28:0)             | C35H69NO9P     | [M+OAc]-     |
| 678.48 | 678.4716 | 0.0084 | PC(28:0(OH))           | C35H69NO9P     | [M-CH3]-     |

|        |          |        |                    |          |        |
|--------|----------|--------|--------------------|----------|--------|
| 351.29 | 351.2905 | 0.0005 | FA(22:0(Ep,cyclo)) | C22H39O3 | [M-H]- |
| 351.29 | 351.2905 | 0.0005 | FA(22:0(Ke,cyclo)) | C22H39O3 | [M-H]- |
| 351.29 | 351.2905 | 0.0005 | FA(22:1(Ep))       | C22H39O3 | [M-H]- |
| 351.29 | 351.2905 | 0.0005 | FA(22:1(Ke))       | C22H39O3 | [M-H]- |
| 351.29 | 351.2905 | 0.0005 | FA(22:1(OH,cyclo)) | C22H39O3 | [M-H]- |
| 351.29 | 351.2905 | 0.0005 | FA(22:2(OH))       | C22H39O3 | [M-H]- |



## Lipidomics 1: CSF top poslog2fc candidate lipids

| Input Mass | Matched Mass | Delta  | Name                      | Formula        | Ion                      |
|------------|--------------|--------|---------------------------|----------------|--------------------------|
| 454.33     | 454.3292     | 0.0008 | LPC(O-14:0)               | C22H49NO6P     | [M+H] <sup>+</sup>       |
| 454.33     | 454.3316     | 0.0016 | CAR(22:6)                 | C29H44NO3      | [M+H-H2O] <sup>+</sup>   |
| 454.33     | 454.3349     | 0.0049 | NAT(24:2)                 | C26H48NO3S     | [M+H-H2O] <sup>+</sup>   |
| 454.33     | 454.3306     | 0.0006 | SQDG(40:0)                | C49H96O12S     | [M+2H] <sup>2+</sup>     |
| 454.33     | 454.3259     | 0.0041 | PG(46:4)                  | C52H93O10P     | [M-2H] <sup>2-</sup>     |
| 454.33     | 454.3259     | 0.0041 | PG(O-46:5(OH))            | C52H93O10P     | [M-2H] <sup>2-</sup>     |
| 454.33     | 454.3259     | 0.0041 | PG(P-46:4(OH))            | C52H93O10P     | [M-2H] <sup>2-</sup>     |
| 425.3      | 425.3026     | 0.0026 | LPA(O-18:0)               | C21H46O6P      | [M+H] <sup>+</sup>       |
| 425.3      | 425.3028     | 0.0028 | MG(20:0)                  | C23H46O4K      | [M+K] <sup>+</sup>       |
| 425.3      | 425.2962     | 0.0038 | PI(O-36:2)                | C45H87O12P     | [M+2H] <sup>2+</sup>     |
| 425.3      | 425.2962     | 0.0038 | PI(P-36:1)                | C45H87O12P     | [M+2H] <sup>2+</sup>     |
| 425.3      | 425.3038     | 0.0038 | PA(46:6(OH))              | C49H87O9P      | [M+2H] <sup>2+</sup>     |
| 425.3      | 425.3014     | 0.0014 | PA(42:0(OH))              | C45H89O9PNa2   | [M+2Na] <sup>2+</sup>    |
| 425.3      | 425.3061     | 0.0061 | FA(28:5(Ep,cyclo))        | C28H41O3       | [M-H] <sup>-</sup>       |
| 425.3      | 425.3061     | 0.0061 | FA(28:5(Ke,cyclo))        | C28H41O3       | [M-H] <sup>-</sup>       |
| 425.3      | 425.3061     | 0.0061 | FA(28:6(Ep))              | C28H41O3       | [M-H] <sup>-</sup>       |
| 425.3      | 425.3061     | 0.0061 | FA(28:6(Ke))              | C28H41O3       | [M-H] <sup>-</sup>       |
| 425.3      | 425.3061     | 0.0061 | FA(28:6(OH,cyclo))        | C28H41O3       | [M-H] <sup>-</sup>       |
| 425.3      | 425.2909     | 0.0091 | FA(24:0(OH2,Ep2,cyclo))   | C24H41O6       | [M-H] <sup>-</sup>       |
| 425.3      | 425.2909     | 0.0091 | FA(24:0(OH2,Ke2,cyclo))   | C24H41O6       | [M-H] <sup>-</sup>       |
| 425.3      | 425.2909     | 0.0091 | FA(24:0(OH2,Ke,Ep,cyclo)) | C24H41O6       | [M-H] <sup>-</sup>       |
| 425.3      | 425.2909     | 0.0091 | FA(24:0(OH,Ke2,Ep))       | C24H41O6       | [M-H] <sup>-</sup>       |
| 425.3      | 425.2909     | 0.0091 | FA(24:0(OH,Ke,Ep2))       | C24H41O6       | [M-H] <sup>-</sup>       |
| 425.3      | 425.2909     | 0.0091 | FA(24:1(OH2,Ep2))         | C24H41O6       | [M-H] <sup>-</sup>       |
| 425.3      | 425.2909     | 0.0091 | FA(24:1(OH2,Ke2))         | C24H41O6       | [M-H] <sup>-</sup>       |
| 425.3      | 425.2909     | 0.0091 | FA(24:1(OH2,Ke,Ep))       | C24H41O6       | [M-H] <sup>-</sup>       |
| 425.3      | 425.2909     | 0.0091 | FA(24:1(OH3,Ep,cyclo))    | C24H41O6       | [M-H] <sup>-</sup>       |
| 425.3      | 425.2909     | 0.0091 | FA(24:1(OH3,Ke,cyclo))    | C24H41O6       | [M-H] <sup>-</sup>       |
| 425.3      | 425.2909     | 0.0091 | FA(24:2(OH3,Ep))          | C24H41O6       | [M-H] <sup>-</sup>       |
| 425.3      | 425.2909     | 0.0091 | FA(24:2(OH3,Ke))          | C24H41O6       | [M-H] <sup>-</sup>       |
| 425.3      | 425.2909     | 0.0091 | FA(24:2(OH4,cyclo))       | C24H41O6       | [M-H] <sup>-</sup>       |
| 425.3      | 425.2909     | 0.0091 | FA(24:3(OH4))             | C24H41O6       | [M-H] <sup>-</sup>       |
| 425.3      | 425.2909     | 0.0091 | MG(20:3)                  | C24H41O6       | [M+Formate] <sup>-</sup> |
| 425.3      | 425.2973     | 0.0027 | PI(O-36:0)                | C45H87O12P     | [M-2H] <sup>2-</sup>     |
| 425.3      | 425.3049     | 0.0049 | PA(46:4(OH))              | C49H87O9P      | [M-2H] <sup>2-</sup>     |
| 425.3      | 425.3021     | 0.0021 | SQDG(68:10)               | C77H127O12S    | [M-3H] <sup>3-</sup>     |
| 627.58     | 627.5852     | 0.0052 | WE(40:0)                  | C40H80O2Cl     | [M+Cl] <sup>-</sup>      |
| 649.57     | 649.5765     | 0.0065 | DG(38:2)                  | C41H77O5       | [M+H] <sup>+</sup>       |
| 649.57     | 649.5765     | 0.0065 | TG(38:0)                  | C41H77O5       | [M+H-H2O] <sup>+</sup>   |
| 649.57     | 649.5712     | 0.0012 | TG(O-82:8)                | C85H152O5Na2   | [M+2Na] <sup>2+</sup>    |
| 649.57     | 649.5712     | 0.0012 | TG(P-82:7)                | C85H152O5Na2   | [M+2Na] <sup>2+</sup>    |
| 649.57     | 649.5777     | 0.0077 | DG(38:1)                  | C41H77O5       | [M-H] <sup>-</sup>       |
| 649.57     | 649.5777     | 0.0077 | TG(P-38:0)                | C41H77O5       | [M-H] <sup>-</sup>       |
| 649.57     | 649.5696     | 0.0004 | WE(42:3)                  | C42H78O2Cl     | [M+Cl] <sup>-</sup>      |
| 649.57     | 649.5747     | 0.0047 | TG(O-86:12)               | C89H150O5      | [M-2H] <sup>2-</sup>     |
| 649.57     | 649.5747     | 0.0047 | TG(P-86:11)               | C89H150O5      | [M-2H] <sup>2-</sup>     |
| 517.36     | 517.3564     | 0.0036 | PI(O-46:2)                | C55H105O12PNa2 | [M+2Na] <sup>2+</sup>    |

|        |          |        |               |                |              |
|--------|----------|--------|---------------|----------------|--------------|
| 517.36 | 517.3564 | 0.0036 | PI(P-46:1)    | C55H105O12PNa2 | [M+2Na]2+    |
| 517.36 | 517.364  | 0.004  | PA(56:6(OH))  | C59H105O9PNa2  | [M+2Na]2+    |
| 517.36 | 517.3665 | 0.0065 | DG(26:1)      | C29H54O5Cl     | [M+Cl]-      |
| 517.36 | 517.3535 | 0.0065 | MG(26:6)      | C31H49O6       | [M+OAc]-     |
| 517.36 | 517.3599 | 0.0001 | PI(O-50:6)    | C59H103O12P    | [M-2H]2-     |
| 517.36 | 517.3599 | 0.0001 | PI(P-50:5)    | C59H103O12P    | [M-2H]2-     |
| 517.36 | 517.3552 | 0.0048 | SQDG(50:5)    | C59H102O12S    | [M-2H]2-     |
| 607.57 | 607.566  | 0.004  | DG(O-36:2)    | C39H75O4       | [M+H]+       |
| 607.57 | 607.566  | 0.004  | DG(P-36:1)    | C39H75O4       | [M+H]+       |
| 607.57 | 607.566  | 0.004  | DG(36:0)      | C39H75O4       | [M+H-2O]+    |
| 607.57 | 607.566  | 0.004  | TG(O-36:0)    | C39H75O4       | [M+H-2O]+    |
| 607.57 | 607.5772 | 0.0072 | Cer(d38:3)    | C38H75N2O3     | [M+NH4]+     |
| 607.57 | 607.5671 | 0.0029 | DG(O-36:1)    | C39H75O4       | [M-H]-       |
| 607.57 | 607.5671 | 0.0029 | DG(P-36:0)    | C39H75O4       | [M-H]-       |
| 607.57 | 607.5671 | 0.0029 | WE(38:1)      | C39H75O4       | [M+Formate]- |
| 889.77 | 889.7732 | 0.0032 | SM(t46:0)     | C51H106N2O7P   | [M+H]+       |
| 889.77 | 889.7643 | 0.0057 | DG(56:8)      | C59H101O5      | [M+H]+       |
| 889.77 | 889.7643 | 0.0057 | TG(O-56:8)    | C59H101O5      | [M+H]+       |
| 889.77 | 889.7643 | 0.0057 | TG(P-56:7)    | C59H101O5      | [M+H]+       |
| 889.77 | 889.7643 | 0.0057 | TG(56:6)      | C59H101O5      | [M+H-2O]+    |
| 889.77 | 889.7772 | 0.0072 | CE(34:5)      | C61H102O2Na    | [M+Na]+      |
| 889.77 | 889.7619 | 0.0081 | DG(54:5)      | C57H102O5Na    | [M+Na]+      |
| 889.77 | 889.7619 | 0.0081 | TG(O-54:5)    | C57H102O5Na    | [M+Na]+      |
| 889.77 | 889.7619 | 0.0081 | TG(P-54:4)    | C57H102O5Na    | [M+Na]+      |
| 889.77 | 889.7732 | 0.0032 | PE(O-46:1)    | C51H106N2O7P   | [M+NH4]+     |
| 889.77 | 889.7732 | 0.0032 | PE(P-46:0)    | C51H106N2O7P   | [M+NH4]+     |
| 889.77 | 889.7655 | 0.0045 | DG(56:7)      | C59H101O5      | [M-H]-       |
| 889.77 | 889.7655 | 0.0045 | TG(O-56:7)    | C59H101O5      | [M-H]-       |
| 889.77 | 889.7655 | 0.0045 | TG(P-56:6)    | C59H101O5      | [M-H]-       |
| 889.77 | 889.7785 | 0.0085 | DG(O-54:4)    | C57H106O4Cl    | [M+Cl]-      |
| 599.55 | 599.5539 | 0.0039 | WE(38:0)      | C38H76O2Cl     | [M+Cl]-      |
| 607.54 | 607.5449 | 0.0049 | WE(42:7)      | C42H71O2       | [M+H]+       |
| 607.54 | 607.5424 | 0.0024 | WE(40:4)      | C40H72O2Na     | [M+Na]+      |
| 607.54 | 607.5408 | 0.0008 | CAR(30:3)     | C37H71N2O4     | [M+NH4]+     |
| 607.54 | 607.54   | 0      | WE(38:1)      | C38H74O2       | [M+2Na-H]+   |
| 607.54 | 607.546  | 0.006  | WE(42:6)      | C42H71O2       | [M-H]-       |
| 382.3  | 382.2972 | 0.0028 | TG(46:8)      | C49H80O6       | [M+2H]2+     |
| 382.3  | 382.296  | 0.004  | PG(O-36:1)    | C42H85O9P      | [M+2H]2+     |
| 382.3  | 382.296  | 0.004  | PG(P-36:0)    | C42H85O9P      | [M+2H]2+     |
| 382.3  | 382.2963 | 0.0037 | NAE(18:2)     | C22H40NO4      | [M+OAc]-     |
| 382.3  | 382.2983 | 0.0017 | TG(46:6)      | C49H80O6       | [M-2H]2-     |
| 382.3  | 382.3019 | 0.0019 | PS(62:3)      | C68H125NO10P   | [M-3H]3-     |
| 489.47 | 489.4626 | 0.0074 | Cer(t28:0)    | C28H61N2O4     | [M+NH4]+     |
| 489.47 | 489.4677 | 0.0023 | TG(96:4)      | C99H183O6      | [M-3H]3-     |
| 703.54 | 703.5385 | 0.0015 | PE-Cer(t36:2) | C38H76N2O7P    | [M+H]+       |
| 703.54 | 703.5355 | 0.0045 | MGDG(30:0)    | C39H75O10      | [M+H]+       |
| 703.54 | 703.5424 | 0.0024 | WE(48:12)     | C48H72O2Na     | [M+Na]+      |
| 703.54 | 703.5385 | 0.0015 | LPC(30:3)     | C38H76N2O7P    | [M+NH4]+     |
| 703.54 | 703.5467 | 0.0067 | HexCer(t32:2) | C38H75N2O9     | [M+NH4]+     |
| 703.54 | 703.54   | 0      | WE(46:9)      | C46H74O2       | [M+2Na-H]+   |

|        |          |        |               |                 |              |
|--------|----------|--------|---------------|-----------------|--------------|
| 703.54 | 703.5396 | 0.0004 | PE-Cer(t36:1) | C38H76N2O7P     | [M-H]-       |
| 703.54 | 703.5396 | 0.0004 | SM(t34:1)     | C38H76N2O7P     | [M-CH3]-     |
| 777.52 | 777.5181 | 0.0019 | SQDG(32:0)    | C41H77O11S      | [M+H-H2O]+   |
| 777.52 | 777.5276 | 0.0076 | LPI(32:1)     | C41H78O11P      | [M+H-H2O]+   |
| 777.52 | 777.5276 | 0.0076 | PI(O-32:1)    | C41H78O11P      | [M+H-H2O]+   |
| 777.52 | 777.5276 | 0.0076 | PI(P-32:0)    | C41H78O11P      | [M+H-H2O]+   |
| 777.52 | 777.5177 | 0.0023 | PE(38:8)      | C43H74N2O8P     | [M+NH4]+     |
| 777.52 | 777.5195 | 0.0005 | PA(O-40:4)    | C43H79O7PK      | [M+K]+       |
| 777.52 | 777.5195 | 0.0005 | PA(P-40:3)    | C43H79O7PK      | [M+K]+       |
| 777.52 | 777.5247 | 0.0047 | CL(80:12)     | C89H152O17P2    | [M+2H]2+     |
| 777.52 | 777.5223 | 0.0023 | CL(76:6)      | C85H154O17P2Na2 | [M+2Na]2+    |
| 777.52 | 777.523  | 0.003  | DG(46:11)     | C49H74O5Cl      | [M+Cl]-      |
| 777.52 | 777.5287 | 0.0087 | PG(O-34:2)    | C41H78O11P      | [M+Formate]- |
| 777.52 | 777.5287 | 0.0087 | PG(P-34:1)    | C41H78O11P      | [M+Formate]- |
| 777.52 | 777.5287 | 0.0087 | PA(36:1(OH))  | C41H78O11P      | [M+OAc]-     |
| 579.54 | 579.5347 | 0.0053 | DG(O-34:2)    | C37H71O4        | [M+H]+       |
| 579.54 | 579.5347 | 0.0053 | DG(P-34:1)    | C37H71O4        | [M+H]+       |
| 579.54 | 579.5347 | 0.0053 | DG(34:0)      | C37H71O4        | [M+H-H2O]+   |
| 579.54 | 579.5499 | 0.0099 | CE(14:0)      | C41H71O         | [M+H-H2O]+   |
| 579.54 | 579.5459 | 0.0059 | Cer(d36:3)    | C36H71N2O3      | [M+NH4]+     |
| 579.54 | 579.5358 | 0.0042 | DG(O-18:1)    | C37H71O4        | [M-H]-       |
| 579.54 | 579.5358 | 0.0042 | DG(O-34:1)    | C37H71O4        | [M-H]-       |
| 579.54 | 579.5358 | 0.0042 | DG(P-34:0)    | C37H71O4        | [M-H]-       |
| 579.54 | 579.5358 | 0.0042 | WE(36:1)      | C37H71O4        | [M+Formate]- |
| 575.5  | 575.5034 | 0.0034 | DG(O-34:4)    | C37H67O4        | [M+H]+       |
| 575.5  | 575.5034 | 0.0034 | DG(P-34:3)    | C37H67O4        | [M+H]+       |
| 575.5  | 575.5034 | 0.0034 | MG(34:4)      | C37H67O4        | [M+H]+       |
| 575.5  | 575.5034 | 0.0034 | DG(34:2)      | C37H67O4        | [M+H-H2O]+   |
| 575.5  | 575.501  | 0.001  | DG(O-32:1)    | C35H68O4Na      | [M+Na]+      |
| 575.5  | 575.501  | 0.001  | DG(P-32:0)    | C35H68O4Na      | [M+Na]+      |
| 575.5  | 575.501  | 0.001  | MG(32:1)      | C35H68O4Na      | [M+Na]+      |
| 575.5  | 575.5045 | 0.0045 | DG(O-34:3)    | C37H67O4        | [M-H]-       |
| 575.5  | 575.5045 | 0.0045 | DG(P-34:2)    | C37H67O4        | [M-H]-       |
| 575.5  | 575.5045 | 0.0045 | WE(36:3)      | C37H67O4        | [M+Formate]- |

Lipidomics 1: Plasma top pvalue candidate lipids

| Input Mass | Matched Mass | Delta  | Name                   | Formula        | Ion                      |
|------------|--------------|--------|------------------------|----------------|--------------------------|
| 482.36     | 482.3605     | 0.0007 | LPC(O-16:0)            | C24H53NO6P     | [M+H] <sup>+</sup>       |
| 482.36     | 482.3662     | 0.005  | NAT(26:2)              | C28H52NO3S     | [M+H-H2O] <sup>+</sup>   |
| 482.36     | 482.3606     | 0.0006 | Cer(t26:0)             | C26H53NO4K     | [M+K] <sup>+</sup>       |
| 482.36     | 482.3619     | 0.0007 | SQDG(44:0)             | C53H104O12S    | [M+2H] <sup>2+</sup>     |
| 482.36     | 482.3572     | 0.004  | PG(50:4)               | C56H101O10P    | [M-2H] <sup>2-</sup>     |
| 482.36     | 482.3572     | 0.004  | PG(O-50:5(OH))         | C56H101O10P    | [M-2H] <sup>2-</sup>     |
| 482.36     | 482.3572     | 0.004  | PG(P-50:4(OH))         | C56H101O10P    | [M-2H] <sup>2-</sup>     |
| 483.36     | 483.3557     | 0.0084 | LysoSM(t18:0)          | C23H52N2O6P    | [M+H] <sup>+</sup>       |
| 483.36     | 483.3557     | 0.0084 | LPE(P-18:0)            | C23H52N2O6P    | [M+NH4] <sup>+</sup>     |
| 483.36     | 483.3557     | 0.0084 | PE(O-18:1)             | C23H52N2O6P    | [M+NH4] <sup>+</sup>     |
| 483.36     | 483.3557     | 0.0084 | PE(P-18:0)             | C23H52N2O6P    | [M+NH4] <sup>+</sup>     |
| 483.36     | 483.3599     | 0.0042 | WE(30:4)               | C30H52O2K      | [M+K] <sup>+</sup>       |
| 483.36     | 483.3639     | 0.0002 | PG(50:5)               | C56H103O10P    | [M+2H] <sup>2+</sup>     |
| 483.36     | 483.3639     | 0.0002 | PG(O-50:6(OH))         | C56H103O10P    | [M+2H] <sup>2+</sup>     |
| 483.36     | 483.3639     | 0.0002 | PG(P-50:5(OH))         | C56H103O10P    | [M+2H] <sup>2+</sup>     |
| 483.36     | 483.3615     | 0.0026 | PG(O-46:0(OH))         | C52H105O10PNa2 | [M+2Na] <sup>2+</sup>    |
| 483.36     | 483.3691     | 0.005  | FA(28:0(OH2,Ep2))      | C28H51O6       | [M-H] <sup>-</sup>       |
| 483.36     | 483.3691     | 0.005  | FA(28:0(OH2,Ke2))      | C28H51O6       | [M-H] <sup>-</sup>       |
| 483.36     | 483.3691     | 0.005  | FA(28:0(OH2,Ke,Ep))    | C28H51O6       | [M-H] <sup>-</sup>       |
| 483.36     | 483.3691     | 0.005  | FA(28:0(OH3,Ep,cyclo)) | C28H51O6       | [M-H] <sup>-</sup>       |
| 483.36     | 483.3691     | 0.005  | FA(28:0(OH3,Ke,cyclo)) | C28H51O6       | [M-H] <sup>-</sup>       |
| 483.36     | 483.3691     | 0.005  | FA(28:1(OH3,Ep))       | C28H51O6       | [M-H] <sup>-</sup>       |
| 483.36     | 483.3691     | 0.005  | FA(28:1(OH3,Ke))       | C28H51O6       | [M-H] <sup>-</sup>       |
| 483.36     | 483.3691     | 0.005  | FA(28:1(OH4,cyclo))    | C28H51O6       | [M-H] <sup>-</sup>       |
| 483.36     | 483.3691     | 0.005  | FA(28:2(OH4))          | C28H51O6       | [M-H] <sup>-</sup>       |
| 483.36     | 483.3691     | 0.005  | MG(24:2)               | C28H51O6       | [M+Formate] <sup>-</sup> |
| 483.36     | 483.365      | 0.0009 | PG(50:3)               | C56H103O10P    | [M-2H] <sup>2-</sup>     |
| 483.36     | 483.365      | 0.0009 | PG(O-50:4(OH))         | C56H103O10P    | [M-2H] <sup>2-</sup>     |
| 483.36     | 483.365      | 0.0009 | PG(P-50:3(OH))         | C56H103O10P    | [M-2H] <sup>2-</sup>     |
| 911.71     | 911.7099     | 0.0017 | PA(50:3(OH))           | C53H100O9P     | [M+H] <sup>+</sup>       |
| 911.71     | 911.7075     | 0.0007 | PA(48:0(OH))           | C51H101O9PNa   | [M+Na] <sup>+</sup>      |
| 911.71     | 911.7059     | 0.0023 | PI-Cer(d42:0)          | C48H100N2O11P  | [M+NH4] <sup>+</sup>     |
| 911.71     | 911.7111     | 0.0028 | PA(50:2(OH))           | C53H100O9P     | [M-H] <sup>-</sup>       |
| 911.71     | 911.7111     | 0.0028 | PA(O-48:3)             | C53H100O9P     | [M+OAc] <sup>-</sup>     |
| 911.71     | 911.7111     | 0.0028 | PA(P-48:2)             | C53H100O9P     | [M+OAc] <sup>-</sup>     |
| 634.45     | 634.4442     | 0.0075 | PE(28:1)               | C33H65NO8P     | [M+H] <sup>+</sup>       |
| 634.45     | 634.4442     | 0.0075 | PE(28:0(OH))           | C33H65NO8P     | [M+H-H2O] <sup>+</sup>   |
| 634.45     | 634.4525     | 0.0007 | MGDG(24:1)             | C33H64NO10     | [M+NH4] <sup>+</sup>     |
| 634.45     | 634.4442     | 0.0075 | PA(30:2)               | C33H65NO8P     | [M+NH4] <sup>+</sup>     |
| 634.45     | 634.4556     | 0.0038 | PI(62:4)               | C71H131O13PNa2 | [M+2Na] <sup>2+</sup>    |
| 634.45     | 634.4453     | 0.0064 | PE(28:0)               | C33H65NO8P     | [M-H] <sup>-</sup>       |
| 634.45     | 634.4453     | 0.0064 | PE(P-28:0(OH))         | C33H65NO8P     | [M-H] <sup>-</sup>       |
| 634.45     | 634.4536     | 0.0018 | HexCer(d26:0)          | C33H64NO10     | [M+Formate] <sup>-</sup> |
| 634.45     | 634.4453     | 0.0064 | CerP(d32:1)            | C33H65NO8P     | [M+Formate] <sup>-</sup> |
| 634.45     | 634.4453     | 0.0064 | PC(26:0)               | C33H65NO8P     | [M-CH3] <sup>-</sup>     |
| 634.45     | 634.4453     | 0.0064 | PC(P-26:0(OH))         | C33H65NO8P     | [M-CH3] <sup>-</sup>     |
| 864.71     | 864.7204     | 0.0055 | PC(O-44:3)             | C52H99NO6P     | [M+H-H2O] <sup>+</sup>   |
| 864.71     | 864.7204     | 0.0055 | PC(P-44:2)             | C52H99NO6P     | [M+H-H2O] <sup>+</sup>   |
| 864.71     | 864.718      | 0.0031 | CerP(d50:1)            | C50H100NO6PNa  | [M+Na] <sup>+</sup>      |
| 864.71     | 864.7076     | 0.0074 | TG(52:8)               | C55H94NO6      | [M+NH4] <sup>+</sup>     |
| 864.71     | 864.7052     | 0.0098 | PG(O-42:1)             | C48H99NO9P     | [M+NH4] <sup>+</sup>     |
| 864.71     | 864.7052     | 0.0098 | PG(P-42:0)             | C48H99NO9P     | [M+NH4] <sup>+</sup>     |
| 678.48     | 678.4704     | 0.008  | PE(30:1(OH))           | C35H69NO9P     | [M+H] <sup>+</sup>       |
| 678.48     | 678.4857     | 0.0072 | LPE(34:5)              | C39H69NO6P     | [M+H-H2O] <sup>+</sup>   |
| 678.48     | 678.4857     | 0.0072 | PE(P-34:4)             | C39H69NO6P     | [M+H-H2O] <sup>+</sup>   |
| 678.48     | 678.4704     | 0.008  | PA(32:2(OH))           | C35H69NO9P     | [M+NH4] <sup>+</sup>     |
| 678.48     | 678.4858     | 0.0073 | CAR(34:6)              | C41H69NO4K     | [M+K] <sup>+</sup>       |
| 678.48     | 678.4716     | 0.0069 | PE(30:0(OH))           | C35H69NO9P     | [M-H] <sup>-</sup>       |
| 678.48     | 678.4717     | 0.0067 | HexCer(d30:1)          | C36H69NO8Cl    | [M+Cl] <sup>-</sup>      |

|        |          |        |                |              |              |
|--------|----------|--------|----------------|--------------|--------------|
| 678.48 | 678.4798 | 0.0013 | HexCer(t28:0)  | C35H68NO11   | [M+Formate]- |
| 678.48 | 678.4716 | 0.0069 | CerP(t34:1)    | C35H69NO9P   | [M+Formate]- |
| 678.48 | 678.4716 | 0.0069 | LPC(26:1)      | C35H69NO9P   | [M+Formate]- |
| 678.48 | 678.4716 | 0.0069 | PC(P-26:0)     | C35H69NO9P   | [M+Formate]- |
| 678.48 | 678.4716 | 0.0069 | LPE(28:1)      | C35H69NO9P   | [M+OAc]-     |
| 678.48 | 678.4716 | 0.0069 | PE(P-28:0)     | C35H69NO9P   | [M+OAc]-     |
| 678.48 | 678.4716 | 0.0069 | PC(28:0(OH))   | C35H69NO9P   | [M-CH3]-     |
| 678.48 | 678.4736 | 0.0049 | PIP(66:4)      | C75H138O16P2 | [M-2H]2-     |
| 651.37 | 651.3632 | 0.0035 | PA(30:4(OH))   | C33H57O9PNa  | [M+Na]+      |
| 651.37 | 651.3608 | 0.0059 | PA(28:1(OH))   | C31H59O9P    | [M+2Na-H]+   |
| 651.37 | 651.3668 | 0      | PA(32:6(OH))   | C35H56O9P    | [M-H]-       |
| 912.72 | 912.7204 | 0.0051 | PC(P-48:6)     | C56H99NO6P   | [M+H-H2O]+   |
| 912.72 | 912.7076 | 0.0078 | TG(56:12)      | C59H94NO6    | [M+NH4]+     |
| 912.72 | 912.7182 | 0.0029 | PE(O-46:0)     | C51H104NO7PK | [M+K]+       |
| 912.72 | 912.7156 | 0.0003 | CerP(d52:2)    | C52H102NO6P  | [M+2Na-H]+   |
| 912.72 | 912.7239 | 0.0085 | HexCer(d46:1)  | C52H101NO8   | [M+2Na-H]+   |
| 912.72 | 912.7063 | 0.009  | PS(O-46:2)     | C52H99NO9P   | [M-H]-       |
| 912.72 | 912.7063 | 0.009  | PS(P-46:1)     | C52H99NO9P   | [M-H]-       |
| 912.72 | 912.7063 | 0.009  | PE(O-46:3)     | C52H99NO9P   | [M+Formate]- |
| 912.72 | 912.7063 | 0.009  | PE(P-46:2)     | C52H99NO9P   | [M+Formate]- |
| 912.72 | 912.7145 | 0.0008 | HexCer(t44:2)  | C52H98NO11   | [M+OAc]-     |
| 912.72 | 912.7063 | 0.009  | PC(O-42:3)     | C52H99NO9P   | [M+OAc]-     |
| 912.72 | 912.7063 | 0.009  | PC(P-42:2)     | C52H99NO9P   | [M+OAc]-     |
| 742.54 | 742.5381 | 0.0008 | PE(36:3)       | C41H77NO8P   | [M+H]+       |
| 742.54 | 742.5381 | 0.0008 | PE(O-36:4(OH)) | C41H77NO8P   | [M+H]+       |
| 742.54 | 742.5381 | 0.0008 | PE(P-36:3(OH)) | C41H77NO8P   | [M+H]+       |
| 742.54 | 742.5381 | 0.0008 | PE(36:2(OH))   | C41H77NO8P   | [M+H-H2O]+   |
| 742.54 | 742.5357 | 0.0016 | PE(34:0)       | C39H78NO8PNa | [M+Na]+      |
| 742.54 | 742.5357 | 0.0016 | PE-NMe2(32:0)  | C39H78NO8PNa | [M+Na]+      |
| 742.54 | 742.5357 | 0.0016 | PE(O-34:1(OH)) | C39H78NO8PNa | [M+Na]+      |
| 742.54 | 742.5357 | 0.0016 | PE(P-34:0(OH)) | C39H78NO8PNa | [M+Na]+      |
| 742.54 | 742.5381 | 0.0008 | PA(38:4)       | C41H77NO8P   | [M+NH4]+     |
| 742.54 | 742.5381 | 0.0008 | PA(O-38:5(OH)) | C41H77NO8P   | [M+NH4]+     |
| 742.54 | 742.5381 | 0.0008 | PA(P-38:4(OH)) | C41H77NO8P   | [M+NH4]+     |
| 742.54 | 742.5464 | 0.0091 | MGDG(32:3)     | C41H76NO10   | [M+NH4]+     |
| 742.54 | 742.5325 | 0.0048 | CL(74:5)       | C83H154O17P2 | [M+2H]2+     |
| 742.54 | 742.5392 | 0.0019 | PE(36:2)       | C41H77NO8P   | [M-H]-       |
| 742.54 | 742.5392 | 0.0019 | PE(O-36:3(OH)) | C41H77NO8P   | [M-H]-       |
| 742.54 | 742.5392 | 0.0019 | PE(P-36:2(OH)) | C41H77NO8P   | [M-H]-       |
| 742.54 | 742.5392 | 0.0019 | CerP(d40:3)    | C41H77NO8P   | [M+Formate]- |
| 742.54 | 742.5392 | 0.0019 | PC(34:2)       | C41H77NO8P   | [M-CH3]-     |
| 742.54 | 742.5392 | 0.0019 | PC(O-34:3(OH)) | C41H77NO8P   | [M-CH3]-     |
| 742.54 | 742.5392 | 0.0019 | PC(P-34:2(OH)) | C41H77NO8P   | [M-CH3]-     |
| 742.54 | 742.5336 | 0.0037 | CL(74:3)       | C83H154O17P2 | [M-2H]2-     |
| 596.50 | 596.5037 | 0.006  | CAR(32:5)      | C39H66NO3    | [M+H-H2O]+   |
| 596.50 | 596.4969 | 0.0008 | PG(66:4)       | C72H137O10P  | [M+2H]2+     |
| 596.50 | 596.4896 | 0.0082 | Cer(t34:2)     | C35H66NO6    | [M+Formate]- |
| 596.50 | 596.4896 | 0.0082 | CAR(26:1)      | C35H66NO6    | [M+OAc]-     |
| 708.46 | 708.4599 | 0.0019 | PE(34:6)       | C39H67NO8P   | [M+H]+       |
| 708.46 | 708.4599 | 0.0019 | PE(34:5(OH))   | C39H67NO8P   | [M+H-H2O]+   |
| 708.46 | 708.4575 | 0.0005 | PE(32:3)       | C37H68NO8PNa | [M+Na]+      |
| 708.46 | 708.4599 | 0.0019 | PA(36:7)       | C39H67NO8P   | [M+NH4]+     |
| 708.46 | 708.4543 | 0.0037 | CL(70:11)      | C79H134O17P2 | [M+2H]2+     |
| 708.46 | 708.4551 | 0.0029 | PE(30:0)       | C35H70NO8P   | [M+2Na-H]+   |
| 708.46 | 708.4551 | 0.0029 | PE-NMe2(28:0)  | C35H70NO8P   | [M+2Na-H]+   |
| 708.46 | 708.4551 | 0.0029 | PE(O-30:1(OH)) | C35H70NO8P   | [M+2Na-H]+   |
| 708.46 | 708.4551 | 0.0029 | PE(P-30:0(OH)) | C35H70NO8P   | [M+2Na-H]+   |
| 708.46 | 708.461  | 0.003  | PE(34:5)       | C39H67NO8P   | [M-H]-       |
| 708.46 | 708.461  | 0.003  | PC(32:5)       | C39H67NO8P   | [M-CH3]-     |
| 708.46 | 708.4554 | 0.0026 | CL(70:9)       | C79H134O17P2 | [M-2H]2-     |
| 896.68 | 896.6869 | 0.0025 | CerP(t50:1)    | C50H100NO7PK | [M+K]+       |
| 896.68 | 896.6869 | 0.0025 | PC(O-42:1)     | C50H100NO7PK | [M+K]+       |
| 896.68 | 896.6869 | 0.0025 | PC(P-42:0)     | C50H100NO7PK | [M+K]+       |

|        |          |        |                       |                 |              |
|--------|----------|--------|-----------------------|-----------------|--------------|
| 896.68 | 896.675  | 0.0093 | PE(46:3(OH))          | C51H95NO9P      | [M-H]-       |
| 896.68 | 896.6881 | 0.0037 | PE(O-44:0(OH))        | C49H100NO8PCI   | [M+Cl]-      |
| 896.68 | 896.675  | 0.0093 | PC(O-42:4)            | C51H95NO9P      | [M+Formate]- |
| 896.68 | 896.675  | 0.0093 | PC(P-42:3)            | C51H95NO9P      | [M+Formate]- |
| 896.68 | 896.675  | 0.0093 | PE(O-44:4)            | C51H95NO9P      | [M+OAc]-     |
| 896.68 | 896.675  | 0.0093 | PE(P-44:3)            | C51H95NO9P      | [M+OAc]-     |
| 896.68 | 896.675  | 0.0093 | PC(44:3(OH))          | C51H95NO9P      | [M-CH3]-     |
| 776.57 | 776.58   | 0.0055 | PC(34:1(OH))          | C42H83NO9P      | [M+H]+       |
| 776.57 | 776.58   | 0.0055 | PS(O-36:1)            | C42H83NO9P      | [M+H]+       |
| 776.57 | 776.58   | 0.0055 | PS(P-36:0)            | C42H83NO9P      | [M+H]+       |
| 776.57 | 776.58   | 0.0055 | PS(O-36:0(OH))        | C42H83NO9P      | [M+H-H2O]+   |
| 776.57 | 776.58   | 0.0055 | PG(O-36:3)            | C42H83NO9P      | [M+NH4]+     |
| 776.57 | 776.58   | 0.0055 | PG(P-36:2)            | C42H83NO9P      | [M+NH4]+     |
| 776.57 | 776.5811 | 0.0066 | PS(O-36:0)            | C42H83NO9P      | [M-H]-       |
| 776.57 | 776.5811 | 0.0066 | PE(O-36:1)            | C42H83NO9P      | [M+Formate]- |
| 776.57 | 776.5811 | 0.0066 | PE(P-36:0)            | C42H83NO9P      | [M+Formate]- |
| 776.57 | 776.5811 | 0.0066 | CerP(t40:1)           | C42H83NO9P      | [M+OAc]-     |
| 776.57 | 776.5811 | 0.0066 | LPC(32:1)             | C42H83NO9P      | [M+OAc]-     |
| 776.57 | 776.5811 | 0.0066 | PC(O-32:1)            | C42H83NO9P      | [M+OAc]-     |
| 776.57 | 776.5811 | 0.0066 | PC(P-32:0)            | C42H83NO9P      | [M+OAc]-     |
| 989.70 | 989.6994 | 0.0018 | PA(58:12)             | C61H98O8P       | [M+H]+       |
| 989.70 | 989.7076 | 0.0065 | MGDG(52:11)           | C61H97O10       | [M+H]+       |
| 989.70 | 989.6994 | 0.0018 | PA(58:11(OH))         | C61H98O8P       | [M+H-H2O]+   |
| 989.70 | 989.7052 | 0.0041 | MGDG(50:8)            | C59H98O10Na     | [M+Na]+      |
| 989.70 | 989.697  | 0.0042 | PA(56:9)              | C59H99O8PNa     | [M+Na]+      |
| 989.70 | 989.6954 | 0.0058 | PS(50:8)              | C56H98N2O10P    | [M+NH4]+     |
| 989.70 | 989.6995 | 0.0017 | TG(60:12)             | C63H98O6K       | [M+K]+       |
| 989.70 | 989.6971 | 0.004  | PG(O-50:5)            | C56H103O9PK     | [M+K]+       |
| 989.70 | 989.6971 | 0.004  | PG(P-50:4)            | C56H103O9PK     | [M+K]+       |
| 989.70 | 989.7028 | 0.0017 | MGDG(48:5)            | C57H100O10      | [M+2Na-H]+   |
| 989.70 | 989.6946 | 0.0066 | PA(54:6)              | C57H101O8P      | [M+2Na-H]+   |
| 989.70 | 989.6946 | 0.0066 | PA(P-54:6(OH))        | C57H101O8P      | [M+2Na-H]+   |
| 989.70 | 989.7005 | 0.0007 | PA(58:11)             | C61H98O8P       | [M-H]-       |
| 989.70 | 989.7087 | 0.0076 | MGDG(52:10)           | C61H97O10       | [M-H]-       |
| 989.70 | 989.7064 | 0.0052 | PG(46:2(OH))          | C54H102O13P     | [M+OAc]-     |
| 365.27 | 365.2697 | 0      | FA(22:0(Ep2,cyclo))   | C22H37O4        | [M-H]-       |
| 365.27 | 365.2697 | 0      | FA(22:0(Ke2,cyclo))   | C22H37O4        | [M-H]-       |
| 365.27 | 365.2697 | 0      | FA(22:0(Ke,Ep,cyclo)) | C22H37O4        | [M-H]-       |
| 365.27 | 365.2697 | 0      | FA(22:1(Ep2))         | C22H37O4        | [M-H]-       |
| 365.27 | 365.2697 | 0      | FA(22:1(Ke2))         | C22H37O4        | [M-H]-       |
| 365.27 | 365.2697 | 0      | FA(22:1(Ke,Ep))       | C22H37O4        | [M-H]-       |
| 365.27 | 365.2697 | 0      | FA(22:1(OH,Ep,cyclo)) | C22H37O4        | [M-H]-       |
| 365.27 | 365.2697 | 0      | FA(22:1(OH,Ke,cyclo)) | C22H37O4        | [M-H]-       |
| 365.27 | 365.2697 | 0      | FA(22:2(OH2,cyclo))   | C22H37O4        | [M-H]-       |
| 365.27 | 365.2697 | 0      | FA(22:2(OH,Ep))       | C22H37O4        | [M-H]-       |
| 365.27 | 365.2697 | 0      | FA(22:2(OH,Ke))       | C22H37O4        | [M-H]-       |
| 365.27 | 365.2697 | 0      | FA(22:3(OH2))         | C22H37O4        | [M-H]-       |
| 365.27 | 365.2697 | 0      | WE(20:3)              | C22H37O4        | [M+OAc]-     |
| 365.27 | 365.2708 | 0.0011 | SQDG(54:2)            | C63H115O12S     | [M-3H]3-     |
| 365.27 | 365.267  | 0.0028 | PG(60:8)              | C66H112O10P     | [M-3H]3-     |
| 834.59 | 834.5937 | 0.0041 | LacCer(d32:1)         | C44H84NO13      | [M+H]+       |
| 834.59 | 834.5855 | 0.0042 | PI-Cer(d38:2)         | C44H85NO11P     | [M+H]+       |
| 834.59 | 834.5855 | 0.0042 | PS(38:1(OH))          | C44H85NO11P     | [M+H]+       |
| 834.59 | 834.5937 | 0.0041 | LacCer(t32:0)         | C44H84NO13      | [M+H-H2O]+   |
| 834.59 | 834.5855 | 0.0042 | PI-Cer(t38:1)         | C44H85NO11P     | [M+H-H2O]+   |
| 834.59 | 834.5983 | 0.0087 | PC(38:3)              | C46H86NO8PNa    | [M+Na]+      |
| 834.59 | 834.5983 | 0.0087 | PC(O-38:4(OH))        | C46H86NO8PNa    | [M+Na]+      |
| 834.59 | 834.5983 | 0.0087 | PC(P-38:3(OH))        | C46H86NO8PNa    | [M+Na]+      |
| 834.59 | 834.5855 | 0.0042 | PG(38:3(OH))          | C44H85NO11P     | [M+NH4]+     |
| 834.59 | 834.5927 | 0.0031 | CL(84:5)              | C93H172O17P2Na2 | [M+2Na]2+    |
| 834.59 | 834.5959 | 0.0063 | PC(36:0)              | C44H88NO8P      | [M+2Na-H]+   |
| 834.59 | 834.5959 | 0.0063 | PC(O-36:1(OH))        | C44H88NO8P      | [M+2Na-H]+   |
| 834.59 | 834.5959 | 0.0063 | PC(P-36:0(OH))        | C44H88NO8P      | [M+2Na-H]+   |

|        |          |        |               |              |              |
|--------|----------|--------|---------------|--------------|--------------|
| 834.59 | 834.5866 | 0.0031 | PI-Cer(d38:1) | C44H85NO11P  | [M-H]-       |
| 834.59 | 834.5866 | 0.0031 | PS(38:0(OH))  | C44H85NO11P  | [M-H]-       |
| 834.59 | 834.5948 | 0.0052 | LacCer(d32:0) | C44H84NO13   | [M-H]-       |
| 834.59 | 834.5866 | 0.0031 | PE(38:1(OH))  | C44H85NO11P  | [M+Formate]- |
| 834.59 | 834.5866 | 0.0031 | PC(34:1(OH))  | C44H85NO11P  | [M+OAc]-     |
| 834.59 | 834.5866 | 0.0031 | PS(O-36:1)    | C44H85NO11P  | [M+OAc]-     |
| 834.59 | 834.5866 | 0.0031 | PS(P-36:0)    | C44H85NO11P  | [M+OAc]-     |
| 384.19 | 384.1937 | 0.0002 | DGDG(20:1)    | C35H62O15Na2 | [M+2Na]2+    |
| 384.19 | 384.1972 | 0.0033 | DGDG(24:5)    | C39H60O15    | [M-2H]2-     |
| 932.57 | 932.5706 | 0.005  | MIPC(t32:0)   | C44H87NO17P  | [M+H]+       |
| 932.57 | 932.5566 | 0.009  | PE(48:11)     | C53H84NO8PK  | [M+K]+       |
| 932.57 | 932.5752 | 0.0096 | PE(46:8(OH))  | C51H86NO9P   | [M+2Na-H]+   |
| 932.57 | 932.5578 | 0.0079 | PC(44:10(OH)) | C52H84NO9PCI | [M+Cl]-      |
| 932.57 | 932.5658 | 0.0002 | PS(44:8)      | C51H83NO12P  | [M+Formate]- |

## Lipidomics 1: Plasma top neg log2fc candidate lipids

| Input Mass | Matched Mass | Delta  | Name                   | Formula        | Ion          |
|------------|--------------|--------|------------------------|----------------|--------------|
| 388.03     | 388.03       | 0.0004 | TG(74:2)               | C77H143O6      | [M-3H]3-     |
| 725.54     | 725.5327     | 0.0031 | PG(O-32:0(OH))         | C38H78O10P     | [M+H]+       |
| 725.54     | 725.5439     | 0.0082 | PE(32:0(OH))           | C37H78N2O9P    | [M+NH4]+     |
| 725.54     | 725.5455     | 0.0097 | DG(P-42:6)             | C45H76O4       | [M+2Na-H]+   |
| 725.54     | 725.537      | 0.0012 | PE-Cer(d36:0)          | C38H79N2O6PCl  | [M+Cl]-      |
| 725.54     | 725.5362     | 0.0004 | DG(40:7)               | C45H73O7       | [M+OAc]-     |
| 678.48     | 678.4704     | 0.008  | PE(30:1(OH))           | C35H69NO9P     | [M+H]+       |
| 678.48     | 678.4857     | 0.0072 | LPE(34:5)              | C39H69NO6P     | [M+H-H2O]+   |
| 678.48     | 678.4857     | 0.0072 | PE(P-34:4)             | C39H69NO6P     | [M+H-H2O]+   |
| 678.48     | 678.4704     | 0.008  | PA(32:2(OH))           | C35H69NO9P     | [M+NH4]+     |
| 678.48     | 678.4858     | 0.0073 | CAR(34:6)              | C41H69NO4K     | [M+K]+       |
| 678.48     | 678.4716     | 0.0069 | PE(30:0(OH))           | C35H69NO9P     | [M-H]-       |
| 678.48     | 678.4717     | 0.0067 | HexCer(d30:1)          | C36H69NO8Cl    | [M+Cl]-      |
| 678.48     | 678.4798     | 0.0013 | HexCer(t28:0)          | C35H68NO11     | [M+Formate]- |
| 678.48     | 678.4716     | 0.0069 | CerP(t34:1)            | C35H69NO9P     | [M+Formate]- |
| 678.48     | 678.4716     | 0.0069 | LPC(26:1)              | C35H69NO9P     | [M+Formate]- |
| 678.48     | 678.4716     | 0.0069 | PC(P-26:0)             | C35H69NO9P     | [M+Formate]- |
| 678.48     | 678.4716     | 0.0069 | LPE(28:1)              | C35H69NO9P     | [M+OAc]-     |
| 678.48     | 678.4716     | 0.0069 | PE(P-28:0)             | C35H69NO9P     | [M+OAc]-     |
| 678.48     | 678.4716     | 0.0069 | PC(28:0(OH))           | C35H69NO9P     | [M-CH3]-     |
| 678.48     | 678.4736     | 0.0049 | PIP(66:4)              | C75H138O16P2   | [M-2H]2-     |
| 483.36     | 483.3557     | 0.0084 | LysoSM(t18:0)          | C23H52N2O6P    | [M+H]+       |
| 483.36     | 483.3557     | 0.0084 | LPE(P-18:0)            | C23H52N2O6P    | [M+NH4]+     |
| 483.36     | 483.3557     | 0.0084 | PE(O-18:1)             | C23H52N2O6P    | [M+NH4]+     |
| 483.36     | 483.3557     | 0.0084 | PE(P-18:0)             | C23H52N2O6P    | [M+NH4]+     |
| 483.36     | 483.3599     | 0.0042 | WE(30:4)               | C30H52O2K      | [M+K]+       |
| 483.36     | 483.3639     | 0.0002 | PG(50:5)               | C56H103O10P    | [M+2H]2+     |
| 483.36     | 483.3639     | 0.0002 | PG(O-50:6(OH))         | C56H103O10P    | [M+2H]2+     |
| 483.36     | 483.3639     | 0.0002 | PG(P-50:5(OH))         | C56H103O10P    | [M+2H]2+     |
| 483.36     | 483.3615     | 0.0026 | PG(O-46:0(OH))         | C52H105O10PNa2 | [M+2Na]2+    |
| 483.36     | 483.3691     | 0.005  | FA(28:0(OH2,Ep2))      | C28H51O6       | [M-H]-       |
| 483.36     | 483.3691     | 0.005  | FA(28:0(OH2,Ke2))      | C28H51O6       | [M-H]-       |
| 483.36     | 483.3691     | 0.005  | FA(28:0(OH2,Ke,Ep))    | C28H51O6       | [M-H]-       |
| 483.36     | 483.3691     | 0.005  | FA(28:0(OH3,Ep,cyclo)) | C28H51O6       | [M-H]-       |
| 483.36     | 483.3691     | 0.005  | FA(28:0(OH3,Ke,cyclo)) | C28H51O6       | [M-H]-       |
| 483.36     | 483.3691     | 0.005  | FA(28:1(OH3,Ep))       | C28H51O6       | [M-H]-       |
| 483.36     | 483.3691     | 0.005  | FA(28:1(OH3,Ke))       | C28H51O6       | [M-H]-       |
| 483.36     | 483.3691     | 0.005  | FA(28:1(OH4,cyclo))    | C28H51O6       | [M-H]-       |
| 483.36     | 483.3691     | 0.005  | FA(28:2(OH4))          | C28H51O6       | [M-H]-       |
| 483.36     | 483.3691     | 0.005  | MG(24:2)               | C28H51O6       | [M+Formate]- |
| 483.36     | 483.365      | 0.0009 | PG(50:3)               | C56H103O10P    | [M-2H]2-     |
| 483.36     | 483.365      | 0.0009 | PG(O-50:4(OH))         | C56H103O10P    | [M-2H]2-     |
| 483.36     | 483.365      | 0.0009 | PG(P-50:3(OH))         | C56H103O10P    | [M-2H]2-     |
| 692.46     | 692.465      | 0.0024 | PE(34:5)               | C39H67NO7P     | [M+H-H2O]+   |
| 692.46     | 692.4626     | 0      | LPE(32:4)              | C37H68NO7PNa   | [M+Na]+      |
| 692.46     | 692.4602     | 0.0024 | LPE(30:1)              | C35H70NO7P     | [M+2Na-H]+   |
| 692.46     | 692.4602     | 0.0024 | PE(O-30:1)             | C35H70NO7P     | [M+2Na-H]+   |
| 692.46     | 692.4602     | 0.0024 | PE(P-30:0)             | C35H70NO7P     | [M+2Na-H]+   |
| 692.46     | 692.4661     | 0.0035 | LPE(34:6)              | C39H67NO7P     | [M-H]-       |
| 384.19     | 384.1937     | 0.0002 | DGDG(20:1)             | C35H62O15Na2   | [M+2Na]2+    |
| 384.19     | 384.1972     | 0.0033 | DGDG(24:5)             | C39H60O15      | [M-2H]2-     |
| 406.33     | 406.3316     | 0.0024 | CAR(16:2)              | C25H44NO3      | [M+H-H2O]+   |
| 406.33     | 406.3316     | 0.0024 | CAR(18:2)              | C25H44NO3      | [M+H-H2O]+   |
| 406.33     | 406.3312     | 0.002  | DG(O-48:6)             | C51H90O4Na2    | [M+2Na]2+    |
| 406.33     | 406.3312     | 0.002  | DG(P-48:5)             | C51H90O4Na2    | [M+2Na]2+    |
| 406.33     | 406.3261     | 0.003  | PC(68:8)               | C76H133NO8P    | [M-3H]3-     |
| 482.36     | 482.3605     | 0.0007 | LPC(O-16:0)            | C24H53NO6P     | [M+H]+       |
| 482.36     | 482.3662     | 0.005  | NAT(26:2)              | C28H52NO3S     | [M+H-H2O]+   |
| 482.36     | 482.3606     | 0.0006 | Cer(t26:0)             | C26H53NO4K     | [M+K]+       |



|        |          |        |                        |                 |              |
|--------|----------|--------|------------------------|-----------------|--------------|
| 482.36 | 482.3619 | 0.0007 | SQDG(44:0)             | C53H104O12S     | [M+2H]2+     |
| 482.36 | 482.3572 | 0.004  | PG(50:4)               | C56H101O10P     | [M-2H]2-     |
| 482.36 | 482.3572 | 0.004  | PG(O-50:5(OH))         | C56H101O10P     | [M-2H]2-     |
| 482.36 | 482.3572 | 0.004  | PG(P-50:4(OH))         | C56H101O10P     | [M-2H]2-     |
| 339.25 | 339.2541 | 0.0034 | FA(20:0(Ep2))          | C20H35O4        | [M-H]-       |
| 339.25 | 339.2541 | 0.0034 | FA(20:0(Ke2))          | C20H35O4        | [M-H]-       |
| 339.25 | 339.2541 | 0.0034 | FA(20:0(Ke,Ep))        | C20H35O4        | [M-H]-       |
| 339.25 | 339.2541 | 0.0034 | FA(20:0(OH,Ep,cyclo))  | C20H35O4        | [M-H]-       |
| 339.25 | 339.2541 | 0.0034 | FA(20:0(OH,Ke,cyclo))  | C20H35O4        | [M-H]-       |
| 339.25 | 339.2541 | 0.0034 | FA(20:1(OH2,cyclo))    | C20H35O4        | [M-H]-       |
| 339.25 | 339.2541 | 0.0034 | FA(20:1(OH,Ep))        | C20H35O4        | [M-H]-       |
| 339.25 | 339.2541 | 0.0034 | FA(20:1(OH,Ke))        | C20H35O4        | [M-H]-       |
| 339.25 | 339.2541 | 0.0034 | FA(20:2(OH2))          | C20H35O4        | [M-H]-       |
| 339.25 | 339.2541 | 0.0034 | WE(18:2)               | C20H35O4        | [M+OAc]-     |
| 339.25 | 339.2513 | 0.0006 | PG(54:5)               | C60H106O10P     | [M-3H]3-     |
| 339.25 | 339.2513 | 0.0006 | PG(O-54:6(OH))         | C60H106O10P     | [M-3H]3-     |
| 339.25 | 339.2513 | 0.0006 | PG(P-54:5(OH))         | C60H106O10P     | [M-3H]3-     |
| 634.45 | 634.4442 | 0.0075 | PE(28:1)               | C33H65NO8P      | [M+H]+       |
| 634.45 | 634.4442 | 0.0075 | PE(28:0(OH))           | C33H65NO8P      | [M+H-H2O]+   |
| 634.45 | 634.4525 | 0.0007 | MGDG(24:1)             | C33H64NO10      | [M+NH4]+     |
| 634.45 | 634.4442 | 0.0075 | PA(30:2)               | C33H65NO8P      | [M+NH4]+     |
| 634.45 | 634.4556 | 0.0038 | PI(62:4)               | C71H131O13PNa2  | [M+2Na]2+    |
| 634.45 | 634.4453 | 0.0064 | PE(28:0)               | C33H65NO8P      | [M-H]-       |
| 634.45 | 634.4453 | 0.0064 | PE(P-28:0(OH))         | C33H65NO8P      | [M-H]-       |
| 634.45 | 634.4536 | 0.0018 | HexCer(d26:0)          | C33H64NO10      | [M+Formate]- |
| 634.45 | 634.4453 | 0.0064 | CerP(d32:1)            | C33H65NO8P      | [M+Formate]- |
| 634.45 | 634.4453 | 0.0064 | PC(26:0)               | C33H65NO8P      | [M-CH3]-     |
| 634.45 | 634.4453 | 0.0064 | PC(P-26:0(OH))         | C33H65NO8P      | [M-CH3]-     |
| 651.37 | 651.3632 | 0.0035 | PA(30:4(OH))           | C33H57O9PNa     | [M+Na]+      |
| 651.37 | 651.3608 | 0.0059 | PA(28:1(OH))           | C31H59O9P       | [M+2Na-H]+   |
| 651.37 | 651.3668 | 0      | PA(32:6(OH))           | C35H56O9P       | [M-H]-       |
| 576.38 | 576.3742 | 0.0057 | MGDG(20:2)             | C29H54NO10      | [M+NH4]+     |
| 576.38 | 576.379  | 0.0009 | LPC(O-20:0)            | C28H60NO6PK     | [M+K]+       |
| 576.38 | 576.3797 | 0.0002 | PI(58:12)              | C67H109O13P     | [M+2H]2+     |
| 576.38 | 576.3839 | 0.004  | DGDG(52:11)            | C67H108O15      | [M+2H]2+     |
| 576.38 | 576.3815 | 0.0016 | DGDG(48:5)             | C63H110O15Na2   | [M+2Na]2+    |
| 576.38 | 576.3773 | 0.0026 | PI(54:6)               | C63H111O13PNa2  | [M+2Na]2+    |
| 576.38 | 576.3773 | 0.0026 | PI(P-54:6(OH))         | C63H111O13PNa2  | [M+2Na]2+    |
| 576.38 | 576.3808 | 0.0009 | PI(58:10)              | C67H109O13P     | [M-2H]2-     |
| 596.50 | 596.5037 | 0.006  | CAR(32:5)              | C39H66NO3       | [M+H-H2O]+   |
| 596.50 | 596.4969 | 0.0008 | PG(66:4)               | C72H137O10P     | [M+2H]2+     |
| 596.50 | 596.4896 | 0.0082 | Cer(t34:2)             | C35H66NO6       | [M+Formate]- |
| 596.50 | 596.4896 | 0.0082 | CAR(26:1)              | C35H66NO6       | [M+OAc]-     |
| 495.41 | 495.4035 | 0.0022 | SM(t50:0)              | C55H113N2O7PNa2 | [M+2Na]2+    |
| 495.41 | 495.4148 | 0.0091 | WE(30:1)               | C30H58O2        | [M+2Na-H]+   |
| 495.41 | 495.4055 | 0.0002 | FA(30:0(OH2,Ep,cyclo)) | C30H55O5        | [M-H]-       |
| 495.41 | 495.4055 | 0.0002 | FA(30:0(OH2,Ke,cyclo)) | C30H55O5        | [M-H]-       |
| 495.41 | 495.4055 | 0.0002 | FA(30:0(OH,Ep2))       | C30H55O5        | [M-H]-       |
| 495.41 | 495.4055 | 0.0002 | FA(30:0(OH,Ke2))       | C30H55O5        | [M-H]-       |
| 495.41 | 495.4055 | 0.0002 | FA(30:0(OH,Ke,Ep))     | C30H55O5        | [M-H]-       |
| 495.41 | 495.4055 | 0.0002 | FA(30:1(OH2,Ep))       | C30H55O5        | [M-H]-       |
| 495.41 | 495.4055 | 0.0002 | FA(30:1(OH2,Ke))       | C30H55O5        | [M-H]-       |
| 495.41 | 495.4055 | 0.0002 | FA(30:1(OH3,cyclo))    | C30H55O5        | [M-H]-       |
| 495.41 | 495.4055 | 0.0002 | FA(30:2(OH3))          | C30H55O5        | [M-H]-       |
| 495.41 | 495.4026 | 0.0032 | DG(64:12)              | C67H106O5       | [M-2H]2-     |
| 495.41 | 495.4026 | 0.0032 | TG(O-64:12)            | C67H106O5       | [M-2H]2-     |
| 495.41 | 495.4026 | 0.0032 | TG(P-64:11)            | C67H106O5       | [M-2H]2-     |
| 411.38 | 411.3844 | 0.0001 | FA(26:0(OH))           | C26H51O3        | [M-H]-       |

Lipidomics 1: Plasma top pos log2fc candidate lipids

| Input Mass | Matched Mass | Delta  | Name                | Formula         | Ion          |
|------------|--------------|--------|---------------------|-----------------|--------------|
| 702.50     | 702.5044     | 0.0086 | PC(O-28:0(OH))      | C36H74NO8PNa    | [M+Na]+      |
| 873.65     | 873.6432     | 0.01   | SM(t42:2)           | C47H93N2O7P     | [M+2Na-H]+   |
| 873.65     | 873.6622     | 0.009  | SM(d44:3)           | C49H95N2O6PCI   | [M+Cl]-      |
| 873.65     | 873.6614     | 0.0082 | DG(52:10)           | C56H89O7        | [M+Formate]- |
| 873.65     | 873.659      | 0.0059 | PA(44:1)            | C49H94O10P      | [M+OAc]-     |
| 873.65     | 873.659      | 0.0059 | PA(O-44:2(OH))      | C49H94O10P      | [M+OAc]-     |
| 873.65     | 873.659      | 0.0059 | PA(P-44:1(OH))      | C49H94O10P      | [M+OAc]-     |
| 676.47     | 676.47       | 0.0016 | LPE(34:6)           | C39H67NO6P      | [M+H-H2O]+   |
| 676.47     | 676.4641     | 0.0043 | HexCer(t28:1)       | C35H66NO11      | [M+Formate]- |
| 283.26     | 283.2632     | 0.0012 | WE(18:1)            | C18H35O2        | [M+H]+       |
| 283.26     | 283.2632     | 0.0012 | FAHFA(O-36:1)       | C36H70O4        | [M+2H]2+     |
| 283.26     | 283.2643     | 0.0001 | FA(18:0)            | C18H35O2        | [M-H]-       |
| 283.26     | 283.2643     | 0.0001 | WE(18:0)            | C18H35O2        | [M-H]-       |
| 513.42     | 513.4217     | 0.0018 | SM(d54:2)           | C59H117N2O6PNa2 | [M+2Na]2+    |
| 513.42     | 513.4161     | 0.0038 | FA(30:0(OH3,Ep))    | C30H57O6        | [M-H]-       |
| 513.42     | 513.4161     | 0.0038 | FA(30:0(OH3,Ke))    | C30H57O6        | [M-H]-       |
| 513.42     | 513.4161     | 0.0038 | FA(30:0(OH4,cyclo)) | C30H57O6        | [M-H]-       |
| 513.42     | 513.4161     | 0.0038 | FA(30:1(OH4))       | C30H57O6        | [M-H]-       |
| 513.42     | 513.4161     | 0.0038 | DG(P-26:0)          | C30H57O6        | [M+Formate]- |
| 513.42     | 513.4161     | 0.0038 | MG(26:1)            | C30H57O6        | [M+Formate]- |
| 805.61     | 805.6065     | 0.0024 | PE(38:2(OH))        | C43H86N2O9P     | [M+NH4]+     |
| 805.61     | 805.617      | 0.008  | SM(d38:0)           | C43H89N2O6P     | [M+2Na-H]+   |
| 805.61     | 805.6118     | 0.0029 | TG(46:4)            | C49H86O6Cl      | [M+Cl]-      |
| 805.61     | 805.5996     | 0.0094 | PE-Cer(d42:2)       | C44H87N2O6PCI   | [M+Cl]-      |
| 805.61     | 805.6077     | 0.0013 | PE-Cer(t40:1)       | C43H86N2O9P     | [M+Formate]- |
| 805.61     | 805.6077     | 0.0013 | SM(t36:1)           | C43H86N2O9P     | [M+OAc]-     |
| 864.71     | 864.7204     | 0.0055 | PC(O-44:3)          | C52H99NO6P      | [M+H-H2O]+   |
| 864.71     | 864.7204     | 0.0055 | PC(P-44:2)          | C52H99NO6P      | [M+H-H2O]+   |
| 864.71     | 864.718      | 0.0031 | CerP(d50:1)         | C50H100NO6PNa   | [M+Na]+      |
| 864.71     | 864.7076     | 0.0074 | TG(52:8)            | C55H94NO6       | [M+NH4]+     |
| 864.71     | 864.7052     | 0.0098 | PG(O-42:1)          | C48H99NO9P      | [M+NH4]+     |
| 864.71     | 864.7052     | 0.0098 | PG(P-42:0)          | C48H99NO9P      | [M+NH4]+     |
| 911.71     | 911.7099     | 0.0017 | PA(50:3(OH))        | C53H100O9P      | [M+H]+       |
| 911.71     | 911.7075     | 0.0007 | PA(48:0(OH))        | C51H101O9PNa    | [M+Na]+      |
| 911.71     | 911.7059     | 0.0023 | PI-Cer(d42:0)       | C48H100N2O11P   | [M+NH4]+     |
| 911.71     | 911.7111     | 0.0028 | PA(50:2(OH))        | C53H100O9P      | [M-H]-       |
| 911.71     | 911.7111     | 0.0028 | PA(O-48:3)          | C53H100O9P      | [M+OAc]-     |
| 911.71     | 911.7111     | 0.0028 | PA(P-48:2)          | C53H100O9P      | [M+OAc]-     |
| 896.68     | 896.6869     | 0.0025 | CerP(t50:1)         | C50H100NO7PK    | [M+K]+       |
| 896.68     | 896.6869     | 0.0025 | PC(O-42:1)          | C50H100NO7PK    | [M+K]+       |
| 896.68     | 896.6869     | 0.0025 | PC(P-42:0)          | C50H100NO7PK    | [M+K]+       |
| 896.68     | 896.675      | 0.0093 | PE(46:3(OH))        | C51H95NO9P      | [M-H]-       |
| 896.68     | 896.6881     | 0.0037 | PE(O-44:0(OH))      | C49H100NO8PCI   | [M+Cl]-      |
| 896.68     | 896.675      | 0.0093 | PC(O-42:4)          | C51H95NO9P      | [M+Formate]- |
| 896.68     | 896.675      | 0.0093 | PC(P-42:3)          | C51H95NO9P      | [M+Formate]- |
| 896.68     | 896.675      | 0.0093 | PE(O-44:4)          | C51H95NO9P      | [M+OAc]-     |
| 896.68     | 896.675      | 0.0093 | PE(P-44:3)          | C51H95NO9P      | [M+OAc]-     |
| 896.68     | 896.675      | 0.0093 | PC(44:3(OH))        | C51H95NO9P      | [M-CH3]-     |
| 912.72     | 912.7204     | 0.0051 | PC(P-48:6)          | C56H99NO6P      | [M+H-H2O]+   |
| 912.72     | 912.7076     | 0.0078 | TG(56:12)           | C59H94NO6       | [M+NH4]+     |
| 912.72     | 912.7182     | 0.0029 | PE(O-46:0)          | C51H104NO7PK    | [M+K]+       |
| 912.72     | 912.7156     | 0.0003 | CerP(d52:2)         | C52H102NO6P     | [M+2Na-H]+   |
| 912.72     | 912.7239     | 0.0085 | HexCer(d46:1)       | C52H101NO8      | [M+2Na-H]+   |
| 912.72     | 912.7063     | 0.009  | PS(O-46:2)          | C52H99NO9P      | [M-H]-       |
| 912.72     | 912.7063     | 0.009  | PS(P-46:1)          | C52H99NO9P      | [M-H]-       |
| 912.72     | 912.7063     | 0.009  | PE(O-46:3)          | C52H99NO9P      | [M+Formate]- |
| 912.72     | 912.7063     | 0.009  | PE(P-46:2)          | C52H99NO9P      | [M+Formate]- |
| 912.72     | 912.7145     | 0.0008 | HexCer(t44:2)       | C52H98NO11      | [M+OAc]-     |
| 912.72     | 912.7063     | 0.009  | PC(O-42:3)          | C52H99NO9P      | [M+OAc]-     |

|        |          |        |                       |              |              |
|--------|----------|--------|-----------------------|--------------|--------------|
| 912.72 | 912.7063 | 0.009  | PC(P-42:2)            | C52H99NO9P   | [M+OAc]-     |
| 369.35 | 369.3475 | 0.0038 | NAE(20:2)             | C22H45N2O2   | [M+NH4]+     |
| 369.35 | 369.3545 | 0.0032 | DG(44:0)              | C47H94O5     | [M+2H]2+     |
| 369.35 | 369.3545 | 0.0032 | TG(O-44:0)            | C47H94O5     | [M+2H]2+     |
| 499.38 | 499.3793 | 0.0037 | FA(32:3(Ep2,cyclo))   | C32H51O4     | [M-H]-       |
| 499.38 | 499.3793 | 0.0037 | FA(32:3(Ke2,cyclo))   | C32H51O4     | [M-H]-       |
| 499.38 | 499.3793 | 0.0037 | FA(32:3(Ke,Ep,cyclo)) | C32H51O4     | [M-H]-       |
| 499.38 | 499.3793 | 0.0037 | FA(32:4(Ep2))         | C32H51O4     | [M-H]-       |
| 499.38 | 499.3793 | 0.0037 | FA(32:4(Ke2))         | C32H51O4     | [M-H]-       |
| 499.38 | 499.3793 | 0.0037 | FA(32:4(Ke,Ep))       | C32H51O4     | [M-H]-       |
| 499.38 | 499.3793 | 0.0037 | FA(32:4(OH,Ep,cyclo)) | C32H51O4     | [M-H]-       |
| 499.38 | 499.3793 | 0.0037 | FA(32:4(OH,Ke,cyclo)) | C32H51O4     | [M-H]-       |
| 499.38 | 499.3793 | 0.0037 | FA(32:5(OH2,cyclo))   | C32H51O4     | [M-H]-       |
| 499.38 | 499.3793 | 0.0037 | FA(32:5(OH,Ep))       | C32H51O4     | [M-H]-       |
| 499.38 | 499.3793 | 0.0037 | FA(32:5(OH,Ke))       | C32H51O4     | [M-H]-       |
| 499.38 | 499.3793 | 0.0037 | FA(32:6(OH2))         | C32H51O4     | [M-H]-       |
| 776.57 | 776.58   | 0.0055 | PC(34:1(OH))          | C42H83NO9P   | [M+H]+       |
| 776.57 | 776.58   | 0.0055 | PS(O-36:1)            | C42H83NO9P   | [M+H]+       |
| 776.57 | 776.58   | 0.0055 | PS(P-36:0)            | C42H83NO9P   | [M+H]+       |
| 776.57 | 776.58   | 0.0055 | PS(O-36:0(OH))        | C42H83NO9P   | [M+H-H2O]+   |
| 776.57 | 776.58   | 0.0055 | PG(O-36:3)            | C42H83NO9P   | [M+NH4]+     |
| 776.57 | 776.58   | 0.0055 | PG(P-36:2)            | C42H83NO9P   | [M+NH4]+     |
| 776.57 | 776.5811 | 0.0066 | PS(O-36:0)            | C42H83NO9P   | [M-H]-       |
| 776.57 | 776.5811 | 0.0066 | PE(O-36:1)            | C42H83NO9P   | [M+Formate]- |
| 776.57 | 776.5811 | 0.0066 | PE(P-36:0)            | C42H83NO9P   | [M+Formate]- |
| 776.57 | 776.5811 | 0.0066 | CerP(t40:1)           | C42H83NO9P   | [M+OAc]-     |
| 776.57 | 776.5811 | 0.0066 | LPC(32:1)             | C42H83NO9P   | [M+OAc]-     |
| 776.57 | 776.5811 | 0.0066 | PC(O-32:1)            | C42H83NO9P   | [M+OAc]-     |
| 776.57 | 776.5811 | 0.0066 | PC(P-32:0)            | C42H83NO9P   | [M+OAc]-     |
| 591.43 | 591.432  | 0.0032 | PI(58:5(OH))          | C67H123O14P  | [M+2H]2+     |
| 591.43 | 591.4278 | 0.001  | TG(74:17)             | C77H116O6Na2 | [M+2Na]2+    |
| 591.43 | 591.436  | 0.0072 | MG(32:4)              | C35H62O4     | [M+2Na-H]+   |
| 591.43 | 591.4266 | 0.0021 | DG(30:4)              | C35H59O7     | [M+OAc]-     |
| 591.43 | 591.4331 | 0.0043 | PI(58:3(OH))          | C67H123O14P  | [M-2H]2-     |
| 678.48 | 678.4704 | 0.008  | PE(30:1(OH))          | C35H69NO9P   | [M+H]+       |
| 678.48 | 678.4857 | 0.0072 | LPE(34:5)             | C39H69NO6P   | [M+H-H2O]+   |
| 678.48 | 678.4857 | 0.0072 | PE(P-34:4)            | C39H69NO6P   | [M+H-H2O]+   |
| 678.48 | 678.4704 | 0.008  | PA(32:2(OH))          | C35H69NO9P   | [M+NH4]+     |
| 678.48 | 678.4858 | 0.0074 | CAR(34:6)             | C41H69NO4K   | [M+K]+       |
| 678.48 | 678.4716 | 0.0069 | PE(30:0(OH))          | C35H69NO9P   | [M-H]-       |
| 678.48 | 678.4717 | 0.0067 | HexCer(d30:1)         | C36H69NO8Cl  | [M+Cl]-      |
| 678.48 | 678.4798 | 0.0013 | HexCer(t28:0)         | C35H68NO11   | [M+Formate]- |
| 678.48 | 678.4716 | 0.0069 | CerP(t34:1)           | C35H69NO9P   | [M+Formate]- |
| 678.48 | 678.4716 | 0.0069 | LPC(26:1)             | C35H69NO9P   | [M+Formate]- |
| 678.48 | 678.4716 | 0.0069 | PC(P-26:0)            | C35H69NO9P   | [M+Formate]- |
| 678.48 | 678.4716 | 0.0069 | LPE(28:1)             | C35H69NO9P   | [M+OAc]-     |
| 678.48 | 678.4716 | 0.0069 | PE(P-28:0)            | C35H69NO9P   | [M+OAc]-     |
| 678.48 | 678.4716 | 0.0069 | PC(28:0(OH))          | C35H69NO9P   | [M-CH3]-     |
| 678.48 | 678.4736 | 0.0049 | PIP(66:4)             | C75H138O16P2 | [M-2H]2-     |
| 932.57 | 932.5706 | 0.005  | MIPC(t32:0)           | C44H87NO17P  | [M+H]+       |
| 932.57 | 932.5566 | 0.009  | PE(48:11)             | C53H84NO8PK  | [M+K]+       |
| 932.57 | 932.5752 | 0.0096 | PE(46:8(OH))          | C51H86NO9P   | [M+2Na-H]+   |
| 932.57 | 932.5578 | 0.0079 | PC(44:10(OH))         | C52H84NO9PCI | [M+Cl]-      |
| 932.57 | 932.5658 | 0.0002 | PS(44:8)              | C51H83NO12P  | [M+Formate]- |
| 989.70 | 989.6994 | 0.0018 | PA(58:12)             | C61H98O8P    | [M+H]+       |
| 989.70 | 989.7076 | 0.0065 | MGDG(52:11)           | C61H97O10    | [M+H]+       |
| 989.70 | 989.6994 | 0.0018 | PA(58:11(OH))         | C61H98O8P    | [M+H-H2O]+   |
| 989.70 | 989.7052 | 0.0041 | MGDG(50:8)            | C59H98O10Na  | [M+Na]+      |
| 989.70 | 989.697  | 0.0042 | PA(56:9)              | C59H99O8PNa  | [M+Na]+      |
| 989.70 | 989.6954 | 0.0058 | PS(50:8)              | C56H98N2O10P | [M+NH4]+     |
| 989.70 | 989.6995 | 0.0017 | TG(60:12)             | C63H98O6K    | [M+K]+       |
| 989.70 | 989.6971 | 0.004  | PG(O-50:5)            | C56H103O9PK  | [M+K]+       |
| 989.70 | 989.6971 | 0.004  | PG(P-50:4)            | C56H103O9PK  | [M+K]+       |

|        |          |        |                |             |                        |
|--------|----------|--------|----------------|-------------|------------------------|
| 989.70 | 989.7028 | 0.0017 | MGDG(48:5)     | C57H100O10  | [M+2Na-H] <sup>+</sup> |
| 989.70 | 989.6946 | 0.0066 | PA(54:6)       | C57H101O8P  | [M+2Na-H] <sup>+</sup> |
| 989.70 | 989.6946 | 0.0066 | PA(P-54:6(OH)) | C57H101O8P  | [M+2Na-H] <sup>+</sup> |
| 989.70 | 989.7005 | 0.0007 | PA(58:11)      | C61H98O8P   | [M-H] <sup>-</sup>     |
| 989.70 | 989.7087 | 0.0076 | MGDG(52:10)    | C61H97O10   | [M-H] <sup>-</sup>     |
| 989.70 | 989.7064 | 0.0052 | PG(46:2(OH))   | C54H102O13P | [M+OAc] <sup>-</sup>   |

**Lipidomics 1: Urine top pvalue candidate lipids**

| Input Mass | Matched Mass | Delta  | Name                  | Formula       | Ion          |
|------------|--------------|--------|-----------------------|---------------|--------------|
| 195.07     | 195.0663     | 0.0003 | FA(10:1(Ep2,cyclo))   | C10H11O4      | [M-H]-       |
| 195.07     | 195.0663     | 0.0003 | FA(10:1(Ke2,cyclo))   | C10H11O4      | [M-H]-       |
| 195.07     | 195.0663     | 0.0003 | FA(10:1(Ke,Ep,cyclo)) | C10H11O4      | [M-H]-       |
| 195.07     | 195.0663     | 0.0003 | FA(10:2(Ep2))         | C10H11O4      | [M-H]-       |
| 195.07     | 195.0663     | 0.0003 | FA(10:2(Ke2))         | C10H11O4      | [M-H]-       |
| 195.07     | 195.0663     | 0.0003 | FA(10:2(Ke,Ep))       | C10H11O4      | [M-H]-       |
| 195.07     | 195.0663     | 0.0003 | FA(10:2(OH,Ep,cyclo)) | C10H11O4      | [M-H]-       |
| 195.07     | 195.0663     | 0.0003 | FA(10:2(OH,Ke,cyclo)) | C10H11O4      | [M-H]-       |
| 926.64     | 926.6399     | 0.0029 | PE(P-48:6)            | C53H94NO7PK   | [M+K]+       |
| 926.64     | 926.6411     | 0.0017 | PC(44:5)              | C52H94NO8PCI  | [M+Cl]-      |
| 926.64     | 926.6411     | 0.0017 | PC(O-44:6(OH))        | C52H94NO8PCI  | [M+Cl]-      |
| 926.64     | 926.6411     | 0.0017 | PC(P-44:5(OH))        | C52H94NO8PCI  | [M+Cl]-      |
| 926.64     | 926.6341     | 0.0088 | LacCer(d36:0)         | C48H93NO13Cl  | [M+Cl]-      |
| 926.64     | 926.6492     | 0.0063 | PC(42:4(OH))          | C51H93NO11P   | [M+Formate]- |
| 926.64     | 926.6492     | 0.0063 | PS(O-44:4)            | C51H93NO11P   | [M+Formate]- |
| 926.64     | 926.6492     | 0.0063 | PS(P-44:3)            | C51H93NO11P   | [M+Formate]- |
| 926.64     | 926.6339     | 0.0089 | PI-Cer(t40:0)         | C47H93NO14P   | [M+Formate]- |
| 926.64     | 926.6492     | 0.0063 | PE(44:4(OH))          | C51H93NO11P   | [M+OAc]-     |
| 700.31     | 700.307      | 0.0071 | MIPC(m16:0)           | C28H56NO14PK  | [M+K]+       |
| 452.39     | 452.3924     | 0.0025 | PA(O-50:0(OH))        | C53H109O8P    | [M+2H]2+     |
| 452.39     | 452.3981     | 0.0031 | PE-Cer(t50:0)         | C52H109N2O7P  | [M+2H]2+     |
| 452.39     | 452.3989     | 0.0039 | WE(60:7)              | C60H106O2Na2  | [M+2Na]2+    |
| 299.13     | 299.1289     | 0.0033 | FA(18:5(Ep2,cyclo))   | C18H19O4      | [M-H]-       |
| 299.13     | 299.1289     | 0.0033 | FA(18:5(Ke2,cyclo))   | C18H19O4      | [M-H]-       |
| 299.13     | 299.1289     | 0.0033 | FA(18:5(Ke,Ep,cyclo)) | C18H19O4      | [M-H]-       |
| 597.01     | 597.0127     | 0.002  | PC(64:3(OH))          | C72H140NO9P   | [M+2H]2+     |
| 597.01     | 597.0138     | 0.0031 | PC(64:1(OH))          | C72H140NO9P   | [M-2H]2-     |
| 628.59     | 628.5874     | 0.0001 | Cer(t38:0(OH))        | C38H78NO5     | [M+H]+       |
| 250.18     | 250.1733     | 0.0042 | LPG(O-18:0)           | C24H53O8P     | [M+2H]2+     |
| 501.38     | 501.3797     | 0.0035 | PG(O-50:2)            | C56H109O9PNa2 | [M+2Na]2+    |
| 501.38     | 501.3797     | 0.0035 | PG(P-50:1)            | C56H109O9PNa2 | [M+2Na]2+    |
| 501.38     | 501.3809     | 0.0047 | TG(60:9)              | C63H104O6Na2  | [M+2Na]2+    |
| 501.38     | 501.3797     | 0.0035 | FA(28:0(OH4,Ep))      | C28H53O7      | [M-H]-       |
| 501.38     | 501.3797     | 0.0035 | FA(28:0(OH4,Ke))      | C28H53O7      | [M-H]-       |
| 501.38     | 501.3716     | 0.0045 | MG(26:2)              | C29H54O4Cl    | [M+Cl]-      |
| 501.38     | 501.3797     | 0.0035 | DG(24:0)              | C28H53O7      | [M+Formate]- |
| 756.63     | 756.6348     | 0.0002 | HexCer(d38:1)         | C44H86NO8     | [M+H]+       |
| 756.63     | 756.6265     | 0.0084 | CerP(d44:2)           | C44H87NO6P    | [M+H]+       |
| 756.63     | 756.6348     | 0.0002 | HexCer(t38:0)         | C44H86NO8     | [M+H-H2O]+   |
| 756.63     | 756.6265     | 0.0084 | CerP(t44:1)           | C44H87NO6P    | [M+H-H2O]+   |
| 756.63     | 756.6265     | 0.0084 | PC(O-36:1)            | C44H87NO6P    | [M+H-H2O]+   |
| 756.63     | 756.6265     | 0.0084 | PC(P-36:0)            | C44H87NO6P    | [M+H-H2O]+   |
| 756.63     | 756.6359     | 0.0009 | HexCer(d38:0)         | C44H86NO8     | [M-H]-       |
| 756.63     | 756.6277     | 0.0073 | CerP(d44:1)           | C44H87NO6P    | [M-H]-       |
| 779.62     | 779.6273     | 0.0076 | PC(34:0)              | C42H88N2O8P   | [M+NH4]+     |
| 779.62     | 779.6273     | 0.0076 | PC(O-34:1(OH))        | C42H88N2O8P   | [M+NH4]+     |
| 779.62     | 779.6273     | 0.0076 | PC(P-34:0(OH))        | C42H88N2O8P   | [M+NH4]+     |
| 779.62     | 779.6273     | 0.0076 | PE-NMe(36:0)          | C42H88N2O8P   | [M+NH4]+     |
| 779.62     | 779.6103     | 0.0094 | WE(52:10)             | C52H84O2K     | [M+K]+       |
| 426.29     | 426.287      | 0.0016 | MGDG(42:10)           | C51H80O10     | [M+2H]2+     |
| 426.29     | 426.2829     | 0.0025 | PA(48:11)             | C51H81O8P     | [M+2H]2+     |
| 426.29     | 426.2846     | 0.0008 | MGDG(38:4)            | C47H82O10Na2  | [M+2Na]2+    |
| 426.29     | 426.2805     | 0.005  | PA(44:5)              | C47H83O8PNa2  | [M+2Na]2+    |
| 426.29     | 426.2805     | 0.005  | PA(O-44:6(OH))        | C47H83O8PNa2  | [M+2Na]2+    |
| 426.29     | 426.2805     | 0.005  | PA(P-44:5(OH))        | C47H83O8PNa2  | [M+2Na]2+    |
| 426.29     | 426.2861     | 0.0007 | CAR(14:2)             | C23H40NO6     | [M+OAc]-     |
| 426.29     | 426.284      | 0.0014 | PA(48:9)              | C51H81O8P     | [M-2H]2-     |
| 426.29     | 426.2881     | 0.0027 | MGDG(42:8)            | C51H80O10     | [M-2H]2-     |
| 778.62     | 778.6109     | 0.0041 | PC(O-38:4)            | C46H85NO6P    | [M+H-H2O]+   |
| 778.62     | 778.6109     | 0.0041 | PC(P-38:3)            | C46H85NO6P    | [M+H-H2O]+   |

|        |          |        |                     |               |            |
|--------|----------|--------|---------------------|---------------|------------|
| 778.62 | 778.6167 | 0.0017 | HexCer(d38:1)       | C44H85NO8Na   | [M+Na]+    |
| 778.62 | 778.6085 | 0.0065 | CerP(d44:2)         | C44H86NO6PNa  | [M+Na]+    |
| 778.62 | 778.6202 | 0.0052 | HexCer(d40:3)       | C46H84NO8     | [M-H]-     |
| 300.13 | 300.1207 | 0.0084 | LPC(2:0)            | C10H23NO7P    | [M+H]+     |
| 537.39 | 537.3914 | 0.0031 | MG(30:6)            | C33H54O4Na    | [M+Na]+    |
| 537.39 | 537.3979 | 0.0034 | PA(60:6)            | C63H113O8PNa2 | [M+2Na]2+  |
| 537.39 | 537.389  | 0.0055 | MG(28:3)            | C31H56O4      | [M+2Na-H]+ |
| 201.12 | 201.1132 | 0.0025 | FA(10:0(OH2,cyclo)) | C10H17O4      | [M-H]-     |
| 201.12 | 201.1132 | 0.0025 | FA(10:0(OH,Ep))     | C10H17O4      | [M-H]-     |
| 201.12 | 201.1132 | 0.0025 | FA(10:0(OH,Ke))     | C10H17O4      | [M-H]-     |
| 201.12 | 201.1132 | 0.0025 | FA(10:1(OH2))       | C10H17O4      | [M-H]-     |
| 203.11 | 203.1066 | 0.0001 | LPA(16:1)           | C19H35O7P     | [M-2H]2-   |
| 203.11 | 203.107  | 0.0003 | LPG(26:6)           | C32H50O9P     | [M-3H]3-   |

**Lipidomics 1: Urine top neg log2fc candidate lipids**

| Input Mass | Matched Mass | Delta  | Name                       | Formula         | Ion          |
|------------|--------------|--------|----------------------------|-----------------|--------------|
| 570.31     | 570.3049     | 0.0008 | LPS(18:0)                  | C25H49NO11P     | [M+Formate]- |
| 695.39     | 695.4023     | 0.0086 | LPA(34:6)                  | C37H63O7P       | [M+2Na-H]+   |
| 695.39     | 695.393      | 0.0007 | PA(32:6)                   | C37H60O10P      | [M+OAc]-     |
| 695.39     | 695.4012     | 0.0076 | MGDG(26:5)                 | C37H59O12       | [M+OAc]-     |
| 516.30     | 516.2933     | 0.0018 | HexSph(t18:1)              | C24H47NO8K      | [M+K]+       |
| 516.30     | 516.2863     | 0.0089 | LPE(18:0)                  | C23H48NO7PCI    | [M+Cl]-      |
| 570.31     | 570.3049     | 0.0008 | LPS(18:0)                  | C25H49NO11P     | [M+Formate]- |
| 571.31     | 571.3172     | 0.0084 | PA(24:0)                   | C27H53O8PCI     | [M+Cl]-      |
| 571.31     | 571.3042     | 0.0047 | LPA(24:5)                  | C29H48O9P       | [M+OAc]-     |
| 517.30     | 517.2925     | 0.0071 | LPG(20:3)                  | C26H46O8P       | [M+H-H2O]+   |
| 517.30     | 517.3037     | 0.0041 | LPE(20:5)                  | C25H46N2O7P     | [M+NH4]+     |
| 517.30     | 517.2954     | 0.0042 | DGDG(40:8)                 | C55H88O15Na2    | [M+2Na]2+    |
| 517.30     | 517.2989     | 0.0007 | DGDG(44:12)                | C59H86O15       | [M-2H]2-     |
| 572.31     | 572.3113     | 0.0004 | LPE(22:2)                  | C27H52NO7PK     | [M+K]+       |
| 572.31     | 572.3125     | 0.0008 | LPS(P-20:0)                | C26H52NO8PCI    | [M+Cl]-      |
| 465.26     | 465.2612     | 0.0046 | LPG(16:1)                  | C22H42O8P       | [M+H-H2O]+   |
| 465.26     | 465.249      | 0.0075 | LysoSM(t14:0)              | C19H43N2O6PK    | [M+K]+       |
| 465.26     | 465.26       | 0.0034 | PI(38:5)                   | C47H81O13PNa2   | [M+2Na]2+    |
| 465.26     | 465.26       | 0.0034 | PI(O-38:6(OH))             | C47H81O13PNa2   | [M+2Na]2+    |
| 465.26     | 465.26       | 0.0034 | PI(P-38:5(OH))             | C47H81O13PNa2   | [M+2Na]2+    |
| 465.26     | 465.2623     | 0.0057 | CPA(18:0)                  | C22H42O8P       | [M+Formate]- |
| 573.31     | 573.3163     | 0.002  | PA(24:1(OH))               | C27H51O9PNa     | [M+Na]+      |
| 573.31     | 573.3069     | 0.0073 | FA(32:4(OH3,Ke2,Ep2,cyc))  | C32H45O9        | [M-H]-       |
| 573.31     | 573.3069     | 0.0073 | FA(32:5(OH3,Ke2,Ep2))      | C32H45O9        | [M-H]-       |
| 573.31     | 573.3069     | 0.0073 | FA(32:5(OH4,Ke2,Ep,cyclo)) | C32H45O9        | [M-H]-       |
| 573.31     | 573.3069     | 0.0073 | FA(32:5(OH4,Ke,Ep2,cyclo)) | C32H45O9        | [M-H]-       |
| 573.31     | 573.3069     | 0.0073 | FA(32:6(OH4,Ke,Ep))        | C32H45O9        | [M-H]-       |
| 573.31     | 573.3069     | 0.0073 | FA(32:6(OH4,Ke,Ep2))       | C32H45O9        | [M-H]-       |
| 573.31     | 573.3198     | 0.0056 | LPA(24:4)                  | C29H50O9P       | [M+OAc]-     |
| 574.32     | 574.3139     | 0.0026 | LPS(22:4)                  | C28H49NO9P      | [M+H]+       |
| 574.32     | 574.3198     | 0.0032 | LacSph(m14:1)              | C26H49NO11Na    | [M+Na]+      |
| 574.32     | 574.3115     | 0.0051 | LPS(20:1)                  | C26H50NO9PNa    | [M+Na]+      |
| 574.32     | 574.3139     | 0.0026 | LPG(22:6)                  | C28H49NO9P      | [M+NH4]+     |
| 574.32     | 574.316      | 0.0006 | PIP(52:12)                 | C61H98O16P2     | [M+2H]2+     |
| 574.32     | 574.3135     | 0.003  | PIP(48:6)                  | C57H100O16P2Na2 | [M+2Na]2+    |
| 574.32     | 574.3135     | 0.003  | PIP(P-48:6(OH))            | C57H100O16P2Na2 | [M+2Na]2+    |
| 574.32     | 574.3151     | 0.0015 | LPE(22:4)                  | C28H49NO9P      | [M+Formate]- |
| 574.32     | 574.3151     | 0.0015 | LPC(18:4)                  | C28H49NO9P      | [M+OAc]-     |
| 574.32     | 574.3171     | 0.0005 | PIP(52:10)                 | C61H98O16P2     | [M-2H]2-     |
| 195.07     | 195.0663     | 0.0003 | FA(10:1(Ep2,cyclo))        | C10H11O4        | [M-H]-       |
| 195.07     | 195.0663     | 0.0003 | FA(10:1(Ke2,cyclo))        | C10H11O4        | [M-H]-       |
| 195.07     | 195.0663     | 0.0003 | FA(10:1(Ke,Ep,cyclo))      | C10H11O4        | [M-H]-       |
| 195.07     | 195.0663     | 0.0003 | FA(10:2(Ep2))              | C10H11O4        | [M-H]-       |
| 195.07     | 195.0663     | 0.0003 | FA(10:2(Ke2))              | C10H11O4        | [M-H]-       |
| 195.07     | 195.0663     | 0.0003 | FA(10:2(Ke,Ep))            | C10H11O4        | [M-H]-       |
| 195.07     | 195.0663     | 0.0003 | FA(10:2(OH,Ep,cyclo))      | C10H11O4        | [M-H]-       |
| 195.07     | 195.0663     | 0.0003 | FA(10:2(OH,Ke,cyclo))      | C10H11O4        | [M-H]-       |
| 206.12     | 206.1169     | 0.0009 | LacSph(d18:2)              | C30H52NO12      | [M-3H]3-     |
| 256.15     | 256.1552     | 0.0003 | LPG(18:1)                  | C24H49O9P       | [M+2H]2+     |
| 256.15     | 256.1554     | 0.0006 | CAR(6:1)                   | C13H22NO4       | [M-H]-       |
| 619.36     | 619.3734     | 0.0088 | LPA(30:5)                  | C33H57O7PNa     | [M+Na]+      |
| 619.36     | 619.3718     | 0.0072 | LPS(24:4)                  | C30H56N2O9P     | [M+NH4]+     |
| 619.36     | 619.371      | 0.0064 | LPA(28:2)                  | C31H59O7P       | [M+2Na-H]+   |
| 619.36     | 619.3699     | 0.0053 | MGDG(20:1)                 | C31H55O12       | [M+OAc]-     |
| 530.31     | 530.3217     | 0.0099 | LPE(20:1)                  | C25H50NO7PNa    | [M+Na]+      |
| 530.31     | 530.3161     | 0.0043 | PIP(O-42:1)                | C51H100O15P2Na2 | [M+2Na]2+    |
| 530.31     | 530.3161     | 0.0043 | PIP(P-42:0)                | C51H100O15P2Na2 | [M+2Na]2+    |
| 530.31     | 530.3076     | 0.0041 | NAT(26:4)                  | C28H49NO4SCI    | [M+Cl]-      |
| 530.31     | 530.3019     | 0.0099 | LPC(16:0)                  | C24H50NO7PCI    | [M+Cl]-      |
| 530.31     | 530.3019     | 0.0099 | PC(O-16:0)                 | C24H50NO7PCI    | [M+Cl]-      |

|        |          |        |                |                |                          |
|--------|----------|--------|----------------|----------------|--------------------------|
| 538.34 | 538.3503 | 0.0099 | LPS(P-20:0)    | C26H53NO8P     | [M+H] <sup>+</sup>       |
| 538.34 | 538.3327 | 0.0078 | NAT(26:2)      | C28H53NO4SK    | [M+K] <sup>+</sup>       |
| 538.34 | 538.3447 | 0.0042 | PIP(44:0(OH))  | C53H106O17P2   | [M+2H] <sup>2+</sup>     |
| 947.62 | 947.609  | 0.0092 | DGDG(38:6)     | C53H87O14      | [M+H-H2O] <sup>+</sup>   |
| 947.62 | 947.6136 | 0.0046 | PA(52:10(OH))  | C55H89O9PNa    | [M+Na] <sup>+</sup>      |
| 947.62 | 947.612  | 0.0062 | PS(46:9(OH))   | C52H88N2O11P   | [M+NH4] <sup>+</sup>     |
| 947.62 | 947.6138 | 0.0045 | PG(46:5)       | C52H93O10PK    | [M+K] <sup>+</sup>       |
| 947.62 | 947.6138 | 0.0045 | PG(O-46:6(OH)) | C52H93O10PK    | [M+K] <sup>+</sup>       |
| 947.62 | 947.6138 | 0.0045 | PG(P-46:5(OH)) | C52H93O10PK    | [M+K] <sup>+</sup>       |
| 947.62 | 947.6112 | 0.007  | PA(50:7(OH))   | C53H91O9P      | [M+2Na-H] <sup>+</sup>   |
| 947.62 | 947.6172 | 0.0011 | PA(54:12(OH))  | C57H88O9P      | [M-H] <sup>-</sup>       |
| 947.62 | 947.6135 | 0.0047 | SQDG(40:2)     | C50H91O14S     | [M+Formate] <sup>-</sup> |
| 947.62 | 947.623  | 0.0048 | PI(O-40:3)     | C50H92O14P     | [M+Formate] <sup>-</sup> |
| 947.62 | 947.623  | 0.0048 | PI(P-40:2)     | C50H92O14P     | [M+Formate] <sup>-</sup> |
| 821.57 | 821.5691 | 0.002  | PA(44:6(OH))   | C47H82O9P      | [M+H] <sup>+</sup>       |
| 821.57 | 821.5667 | 0.0004 | PA(42:3(OH))   | C45H83O9PNa    | [M+Na] <sup>+</sup>      |
| 821.57 | 821.5651 | 0.002  | PI-Cer(d36:3)  | C42H82N2O11P   | [M+NH4] <sup>+</sup>     |
| 821.57 | 821.5651 | 0.002  | PS(36:2(OH))   | C42H82N2O11P   | [M+NH4] <sup>+</sup>     |
| 821.57 | 821.5733 | 0.0063 | LacCer(d30:2)  | C42H81N2O13    | [M+NH4] <sup>+</sup>     |
| 821.57 | 821.5643 | 0.0028 | PA(40:0(OH))   | C43H85O9P      | [M+2Na-H] <sup>+</sup>   |
| 821.57 | 821.5702 | 0.0032 | PA(44:5(OH))   | C47H82O9P      | [M-H] <sup>-</sup>       |
| 821.57 | 821.5702 | 0.0032 | PA(O-42:6)     | C47H82O9P      | [M+OAc] <sup>-</sup>     |
| 821.57 | 821.5702 | 0.0032 | PA(P-42:5)     | C47H82O9P      | [M+OAc] <sup>-</sup>     |
| 555.28 | 555.2929 | 0.0097 | LPI(16:0)      | C25H48O11P     | [M+H-H2O] <sup>+</sup>   |
| 555.28 | 555.2847 | 0.0016 | LPA(24:3)      | C27H49O7PK     | [M+K] <sup>+</sup>       |
| 555.28 | 555.2875 | 0.0043 | PIP(44:5(OH))  | C53H94O17P2Na2 | [M+2Na] <sup>2+</sup>    |



**Lipidomics 1: Urine top pos log2fc candidate lipids**

| <b>Input Mass</b> | <b>Matched Mass</b> | <b>Delta</b> | <b>Name</b>         | <b>Formula</b> | <b>Ion</b>   |
|-------------------|---------------------|--------------|---------------------|----------------|--------------|
| 343.23            | 343.2356            | 0.0073       | S1P(d14:0)          | C14H36N2O5P    | [M+NH4]+     |
| 343.23            | 343.2256            | 0.0027       | PA(34:4(OH))        | C37H67O9P      | [M+2H]2+     |
| 343.23            | 343.2279            | 0.0004       | FA(22:4(Ep,cyclo))  | C22H31O3       | [M-H]-       |
| 343.23            | 343.2279            | 0.0004       | FA(22:4(Ke,cyclo))  | C22H31O3       | [M-H]-       |
| 343.23            | 343.2279            | 0.0004       | FA(22:5(Ep))        | C22H31O3       | [M-H]-       |
| 343.23            | 343.2279            | 0.0004       | FA(22:5(Ke))        | C22H31O3       | [M-H]-       |
| 343.23            | 343.2279            | 0.0004       | FA(22:5(OH,cyclo))  | C22H31O3       | [M-H]-       |
| 343.23            | 343.2279            | 0.0004       | FA(22:6(OH))        | C22H31O3       | [M-H]-       |
| 343.23            | 343.2267            | 0.0016       | PA(34:2(OH))        | C37H67O9P      | [M-2H]2-     |
| 664.46            | 664.4548            | 0.0083       | LPS(28:1)           | C34H67NO9P     | [M+H]+       |
| 664.46            | 664.4548            | 0.0083       | PC(26:1(OH))        | C34H67NO9P     | [M+H]+       |
| 664.46            | 664.4548            | 0.0083       | PS(P-28:0)          | C34H67NO9P     | [M+H]+       |
| 664.46            | 664.47              | 0.007        | LPC(30:5)           | C38H67NO6P     | [M+H-H2O]+   |
| 664.46            | 664.4548            | 0.0083       | PS(O-28:0(OH))      | C34H67NO9P     | [M+H-H2O]+   |
| 664.46            | 664.4676            | 0.0046       | CerP(d36:3)         | C36H68NO6PNa   | [M+Na]+      |
| 664.46            | 664.4548            | 0.0083       | LPG(28:3)           | C34H67NO9P     | [M+NH4]+     |
| 664.46            | 664.4652            | 0.0022       | CerP(d34:0)         | C34H70NO6P     | [M+2Na-H]+   |
| 664.46            | 664.4559            | 0.0072       | LPS(28:0)           | C34H67NO9P     | [M-H]-       |
| 664.46            | 664.4559            | 0.0072       | PS(O-28:0)          | C34H67NO9P     | [M-H]-       |
| 664.46            | 664.4559            | 0.0072       | LPE(28:1)           | C34H67NO9P     | [M+Formate]- |
| 664.46            | 664.4559            | 0.0072       | PE(P-28:0)          | C34H67NO9P     | [M+Formate]- |
| 664.46            | 664.4641            | 0.0011       | HexCer(t26:0)       | C34H66NO11     | [M+OAc]-     |
| 664.46            | 664.4616            | 0.0014       | NAT(34:5)           | C38H66NO6S     | [M+OAc]-     |
| 664.46            | 664.4559            | 0.0072       | CerP(t32:1)         | C34H67NO9P     | [M+OAc]-     |
| 664.46            | 664.4559            | 0.0072       | LPC(24:1)           | C34H67NO9P     | [M+OAc]-     |
| 201.12            | 201.1132            | 0.0025       | FA(10:0(OH2,cyclo)) | C10H17O4       | [M-H]-       |
| 201.12            | 201.1132            | 0.0025       | FA(10:0(OH,Ep))     | C10H17O4       | [M-H]-       |
| 201.12            | 201.1132            | 0.0025       | FA(10:0(OH,Ke))     | C10H17O4       | [M-H]-       |
| 201.12            | 201.1132            | 0.0025       | FA(10:1(OH2))       | C10H17O4       | [M-H]-       |

**Lipidomics 2: CSF top pvalue candidate lipids**

| Input Mass | Matched Mass | Delta  | Name                     | Formula       | Ion                      |
|------------|--------------|--------|--------------------------|---------------|--------------------------|
| 474.35     | 474.3578     | 0.0093 | CAR(22:5)                | C29H48NO4     | [M+H] <sup>+</sup>       |
| 474.35     | 474.3554     | 0.0069 | CAR(20:2)                | C27H49NO4Na   | [M+Na] <sup>+</sup>      |
| 663.47     | 663.4595     | 0.0057 | PA(32:1(OH))             | C35H68O9P     | [M+H] <sup>+</sup>       |
| 663.47     | 663.4748     | 0.0095 | PA(O-36:5)               | C39H68O6P     | [M+H-H2O] <sup>+</sup>   |
| 663.47     | 663.4748     | 0.0095 | PA(P-36:4)               | C39H68O6P     | [M+H-H2O] <sup>+</sup>   |
| 663.47     | 663.4749     | 0.0096 | DG(P-38:6)               | C41H68O4K     | [M+K] <sup>+</sup>       |
| 663.47     | 663.4607     | 0.0046 | PA(32:0(OH))             | C35H68O9P     | [M-H] <sup>-</sup>       |
| 663.47     | 663.4719     | 0.0066 | SM(d28:1)                | C34H68N2O8P   | [M+Formate] <sup>-</sup> |
| 663.47     | 663.4607     | 0.0046 | LPA(30:1)                | C35H68O9P     | [M+OAc] <sup>-</sup>     |
| 663.47     | 663.4607     | 0.0046 | PA(O-30:1)               | C35H68O9P     | [M+OAc] <sup>-</sup>     |
| 663.47     | 663.4607     | 0.0046 | PA(P-30:0)               | C35H68O9P     | [M+OAc] <sup>-</sup>     |
| 663.47     | 663.4719     | 0.0066 | PE-Cer(d30:1)            | C34H68N2O8P   | [M+OAc] <sup>-</sup>     |
| 358.20     | 358.2022     | 0.0006 | NAT(14:0)                | C16H33NO4SNa  | [M+Na] <sup>+</sup>      |
| 358.20     | 358.1965     | 0.0052 | CAR(10:1)                | C17H31NO4     | [M+2Na-H] <sup>+</sup>   |
| 805.62     | 805.6317     | 0.0081 | PA(42:0(OH))             | C45H90O9P     | [M+H] <sup>+</sup>       |
| 805.62     | 805.6194     | 0.0042 | SM(d40:3)                | C45H87N2O6PNa | [M+Na] <sup>+</sup>      |
| 805.62     | 805.6259     | 0.0023 | WE(54:11)                | C54H86O2K     | [M+K] <sup>+</sup>       |
| 805.62     | 805.617      | 0.0066 | SM(d38:0)                | C43H89N2O6P   | [M+2Na-H] <sup>+</sup>   |
| 805.62     | 805.6328     | 0.0092 | PA(O-40:0)               | C45H90O9P     | [M+OAc] <sup>-</sup>     |
| 527.16     | 527.1654     | 0.0029 | LPI(10:0)                | C19H37O12PK   | [M+K] <sup>+</sup>       |
| 716.38     | 716.3874     | 0.0076 | PE(30:4(OH))             | C35H62NO9P    | [M+2Na-H] <sup>+</sup>   |
| 716.38     | 716.37       | 0.0098 | LPS(30:6)                | C36H60NO9PCI  | [M+Cl] <sup>-</sup>      |
| 716.38     | 716.378      | 0.0018 | PS(28:4)                 | C35H59NO12P   | [M+Formate] <sup>-</sup> |
| 321.03     | 321.0252     | 0.0088 | FA(14:4(OH3,Ke2,Ep2,cy)) | C14H9O9       | [M-H] <sup>-</sup>       |
| 609.40     | 609.4008     | 0.0039 | FA(34:0(OH3,Ke2,Ep2,cy)) | C34H57O9      | [M-H] <sup>-</sup>       |
| 609.40     | 609.4008     | 0.0039 | FA(34:1(OH3,Ke2,Ep2))    | C34H57O9      | [M-H] <sup>-</sup>       |
| 609.40     | 609.4008     | 0.0039 | FA(34:1(OH4,Ke,Ep2,cy))  | C34H57O9      | [M-H] <sup>-</sup>       |
| 609.40     | 609.4008     | 0.0039 | FA(34:1(OH4,Ke,Ep2,cy))  | C34H57O9      | [M-H] <sup>-</sup>       |
| 609.40     | 609.4008     | 0.0039 | FA(34:2(OH4,Ke2,Ep))     | C34H57O9      | [M-H] <sup>-</sup>       |
| 609.40     | 609.4008     | 0.0039 | FA(34:2(OH4,Ke,Ep2))     | C34H57O9      | [M-H] <sup>-</sup>       |
| 609.40     | 609.3886     | 0.0083 | PE-Cer(t26:1)            | C29H58N2O9P   | [M+Formate] <sup>-</sup> |
| 931.45     | 931.4368     | 0.0094 | PIP(36:8)                | C45H73O16P2   | [M+H] <sup>+</sup>       |
| 931.45     | 931.4368     | 0.0094 | PIP(36:7(OH))            | C45H73O16P2   | [M+H-H2O] <sup>+</sup>   |
| 931.45     | 931.437      | 0.0093 | PI(38:9(OH))             | C47H73O14PK   | [M+K] <sup>+</sup>       |
| 931.45     | 931.4379     | 0.0083 | PIP(36:7)                | C45H73O16P2   | [M-H] <sup>-</sup>       |
| 931.45     | 931.451      | 0.0048 | LPIP(34:4)               | C43H78O15P2Cl | [M+Cl] <sup>-</sup>      |
| 931.45     | 931.451      | 0.0048 | PIP(O-34:4)              | C43H78O15P2Cl | [M+Cl] <sup>-</sup>      |
| 931.45     | 931.451      | 0.0048 | PIP(P-34:3)              | C43H78O15P2Cl | [M+Cl] <sup>-</sup>      |
| 897.67     | 897.6732     | 0.0076 | PA(52:7)                 | C55H94O7P     | [M+H-H2O] <sup>+</sup>   |
| 897.67     | 897.6708     | 0.0052 | PA(O-50:6)               | C53H95O7PNa   | [M+Na] <sup>+</sup>      |
| 897.67     | 897.6708     | 0.0052 | PA(P-50:5)               | C53H95O7PNa   | [M+Na] <sup>+</sup>      |
| 897.67     | 897.6621     | 0.0035 | LacCer(t34:0)            | C46H93N2O14   | [M+NH4] <sup>+</sup>     |
| 897.67     | 897.6691     | 0.0036 | PC(42:5(OH))             | C50H94N2O9P   | [M+NH4] <sup>+</sup>     |
| 897.67     | 897.6691     | 0.0036 | PS(O-44:5)               | C50H94N2O9P   | [M+NH4] <sup>+</sup>     |
| 897.67     | 897.6691     | 0.0036 | PS(P-44:4)               | C50H94N2O9P   | [M+NH4] <sup>+</sup>     |
| 897.67     | 897.6733     | 0.0077 | DG(54:9)                 | C57H94O5K     | [M+K] <sup>+</sup>       |
| 897.67     | 897.6733     | 0.0077 | TG(O-54:9)               | C57H94O5K     | [M+K] <sup>+</sup>       |
| 897.67     | 897.6733     | 0.0077 | TG(P-54:8)               | C57H94O5K     | [M+K] <sup>+</sup>       |
| 897.67     | 897.6684     | 0.0028 | PA(O-48:3)               | C51H97O7P     | [M+2Na-H] <sup>+</sup>   |
| 897.67     | 897.6684     | 0.0028 | PA(P-48:2)               | C51H97O7P     | [M+2Na-H] <sup>+</sup>   |
| 897.67     | 897.6614     | 0.0042 | DG(54:12)                | C58H89O7      | [M+Formate] <sup>-</sup> |
| 897.67     | 897.6673     | 0.0017 | MGDG(40:2)               | C51H93O12     | [M+OAc] <sup>-</sup>     |
| 897.67     | 897.659      | 0.0066 | PA(46:3)                 | C51H94O10P    | [M+OAc] <sup>-</sup>     |
| 897.67     | 897.659      | 0.0066 | PA(O-46:4(OH))           | C51H94O10P    | [M+OAc] <sup>-</sup>     |
| 897.67     | 897.659      | 0.0066 | PA(P-46:3(OH))           | C51H94O10P    | [M+OAc] <sup>-</sup>     |
| 672.54     | 672.5409     | 0.0026 | HexCer(d32:1)            | C38H74NO8     | [M+H] <sup>+</sup>       |
| 672.54     | 672.5409     | 0.0026 | HexCer(t32:0)            | C38H74NO8     | [M+H-H2O] <sup>+</sup>   |
| 672.54     | 672.5513     | 0.0078 | Cer(t38:0(OH))           | C38H77NO5     | [M+2Na-H] <sup>+</sup>   |
| 672.54     | 672.542      | 0.0015 | HexCer(d32:0)            | C38H74NO8     | [M-H] <sup>-</sup>       |
| 672.54     | 672.5338     | 0.0098 | CerP(d38:1)              | C38H75NO6P    | [M-H] <sup>-</sup>       |

|        |          |        |                |                      |                          |
|--------|----------|--------|----------------|----------------------|--------------------------|
| 685.44 | 685.4439 | 0.0075 | PA(34:4(OH))   | C37H66O9P            | [M+H] <sup>+</sup>       |
| 685.44 | 685.4286 | 0.0078 | LPI(24:0)      | C33H66O12P           | [M+H] <sup>+</sup>       |
| 685.44 | 685.4415 | 0.0051 | PA(32:1(OH))   | C35H67O9PNa          | [M+Na] <sup>+</sup>      |
| 685.44 | 685.4399 | 0.0035 | PI-Cer(d26:1)  | C32H66N2O11P         | [M+NH4] <sup>+</sup>     |
| 685.44 | 685.4399 | 0.0035 | PS(26:0(OH))   | C32H66N2O11P         | [M+NH4] <sup>+</sup>     |
| 685.44 | 685.4304 | 0.0061 | SHexCer(d26:1) | C32H65N2O11S         | [M+NH4] <sup>+</sup>     |
| 685.44 | 685.4317 | 0.0047 | PE-Cer(t32:2)  | C34H67N2O7PK         | [M+K] <sup>+</sup>       |
| 685.44 | 685.4288 | 0.0077 | MGDG(26:0)     | C35H66O10K           | [M+K] <sup>+</sup>       |
| 685.44 | 685.445  | 0.0086 | PA(34:3(OH))   | C37H66O9P            | [M-H] <sup>-</sup>       |
| 685.44 | 685.4297 | 0.0067 | PG(O-26:0(OH)) | C33H66O12P           | [M+Formate] <sup>-</sup> |
| 685.44 | 685.445  | 0.0086 | LPA(32:4)      | C37H66O9P            | [M+OAc] <sup>-</sup>     |
| 956.21 | 956.2038 | 0.0076 | CoA(10:1(Ke))  | C31H50N7O18P3<br>SNa | [M+Na] <sup>+</sup>      |
| 956.21 | 956.2038 | 0.0076 | CoA(10:1(OH))  | C31H50N7O18P3<br>SNa | [M+Na] <sup>+</sup>      |
| 956.21 | 956.2204 | 0.0089 | CoA(10:0)      | C31H54N7O17P3<br>SCI | [M+Cl] <sup>-</sup>      |
| 380.35 | 380.3523 | 0.0022 | NAE(22:2)      | C24H46NO2            | [M+H] <sup>+</sup>       |
| 380.35 | 380.3523 | 0.0022 | WE(24:3)       | C24H46NO2            | [M+NH4] <sup>+</sup>     |
| 380.35 | 380.3534 | 0.0033 | NAE(22:1)      | C24H46NO2            | [M-H] <sup>-</sup>       |
| 443.33 | 443.3378 | 0.0033 | MG(20:1)       | C25H47O6             | [M+OAc] <sup>-</sup>     |
| 678.48 | 678.4704 | 0.0084 | PE(30:1(OH))   | C35H69NO9P           | [M+H] <sup>+</sup>       |
| 678.48 | 678.4857 | 0.0068 | LPE(34:5)      | C39H69NO6P           | [M+H-H2O] <sup>+</sup>   |
| 678.48 | 678.4857 | 0.0068 | PE(P-34:4)     | C39H69NO6P           | [M+H-H2O] <sup>+</sup>   |
| 678.48 | 678.4704 | 0.0084 | PA(32:2(OH))   | C35H69NO9P           | [M+NH4] <sup>+</sup>     |
| 678.48 | 678.4858 | 0.007  | CAR(34:6)      | C41H69NO4K           | [M+K] <sup>+</sup>       |
| 678.48 | 678.4716 | 0.0073 | PE(30:0(OH))   | C35H69NO9P           | [M-H] <sup>-</sup>       |
| 678.48 | 678.4717 | 0.0071 | HexCer(d30:1)  | C36H69NO8Cl          | [M+Cl] <sup>-</sup>      |
| 678.48 | 678.4798 | 0.0009 | HexCer(t28:0)  | C35H68NO11           | [M+Formate] <sup>-</sup> |
| 678.48 | 678.4716 | 0.0073 | CerP(t34:1)    | C35H69NO9P           | [M+Formate] <sup>-</sup> |
| 678.48 | 678.4716 | 0.0073 | LPC(26:1)      | C35H69NO9P           | [M+Formate] <sup>-</sup> |
| 678.48 | 678.4716 | 0.0073 | PC(P-26:0)     | C35H69NO9P           | [M+Formate] <sup>-</sup> |
| 678.48 | 678.4716 | 0.0073 | LPE(28:1)      | C35H69NO9P           | [M+OAc] <sup>-</sup>     |
| 678.48 | 678.4716 | 0.0073 | PE(P-28:0)     | C35H69NO9P           | [M+OAc] <sup>-</sup>     |
| 678.48 | 678.4716 | 0.0073 | PC(28:0(OH))   | C35H69NO9P           | [M-CH3] <sup>-</sup>     |
| 559.48 | 559.4873 | 0.0029 | WE(40:8)       | C40H63O              | [M+H-H2O] <sup>+</sup>   |

## Lipidomics 2: CSF top neg log2FC candidate lipids

| Input Mass | Matched Mass | Delta  | Name                  | Formula      | Ion                      |
|------------|--------------|--------|-----------------------|--------------|--------------------------|
| 678.48     | 678.4704     | 0.0084 | PE(30:1(OH))          | C35H69NO9P   | [M+H] <sup>+</sup>       |
| 678.48     | 678.4857     | 0.0068 | LPE(34:5)             | C39H69NO6P   | [M+H-H2O] <sup>+</sup>   |
| 678.48     | 678.4857     | 0.0068 | PE(P-34:4)            | C39H69NO6P   | [M+H-H2O] <sup>+</sup>   |
| 678.48     | 678.4704     | 0.0084 | PA(32:2(OH))          | C35H69NO9P   | [M+NH4] <sup>+</sup>     |
| 678.48     | 678.4858     | 0.0069 | CAR(34:6)             | C41H69NO4K   | [M+K] <sup>+</sup>       |
| 678.48     | 678.4716     | 0.0073 | PE(30:0(OH))          | C35H69NO9P   | [M-H] <sup>-</sup>       |
| 678.48     | 678.4717     | 0.0072 | HexCer(d30:1)         | C36H69NO8Cl  | [M+Cl] <sup>-</sup>      |
| 678.48     | 678.4798     | 0.0009 | HexCer(t28:0)         | C35H68NO11   | [M+Formate] <sup>-</sup> |
| 678.48     | 678.4716     | 0.0073 | CerP(t34:1)           | C35H69NO9P   | [M+Formate] <sup>-</sup> |
| 678.48     | 678.4716     | 0.0073 | LPC(26:1)             | C35H69NO9P   | [M+Formate] <sup>-</sup> |
| 678.48     | 678.4716     | 0.0073 | PC(P-26:0)            | C35H69NO9P   | [M+Formate] <sup>-</sup> |
| 678.48     | 678.4716     | 0.0073 | LPE(28:1)             | C35H69NO9P   | [M+OAc] <sup>-</sup>     |
| 678.48     | 678.4716     | 0.0073 | PE(P-28:0)            | C35H69NO9P   | [M+OAc] <sup>-</sup>     |
| 678.48     | 678.4716     | 0.0073 | PC(28:0(OH))          | C35H69NO9P   | [M-CH3] <sup>-</sup>     |
| 540.45     | 540.4445     | 0.0017 | NAT(30:1)             | C32H62NO3S   | [M+H-H2O] <sup>+</sup>   |
| 540.45     | 540.4411     | 0.0051 | CAR(28:5)             | C35H58NO3    | [M+H-H2O] <sup>+</sup>   |
| 413.27     | 413.2697     | 0.0036 | FA(26:4(Ep2,cyclo))   | C26H37O4     | [M-H] <sup>-</sup>       |
| 413.27     | 413.2697     | 0.0036 | FA(26:4(Ke2,cyclo))   | C26H37O4     | [M-H] <sup>-</sup>       |
| 413.27     | 413.2697     | 0.0036 | FA(26:4(Ke,Ep,cyclo)) | C26H37O4     | [M-H] <sup>-</sup>       |
| 413.27     | 413.2697     | 0.0036 | FA(26:5(Ep2))         | C26H37O4     | [M-H] <sup>-</sup>       |
| 413.27     | 413.2697     | 0.0036 | FA(26:5(Ke2))         | C26H37O4     | [M-H] <sup>-</sup>       |
| 413.27     | 413.2697     | 0.0036 | FA(26:5(Ke,Ep))       | C26H37O4     | [M-H] <sup>-</sup>       |
| 413.27     | 413.2697     | 0.0036 | FA(26:5(OH,Ep,cyclo)) | C26H37O4     | [M-H] <sup>-</sup>       |
| 413.27     | 413.2697     | 0.0036 | FA(26:5(OH,Ke,cyclo)) | C26H37O4     | [M-H] <sup>-</sup>       |
| 413.27     | 413.2697     | 0.0036 | FA(26:6(OH2,cyclo))   | C26H37O4     | [M-H] <sup>-</sup>       |
| 413.27     | 413.2697     | 0.0036 | FA(26:6(OH,Ep))       | C26H37O4     | [M-H] <sup>-</sup>       |
| 413.27     | 413.2697     | 0.0036 | FA(26:6(OH,Ke))       | C26H37O4     | [M-H] <sup>-</sup>       |
| 217.10     | 217.1082     | 0.0035 | FA(10:0(OH2,Ep))      | C10H17O5     | [M-H] <sup>-</sup>       |
| 217.10     | 217.1082     | 0.0035 | FA(10:0(OH2,Ke))      | C10H17O5     | [M-H] <sup>-</sup>       |
| 217.10     | 217.1082     | 0.0035 | FA(10:0(OH3,cyclo))   | C10H17O5     | [M-H] <sup>-</sup>       |
| 217.10     | 217.1082     | 0.0035 | FA(10:1(OH3))         | C10H17O5     | [M-H] <sup>-</sup>       |
| 503.38     | 503.3742     | 0.0039 | DG(28:4)              | C31H51O5     | [M-H] <sup>-</sup>       |
| 503.38     | 503.3873     | 0.0091 | DG(P-26:0)            | C29H56O4Cl   | [M+Cl] <sup>-</sup>      |
| 503.38     | 503.3873     | 0.0091 | MG(26:1)              | C29H56O4Cl   | [M+Cl] <sup>-</sup>      |
| 432.28     | 432.2849     | 0.0041 | S1P(d20:0)            | C20H44NO5PNa | [M+Na] <sup>+</sup>      |
| 432.28     | 432.2886     | 0.0078 | CAR(16:1)             | C23H43NO4Cl  | [M+Cl] <sup>-</sup>      |
| 507.33     | 507.3205     | 0.0081 | LysoSM(d18:2)         | C24H48N2O7P  | [M+Formate] <sup>-</sup> |
| 503.38     | 503.3742     | 0.0039 | DG(28:4)              | C31H51O5     | [M-H] <sup>-</sup>       |
| 503.38     | 503.3873     | 0.0092 | DG(P-26:0)            | C29H56O4Cl   | [M+Cl] <sup>-</sup>      |
| 503.38     | 503.3873     | 0.0092 | MG(26:1)              | C29H56O4Cl   | [M+Cl] <sup>-</sup>      |
| 503.38     | 503.3742     | 0.0039 | DG(28:4)              | C31H51O5     | [M-H] <sup>-</sup>       |
| 503.38     | 503.3873     | 0.0091 | DG(P-26:0)            | C29H56O4Cl   | [M+Cl] <sup>-</sup>      |
| 503.38     | 503.3873     | 0.0091 | MG(26:1)              | C29H56O4Cl   | [M+Cl] <sup>-</sup>      |
| 848.63     | 848.6375     | 0.0077 | PS(40:0)              | C46H91NO10P  | [M+H] <sup>+</sup>       |
| 848.63     | 848.6375     | 0.0077 | PS(O-40:1(OH))        | C46H91NO10P  | [M+H] <sup>+</sup>       |
| 848.63     | 848.6375     | 0.0077 | PS(P-40:0(OH))        | C46H91NO10P  | [M+H] <sup>+</sup>       |
| 848.63     | 848.628      | 0.0018 | SHexCer(d40:0)        | C46H90NO10S  | [M+H-H2O] <sup>+</sup>   |
| 848.63     | 848.6375     | 0.0077 | PI-Cer(d40:0)         | C46H91NO10P  | [M+H-H2O] <sup>+</sup>   |
| 848.63     | 848.6246     | 0.0052 | MGDG(40:6)            | C49H86NO10   | [M+NH4] <sup>+</sup>     |
| 848.63     | 848.6375     | 0.0077 | PG(40:2)              | C46H91NO10P  | [M+NH4] <sup>+</sup>     |
| 848.63     | 848.6375     | 0.0077 | PG(O-40:3(OH))        | C46H91NO10P  | [M+NH4] <sup>+</sup>     |
| 848.63     | 848.6375     | 0.0077 | PG(P-40:2(OH))        | C46H91NO10P  | [M+NH4] <sup>+</sup>     |
| 848.63     | 848.6376     | 0.0078 | HexCer(d42:2)         | C48H91NO8K   | [M+K] <sup>+</sup>       |
| 848.63     | 848.6386     | 0.0088 | PS(O-40:0(OH))        | C46H91NO10P  | [M-H] <sup>-</sup>       |
| 848.63     | 848.6306     | 0.0007 | PE(O-42:2)            | C47H92NO7PCl | [M+Cl] <sup>-</sup>      |
| 848.63     | 848.6306     | 0.0007 | PE(P-42:1)            | C47H92NO7PCl | [M+Cl] <sup>-</sup>      |
| 848.63     | 848.6386     | 0.0088 | PE(40:0)              | C46H91NO10P  | [M+Formate] <sup>-</sup> |
| 848.63     | 848.6386     | 0.0088 | PE(O-40:1(OH))        | C46H91NO10P  | [M+Formate] <sup>-</sup> |
| 848.63     | 848.6386     | 0.0088 | PE(P-40:0(OH))        | C46H91NO10P  | [M+Formate] <sup>-</sup> |
| 848.63     | 848.6386     | 0.0088 | PC(36:0)              | C46H91NO10P  | [M+OAc] <sup>-</sup>     |

|        |          |        |                     |              |              |
|--------|----------|--------|---------------------|--------------|--------------|
| 848.63 | 848.6386 | 0.0088 | PC(O-36:1(OH))      | C46H91NO10P  | [M+OAc]-     |
| 848.63 | 848.6386 | 0.0088 | PC(P-36:0(OH))      | C46H91NO10P  | [M+OAc]-     |
| 722.50 | 722.5119 | 0.0076 | PE(P-36:5)          | C41H73NO7P   | [M+H]+       |
| 722.50 | 722.5119 | 0.0076 | PE(36:4)            | C41H73NO7P   | [M+H-H2O]+   |
| 722.50 | 722.5119 | 0.0076 | PE(O-36:5(OH))      | C41H73NO7P   | [M+H-H2O]+   |
| 722.50 | 722.5119 | 0.0076 | PE(P-36:4(OH))      | C41H73NO7P   | [M+H-H2O]+   |
| 722.50 | 722.5095 | 0.0052 | PE(O-34:3)          | C39H74NO7PNa | [M+Na]+      |
| 722.50 | 722.5095 | 0.0052 | PE(P-34:2)          | C39H74NO7PNa | [M+Na]+      |
| 722.50 | 722.5119 | 0.0076 | PA(P-38:6)          | C41H73NO7P   | [M+NH4]+     |
| 722.50 | 722.5071 | 0.0028 | LPE(32:0)           | C37H76NO7P   | [M+2Na-H]+   |
| 722.50 | 722.5071 | 0.0028 | PE(O-32:0)          | C37H76NO7P   | [M+2Na-H]+   |
| 722.50 | 722.513  | 0.0087 | PE(O-36:5)          | C41H73NO7P   | [M-H]-       |
| 722.50 | 722.513  | 0.0087 | PE(P-36:4)          | C41H73NO7P   | [M-H]-       |
| 722.50 | 722.4979 | 0.0064 | HexCer(t32:1)       | C38H73NO9Cl  | [M+Cl]-      |
| 722.50 | 722.4978 | 0.0065 | PC(28:0)            | C37H73NO10P  | [M+Formate]- |
| 722.50 | 722.4978 | 0.0065 | PC(P-28:0(OH))      | C37H73NO10P  | [M+Formate]- |
| 722.50 | 722.4978 | 0.0065 | PE(30:0)            | C37H73NO10P  | [M+OAc]-     |
| 722.50 | 722.4978 | 0.0065 | PE-NMe2(28:0)       | C37H73NO10P  | [M+OAc]-     |
| 722.50 | 722.4978 | 0.0065 | PE(O-30:1(OH))      | C37H73NO10P  | [M+OAc]-     |
| 722.50 | 722.4978 | 0.0065 | PE(P-30:0(OH))      | C37H73NO10P  | [M+OAc]-     |
| 722.50 | 722.513  | 0.0087 | PC(P-34:4)          | C41H73NO7P   | [M-CH3]-     |
| 678.48 | 678.4704 | 0.0085 | PE(30:1(OH))        | C35H69NO9P   | [M+H]+       |
| 678.48 | 678.4857 | 0.0067 | LPE(34:5)           | C39H69NO6P   | [M+H-H2O]+   |
| 678.48 | 678.4857 | 0.0067 | PE(P-34:4)          | C39H69NO6P   | [M+H-H2O]+   |
| 678.48 | 678.4704 | 0.0085 | PA(32:2(OH))        | C35H69NO9P   | [M+NH4]+     |
| 678.48 | 678.4858 | 0.0068 | CAR(34:6)           | C41H69NO4K   | [M+K]+       |
| 678.48 | 678.4716 | 0.0074 | PE(30:0(OH))        | C35H69NO9P   | [M-H]-       |
| 678.48 | 678.4717 | 0.0072 | HexCer(d30:1)       | C36H69NO8Cl  | [M+Cl]-      |
| 678.48 | 678.4798 | 0.0008 | HexCer(t28:0)       | C35H68NO11   | [M+Formate]- |
| 678.48 | 678.4716 | 0.0074 | CerP(t34:1)         | C35H69NO9P   | [M+Formate]- |
| 678.48 | 678.4716 | 0.0074 | LPC(26:1)           | C35H69NO9P   | [M+Formate]- |
| 678.48 | 678.4716 | 0.0074 | PC(P-26:0)          | C35H69NO9P   | [M+Formate]- |
| 678.48 | 678.4716 | 0.0074 | LPE(28:1)           | C35H69NO9P   | [M+OAc]-     |
| 678.48 | 678.4716 | 0.0074 | PE(P-28:0)          | C35H69NO9P   | [M+OAc]-     |
| 678.48 | 678.4716 | 0.0074 | PC(28:0(OH))        | C35H69NO9P   | [M-CH3]-     |
| 458.35 | 458.3407 | 0.0068 | Cer(d26:2)          | C26H49NO3Cl  | [M+Cl]-      |
| 458.35 | 458.3487 | 0.0013 | CAR(16:0)           | C25H48NO6    | [M+OAc]-     |
| 305.16 | 305.1606 | 0.0038 | FA(14:0(OH4,Ep))    | C14H25O7     | [M-H]-       |
| 305.16 | 305.1606 | 0.0038 | FA(14:0(OH4,Ke))    | C14H25O7     | [M-H]-       |
| 217.10 | 217.1082 | 0.0035 | FA(10:0(OH2,Ep))    | C10H17O5     | [M-H]-       |
| 217.10 | 217.1082 | 0.0035 | FA(10:0(OH2,Ke))    | C10H17O5     | [M-H]-       |
| 217.10 | 217.1082 | 0.0035 | FA(10:0(OH3,cyclo)) | C10H17O5     | [M-H]-       |
| 217.10 | 217.1082 | 0.0035 | FA(10:1(OH3))       | C10H17O5     | [M-H]-       |

**Lipidomics 2: CSF top neg log2FC candidate lipids**

| Input Mass | Matched Mass | Delta  | Name                  | Formula      | Ion                      |
|------------|--------------|--------|-----------------------|--------------|--------------------------|
| 678.48     | 678.4704     | 0.0084 | PE(30:1(OH))          | C35H69NO9P   | [M+H] <sup>+</sup>       |
| 678.48     | 678.4857     | 0.0068 | LPE(34:5)             | C39H69NO6P   | [M+H-H2O] <sup>+</sup>   |
| 678.48     | 678.4857     | 0.0068 | PE(P-34:4)            | C39H69NO6P   | [M+H-H2O] <sup>+</sup>   |
| 678.48     | 678.4704     | 0.0084 | PA(32:2(OH))          | C35H69NO9P   | [M+NH4] <sup>+</sup>     |
| 678.48     | 678.4858     | 0.0069 | CAR(34:6)             | C41H69NO4K   | [M+K] <sup>+</sup>       |
| 678.48     | 678.4716     | 0.0073 | PE(30:0(OH))          | C35H69NO9P   | [M-H] <sup>-</sup>       |
| 678.48     | 678.4717     | 0.0072 | HexCer(d30:1)         | C36H69NO8Cl  | [M+Cl] <sup>-</sup>      |
| 678.48     | 678.4798     | 0.0009 | HexCer(t28:0)         | C35H68NO11   | [M+Formate] <sup>-</sup> |
| 678.48     | 678.4716     | 0.0073 | CerP(t34:1)           | C35H69NO9P   | [M+Formate] <sup>-</sup> |
| 678.48     | 678.4716     | 0.0073 | LPC(26:1)             | C35H69NO9P   | [M+Formate] <sup>-</sup> |
| 678.48     | 678.4716     | 0.0073 | PC(P-26:0)            | C35H69NO9P   | [M+Formate] <sup>-</sup> |
| 678.48     | 678.4716     | 0.0073 | LPE(28:1)             | C35H69NO9P   | [M+OAc] <sup>-</sup>     |
| 678.48     | 678.4716     | 0.0073 | PE(P-28:0)            | C35H69NO9P   | [M+OAc] <sup>-</sup>     |
| 678.48     | 678.4716     | 0.0073 | PC(28:0(OH))          | C35H69NO9P   | [M-CH3] <sup>-</sup>     |
| 540.45     | 540.4445     | 0.0017 | NAT(30:1)             | C32H62NO3S   | [M+H-H2O] <sup>+</sup>   |
| 540.45     | 540.4411     | 0.0051 | CAR(28:5)             | C35H58NO3    | [M+H-H2O] <sup>+</sup>   |
| 413.27     | 413.2697     | 0.0036 | FA(26:4(Ep2,cyclo))   | C26H37O4     | [M-H] <sup>-</sup>       |
| 413.27     | 413.2697     | 0.0036 | FA(26:4(Ke2,cyclo))   | C26H37O4     | [M-H] <sup>-</sup>       |
| 413.27     | 413.2697     | 0.0036 | FA(26:4(Ke,Ep,cyclo)) | C26H37O4     | [M-H] <sup>-</sup>       |
| 413.27     | 413.2697     | 0.0036 | FA(26:5(Ep2))         | C26H37O4     | [M-H] <sup>-</sup>       |
| 413.27     | 413.2697     | 0.0036 | FA(26:5(Ke2))         | C26H37O4     | [M-H] <sup>-</sup>       |
| 413.27     | 413.2697     | 0.0036 | FA(26:5(Ke,Ep))       | C26H37O4     | [M-H] <sup>-</sup>       |
| 413.27     | 413.2697     | 0.0036 | FA(26:5(OH,Ep,cyclo)) | C26H37O4     | [M-H] <sup>-</sup>       |
| 413.27     | 413.2697     | 0.0036 | FA(26:5(OH,Ke,cyclo)) | C26H37O4     | [M-H] <sup>-</sup>       |
| 413.27     | 413.2697     | 0.0036 | FA(26:6(OH2,cyclo))   | C26H37O4     | [M-H] <sup>-</sup>       |
| 413.27     | 413.2697     | 0.0036 | FA(26:6(OH,Ep))       | C26H37O4     | [M-H] <sup>-</sup>       |
| 413.27     | 413.2697     | 0.0036 | FA(26:6(OH,Ke))       | C26H37O4     | [M-H] <sup>-</sup>       |
| 217.10     | 217.1082     | 0.0035 | FA(10:0(OH2,Ep))      | C10H17O5     | [M-H] <sup>-</sup>       |
| 217.10     | 217.1082     | 0.0035 | FA(10:0(OH2,Ke))      | C10H17O5     | [M-H] <sup>-</sup>       |
| 217.10     | 217.1082     | 0.0035 | FA(10:0(OH3,cyclo))   | C10H17O5     | [M-H] <sup>-</sup>       |
| 217.10     | 217.1082     | 0.0035 | FA(10:1(OH3))         | C10H17O5     | [M-H] <sup>-</sup>       |
| 503.38     | 503.3742     | 0.0039 | DG(28:4)              | C31H51O5     | [M-H] <sup>-</sup>       |
| 503.38     | 503.3873     | 0.0091 | DG(P-26:0)            | C29H56O4Cl   | [M+Cl] <sup>-</sup>      |
| 503.38     | 503.3873     | 0.0091 | MG(26:1)              | C29H56O4Cl   | [M+Cl] <sup>-</sup>      |
| 432.28     | 432.2849     | 0.0041 | S1P(d20:0)            | C20H44NO5PNa | [M+Na] <sup>+</sup>      |
| 432.28     | 432.2886     | 0.0078 | CAR(16:1)             | C23H43NO4Cl  | [M+Cl] <sup>-</sup>      |
| 507.33     | 507.3205     | 0.0081 | LysoSM(d18:2)         | C24H48N2O7P  | [M+Formate] <sup>-</sup> |
| 503.38     | 503.3742     | 0.0039 | DG(28:4)              | C31H51O5     | [M-H] <sup>-</sup>       |
| 503.38     | 503.3873     | 0.0092 | DG(P-26:0)            | C29H56O4Cl   | [M+Cl] <sup>-</sup>      |
| 503.38     | 503.3873     | 0.0092 | MG(26:1)              | C29H56O4Cl   | [M+Cl] <sup>-</sup>      |
| 503.38     | 503.3742     | 0.0039 | DG(28:4)              | C31H51O5     | [M-H] <sup>-</sup>       |
| 503.38     | 503.3873     | 0.0091 | DG(P-26:0)            | C29H56O4Cl   | [M+Cl] <sup>-</sup>      |
| 503.38     | 503.3873     | 0.0091 | MG(26:1)              | C29H56O4Cl   | [M+Cl] <sup>-</sup>      |
| 848.63     | 848.6375     | 0.0077 | PS(40:0)              | C46H91NO10P  | [M+H] <sup>+</sup>       |
| 848.63     | 848.6375     | 0.0077 | PS(O-40:1(OH))        | C46H91NO10P  | [M+H] <sup>+</sup>       |
| 848.63     | 848.6375     | 0.0077 | PS(P-40:0(OH))        | C46H91NO10P  | [M+H] <sup>+</sup>       |
| 848.63     | 848.628      | 0.0018 | SHexCer(d40:0)        | C46H90NO10S  | [M+H-H2O] <sup>+</sup>   |
| 848.63     | 848.6375     | 0.0077 | PI-Cer(d40:0)         | C46H91NO10P  | [M+H-H2O] <sup>+</sup>   |
| 848.63     | 848.6246     | 0.0052 | MGDG(40:6)            | C49H86NO10   | [M+NH4] <sup>+</sup>     |
| 848.63     | 848.6375     | 0.0077 | PG(40:2)              | C46H91NO10P  | [M+NH4] <sup>+</sup>     |
| 848.63     | 848.6375     | 0.0077 | PG(O-40:3(OH))        | C46H91NO10P  | [M+NH4] <sup>+</sup>     |
| 848.63     | 848.6375     | 0.0077 | PG(P-40:2(OH))        | C46H91NO10P  | [M+NH4] <sup>+</sup>     |
| 848.63     | 848.6376     | 0.0078 | HexCer(d42:2)         | C48H91NO8K   | [M+K] <sup>+</sup>       |
| 848.63     | 848.6386     | 0.0088 | PS(O-40:0(OH))        | C46H91NO10P  | [M-H] <sup>-</sup>       |
| 848.63     | 848.6306     | 0.0007 | PE(O-42:2)            | C47H92NO7PCl | [M+Cl] <sup>-</sup>      |
| 848.63     | 848.6306     | 0.0007 | PE(P-42:1)            | C47H92NO7PCl | [M+Cl] <sup>-</sup>      |
| 848.63     | 848.6386     | 0.0088 | PE(40:0)              | C46H91NO10P  | [M+Formate] <sup>-</sup> |
| 848.63     | 848.6386     | 0.0088 | PE(O-40:1(OH))        | C46H91NO10P  | [M+Formate] <sup>-</sup> |
| 848.63     | 848.6386     | 0.0088 | PE(P-40:0(OH))        | C46H91NO10P  | [M+Formate] <sup>-</sup> |
| 848.63     | 848.6386     | 0.0088 | PC(36:0)              | C46H91NO10P  | [M+OAc] <sup>-</sup>     |

|        |          |        |                     |              |              |
|--------|----------|--------|---------------------|--------------|--------------|
| 848.63 | 848.6386 | 0.0088 | PC(O-36:1(OH))      | C46H91NO10P  | [M+OAc]-     |
| 848.63 | 848.6386 | 0.0088 | PC(P-36:0(OH))      | C46H91NO10P  | [M+OAc]-     |
| 722.50 | 722.5119 | 0.0076 | PE(P-36:5)          | C41H73NO7P   | [M+H]+       |
| 722.50 | 722.5119 | 0.0076 | PE(36:4)            | C41H73NO7P   | [M+H-H2O]+   |
| 722.50 | 722.5119 | 0.0076 | PE(O-36:5(OH))      | C41H73NO7P   | [M+H-H2O]+   |
| 722.50 | 722.5119 | 0.0076 | PE(P-36:4(OH))      | C41H73NO7P   | [M+H-H2O]+   |
| 722.50 | 722.5095 | 0.0052 | PE(O-34:3)          | C39H74NO7PNa | [M+Na]+      |
| 722.50 | 722.5095 | 0.0052 | PE(P-34:2)          | C39H74NO7PNa | [M+Na]+      |
| 722.50 | 722.5119 | 0.0076 | PA(P-38:6)          | C41H73NO7P   | [M+NH4]+     |
| 722.50 | 722.5071 | 0.0028 | LPE(32:0)           | C37H76NO7P   | [M+2Na-H]+   |
| 722.50 | 722.5071 | 0.0028 | PE(O-32:0)          | C37H76NO7P   | [M+2Na-H]+   |
| 722.50 | 722.513  | 0.0087 | PE(O-36:5)          | C41H73NO7P   | [M-H]-       |
| 722.50 | 722.513  | 0.0087 | PE(P-36:4)          | C41H73NO7P   | [M-H]-       |
| 722.50 | 722.4979 | 0.0064 | HexCer(t32:1)       | C38H73NO9Cl  | [M+Cl]-      |
| 722.50 | 722.4978 | 0.0065 | PC(28:0)            | C37H73NO10P  | [M+Formate]- |
| 722.50 | 722.4978 | 0.0065 | PC(P-28:0(OH))      | C37H73NO10P  | [M+Formate]- |
| 722.50 | 722.4978 | 0.0065 | PE(30:0)            | C37H73NO10P  | [M+OAc]-     |
| 722.50 | 722.4978 | 0.0065 | PE-NMe2(28:0)       | C37H73NO10P  | [M+OAc]-     |
| 722.50 | 722.4978 | 0.0065 | PE(O-30:1(OH))      | C37H73NO10P  | [M+OAc]-     |
| 722.50 | 722.4978 | 0.0065 | PE(P-30:0(OH))      | C37H73NO10P  | [M+OAc]-     |
| 722.50 | 722.513  | 0.0087 | PC(P-34:4)          | C41H73NO7P   | [M-CH3]-     |
| 678.48 | 678.4704 | 0.0085 | PE(30:1(OH))        | C35H69NO9P   | [M+H]+       |
| 678.48 | 678.4857 | 0.0067 | LPE(34:5)           | C39H69NO6P   | [M+H-H2O]+   |
| 678.48 | 678.4857 | 0.0067 | PE(P-34:4)          | C39H69NO6P   | [M+H-H2O]+   |
| 678.48 | 678.4704 | 0.0085 | PA(32:2(OH))        | C35H69NO9P   | [M+NH4]+     |
| 678.48 | 678.4858 | 0.0068 | CAR(34:6)           | C41H69NO4K   | [M+K]+       |
| 678.48 | 678.4716 | 0.0074 | PE(30:0(OH))        | C35H69NO9P   | [M-H]-       |
| 678.48 | 678.4717 | 0.0072 | HexCer(d30:1)       | C36H69NO8Cl  | [M+Cl]-      |
| 678.48 | 678.4798 | 0.0008 | HexCer(t28:0)       | C35H68NO11   | [M+Formate]- |
| 678.48 | 678.4716 | 0.0074 | CerP(t34:1)         | C35H69NO9P   | [M+Formate]- |
| 678.48 | 678.4716 | 0.0074 | LPC(26:1)           | C35H69NO9P   | [M+Formate]- |
| 678.48 | 678.4716 | 0.0074 | PC(P-26:0)          | C35H69NO9P   | [M+Formate]- |
| 678.48 | 678.4716 | 0.0074 | LPE(28:1)           | C35H69NO9P   | [M+OAc]-     |
| 678.48 | 678.4716 | 0.0074 | PE(P-28:0)          | C35H69NO9P   | [M+OAc]-     |
| 678.48 | 678.4716 | 0.0074 | PC(28:0(OH))        | C35H69NO9P   | [M-CH3]-     |
| 458.35 | 458.3407 | 0.0068 | Cer(d26:2)          | C26H49NO3Cl  | [M+Cl]-      |
| 458.35 | 458.3487 | 0.0013 | CAR(16:0)           | C25H48NO6    | [M+OAc]-     |
| 305.16 | 305.1606 | 0.0038 | FA(14:0(OH4,Ep))    | C14H25O7     | [M-H]-       |
| 305.16 | 305.1606 | 0.0038 | FA(14:0(OH4,Ke))    | C14H25O7     | [M-H]-       |
| 217.10 | 217.1082 | 0.0035 | FA(10:0(OH2,Ep))    | C10H17O5     | [M-H]-       |
| 217.10 | 217.1082 | 0.0035 | FA(10:0(OH2,Ke))    | C10H17O5     | [M-H]-       |
| 217.10 | 217.1082 | 0.0035 | FA(10:0(OH3,cyclo)) | C10H17O5     | [M-H]-       |
| 217.10 | 217.1082 | 0.0035 | FA(10:1(OH3))       | C10H17O5     | [M-H]-       |

#### Lipidomics 2: CSF top pos log2FC candidate lipids

| Input Mass | Matched Mass | Delta  | Name           | Formula     | Ion          |
|------------|--------------|--------|----------------|-------------|--------------|
| 475.32     | 475.3183     | 0.0059 | LPA(22:1)      | C25H48O6P   | [M+H-H2O]+   |
| 475.32     | 475.3159     | 0.0083 | LPA(O-20:0)    | C23H49O6PNa | [M+Na]+      |
| 475.32     | 475.3159     | 0.0083 | PA(O-20:0)     | C23H49O6PNa | [M+Na]+      |
| 475.32     | 475.3184     | 0.0058 | MG(24:3)       | C27H48O4K   | [M+K]+       |
| 507.33     | 507.3205     | 0.0081 | LysoSM(d18:2)  | C24H48N2O7P | [M+Formate]- |
| 372.28     | 372.2897     | 0.0095 | NAE(22:6)      | C24H38NO2   | [M+H]+       |
| 372.28     | 372.2873     | 0.0071 | NAE(20:3)      | C22H39NO2Na | [M+Na]+      |
| 372.28     | 372.2849     | 0.0047 | NAE(18:0)      | C20H41NO2   | [M+2Na-H]+   |
| 372.28     | 372.2849     | 0.0047 | Sph(d20:1)     | C20H41NO2   | [M+2Na-H]+   |
| 527.16     | 527.1654     | 0.0029 | LPI(10:0)      | C19H37O12PK | [M+K]+       |
| 649.45     | 649.4439     | 0.0051 | LPG(28:2)      | C34H66O9P   | [M+H]+       |
| 649.45     | 649.4439     | 0.0051 | PG(28:0)       | C34H66O9P   | [M+H-H2O]+   |
| 649.45     | 649.4439     | 0.0051 | PG(P-28:0(OH)) | C34H66O9P   | [M+H-H2O]+   |
| 649.45     | 649.4551     | 0.0061 | PE(28:2)       | C33H66N2O8P | [M+NH4]+     |
| 649.45     | 649.445      | 0.004  | LPG(28:1)      | C34H66O9P   | [M-H]-       |

|        |          |        |                             |               |              |
|--------|----------|--------|-----------------------------|---------------|--------------|
| 649.45 | 649.445  | 0.004  | PG(P-28:0)                  | C34H66O9P     | [M-H]-       |
| 649.45 | 649.445  | 0.004  | LPA(30:1)                   | C34H66O9P     | [M+Formate]- |
| 649.45 | 649.445  | 0.004  | PA(O-30:1)                  | C34H66O9P     | [M+Formate]- |
| 649.45 | 649.445  | 0.004  | PA(P-30:0)                  | C34H66O9P     | [M+Formate]- |
| 649.45 | 649.4562 | 0.0072 | PE-Cer(d30:1)               | C33H66N2O8P   | [M+Formate]- |
| 649.45 | 649.4562 | 0.0072 | SM(d26:1)                   | C33H66N2O8P   | [M+OAc]-     |
| 443.33 | 443.3378 | 0.0033 | MG(20:1)                    | C25H47O6      | [M+OAc]-     |
| 443.33 | 443.3378 | 0.0033 | MG(20:1)                    | C25H47O6      | [M+OAc]-     |
| 358.20 | 358.2022 | 0.0006 | NAT(14:0)                   | C16H33NO4SNa  | [M+Na]+      |
| 358.20 | 358.1965 | 0.0051 | CAR(10:1)                   | C17H31NO4     | [M+2Na-H]+   |
| 321.03 | 321.0252 | 0.0088 | FA(14:4(OH3,Ke2,Ep2,cyclo)) | C14H9O9       | [M-H]-       |
| 607.40 | 607.3969 | 0.0066 | PA(28:1(OH))                | C31H60O9P     | [M+H]+       |
| 607.40 | 607.4122 | 0.0086 | LPA(32:5)                   | C35H60O6P     | [M+H-H2O]+   |
| 607.40 | 607.3981 | 0.0055 | PA(28:0(OH))                | C31H60O9P     | [M-H]-       |
| 607.40 | 607.3981 | 0.0055 | LPA(26:1)                   | C31H60O9P     | [M+OAc]-     |
| 607.40 | 607.3981 | 0.0055 | PA(P-26:0)                  | C31H60O9P     | [M+OAc]-     |
| 607.40 | 607.4093 | 0.0057 | PE-Cer(d26:1)               | C30H60N2O8P   | [M+OAc]-     |
| 693.48 | 693.4701 | 0.0069 | PG(30:1)                    | C36H70O10P    | [M+H]+       |
| 693.48 | 693.4701 | 0.0069 | PG(P-30:1(OH))              | C36H70O10P    | [M+H]+       |
| 693.48 | 693.4701 | 0.0069 | PG(30:0(OH))                | C36H70O10P    | [M+H-H2O]+   |
| 693.48 | 693.4813 | 0.0043 | PE(30:2(OH))                | C35H70N2O9P   | [M+NH4]+     |
| 693.48 | 693.4712 | 0.0058 | PG(30:0)                    | C36H70O10P    | [M-H]-       |
| 693.48 | 693.4712 | 0.0058 | PG(O-30:1(OH))              | C36H70O10P    | [M-H]-       |
| 693.48 | 693.4712 | 0.0058 | PG(P-30:0(OH))              | C36H70O10P    | [M-H]-       |
| 693.48 | 693.4744 | 0.0026 | PE-Cer(d34:2)               | C36H71N2O6PCl | [M+Cl]-      |
| 693.48 | 693.4866 | 0.0096 | TG(38:4)                    | C41H70O6Cl    | [M+Cl]-      |
| 693.48 | 693.4825 | 0.0054 | PE-Cer(t32:1)               | C35H70N2O9P   | [M+Formate]- |
| 693.48 | 693.4712 | 0.0058 | PA(32:0)                    | C36H70O10P    | [M+Formate]- |
| 693.48 | 693.4712 | 0.0058 | PA(O-32:1(OH))              | C36H70O10P    | [M+Formate]- |
| 693.48 | 693.4712 | 0.0058 | PA(P-32:0(OH))              | C36H70O10P    | [M+Formate]- |
| 693.48 | 693.4736 | 0.0034 | DG(38:9)                    | C43H65O7      | [M+OAc]-     |
| 693.48 | 693.4825 | 0.0054 | SM(t28:1)                   | C35H70N2O9P   | [M+OAc]-     |
| 460.33 | 460.3269 | 0.0059 | HexSph(d18:2)               | C24H46NO7     | [M+H]+       |
| 460.33 | 460.3269 | 0.0059 | HexSph(t18:1)               | C24H46NO7     | [M+H-H2O]+   |
| 460.33 | 460.328  | 0.0047 | HexSph(d18:1)               | C24H46NO7     | [M-H]-       |
| 283.26 | 283.2632 | 0.0001 | WE(18:1)                    | C18H35O2      | [M+H]+       |
| 283.26 | 283.2643 | 0.001  | FA(18:0)                    | C18H35O2      | [M-H]-       |
| 283.26 | 283.2643 | 0.001  | WE(18:0)                    | C18H35O2      | [M-H]-       |
| 716.38 | 716.3874 | 0.0076 | PE(30:4(OH))                | C35H62NO9P    | [M+2Na-H]+   |
| 716.38 | 716.37   | 0.0098 | LPS(30:6)                   | C36H60NO9PCl  | [M+Cl]-      |
| 716.38 | 716.378  | 0.0018 | PS(28:4)                    | C35H59NO12P   | [M+Formate]- |
| 558.49 | 558.4857 | 0.0088 | Cer(d34:2)                  | C34H65NO3Na   | [M+Na]+      |
| 558.49 | 558.5022 | 0.0078 | Cer(m34:0)                  | C34H69NO2Cl   | [M+Cl]-      |
| 558.49 | 558.5022 | 0.0078 | NAE(32:0)                   | C34H69NO2Cl   | [M+Cl]-      |



**Lipidomics 2: Plasma top pvalue candidate lipids**

| Input Mass | Matched Mass | Delta  | Name                | Formula       | Ion          |
|------------|--------------|--------|---------------------|---------------|--------------|
| 900.33     | 900.339      | 0.007  | M(IP)2C(d16:1)      | C34H64NO22P2  | [M+H-H2O]+   |
| 747.51     | 747.5171     | 0.0041 | LBPA(34:2)          | C40H76O10P    | [M+H]+       |
| 747.51     | 747.5171     | 0.0041 | PG(34:2)            | C40H76O10P    | [M+H]+       |
| 747.51     | 747.5171     | 0.0041 | PG(O-34:3(OH))      | C40H76O10P    | [M+H]+       |
| 747.51     | 747.5171     | 0.0041 | PG(P-34:2(OH))      | C40H76O10P    | [M+H]+       |
| 747.51     | 747.5042     | 0.0088 | MGDG(34:6)          | C43H71O10     | [M+H]+       |
| 747.51     | 747.5171     | 0.0041 | PG(34:1(OH))        | C40H76O10P    | [M+H-H2O]+   |
| 747.51     | 747.5147     | 0.0017 | PG(O-32:0(OH))      | C38H77O10PNa  | [M+Na]+      |
| 747.51     | 747.5182     | 0.0052 | LBPA(34:1)          | C40H76O10P    | [M-H]-       |
| 747.51     | 747.5182     | 0.0052 | PG(34:1)            | C40H76O10P    | [M-H]-       |
| 747.51     | 747.5182     | 0.0052 | PG(O-34:2(OH))      | C40H76O10P    | [M-H]-       |
| 747.51     | 747.5182     | 0.0052 | PG(P-34:1(OH))      | C40H76O10P    | [M-H]-       |
| 747.51     | 747.5053     | 0.0077 | MGDG(34:5)          | C43H71O10     | [M-H]-       |
| 747.51     | 747.5101     | 0.0029 | PA(O-38:3)          | C41H77O7PCI   | [M+Cl]-      |
| 747.51     | 747.5101     | 0.0029 | PA(P-38:2)          | C41H77O7PCI   | [M+Cl]-      |
| 747.51     | 747.5213     | 0.0083 | PE-Cer(d38:3)       | C40H77N2O6PCI | [M+Cl]-      |
| 747.51     | 747.5182     | 0.0052 | PA(36:1)            | C40H76O10P    | [M+Formate]- |
| 747.51     | 747.5182     | 0.0052 | PA(O-36:2(OH))      | C40H76O10P    | [M+Formate]- |
| 747.51     | 747.5182     | 0.0052 | PA(P-36:1(OH))      | C40H76O10P    | [M+Formate]- |
| 747.51     | 747.5205     | 0.0075 | DG(42:10)           | C47H71O7      | [M+OAc]-     |
| 401.29     | 401.2816     | 0.0064 | WE(24:3)            | C24H42O2K     | [M+K]+       |
| 401.29     | 401.2909     | 0.0029 | FA(22:0(OH3,Ep))    | C22H41O6      | [M-H]-       |
| 401.29     | 401.2909     | 0.0029 | FA(22:0(OH3,Ke))    | C22H41O6      | [M-H]-       |
| 401.29     | 401.2909     | 0.0029 | FA(22:0(OH4,cyclo)) | C22H41O6      | [M-H]-       |
| 401.29     | 401.2909     | 0.0029 | FA(22:1(OH4))       | C22H41O6      | [M-H]-       |
| 401.29     | 401.2909     | 0.0029 | MG(18:1)            | C22H41O6      | [M+Formate]- |
| 358.20     | 358.2022     | 0.0012 | NAT(14:0)           | C16H33NO4SNa  | [M+Na]+      |
| 358.20     | 358.1965     | 0.0045 | CAR(10:1)           | C17H31NO4     | [M+2Na-H]+   |
| 591.35     | 591.3528     | 0.0018 | MGDG(24:5)          | C33H51O9      | [M+H-H2O]+   |
| 591.35     | 591.3421     | 0.0089 | LPA(28:5)           | C31H53O7PNa   | [M+Na]+      |
| 591.35     | 591.3509     | 0.0001 | PE-Cer(d26:2)       | C28H55N2O6P   | [M+2Na-H]+   |
| 925.65     | 925.6528     | 0.0018 | PG(46:5(OH))        | C52H94O11P    | [M+H]+       |
| 925.65     | 925.6504     | 0.0006 | PG(44:2(OH))        | C50H95O11PNa  | [M+Na]+      |
| 925.65     | 925.6429     | 0.0081 | PC(46:11)           | C54H90N2O8P   | [M+NH4]+     |
| 925.65     | 925.6539     | 0.0029 | PG(46:4(OH))        | C52H94O11P    | [M-H]-       |
| 925.65     | 925.6541     | 0.0031 | MGDG(44:4)          | C53H94O10Cl   | [M+Cl]-      |
| 925.65     | 925.6459     | 0.0051 | PA(50:5)            | C53H95O8PCI   | [M+Cl]-      |
| 925.65     | 925.6459     | 0.0051 | PA(O-50:6(OH))      | C53H95O8PCI   | [M+Cl]-      |
| 925.65     | 925.6459     | 0.0051 | PA(P-50:5(OH))      | C53H95O8PCI   | [M+Cl]-      |
| 925.65     | 925.6539     | 0.0029 | PA(48:4(OH))        | C52H94O11P    | [M+Formate]- |
| 925.65     | 925.6539     | 0.0029 | PG(O-44:5)          | C52H94O11P    | [M+OAc]-     |
| 925.65     | 925.6539     | 0.0029 | PG(P-44:4)          | C52H94O11P    | [M+OAc]-     |
| 925.65     | 925.6563     | 0.0053 | TG(54:12)           | C59H89O8      | [M+OAc]-     |
| 753.56     | 753.564      | 0.005  | PG(O-34:0(OH))      | C40H82O10P    | [M+H]+       |
| 753.56     | 753.5511     | 0.0079 | MGDG(34:3)          | C43H77O10     | [M+H]+       |

|        |          |        |                |               |              |
|--------|----------|--------|----------------|---------------|--------------|
| 753.56 | 753.5517 | 0.0073 | PE-Cer(t38:2)  | C40H79N2O7PNa | [M+Na]+      |
| 753.56 | 753.5541 | 0.0049 | LPC(34:6)      | C42H78N2O7P   | [M+NH4]+     |
| 753.56 | 753.5557 | 0.0033 | WE(50:12)      | C50H76O2      | [M+2Na-H]+   |
| 753.56 | 753.5522 | 0.0068 | MGDG(34:2)     | C43H77O10     | [M-H]-       |
| 753.56 | 753.5571 | 0.0019 | PA(O-38:0)     | C41H83O7PCI   | [M+Cl]-      |
| 753.56 | 753.5683 | 0.0093 | PE-Cer(d38:0)  | C40H83N2O6PCI | [M+Cl]-      |
| 753.56 | 753.5675 | 0.0085 | DG(42:7)       | C47H77O7      | [M+OAc]-     |
| 975.63 | 975.6226 | 0.0074 | SQDG(46:8)     | C55H91O12S    | [M+H]+       |
| 975.63 | 975.6321 | 0.0021 | PI(46:7)       | C55H92O12P    | [M+H-H2O]+   |
| 975.63 | 975.6297 | 0.0003 | PI(O-44:6)     | C53H93O12PNa  | [M+Na]+      |
| 975.63 | 975.6297 | 0.0003 | PI(P-44:5)     | C53H93O12PNa  | [M+Na]+      |
| 975.63 | 975.6202 | 0.0098 | SQDG(44:5)     | C53H92O12SNa  | [M+Na]+      |
| 975.63 | 975.6322 | 0.0022 | MGDG(48:9)     | C57H92O10K    | [M+K]+       |
| 975.63 | 975.624  | 0.006  | PA(54:10)      | C57H93O8PK    | [M+K]+       |
| 975.63 | 975.6273 | 0.0027 | PI(O-42:3)     | C51H95O12P    | [M+2Na-H]+   |
| 975.63 | 975.6273 | 0.0027 | PI(P-42:2)     | C51H95O12P    | [M+2Na-H]+   |
| 975.63 | 975.6237 | 0.0063 | SQDG(46:7)     | C55H91O12S    | [M-H]-       |
| 975.63 | 975.6332 | 0.0032 | PG(48:8)       | C55H92O12P    | [M+Formate]- |
| 975.63 | 975.6203 | 0.0097 | MGDG(48:12)    | C58H87O12     | [M+Formate]- |
| 975.63 | 975.6262 | 0.0038 | DGDG(34:2)     | C51H91O17     | [M+OAc]-     |
| 767.66 | 767.6676 | 0.0096 | WE(52:8)       | C52H88O2Na    | [M+Na]+      |
| 767.66 | 767.6652 | 0.0072 | WE(50:5)       | C50H90O2      | [M+2Na-H]+   |
| 731.58 | 731.5698 | 0.0092 | PE-Cer(t38:2)  | C40H80N2O7P   | [M+H]+       |
| 731.58 | 731.5737 | 0.0053 | WE(50:12)      | C50H76O2Na    | [M+Na]+      |
| 731.58 | 731.578  | 0.001  | HexCer(t34:2)  | C40H79N2O9    | [M+NH4]+     |
| 731.58 | 731.5698 | 0.0092 | PC(O-32:3)     | C40H80N2O7P   | [M+NH4]+     |
| 731.58 | 731.5713 | 0.0077 | WE(48:9)       | C48H78O2      | [M+2Na-H]+   |
| 731.58 | 731.5709 | 0.0081 | PE-Cer(t38:1)  | C40H80N2O7P   | [M-H]-       |
| 731.58 | 731.5831 | 0.0041 | DG(40:4)       | C45H79O7      | [M+OAc]-     |
| 731.58 | 731.5709 | 0.0081 | SM(t36:1)      | C40H80N2O7P   | [M-CH3]-     |
| 806.51 | 806.5083 | 0.0013 | SQDG(32:3)     | C41H76NO12S   | [M+NH4]+     |
| 806.51 | 806.5097 | 0.0027 | PE(38:4)       | C43H78NO8PK   | [M+K]+       |
| 806.51 | 806.5097 | 0.0027 | PE(O-38:5(OH)) | C43H78NO8PK   | [M+K]+       |
| 806.51 | 806.5097 | 0.0027 | PE(P-38:4(OH)) | C43H78NO8PK   | [M+K]+       |
| 806.51 | 806.4978 | 0.0092 | PS(38:6)       | C44H73NO10P   | [M-H]-       |
| 806.51 | 806.4978 | 0.0092 | PS(P-38:6(OH)) | C44H73NO10P   | [M-H]-       |
| 806.51 | 806.5108 | 0.0038 | PC(34:3(OH))   | C42H78NO9PCI  | [M+Cl]-      |
| 806.51 | 806.5108 | 0.0038 | PS(O-36:3)     | C42H78NO9PCI  | [M+Cl]-      |
| 806.51 | 806.5108 | 0.0038 | PS(P-36:2)     | C42H78NO9PCI  | [M+Cl]-      |
| 806.51 | 806.4978 | 0.0092 | PE(38:7)       | C44H73NO10P   | [M+Formate]- |
| 805.56 | 805.5589 | 0.0029 | PI(O-34:1)     | C43H82O11P    | [M+H-H2O]+   |
| 805.56 | 805.5589 | 0.0029 | PI(P-34:0)     | C43H82O11P    | [M+H-H2O]+   |
| 805.56 | 805.5494 | 0.0066 | SQDG(34:0)     | C43H81O11S    | [M+H-H2O]+   |
| 805.56 | 805.549  | 0.007  | PE(40:8)       | C45H78N2O8P   | [M+NH4]+     |
| 805.56 | 805.5508 | 0.0052 | PA(O-42:4)     | C45H83O7PK    | [M+K]+       |
| 805.56 | 805.5508 | 0.0052 | PA(P-42:3)     | C45H83O7PK    | [M+K]+       |
| 805.56 | 805.5543 | 0.0017 | DG(48:11)      | C51H78O5Cl    | [M+Cl]-      |

|        |          |        |                |              |              |
|--------|----------|--------|----------------|--------------|--------------|
| 805.56 | 805.56   | 0.004  | PG(O-36:2)     | C43H82O11P   | [M+Formate]- |
| 805.56 | 805.56   | 0.004  | PG(P-36:1)     | C43H82O11P   | [M+Formate]- |
| 805.56 | 805.56   | 0.004  | PA(38:1(OH))   | C43H82O11P   | [M+OAc]-     |
| 959.64 | 959.65   | 0.008  | PA(54:10)      | C57H93O8PNa  | [M+Na]+      |
| 959.64 | 959.6484 | 0.0064 | PS(48:9)       | C54H92N2O10P | [M+NH4]+     |
| 959.64 | 959.6502 | 0.0082 | PG(O-48:6)     | C54H97O9PK   | [M+K]+       |
| 959.64 | 959.6502 | 0.0082 | PG(P-48:5)     | C54H97O9PK   | [M+K]+       |
| 959.64 | 959.6476 | 0.0056 | PA(52:7)       | C55H95O8P    | [M+2Na-H]+   |
| 959.64 | 959.6361 | 0.0059 | PI(O-40:0(OH)) | C49H97O13PCl | [M+Cl]-      |
| 959.64 | 959.6383 | 0.0037 | PA(50:8(OH))   | C55H92O11P   | [M+OAc]-     |
| 730.57 | 730.5745 | 0.0005 | PE(O-36:2)     | C41H81NO7P   | [M+H]+       |
| 730.57 | 730.5745 | 0.0005 | PE(P-36:1)     | C41H81NO7P   | [M+H]+       |
| 730.57 | 730.5745 | 0.0005 | PE(36:0)       | C41H81NO7P   | [M+H-H2O]+   |
| 730.57 | 730.5745 | 0.0005 | PE(O-36:1(OH)) | C41H81NO7P   | [M+H-H2O]+   |
| 730.57 | 730.5745 | 0.0005 | PE(P-36:0(OH)) | C41H81NO7P   | [M+H-H2O]+   |
| 730.57 | 730.5745 | 0.0005 | PA(O-38:3)     | C41H81NO7P   | [M+NH4]+     |
| 730.57 | 730.5745 | 0.0005 | PA(P-38:2)     | C41H81NO7P   | [M+NH4]+     |
| 730.57 | 730.5756 | 0.0016 | PE(O-36:1)     | C41H81NO7P   | [M-H]-       |
| 730.57 | 730.5756 | 0.0016 | PE(P-36:0)     | C41H81NO7P   | [M-H]-       |
| 730.57 | 730.5756 | 0.0016 | PC(O-34:1)     | C41H81NO7P   | [M-CH3]-     |
| 730.57 | 730.5756 | 0.0016 | PC(P-34:0)     | C41H81NO7P   | [M-CH3]-     |
| 752.56 | 752.5589 | 0.0029 | PE(O-38:5)     | C43H79NO7P   | [M+H]+       |
| 752.56 | 752.5589 | 0.0029 | PE(P-38:4)     | C43H79NO7P   | [M+H]+       |
| 752.56 | 752.5589 | 0.0029 | PE(38:3)       | C43H79NO7P   | [M+H-H2O]+   |
| 752.56 | 752.5589 | 0.0029 | PE(O-38:4(OH)) | C43H79NO7P   | [M+H-H2O]+   |
| 752.56 | 752.5589 | 0.0029 | PE(P-38:3(OH)) | C43H79NO7P   | [M+H-H2O]+   |
| 752.56 | 752.5565 | 0.0005 | PE(O-36:2)     | C41H80NO7PNa | [M+Na]+      |
| 752.56 | 752.5565 | 0.0005 | PE(P-36:1)     | C41H80NO7PNa | [M+Na]+      |
| 752.56 | 752.5589 | 0.0029 | PA(O-40:6)     | C43H79NO7P   | [M+NH4]+     |
| 752.56 | 752.5589 | 0.0029 | PA(P-40:5)     | C43H79NO7P   | [M+NH4]+     |
| 752.56 | 752.56   | 0.004  | PE(O-38:4)     | C43H79NO7P   | [M-H]-       |
| 752.56 | 752.56   | 0.004  | PE(P-38:3)     | C43H79NO7P   | [M-H]-       |
| 752.56 | 752.56   | 0.004  | PC(O-36:4)     | C43H79NO7P   | [M-CH3]-     |
| 752.56 | 752.56   | 0.004  | PC(P-36:3)     | C43H79NO7P   | [M-CH3]-     |
| 808.66 | 808.6578 | 0.0028 | PC(O-40:3)     | C48H91NO6P   | [M+H-H2O]+   |
| 808.66 | 808.6578 | 0.0028 | PC(P-40:2)     | C48H91NO6P   | [M+H-H2O]+   |
| 808.66 | 808.6554 | 0.0004 | CerP(d46:1)    | C46H92NO6PNa | [M+Na]+      |
| 808.66 | 808.6637 | 0.0087 | HexCer(d40:0)  | C46H91NO8Na  | [M+Na]+      |
| 707.69 | 707.6923 | 0.0073 | WE(44:0)       | C46H91O4     | [M+OAc]-     |

#### Lipidomics 2: Plasma top neg log2FC candidate lipids

| Input Mass | Matched Mass | Delta  | Name           | Formula      | Ion        |
|------------|--------------|--------|----------------|--------------|------------|
| 722.50     | 722.5119     | 0.0079 | PE(P-36:5)     | C41H73NO7P   | [M+H]+     |
| 722.50     | 722.5119     | 0.0079 | PE(36:4)       | C41H73NO7P   | [M+H-H2O]+ |
| 722.50     | 722.5119     | 0.0079 | PE(O-36:5(OH)) | C41H73NO7P   | [M+H-H2O]+ |
| 722.50     | 722.5119     | 0.0079 | PE(P-36:4(OH)) | C41H73NO7P   | [M+H-H2O]+ |
| 722.50     | 722.5095     | 0.0055 | PE(O-34:3)     | C39H74NO7PNa | [M+Na]+    |

|        |          |        |                        |              |              |
|--------|----------|--------|------------------------|--------------|--------------|
| 722.50 | 722.5095 | 0.0055 | PE(P-34:2)             | C39H74NO7PNa | [M+Na]+      |
| 722.50 | 722.5119 | 0.0079 | PA(P-38:6)             | C41H73NO7P   | [M+NH4]+     |
| 722.50 | 722.5071 | 0.0031 | LPE(32:0)              | C37H76NO7P   | [M+2Na-H]+   |
| 722.50 | 722.5071 | 0.0031 | PE(O-32:0)             | C37H76NO7P   | [M+2Na-H]+   |
| 722.50 | 722.513  | 0.009  | PE(O-36:5)             | C41H73NO7P   | [M-H]-       |
| 722.50 | 722.513  | 0.009  | PE(P-36:4)             | C41H73NO7P   | [M-H]-       |
| 722.50 | 722.4979 | 0.0061 | HexCer(t32:1)          | C38H73NO9Cl  | [M+Cl]-      |
| 722.50 | 722.4978 | 0.0062 | PC(28:0)               | C37H73NO10P  | [M+Formate]- |
| 722.50 | 722.4978 | 0.0062 | PC(P-28:0(OH))         | C37H73NO10P  | [M+Formate]- |
| 722.50 | 722.4978 | 0.0062 | PE(30:0)               | C37H73NO10P  | [M+OAc]-     |
| 722.50 | 722.4978 | 0.0062 | PE-NMe2(28:0)          | C37H73NO10P  | [M+OAc]-     |
| 722.50 | 722.4978 | 0.0062 | PE(O-30:1(OH))         | C37H73NO10P  | [M+OAc]-     |
| 722.50 | 722.4978 | 0.0062 | PE(P-30:0(OH))         | C37H73NO10P  | [M+OAc]-     |
| 722.50 | 722.513  | 0.009  | PC(P-34:4)             | C41H73NO7P   | [M-CH3]-     |
| 454.34 | 454.3292 | 0.0078 | LPC(O-14:0)            | C22H49NO6P   | [M+H]+       |
| 454.34 | 454.3349 | 0.0021 | NAT(24:2)              | C26H48NO3S   | [M+H-H2O]+   |
| 454.34 | 454.3316 | 0.0054 | CAR(22:6)              | C29H44NO3    | [M+H-H2O]+   |
| 454.34 | 454.3404 | 0.0034 | LysoSM(d16:1)          | C21H49N3O5P  | [M+NH4]+     |
| 590.43 | 590.418  | 0.008  | LPE(26:2)              | C31H61NO7P   | [M+H]+       |
| 590.43 | 590.418  | 0.008  | PE(26:0)               | C31H61NO7P   | [M+H-H2O]+   |
| 590.43 | 590.418  | 0.008  | PE-NMe2(24:0)          | C31H61NO7P   | [M+H-H2O]+   |
| 590.43 | 590.418  | 0.008  | PE(P-26:0(OH))         | C31H61NO7P   | [M+H-H2O]+   |
| 590.43 | 590.418  | 0.008  | LPA(28:3)              | C31H61NO7P   | [M+NH4]+     |
| 590.43 | 590.4191 | 0.0069 | LPE(26:1)              | C31H61NO7P   | [M-H]-       |
| 590.43 | 590.4191 | 0.0069 | PE(P-26:0)             | C31H61NO7P   | [M-H]-       |
| 900.33 | 900.339  | 0.007  | M(IP)2C(d16:1)         | C34H64NO22P2 | [M+H-H2O]+   |
| 634.45 | 634.4442 | 0.0078 | PE(28:1)               | C33H65NO8P   | [M+H]+       |
| 634.45 | 634.4442 | 0.0078 | PE(28:0(OH))           | C33H65NO8P   | [M+H-H2O]+   |
| 634.45 | 634.4525 | 0.0005 | MGDG(24:1)             | C33H64NO10   | [M+NH4]+     |
| 634.45 | 634.4442 | 0.0078 | PA(30:2)               | C33H65NO8P   | [M+NH4]+     |
| 634.45 | 634.4453 | 0.0067 | PE(28:0)               | C33H65NO8P   | [M-H]-       |
| 634.45 | 634.4453 | 0.0067 | PE(P-28:0(OH))         | C33H65NO8P   | [M-H]-       |
| 634.45 | 634.4536 | 0.0016 | HexCer(d26:0)          | C33H64NO10   | [M+Formate]- |
| 634.45 | 634.4453 | 0.0067 | CerP(d32:1)            | C33H65NO8P   | [M+Formate]- |
| 634.45 | 634.4453 | 0.0067 | PC(26:0)               | C33H65NO8P   | [M-CH3]-     |
| 634.45 | 634.4453 | 0.0067 | PC(P-26:0(OH))         | C33H65NO8P   | [M-CH3]-     |
| 699.53 | 699.5347 | 0.0037 | DG(44:10)              | C47H71O4     | [M+H-H2O]+   |
| 699.53 | 699.5299 | 0.0011 | DG(O-40:6)             | C43H74O4     | [M+2Na-H]+   |
| 699.53 | 699.5299 | 0.0011 | DG(P-40:5)             | C43H74O4     | [M+2Na-H]+   |
| 699.53 | 699.5336 | 0.0026 | TG(38:1)               | C41H76O6Cl   | [M+Cl]-      |
| 699.53 | 699.5358 | 0.0048 | WE(46:11)              | C47H71O4     | [M+Formate]- |
| 395.36 | 395.352  | 0.004  | MG(22:1)               | C25H47O3     | [M+H-H2O]+   |
| 395.36 | 395.3496 | 0.0064 | MG(O-20:0)             | C23H48O3Na   | [M+Na]+      |
| 513.35 | 513.3586 | 0.0056 | FA(32:3(Ke2,Ep,cyclo)) | C32H49O5     | [M-H]-       |
| 513.35 | 513.3586 | 0.0056 | FA(32:3(Ke,Ep2,cyclo)) | C32H49O5     | [M-H]-       |
| 513.35 | 513.3586 | 0.0056 | FA(32:4(Ke2,Ep))       | C32H49O5     | [M-H]-       |
| 513.35 | 513.3586 | 0.0056 | FA(32:4(Ke,Ep2))       | C32H49O5     | [M-H]-       |

|        |          |        |                           |              |              |
|--------|----------|--------|---------------------------|--------------|--------------|
| 513.35 | 513.3586 | 0.0056 | FA(32:4(OH,Ep2,cyclo))    | C32H49O5     | [M-H]-       |
| 513.35 | 513.3586 | 0.0056 | FA(32:4(OH,Ke2,cyclo))    | C32H49O5     | [M-H]-       |
| 513.35 | 513.3586 | 0.0056 | FA(32:4(OH,Ke,Ep,cyclo))  | C32H49O5     | [M-H]-       |
| 513.35 | 513.3586 | 0.0056 | FA(32:5(OH2,Ep,cyclo))    | C32H49O5     | [M-H]-       |
| 513.35 | 513.3586 | 0.0056 | FA(32:5(OH2,Ke,cyclo))    | C32H49O5     | [M-H]-       |
| 513.35 | 513.3586 | 0.0056 | FA(32:5(OH,Ep2))          | C32H49O5     | [M-H]-       |
| 513.35 | 513.3586 | 0.0056 | FA(32:5(OH,Ke2))          | C32H49O5     | [M-H]-       |
| 513.35 | 513.3586 | 0.0056 | FA(32:5(OH,Ke,Ep))        | C32H49O5     | [M-H]-       |
| 513.35 | 513.3586 | 0.0056 | FA(32:6(OH2,Ep))          | C32H49O5     | [M-H]-       |
| 513.35 | 513.3586 | 0.0056 | FA(32:6(OH2,Ke))          | C32H49O5     | [M-H]-       |
| 513.35 | 513.3586 | 0.0056 | FA(32:6(OH3,cyclo))       | C32H49O5     | [M-H]-       |
| 513.35 | 513.3433 | 0.0097 | FA(28:0(OH3,Ke2,Ep))      | C28H49O8     | [M-H]-       |
| 513.35 | 513.3433 | 0.0097 | FA(28:0(OH3,Ke,Ep2))      | C28H49O8     | [M-H]-       |
| 513.35 | 513.3433 | 0.0097 | FA(28:0(OH4,Ep2,cyclo))   | C28H49O8     | [M-H]-       |
| 513.35 | 513.3433 | 0.0097 | FA(28:0(OH4,Ke2,cyclo))   | C28H49O8     | [M-H]-       |
| 513.35 | 513.3433 | 0.0097 | FA(28:0(OH4,Ke,Ep,cyclo)) | C28H49O8     | [M-H]-       |
| 513.35 | 513.3433 | 0.0097 | FA(28:1(OH4,Ep2))         | C28H49O8     | [M-H]-       |
| 513.35 | 513.3433 | 0.0097 | FA(28:1(OH4,Ke2))         | C28H49O8     | [M-H]-       |
| 513.35 | 513.3433 | 0.0097 | FA(28:1(OH4,Ke,Ep))       | C28H49O8     | [M-H]-       |
| 672.54 | 672.5409 | 0.0021 | HexCer(d32:1)             | C38H74NO8    | [M+H]+       |
| 672.54 | 672.5409 | 0.0021 | HexCer(t32:0)             | C38H74NO8    | [M+H-H2O]+   |
| 672.54 | 672.5513 | 0.0083 | Cer(t38:0(OH))            | C38H77NO5    | [M+2Na-H]+   |
| 672.54 | 672.542  | 0.001  | HexCer(d32:0)             | C38H74NO8    | [M-H]-       |
| 672.54 | 672.5338 | 0.0092 | CerP(d38:1)               | C38H75NO6P   | [M-H]-       |
| 513.42 | 513.4161 | 0.0029 | FA(30:0(OH3,Ep))          | C30H57O6     | [M-H]-       |
| 513.42 | 513.4161 | 0.0029 | FA(30:0(OH3,Ke))          | C30H57O6     | [M-H]-       |
| 513.42 | 513.4161 | 0.0029 | FA(30:0(OH4,cyclo))       | C30H57O6     | [M-H]-       |
| 513.42 | 513.4161 | 0.0029 | FA(30:1(OH4))             | C30H57O6     | [M-H]-       |
| 513.42 | 513.4161 | 0.0029 | DG(P-26:0)                | C30H57O6     | [M+Formate]- |
| 513.42 | 513.4161 | 0.0029 | MG(26:1)                  | C30H57O6     | [M+Formate]- |
| 888.65 | 888.6477 | 0.0043 | PC(44:7)                  | C52H91NO8P   | [M+H]+       |
| 888.65 | 888.6477 | 0.0043 | PC(44:6(OH))              | C52H91NO8P   | [M+H-H2O]+   |
| 888.65 | 888.6477 | 0.0043 | PS(O-46:6)                | C52H91NO8P   | [M+H-H2O]+   |
| 888.65 | 888.6477 | 0.0043 | PS(P-46:5)                | C52H91NO8P   | [M+H-H2O]+   |
| 888.65 | 888.6453 | 0.0067 | PC(42:4)                  | C50H92NO8PNa | [M+Na]+      |
| 888.65 | 888.6453 | 0.0067 | PC(O-42:5(OH))            | C50H92NO8PNa | [M+Na]+      |
| 888.65 | 888.6453 | 0.0067 | PC(P-42:4(OH))            | C50H92NO8PNa | [M+Na]+      |
| 888.65 | 888.6429 | 0.0091 | PC(40:1)                  | C48H94NO8P   | [M+2Na-H]+   |
| 888.65 | 888.6429 | 0.0091 | PC(O-40:2(OH))            | C48H94NO8P   | [M+2Na-H]+   |
| 888.65 | 888.6429 | 0.0091 | PC(P-40:1(OH))            | C48H94NO8P   | [M+2Na-H]+   |
| 888.65 | 888.6619 | 0.0099 | PC(O-42:3)                | C50H96NO7PCI | [M+Cl]-      |
| 888.65 | 888.6619 | 0.0099 | PC(P-42:2)                | C50H96NO7PCI | [M+Cl]-      |
| 975.63 | 975.6226 | 0.0074 | SQDG(46:8)                | C55H91O12S   | [M+H]+       |
| 975.63 | 975.6321 | 0.0021 | PI(46:7)                  | C55H92O12P   | [M+H-H2O]+   |
| 975.63 | 975.6297 | 0.0003 | PI(O-44:6)                | C53H93O12PNa | [M+Na]+      |
| 975.63 | 975.6297 | 0.0003 | PI(P-44:5)                | C53H93O12PNa | [M+Na]+      |
| 975.63 | 975.6202 | 0.0098 | SQDG(44:5)                | C53H92O12SNa | [M+Na]+      |

|        |          |        |                |                |              |
|--------|----------|--------|----------------|----------------|--------------|
| 975.63 | 975.6322 | 0.0022 | MGDG(48:9)     | C57H92O10K     | [M+K]+       |
| 975.63 | 975.624  | 0.006  | PA(54:10)      | C57H93O8PK     | [M+K]+       |
| 975.63 | 975.6273 | 0.0027 | PI(O-42:3)     | C51H95O12P     | [M+2Na-H]+   |
| 975.63 | 975.6273 | 0.0027 | PI(P-42:2)     | C51H95O12P     | [M+2Na-H]+   |
| 975.63 | 975.6237 | 0.0063 | SQDG(46:7)     | C55H91O12S     | [M-H]-       |
| 975.63 | 975.6332 | 0.0032 | PG(48:8)       | C55H92O12P     | [M+Formate]- |
| 975.63 | 975.6203 | 0.0097 | MGDG(48:12)    | C58H87O12      | [M+Formate]- |
| 975.63 | 975.6262 | 0.0038 | DGDG(34:2)     | C51H91O17      | [M+OAc]-     |
| 788.46 | 788.4589 | 0.0041 | SHexCer(t32:2) | C38H71NO12SNa  | [M+Na]+      |
| 788.46 | 788.4684 | 0.0054 | PI-Cer(t32:2)  | C38H72NO12PNa  | [M+Na]+      |
| 788.46 | 788.4627 | 0.0003 | PC(34:6)       | C42H72NO8PK    | [M+K]+       |
| 788.46 | 788.4557 | 0.0073 | LacCer(d26:1)  | C38H71NO13K    | [M+K]+       |
| 788.46 | 788.4639 | 0.0009 | PE(36:5(OH))   | C41H72NO9PCI   | [M+Cl]-      |
| 788.46 | 788.4719 | 0.0089 | PS(32:3)       | C40H71NO12P    | [M+OAc]-     |
| 1010.7 | 1010.720 | 0.0028 | PC(52:10(OH))  | C60H101NO9P    | [M+H]+       |
| 1010.7 | 1010.720 | 0.0028 | PS(54:8)       | C60H101NO9P    | [M+H-H2O]+   |
| 1010.7 | 1010.718 | 0.0004 | PC(50:7(OH))   | C58H102NO9PNa  | [M+Na]+      |
| 1010.7 | 1010.718 | 0.0004 | PS(P-52:6)     | C58H102NO9PNa  | [M+Na]+      |
| 1010.7 | 1010.711 | 0.0066 | LacCer(t42:2)  | C54H101NO14Na  | [M+Na]+      |
| 1010.7 | 1010.726 | 0.0087 | PI(44:1(OH))   | C53H105NO14P   | [M+NH4]+     |
| 1010.7 | 1010.716 | 0.002  | PC(48:4(OH))   | C56H104NO9P    | [M+2Na-H]+   |
| 1010.7 | 1010.716 | 0.002  | PS(O-50:4)     | C56H104NO9P    | [M+2Na-H]+   |
| 1010.7 | 1010.716 | 0.002  | PS(P-50:3)     | C56H104NO9P    | [M+2Na-H]+   |
| 1010.7 | 1010.719 | 0.0018 | PI-Cer(d48:1)  | C54H106NO11PCI | [M+Cl]-      |
| 1010.7 | 1010.719 | 0.0018 | PS(48:0(OH))   | C54H106NO11PCI | [M+Cl]-      |
| 1010.7 | 1010.710 | 0.0078 | SHexCer(d48:1) | C54H105NO11SCI | [M+Cl]-      |
| 1010.7 | 1010.718 | 0.0003 | SHexCer(t46:0) | C53H104NO14S   | [M+Formate]- |
| 1010.7 | 1010.727 | 0.0098 | PI-Cer(t46:0)  | C53H105NO14P   | [M+Formate]- |

**Lipidomics 2: Plasma top pos log2FC candidate lipids**

| Input Mass | Matched Mass | Delta  | Name           | Formula       | Ion          |
|------------|--------------|--------|----------------|---------------|--------------|
| 532.39     | 532.3819     | 0.0091 | NAT(30:5)      | C32H54NO3S    | [M+H-H2O]+   |
| 358.20     | 358.2022     | 0.0002 | NAT(14:0)      | C16H33NO4SNa  | [M+Na]+      |
| 358.20     | 358.1965     | 0.0055 | CAR(10:1)      | C17H31NO4     | [M+2Na-H]+   |
| 610.51     | 610.5146     | 0.0036 | Cer(d36:1)     | C36H71NO3     | [M+2Na-H]+   |
| 610.51     | 610.5052     | 0.0058 | CAR(28:1)      | C36H68NO6     | [M+Formate]- |
| 610.51     | 610.5052     | 0.0058 | Cer(t34:2)     | C36H68NO6     | [M+OAc]-     |
| 663.45     | 663.4595     | 0.0085 | PA(32:1(OH))   | C35H68O9P     | [M+H]+       |
| 663.45     | 663.4538     | 0.0028 | WE(44:12)      | C44H64O2K     | [M+K]+       |
| 663.45     | 663.4448     | 0.0062 | SM(d28:1)      | C33H67N2O6P   | [M+2Na-H]+   |
| 663.45     | 663.4607     | 0.0097 | PA(32:0(OH))   | C35H68O9P     | [M-H]-       |
| 663.45     | 663.4607     | 0.0097 | LPA(30:1)      | C35H68O9P     | [M+OAc]-     |
| 663.45     | 663.4607     | 0.0097 | PA(O-30:1)     | C35H68O9P     | [M+OAc]-     |
| 663.45     | 663.4607     | 0.0097 | PA(P-30:0)     | C35H68O9P     | [M+OAc]-     |
| 665.44     | 665.4388     | 0.0008 | PG(28:1)       | C34H66O10P    | [M+H]+       |
| 665.44     | 665.4388     | 0.0008 | PG(28:0(OH))   | C34H66O10P    | [M+H-H2O]+   |
| 665.44     | 665.4399     | 0.0019 | PG(28:0)       | C34H66O10P    | [M-H]-       |
| 665.44     | 665.4399     | 0.0019 | PG(P-28:0(OH)) | C34H66O10P    | [M-H]-       |
| 665.44     | 665.4431     | 0.0051 | PE-Cer(d32:2)  | C34H67N2O6PCI | [M+Cl]-      |
| 665.44     | 665.4319     | 0.0061 | PA(P-32:1)     | C35H67O7PCI   | [M+Cl]-      |
| 665.44     | 665.4399     | 0.0019 | PA(30:0)       | C34H66O10P    | [M+Formate]- |
| 665.44     | 665.4399     | 0.0019 | PA(O-30:1(OH)) | C34H66O10P    | [M+Formate]- |
| 665.44     | 665.4399     | 0.0019 | PA(P-30:0(OH)) | C34H66O10P    | [M+Formate]- |
| 773.49     | 773.4868     | 0.0072 | SQDG(32:2)     | C41H73O11S    | [M+H-H2O]+   |
| 773.49     | 773.4882     | 0.0058 | PA(O-40:6)     | C43H75O7PK    | [M+K]+       |
| 773.49     | 773.4882     | 0.0058 | PA(P-40:5)     | C43H75O7PK    | [M+K]+       |
| 773.49     | 773.4974     | 0.0034 | LPG(34:4)      | C41H74O11P    | [M+Formate]- |
| 773.49     | 773.4974     | 0.0034 | PG(O-34:4)     | C41H74O11P    | [M+Formate]- |
| 773.49     | 773.4974     | 0.0034 | PG(P-34:3)     | C41H74O11P    | [M+Formate]- |
| 773.49     | 773.4974     | 0.0034 | PA(36:3(OH))   | C41H74O11P    | [M+OAc]-     |
| 328.22     | 328.2248     | 0.0068 | Sph(t16:0)     | C16H35NO3K    | [M+K]+       |
| 436.31     | 436.3186     | 0.0086 | LPC(O-14:0)    | C22H47NO5P    | [M+H-H2O]+   |
| 436.31     | 436.3033     | 0.0067 | CAR(16:1(OH))  | C23H43NO5Na   | [M+Na]+      |
| 772.49     | 772.4912     | 0.0022 | PC(36:8(OH))   | C44H71NO8P    | [M+H-H2O]+   |
| 772.49     | 772.4888     | 0.0002 | PC(34:6)       | C42H72NO8PNa  | [M+Na]+      |
| 772.49     | 772.4818     | 0.0072 | LacCer(d26:1)  | C38H71NO13Na  | [M+Na]+      |
| 772.49     | 772.4888     | 0.0002 | PPA(34:1)      | C37H76NO11P2  | [M+NH4]+     |
| 772.49     | 772.4971     | 0.0081 | PI(28:0)       | C37H75NO13P   | [M+NH4]+     |
| 772.49     | 772.4971     | 0.0081 | PI(P-28:0(OH)) | C37H75NO13P   | [M+NH4]+     |
| 772.49     | 772.4889     | 0.0001 | PE(34:1(OH))   | C39H76NO9PK   | [M+K]+       |
| 772.49     | 772.4864     | 0.0026 | PC(32:3)       | C40H74NO8P    | [M+2Na-H]+   |
| 772.49     | 772.4901     | 0.0011 | PS(O-32:0(OH)) | C38H76NO10PCI | [M+Cl]-      |
| 609.51     | 609.5089     | 0.0019 | TG(34:1)       | C37H69O6      | [M+H]+       |
| 609.51     | 609.503      | 0.004  | WE(44:11)      | C44H65O       | [M+H-H2O]+   |
| 609.51     | 609.51       | 0.003  | TG(34:0)       | C37H69O6      | [M-H]-       |
| 609.51     | 609.51       | 0.003  | FAHFA(O-36:1)  | C37H69O6      | [M+Formate]- |

|        |          |        |                    |             |            |
|--------|----------|--------|--------------------|-------------|------------|
| 609.51 | 609.51   | 0.003  | DG(P-18:1)         | C37H69O6    | [M+OAc]-   |
| 609.51 | 609.51   | 0.003  | DG(P-32:1)         | C37H69O6    | [M+OAc]-   |
| 401.32 | 401.3061 | 0.0089 | FA(26:3(Ep,cyclo)) | C26H41O3    | [M-H]-     |
| 401.32 | 401.3061 | 0.0089 | FA(26:3(Ke,cyclo)) | C26H41O3    | [M-H]-     |
| 401.32 | 401.3061 | 0.0089 | FA(26:4(Ep))       | C26H41O3    | [M-H]-     |
| 401.32 | 401.3061 | 0.0089 | FA(26:4(Ke))       | C26H41O3    | [M-H]-     |
| 401.32 | 401.3061 | 0.0089 | FA(26:4(OH,cyclo)) | C26H41O3    | [M-H]-     |
| 401.32 | 401.3061 | 0.0089 | FA(26:5(OH))       | C26H41O3    | [M-H]-     |
| 401.32 | 401.3192 | 0.0042 | WE(24:1)           | C24H46O2Cl  | [M+Cl]-    |
| 608.50 | 608.4989 | 0.0051 | Cer(d36:2)         | C36H69NO3   | [M+2Na-H]+ |
| 651.41 | 651.402  | 0.005  | LPG(30:6)          | C36H60O8P   | [M+H-H2O]+ |
| 651.41 | 651.4085 | 0.0015 | SM(t26:1)          | C31H63N2O7P | [M+2Na-H]+ |
| 309.28 | 309.2788 | 0.0002 | WE(20:2)           | C20H37O2    | [M+H]+     |
| 309.28 | 309.2799 | 0.0009 | FA(20:0(cyclo))    | C20H37O2    | [M-H]-     |
| 309.28 | 309.2799 | 0.0009 | FA(20:1)           | C20H37O2    | [M-H]-     |
| 309.28 | 309.2799 | 0.0009 | WE(20:1)           | C20H37O2    | [M-H]-     |
| 595.38 | 595.3758 | 0.0062 | LPA(30:6)          | C33H56O7P   | [M+H]+     |
| 595.38 | 595.3841 | 0.0021 | MGDG(24:3)         | C33H55O9    | [M+H-H2O]+ |
| 595.38 | 595.3758 | 0.0062 | PA(30:4)           | C33H56O7P   | [M+H-H2O]+ |
| 595.38 | 595.3734 | 0.0086 | LPA(28:3)          | C31H57O7PNa | [M+Na]+    |
| 595.38 | 595.3759 | 0.0061 | DG(32:6)           | C35H56O5K   | [M+K]+     |
| 595.38 | 595.3822 | 0.0002 | PE-Cer(d26:0)      | C28H59N2O6P | [M+2Na-H]+ |
| 595.38 | 595.3769 | 0.0051 | LPA(30:5)          | C33H56O7P   | [M-H]-     |
| 437.31 | 437.3139 | 0.0001 | LysoSM(d16:1)      | C21H46N2O5P | [M+H]+     |
| 437.31 | 437.3139 | 0.0001 | LysoSM(t16:0)      | C21H46N2O5P | [M+H-H2O]+ |
| 437.31 | 437.315  | 0.001  | LysoSM(d16:0)      | C21H46N2O5P | [M-H]-     |
| 429.28 | 429.2782 | 0.0049 | NAT(20:4)          | C22H41N2O4S | [M+NH4]+   |
| 597.39 | 597.3915 | 0.0035 | LPA(30:5)          | C33H58O7P   | [M+H]+     |
| 597.39 | 597.3915 | 0.0035 | PA(30:3)           | C33H58O7P   | [M+H-H2O]+ |
| 597.39 | 597.3891 | 0.0011 | LPA(28:2)          | C31H59O7PNa | [M+Na]+    |
| 597.39 | 597.3874 | 0.0006 | LPS(22:1)          | C28H58N2O9P | [M+NH4]+   |
| 597.39 | 597.3957 | 0.0077 | LacSph(m16:1)      | C28H57N2O11 | [M+NH4]+   |
| 597.39 | 597.3916 | 0.0036 | DG(32:5)           | C35H58O5K   | [M+K]+     |
| 597.39 | 597.3926 | 0.0046 | LPA(30:4)          | C33H58O7P   | [M-H]-     |
| 463.30 | 463.3065 | 0.0035 | MG(22:5)           | C27H43O6    | [M+OAc]-   |



**Lipidomics 2: Urine top pvalue candidate lipids**

| Input Mass | Matched Mass | Delta  | Name                | Formula       | Ion          |
|------------|--------------|--------|---------------------|---------------|--------------|
| 532.35     | 532.3491     | 0.0049 | HexSph(d20:2)       | C27H50NO9     | [M+Formate]- |
| 490.34     | 490.3457     | 0.0019 | NAE(28:6)           | C30H49NO2Cl   | [M+Cl]-      |
| 487.32     | 487.3271     | 0.0023 | LysoSM(d18:1)       | C23H49N2O5PNa | [M+Na]+      |
| 487.32     | 487.3277     | 0.0028 | FA(26:0(OH4,Ep2))   | C26H47O8      | [M-H]-       |
| 487.32     | 487.3277     | 0.0028 | FA(26:0(OH4,Ke2))   | C26H47O8      | [M-H]-       |
| 487.32     | 487.3277     | 0.0028 | FA(26:0(OH4,Ke,Ep)) | C26H47O8      | [M-H]-       |
| 502.37     | 502.3749     | 0.0005 | CAR(18:0(OH))       | C27H52NO7     | [M+OAc]-     |
| 488.33     | 488.3347     | 0.007  | LPG(O-16:0)         | C22H51NO8P    | [M+NH4]+     |
| 488.33     | 488.3322     | 0.0045 | CAR(18:0(OH))       | C25H49NO5     | [M+2Na-H]+   |
| 488.33     | 488.3229     | 0.0048 | CAR(16:0(COOH))     | C25H46NO8     | [M+OAc]-     |
| 354.34     | 354.3366     | 0      | NAE(20:1)           | C22H44NO2     | [M+H]+       |
| 354.34     | 354.3367     | 0      | WE(22:2)            | C22H44NO2     | [M+NH4]+     |
| 354.34     | 354.3378     | 0.0011 | NAE(20:0)           | C22H44NO2     | [M-H]-       |
| 606.43     | 606.4212     | 0.0069 | MGDG(22:1)          | C31H60NO10    | [M+NH4]+     |
| 619.44     | 619.4416     | 0.0015 | MGDG(24:0)          | C33H63O10     | [M+H]+       |
| 619.44     | 619.4446     | 0.0045 | PE-Cer(t30:2)       | C32H64N2O7P   | [M+H]+       |
| 619.44     | 619.4333     | 0.0067 | PA(30:1)            | C33H64O8P     | [M+H]+       |
| 619.44     | 619.4333     | 0.0067 | PA(P-30:1(OH))      | C33H64O8P     | [M+H]+       |
| 619.44     | 619.4333     | 0.0067 | PA(30:0(OH))        | C33H64O8P     | [M+H-H2O]+   |
| 619.44     | 619.4446     | 0.0045 | LPC(24:3)           | C32H64N2O7P   | [M+NH4]+     |
| 619.44     | 619.4461     | 0.0061 | WE(40:9)            | C40H62O2      | [M+2Na-H]+   |
| 619.44     | 619.4344     | 0.0056 | PA(30:0)            | C33H64O8P     | [M-H]-       |
| 619.44     | 619.4344     | 0.0056 | PA(O-30:1(OH))      | C33H64O8P     | [M-H]-       |
| 619.44     | 619.4344     | 0.0056 | PA(P-30:0(OH))      | C33H64O8P     | [M-H]-       |
| 619.44     | 619.4457     | 0.0056 | PE-Cer(t30:1)       | C32H64N2O7P   | [M-H]-       |
| 619.44     | 619.4457     | 0.0056 | SM(t28:1)           | C32H64N2O7P   | [M-CH3]-     |
| 575.38     | 575.3707     | 0.0067 | LPG(24:2)           | C30H56O8P     | [M+H-H2O]+   |
| 575.38     | 575.382      | 0.0046 | LPE(24:4)           | C29H56N2O7P   | [M+NH4]+     |
| 575.38     | 575.3683     | 0.0091 | DG(30:5)            | C33H54O5      | [M+2Na-H]+   |
| 621.51     | 621.4966     | 0.0095 | SM(d28:0)           | C33H70N2O6P   | [M+H]+       |
| 621.51     | 621.5007     | 0.0054 | WE(40:5)            | C40H70O2K     | [M+K]+       |
| 621.51     | 621.51       | 0.0039 | DG(O-34:3)          | C38H69O6      | [M+Formate]- |
| 621.51     | 621.51       | 0.0039 | DG(P-34:2)          | C38H69O6      | [M+Formate]- |
| 589.56     | 589.5554     | 0.0008 | DG(O-36:2)          | C39H73O3      | [M+H-H2O]+   |
| 589.56     | 589.5554     | 0.0008 | DG(P-36:1)          | C39H73O3      | [M+H-H2O]+   |
| 589.56     | 589.5514     | 0.0048 | Cer(t34:0(OH))      | C34H73N2O5    | [M+NH4]+     |
| 698.37     | 698.3768     | 0.008  | PE(30:5)            | C35H60NO8P    | [M+2Na-H]+   |
| 698.37     | 698.3675     | 0.0014 | LPS(28:6)           | C35H57NO11P   | [M+Formate]- |
| 772.49     | 772.4912     | 0.002  | PC(36:8(OH))        | C44H71NO8P    | [M+H-H2O]+   |
| 772.49     | 772.4888     | 0.0004 | PC(34:6)            | C42H72NO8PNa  | [M+Na]+      |
| 772.49     | 772.4818     | 0.0074 | LacCer(d26:1)       | C38H71NO13Na  | [M+Na]+      |
| 772.49     | 772.4888     | 0.0003 | PPA(34:1)           | C37H76NO11P2  | [M+NH4]+     |
| 772.49     | 772.4971     | 0.0079 | PI(28:0)            | C37H75NO13P   | [M+NH4]+     |
| 772.49     | 772.4971     | 0.0079 | PI(P-28:0(OH))      | C37H75NO13P   | [M+NH4]+     |
| 772.49     | 772.4889     | 0.0002 | PE(34:1(OH))        | C39H76NO9PK   | [M+K]+       |
| 772.49     | 772.4864     | 0.0028 | PC(32:3)            | C40H74NO8P    | [M+2Na-H]+   |
| 772.49     | 772.4901     | 0.0009 | PS(O-32:0(OH))      | C38H76NO10PCl | [M+Cl]-      |
| 527.16     | 527.1654     | 0.0029 | LPI(10:0)           | C19H37O12PK   | [M+K]+       |
| 441.36     | 441.3703     | 0.0091 | WE(28:3)            | C28H50O2Na    | [M+Na]+      |
| 441.36     | 441.3687     | 0.0074 | CAR(16:2)           | C25H49N2O4    | [M+NH4]+     |
| 441.36     | 441.3687     | 0.0074 | CAR(18:2)           | C25H49N2O4    | [M+NH4]+     |
| 441.36     | 441.3679     | 0.0067 | WE(26:0)            | C26H52O2      | [M+2Na-H]+   |
| 441.36     | 441.3586     | 0.0027 | FA(26:0(OH2,Ep))    | C26H49O5      | [M-H]-       |
| 441.36     | 441.3586     | 0.0027 | FA(26:0(OH2,Ke))    | C26H49O5      | [M-H]-       |
| 441.36     | 441.3586     | 0.0027 | FA(26:0(OH3,cyclo)) | C26H49O5      | [M-H]-       |
| 441.36     | 441.3586     | 0.0027 | FA(26:1(OH3))       | C26H49O5      | [M-H]-       |

**Lipidomics 2: Urine top neg log2FC candidate lipids**

| Input Mass | Matched Mass | Delta  | Name                   | Formula       | Ion                      |
|------------|--------------|--------|------------------------|---------------|--------------------------|
| 722.50     | 722.5119     | 0.0081 | PE(P-36:5)             | C41H73NO7P    | [M+H] <sup>+</sup>       |
| 722.50     | 722.5119     | 0.0081 | PE(36:4)               | C41H73NO7P    | [M+H-H2O] <sup>+</sup>   |
| 722.50     | 722.5119     | 0.0081 | PE(O-36:5(OH))         | C41H73NO7P    | [M+H-H2O] <sup>+</sup>   |
| 722.50     | 722.5119     | 0.0081 | PE(P-36:4(OH))         | C41H73NO7P    | [M+H-H2O] <sup>+</sup>   |
| 722.50     | 722.5095     | 0.0057 | PE(O-34:3)             | C39H74NO7PNa  | [M+Na] <sup>+</sup>      |
| 722.50     | 722.5095     | 0.0057 | PE(P-34:2)             | C39H74NO7PNa  | [M+Na] <sup>+</sup>      |
| 722.50     | 722.5119     | 0.0081 | PA(P-38:6)             | C41H73NO7P    | [M+NH4] <sup>+</sup>     |
| 722.50     | 722.5071     | 0.0033 | LPE(32:0)              | C37H76NO7P    | [M+2Na-H] <sup>+</sup>   |
| 722.50     | 722.5071     | 0.0033 | PE(O-32:0)             | C37H76NO7P    | [M+2Na-H] <sup>+</sup>   |
| 722.50     | 722.513      | 0.0092 | PE(O-36:5)             | C41H73NO7P    | [M-H] <sup>-</sup>       |
| 722.50     | 722.513      | 0.0092 | PE(P-36:4)             | C41H73NO7P    | [M-H] <sup>-</sup>       |
| 722.50     | 722.4979     | 0.0059 | HexCer(t32:1)          | C38H73NO9Cl   | [M+Cl] <sup>-</sup>      |
| 722.50     | 722.4978     | 0.006  | PC(28:0)               | C37H73NO10P   | [M+Formate] <sup>-</sup> |
| 722.50     | 722.4978     | 0.006  | PC(P-28:0(OH))         | C37H73NO10P   | [M+Formate] <sup>-</sup> |
| 722.50     | 722.4978     | 0.006  | PE(30:0)               | C37H73NO10P   | [M+OAc] <sup>-</sup>     |
| 722.50     | 722.4978     | 0.006  | PE-NMe2(28:0)          | C37H73NO10P   | [M+OAc] <sup>-</sup>     |
| 722.50     | 722.4978     | 0.006  | PE(O-30:1(OH))         | C37H73NO10P   | [M+OAc] <sup>-</sup>     |
| 722.50     | 722.4978     | 0.006  | PE(P-30:0(OH))         | C37H73NO10P   | [M+OAc] <sup>-</sup>     |
| 722.50     | 722.513      | 0.0092 | PC(P-34:4)             | C41H73NO7P    | [M-CH3] <sup>-</sup>     |
| 500.36     | 500.3686     | 0.0075 | CAR(20:0)              | C27H53NO4     | [M+2Na-H] <sup>+</sup>   |
| 331.18     | 331.1762     | 0.0042 | FA(16:0(OH3,Ep2))      | C16H27O7      | [M-H] <sup>-</sup>       |
| 331.18     | 331.1762     | 0.0042 | FA(16:0(OH3,Ke2))      | C16H27O7      | [M-H] <sup>-</sup>       |
| 331.18     | 331.1762     | 0.0042 | FA(16:0(OH3,Ke,Ep))    | C16H27O7      | [M-H] <sup>-</sup>       |
| 331.18     | 331.1762     | 0.0042 | FA(16:0(OH4,Ep,cyclo)) | C16H27O7      | [M-H] <sup>-</sup>       |
| 331.18     | 331.1762     | 0.0042 | FA(16:0(OH4,Ke,cyclo)) | C16H27O7      | [M-H] <sup>-</sup>       |
| 331.18     | 331.1762     | 0.0042 | FA(16:1(OH4,Ep))       | C16H27O7      | [M-H] <sup>-</sup>       |
| 331.18     | 331.1762     | 0.0042 | FA(16:1(OH4,Ke))       | C16H27O7      | [M-H] <sup>-</sup>       |
| 502.37     | 502.3749     | 0.0006 | CAR(18:0(OH))          | C27H52NO7     | [M+OAc] <sup>-</sup>     |
| 464.25     | 464.2538     | 0.0001 | S1P(t20:0)             | C20H44NO6PK   | [M+K] <sup>+</sup>       |
| 922.75     | 922.7401     | 0.0064 | CerP(t52:0)            | C52H106NO7PCl | [M+Cl] <sup>-</sup>      |
| 922.75     | 922.7401     | 0.0064 | PC(O-44:0)             | C52H106NO7PCl | [M+Cl] <sup>-</sup>      |
| 571.31     | 571.3172     | 0.0088 | PA(24:0)               | C27H53O8PCl   | [M+Cl] <sup>-</sup>      |
| 571.31     | 571.3042     | 0.0043 | LPA(24:5)              | C29H48O9P     | [M+OAc] <sup>-</sup>     |
| 413.27     | 413.2697     | 0.0036 | FA(26:4(Ep2,cyclo))    | C26H37O4      | [M-H] <sup>-</sup>       |
| 413.27     | 413.2697     | 0.0036 | FA(26:4(Ke2,cyclo))    | C26H37O4      | [M-H] <sup>-</sup>       |
| 413.27     | 413.2697     | 0.0036 | FA(26:4(Ke,Ep,cyclo))  | C26H37O4      | [M-H] <sup>-</sup>       |
| 413.27     | 413.2697     | 0.0036 | FA(26:5(Ep2))          | C26H37O4      | [M-H] <sup>-</sup>       |
| 413.27     | 413.2697     | 0.0036 | FA(26:5(Ke2))          | C26H37O4      | [M-H] <sup>-</sup>       |
| 413.27     | 413.2697     | 0.0036 | FA(26:5(Ke,Ep))        | C26H37O4      | [M-H] <sup>-</sup>       |
| 413.27     | 413.2697     | 0.0036 | FA(26:5(OH,Ep,cyclo))  | C26H37O4      | [M-H] <sup>-</sup>       |
| 413.27     | 413.2697     | 0.0036 | FA(26:5(OH,Ke,cyclo))  | C26H37O4      | [M-H] <sup>-</sup>       |
| 413.27     | 413.2697     | 0.0036 | FA(26:6(OH2,cyclo))    | C26H37O4      | [M-H] <sup>-</sup>       |
| 413.27     | 413.2697     | 0.0036 | FA(26:6(OH,Ep))        | C26H37O4      | [M-H] <sup>-</sup>       |
| 413.27     | 413.2697     | 0.0036 | FA(26:6(OH,Ke))        | C26H37O4      | [M-H] <sup>-</sup>       |
| 217.10     | 217.1082     | 0.0034 | FA(10:0(OH2,Ep))       | C10H17O5      | [M-H] <sup>-</sup>       |
| 217.10     | 217.1082     | 0.0034 | FA(10:0(OH2,Ke))       | C10H17O5      | [M-H] <sup>-</sup>       |
| 217.10     | 217.1082     | 0.0034 | FA(10:0(OH3,cyclo))    | C10H17O5      | [M-H] <sup>-</sup>       |
| 217.10     | 217.1082     | 0.0034 | FA(10:1(OH3))          | C10H17O5      | [M-H] <sup>-</sup>       |

## Lipidomics 2: Urine top pos log2FC candidate lipids

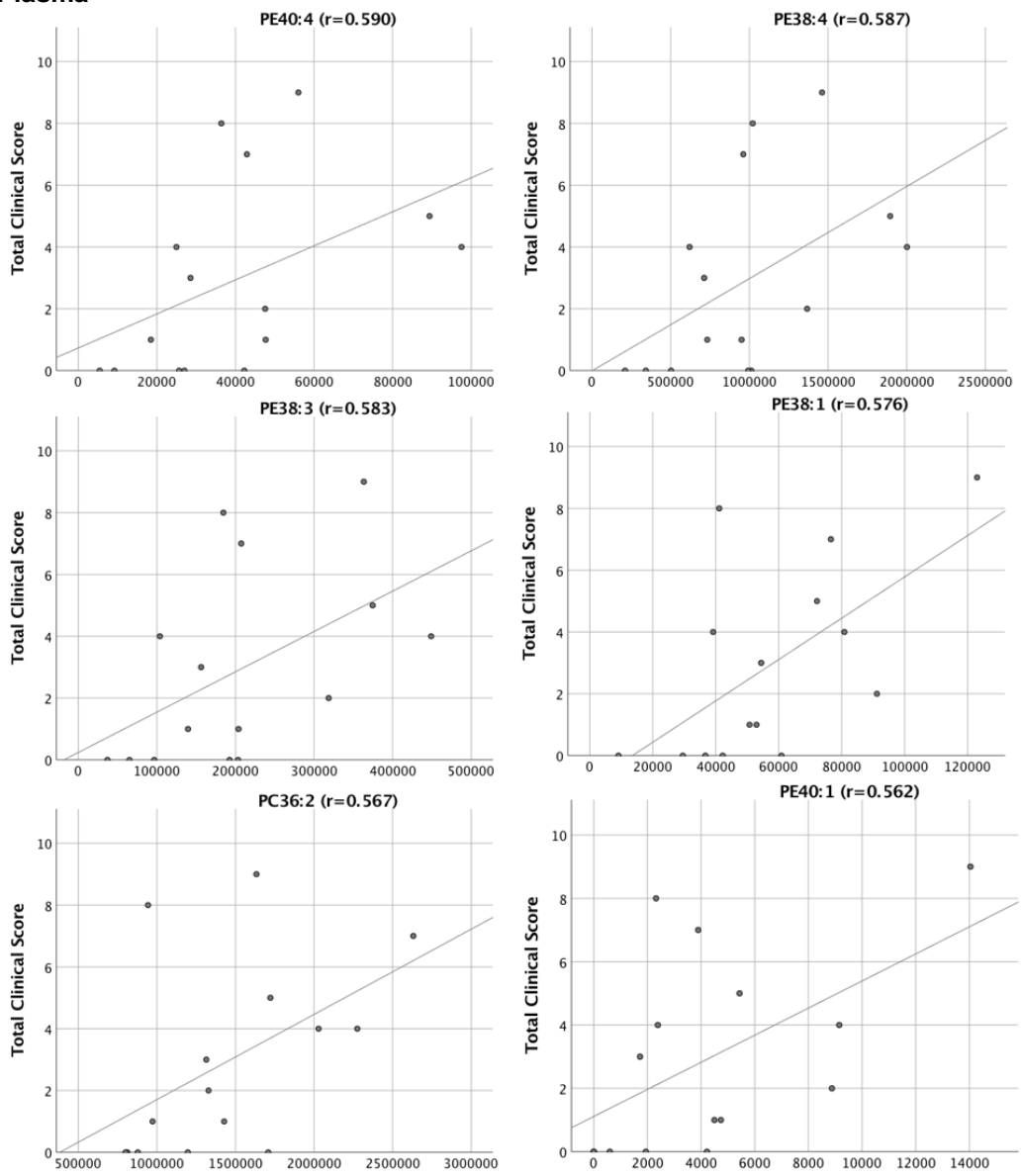
| Input Mass | Matched Mass | Delta  | Name           | Formula       | Ion                      |
|------------|--------------|--------|----------------|---------------|--------------------------|
| 330.34     | 330.3366     | 0.0002 | Sph(d20:0)     | C20H44NO2     | [M+H] <sup>+</sup>       |
| 330.34     | 330.3366     | 0.0002 | WE(20:0)       | C20H44NO2     | [M+NH4] <sup>+</sup>     |
| 791.55     | 791.5433     | 0.0048 | PG(36:2(OH))   | C42H80O11P    | [M+H] <sup>+</sup>       |
| 791.55     | 791.5561     | 0.008  | DG(46:9)       | C49H78O5      | [M+2Na-H] <sup>+</sup>   |
| 791.55     | 791.5444     | 0.0037 | PG(36:1(OH))   | C42H80O11P    | [M-H] <sup>-</sup>       |
| 791.55     | 791.5475     | 0.0005 | PE-Cer(t40:3)  | C42H81N2O7PCI | [M+Cl] <sup>-</sup>      |
| 791.55     | 791.5446     | 0.0035 | MGDG(34:1)     | C43H80O10Cl   | [M+Cl] <sup>-</sup>      |
| 791.55     | 791.5444     | 0.0037 | PA(38:1(OH))   | C42H80O11P    | [M+Formate] <sup>-</sup> |
| 791.55     | 791.5444     | 0.0037 | PG(O-34:2)     | C42H80O11P    | [M+OAc] <sup>-</sup>     |
| 791.55     | 791.5444     | 0.0037 | PG(P-34:1)     | C42H80O11P    | [M+OAc] <sup>-</sup>     |
| 595.38     | 595.3758     | 0.0059 | LPA(30:6)      | C33H56O7P     | [M+H] <sup>+</sup>       |
| 595.38     | 595.3841     | 0.0023 | MGDG(24:3)     | C33H55O9      | [M+H-H2O] <sup>+</sup>   |
| 595.38     | 595.3758     | 0.0059 | PA(30:4)       | C33H56O7P     | [M+H-H2O] <sup>+</sup>   |
| 595.38     | 595.3734     | 0.0083 | LPA(28:3)      | C31H57O7PNa   | [M+Na] <sup>+</sup>      |
| 595.38     | 595.3718     | 0.01   | LPS(22:2)      | C28H56N2O9P   | [M+NH4] <sup>+</sup>     |
| 595.38     | 595.3759     | 0.0058 | DG(32:6)       | C35H56O5K     | [M+K] <sup>+</sup>       |
| 595.38     | 595.3822     | 0.0005 | PE-Cer(d26:0)  | C28H59N2O6P   | [M+2Na-H] <sup>+</sup>   |
| 595.38     | 595.3769     | 0.0048 | LPA(30:5)      | C33H56O7P     | [M-H] <sup>-</sup>       |
| 747.52     | 747.5171     | 0.0052 | LBPA(34:2)     | C40H76O10P    | [M+H] <sup>+</sup>       |
| 747.52     | 747.5171     | 0.0052 | PG(34:2)       | C40H76O10P    | [M+H] <sup>+</sup>       |
| 747.52     | 747.5171     | 0.0052 | PG(O-34:3(OH)) | C40H76O10P    | [M+H] <sup>+</sup>       |
| 747.52     | 747.5171     | 0.0052 | PG(P-34:2(OH)) | C40H76O10P    | [M+H] <sup>+</sup>       |
| 747.52     | 747.5171     | 0.0052 | PG(34:1(OH))   | C40H76O10P    | [M+H-H2O] <sup>+</sup>   |
| 747.52     | 747.5147     | 0.0076 | PG(O-32:0(OH)) | C38H77O10PNa  | [M+Na] <sup>+</sup>      |
| 747.52     | 747.5283     | 0.0061 | PE(34:3(OH))   | C39H76N2O9P   | [M+NH4] <sup>+</sup>     |
| 747.52     | 747.5182     | 0.0041 | LBPA(34:1)     | C40H76O10P    | [M-H] <sup>-</sup>       |
| 747.52     | 747.5182     | 0.0041 | PG(34:1)       | C40H76O10P    | [M-H] <sup>-</sup>       |
| 747.52     | 747.5182     | 0.0041 | PG(O-34:2(OH)) | C40H76O10P    | [M-H] <sup>-</sup>       |
| 747.52     | 747.5182     | 0.0041 | PG(P-34:1(OH)) | C40H76O10P    | [M-H] <sup>-</sup>       |
| 747.52     | 747.5213     | 0.0009 | PE-Cer(d38:3)  | C40H77N2O6PCI | [M+Cl] <sup>-</sup>      |
| 747.52     | 747.5182     | 0.0041 | PA(36:1)       | C40H76O10P    | [M+Formate] <sup>-</sup> |
| 747.52     | 747.5182     | 0.0041 | PA(O-36:2(OH)) | C40H76O10P    | [M+Formate] <sup>-</sup> |
| 747.52     | 747.5182     | 0.0041 | PA(P-36:1(OH)) | C40H76O10P    | [M+Formate] <sup>-</sup> |
| 747.52     | 747.5264     | 0.0042 | MGDG(30:0)     | C40H75O12     | [M+Formate] <sup>-</sup> |
| 747.52     | 747.5294     | 0.0072 | PE-Cer(t36:2)  | C39H76N2O9P   | [M+Formate] <sup>-</sup> |
| 747.52     | 747.5205     | 0.0017 | DG(42:10)      | C47H71O7      | [M+OAc] <sup>-</sup>     |
| 747.52     | 747.5294     | 0.0072 | SM(t32:2)      | C39H76N2O9P   | [M+OAc] <sup>-</sup>     |
| 703.50     | 703.4908     | 0.0058 | PG(32:1)       | C38H72O9P     | [M+H-H2O] <sup>+</sup>   |
| 703.50     | 703.4908     | 0.0058 | PG(P-32:1(OH)) | C38H72O9P     | [M+H-H2O] <sup>+</sup>   |
| 703.50     | 703.4884     | 0.0082 | LPG(30:0)      | C36H73O9PNa   | [M+Na] <sup>+</sup>      |
| 703.50     | 703.4884     | 0.0082 | PG(O-30:0)     | C36H73O9PNa   | [M+Na] <sup>+</sup>      |
| 703.50     | 703.5021     | 0.0055 | PE(32:3)       | C37H72N2O8P   | [M+NH4] <sup>+</sup>     |
| 703.50     | 703.4884     | 0.0082 | TG(38:4)       | C41H70O6      | [M+2Na-H] <sup>+</sup>   |
| 703.50     | 703.492      | 0.0046 | PG(P-32:1)     | C38H72O9P     | [M-H] <sup>-</sup>       |
| 703.50     | 703.492      | 0.0046 | PA(O-34:2)     | C38H72O9P     | [M+Formate] <sup>-</sup> |
| 703.50     | 703.492      | 0.0046 | PA(P-34:1)     | C38H72O9P     | [M+Formate] <sup>-</sup> |
| 703.50     | 703.5032     | 0.0066 | PE-Cer(d34:2)  | C37H72N2O8P   | [M+Formate] <sup>-</sup> |
| 703.50     | 703.5032     | 0.0066 | SM(d30:2)      | C37H72N2O8P   | [M+OAc] <sup>-</sup>     |
| 617.45     | 617.4564     | 0.0063 | DG(38:9)       | C41H61O4      | [M+H-H2O] <sup>+</sup>   |
| 617.45     | 617.4516     | 0.0015 | DG(P-34:4)     | C37H64O4      | [M+2Na-H] <sup>+</sup>   |
| 617.45     | 617.4516     | 0.0015 | MG(34:5)       | C37H64O4      | [M+2Na-H] <sup>+</sup>   |
| 617.45     | 617.4553     | 0.0053 | TG(32:0)       | C35H66O6Cl    | [M+Cl] <sup>-</sup>      |
| 617.45     | 617.4575     | 0.0075 | WE(40:10)      | C41H61O4      | [M+Formate] <sup>-</sup> |
| 617.45     | 617.4423     | 0.0078 | DG(32:5)       | C37H61O7      | [M+OAc] <sup>-</sup>     |
| 903.57     | 903.5593     | 0.0073 | PI(38:4(OH))   | C47H84O14P    | [M+H] <sup>+</sup>       |
| 903.57     | 903.5651     | 0.0015 | SQDG(42:7)     | C51H83O11S    | [M+H-H2O] <sup>+</sup>   |
| 903.57     | 903.5569     | 0.0097 | PI(36:1(OH))   | C45H85O14PNa  | [M+Na] <sup>+</sup>      |
| 903.57     | 903.5604     | 0.0062 | PI(38:3(OH))   | C47H84O14P    | [M-H] <sup>-</sup>       |
| 903.57     | 903.5735     | 0.0069 | PI(O-36:0(OH)) | C45H89O13PCI  | [M+Cl] <sup>-</sup>      |
| 903.57     | 903.5604     | 0.0062 | PI(O-36:4)     | C47H84O14P    | [M+OAc] <sup>-</sup>     |

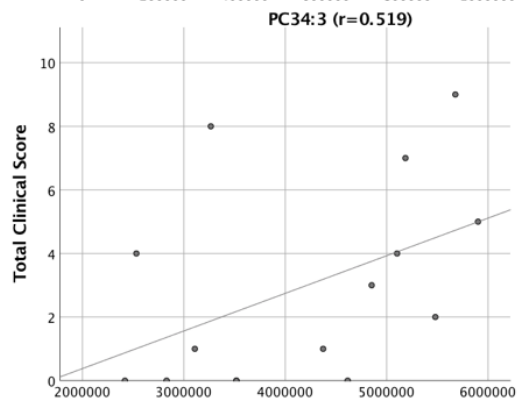
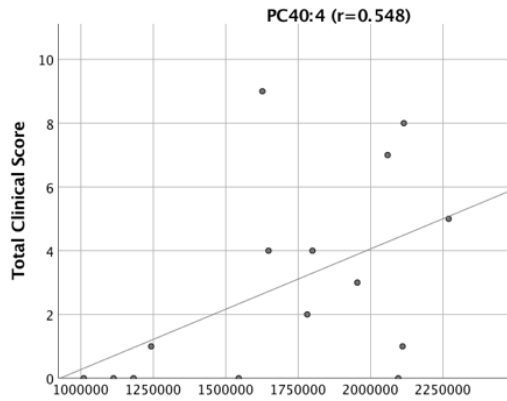
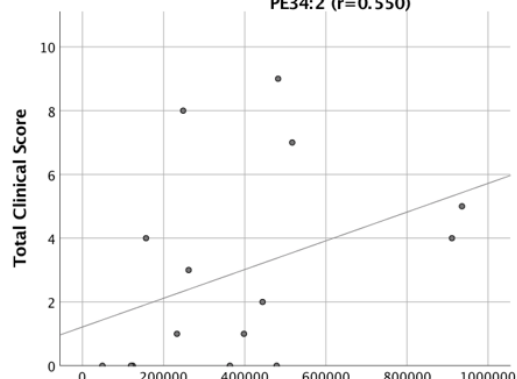
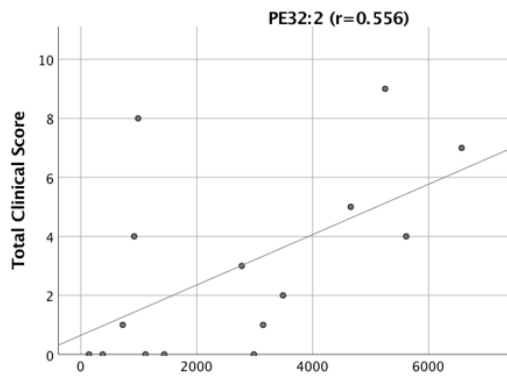
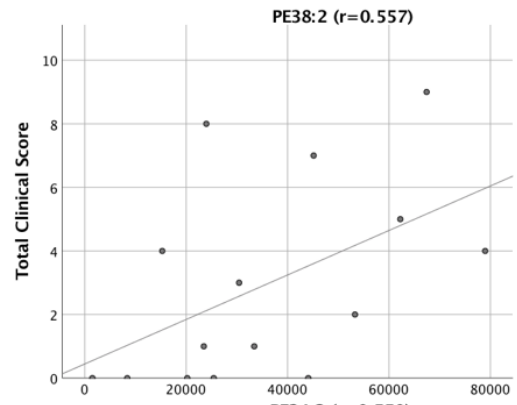
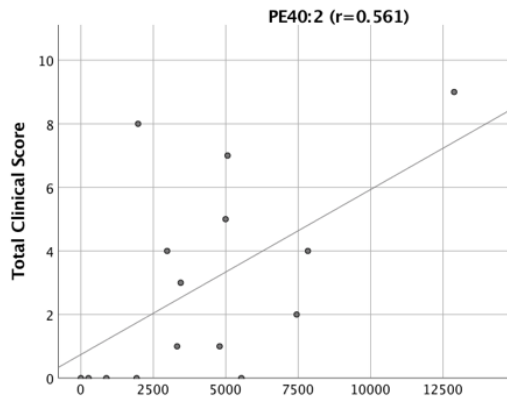
|        |          |        |                |               |              |
|--------|----------|--------|----------------|---------------|--------------|
| 903.57 | 903.5604 | 0.0062 | PI(P-36:3)     | C47H84O14P    | [M+OAc]-     |
| 903.57 | 903.5757 | 0.0091 | PA(46:8(OH))   | C51H84O11P    | [M+OAc]-     |
| 704.50 | 704.4861 | 0.0095 | PE(32:2(OH))   | C37H71NO9P    | [M+H]+       |
| 704.50 | 704.5013 | 0.0057 | PE(P-36:5)     | C41H71NO6P    | [M+H-H2O]+   |
| 704.50 | 704.4861 | 0.0095 | PA(34:3(OH))   | C37H71NO9P    | [M+NH4]+     |
| 704.50 | 704.4872 | 0.0084 | PE(32:1(OH))   | C37H71NO9P    | [M-H]-       |
| 704.50 | 704.4874 | 0.0082 | HexCer(d32:2)  | C38H71NO8Cl   | [M+Cl]-      |
| 704.50 | 704.4954 | 0.0002 | HexCer(t30:1)  | C37H70NO11    | [M+Formate]- |
| 704.50 | 704.4872 | 0.0084 | CerP(t36:2)    | C37H71NO9P    | [M+Formate]- |
| 704.50 | 704.4872 | 0.0084 | LPC(28:2)      | C37H71NO9P    | [M+Formate]- |
| 704.50 | 704.4872 | 0.0084 | LPE(30:2)      | C37H71NO9P    | [M+OAc]-     |
| 704.50 | 704.4872 | 0.0084 | PE(P-30:1)     | C37H71NO9P    | [M+OAc]-     |
| 704.50 | 704.4872 | 0.0084 | PC(30:1(OH))   | C37H71NO9P    | [M-CH3]-     |
| 745.63 | 745.6341 | 0.0012 | TG(44:3)       | C47H85O6      | [M+H]+       |
| 745.63 | 745.6317 | 0.0012 | TG(42:0)       | C45H86O6Na    | [M+Na]+      |
| 745.63 | 745.63   | 0.0028 | DGCC(32:0)     | C42H85N2O8    | [M+NH4]+     |
| 745.63 | 745.63   | 0.0028 | HexCer(d36:1)  | C42H85N2O8    | [M+NH4]+     |
| 745.63 | 745.6259 | 0.0069 | CE(22:1)       | C49H86O2K     | [M+K]+       |
| 745.63 | 745.6352 | 0.0024 | TG(44:2)       | C47H85O6      | [M-H]-       |
| 745.63 | 745.6229 | 0.0099 | PE-Cer(d40:0)  | C42H86N2O6P   | [M-H]-       |
| 745.63 | 745.6352 | 0.0024 | DG(O-42:4)     | C47H85O6      | [M+OAc]-     |
| 745.63 | 745.6352 | 0.0024 | DG(P-42:3)     | C47H85O6      | [M+OAc]-     |
| 745.63 | 745.6229 | 0.0099 | SM(d38:0)      | C42H86N2O6P   | [M-CH3]-     |
| 659.47 | 659.4646 | 0.0051 | LPG(30:2)      | C36H68O8P     | [M+H-H2O]+   |
| 659.47 | 659.4646 | 0.0051 | PG(P-30:1)     | C36H68O8P     | [M+H-H2O]+   |
| 659.47 | 659.4735 | 0.0037 | SM(t28:0)      | C33H69N2O7PNa | [M+Na]+      |
| 659.47 | 659.4646 | 0.0052 | DG(38:8)       | C41H64O5Na    | [M+Na]+      |
| 659.47 | 659.4759 | 0.0061 | LPE(30:4)      | C35H68N2O7P   | [M+NH4]+     |
| 659.47 | 659.4622 | 0.0076 | DG(36:5)       | C39H66O5      | [M+2Na-H]+   |
| 659.47 | 659.4681 | 0.0017 | DG(40:10)      | C43H63O5      | [M-H]-       |
| 659.47 | 659.477  | 0.0072 | PE-Cer(t33:2)  | C35H68N2O7P   | [M-H]-       |
| 659.47 | 659.46   | 0.0097 | WE(44:12)      | C44H64O2Cl    | [M+Cl]-      |
| 795.51 | 795.5042 | 0.0028 | MGDG(38:10)    | C47H71O10     | [M+H]+       |
| 795.51 | 795.5018 | 0.0052 | MGDG(36:7)     | C45H72O10Na   | [M+Na]+      |
| 795.51 | 795.5147 | 0.0076 | PG(36:3)       | C42H77O10PNa  | [M+Na]+      |
| 795.51 | 795.5147 | 0.0076 | PG(O-36:4(OH)) | C42H77O10PNa  | [M+Na]+      |
| 795.51 | 795.5147 | 0.0076 | PG(P-36:3(OH)) | C42H77O10PNa  | [M+Na]+      |
| 795.51 | 795.5122 | 0.0052 | PG(34:0)       | C40H79O10P    | [M+2Na-H]+   |
| 795.51 | 795.5122 | 0.0052 | PG(O-34:1(OH)) | C40H79O10P    | [M+2Na-H]+   |
| 795.51 | 795.5122 | 0.0052 | PG(P-34:0(OH)) | C40H79O10P    | [M+2Na-H]+   |
| 795.51 | 795.4994 | 0.0076 | MGDG(34:4)     | C43H74O10     | [M+2Na-H]+   |
| 795.51 | 795.5053 | 0.0017 | MGDG(38:9)     | C47H71O10     | [M-H]-       |
| 795.51 | 795.497  | 0.01   | PA(44:10)      | C47H72O8P     | [M-H]-       |
| 795.51 | 795.5101 | 0.0031 | PA(P-42:6)     | C45H77O7PCl   | [M+Cl]-      |
| 795.51 | 795.5029 | 0.0041 | PG(32:1(OH))   | C40H76O13P    | [M+OAc]-     |
| 742.57 | 742.5745 | 0.006  | PC(O-34:3)     | C42H81NO7P    | [M+H]+       |
| 742.57 | 742.5745 | 0.006  | PC(P-34:2)     | C42H81NO7P    | [M+H]+       |
| 742.57 | 742.5745 | 0.006  | PC(34:1)       | C42H81NO7P    | [M+H-H2O]+   |
| 742.57 | 742.5745 | 0.006  | PC(O-34:2(OH)) | C42H81NO7P    | [M+H-H2O]+   |
| 742.57 | 742.5745 | 0.006  | PC(P-34:1(OH)) | C42H81NO7P    | [M+H-H2O]+   |
| 742.57 | 742.5721 | 0.0036 | CerP(t40:0)    | C40H82NO7PNa  | [M+Na]+      |
| 742.57 | 742.5721 | 0.0036 | LPC(32:0)      | C40H82NO7PNa  | [M+Na]+      |
| 742.57 | 742.5721 | 0.0036 | PC(O-32:0)     | C40H82NO7PNa  | [M+Na]+      |
| 742.57 | 742.5593 | 0.0092 | PG(O-32:0(OH)) | C38H81NO10P   | [M+NH4]+     |
| 742.57 | 742.5756 | 0.0071 | CerP(t42:2)    | C42H81NO7P    | [M-H]-       |
| 311.29 | 311.2945 | 0.0002 | WE(20:1)       | C20H39O2      | [M+H]+       |
| 311.29 | 311.2956 | 0.0013 | FA(20:0)       | C20H39O2      | [M-H]-       |
| 311.29 | 311.2956 | 0.0013 | WE(20:0)       | C20H39O2      | [M-H]-       |
| 823.76 | 823.7538 | 0.0056 | DG(O-52:6)     | C55H99O4      | [M+H]+       |
| 823.76 | 823.7538 | 0.0056 | DG(P-52:5)     | C55H99O4      | [M+H]+       |
| 823.76 | 823.7538 | 0.0056 | DG(52:4)       | C55H99O4      | [M+H-H2O]+   |
| 823.76 | 823.7538 | 0.0056 | TG(O-52:4)     | C55H99O4      | [M+H-H2O]+   |
| 823.76 | 823.7538 | 0.0056 | TG(P-52:3)     | C55H99O4      | [M+H-H2O]+   |

|        |          |        |              |               |              |
|--------|----------|--------|--------------|---------------|--------------|
| 823.76 | 823.769  | 0.0096 | CE(32:4)     | C59H99O       | [M+H-H2O]+   |
| 823.76 | 823.7514 | 0.008  | DG(O-50:3)   | C53H100O4Na   | [M+Na]+      |
| 823.76 | 823.7514 | 0.008  | DG(P-50:2)   | C53H100O4Na   | [M+Na]+      |
| 823.76 | 823.7668 | 0.0074 | WE(54:2)     | C54H104O2K    | [M+K]+       |
| 823.76 | 823.7549 | 0.0045 | DG(O-52:5)   | C55H99O4      | [M-H]-       |
| 823.76 | 823.7549 | 0.0045 | DG(P-52:4)   | C55H99O4      | [M-H]-       |
| 823.76 | 823.7549 | 0.0045 | WE(54:5)     | C55H99O4      | [M+Formate]- |
| 823.76 | 823.7549 | 0.0045 | CE(26:0)     | C55H99O4      | [M+OAc]-     |
| 679.42 | 679.4181 | 0.0067 | PG(28:2(OH)) | C34H64O11P    | [M+H]+       |
| 679.42 | 679.4333 | 0.0086 | LPG(32:6)    | C38H64O8P     | [M+H-H2O]+   |
| 679.42 | 679.4309 | 0.0062 | DG(38:9)     | C41H62O5      | [M+2Na-H]+   |
| 679.42 | 679.4192 | 0.0055 | PG(28:1(OH)) | C34H64O11P    | [M-H]-       |
| 679.42 | 679.4194 | 0.0054 | MGDG(26:1)   | C35H64O10Cl   | [M+Cl]-      |
| 679.42 | 679.4192 | 0.0055 | PA(30:1(OH)) | C34H64O11P    | [M+Formate]- |
| 679.42 | 679.4192 | 0.0055 | LPG(26:2)    | C34H64O11P    | [M+OAc]-     |
| 743.57 | 743.5609 | 0.0089 | DG(46:11)    | C49H75O5      | [M+H]+       |
| 743.57 | 743.5674 | 0.0024 | SM(t34:0)    | C39H81N2O7PNa | [M+Na]+      |
| 743.57 | 743.5698 | 0      | PE(O-36:4)   | C41H80N2O7P   | [M+NH4]+     |
| 743.57 | 743.5698 | 0      | PE(P-36:3)   | C41H80N2O7P   | [M+NH4]+     |
| 743.57 | 743.5713 | 0.0015 | CE(22:5)     | C49H78O2      | [M+2Na-H]+   |
| 743.57 | 743.562  | 0.0078 | DG(46:10)    | C49H75O5      | [M-H]-       |
| 743.57 | 743.5751 | 0.0053 | DG(P-44:6)   | C47H80O4Cl    | [M+Cl]-      |
| 663.45 | 663.4595 | 0.0076 | PA(32:1(OH)) | C35H68O9P     | [M+H]+       |
| 663.45 | 663.4538 | 0.0018 | WE(44:12)    | C44H64O2K     | [M+K]+       |
| 663.45 | 663.4448 | 0.0071 | SM(d28:1)    | C33H67N2O6P   | [M+2Na-H]+   |
| 663.45 | 663.4607 | 0.0087 | PA(32:0(OH)) | C35H68O9P     | [M-H]-       |
| 663.45 | 663.4607 | 0.0087 | LPA(30:1)    | C35H68O9P     | [M+OAc]-     |
| 663.45 | 663.4607 | 0.0087 | PA(O-30:1)   | C35H68O9P     | [M+OAc]-     |
| 663.45 | 663.4607 | 0.0087 | PA(P-30:0)   | C35H68O9P     | [M+OAc]-     |

# CLINICAL CORRELATION

## Plasma

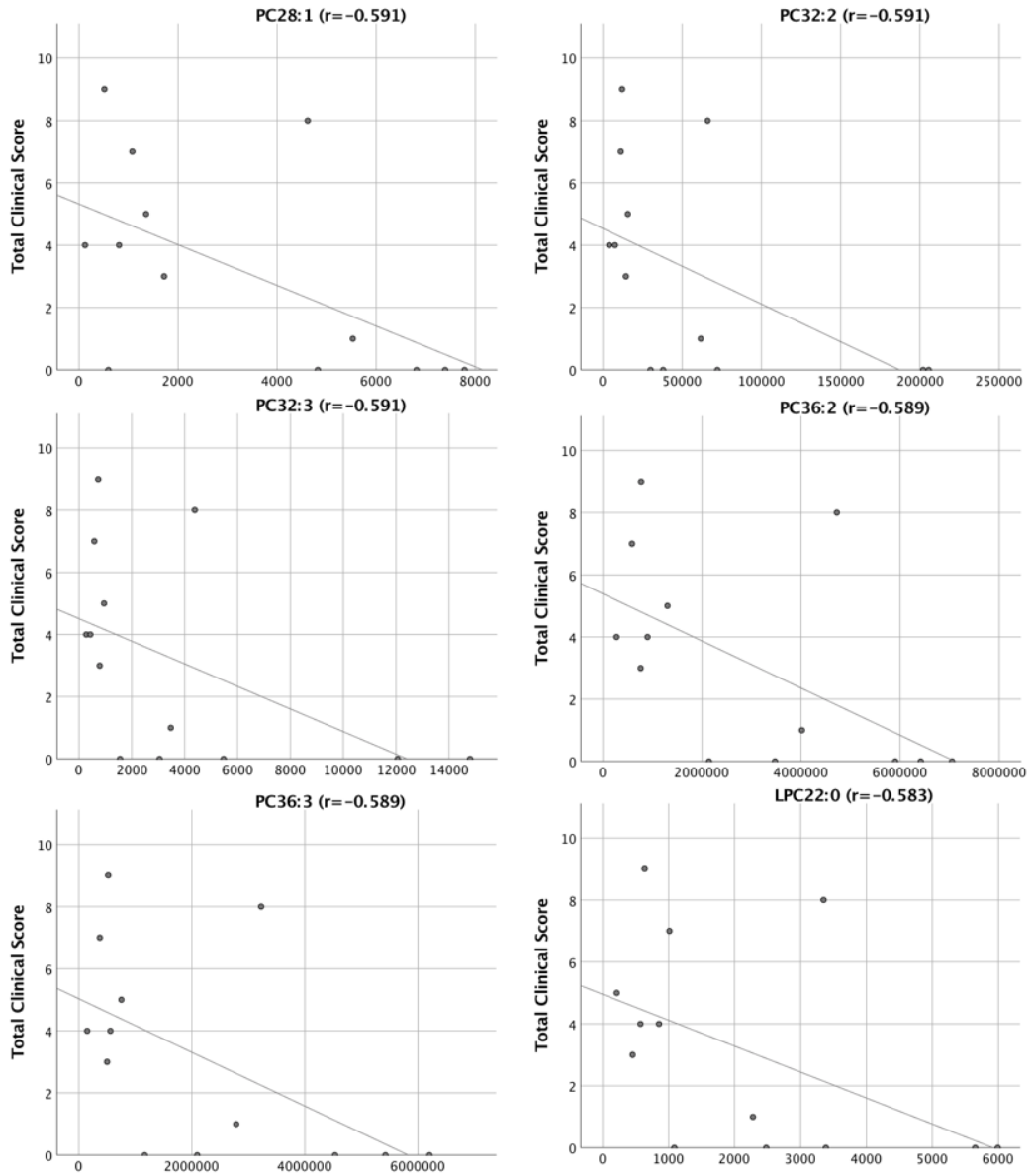


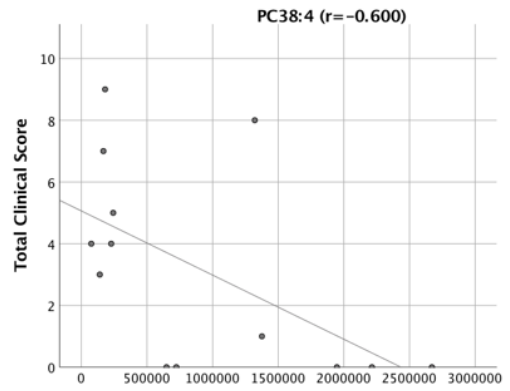
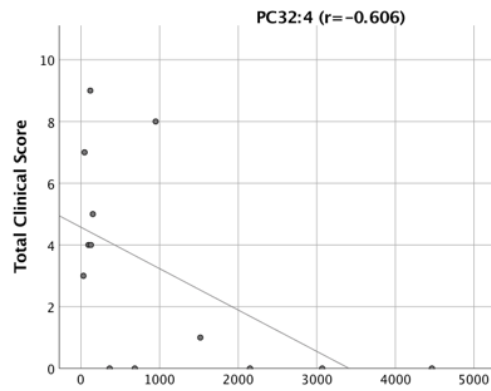
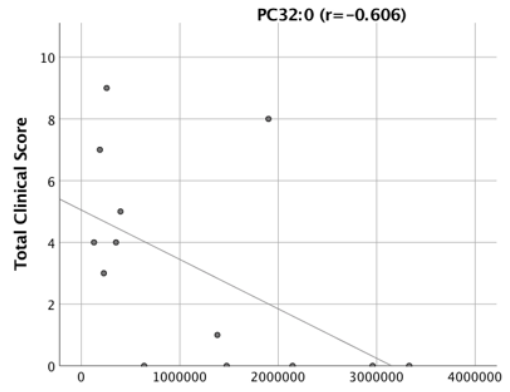
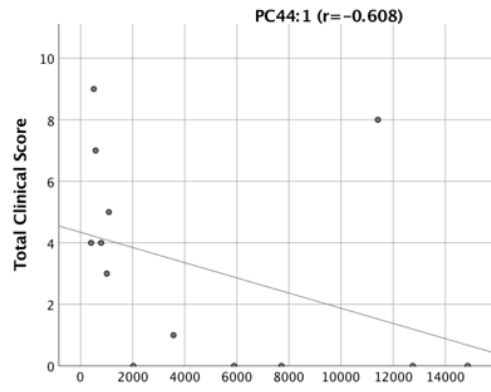
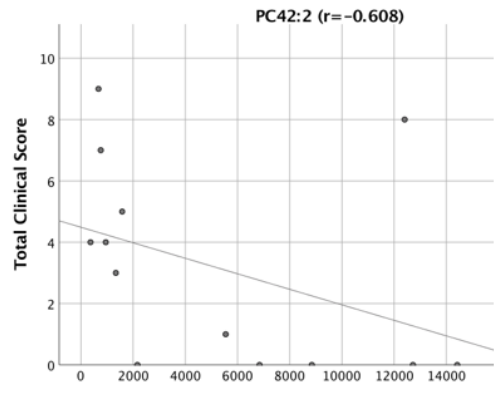
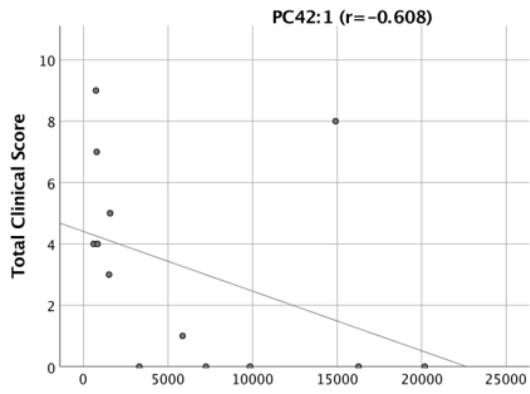


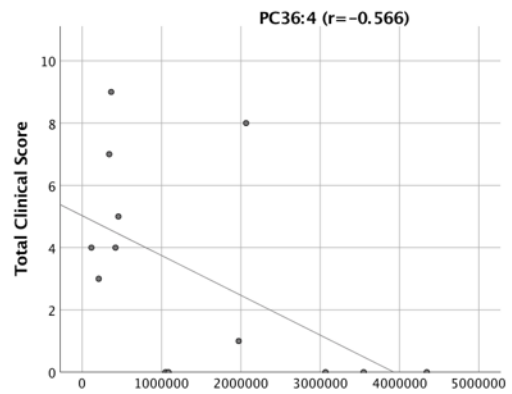
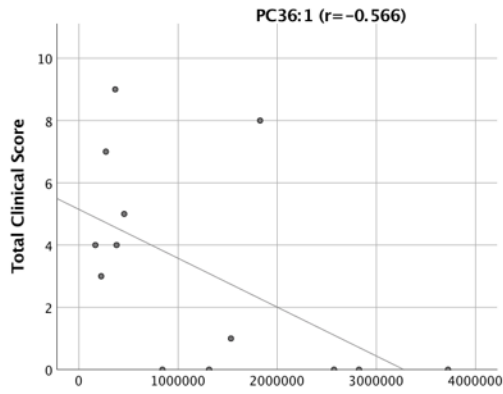
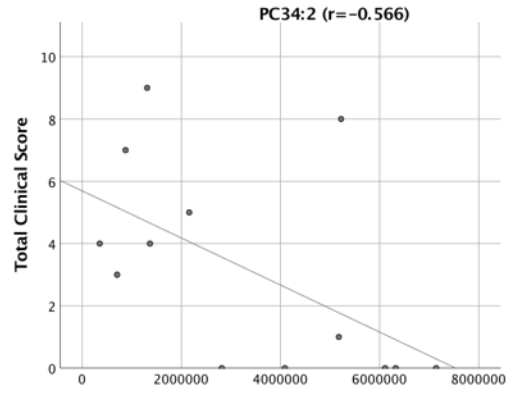
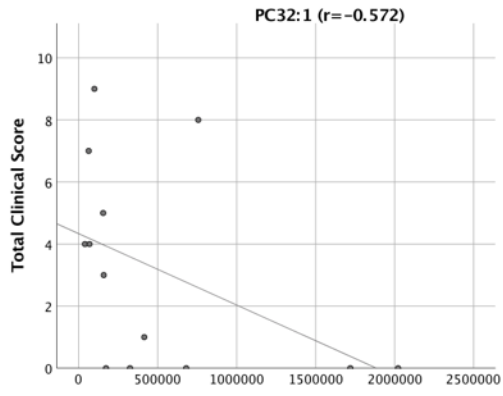
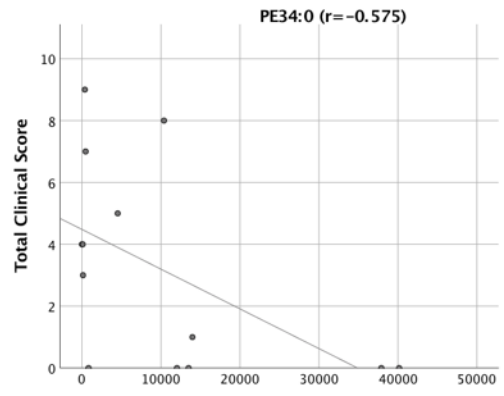
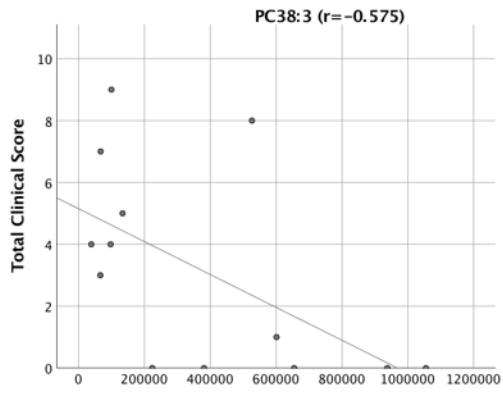
| LIPID         | R       | PVALUE    |
|---------------|---------|-----------|
| PLASMAPE38:0  | .692**  | 0.004233  |
| PLASMALPC14:1 | .678**  | 0.0054966 |
| PLASMAPE40:3  | .676**  | 0.0056735 |
| PLASMALPE12:4 | -.674** | 0.0058549 |
| PLASMAPE36:0  | .645**  | 0.009431  |
| PLASMAPE32:1  | .634*   | 0.0111429 |
| PLASMAPE36:4  | .629*   | 0.0120849 |
| PLASMAPE40:4  | .590*   | 0.0205264 |
| PLASMAPE38:4  | .587*   | 0.021519  |
| PLASMAPE38:3  | .583*   | 0.0225478 |
| PLASMALPC12:2 | -.578*  | 0.0241607 |
| PLASMAPE38:1  | .576*   | 0.0247174 |
| PLASMAPC36:2  | .567*   | 0.0276483 |
| PLASMAPC40:0  | -.567*  | 0.0276483 |
| PLASMAPE32:3  | .565*   | 0.0280929 |
| PLASMAPE40:1  | .562*   | 0.0293522 |
| PLASMAPE40:2  | .561*   | 0.0295287 |
| PLASMAPE38:2  | .557*   | 0.0308348 |
| PLASMAPE32:2  | .556*   | 0.0315039 |
| PLASMAPE34:2  | .550*   | 0.033577  |
| PLASMAPC40:4  | .548*   | 0.0342903 |
| PLASMAPC40:1  | -.543*  | 0.0364983 |
| PLASMAPC42:2  | -.523*  | 0.0455112 |
| PLASMAPC34:3  | .519*   | 0.0473121 |

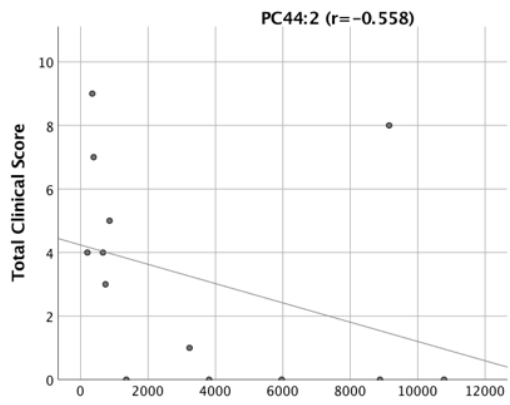
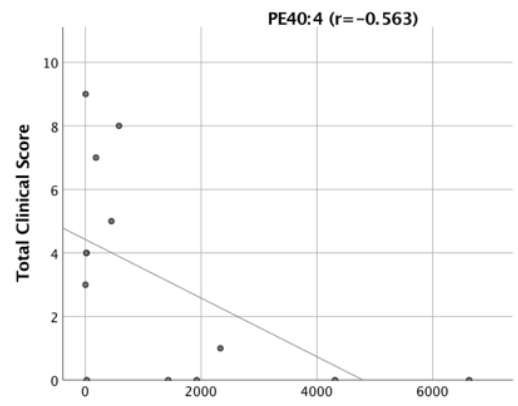
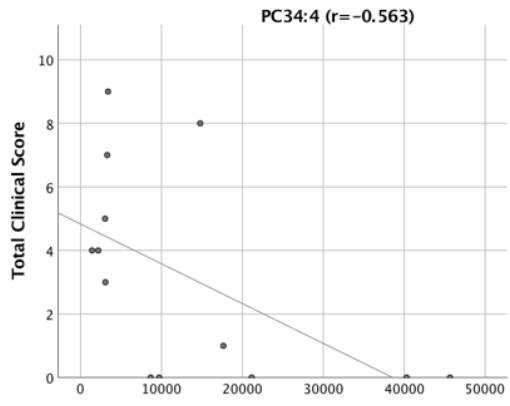
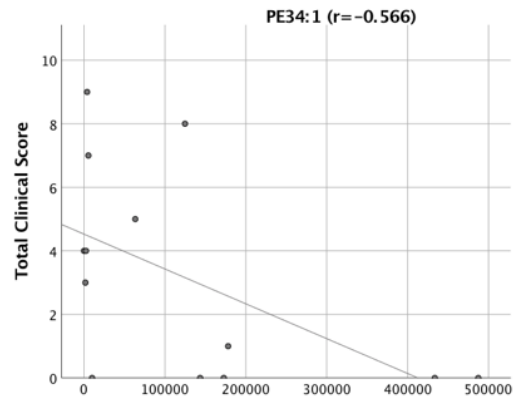
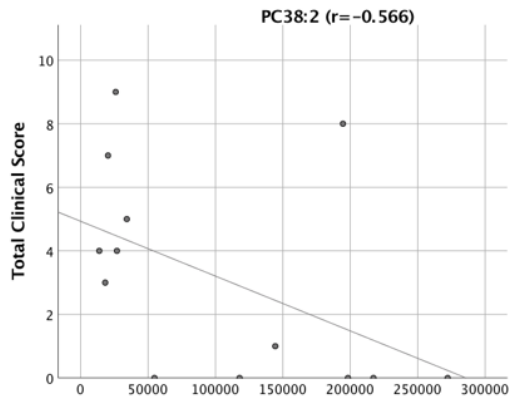


# Urine










| LIPID        | R       | PVALUE    |
|--------------|---------|-----------|
| URINELPC18:0 | -.739** | 0.0039267 |
| URINEPC44:4  | -.668*  | 0.0126    |
| URINEPC28:0  | -.659*  | 0.014211  |
| URINELPC16:0 | -.651*  | 0.0159722 |
| URINEPC30:0  | -.625*  | 0.0222429 |
| URINEPC44:3  | -.611*  | 0.0264302 |
| URINEPC42:1  | -.608*  | 0.0273329 |
| URINEPC42:2  | -.608*  | 0.0273329 |
| URINEPC44:1  | -.608*  | 0.0273329 |
| URINEPC32:0  | -.606*  | 0.028258  |
| URINEPC32:4  | -.606*  | 0.028258  |
| URINEPC38:4  | -.600*  | 0.0301771 |
| URINEPC28:1  | -.591*  | 0.0332325 |
| URINEPC32:2  | -.591*  | 0.0332325 |
| URINEPC32:3  | -.591*  | 0.0332325 |
| URINEPC36:2  | -.589*  | 0.0342994 |
| URINEPC36:3  | -.589*  | 0.0342994 |
| URINELPC22:0 | -.583*  | 0.0365079 |
| URINEPC38:3  | -.575*  | 0.0400119 |
| URINEPE34:0  | -.575*  | 0.0400119 |
| URINEPC32:1  | -.572*  | 0.0412322 |
| URINEPC34:2  | -.566*  | 0.0437532 |
| URINEPC36:1  | -.566*  | 0.0437532 |
| URINEPC36:4  | -.566*  | 0.0437532 |
| URINEPC38:2  | -.566*  | 0.0437532 |
| URINEPE34:1  | -.566*  | 0.0437532 |
| URINEPC34:4  | -.563*  | 0.0450545 |
| URINEPE40:4  | -.563*  | 0.0450545 |
| URINEPC44:2  | -.558*  | 0.0477403 |

## The pathology of lumbosacral lipomas: macroscopic and microscopic disparity have implications for embryogenesis and mode of clinical deterioration

Victoria Jones,<sup>1,2</sup>  Victoria Wykes,<sup>2</sup> Nicki Cohen,<sup>3,4</sup> Dominic Thompson<sup>2</sup> & Tom S Jacques<sup>1,3</sup>

<sup>1</sup>Developmental Biology and Cancer Programme, UCL Institute of Child Health, <sup>2</sup>Department of Neurosurgery, Great Ormond Street Hospital NHS Trust, <sup>3</sup>Department of Histopathology, Great Ormond Street Hospital NHS Trust, and <sup>4</sup>Department of Histopathology, Kings College London, London, UK

Date of submission 23 November 2017  
Accepted for publication 15 January 2018  
Published online Article Accepted 19 January 2018

Jones V, Wykes V, Cohen N, Thompson D & Jacques T S

(2018) *Histopathology* 72, 1136–1144. <https://doi.org/10.1111/his.13469>

### The pathology of lumbosacral lipomas: macroscopic and microscopic disparity have implications for embryogenesis and mode of clinical deterioration

**Aims:** Lumbosacral lipomas (LSL) are congenital disorders of the terminal spinal cord region that have the potential to cause significant spinal cord dysfunction in children. They are of unknown embryogenesis with variable clinical presentation and natural history. It is unclear whether the spinal cord dysfunction reflects a primary developmental dysplasia or whether it occurs secondarily to mechanical traction (spinal cord tethering) with growth. While different anatomical subtypes are recognised and classified according to radiological criteria, these subtypes correlate poorly with clinical prognosis. We have undertaken an analysis of surgical specimens in order to describe the spectrum of histological changes that occur and have correlated the histology with the anatomical type of LSL to determine if there are distinct histological subtypes.

**Methods and results:** The histopathology was reviewed of 64 patients who had undergone surgical

resection of LSL. The presence of additional tissues and cell types were recorded. LSLs were classified from pre-operative magnetic resonance imaging (MRI) scans according to Chapman classification. Ninety-five per cent of the specimens consisted predominantly of mature adipocytes with all containing thickened bands of connective tissue and peripheral nerve fibres, 91% of samples contained ectatic blood vessels with thickened walls, while 22% contained central nervous system (CNS) glial tissue. Additional tissue was identified of both mesodermal and neuroectodermal origin.

**Conclusions:** Our analysis highlights the heterogeneity of tissue types within all samples, not reflected in the nomenclature. The diversity of tissue types, consistent across all subtypes, challenges currently held notions regarding the embryogenesis of LSLs and the assumption that clinical deterioration is due simply to tethering.

**Keywords:** adipocytes, conus medullaris, dysraphism, lipomyelomeningocele, lumbosacral lipoma, spinal cord untethering, tethered cord syndrome

### Introduction

Lumbosacral lipomas (LSL) of the conus medullaris are a common form of spinal malformation. Diagnosis is made typically in infants on the basis of a midline

lumbosacral swelling, sometimes accompanied by local cutaneous manifestations including dermal sinus, skin appendage and capillary haemangioma.<sup>1</sup> At the time of diagnosis there may already be features of distal spinal cord dysfunction, including distal lower limb weakness and asymmetry, talipes deformities and features of neurogenic sphincter impairment; however, as many as 40% of cases are ostensibly asymptomatic at birth. Ultimately, over time all patients are at risk of new or progressive neurological deterioration.<sup>2–4</sup> The role of resection of the lipoma and untethering of the spinal cord in averting neurological and urological deterioration is controversial.<sup>5,6</sup> The essence of this controversy is whether the neurological and urological disability is a result of secondary injury to the terminal spinal cord and cauda equina through a process of mechanical tethering – and thus potentially amenable to surgery – or whether dysfunction is a result of a primary inherent malformation.

Magnetic resonance imaging (MRI) is used to confirm the diagnosis and classify the LSL, depending on its relationship to the conus.<sup>7,8</sup> Although widely used, the classification of LSL is somewhat difficult to apply in practice and, according to most published series, the correlation between LSL type and neurological prognosis has been poor (Figure 1).

It has been established for almost 100 years that congenital spinal lipomas are different from lipomas at other sites.<sup>4</sup> However, despite a wealth of publications during that time on the management and clinical presentation of spinal lipomas, there is surprisingly little in the literature about the histopathology, with one large series, two smaller series<sup>9–13</sup> and a number of case reports often describing the bizarre and unusual.

LSLs are characterised by mature adipocytes, both microscopically and metabolically, surrounded by thickened bands of connective tissue and containing a diverse range of different cell types present from all three germ layers.<sup>14–16</sup> This pathological heterogeneity within LSL has implications both for our understanding of their embryogenesis and the mechanisms underlying clinical deterioration. There have been no previous attempts to correlate histological findings to clinical or radiological features.

A large-scale analysis of 671 patients over 22 years looked collectively at spinal lipomas of the filum and of the conus, and found that 77% were more complex lesions containing more than just adipocytes and collagen bands.<sup>9,11,14</sup>

Walsh *et al.* looked at 20 patients, and again a diverse group was considered including intradural lipomas. This paper showed principally 'the presence

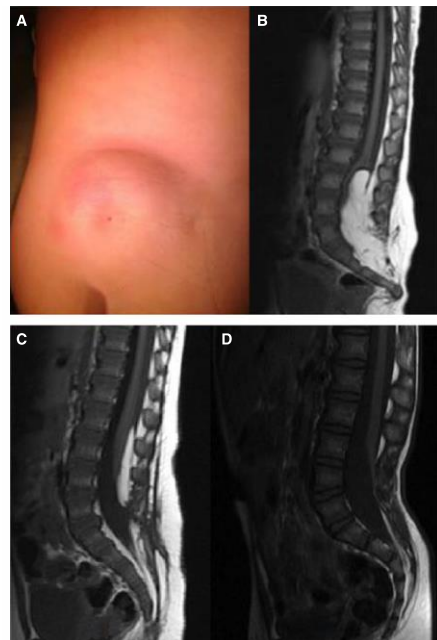


**Figure 1.** A. Lumbosacral lipoma with cutaneous dimple. B–D. Sagittal T1 magnetic resonance imaging (MRI) illustrating different anatomical subtypes of lumbosacral lipomas as described by Chapman. Lipoma tissue is closely adherent to splayed neural tissue forming a lipoma–neuronal placode; the lipoma extends through a defect in the posterior dura and vertebral column, before becoming continuous with the subcutaneous fat. Lumbosacral lipomas (LSLs) are classified based on their radiological appearance and relationship to the conus. C. Dorsal LSL: the interface between the lipoma and spinal cord is above the level of the conus. B. Transitional LSL: the interface includes the conus and the lipoma extends into elements of the cauda equina. D. Caudal LSL: the lipoma extends from the tip of the conus to the end of the thecal sac. Caudal LSL may be referred to alternatively as terminal or filar LSL. Pang *et al.* have recently describe a chaotic form that is most allied to the transitional type, but where the lipoma extends ventrally to the placode and nerve roots.<sup>8</sup> [Colour figure can be viewed at [wileyonlinelibrary.com](http://wileyonlinelibrary.com)]

of large, rather monotonous sheets of mature fat-cells and thick strands of connective tissue. Numerous thin-walled blood vessels were also seen', but 25% (five cases) demonstrated a more diverse range of cell types.<sup>10</sup> The two histopathology series above include lipomas within all radiological subsets.

We present here an intermediate-size series of LSLs including detailed histopathological analysis of post-operative samples. Unlike the above-described series

we have grouped our data based on radiological classification to test the hypothesis that there is a difference in histopathology between different anatomical subtypes.

### Materials and methods

Sixty-four patients underwent resection of LSL and untethering of the spinal cord at Great Ormond Street Hospital between 1998 and 2010. Tissue was removed as part of planned surgical resection and placed in formalin. Routine histopathology sections were performed with haematoxylin and eosin (H&E) staining and immunostaining as part of standard diagnostic analysis. Analysis was performed within the histopathology department by a senior neuropathologist with experience in viewing LSLs (N.C.). Each specimen was analysed for the presence and frequency of tissue and cell type.

Pre-operative radiological MRI was reviewed in all cases. Only complex conus region lipomas were included and T1-weighted axial and sagittal images were used to classify the LSLs as dorsal, caudal, transitional or chaotic. Teratomas and thickened (fatty) filum were excluded (Figure 2).

During the period of this study surgical technique comprised untethering of the spinal cord and subtotal resection of the LSL, leaving a cuff of lipoma adjacent to the neural placode. Neural elements would therefore not be anticipated in the surgical specimens.

Results are stated as percentage, and standard error was calculated to determine the 95% confidence interval (CI) (expressed in brackets).

The study was approved by Great Ormond Street Hospital and UCL Institute of Child Health Research and Development Office (16DD01).

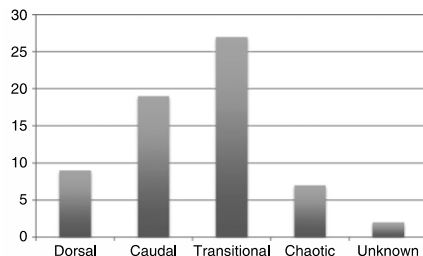


Figure 2. Breakdown of radiological subtypes. For description of classification see legend to Figure 1. It was not possible to classify two cases due to insufficient imaging.

### Results

Of the 64 specimens, 95.3% (95% CI = 87.98) consisted predominantly of mature adipocytes, while the other specimens had a greater proportion of immature adipocytes. All specimens had thickened bands of connective tissue within the adipose tissue. Within this connective tissue, all specimens had small peripheral nerve fibres present; 21.9% (95% CI  $\pm$  10.1) of specimens had central nervous system (CNS) glial cells present within the connective tissue.

Of the 64 specimens, 90.6% (95% CI  $\pm$  7.0) contained blood vessels with enlarged lumina and thickened walls. In 25.9% (95% CI  $\pm$  11.3) of these 58 specimens, these vessels were only located deep within the substance of the adipose tissue rather than at the presumed lipoma boundary. However, two of the cases that did not contain abnormal vessels showed deep vessels at the lipoma boundary (Figure 3). Of the 64 specimens, 48.4% (95% CI  $\pm$  12.2) demonstrated skeletal muscle surrounded by adipose tissue.

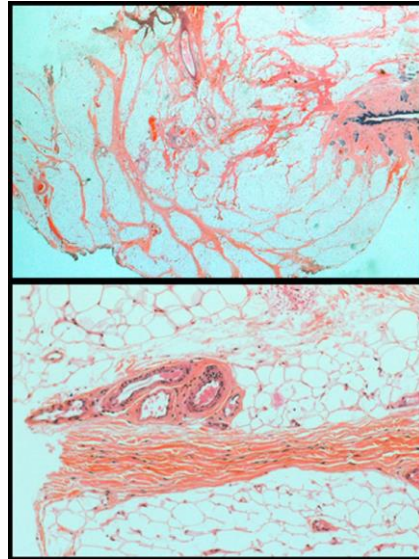


Figure 3. Histology slides of lipoma specimens demonstrating prominent blood vessels: 91% showed blood vessels focused upon the adipose with enlarged lumina and thickened walls and 74% showed similar vessels extending towards the base of the surgical resection adjacent to skeletal muscle.



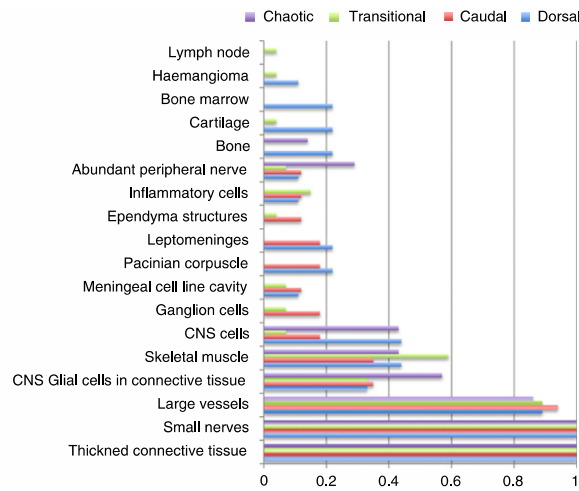


Figure 4. Results as per radiological subtype, expressed as a proportion. For statistical analysis see Supporting Information.

CELLULAR DIVERSITY

A range of other tissue types were also identified with varying degrees of maturity; 15.6% (95% CI ± 8.9) contained glial CNS type tissue (as opposed to individual glial cells commented on above), 14.1% (95% CI ± 8.5) contained meningeal cells, 12.5% (95% CI ± 8.1) contained inflammatory cells (half of which were acute perivascular inflammation in keeping with prolonged surgery, while the other half demonstrated established inflammation with multinucleated/giant cells present), and 9.4% (95% CI = 4.4.19) contained ganglion cells.

In total, 22 (95% CI = 34 ± 11.6) specimens demonstrated differentiated structures, ranging from a cavity lined with meningeal tissue (seven), haemangiomas (two), cavity lined with ependymal tissue (three), lymph node (one), peripheral nerve bundles (six), bone marrow (two), bone (three) and Pacinian corpuscle (five).

The number of blocks analysed for each specimen ranged from one to nine. The diversity of cell and tissue types detected rose steadily and peaked at four blocks. Thereafter, analysis of further blocks did not to add any more findings, with an average number of additional cell types in a sample not rising above 4.1 (Supporting Information).

RELATIONSHIP TO DERMIS

Of the 64 surgical specimens reviewed, 18 contained overlying epidermis and dermis. Epidermis was excised if there was a suspected sinus tract/pit or to aid skin closure; 50 ± 21% of these samples demonstrated a dermal pit. In 77.8 ± 19.2% adnexal structures were identified within the superficial adipose, regardless of whether it connected to the main adipose tissue of the lipoma. In 66.7 ± 21.8%, adipose was identified within the overlying dermis.

ANALYSIS BY RADIOLOGICAL CLASSIFICATION

Chronic inflammation was detected within four of the transitional type lipomas but none of the other groups, although most of these cases had undergone previous lipoma surgery. Despite the larger sample size for transitional lipomas, none demonstrated Pacinian corpuscles. Dermal pits were found in all three subtypes: caudal, dorsal and transitional. Bone marrow was detected only in dorsal lipomas; the significance of this is unclear. There was no further correlation between the different subtypes and degree of cellular diversity and maturity of structures (Figures 4 and 5 and Supporting Information).

© 2018 The Authors. *Histopathology* Published by John Wiley & Sons Ltd, *Histopathology*, 72, 1136–1144.

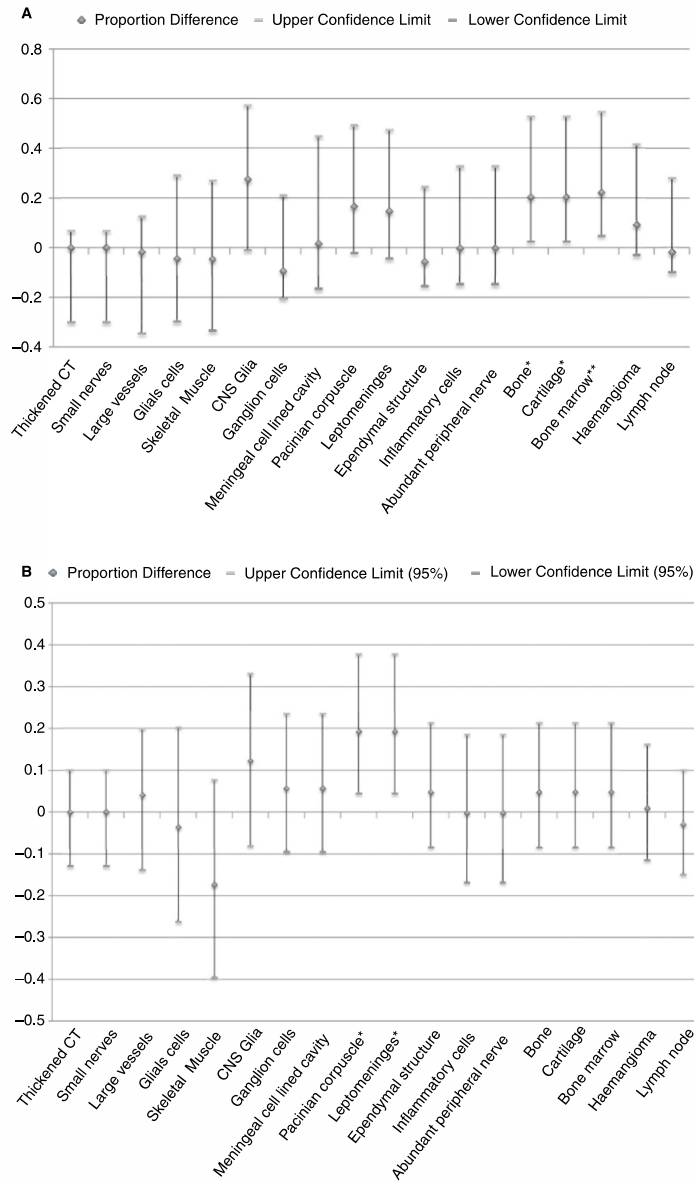


**Figure 5.** A. Subtypes of lipoma were grouped into those proposed to be due to a defect in primary neurulation (dorsal) and those proposed to be due to a defect in secondary neurulation (caudal, transitional and chaotic). Differences in proportion of different cell/tissue types detected were calculated along with 95% confidence intervals (CI) of the difference. \*Values which show significant difference at the 95% CI. This significance is lost at 99% CI for the presence of bone and cartilage but not bone marrow; \*\*difference = 0.222 (0.013, 0.635). B. Subtypes of lipoma were grouped into 'simple' (dorsal and caudal) and 'complex' (transitional and chaotic). Difference in proportion of different cell/tissue types detected was calculated along with 95% CI of the difference. \*Values which show significant difference at the 95% CI. This significance is lost at 99% CI for the presence of Pacinian corpuscles and leptomeninges, difference = 0.192 (-0.014, 0.443).

**Discussion**

Our findings are superficially similar to previous publications with LSLs consisting of mature adipocytes surrounded by thick bands of connective tissue.<sup>9-13</sup> However, we demonstrate a much higher incidence of a number of key features. Within the thickened bands of connective tissue all cases demonstrated peripheral nerve fibres, and 90.6 ± 7.0% of specimens demonstrated enlarged thickened blood vessels. The uniformity of these additional findings, which are not characteristic of non-spinal lipomas, raises the question as to whether the term 'lipoma' is the most accurate name for this pathology. Supporting previous publications on LSL pathology, we propose the term 'conus hamartoma', with LSLs consisting of non-malignant mature cell types in a disorganised

mass with the presence of cell types not usually located in the region.

The frequency of particular cell types also differs from other publications (Figure 6). None of our samples included cells of endodermal origin. Our series specifically excluded sacral teratomas, anterior sacral meningocoeles, Currarino syndrome or myelomeningocoele, as these are fundamentally different dysraphic anomalies and would have confounded the results.

Cells of neuroectodermal origin were present with Pacinian corpuscles and ganglion cells occurring with approximately equal frequency, with glial tissue and meningeal cells being identified more frequently than published previously. A large number of cell types identified within LSL specimens may be derived from or associated with neural crest cells. A number of

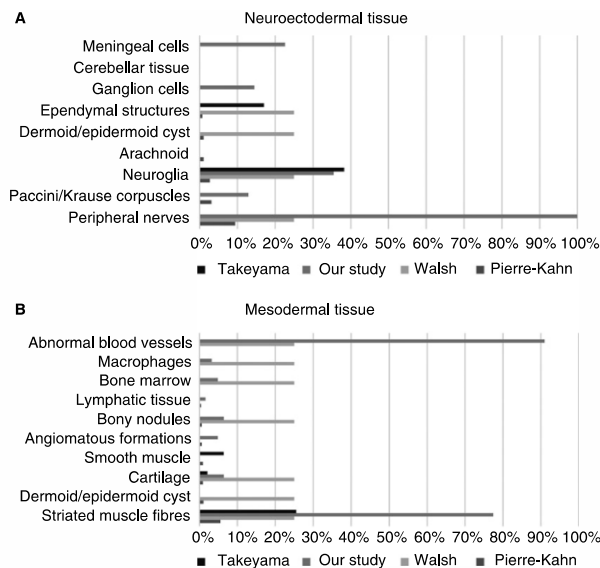


**Figure 6.** A. Comparison with previously published data on frequency of cell types of neuroectodermal origin. B. Comparison with previously published data on frequency of cell types of mesodermal origin.

recent publications have demonstrated the ability of neural crest cells to differentiate into an even larger range of cell types than thought previously, including adipocytes and bone marrow.<sup>17–20</sup> This raises the possibility that neural crest differentiation may have a role in the embryogenesis of LSL and casts doubt on the previous notion of premature dysjunction.

'Complex' LSLs (transitional and chaotic) are related intimately to the conus; indeed, the precise position of the conus may be difficult to identify on MRI in these types. These malformations lie at the interface between primary and secondary neurulation. Some published series indicate that these forms are more likely to result in severe neurological and particularly urological dysfunction.<sup>2</sup> By contrast, 'simple' LSLs (caudal and dorsal) tend to lie on either side, below or above, respectively, the primary–secondary neurulation interface. The conus is identified more readily on MRI in these types of LSL. Although these subtypes seem to present as distinct anatomical entities, there was no correlation with the diversity or maturity of cell types and tissue between complex and simple LSLs (Table 1).

Primary neural tube closure is responsible for formation of the spinal cord above the level of the conus. The remainder of the neural tube, i.e. the conus and filum, forms via secondary neurulation. A mass of neuromesodermal progenitor cells located in the tail bud proliferates to produce a solid rod-like structure which fuses with the primary neural tube. Subsequent cavitation results in completion of formation of the neural tube.<sup>21–23</sup>

As, by definition, caudal and transitional LSLs involve the conus, they are assumed to be related to a defect in the process of secondary neurulation. This is reflected in the high incidence of lipomas associated

with syndromes of complex anorectal and urological malformation [OEIS (omphalocele, exstrophy, imperforate anus, spinal syndrome, cloacal extrophy), VATER (vertebrae, anus, trachea, esophagus, renal)], in which maldevelopment of the caudal cell mass and tail bud are implicated.

A number of different hypotheses have arisen over recent decades regarding the origin of LSL, although none of these have been supported by experimental evidence. McLone *et al.* proposed the theory of premature dysjunction whereby the ectoderm and neuroectoderm separate before closure of the neural tube, thus allowing paraxial mesoderm to migrate into the open neural tube preventing closure and differentiating into fat cells.<sup>24</sup>

Catala proposed the hypothesis of incomplete dysjunction whereby the ectoderm never separates completely from the neuroectoderm and forms a dermal tract that subsequently disrupts normal development around the dorsal spinal cord. As a double-hit model, Catala then proposes that teratogenic cells might be present, inducing abnormal differentiation of the dorsal mesoderm into tissue derived from all three germ layers.<sup>25</sup>

As both these theories involve defects in the process of primary neurulation they can only explain the pathogenesis of dorsal LSLs. In addition, these hypotheses would suggest that a dermal sinus/pit should be associated only with dorsal LSLs.

McLone and Naidich later proposed a role of the tailbud, involved in the process of secondary neurulation, in the formation of caudal LSLs. Similarly, Catala proposed that spinal lipomas associated with sacral agenesis must be due to malfunctions in axis elongation, i.e. the tailbud.<sup>25</sup> On comparing dorsal LSL (thought to be due to a primary neurulation

**Table 1.** Comparison of location, radiological and histological features between simple and complex lumbosacral lipomas

|                            | Simple   | Complex  |
|----------------------------|--|--|
| Previous classification    | Dorsal, caudal*                                  | Transitional, chaotic  |
| Characteristic location    | Dorsal aspect of conus or caudal aspect of conus | Extending from dorsal to caudal aspect of conus, extending ventrally |
| Radiological features (MR) | Associated with bony spina bifida                | Associated with bony spina bifida                                    |
|                            | Preserved conus morphology                       | Conus poorly delineated  |
|                            |  | Rotation of the neural placode                                       |
| Histological features      | Predominantly mature adipocytes                  | Predominantly mature adipocytes                                      |
|                            | Cells of mesodermal and neuroectodermal origin   | Cells of mesodermal and neuroectodermal origin                       |

MR, Magnetic resonance.

\*Lipomas of the filum terminale with intact conus.

defect) with the other LSL subtypes (thought to be due to a secondary neurulation defect) we found no significant difference in the type or diversity of cells present, and particularly the presence of a dermal pit. These data therefore challenge these views on embryogenesis of LSL and suggests a unifying mechanism of pathogenesis, rather than the currently proposed models.

The role of secondary neurulation in conus formation, the lack of an established and proven mechanism and the results of this current pathology study highlight the need to re-examine the theory of embryogenesis of LSL and also our notions of the mechanisms of neurological deterioration. As mentioned above, we propose an alternative embryological origin of spinal lipomas due to maldifferentiation of neural crest cells. Recent literature has indicated that neural crest cells are present within the secondary neural tube as well as the primary neural tube.<sup>26</sup> In addition, our understanding of the cell biology of neural crest cells is expanding rapidly, with neural crest stem cells being identified in a range of different tissue types.<sup>17–20</sup> These cells have the potential to differentiate and even transdifferentiate into the range of cell types seen within the majority of samples within our series.

Historically, all patients underwent early prophylactic surgery due to the pervading assumption that neurological deterioration was inevitable. However, recent evidence suggesting that not all children will ultimately become symptomatic has led to an increasing number of surgeons practising a watch-and-wait policy.<sup>2,3</sup> In keeping with the diverse range of classes and histopathology, clinical deterioration is inconsistent and variable. The presence of mature tissue structures in addition to adipocytes suggests a degree of dysgenesis not described previously, and hints at a cellular mechanism that may contribute to clinical deterioration beyond the mechanical aspect.

The presence of a higher frequency of tissue types within our series may be due to the level of sectioning and analysis. On average, analysis of one block identified 2.9 abnormal cell types, whereas analysis of four blocks revealed on average 4.1 abnormal cell types. Histopathological diagnosis was therefore optimally accurate with analysis of four blocks. With such diverse heterogeneous specimens, it can be assumed that further analysis is likely to reveal further less-frequent cell types. However, our data suggest that abnormal tissue and cells types are dispersed throughout the lipoma tissue, and sufficient analysis is achieved with reviewing four blocks.

In conclusion, our in-depth histopathological analysis of LSL highlights the heterogeneity of cell types within all samples that are not reflected in the current nomenclature. We find no histological difference between radiological subtypes refuting previously proposed theories for separate embryogenesis of the different subtypes. The diversity and maturity of cell types also challenges currently held notions, and may have implications for both the mechanisms of clinical deterioration and the role of surgical intervention. Pure lipomas attached to a fundamentally functional spinal cord are more likely to deteriorate through traction and thus may benefit from untethering surgery. By contrast, more diverse, hamartomatous lipomas (particularly those that occur in the context of other caudal cell mass anomalies) with questionable functional integrity of the conus region would be less likely to benefit from surgery.

### Acknowledgements

The study was supported by the Institute of Child Health, University College London and the Great Ormond Street Hospital NHS Trust, with funding from the Great Ormond Street Children's Charity, Medical Research Council and Smiles with Grace.

### Conflicts of interest

None of the authors have any conflicts of interest to declare.

### References

1. Finn MA, Walker ML. Spinal lipomas: clinical spectrum, embryology, and treatment. *Neurosurg. Focus* 2007; 23: E10.
2. Wykes V, Desai D, Thompson DN. Asymptomatic lumbosacral lipomas – a natural history study. *Childs Nerv. Syst.* 2012; 28: 1731–1739.
3. Kulkarni AV, Pierre-Kahn A, Zerah M. Conservative management of asymptomatic spinal lipomas of the conus. *Neurosurgery* 2004; 54: 868–875.
4. Lassman LP, James CCM. Lumbosacral lipomas: critical survey of 26 cases submitted to laminectomy. *J. Neurol. Neurosurg. Psychiatry* 1967; 30: 174–181.
5. Pang D. Total resection of complex spinal cord lipomas: how, why, and when to operate? *Neurol. Med. Chir. (Tokyo)* 2015; 55: 695–721.
6. Pang D, Zovickian J, Wong ST, Hou YJ, Moes GS. Surgical treatment of complex spinal cord lipomas. *Childs Nerv. Syst.* 2013; 29: 1485–1513.
7. Chapman PH. Congenital intraspinal lipomas: anatomic considerations and surgical treatment. *Childs Brain* 1982; 9: 37.
8. Pang D, Zovickian J, Oviedo A. Long-term outcome of total and near-total resection of spinal cord lipomas and radical

- reconstruction of the neural placode: part I. Surgical technique. *Neurosurgery* 2009; **65**: 511–528; discussion 528–529.
9. Pierre-Kahn A, Zerah M, Renier D et al. Congenital lumbosacral lipomas. *Childs Nerv. Syst.* 1997; **13**: 298–334.
  10. Walsh JW, Markesbery WR. Histological features of congenital lipomas of the lower spinal canal. *J. Neurosurg.* 1980; **52**: 564–569.
  11. Zerah M, Roujeau T, Catala M, Pierre-Kahn A. Spinal lipomas. In Özek M, Cinalli G, Maixner W eds. *Spinal bifida: management and outcome*. Milan: Springer-Verlag, 2008; 445–474.
  12. Lellouch-Tubiana A, Zerah M, Catala M, Brousse N, Pierre-Kahn A. Congenital intraspinal lipomas: histological analysis of 234 cases and review of the literature. *Pediatr. Dev. Pathol.* 1999; **2**: 346–352.
  13. Takeyama J. Spinal hamartoma associated with spinal dysraphism. *Childs Nerv. Syst.* 2006; **22**: 1098–1102.
  14. Dubowitz V, Lober J, Zachary RB. Lipoma of the CAUDA EQUINA. *Arch. Dis. Child.* 1965; **40**: 207–213.
  15. Anderson FM. Occult spinal dysraphism: a series of 73 cases. *Pediatrics* 1975; **55**: 826–835.
  16. Giudicelli Y, Pierre-Khan A, Bourdeaux AM, de Mazancourt P, Lacasa D, Hirsch JF. Are the metabolic characteristics of congenital intraspinal lipoma cells identical to, or different from normal adipocytes? *Childs Nerv. Syst.* 1986; **2**: 290–296.
  17. Billon N, Iannarelli P, Monteiro MC et al. The generation of adipocytes by the neural crest. *Development* 2007; **134**: 2283–2292.
  18. Isern J, Garcia-Garcia A, Martin AM et al. The neural crest is a source of mesenchymal stem cells with specialized hematopoietic stem cell niche function. *Elife* 2014; **3**: e03696.
  19. Paylor B, Joe AW, Rossi FMV, Lemos DR. *In vivo* characterization of neural crest-derived fibro/adipogenic progenitor cells as a likely substrate for craniofacial fibrofatty infiltrating disorders. *Biochem. Biophys. Res. Commun.* 2014; **451**: 148–151.
  20. Sowa Y, Imura T, Numajiri T et al. Adipose stromal cells contain phenotypically distinct adipogenic progenitors derived from neural crest. *PLoS ONE* 2013; **8**: e84206.
  21. Durdag E, Borcek PB, Ocal O, Borcek AO, Emmez H, Baykaner MK. Pathological evaluation of the filum terminale tissue after surgical excision. *Childs Nerv. Syst.* 2015; **31**: 759–763.
  22. Kural C, Guresci S, Simsek GG et al. Histological structure of filum terminale in human fetuses. *J. Neurosurg. Pediatr.* 2014; **13**: 362–367.
  23. Copp AJ, Greene ND. Neural tube defects – disorders of neurulation and related embryonic processes. *Wiley Interdiscip. Rev. Dev. Biol.* 2013; **2**: 213–227.
  24. Naidich T, McLone DG, Mutluer S. A new understanding of dorsal dysraphism with lipoma (lipomyeloschisis): radiologic evaluation and surgical correction. *Am. J. Roentgenol.* 1983; **140**: 1065–1078.
  25. Catala M. Why do we need a new explanation for the emergence of spina bifida with lipoma. *Childs Nerv. Syst.* 1997; **13**: 336–340.
  26. Osorio L, Teillet MA, Palmeirim I, Catala M. Neural crest ontogeny during secondary neurulation: a gene expression pattern study in the chick embryo. *Int. J. Dev. Biol.* 2009; **53**: 641–648.

### Supporting Information

Additional Supporting Information may be found in the online version of this article:

**Figure S1.** (A) Dot plot demonstrating the range of the number of blocks reviewed. (B) Mean number of cell/tissue types detected for specimens based on the number of blocks reviewed. Calculated values for 1, 2, 3, 4, 5, 6 and 9 blocks were 3.0, 3.1, 3.6, 4.1, 3.4, 4.0, 0.1.

**Table S1.** Statistical analysis of data Subtypes of lipoma were grouped into those proposed to be due to a defect in primary neurulation (dorsal) and those proposed to be due to a defect in secondary neurulation (caudal, transitional and chaotic).

**Table S2.** Statistical analysis of data Subtypes of lipoma were grouped into 'simple' (dorsal and caudal) and 'complex' (transitional and chaotic).



## Placode rotation in transitional lumbosacral lipomas: are there implications for origin and mechanism of deterioration?

Victoria Jones<sup>1</sup> · Dominic Thompson<sup>1</sup>

Received: 2 February 2018 / Accepted: 16 March 2018 / Published online: 29 March 2018  
© The Author(s) 2018

### Abstract

**Purpose** Rotation of the lipoma-neural placode has been noted in transitional lumbosacral lipomas. The purpose of this study was to confirm this rotation; that this rotation occurs with a preference to the left, and correlates with clinical symptoms. In addition, this study tests the hypothesis that this rotation occurs through local mechanical forces rather than intrinsic congenital malformation.

**Methods** Lipomas were classified as per the Chapman classification. Degree of rotation of the placode from the coronal plane was recorded along with the presence of herniation outside of the vertebral canal. Abnormalities on urodynamic testing were recorded, along with neuro-orthopaedic signs picked up on formal neuro-physiotherapy assessment.

**Results** Placode rotation occurs more frequently in the transitional group. Regardless of lipoma classification, rotation was much more common to the left. Furthermore, when lateralisation of symptoms was present, this strongly correlated with the direct of rotation. There was no difference in rotation of the placode whether it was within (lipomyelocoele) or without the vertebral canal (lipomyelomeningocoele).

**Conclusions** Placode rotation is a feature of transitional lumbosacral lipomas and may account for the increase in symptoms amongst this subgroup. Herniation of the placode outside the vertebral canal does not increase the risk of rotation suggesting a congenital cause for this finding rather than a purely mechanical explanation.

**Keywords** Dysraphism · Lipomyelomeningocoele · Subtype · Neuro-orthopaedic syndrome · Magnetic resonance imaging

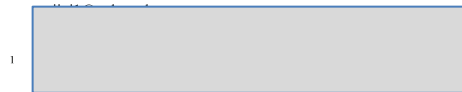
### Introduction

Lumbosacral lipomas (LSLs) are considered to be a form of closed neural tube defect. They account for the most frequent occurrence of closed spinal dysraphism (1 in 4000). Children present at a young age with cutaneous manifestations: a sacral swelling, focal hirsutism or pigmentation, often before neurological symptoms become apparent [5, 7, 20, 25]. As the name suggests, a mass of adipocytes are located at the caudal most aspect of the spinal cord. The mass of predominantly adipocytes is closely adherent to an abnormal caudal spinal cord; the fatty mass then extends through a defect within the dura, a defect in the vertebral lamina, and becomes continuous with

the subcutaneous fat [9, 12, 20, 22]. The timing and extent of surgery remains controversial [16–18, 24], whilst the embryogenesis of this pathology also remains unproven with no animal model in existence [4].

Chapman has classified LSLs based on radiology and surgical anatomy into dorsal, caudal and transitional types according to the site of attachment of the lipoma relative to the conus medullaris [5]. In the dorsal subtype, the interface between lipoma and neural placode is above the conus; the roots of the cauda equina are separate to the lesion and the surgical anatomy tends to be more favourable. By comparison, in the caudal subtype, the tip of the conus becomes continuous with the lipoma and there is a variable association with the roots of the cauda equina. The transitional subtype is allied to the caudal type in that the conus is also involved, the interface between lipoma and neural placode extending for a variable distance from the conus along the dorsolateral aspect of the terminal spinal cord, there is invariable involvement and asymmetry of the roots of the cauda equina. Attempts have been made to correlate radiological findings and anatomical

✉ Victoria Jones



subtype with prognosis; however, although findings have been inconsistent most neurosurgeons would agree that the transitional subtype portends a more severe long-term prognosis, particularly in terms of sphincter continence [23].

In the transitional subtype, the attachment of the lipoma to the neural placode is rarely symmetrical; rather, this interface is typically rotated to one side [10, 20, 22]. This rotation results in some nerve roots emerging more dorsally and therefore having a longer course to their respective nerve root exit foramina whilst the contralateral nerve roots are located deeper and are shorter being closer to their exit foramina. To what extent this rotation is congenital rather than a local mechanical response to growth of the spine and lipoma is unknown; however, the nerve roots on either side are frequently irregular in size, number and point of attachment to the conus suggesting a significant congenital component.

LSLs can be further classified as being associated with herniation of the meninges outside of the vertebral canal, often associated with co-herniation of the caudal spinal cord and neural placode, often referred to as a lipomyelomeningocele (LMM). Alternatively, no herniation of the meninges through the bony defect is often referred to as a lipomyelocoele (LM).

There has been some evidence that neural placode rotation occurs preferentially to one side more than the other. In addition, this asymmetry has also been documented in the location of cutaneous stigmata and manifestations of neuro-orthopaedic syndrome [20]; however, no correlation has yet been established between rotation, symptoms and prognosis. There is, however, an increasing literature on the early developmental origins of laterality and it is postulated that if there were significant tendencies to rotate to one side, this might shed some light on the pathogenesis of lumbosacral lipoma.

The aim of this study is to confirm the presence of placode rotation within LSLs, and in particular that this rotation occurs not only more commonly in the transitional subtype, but also occurs more commonly towards the left. Secondly, we propose that rotation puts mechanical stress on nerve roots and that a rotated neural placode is likely to be correlated with the presence of unilateral symptoms. Finally, we propose that this laterality and rotation can be due to either congenital effects or local mechanical influences. Since herniation of the cord out of the canal is likely to cause significant mechanical effects, one would expect to see a significant difference when herniation is present (lipomyelomeningocele) compared to when it is not present (lipomyelocoele). Alternatively, no difference between lipomyelomeningocele and lipomyelocoele would be more consistent with a primary congenital origin of the rotation.

## Methods

Cases of transitional and non-transitional LSLs were identified from a spinal lipoma database collected at the Great

Ormond Street Hospital (GOSH) over a period of 15 years. Classification was confirmed, as per Chapman classification, by both radiological assessments of T1-weighted axial and sagittal images and at time of surgery. In the case where serial imaging was done over a period of years, all pre-operative images were reviewed. Imaging was further reviewed to identify the neural placode and lipoma with classification of the neural placode as being rotated to either right, left or no significant rotation. Operation notes were then reviewed to confirm radiological rotation.

Direction of rotation as recorded was taken to describe the position of the lipoma in respect to the spinal cord. A placode rotated to the right would be associated with lipoma tissue predominantly extending to the right of the spinal cord whilst nervous tissue remained to the left of the spinal canal. The right nerve roots would be orientated more ventrally and therefore deeper whilst the left nerve roots would be orientated more dorsally. Conversely, a lipoma said to be rotated to the left (Fig. 1) will be associated with a right-sided nerve root lying more superficial and presenting itself earlier at surgical dissection, whilst the left nerve root will lie deep and buried under the mass of the lipoma and the rotated neural placode.

T1-weighted axial and sagittal sections were reviewed to identify the point of the greatest rotation. Axial sections were then further reviewed with identification and marking of the midline. Care was taken to take into account possible rotation of the patient at time of imaging. This was achieved by determining the horizontal plane through the coronal axis of the vertebral body. A separate line was then drawn through the neural placode at the level of greatest rotation. The angle between this and the horizontal was then measured. No rotation was taken to be a neural placode orientated parallel to the horizontal plane. Results were subsequently divided into left

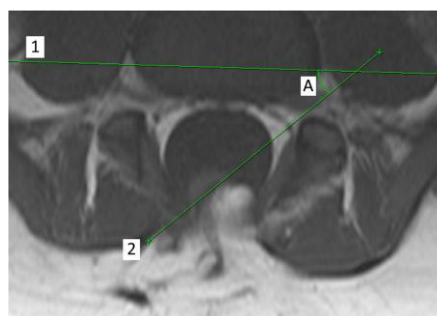


**Fig. 1** Measurement of rotation on T1 axial MR imaging with lipoma-neural placode rotated to the left. Lines that are drawn through coronal plane of vertebral body (1) and coronal plane of lipoma-neural placode at maximal rotation (2). Degree of rotation (A) measured as angle subtended by the plane of the placode (2) and horizontal plane (1)



rotation with the neural placode rotated anti-clockwise from the neutral position and right rotation with the neural placode rotated clockwise from the neutral position.

Any angle less than 20° was taken to be equivocal and not demonstrating any rotation. The thinking behind this decision was firstly to account for any potential error within the method described but secondly to account for the significance of rotation to surgical planning with rotation of less than 20° presenting no significance. Results were subsequently divided into 20–45°, 45–70° and 70–90°.

Clinical notes were then reviewed of the transitional LSLs to look for presence of urological symptoms from history and signs from formal urodynamic testing. Similarly, lateralised neurological symptoms such as pain were identified through the history and neuro-orthopaedic signs were documented from assessment by both a physiotherapist and a neurosurgeon.

Results are expressed as patient numbers followed by a percentage and confidence interval (expressed in brackets). Standard error was calculated to determine the 95% confidence interval, unless otherwise stated. Comparisons between test and control groups were performed by calculating the difference in percentage followed by the standard error of that difference. Results were taken to be significant when the range of the 95% confidence interval did not cross zero.

## Results

A total of 155 cases were reviewed using pre-operative magnetic resonance imaging and intra-operative surgical documentation. LSLs were classified as per Chapman classification.

A total of 52 cases of transitional lumbosacral spinal lipomas were identified and included in the final analysis. Twelve (23.1, 13.7–36.1%) cases were considered to show equivocal or no rotation (as mentioned above, this was taken to be less than a maximum of 20° rotation in either direction). Of the remaining 40 cases, 26 (65.0, 49.5–77.9%) showed rotation to the left between 20 and 90°. Conversely, 14 (35.0, 22.1–50.5%) cases showed rotation to the right between 20 and 90°.

Forty-six control patients with non-transitional LSLs were selected by random number generator and their pre-operative imaging reviewed. Thirty (65.2, 50.8–77.3%) demonstrated no or equivocal rotation, of the remaining 16, 11 (68.8, 44.4–85.8%) demonstrated rotation to the left and 5 (31.3, 14.2–55.6%) demonstrated rotation to the right.

Relative risk of rotation was calculated between the transitional lipoma and non-transitional lipoma group to 2.21. Those children with transitional lipomas are 2.21 times more likely to have a rotated placode—an increase in 121%. Although rotation was much more common amongst the transitional lipomas, there was no significant difference between the directions of rotation between the two groups (Fig. 2).

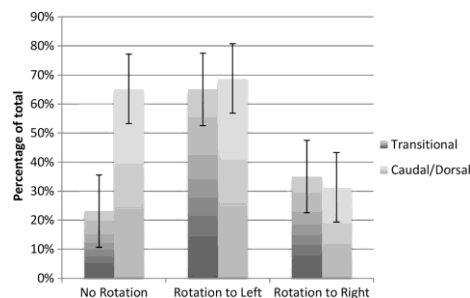


**Fig. 2** Comparison of incidence of direction of rotation between transitional and caudal/dorsal lipomas. Increased rotation is found in transitional lipomas; however, when rotation is present, the incidence of rotation to the left remains consistent between both groups

Twelve (23%) patients were asymptomatic, a further 13 (25%) had only urological symptoms or abnormal findings on urodynamic assessment. A total of 27 (52%) patients had symptoms and/or signs in keeping with neuro-orthopaedic syndrome such as lower limb pain/altered sensation, muscle weakness and foot deformity. There was a clear correlation between direction of rotation of placode and unilateral symptoms (rotation to the left and left sided symptoms 76%, rotation to the right and right sided symptoms 100%) (Fig. 3).

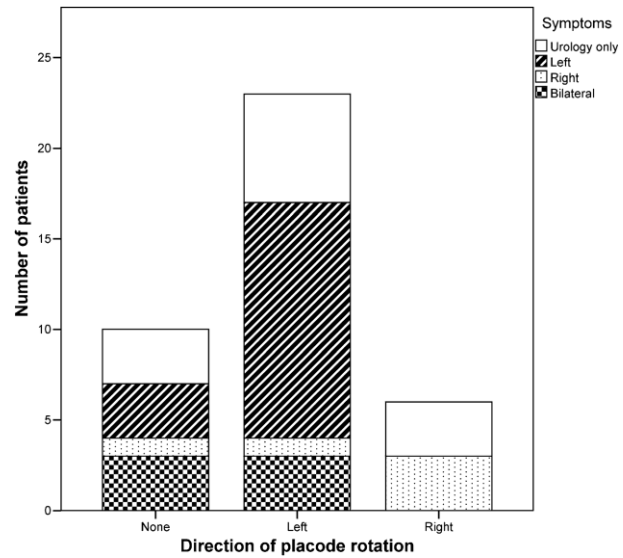
Seventeen lipomyelomeningoceles were identified accounting for 32% of cases and 35 lipomyelocoeles were identified accounting for 67% of cases. Further analysis was then performed to identify any difference in rotation between these two subgroups.

Of the 17 lipomyelomeningoceles, 8 showed rotation to the left (57.1, 32.6–78.6%) and 6 showed rotation to the right (42.9, 21.4–67.4%), whilst 3 cases (17.6, 6.2–41.0%) demonstrated less than 20° rotation or were considered to show equivocal rotation. There was no significant statistical difference between the directions of rotation within this group.

Of the 35 lipomyelocoeles, 17 showed rotation to the left (68.0, 48.4–82.8%) and 8 showed rotation to the right (32.0, 17.2–51.6%), whilst 10 (28.6, 16.3–45.1%) demonstrated less than 20° rotation or were considered to show equivocal rotation. There was no significant statistical difference between the frequency and direction of rotation between the lipomyelocoele and lipomyelomeningocoele groups (Fig. 4).

To further test the hypothesis that placode herniation is associated with increased rotation, the degree of rotation was measured and recorded in groups: < 20°, 20–45°, 45–70° and 70–90°. None of the transitional LSLs demonstrated more than 90° rotation. When lipomyelomeningoceles were rotated to the right, this was most frequently at 70–90° rather than lesser degrees of rotation. Lipomyelocoeles did not demonstrate this same preponderance for being maximally rotated to the right (Tables 1 and 2).

**Fig. 3** Symptoms experienced by patients with radiologically rotated transitional lipoma. Urological symptoms/abnormal findings on formal urodynamic assessment present with similar frequency in all groups. Side of symptoms associated with direction of rotation



**Discussion**

Transitional lumbosacral lipomas are amongst the more difficult lipomas to treat surgically and are those associated with more significant long-term functional impairment. The majority of infants with lipomas are asymptomatic at initial presentation but over half will go onto deteriorate and manifest features of the neuro-orthopaedic syndrome. The pathogenesis of the neurological dysfunction in complex lipomas has been extensively debated; however, the relative contribution of congenital dysplasia of the terminal spinal cord versus

mechanical tethering remains unknown. Hitherto, the lumbosacral lipomas have been considered as a single entity; however, this study of only transitional-type lumbosacral lipomas reveals significant anatomical heterogeneity in this group that might have implications for both our understanding of the cause of lipomas and the variable natural history.

The presence of nerve roots passing through the lipoma itself and the close adherence of the lipoma to nervous tissue at the neural placode requires meticulous dissection with the aid of neurophysiology to ensure the optimum outcome [16–19]. By reviewing our case series of transitional lipomas, we have demonstrated, for the first time, this variation in anatomy of this subtype of LSL.

We have demonstrated an association between transitional LSLs and rotation of the neural placode with rotation being 2.21 times more likely to occur in transitional LSLs. This raises the question as to why this is preferentially occurring in transitional LSLs as supposed to the other subtypes. We have tested the hypothesis that local mechanical factors may have a role by comparing rotation in the presence of placode herniation against the degree of rotation found with no herniation and have not found a significant difference. This highlights the possibility of an intrinsic congenital cause for the formation of transitional lipomas.

We have further demonstrated a correlation with direction of placode rotation and the presence of symptoms on the ventrally tilted side of the placode. It may be tempting to attribute this entirely to the mechanics of a rotated

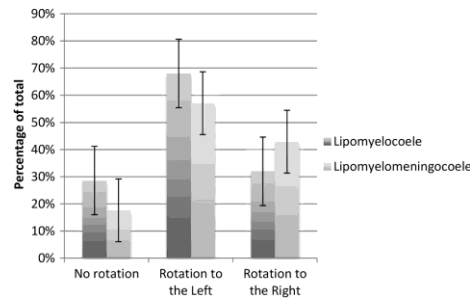


**Fig. 4** Comparison of incidence of direction of rotation between lipomyelocoeles and lipomyelomeningocoeles. There is no significant difference between the two groups

**Table 1** Degree of rotation of neural placode

|       | L70–90 | L45–70 | L20–45 | ±20 | R20–45 | R45–70 | R70–90 | Total |
|-------|--------|--------|--------|-----|--------|--------|--------|-------|
| LM    | 6      | 4      | 7      | 10  | 3      | 4      | 1      | 35    |
| LMM   | 3      | 4      | 1      | 3   | 1      | 1      | 4      | 17    |
| TOTAL | 9      | 8      | 8      | 13  | 4      | 5      | 5      | 52    |

*L* indicates rotation to left, *R* indicates rotation to right

placode with one nerve root being considerably more stretched than the contralateral nerve root. However, pure rotation is likely to put stretch on both nerve roots. This, along with unilateral symptoms in non-rotated lipomas, supports the hypothesis that there is another intrinsic congenital process underlying the pathogenesis and progression of this pathology.

The pathogenesis of lumbosacral lipomas remains undetermined despite a range of theories [4, 7, 13, 15]. It is clear from the spina bifida defect associated with these lipomas that this is a congenital pathology with initiation of pathogenesis occurring prior to the completion of the formation of the caudal vertebrae. Neither a genetic nor an environmental cause has yet been found to cause LSLs, although some large scale genetic screens have suggested associations [3]. The presence of a degree of laterality demonstrated within this paper, with particular reference to transitional LSL, cannot explain the pathogenesis. However, it does raise interesting questions about the pathogenesis process: whether these lipomas form on one side of the embryo body axis, perhaps as a somatic mutation or through “premature disjunction” or whether local anatomy restricts growth of the lipoma such that it preferentially grows on the left more than the right, remains to be answered.

Normal development results in the asymmetry throughout systems of the body, perhaps most noticeably in the cardiovascular and gastrointestinal system. However, more subtle asymmetry is also present within the central nervous system. Regulation of this asymmetry is largely thought to be due to two mechanisms: firstly, the early expression of *lefty2* and *nodal* on the left hand side of the body, and secondly, ongoing signals released by midline structures. Axis determination occurs early in the embryo with the node, primitive streak and even early

endoderm all known to be involved in establishing the left-right body axis. Cilia within the node are thought to help develop a morphogen gradient with local leftwards laminar flow set-up by the nodal cilia. In addition, midline structures are also thought to act as a barrier to diffusion of these signals [11]. Early defects, such as in *nodal*, result in body wide defects—such as *situs inversus*. *Notch* has recently been found to have a role in establishing L-R asymmetry, of note, *notch* is also involved in the differentiation of adipocytes, smooth muscle, blood vessels and neural progenitors to glial cells [2, 6, 14, 21].

In LSLs, none of the surrounding non-spinal anatomy seems to be asymmetrical indicating an otherwise normal axis development. This suggests two hypotheses as to how L-R body patterning might be involved in LSL formation. Firstly, a germ-line mutation might be present which is susceptible to and only manifests in pathology in the presence of local signals. Alternatively, a somatic mutation might be acquired to the left or right, with left-sided mutations occurring more frequently due to the influences of local factors. A comparison can perhaps be made with *Holt–Oram* syndrome in which skeletal manifestations are more commonly seen on the left [8]. Although the transcription factor *TBX5* is known to be mutated in inherited cases an explanation for this laterality remains absent [1].

The analysis within this paper is limited by the small number of cases of lumbosacral lipomas that are encountered, and this is particularly of importance when considering the further analysis of subtypes of transitional LSLs. However, for the first time, we demonstrate the frequency and degree of rotation of the neural placode within this pathology and a correlation with clinical symptoms. This ultimately might have implications towards understanding the embryogenesis of lumbosacral lipomas.

**Table 2** Degree of rotation of neural placode expressed as percentage of total cases by subtype

|       | L70–90 | L45–70 | L20–45 | ±20  | R20–45 | R45–70 | R70–90 | Total |
|-------|--------|--------|--------|------|--------|--------|--------|-------|
| LM    | 17.6   | 11.8   | 20.6   | 26.5 | 8.8    | 11.8   | 2.9    | 100   |
| LMM   | 17.6   | 23.5   | 5.9    | 17.6 | 5.9    | 5.9    | 23.5   | 100   |
| TOTAL | 17.6   | 15.7   | 15.7   | 25.5 | 7.8    | 9.8    | 9.8    | 100   |

*L* indicates rotation to the left, *R* indicates rotation to the right

**Funding** The study was supported by the Institute of Child Health, University College London; Great Ormond Street Hospital NHS Trust and with funding from the Great Ormond Street Children's Charity, Medical Research Council and Smiles with Grace.

### Compliance with ethical standards

**Conflict of interest** The authors declare that they have no conflict of interest.

**Ethical approval** For this type of study, formal consent is not required. Local institution approval was obtained through the research and development department.

**Open Access** This article is distributed under the terms of the Creative Commons Attribution 4.0 International License (<http://creativecommons.org/licenses/by/4.0/>), which permits unrestricted use, distribution, and reproduction in any medium, provided you give appropriate credit to the original author(s) and the source, provide a link to the Creative Commons license, and indicate if changes were made.

### References

- Al-Qattan MM, Abou Al-Shaar H (2015) Molecular basis of the clinical features of Holt–Oram syndrome resulting from missense and extended protein mutations of the TBX5 gene as well as TBX5 intragenic duplications. *Gene* 560:129–136. <https://doi.org/10.1016/j.gene.2015.02.017>
- Andersson ER, Sandberg R, Lendahl U (2011) Notch signaling: simplicity in design, versatility in function. *Development* 138:3593–3612. <https://doi.org/10.1242/dev.063610>
- Bartsch O, Kirmes I, Thiede A, Lechno S, Gocan H, Florian IS, Haaf T, Zechner U, Sabova L, Horn F (2012) Novel VANG1 gene mutations in 144 Slovakian, Romanian and German patients with neural tube defects. *Mol Syndromol* 3:76–81. <https://doi.org/10.1159/000339668>
- Catala M (1997) Why do we need a new explanation for the emergence of spina bifida with lipoma. *Childs Nerv Syst* 13:336–340
- Chapman PH (1982) Congenital intraspinal lipomas: anatomic considerations and surgical treatment. *Childs Brain* 9:37
- Chartoumpakis DV, Palliyaguru DL, Wakabayashi N, Khoo NK, Schoiswohl G, O'Doherty RM, Kensler TW (2015) Notch intracellular domain overexpression in adipocytes confers lipodystrophy in mice. *Mol Metab* 4:543–550. <https://doi.org/10.1016/j.molmet.2015.04.004>
- Finn MA, Walker ML (2007) Spinal lipomas: clinical spectrum, embryology, and treatment. *Neurosurg Focus* 23:E10–E12. <https://doi.org/10.3171/FOC-07/08/E10>
- Holt M, Oram S (1960) Familial heart disease with skeletal malformations. *Br Heart J* 22:236–242
- John W, Walsh WRM (1980) Histological features of congenital lipomas of the lower spinal canal. *J Neurosurg* 52:564–569
- Kulkarni AV, Pierre-Kahn A, Zerah M (2004) Conservative management of asymptomatic spinal lipomas of the conus. *Neurosurgery* 54:868–875. <https://doi.org/10.1227/01.neu.0000114923.76542.81>
- Lee JD, Anderson KV (2008) Morphogenesis of the node and notochord: the cellular basis for the establishment and maintenance of left-right asymmetry in the mouse. *Dev Dyn* 237:3464–3476. <https://doi.org/10.1002/dvdy.21598>
- Lellouch-Tubiana A, Zerah M, Catala M, Brousse N, Pierre-Kahn A (1999) Congenital intraspinal lipomas: histological analysis of 234 cases and review of the literature. *Pediatr Dev Pathol* 2:346–352
- Li YC, Shin S-H, Cho B-K, Lee M-S, Lee Y-J, Hong S-K, Wang K-C (2001) Pathogenesis of lumbosacral lipoma: a test of the 'pre-mature dysfunction' theory. *Pediatr Neurosurg* 34:124–130
- Manderfield LJ, Aghajanian H, Engleka KA, Lim LY, Liu F, Jain R, Li L, Olson EN, Epstein JA (2015) Hippo signaling is required for Notch-dependent smooth muscle differentiation of neural crest. *Development* 142:2962–2971. <https://doi.org/10.1242/dev.125807>
- Naidich T, McLone DG, Mutluer S (1983) A new understanding of dorsal dysraphism with lipoma (lipomyeloschisis): radiologic evaluation and surgical correction. *Am J Roentgenol* 140:1065–1078
- Pang D (2015) Total resection of complex spinal cord lipomas: how, why, and when to operate? *Neurol Med Chir* 55:695–721. <https://doi.org/10.2176/nmc.ra.2014-0442>
- Pang D, Zovickian J, Oviedo A (2009) Long-term outcome of total and near-total resection of spinal cord lipomas and radical reconstruction of the neural placode: part I—surgical technique. *Neurosurgery* 65:511–528; discussion 528–519. <https://doi.org/10.1227/01.NEU.0000350879.02128.80>
- Pang D, Zovickian J, Oviedo A (2010) Long-term outcome of total and near-total resection of spinal cord lipomas and radical reconstruction of the neural placode, part II: outcome analysis and pre-operative profiling. *Neurosurgery* 66:253–273
- Pang D, Zovickian J, Wong ST, Hou YJ, Moes GS (2013) Surgical treatment of complex spinal cord lipomas. *Childs Nerv Syst* 29:1485–1513. <https://doi.org/10.1007/s00381-013-2187-4>
- Pierre-Kahn A, Zerah M, Renier D, Cinalli G, Sainte-Rose C, Lellouch-Tubiana A, Brunelle F, Le Merrer M, Giudicelli Y, Pichon J, Kleinknecht B, Nataf F (1997) Congenital lumbosacral lipomas. *Childs Nerv Syst* 13:298–334
- Przemek GKH (2003) Node and midline defects are associated with left-right development in Delta1 mutant embryos. *Development* 130:3–13. <https://doi.org/10.1242/dev.00176>
- Tortori-Donati P, Andrea R, Biancheri R, Cama A (2001) Magnetic resonance imaging of spinal dysraphism. *Top Magn Reson Imaging* 12:375–409
- Tu A, Hengel AR, Cochrane DD (2016) Radiographic predictors of deterioration in patients with lumbosacral lipomas. *J Neurosurg Pediatr* 18:171–176. <https://doi.org/10.3171/2016.1.PEDS15614>
- Wykes V, Desai D, Thompson DN (2012) Asymptomatic lumbosacral lipomas—a natural history study. *Childs Nerv Syst* 28:1731–1739. <https://doi.org/10.1007/s00381-012-1775-z>
- Zerah M, Roujeau T, Catala M, Pierre-Kahn A (2008) Spinal lipomas. In: Ozek MM, Cinalli G, Maixner W (eds) *Spina bifida: Management and outcome*, first edition. Springer-Verlag Mailand, p 445–474. <https://doi.org/10.1007/978-88-470-0651-5>